Space-based Gamma-Ray Astrophysics

M.Tavani

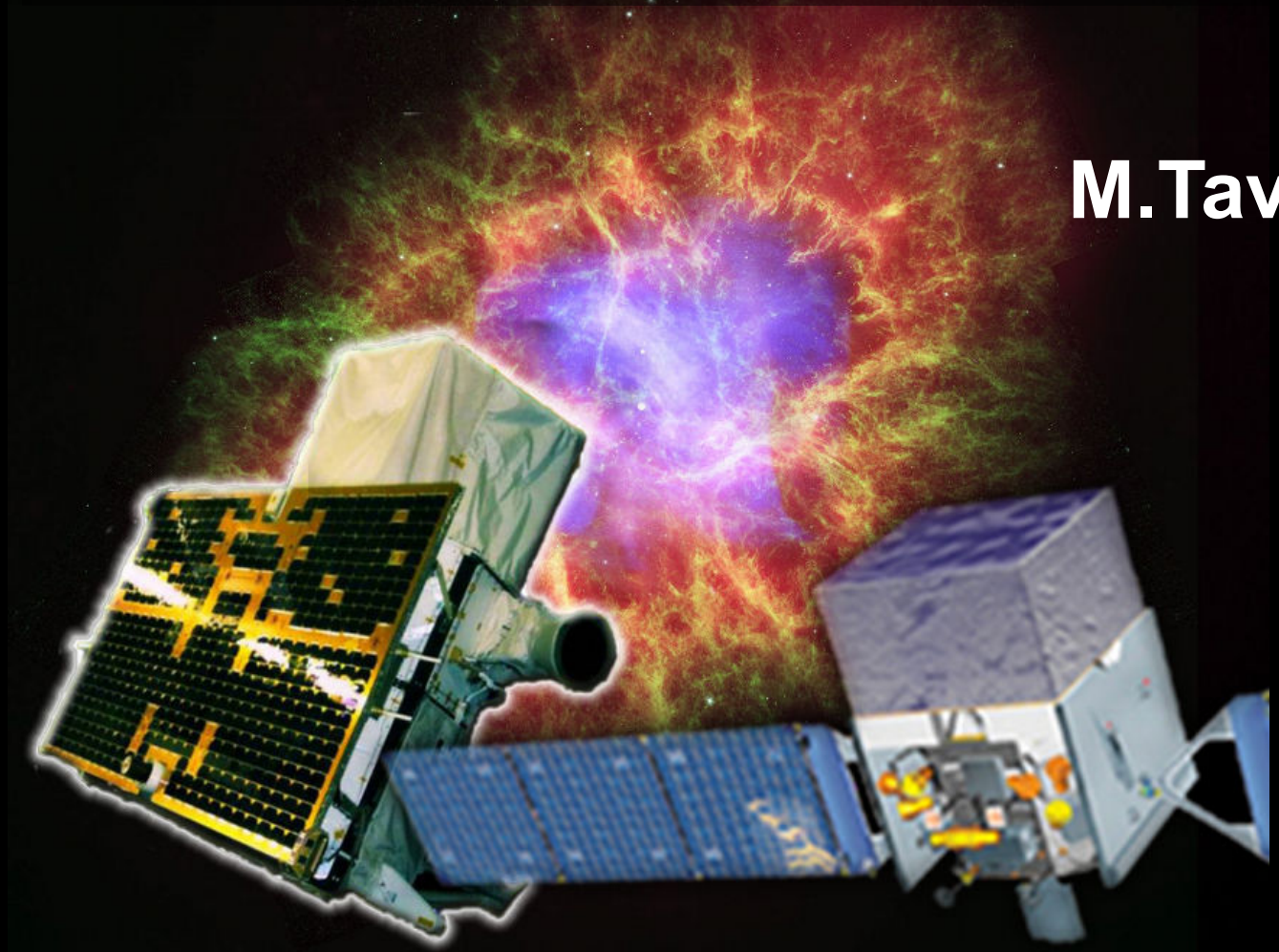

Dublin Summer School on High-Energy Astrophysics, 4-15 July, 2011

cosmic accelerators (hadronic vs. leptonic)

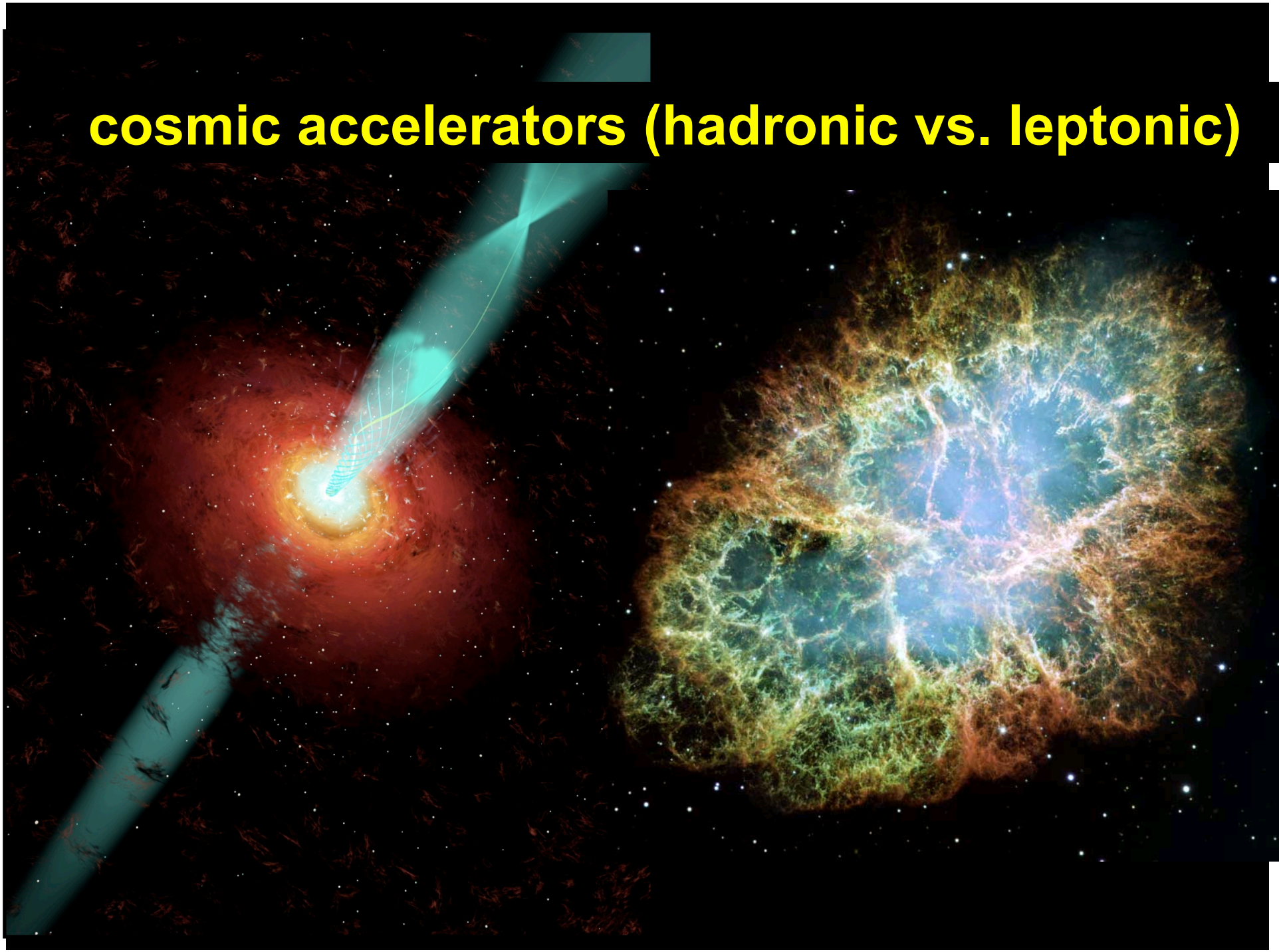

High-energy astrophysics challenges

- unique time for high-energy astrophysics
- more than a dozen observatories/facilities active in the range X-ray/gamma-rays/TeV
- particle acceleration in
  - Neutron stars and PWNe
  - Black holes
  - Supernova Remnants
  - AGNs (blazars)
  - GRBs

Gamma-ray astrophysics above 100 MeV

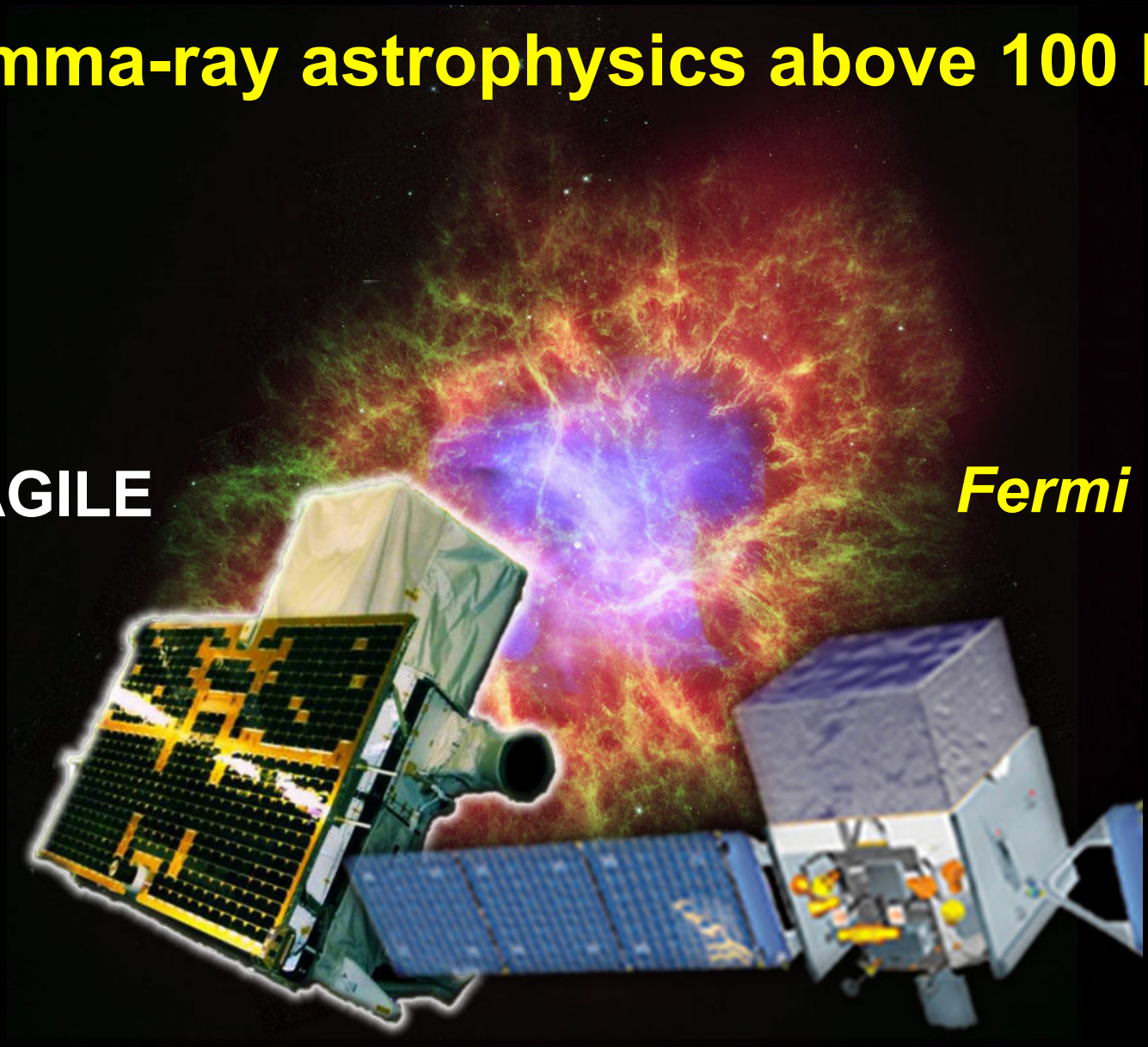

Picture of the day, Feb. 28, 2011, NASA-HEASARC

Gamma-ray astrophysics missions (above 30 MeV)

SAS-2	NASA	Nov. 1972 – July 1973
COS–B	ESA	Aug. 1975 – Apr. 1982
CGRO	NASA	Apr. 1991 – Jun. 2000
AGILE	ASI	April 23, 2007
Fermi	NASA	June 11, 2008

A quick comparison

	AGILE	FERMI-LAT
A_{eff} (100 MeV) (cm^2)	~ 400	~ 400-800
A_{eff} (1 GeV) (cm^2)	~ 500	~ 4000 - 8000
FOV (sr)	2.5	2.5
sky coverage	1/5	whole sky
Energy resolution (~ 400 MeV)	50 %	10 %
PSF (68 % cont. radius) 100 MeV 1 GeV	 3° - 4° < 1°	 4° - 5° < 1°

optical band sky

gamma-ray band (E>100 MeV)

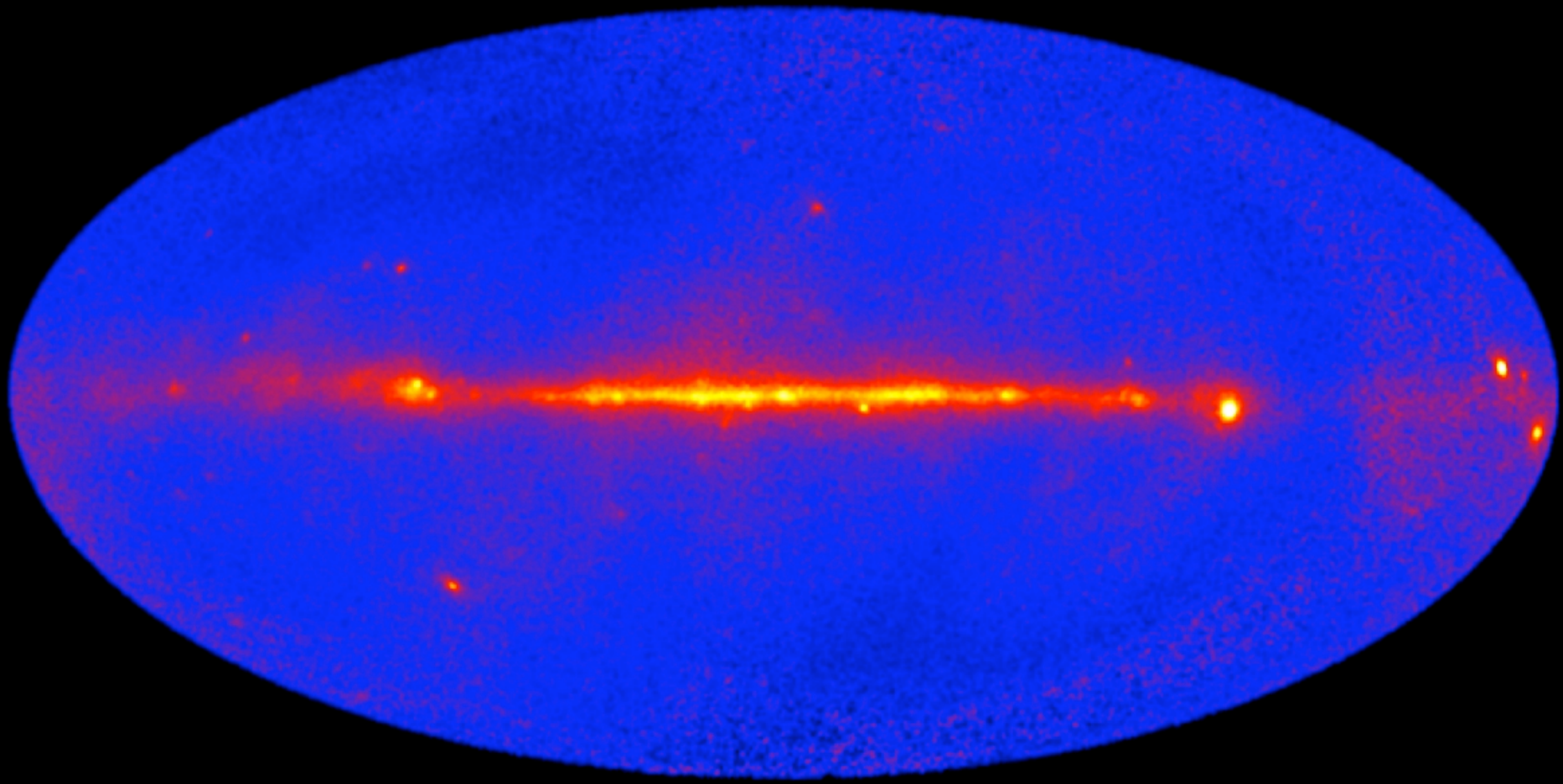

The AGILE gamma-ray sky (E > 100 MeV)
2 year exposure: July 2007 – June 2009

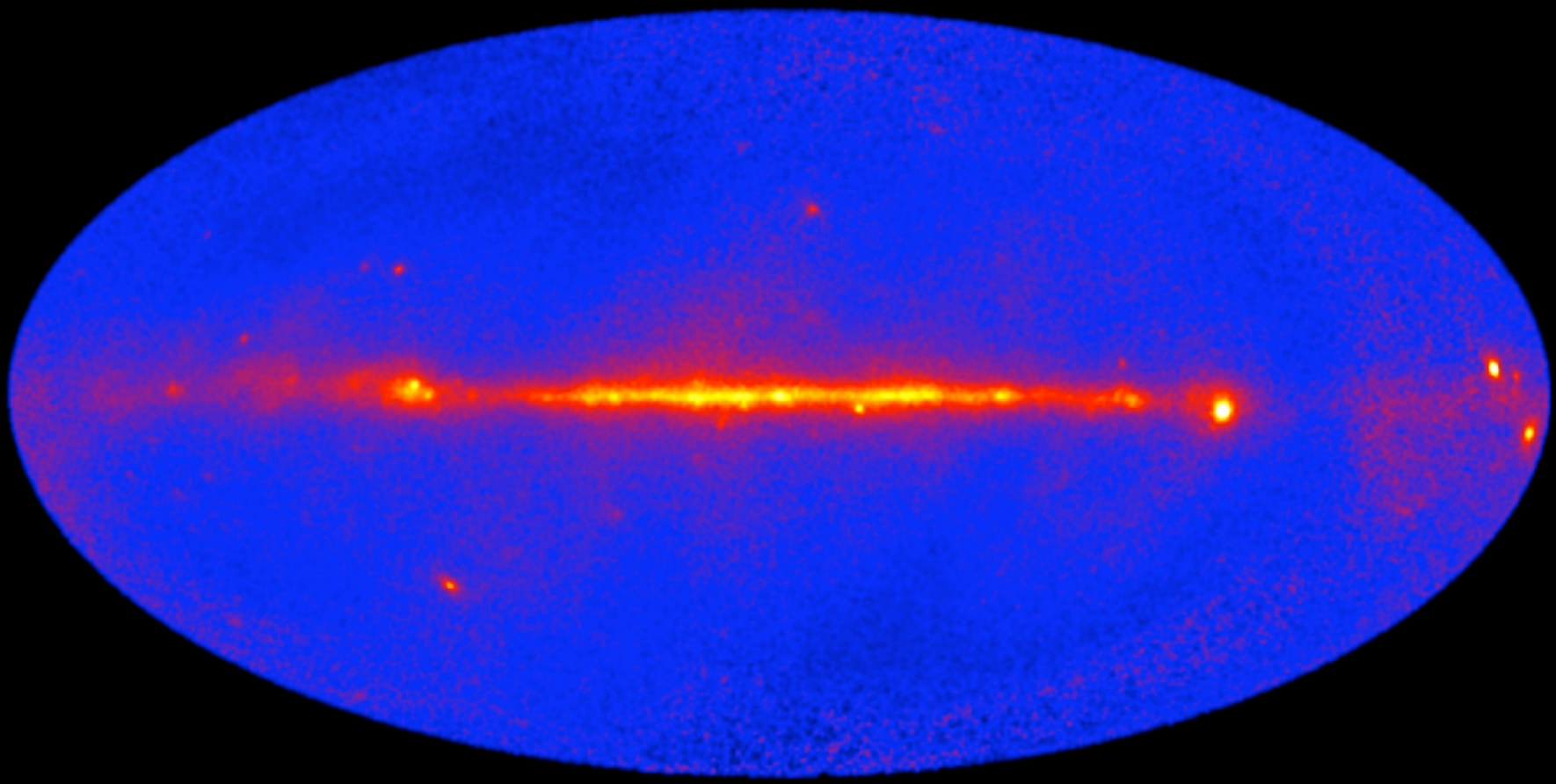

The Gamma-Ray Sky (11 months)

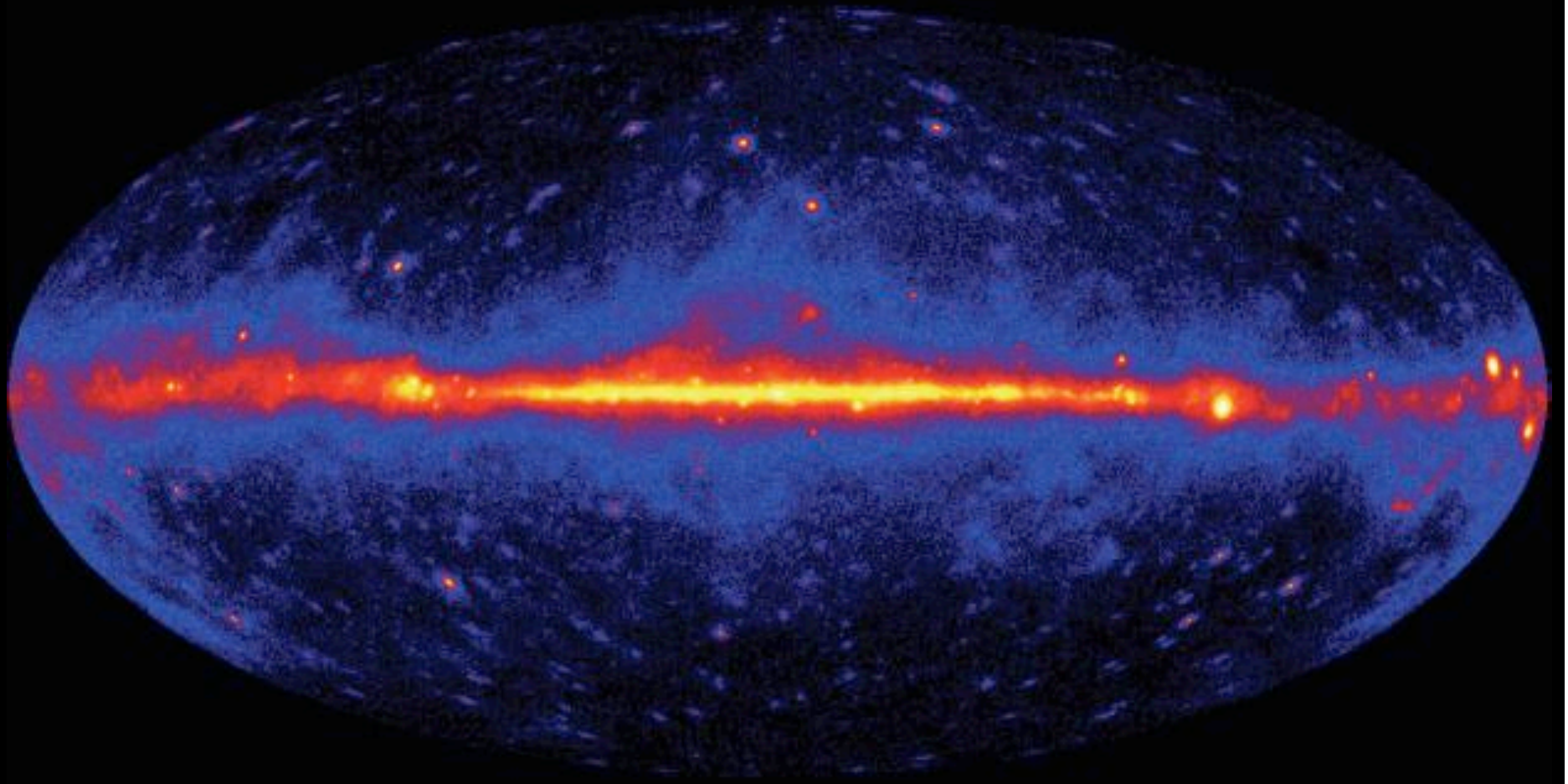

NASA-DOE-Fermi LAT Kollaboration

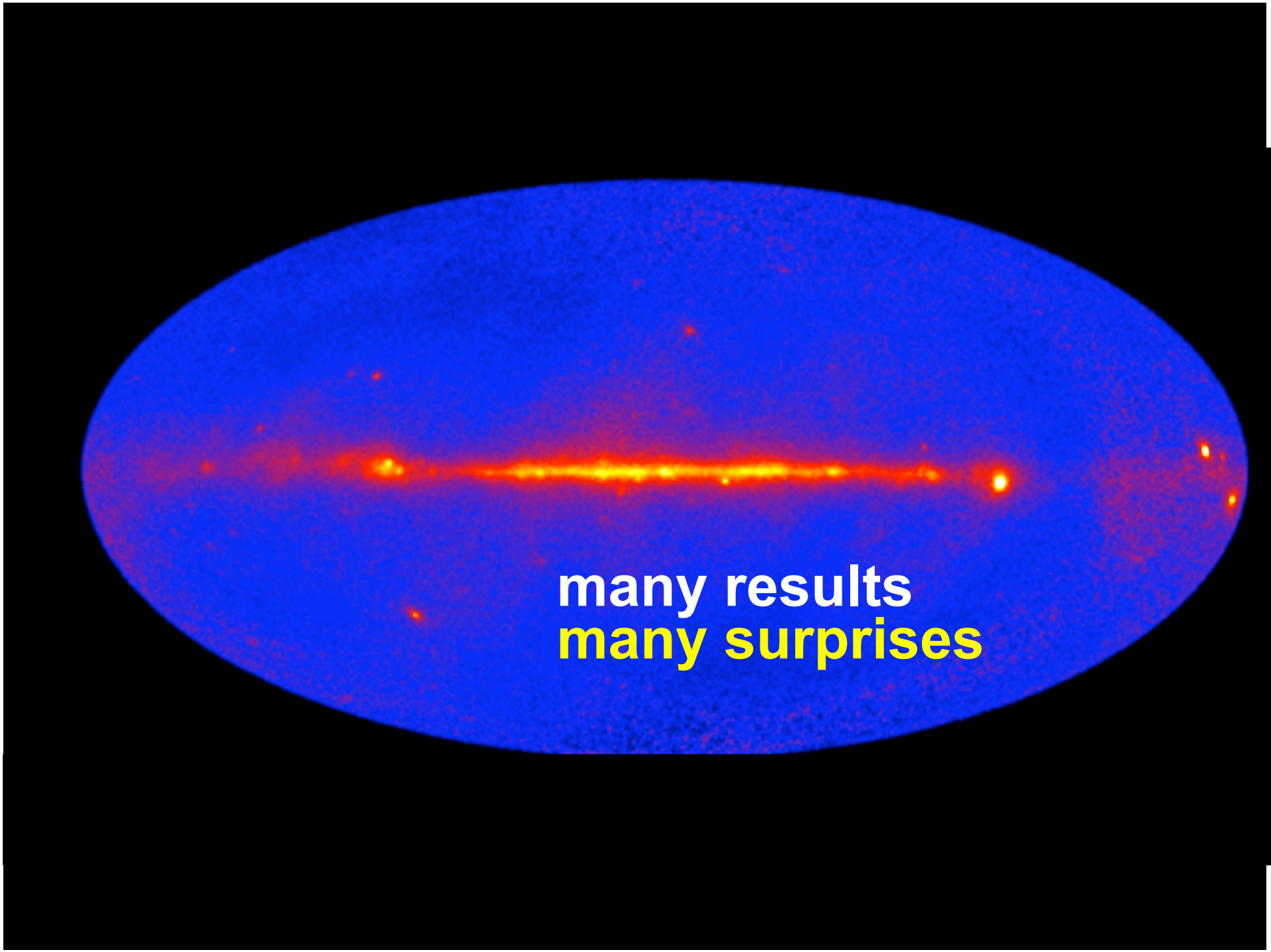
many results
many surprises

AGILE vs. Fermi: sometimes different results

- AGILE-GRID is optimized near 100 MeV, Fermi-LAT at E > 1 GeV

- depending on the season and source position, AGILE and Fermi can have quite different exposure below 1 GeV
  - exposure and off-axis distribution
  - different livetime sequence, different time window

Fermi exposure vs. time (astro-ph/ arXiv :1008.3235)

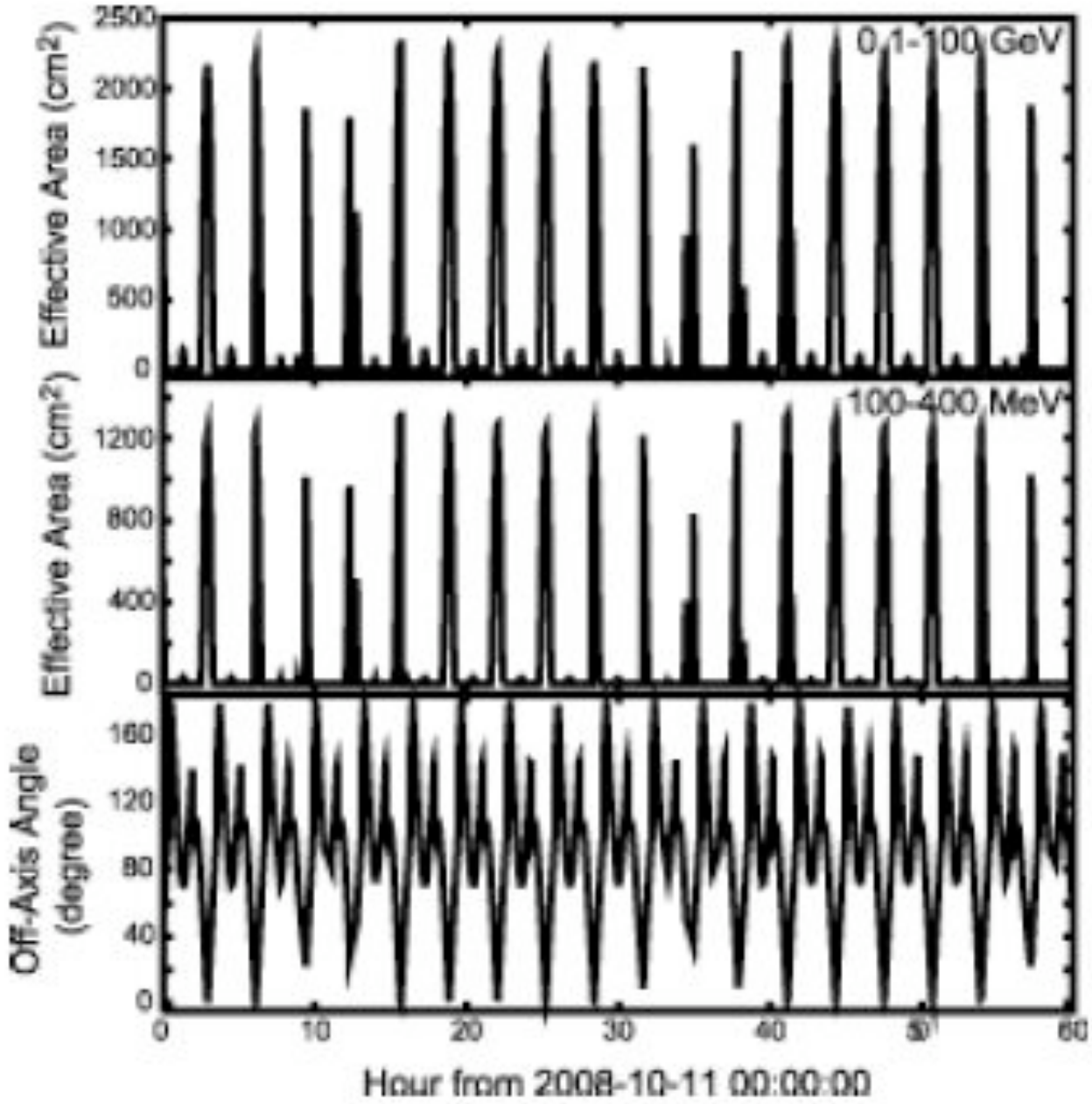

1. Cyg X-3 flare (3 Nov 2008) – pointing mode

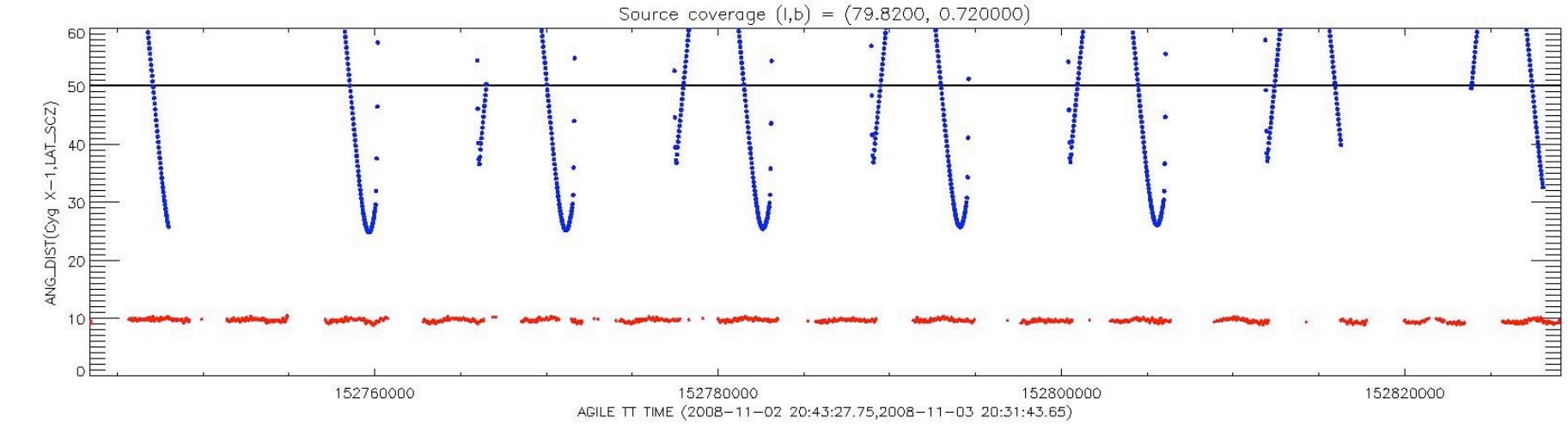

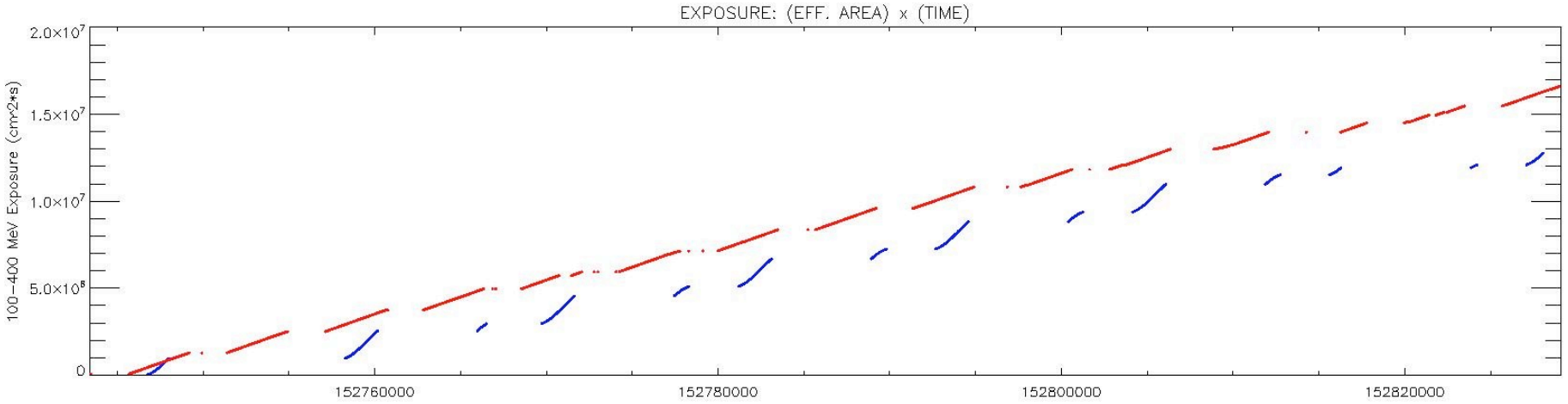

1. Cyg X-3 flare (3 Nov 2008) – pointing mode

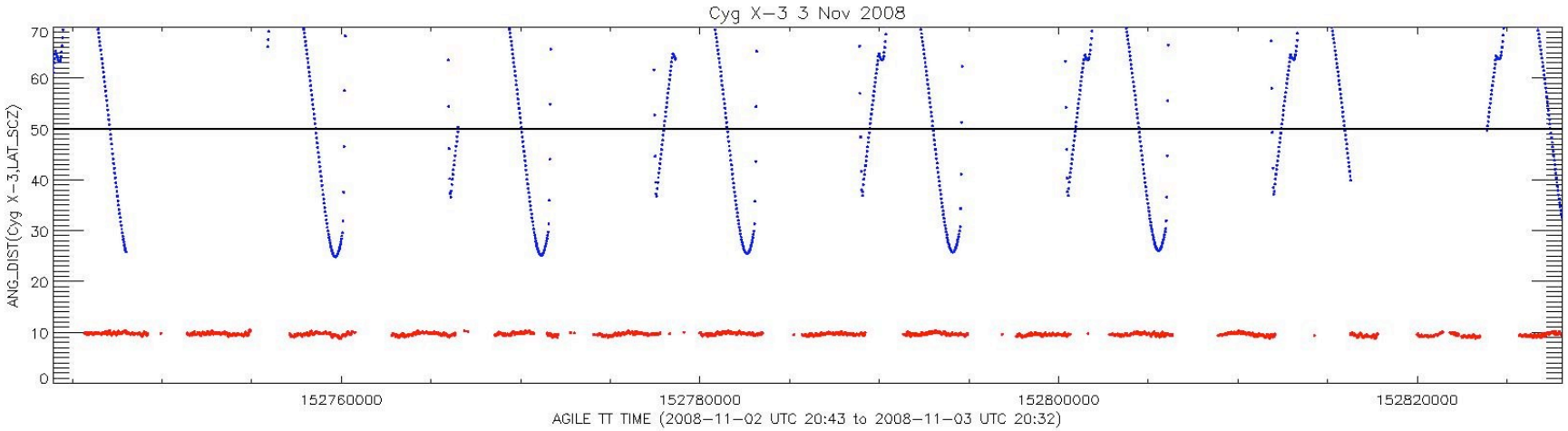

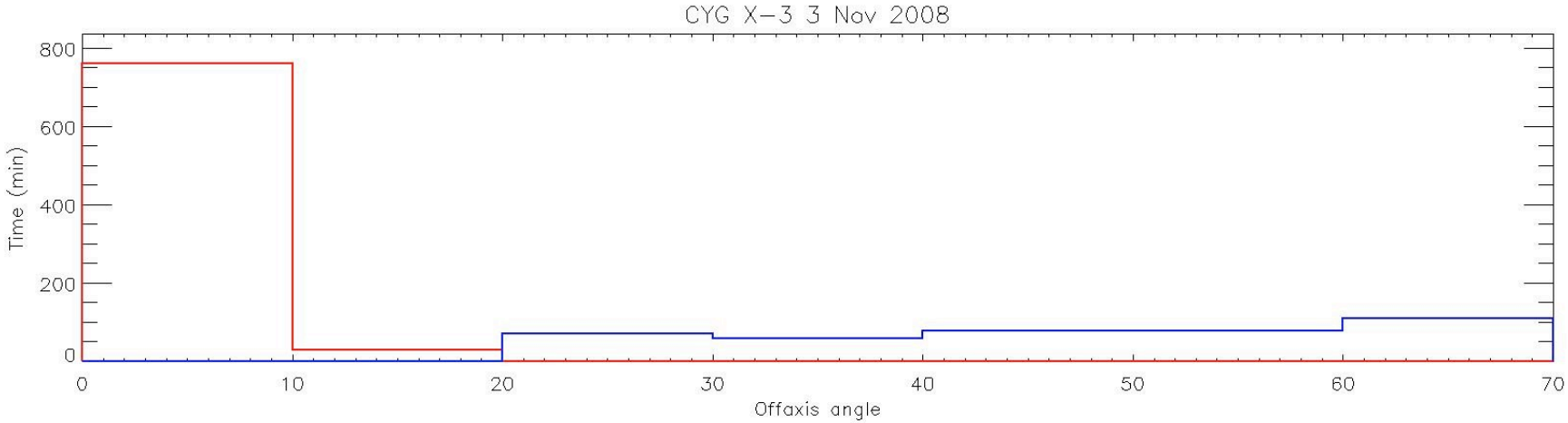

Example: Galactic Centre 2-days integration (13-14 Mar 2010)

AGILE spinning mode vs. Fermi (Sabatini et al. 2010)

Red data (AGILE)
Blue data (Fermi)

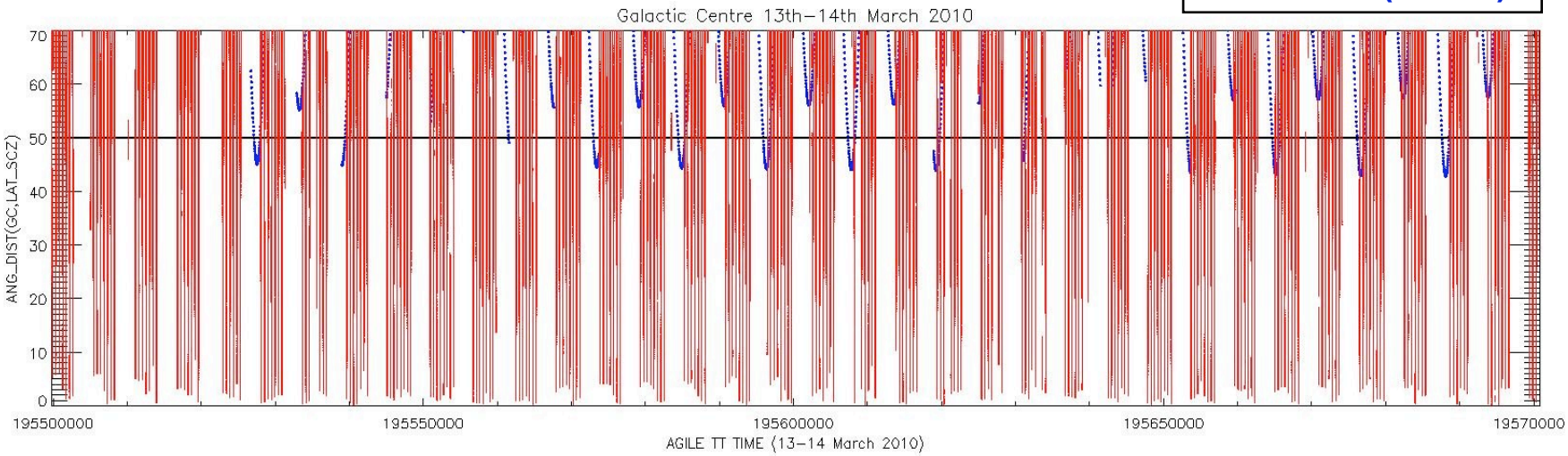

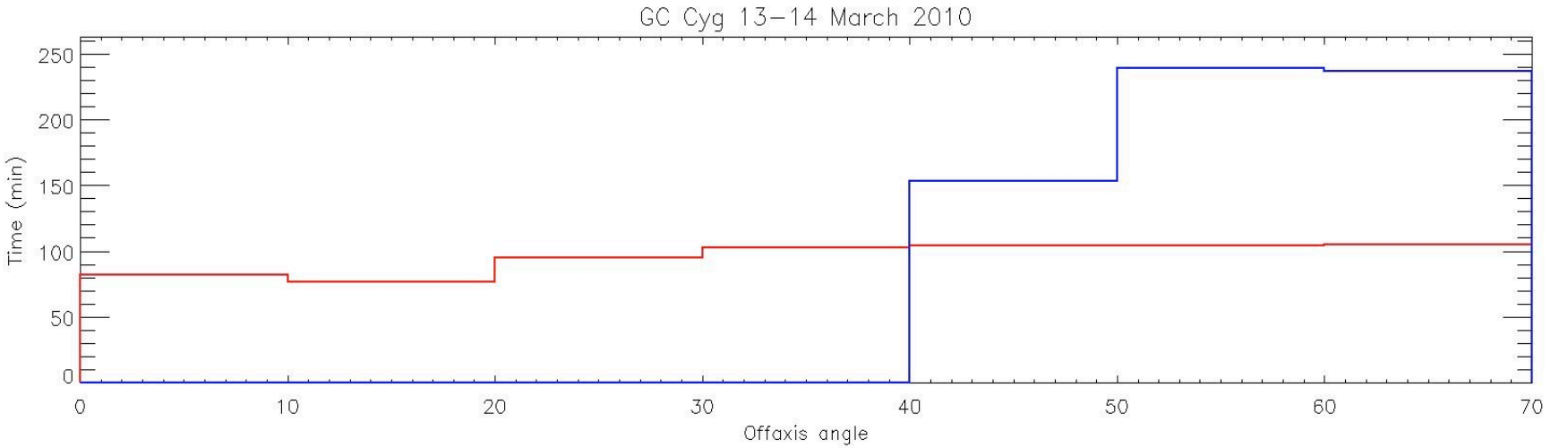

Example: Fermi Galactic Centre 1-month integration (20 Feb-20 Mar 2010)
off-axis angle vs. time and cumulative histogram

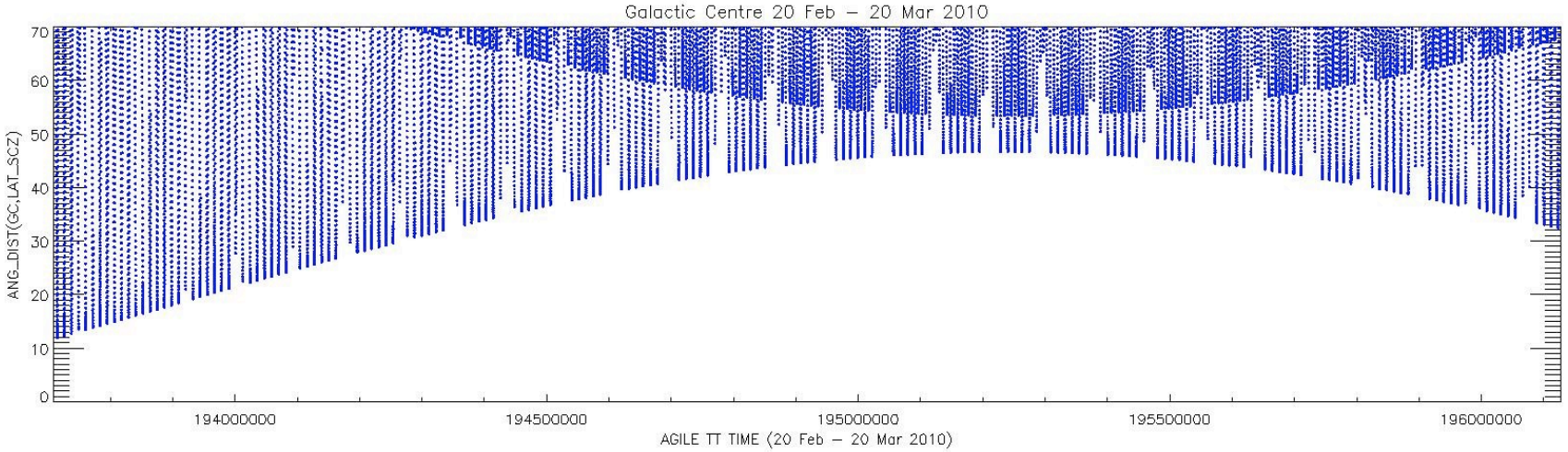

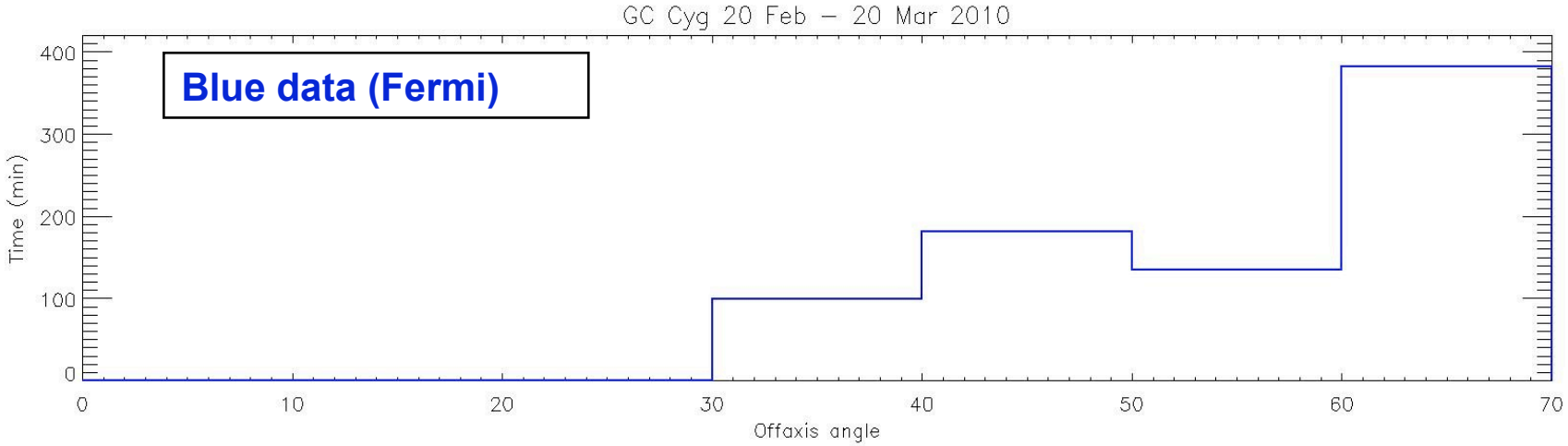

Challenges

- **Compact stars**
  - white dwarfs
  - neutron stars
  - black holes (BH)

- **Particle acceleration**
  - relativistic pulsar winds and nebulae
  - Supernova Remnants
  - relativistic jets
  - accretion disks
  - BH inner regions
  - Hypernovae
  - AGNs

- **Active Galactic Nuclei (AGN)**

Progress

- **Compact stars**
  - **white dwarfs: novae and gamma-ray emission**
  - **neutron stars: pulsars, millisecond pulsars, binary pulsars**
  - **black holes (BH): microquasars (Cygnus X-1, Cygnus X-3)**

- **Particle acceleration**
  - **relativistic pulsar winds and nebulae: Crab Nebula, Vela-X**
  - **Supernova Remnants: origin of cosmic-rays**
  - **relativistic jets: precursor activity and plasmoid ejection**
  - **accretion disks: Cyg X-3 instabilities, BH emission states**
  - **BH inner regions: Galactic Center, GRBs**
  - **Hypernovae: GRBs**
  - **AGNs: blazars**

- **Active Galactic Nuclei (AGN): blazars**

surprises for plasma astrophysics: unexpected discoveries about:

- **Our Galaxy**
- **Blazars and AGNs**
- **Microquasars: Cygnus X-3**
- **Crab Nebula**
- **SNRs and origin of cosmic rays**

Classifications

Type	Number	Percentage of total
Active Galactic Nuclei	832	44%
Candidate Active Galactic Nuclei	268	14%
Unassociated	594	32%
Pulsars (pulsed emission)	86	5%
Pulsars (no pulsations yet)	26	1%
Supernova Remnants/Pulsar Wind Nebulae	60	3%
Globular Clusters	11	< 1%
Other Galaxies	7	< 1%
Binary systems	4	< 1%
TOTAL	1888	100%

Classifications

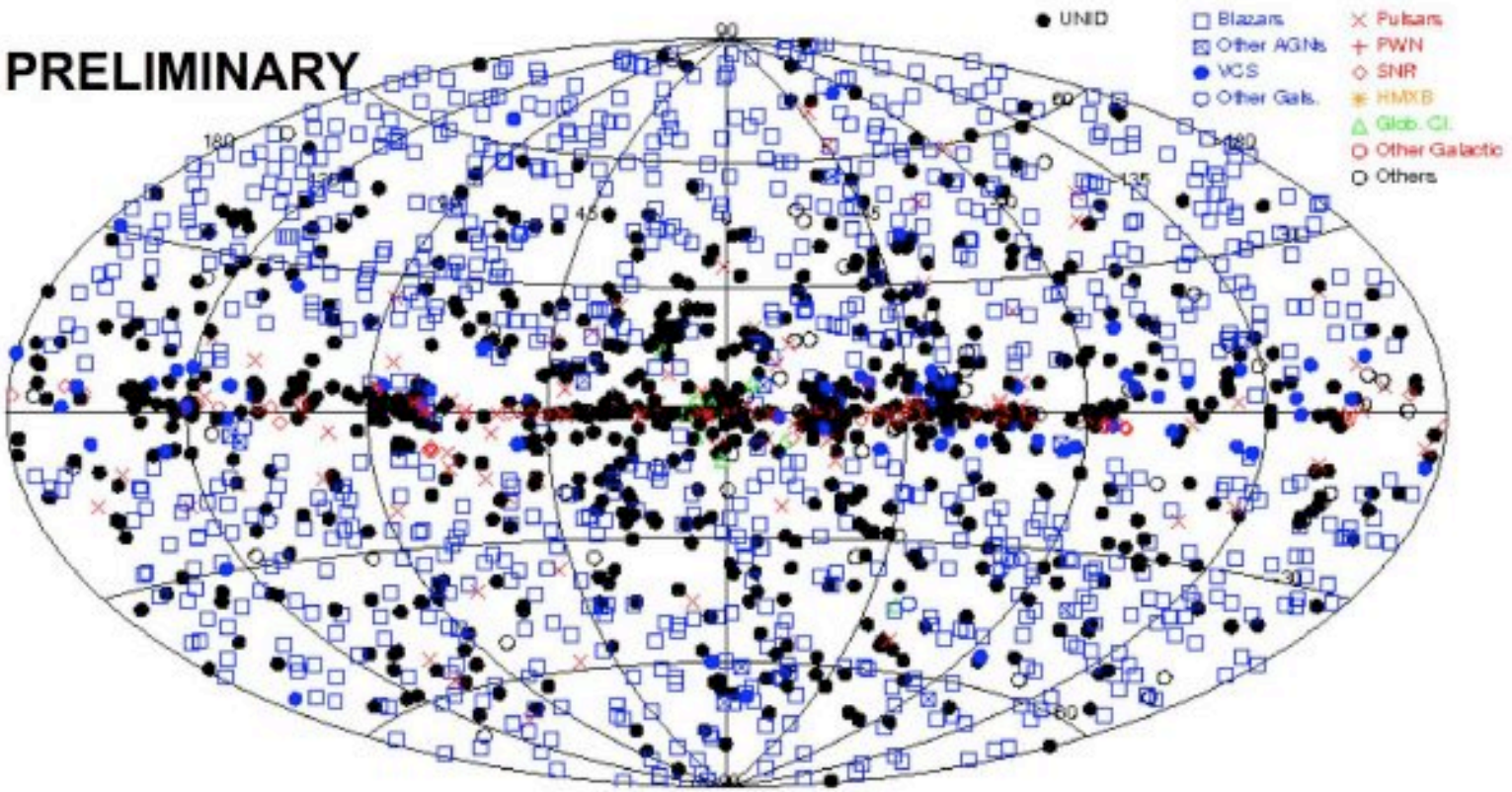

What is Not in the Catalog is Also Important

- Seyfert Galaxies (except for Narrow Line Seyfert 1s)
- Clusters of Galaxies
- Dwarf Spheroidal Galaxies

LAT view of the Galactic interstellar emission

LAT counts above 300 MeV

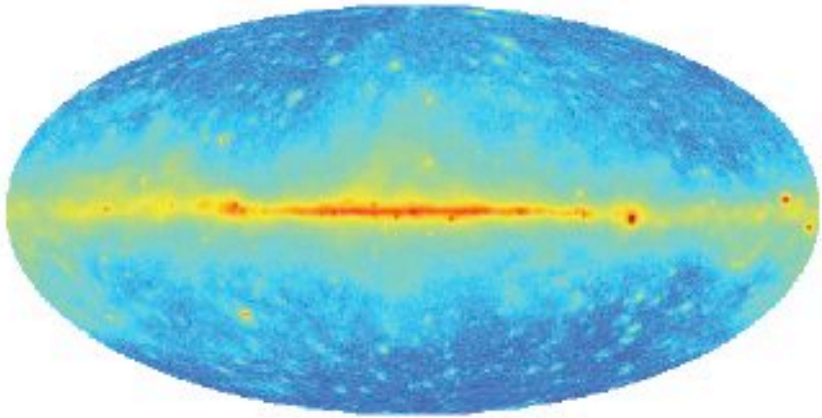

Sources, 2FGL early version

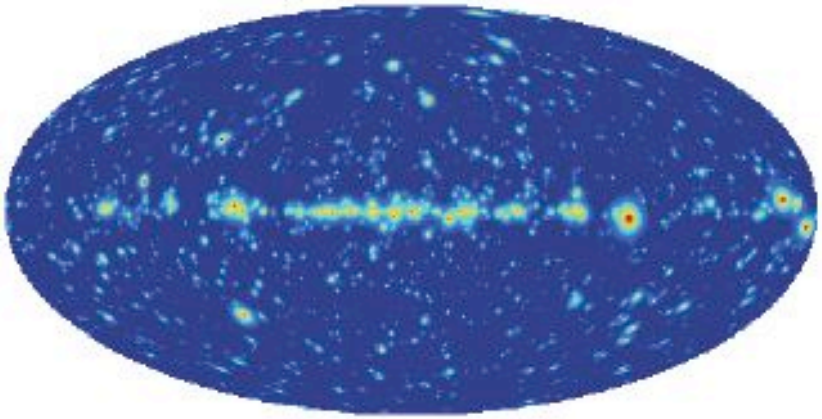

LAT counts minus sources and isotropic

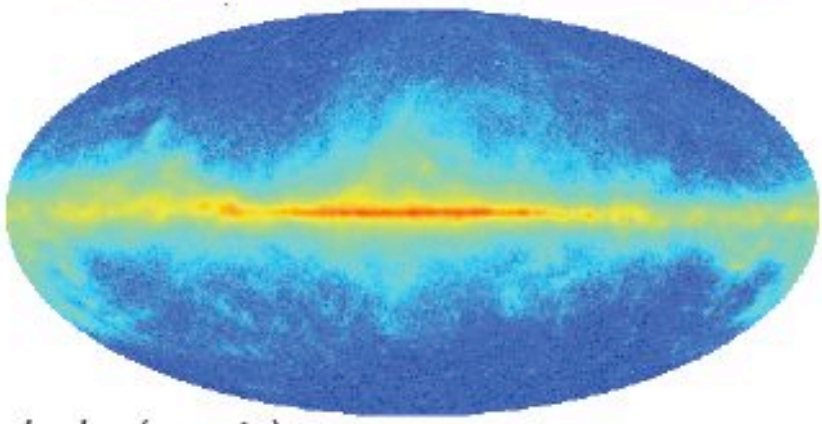

scale: log(counts)

0 3

24 months of data

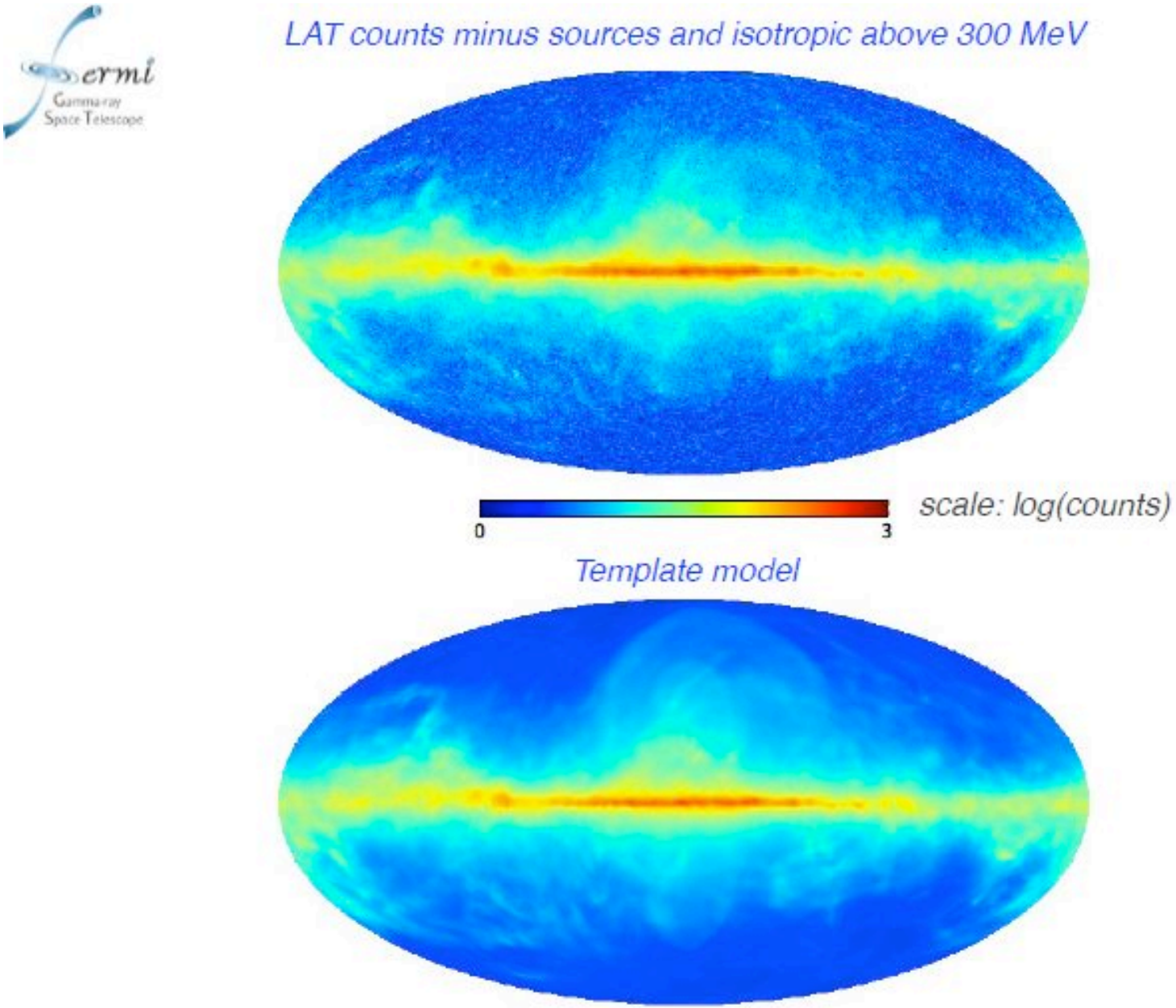
LAT counts minus sources and isotropic above 300 MeV
scale: log(counts)
0
3
Template model

LAT view of the Galactic interstellar emission

LAT counts minus sources and isotropic

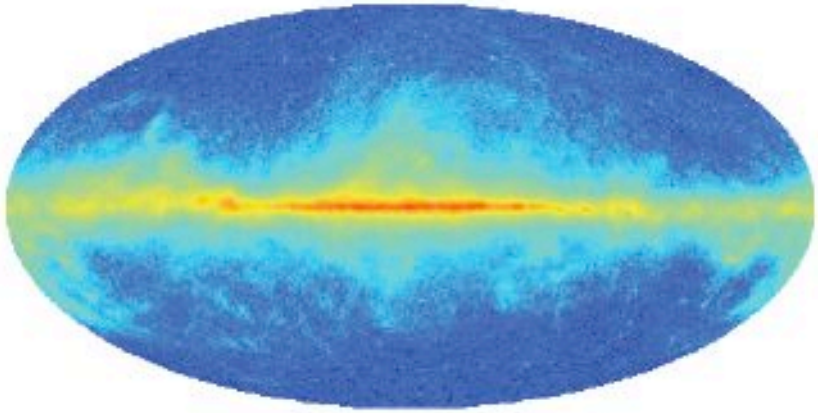

Counts map derived from HI and CO radio surveys. The gas column density distributed in Galactocentric rings was scaled to reproduce the LAT counts

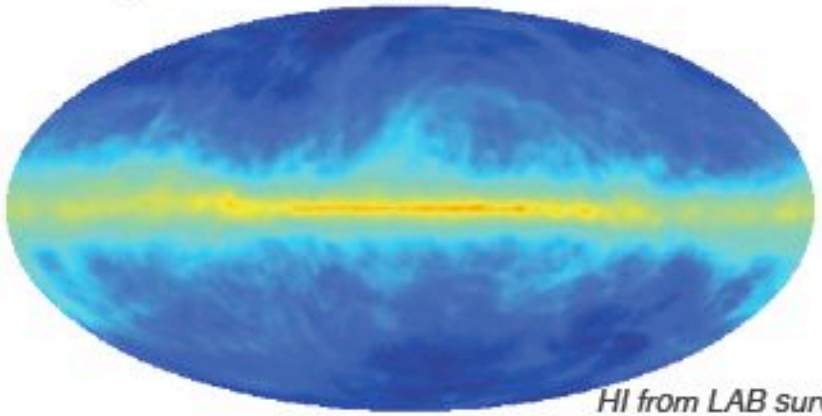

HI from LAB survey

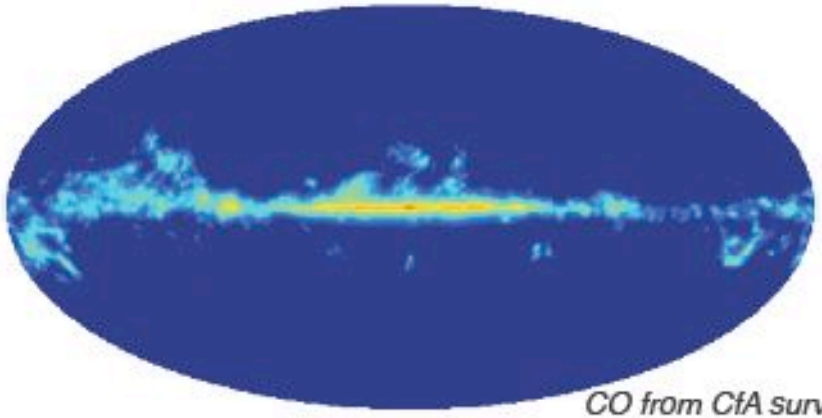

CO from CfA survey

No H_2, γ intensity is proportional to HI column density

γ-ray intensities (sources and IC removed) versus HI column densities

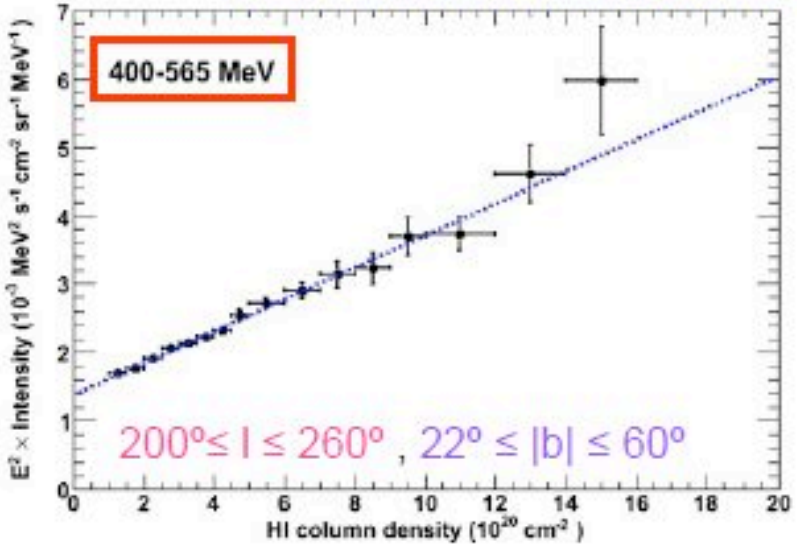

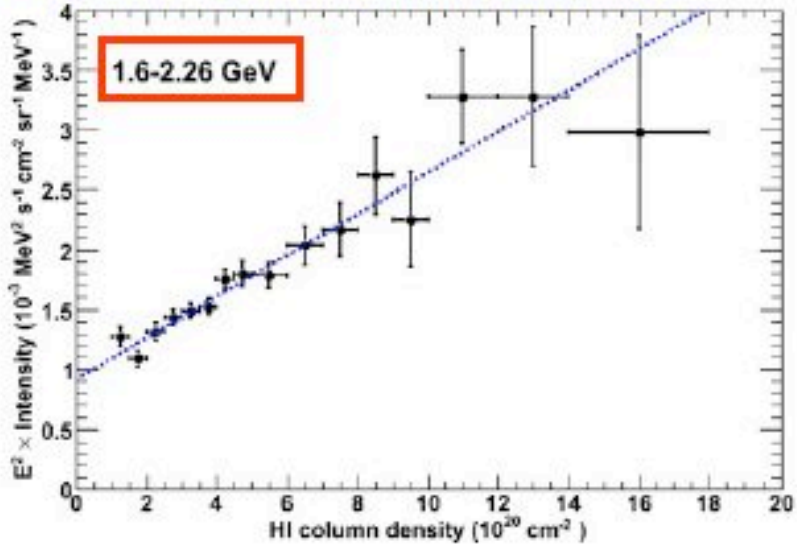

Abdo et al., ApJ 703, 1249 (2009), C.A.: T. Mizuno

The origins of the high energy Milky-Way γ-ray diffuse emission are mainly:

- *decay of π^0 produced in protons/gas collisions*
- *Bremsstrahlung of relativistic electrons in gas*
- *Inverse-Compton of relativistic electrons with ISRF*

Diffuse Emission : study of CR, ISM and ISRF

Inner Galaxy spectrum

a priori model, no special fitting

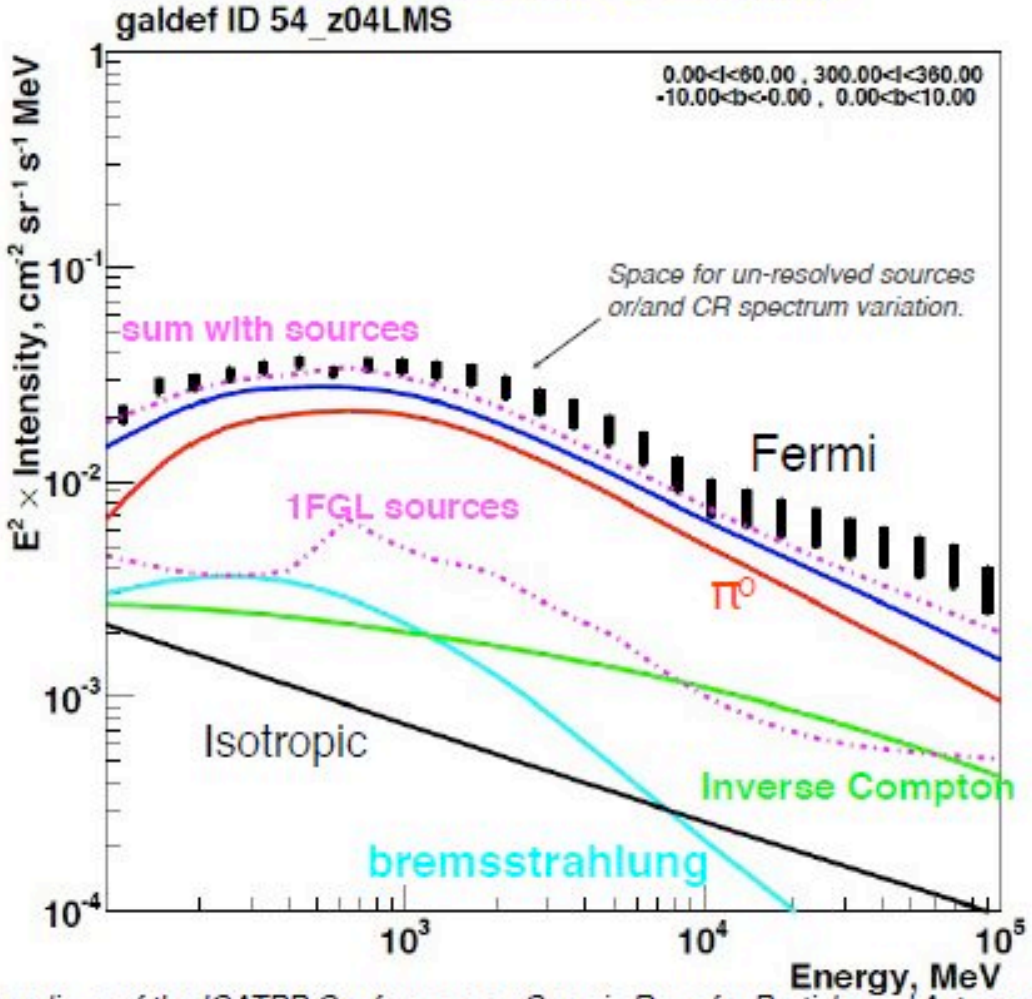

Andy Strong, Proceedings of the ICATPP Conference on Cosmic Rays for Particle and Astroparticle Physics, 2010

Inner Galaxy spectrum: lower energy range with Integral

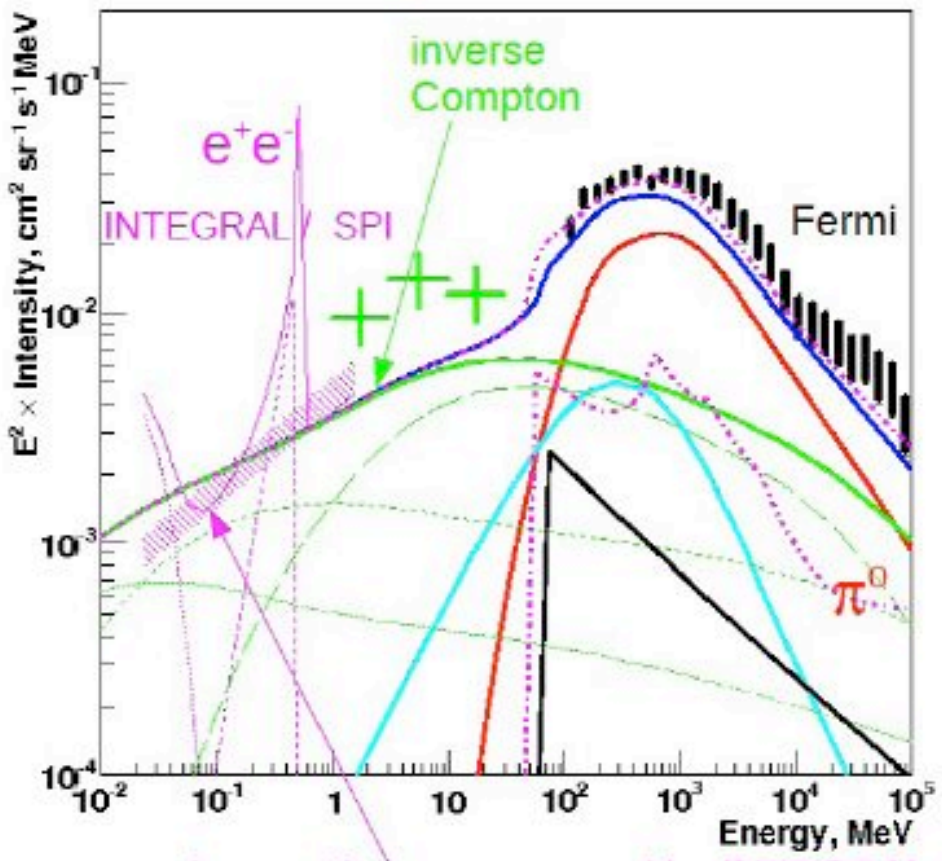

Andy Strong, Proceedings of the ICATPP Conference on Cosmic Rays for Particle and Astroparticle Physics, 2010

Does FERMI see the EGRET GeV excess ?

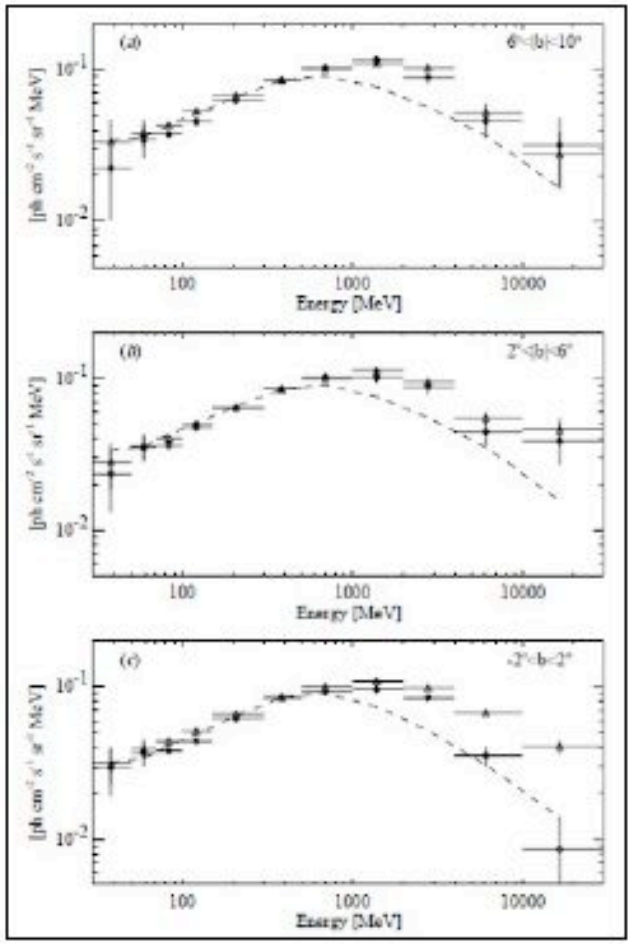

Hunter et al. 1997

Does FERMI see the EGRET GeV excess ?

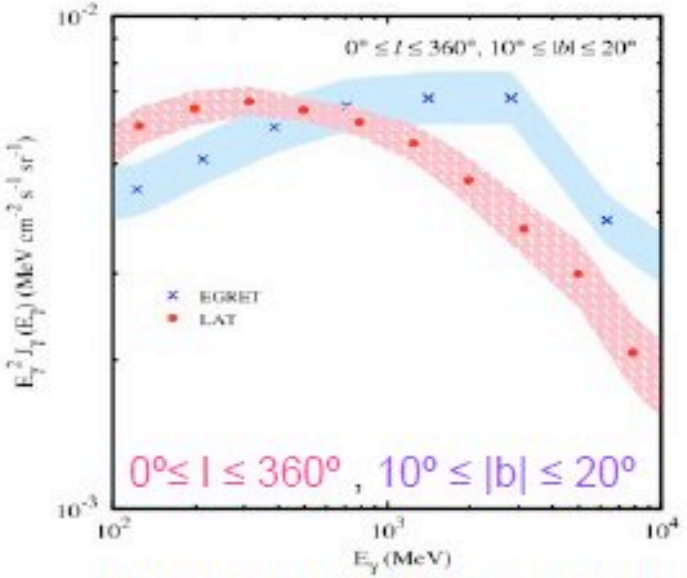

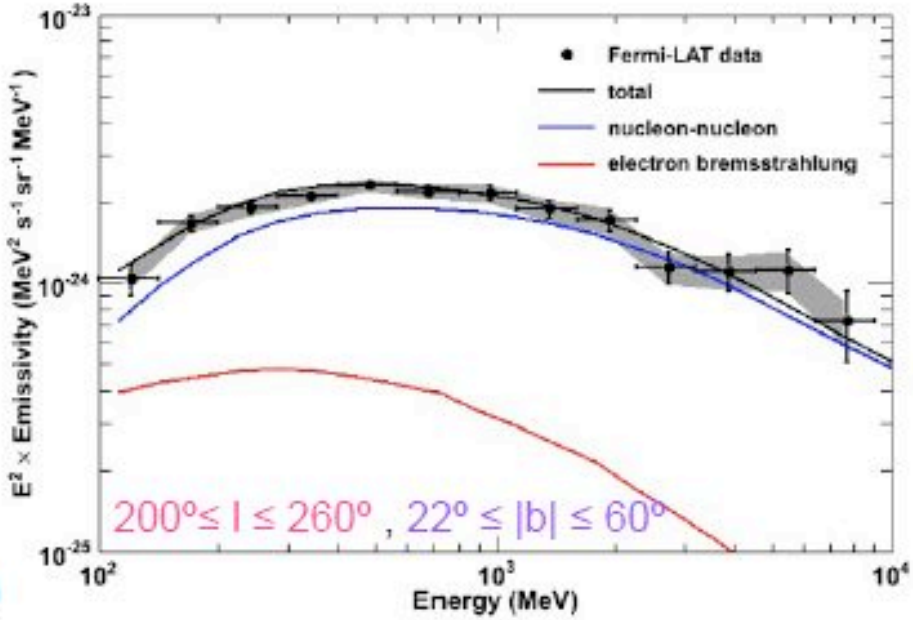

Abdo *et al.*, Phys. Rev. Lett. 103, 251101 (2009)
C.A.: T. Porter, G. Johannesson

LAT spectrum does not confirm the EGRET GeV excess

Galactic Center

Sgr A* is very, very dim…

$L_{sub\text{-}mm} \sim 10^{36}$ erg s^{-1} = 3×10^{-9} L_E

$L_{IR} \sim 10^{35}$ erg s^{-1} = 3×10^{-10} L_E

$L_X \sim 10^{33}$-10^{35} erg s^{-1} = 10^{-12}-10^{-10} L_E

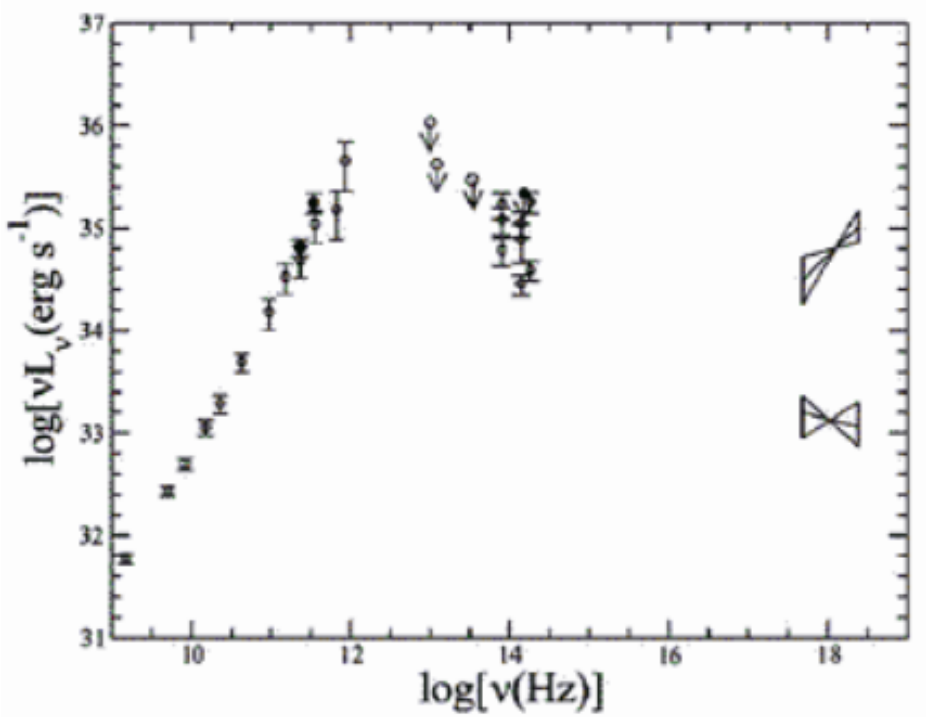

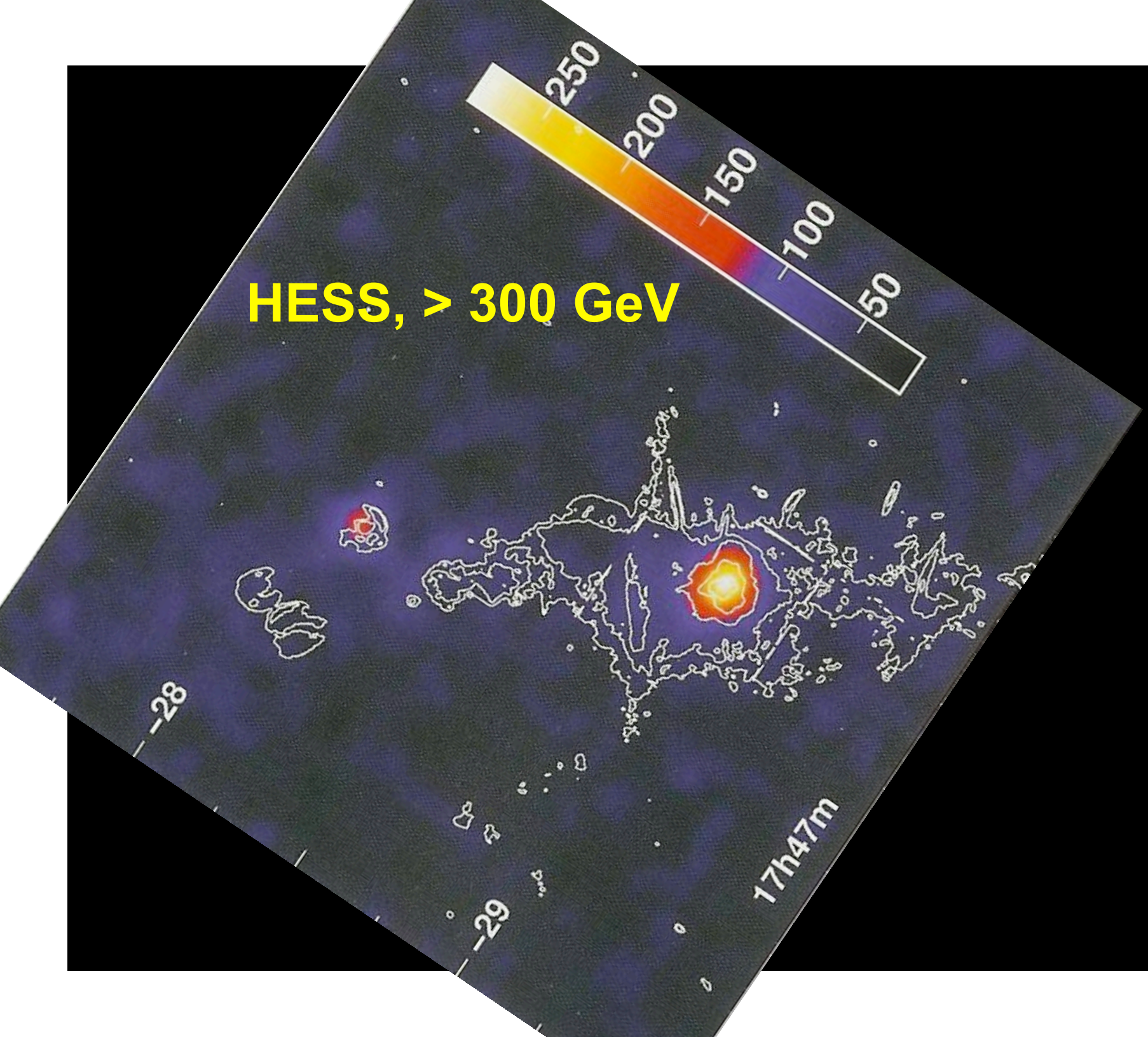
HESS, > 300 GeV
250
200
150
100
50
-28
-29
17h47m

HESS TeV and Chandra

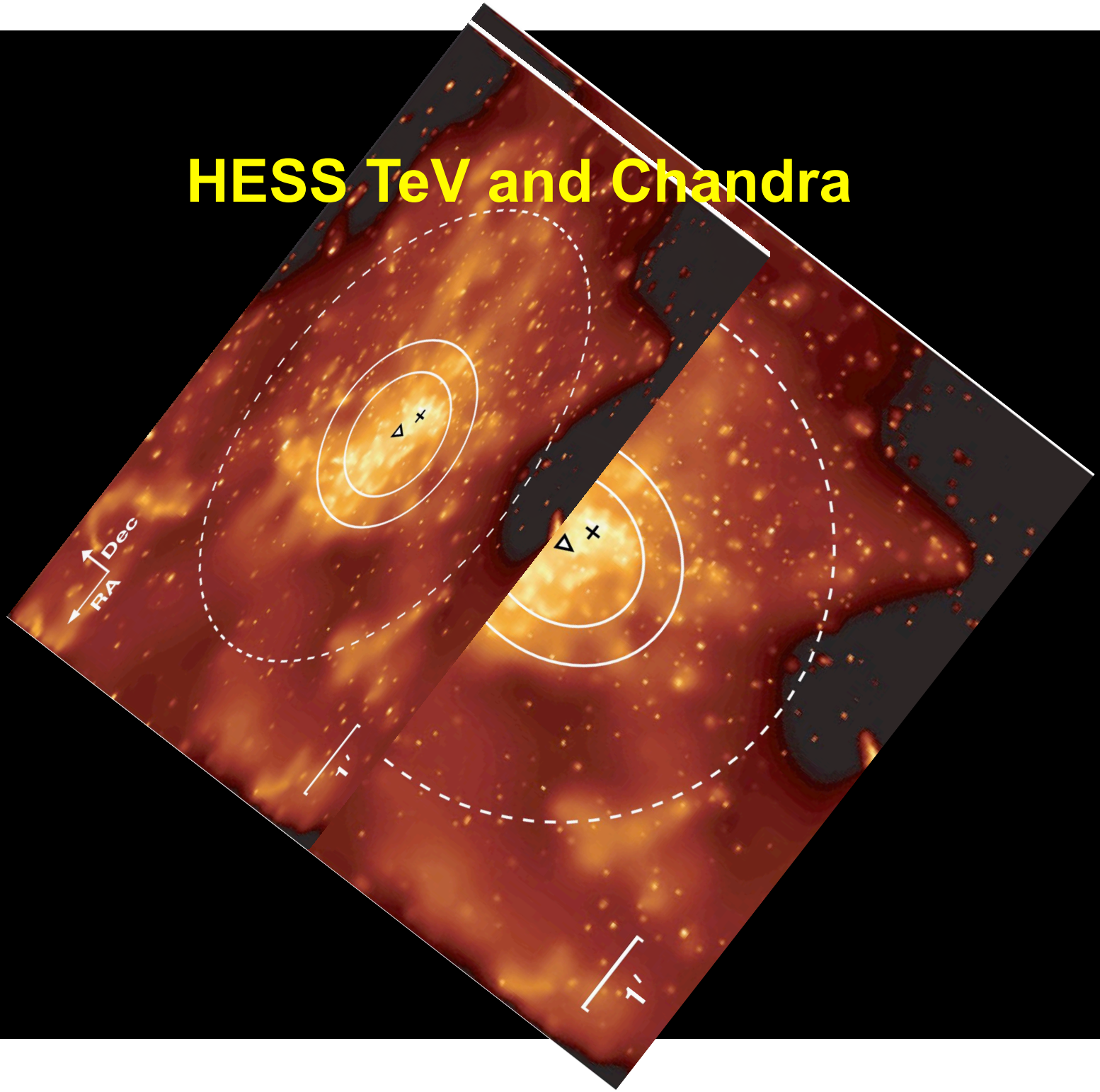

VERITAS observations of the galactic center

- **VERITAS (2010, 15h), sky map:**
  - 12 std.dev. excess @ galactic center:
    fit: longitude = -0.06±0.02, latitude = -0.06±0.01
  - No evidence for variablity
  - Overlay: HESS (GC+diffuse) & Fermi sources
    http://fermi.gsfc.nasa.gov/ssc/data/access/lat/1yr_catalog/
- **Energy spectrum (preliminary):**
  - Flux systematic: ~40% (conservative est.)
    (contemp. Crab LZA: estimate systematics)
  - Compatible with H.E.S.S., Whipple & MAGIC

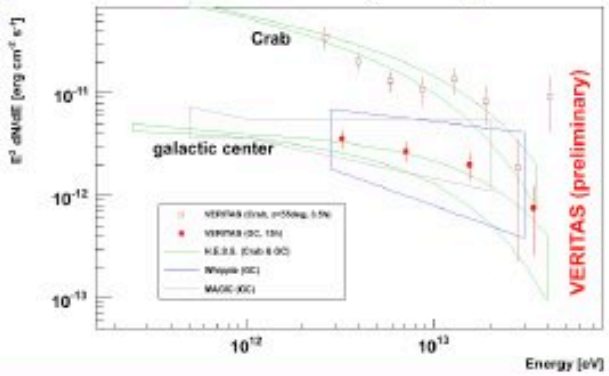

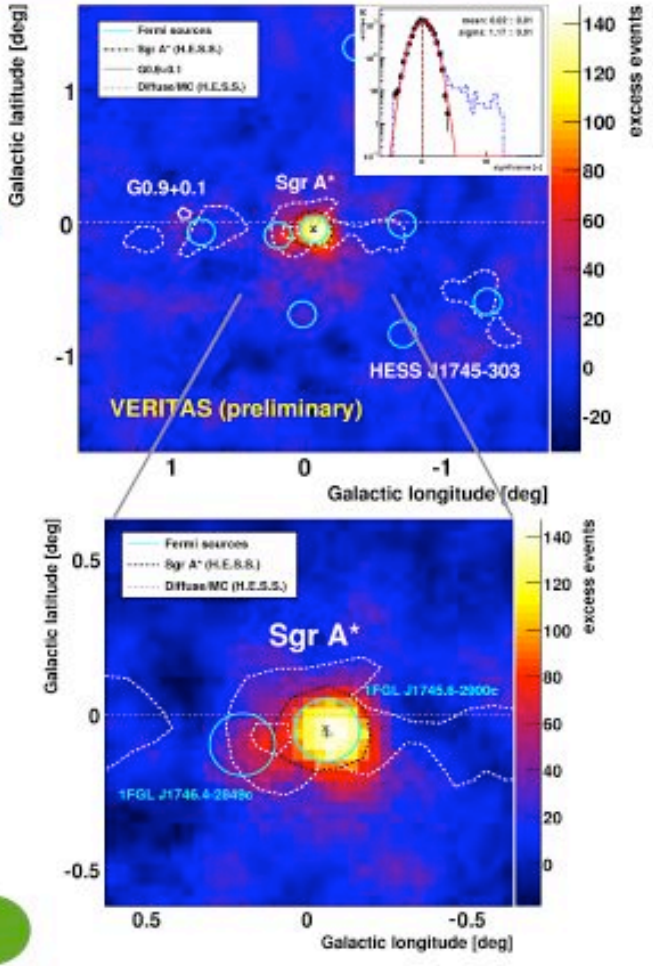

VERITAS: can detect GC (LZA) in ~3h

- **Hadron accelerator around BH:**
  - (1) p's diffuse into ISM (2) pions (3) γ-rays
  - @MeV/GeV: variability ~10^4 yr (old flares)
    @>10 TeV: variability ~10yr (recent flares)
    Chernyakova et al., ApJ, 726, 60 (2011)
- **Hadrons from BH vicinity (2):**
  - Protons accelerated within ~20 Rs
  - Spectral variability for E > 10TeV
    (TeV Spectrum will soften after outburst)
    Ballantyne et al., MNRAS, 410, 152 (2011)
- **BH plerion (leptonic wind):**
  - terminat. shock, TeV γ's via IC, T_{var} ~100 yr
    Atoyan et al., ApJ, 617, L123 (2004)
- **Future: Constrain cutoff energy:**
  - Assume sensitivity x1.3 (upgrade) & 100h

=> Can constrain cutoff energy

Important model input:
cut off & variability @ E>10TeV

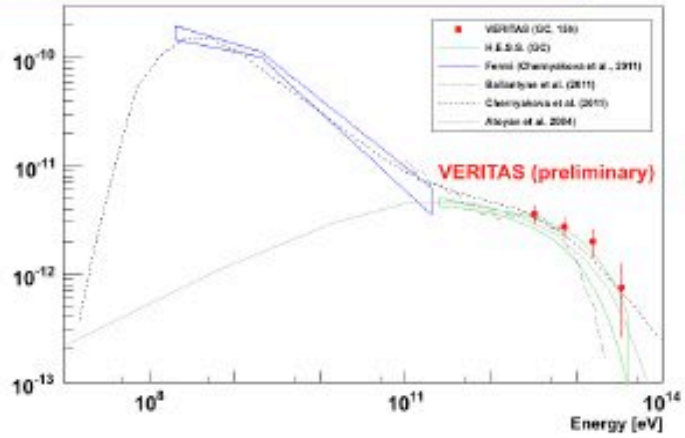

Future VERITAS observations

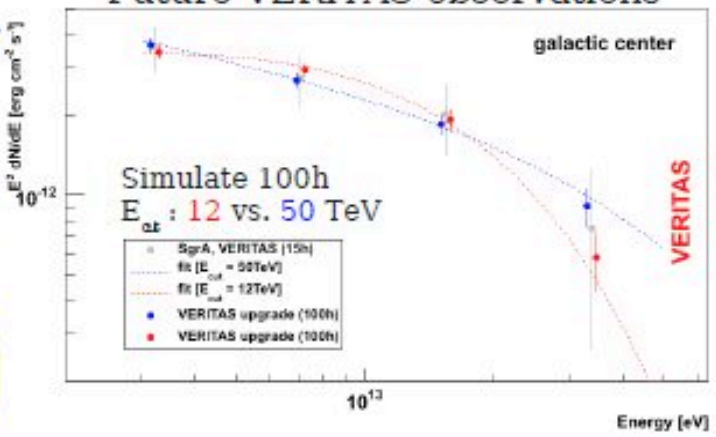

Residual TeV emission (HESS)

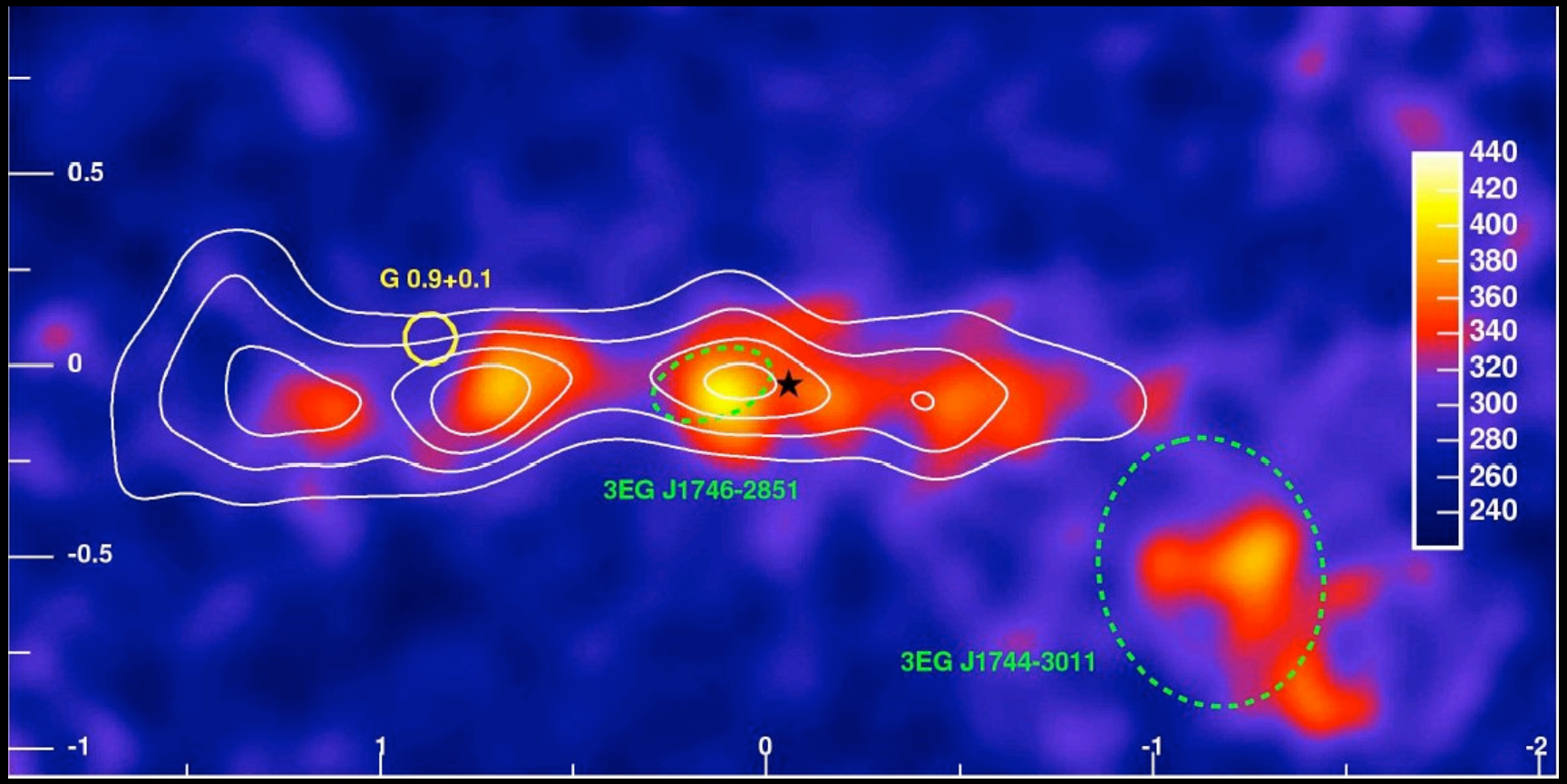

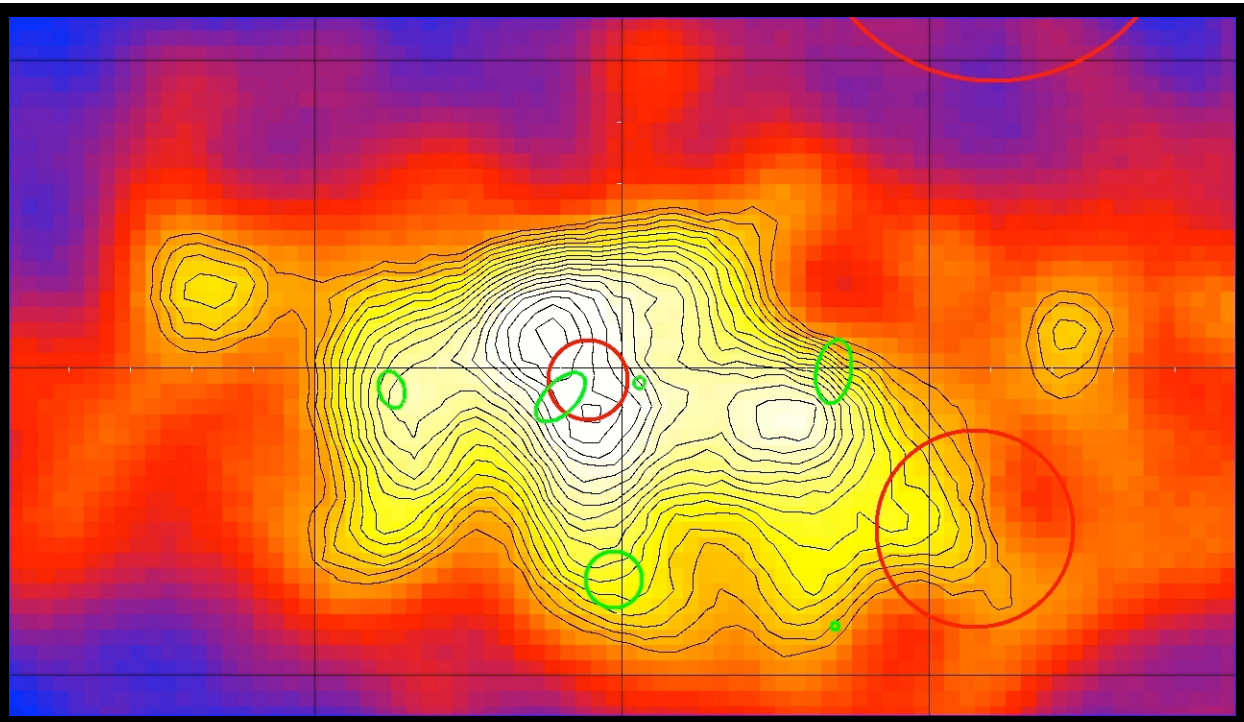

AGILE gamma-ray map (E > 400 MeV)

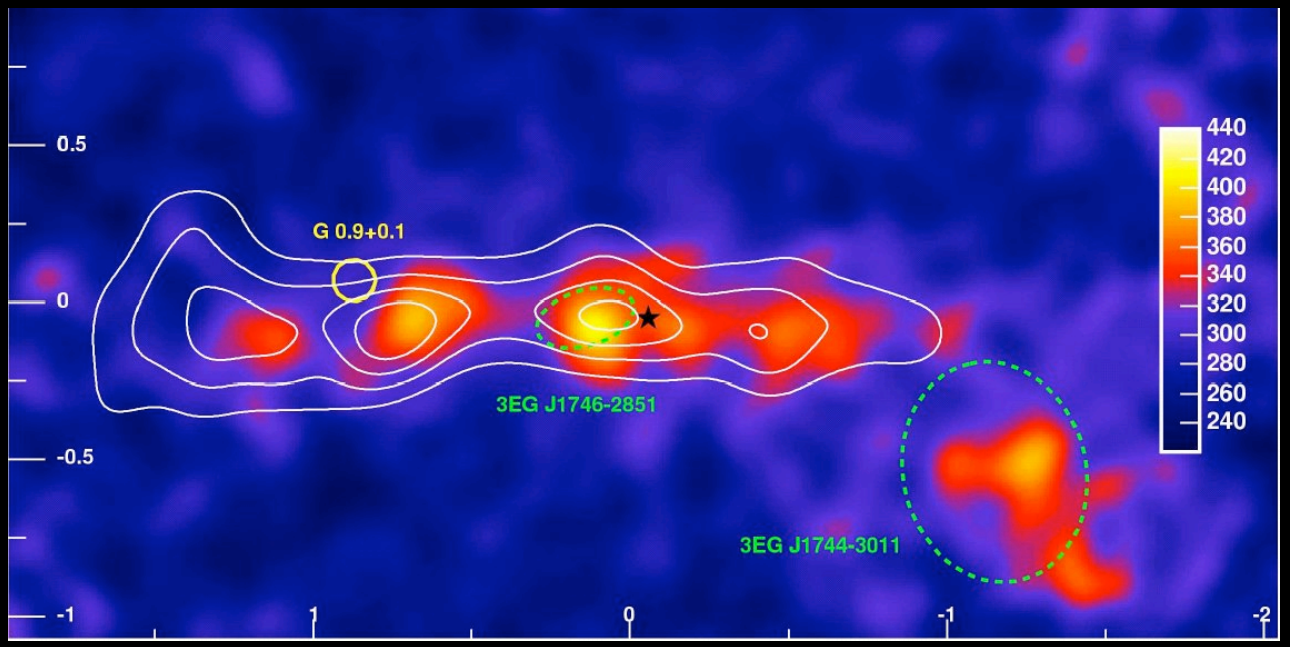

HESS residual TeV map

Galactic Center, AGILE (E > 400 MeV)

(2x2 sq.degree)

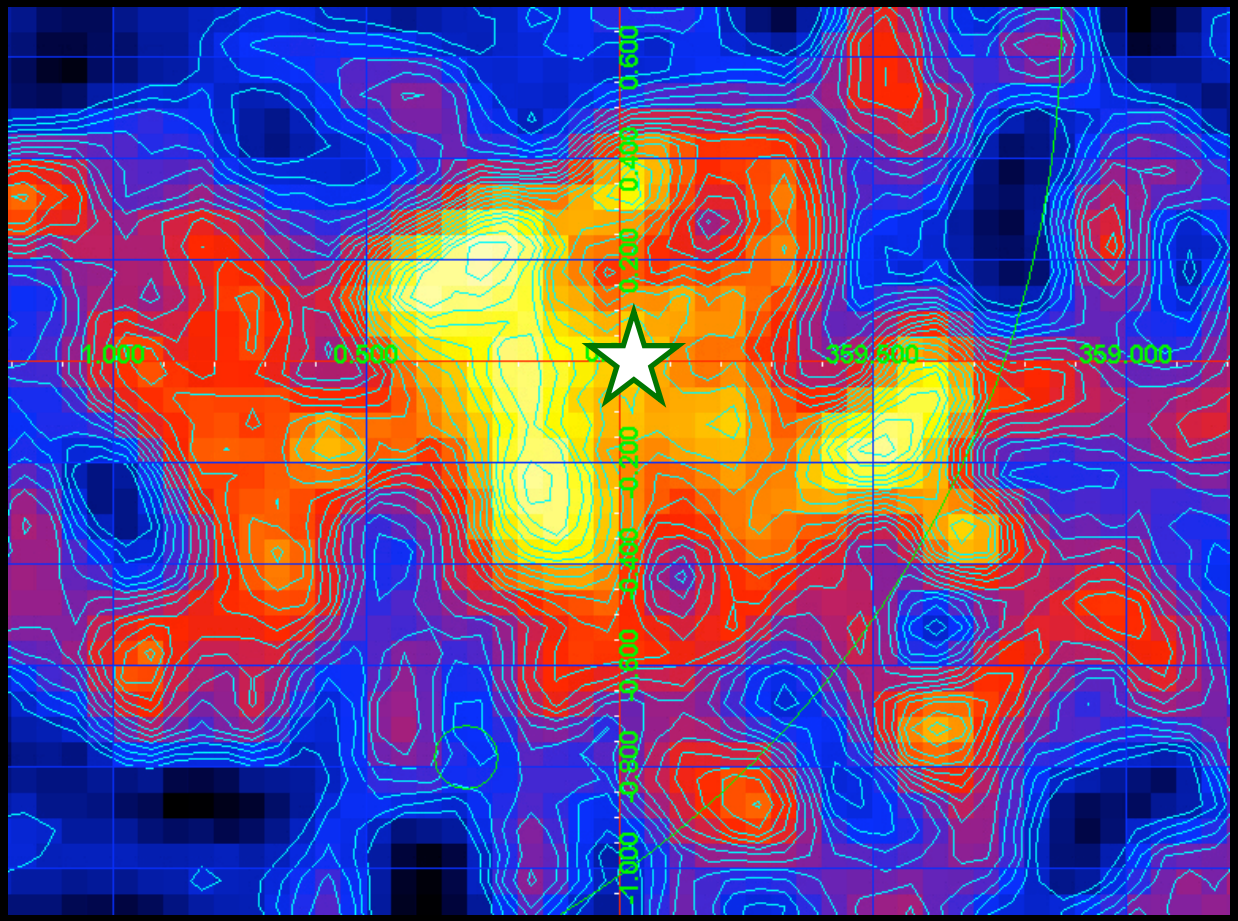

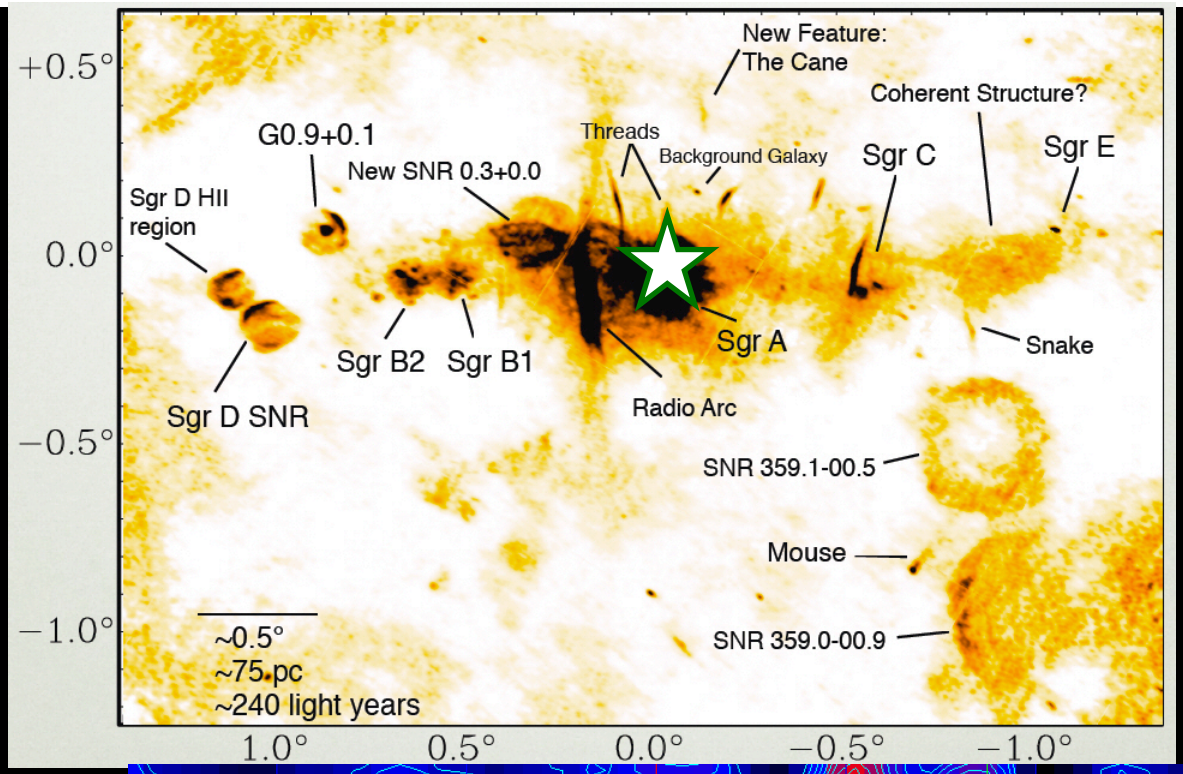
New Feature:
The Cane
Coherent Structure?
G0.9+0.1
Threads
Background Galaxy
Sgr C
Sgr E
New SNR 0.3+0.0
Sgr D HII
region
Sgr A
Snake
Sgr B2
Sgr B1
Sgr D SNR
Radio Arc
SNR 359.1-00.5
Mouse
SNR 359.0-00.9
~0.5°
~75.pc
~240 light years
+0.5°
0.0°
−0.5°
−1.0°
1.0°
0.5°
0.0°
−0.5°
−1.0°

radio

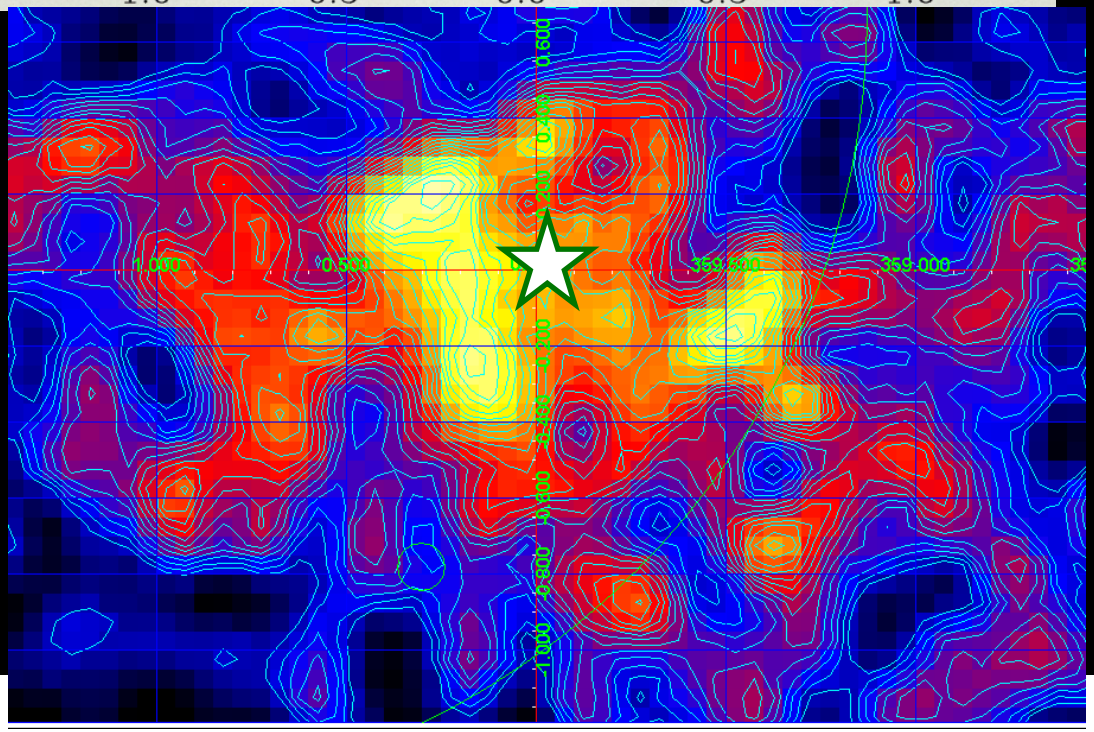

gamma

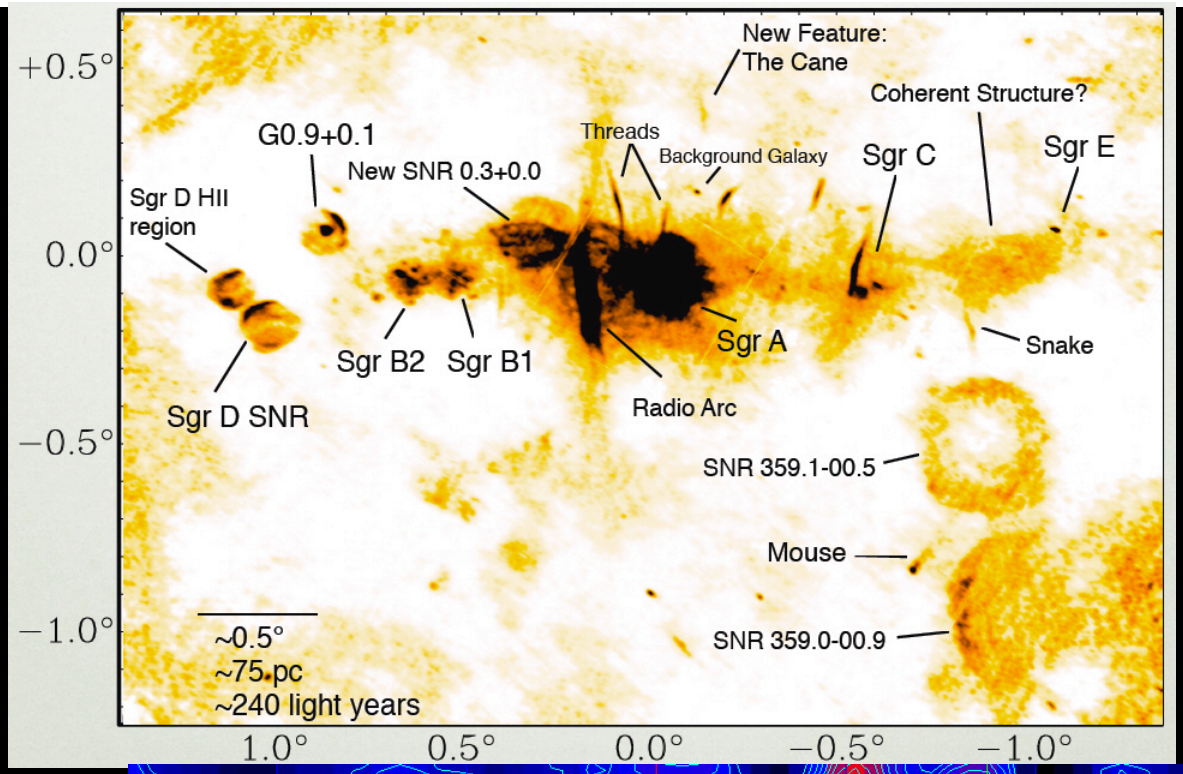
New Feature:
The Cane
Coherent Structure?
G0.9+0.1
Threads
Background Galaxy
Sgr C
Sgr E
New SNR 0.3+0.0
Sgr D HII
region
Sgr A
Snake
Sgr B2
Sgr B1
Sgr D SNR
Radio Arc
SNR 359.1-00.5
Mouse
SNR 359.0-00.9
~0.5°
~75 pc
~240 light years
+0.5°
0.0°
−0.5°
−1.0°
1.0°
0.5°
0.0°
−0.5°
−1.0°

radio

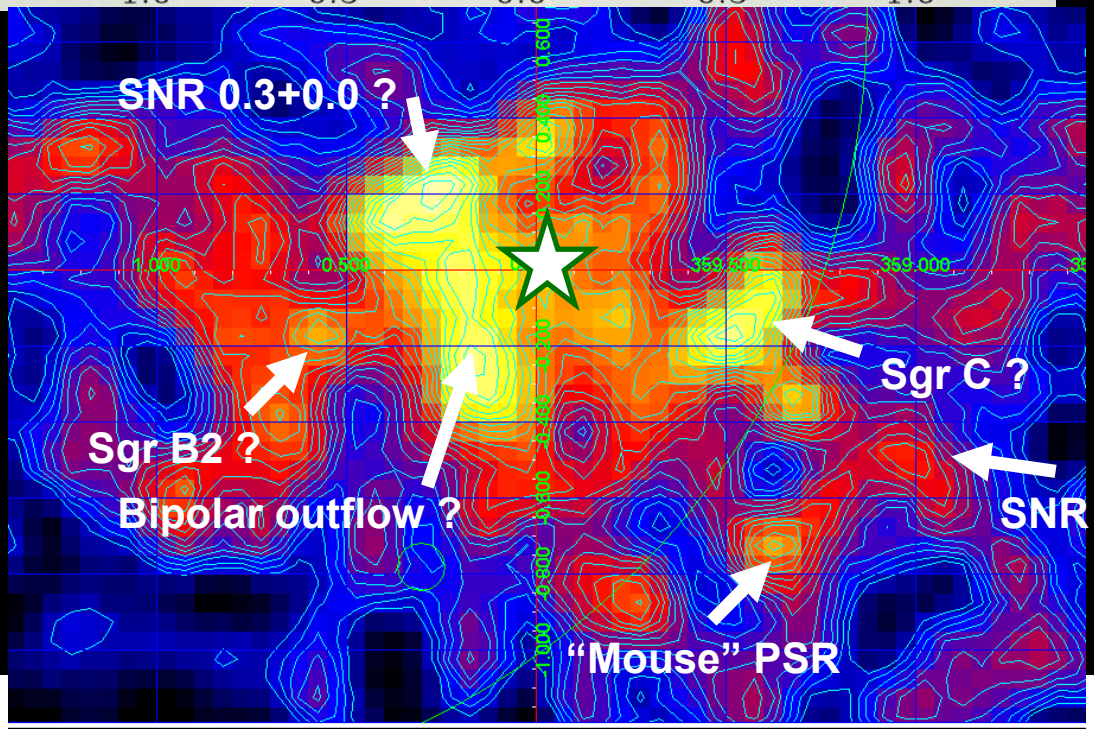
SNR 0.3+0.0 ?
Sgr C ?
Sgr B2 ?
Bipolar outflow ?
SNR 359.1-00.5 ?
"Mouse" PSR

gamma

Example of hard X-ray sources in the GC (Super-AGILE)

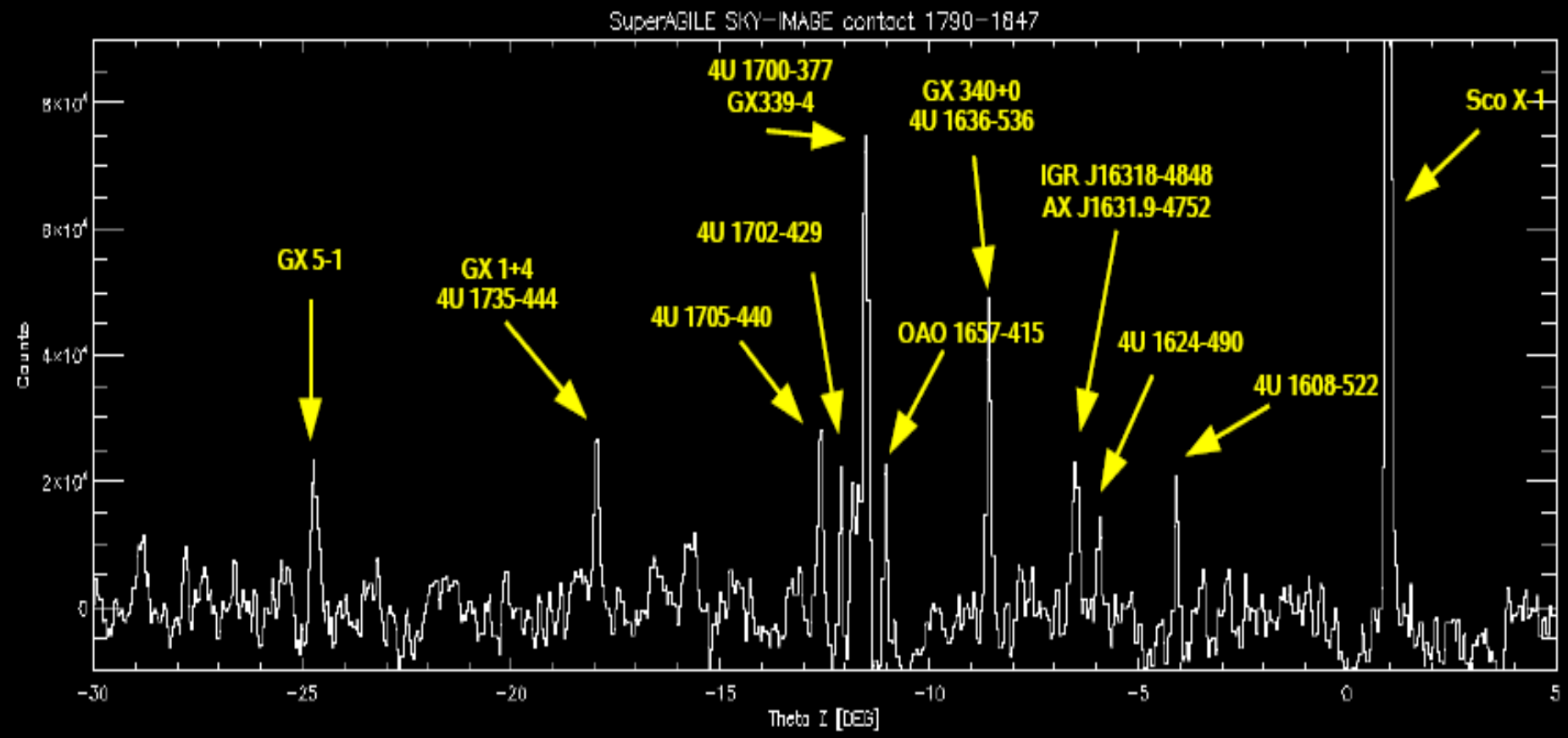

Galactic Center X-ray source variability

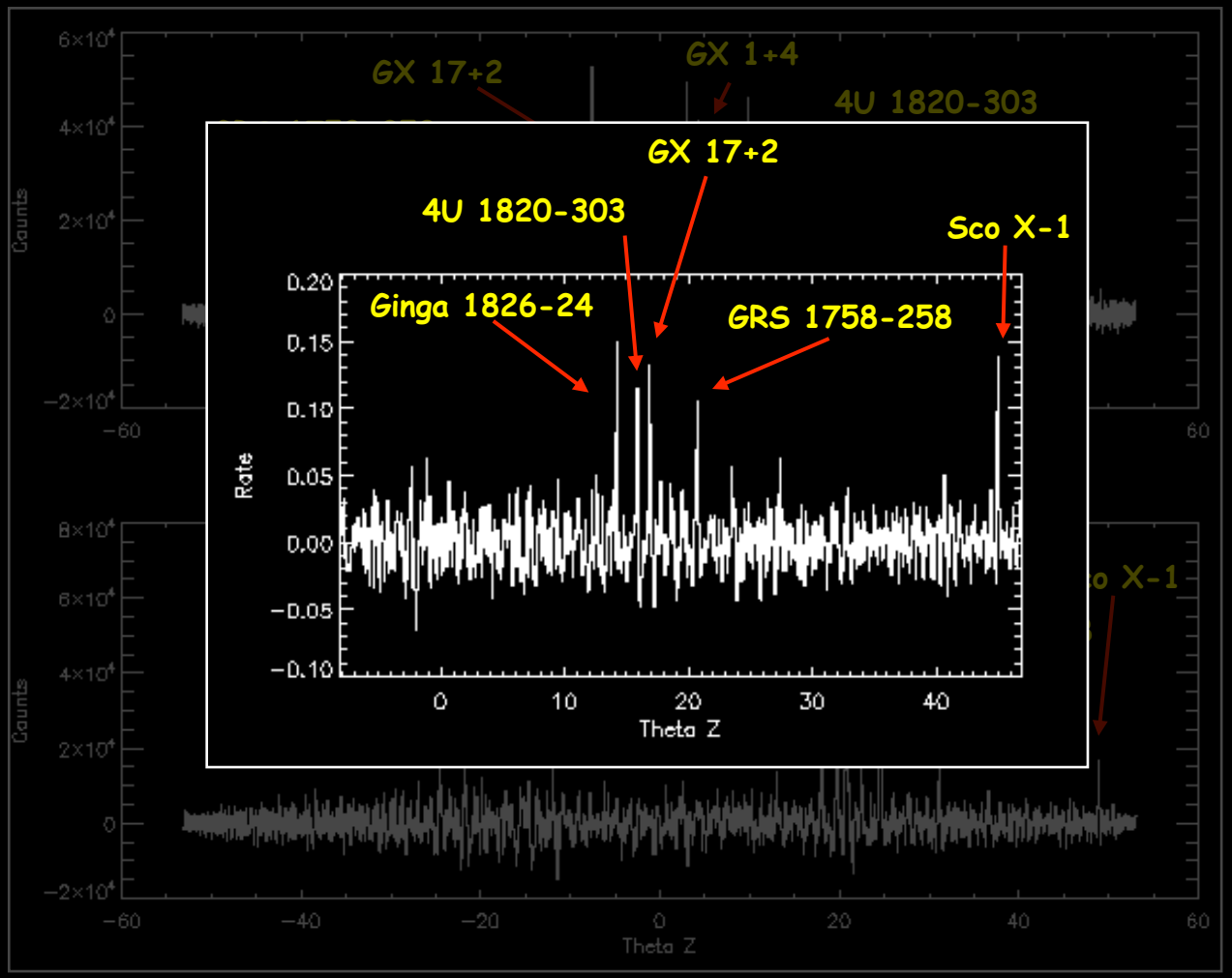

Fermi data reveal giant gamma-ray bubbles

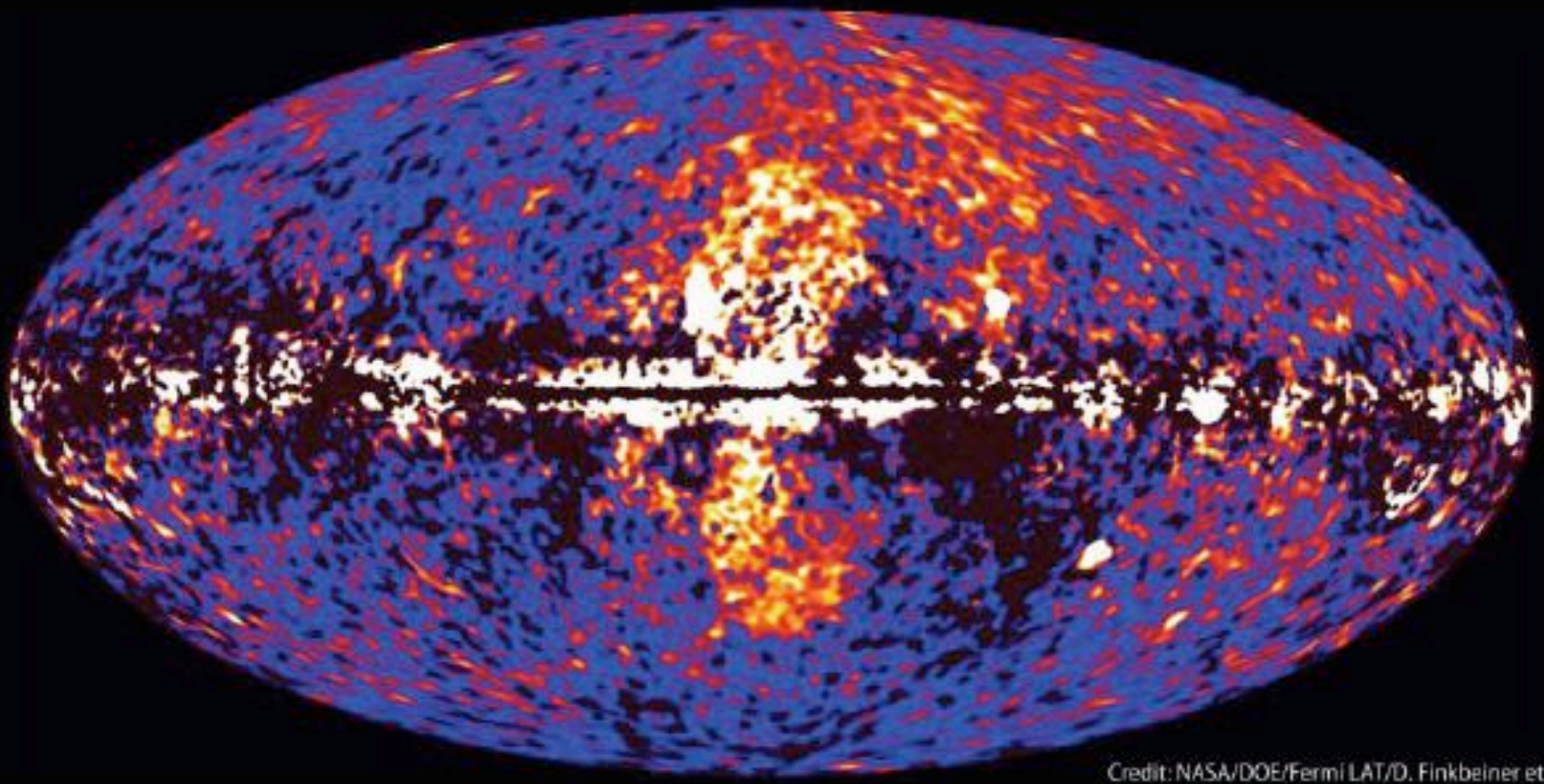

Credit: NASA/DOE/Fermi LAT/D. Finkbeiner et al.

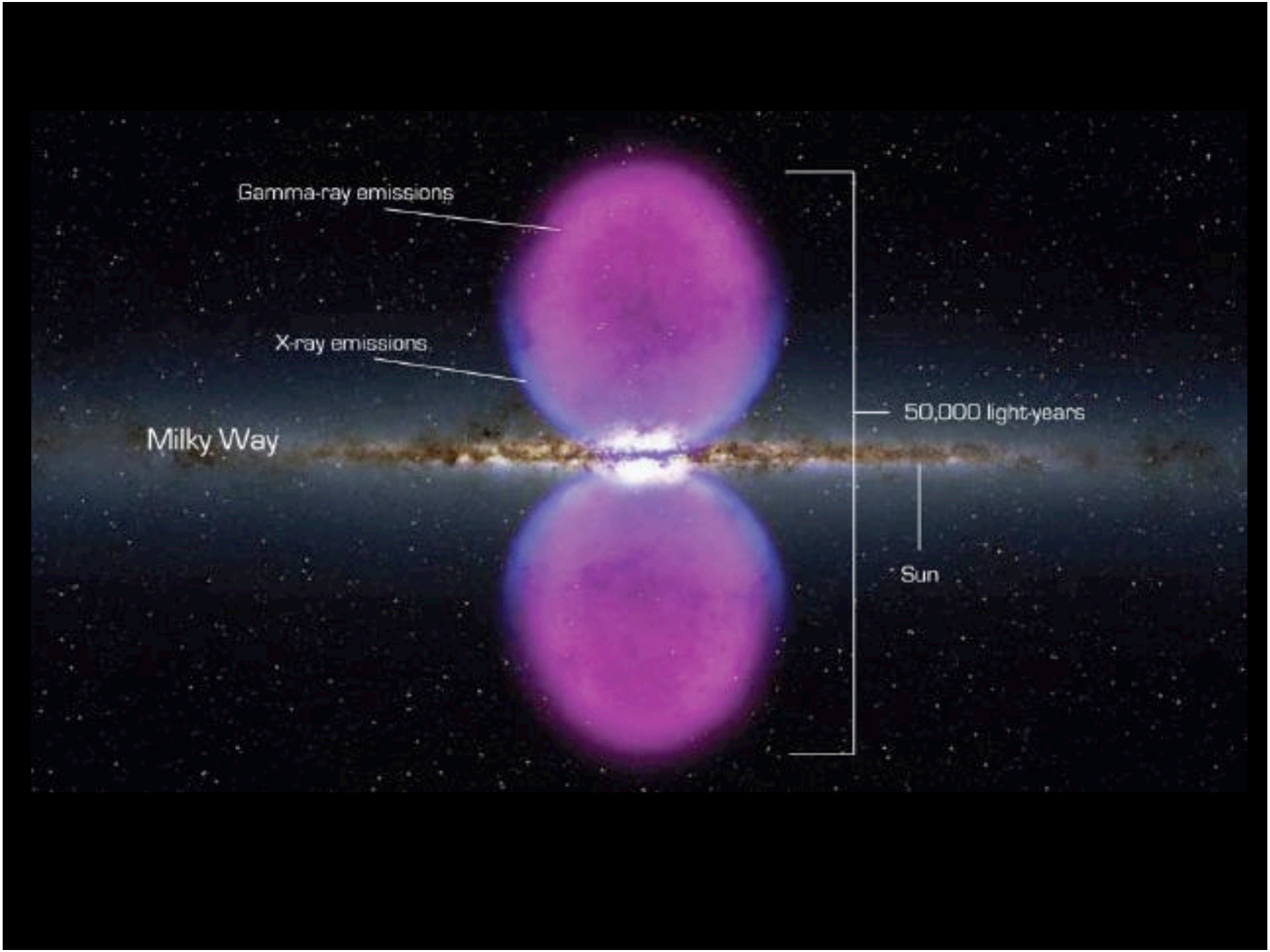
Gamma-ray emissions
X-ray emissions
Milky Way
50,000 light-years
Sun

Radio Jet Activity in Nearby AGN

- Circinus galaxy (D~4 Mpc)
- Radio lobes highly polarized with extent ~6 kpc
- Hosts low-luminosity AGN

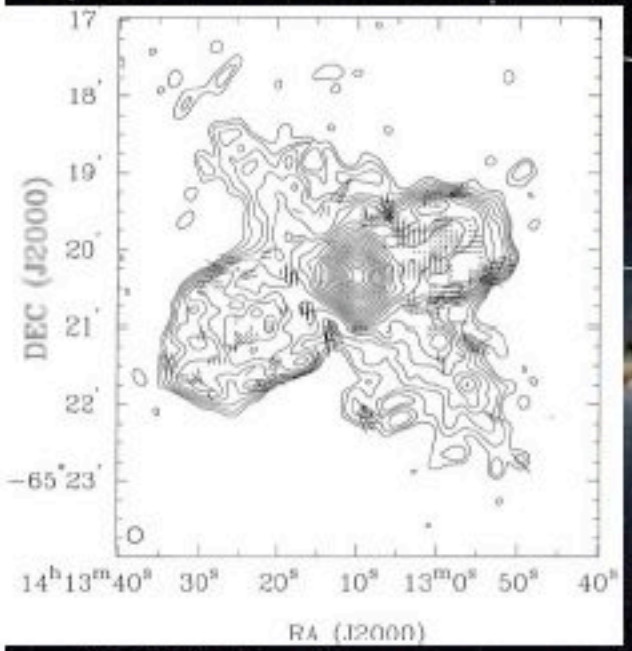

ATCA λ13cm image
Elmouttie et al. (1998)

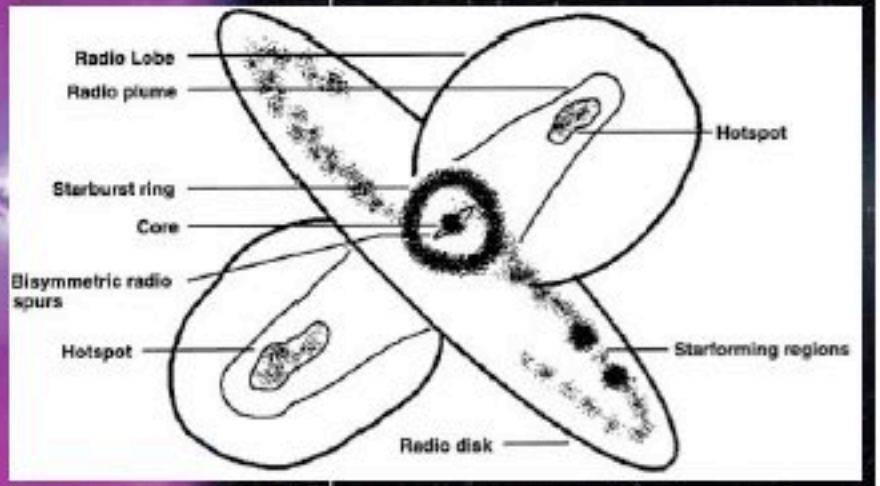

blazars

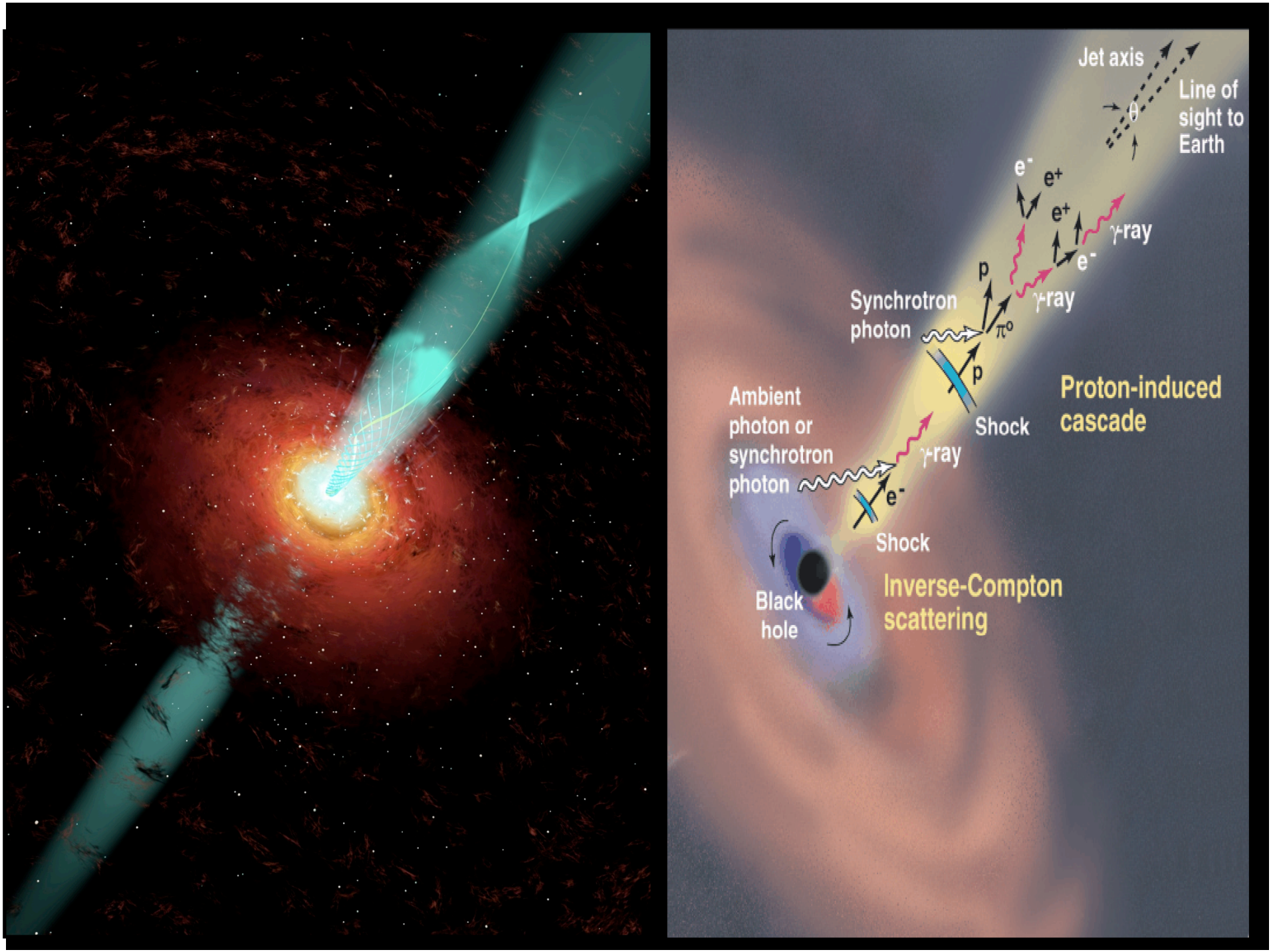
Jet axis
Line of sight to Earth
θ
e-
e+
e+
e-
γ-ray
γ-ray
p
Synchrotron photon
π°
p
Shock
Proton-induced cascade
Ambient photon or synchrotron photon
γ-ray
e-
Shock
Black hole
Inverse-Compton scattering

Radio vs. Gamma Luminosity

MOJAVE

- No simple direct correlation between radio- and gamma-ray luminosity
- Gamma-faint sources over the full range of observed radio luminosities

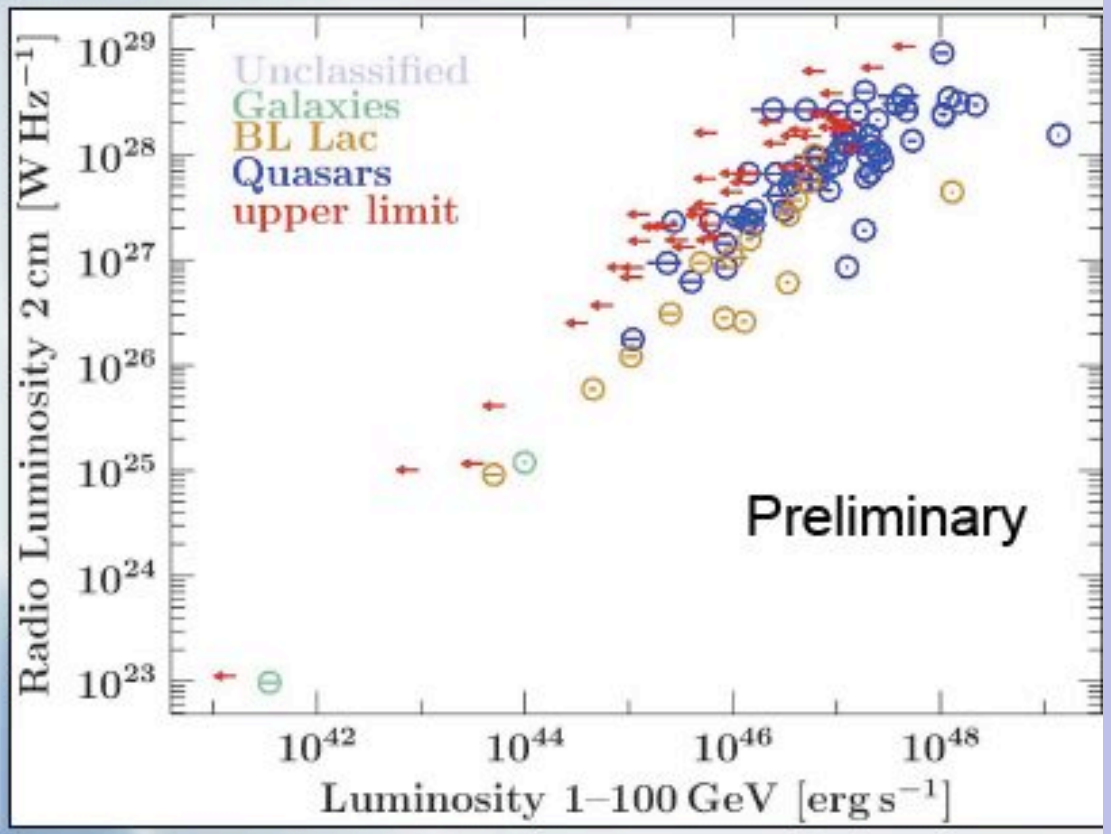

some of the brightest Gamma-ray blazars

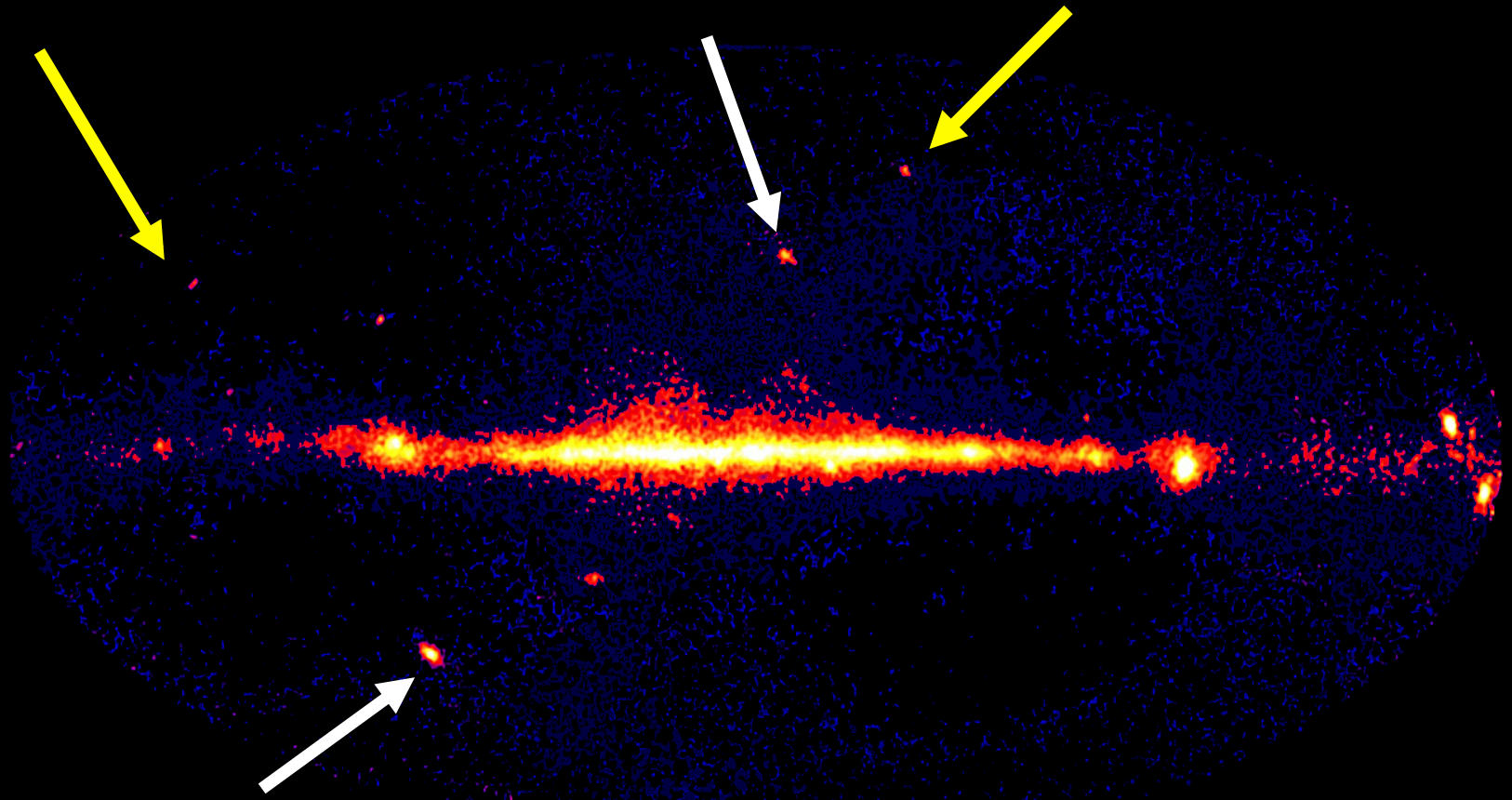

3C 454.3: the *Crazy Diamond*, 7 billion lightyears away…

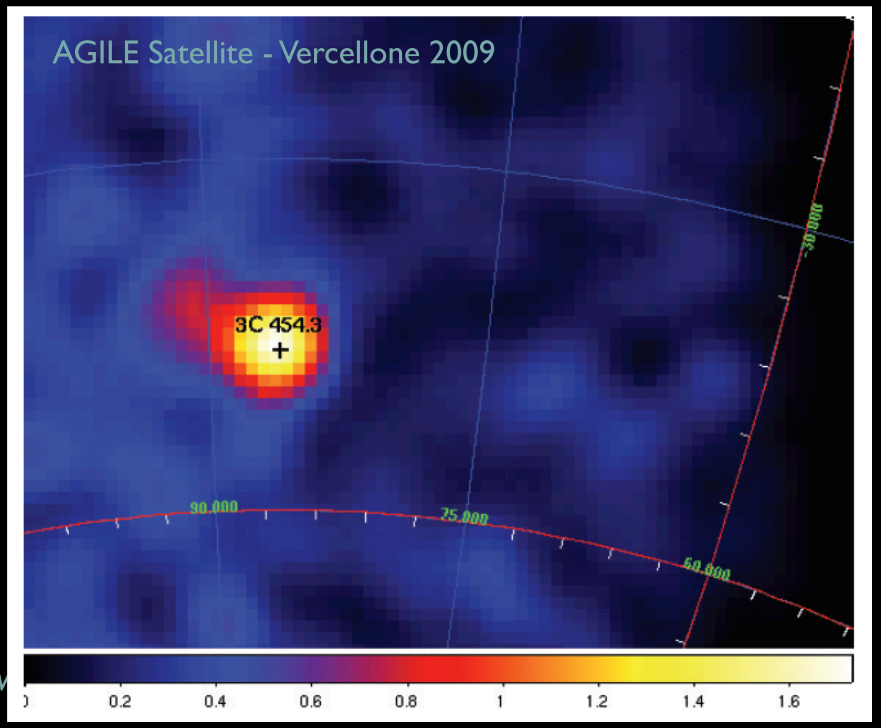

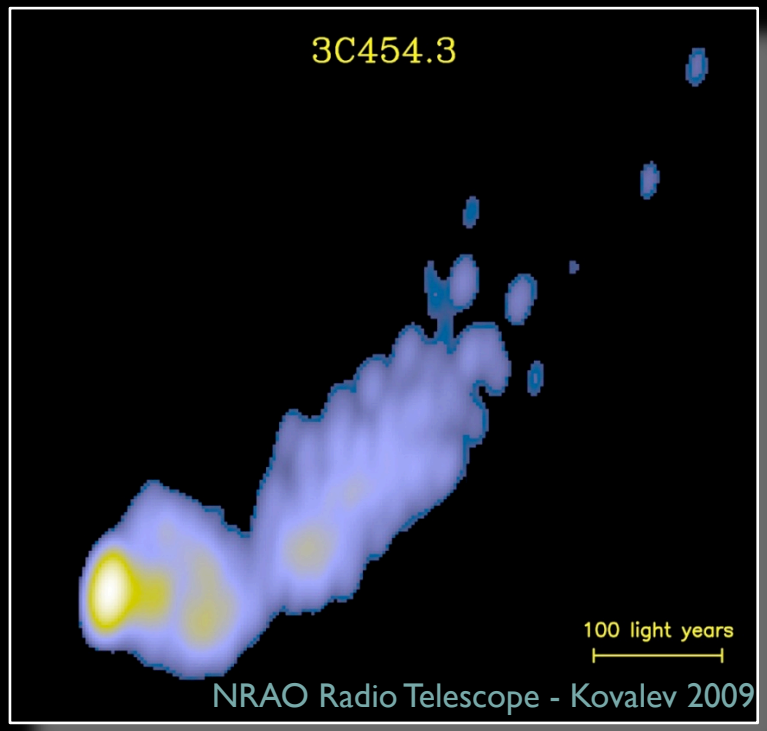

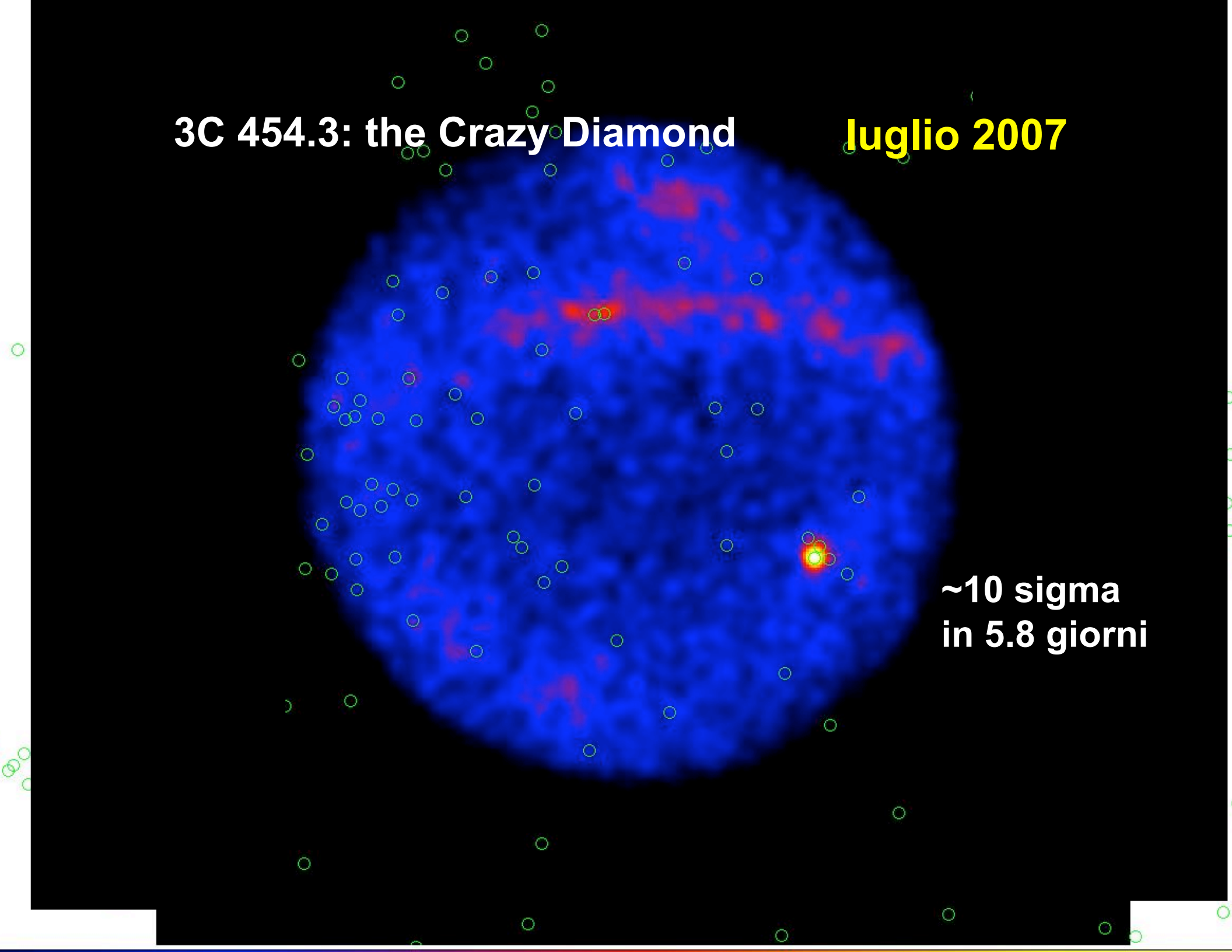
3C 454.3: the Crazy Diamond
luglio 2007
~10 sigma
in 5.8 giorni

3C 454.3: the Crazy Diamond of 2007-2008

(Vercellone et al. 2007-2008-2009, Donnarumma et al. 2009)

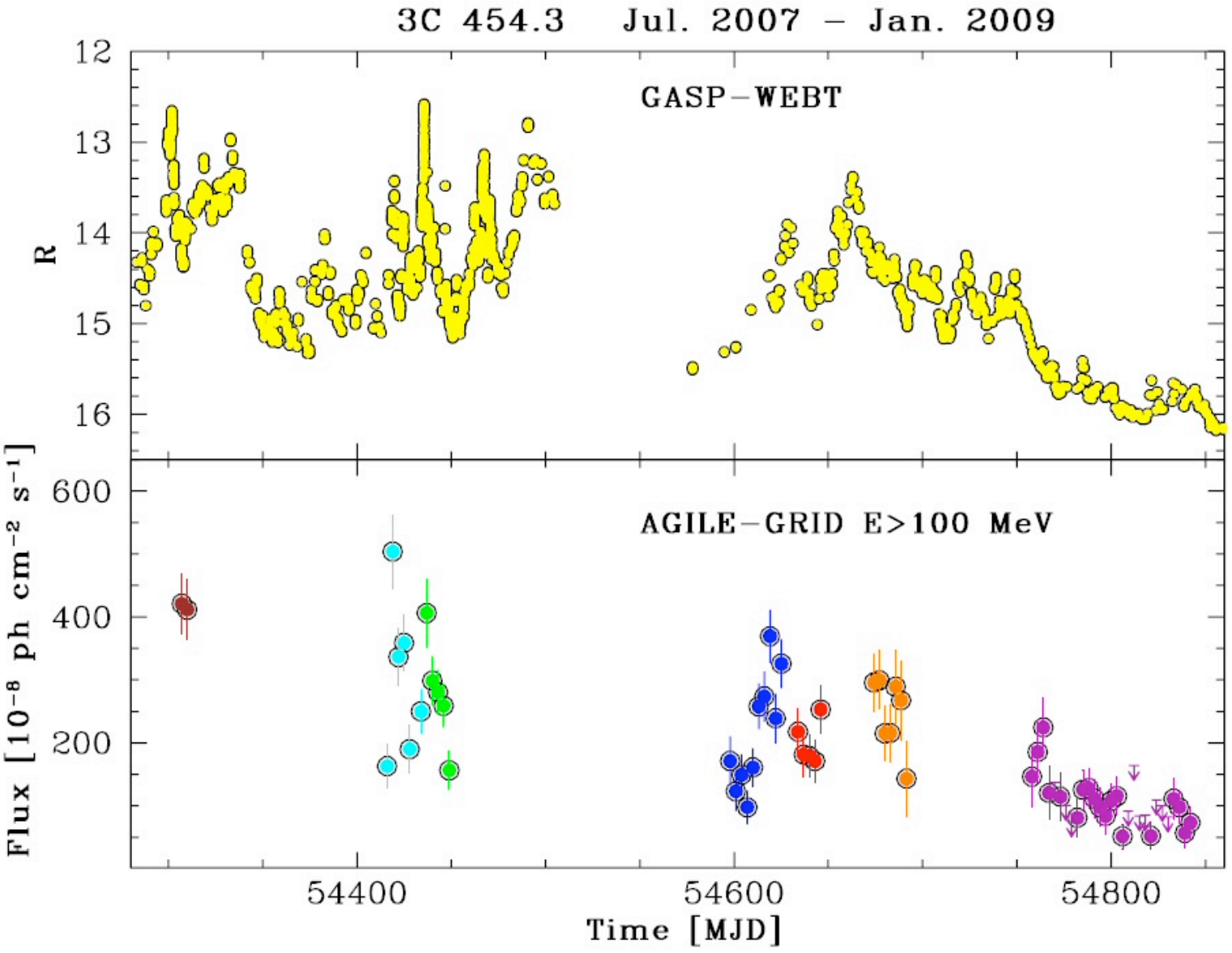

optical

gamma

3C 454.3: Outbursts seen first at mm wavelengths, optical & gamma-ray closely related but do not vary exactly together on short time-scales

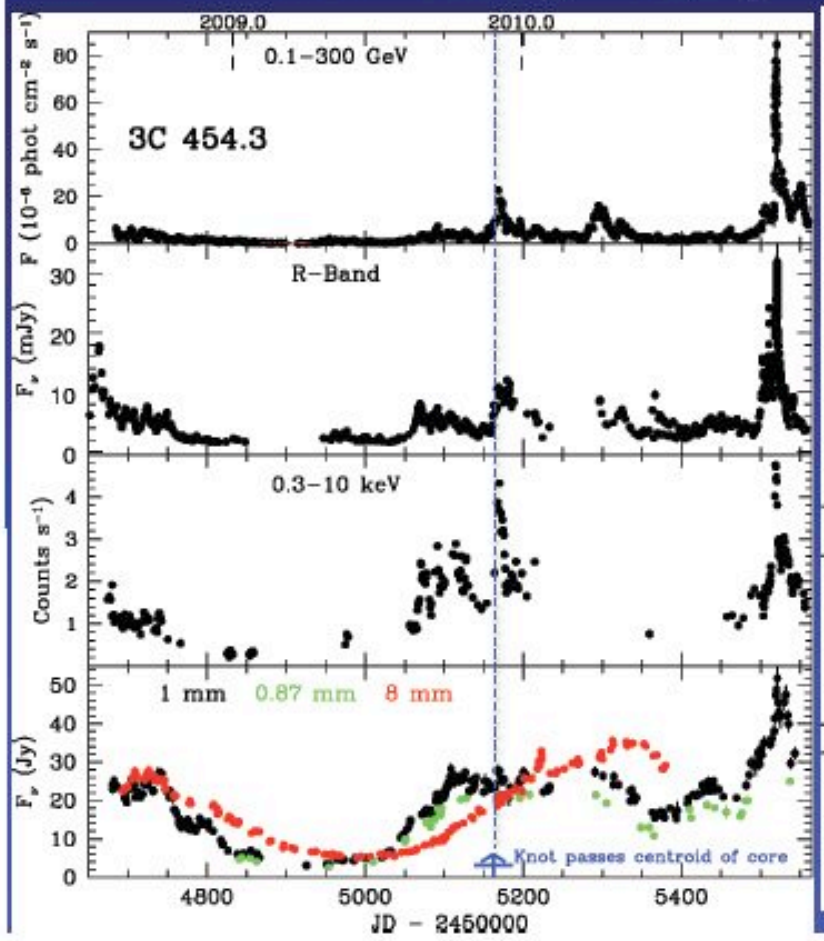

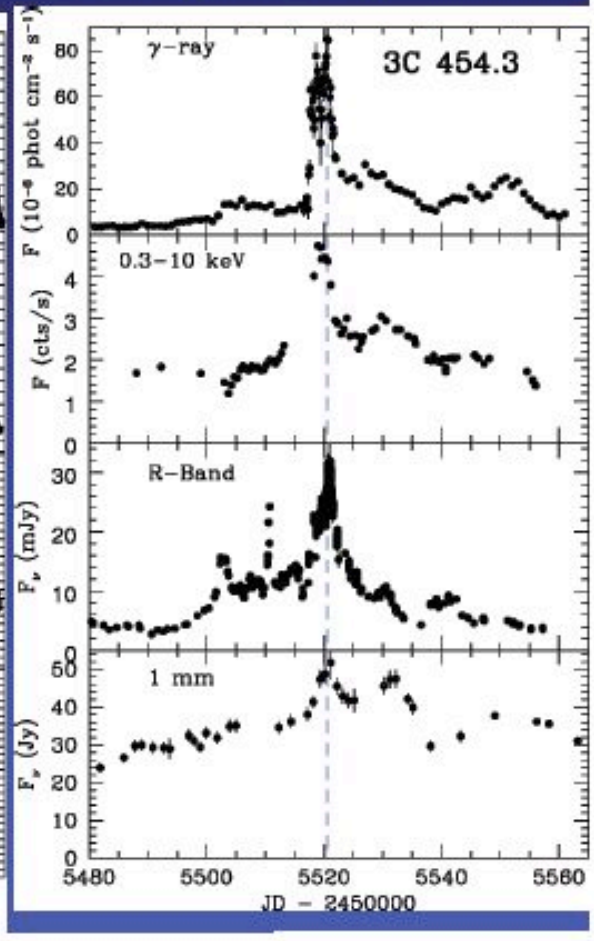

sussulto gamma di 3C 454.3 (3-4 Dic. 2009)

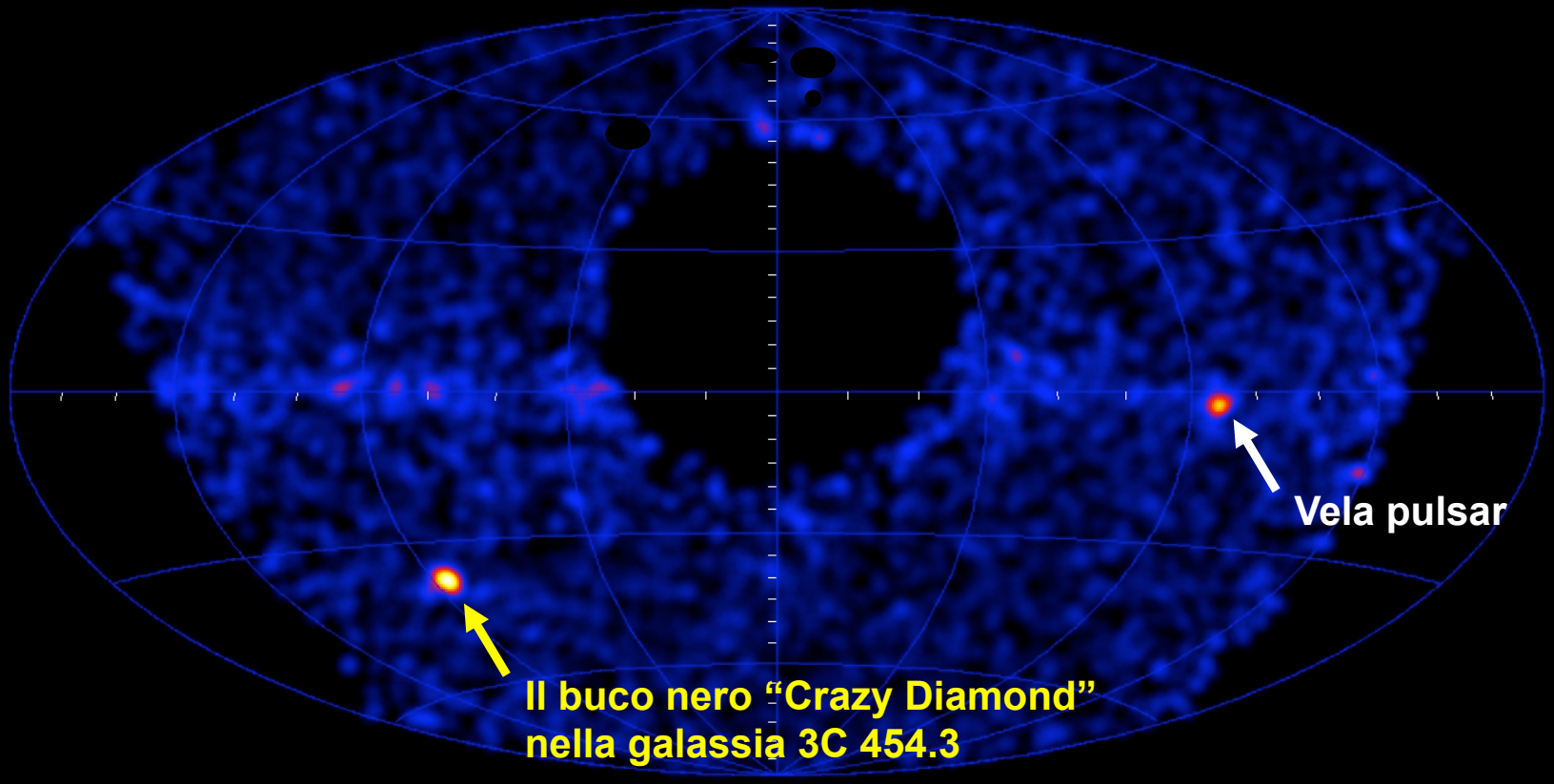

the 3C 454.3 Nov. 2009 flare

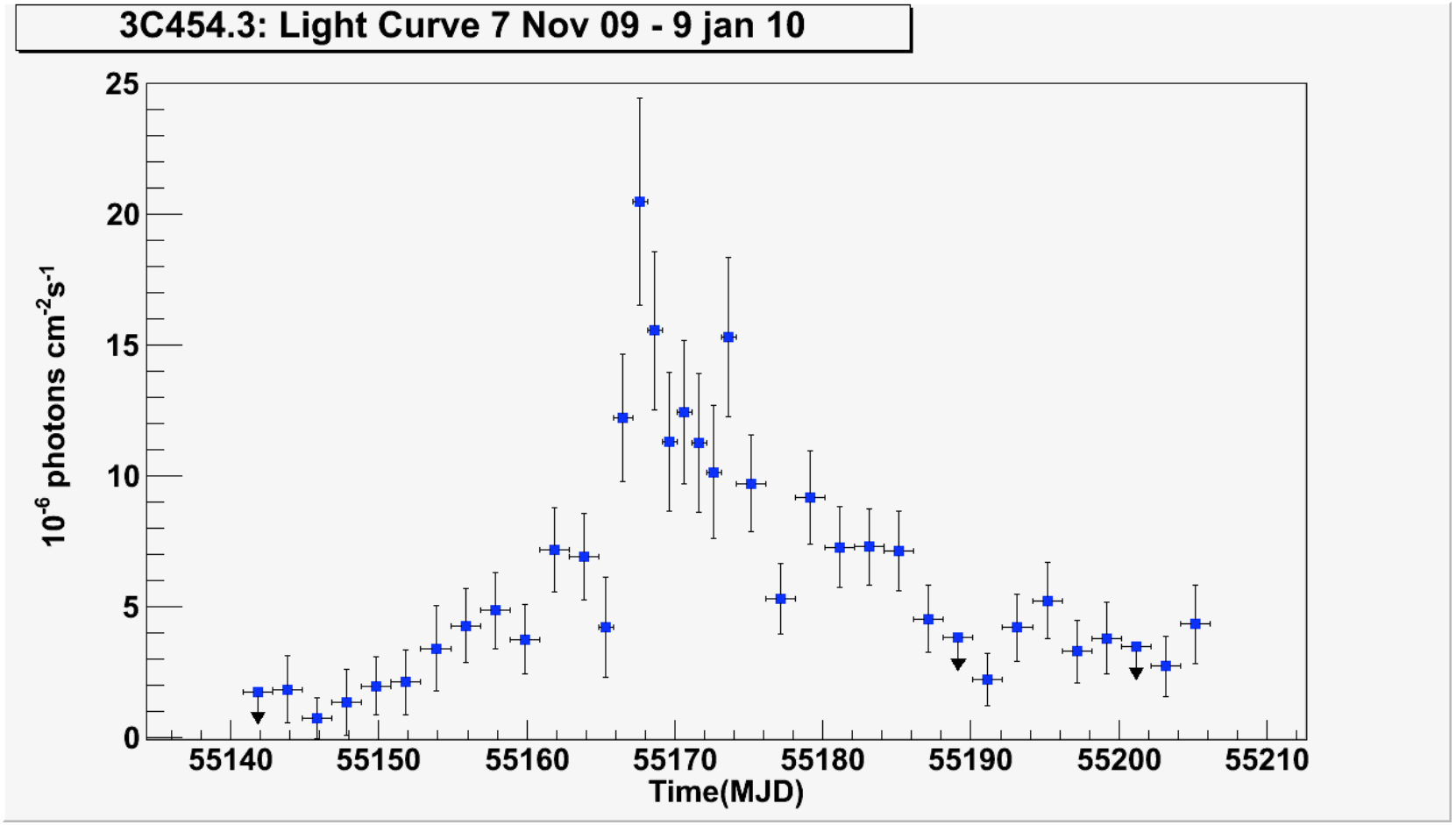

Spectral evolution of 3C 454.3 (Dec. 2009)

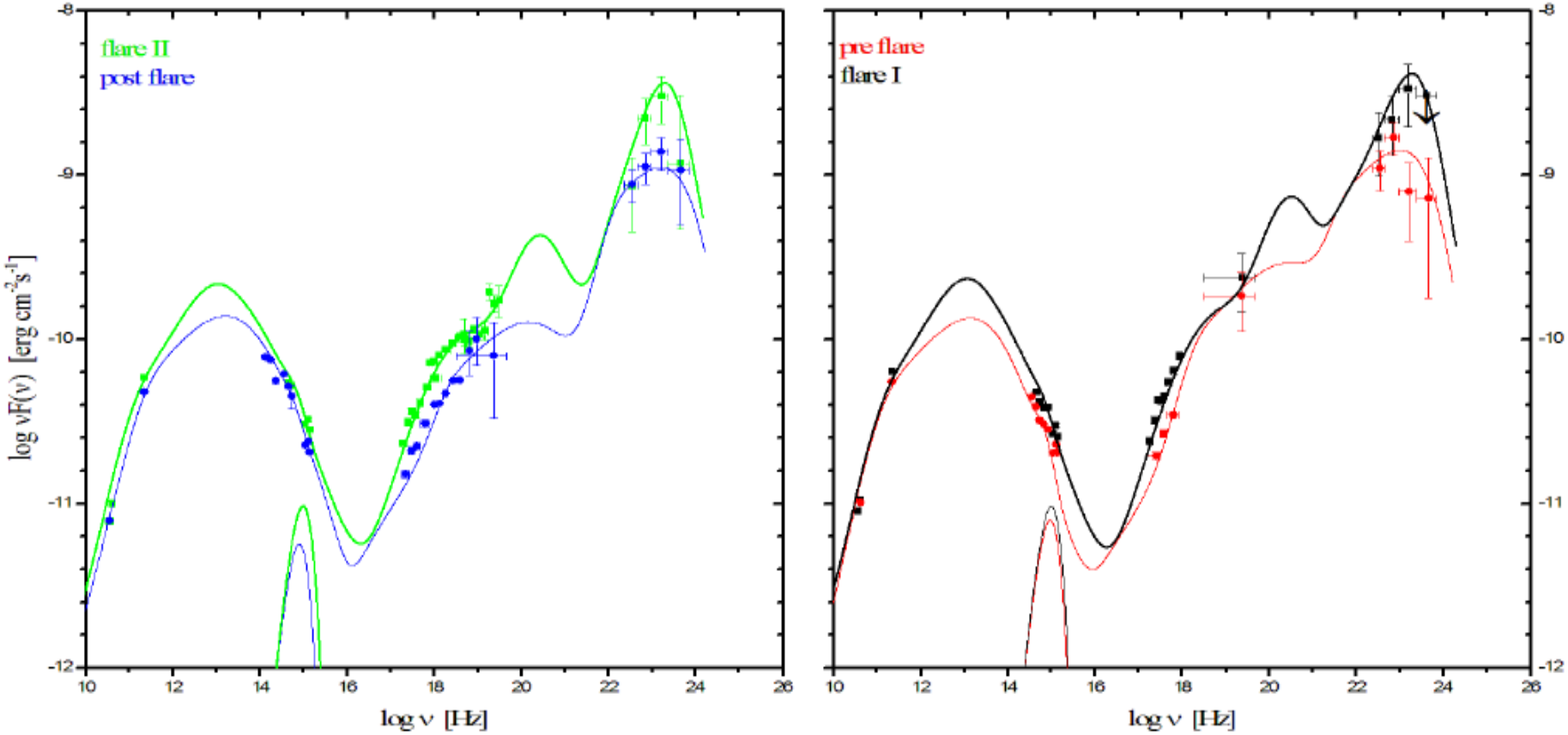

the 3C 454.3 super-flare in Nov.-Dec. 2010

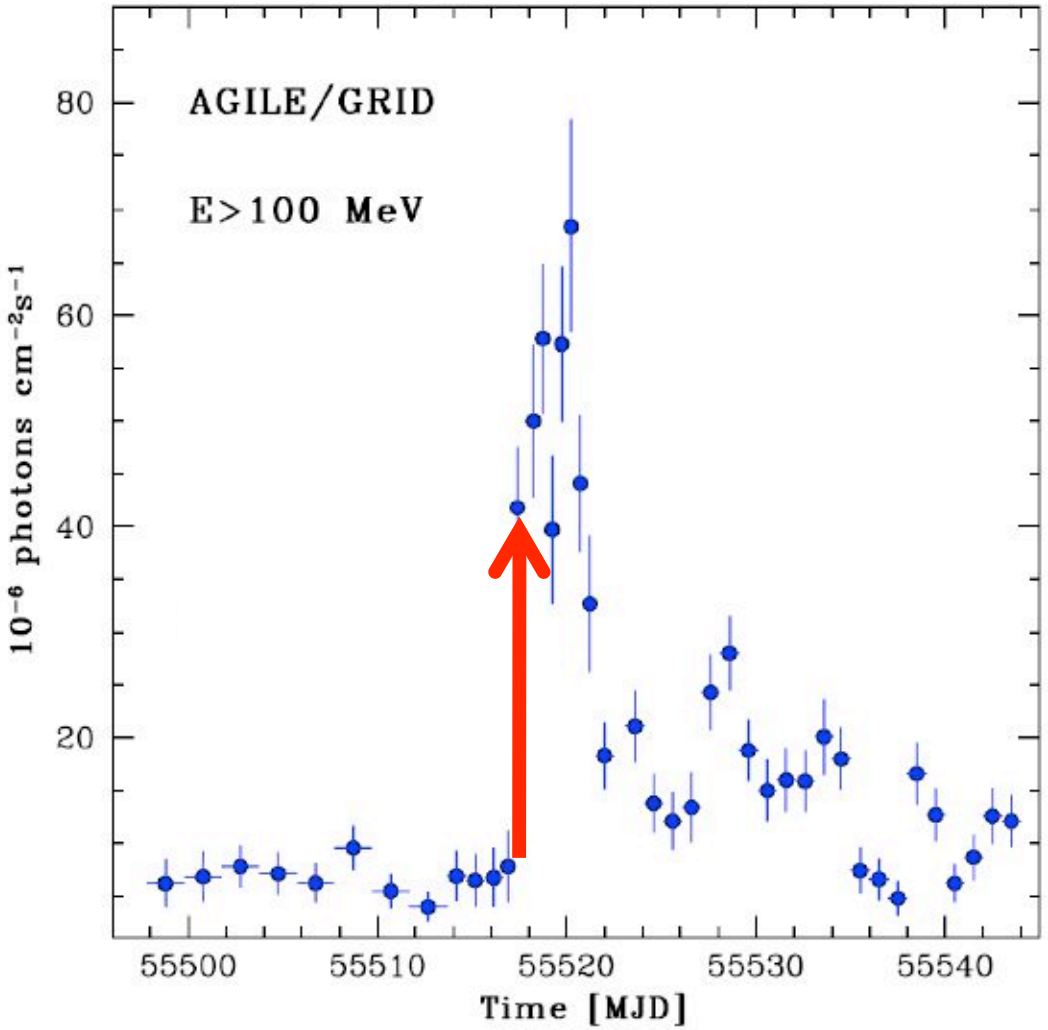

GRID light curve

3C 454.3 superflare (16-19 Nov. 2010)

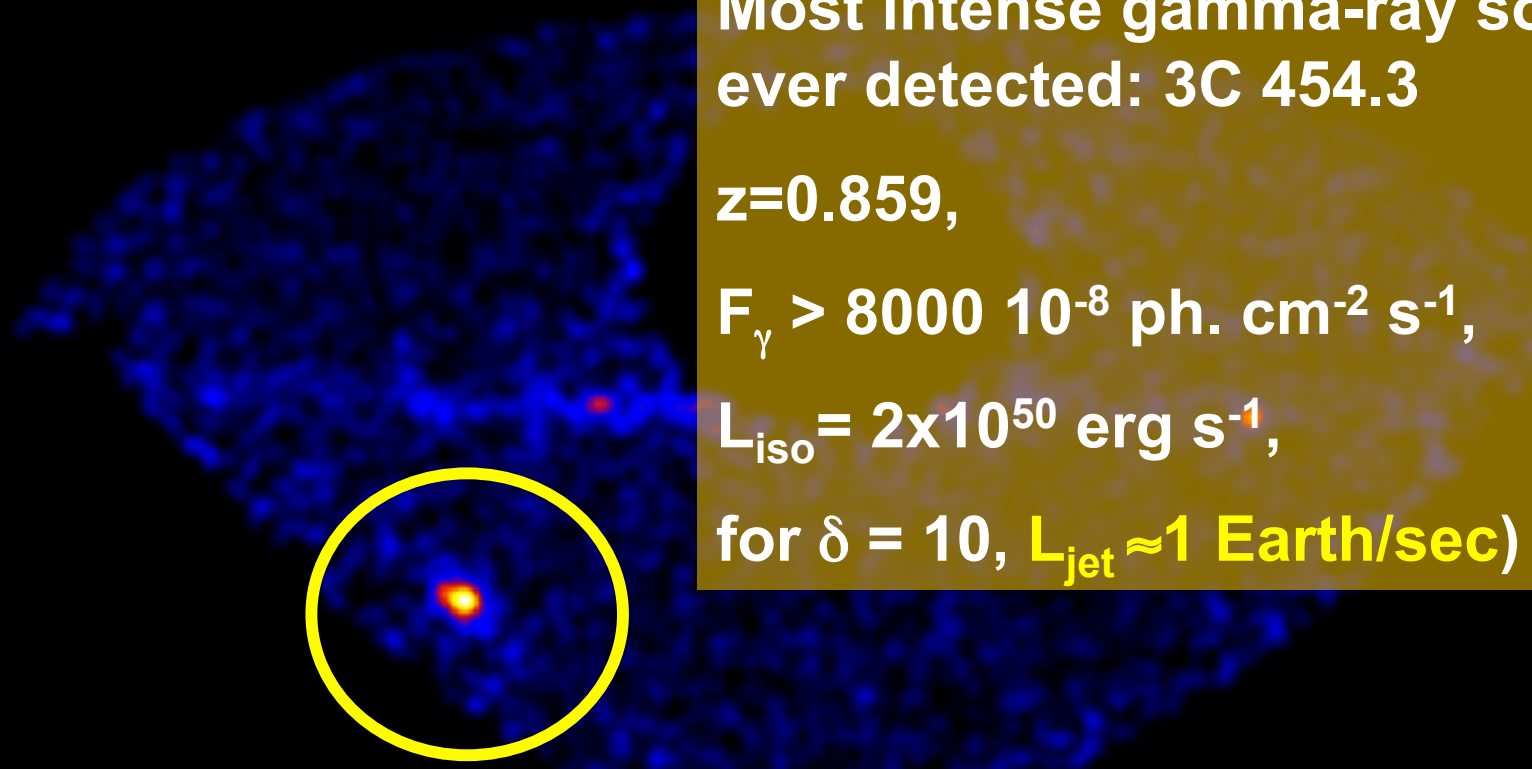

Most intense gamma-ray source ever detected: 3C 454.3

z=0.859,

$F_\gamma > 8000\ 10^{-8}$ ph. cm^{-2} s^{-1},

$L_{iso} = 2 \times 10^{50}$ erg s^{-1},

for $\delta = 10$, $L_{jet} \approx 1$ Earth/sec)

emission spectrum of 3C 454.3, November 2010 (Vercellone et al., 2011)

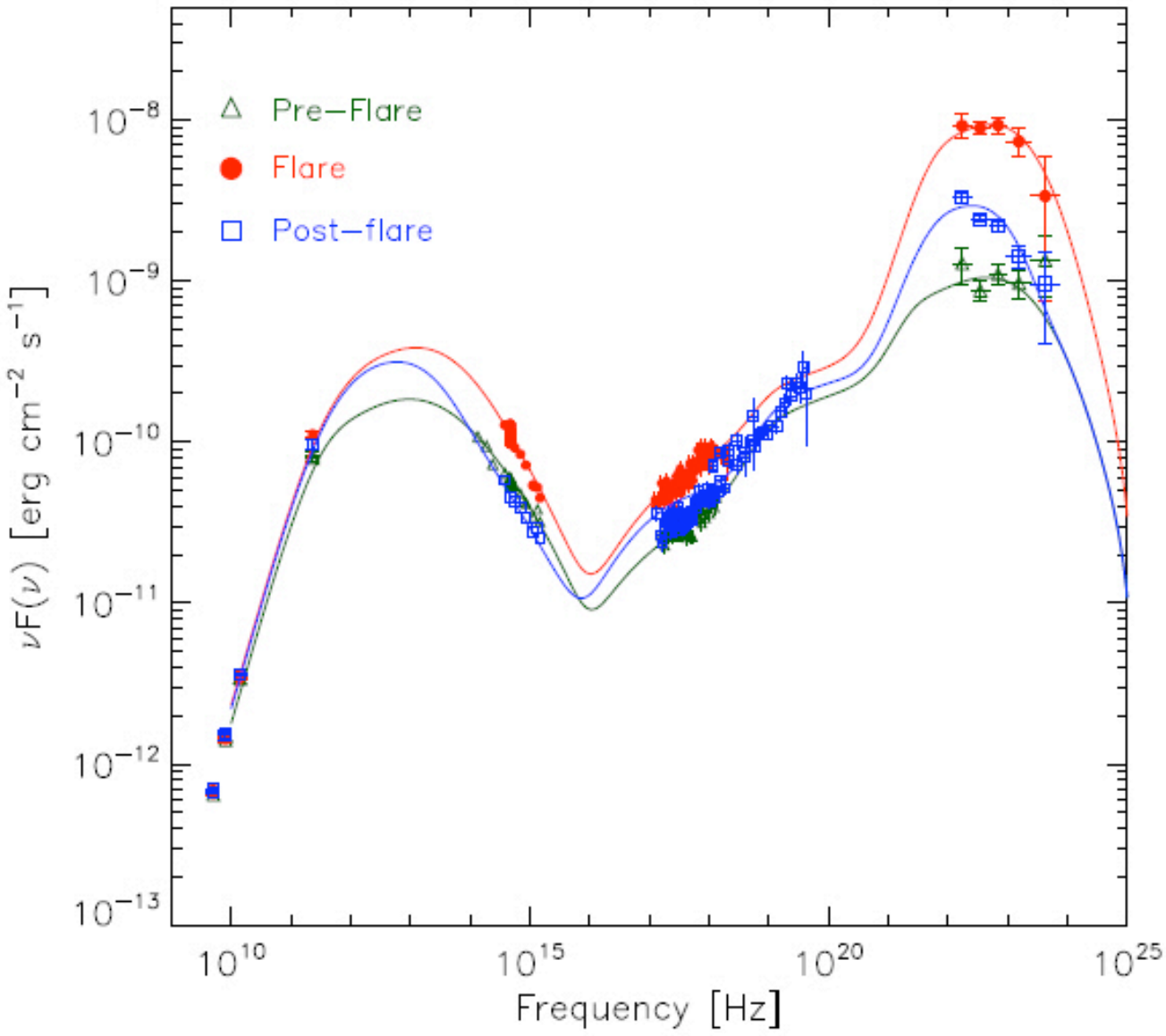

γ-ray νFν spectrum

- preflare and plateau: BPL and PL+expcutoff give similar quality fits, significantly better than Log-parabola
- none of tested functions gives a good fit for the flare period

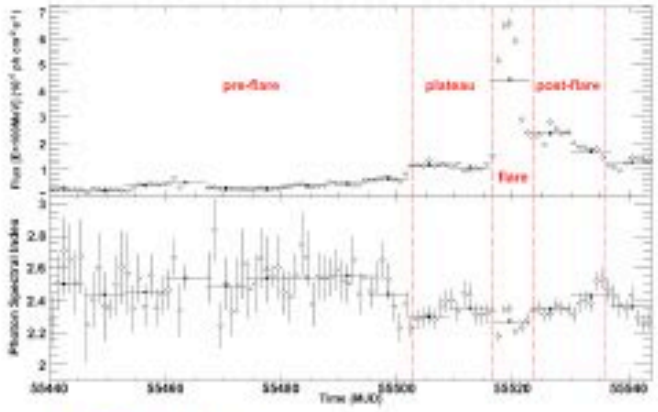

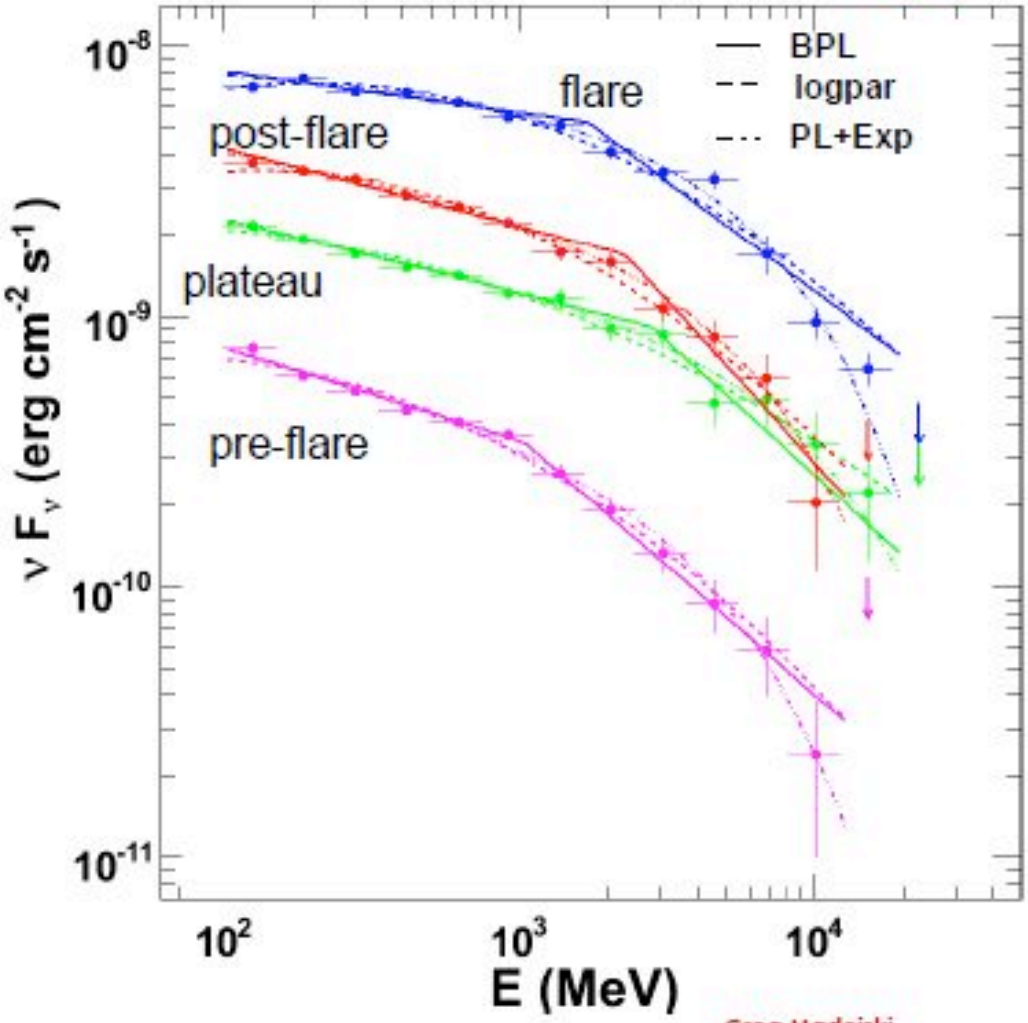

Rome May 2011

Greg Madejski

3C 454 Nov. 2010 flare

- **Energetics**
  - **dE/dt (jet kinetic energy) = M_{Earth} / 10 sec**
  - **L (gamma) = L (iso) / Γ^2 = 1.2x10^{47} erg/s**

3C 454.3: 2010 super-outburst from gamma-ray to mm-wave

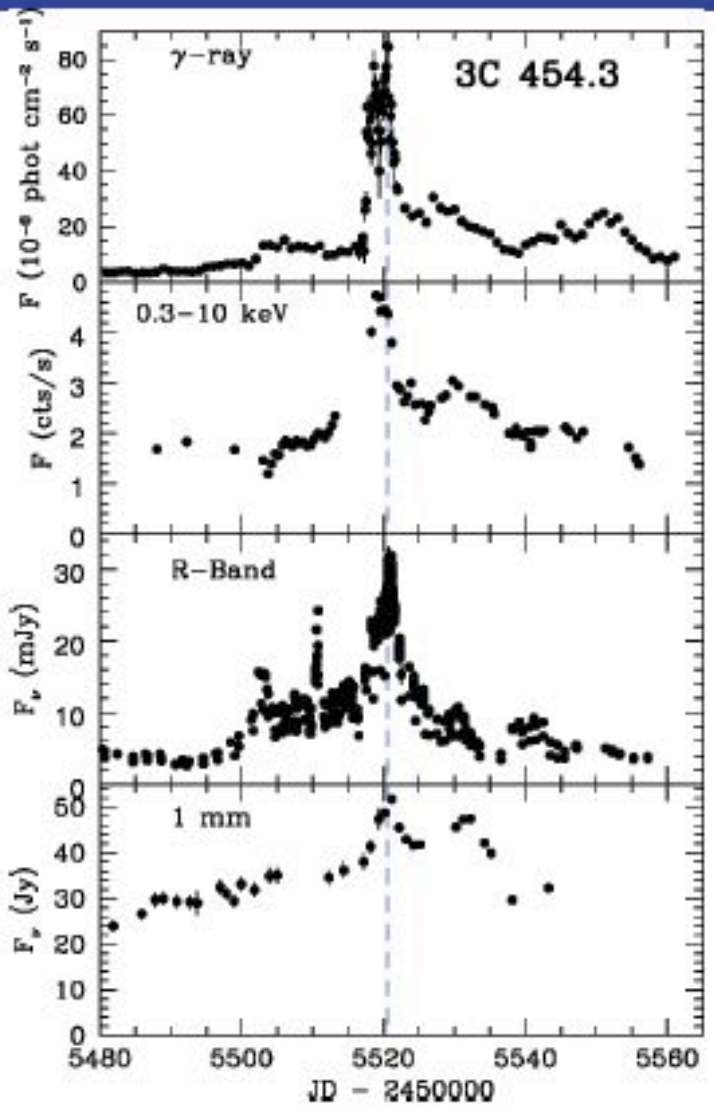

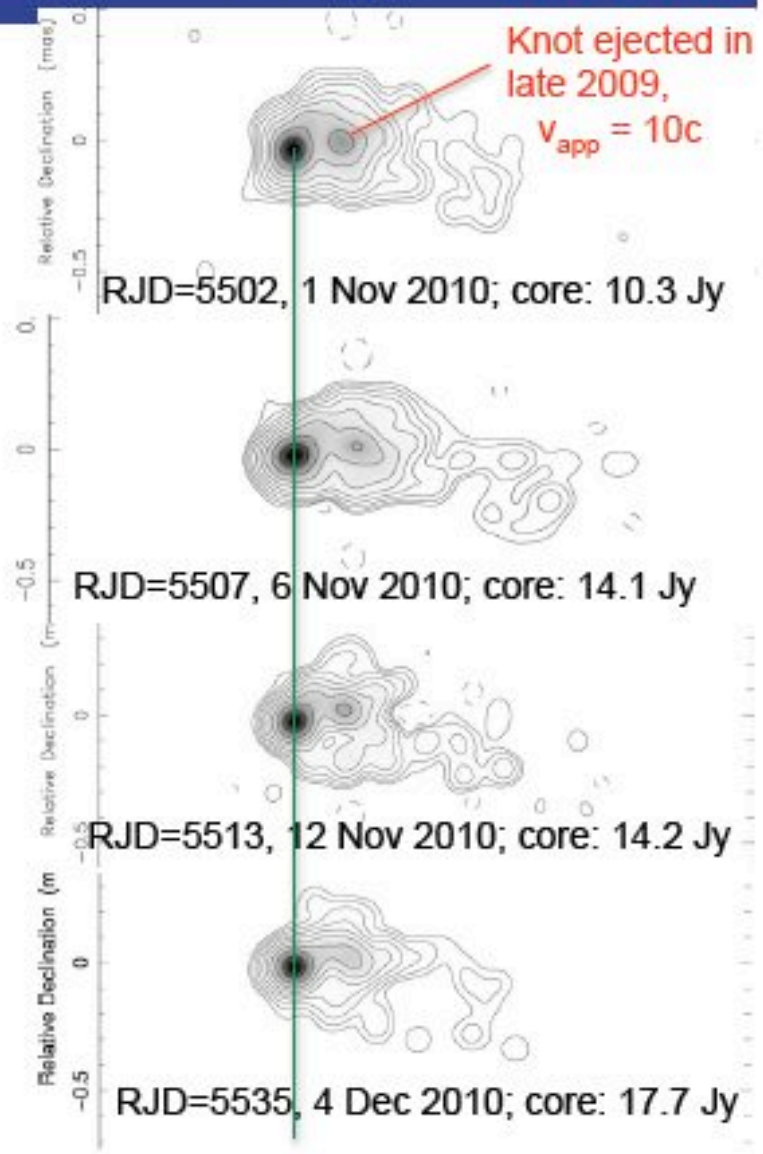

3C 454.3: Knot from mega-outburst moving in new direction

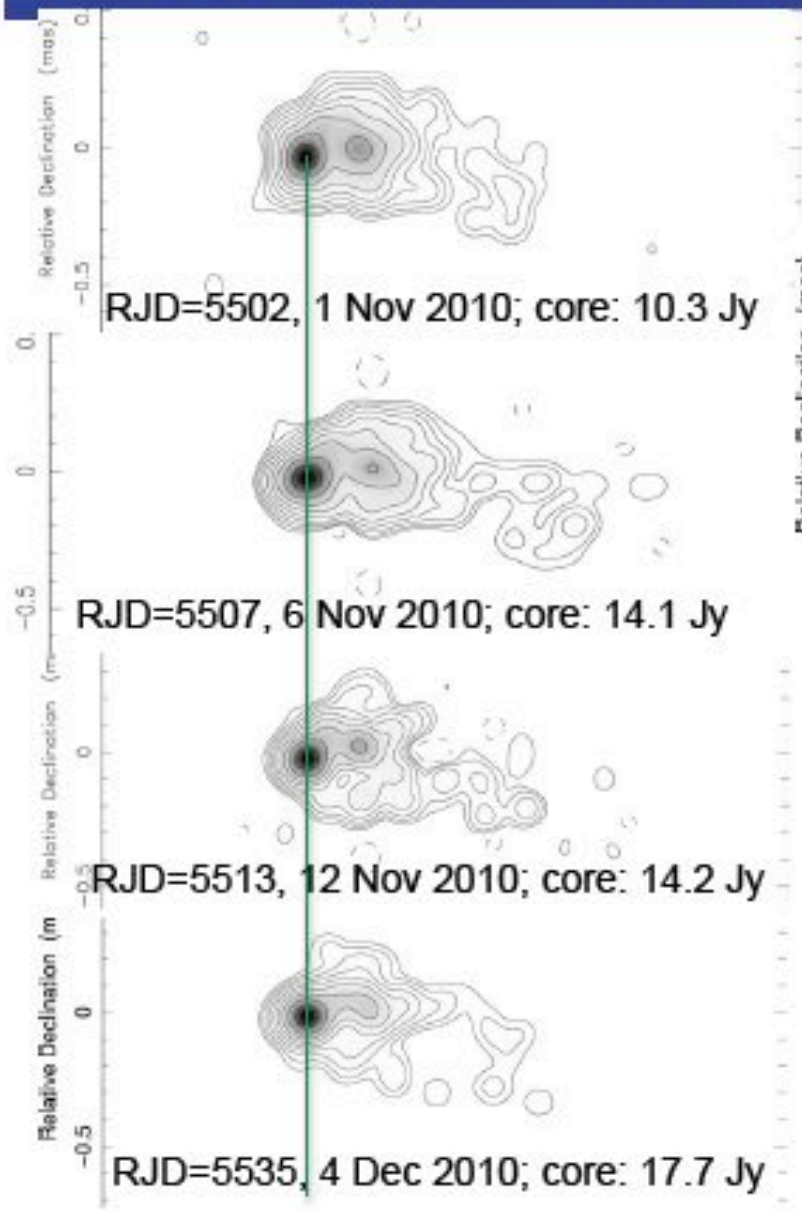

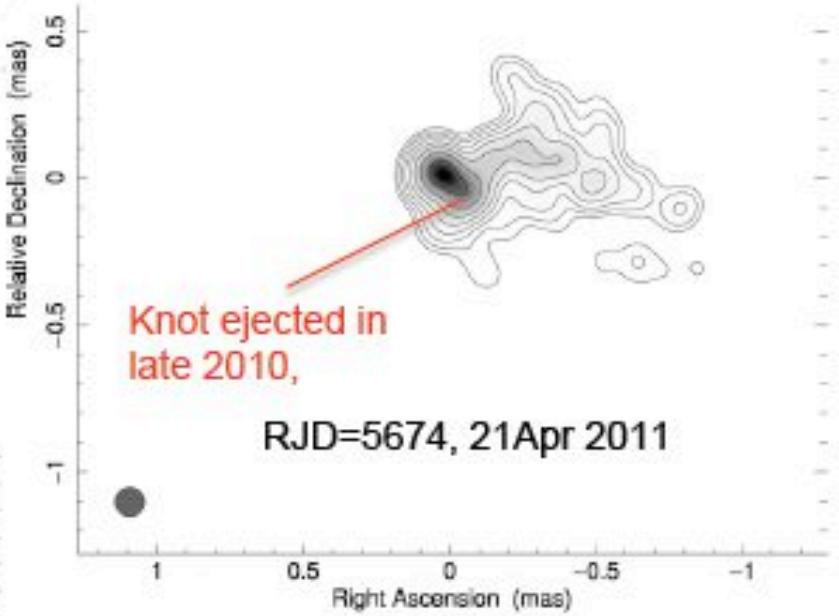

Jorstad et al. (2010 ApJ): core has triple structure, with a flare occurring as a knot passes each feature

3C 279 in 2008-09

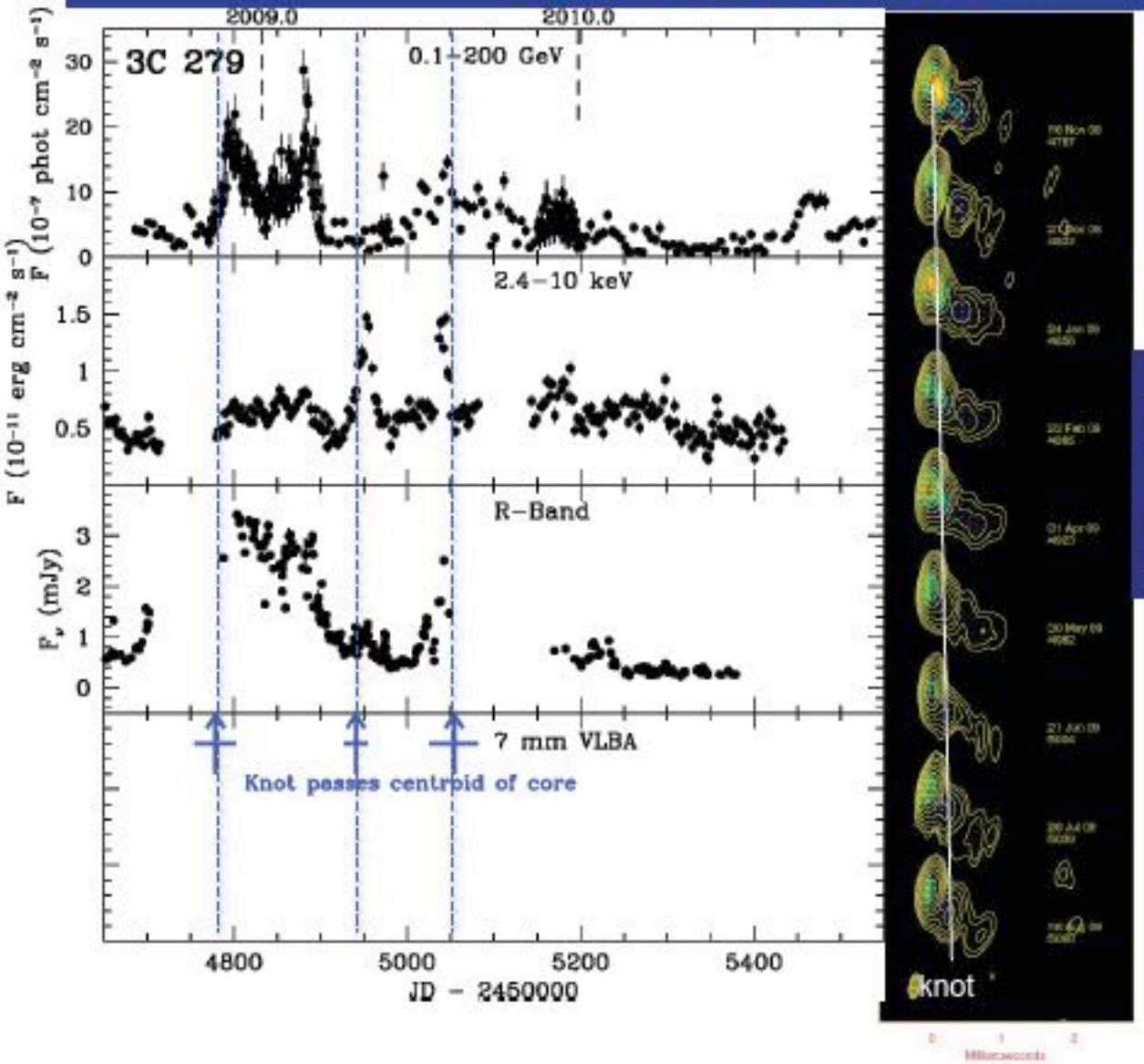

1. High-energy utbursts occur after new superluminal knot appears

2. Note optical/γ-ray general correlation but poor detailed correspondence on short time-scales.

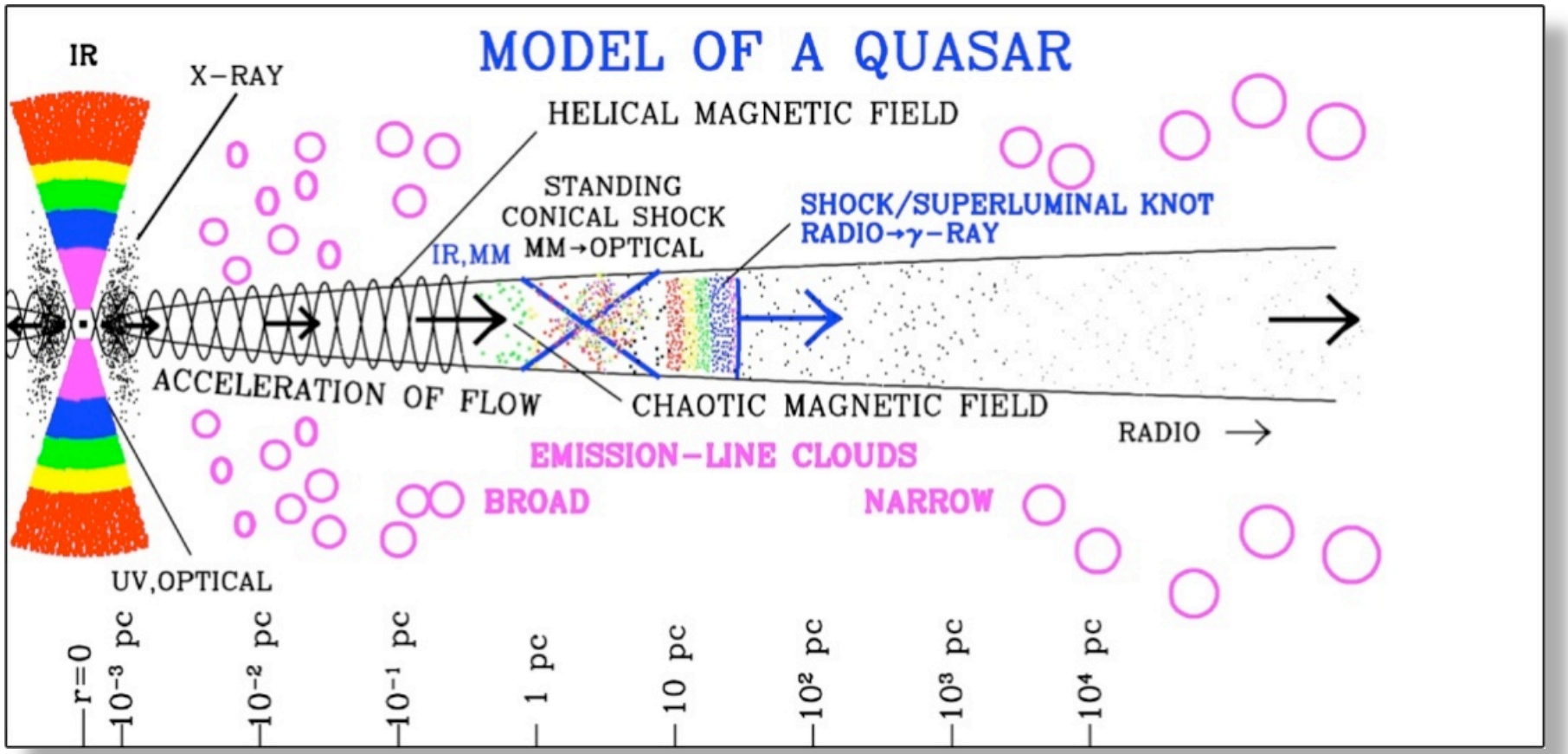
MODEL OF A QUASAR
IR
X-RAY
HELICAL MAGNETIC FIELD
STANDING
CONICAL SHOCK
MM→OPTICAL
IR,MM
SHOCK/SUPERLUMINAL KNOT
RADIO→γ-RAY
ACCELERATION OF FLOW
CHAOTIC MAGNETIC FIELD
RADIO
EMISSION-LINE CLOUDS
BROAD
NARROW
UV,OPTICAL
r=0
10⁻³ pc
10⁻² pc
10⁻¹ pc
1 pc
10 pc
10² pc
10³ pc
10⁴ pc

Seed photons for Inverse Compton (IC)

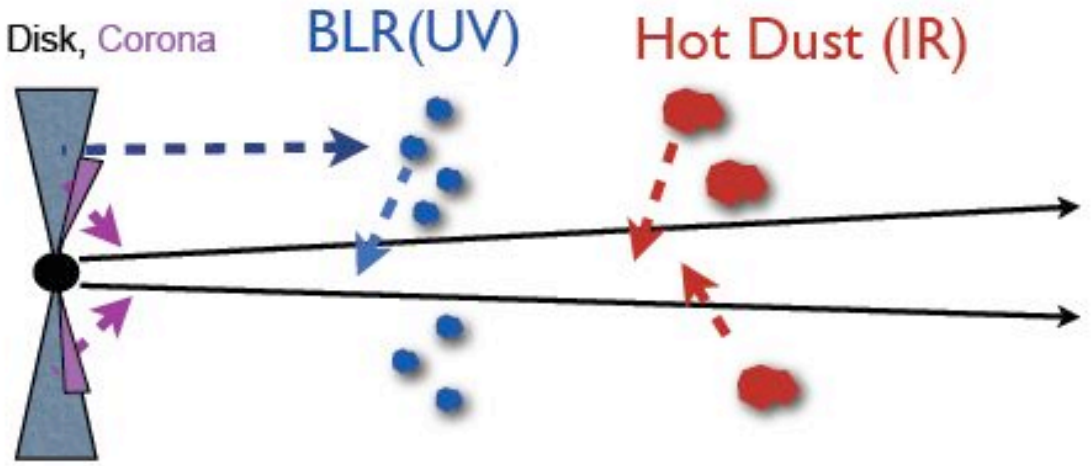

$$R_{BLR} \simeq 0.1 \times L_{46}{}^{1/2}\ \mathrm{pc}$$ (Bentz et al. 2006 ; Kaspi et al. 2007)

$$R_{HD} \simeq 2.5 \times L_{46}{}^{1/2}\ \mathrm{pc}$$ (Cleary et al. 2007 ; Nenkova et al. 2008)

$$R \propto L_{disk}^{1/2} \qquad U_{rad} \propto L/R^2 \sim \mathrm{const.} \sim 10^{-2}\mathrm{erg/cm^3}$$

Basic 0th-order assumptions/approximations:
a) R ~ as above
b) isotropic field (shell)
c) BlackBody spectrum @9eV (0.2 eV)
d) reprocessing factor η~ 10% (20-30%)

(e.g. Ghisellini et al. 2009
Sikora et al. 2009)

Absorption feature by γ-γ interactions

But: the same seed photons for EC are targets for γ-γ interactions.
"Double wall" of target photons !

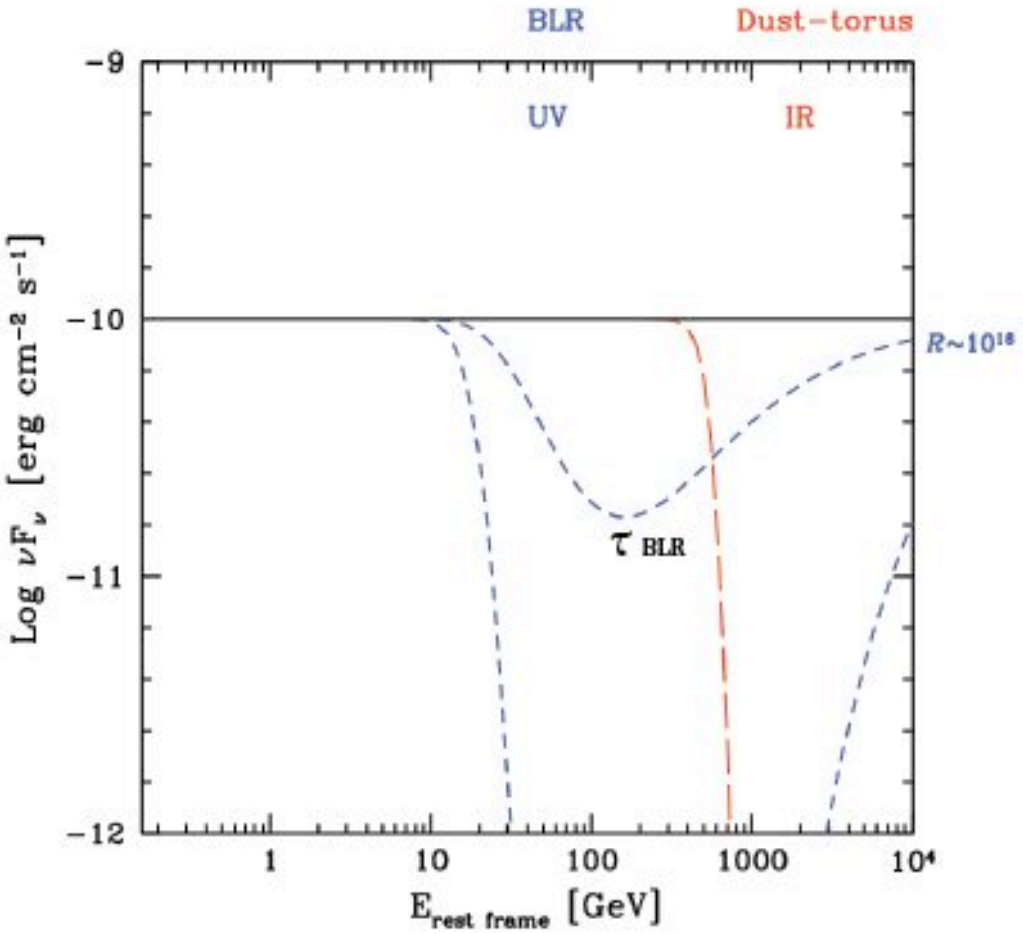

Optical depth τ is high !

U_{rad} ~const ⇒ τ depends only on path length inside BLR/HD

Always not negligible (≥1), even in the minimal case: photon path ~ size of emitting region (typically ~10^{16} cm)

Fermi now samples this energy range for the first time (1-100 GeV rest frame)

NO evidence of strong BLR cut-offs !

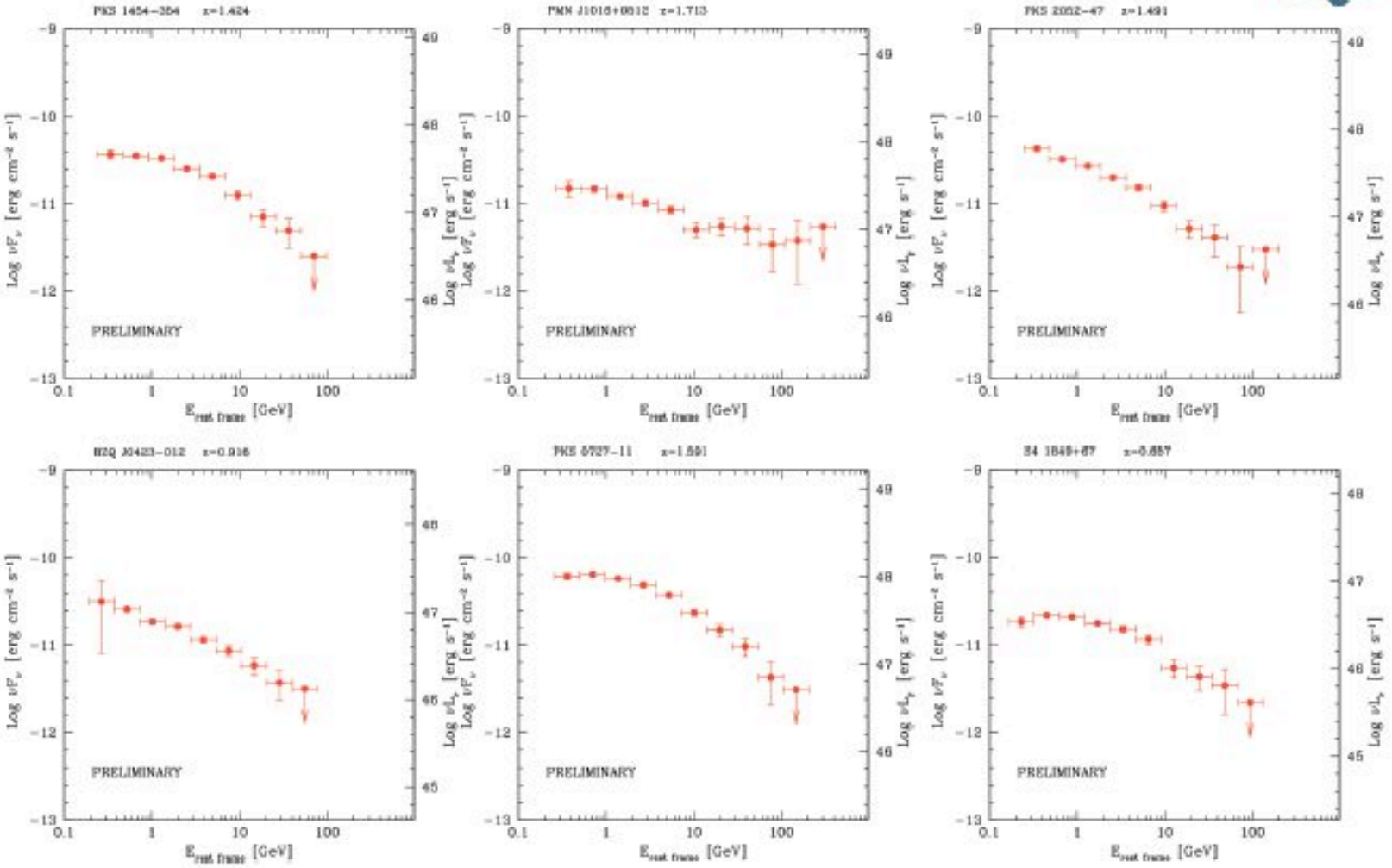

High energy SED

PKS 1221+21

Aleksić et al. ApJL 730 (2011)

- Simultaneous *Fermi*/LAT 2.5 hrs encompassing MAGIC obs.

Tanaka et al. ApJ 2011

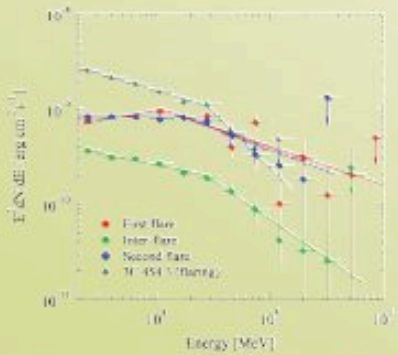

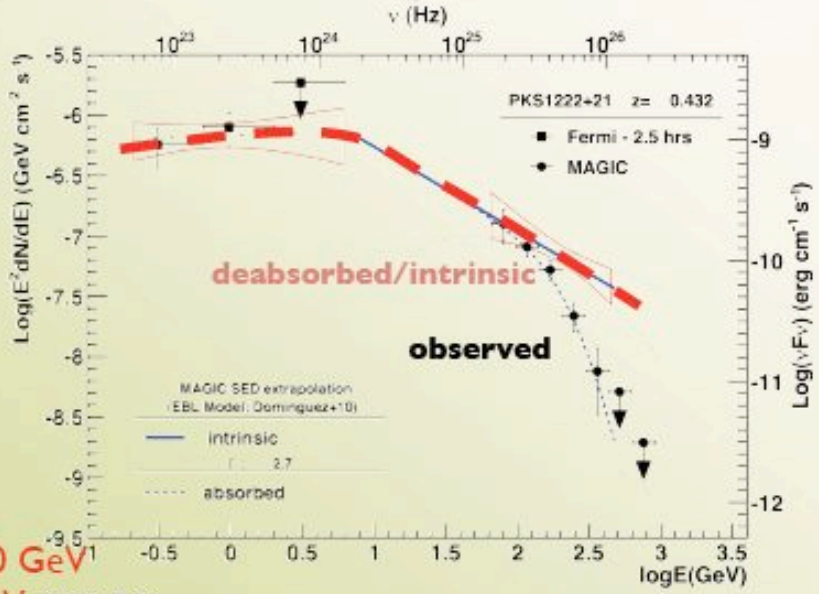

Single component from 2 to 400 GeV

Cutoff excluded at E < ~130 GeV (95% CL)

High energy SED

- Internal absorption + Klein-Nishina break

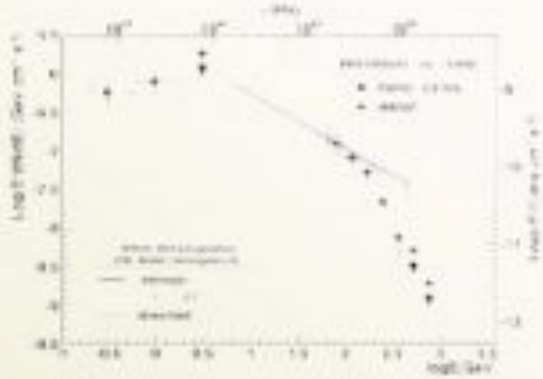

Ghisellini&Tavecchio 2009

Liu&Bai 2006

Inside BLR

$$\nu_{KN} = \frac{4}{3}\gamma^2 \nu_{La} \frac{2\Gamma\delta}{1+z} = 15 \frac{\delta}{\Gamma(1+z)}\ \mathrm{GeV}$$

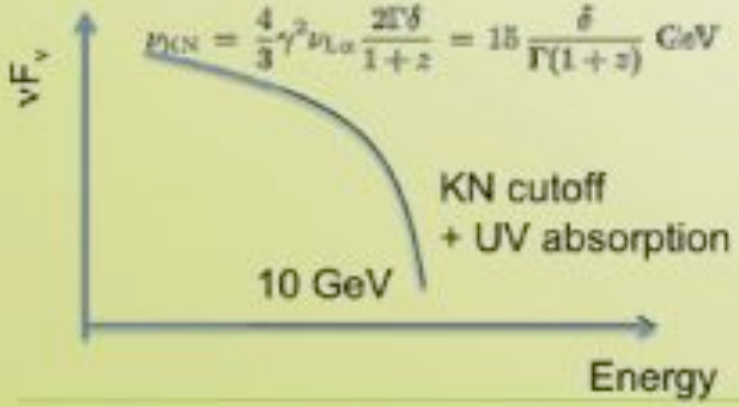

Outside BLR

$$\nu_{KN} = \frac{4}{3}\gamma^2 \nu_{IR} \frac{2\Gamma\delta}{1+z} = 1.2 \frac{\delta}{\Gamma(1+z)}\ \mathrm{TeV}$$

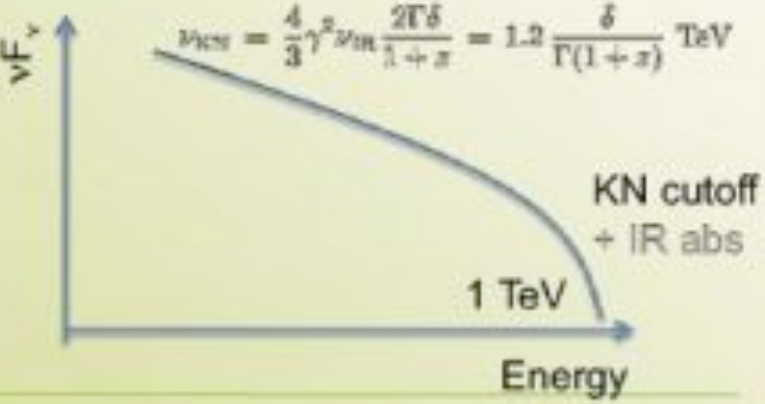

a.Stamerra

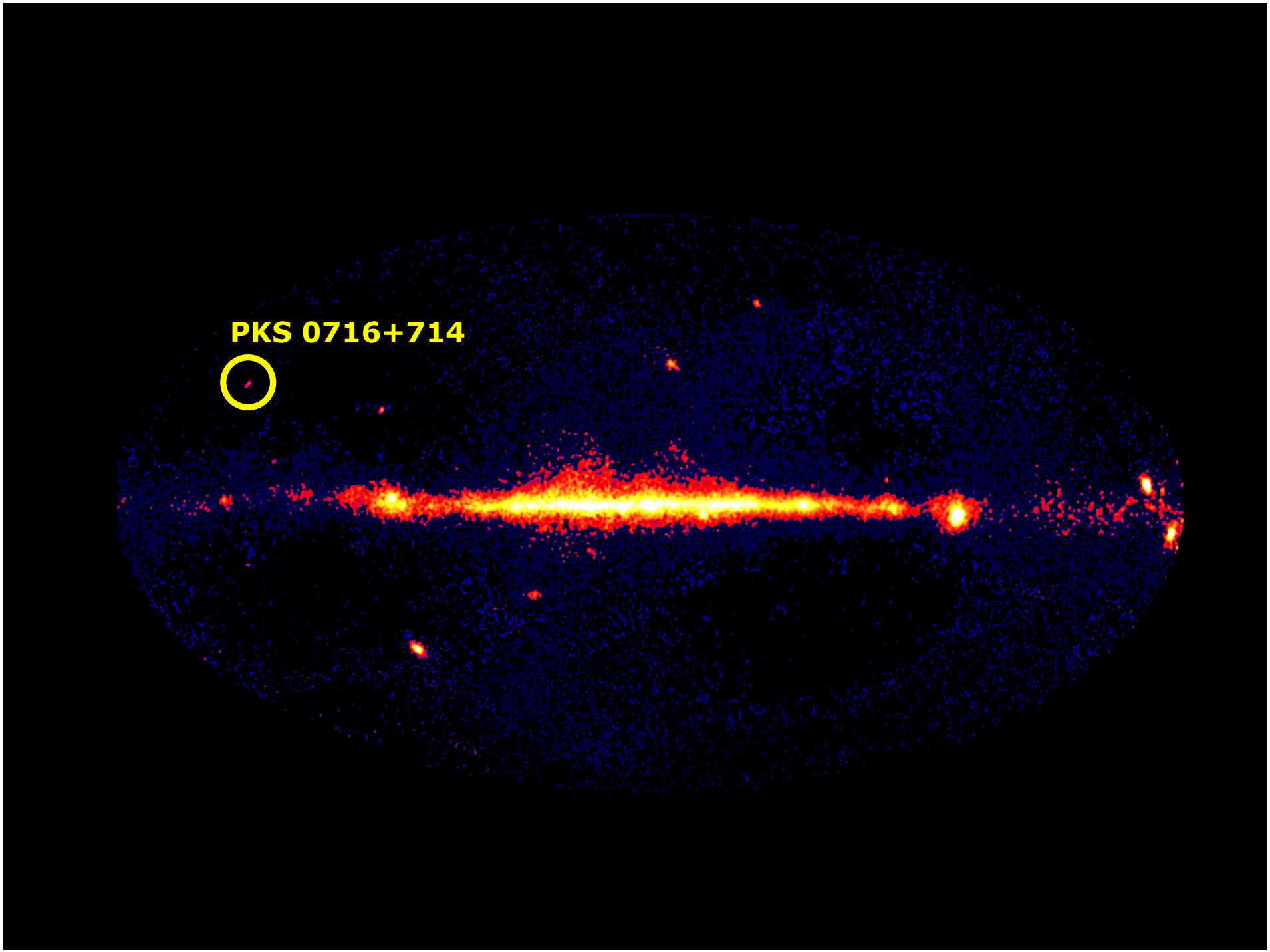
PKS 0716+714

PKS 0716+714 Sep. '07 (Chen et al, 2008)

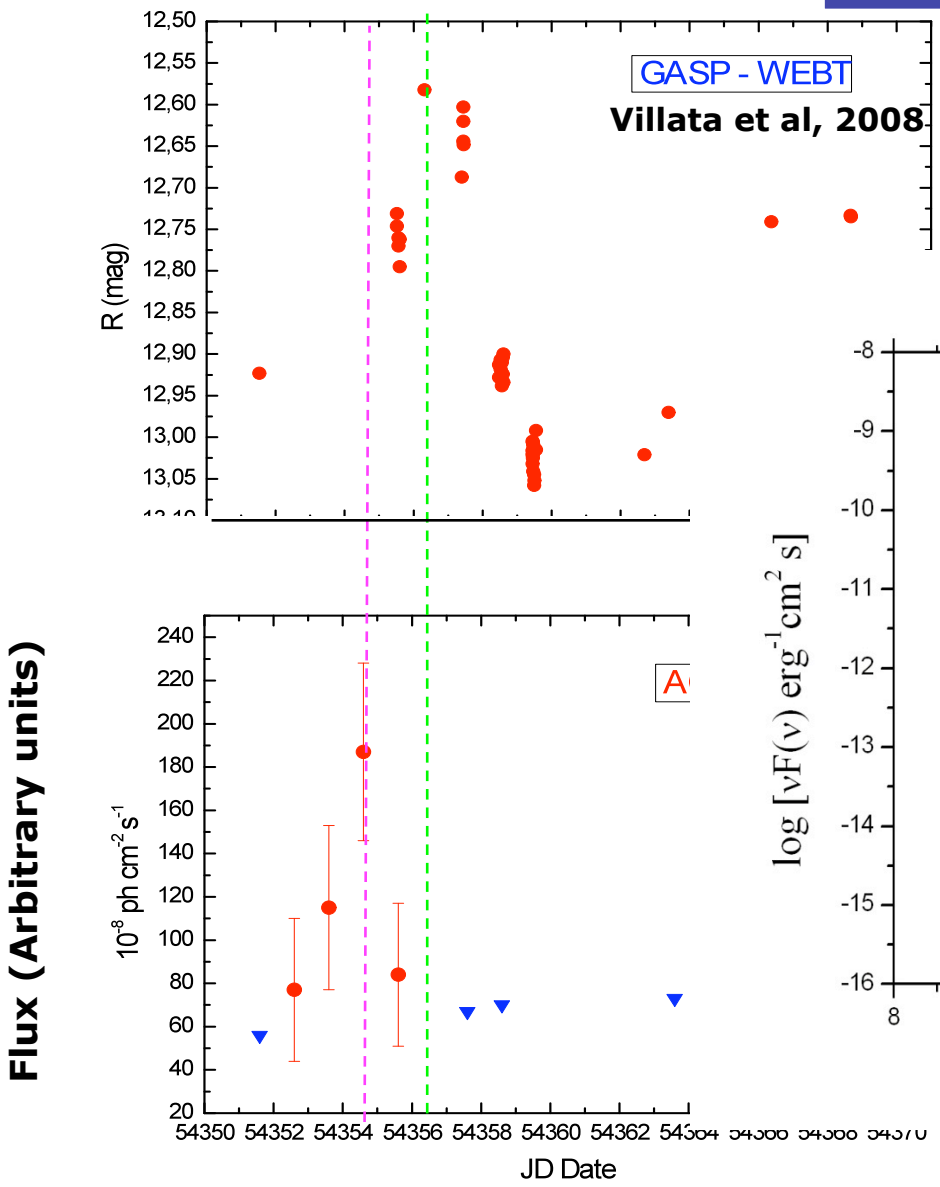

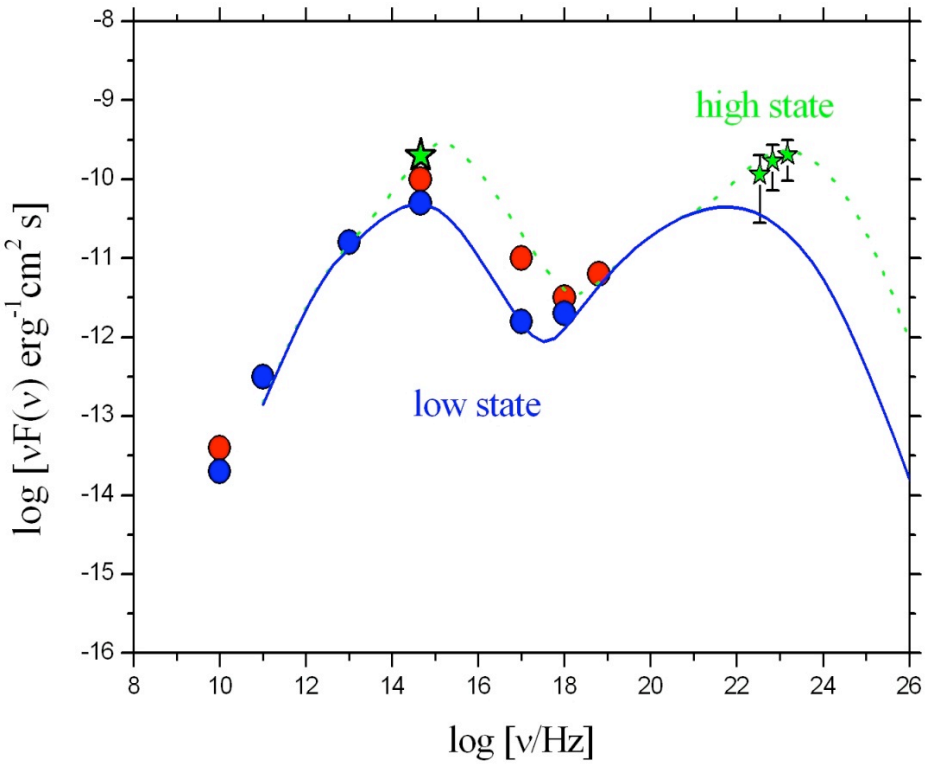

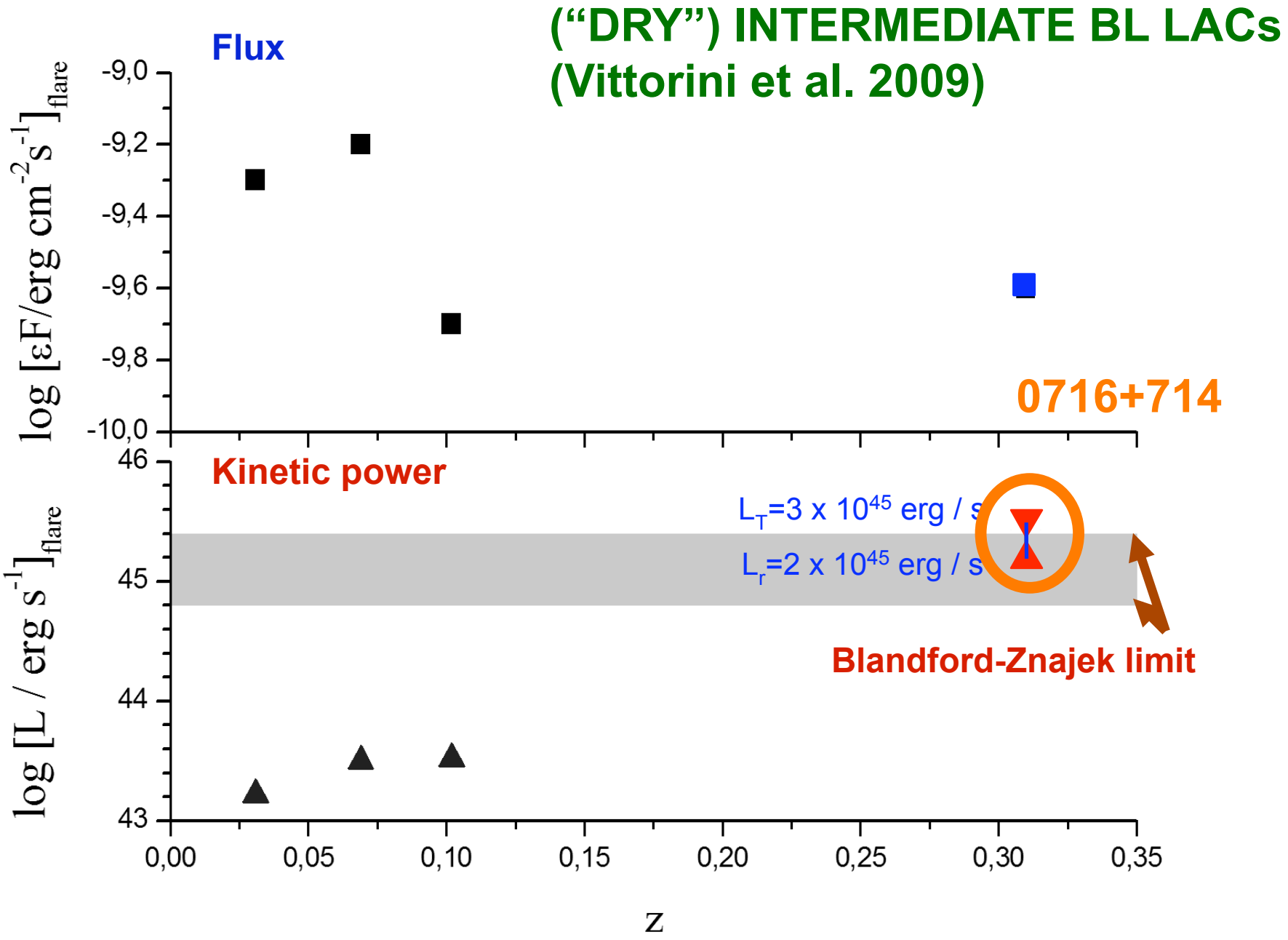
("DRY") INTERMEDIATE BL LACs
(Vittorini et al. 2009)
Flux
log [εF/erg cm-2s-1]flare
-9,0
-9,2
-9,4
-9,6
-9,8
-10,0
0716+714
Kinetic power
log [L / erg s-1]flare
46
45
44
43
LT=3 x 10^45 erg / s
Lr=2 x 10^45 erg / s
Blandford-Znajek limit
0,00
0,05
0,10
0,15
0,20
0,25
0,30
0,35
z

Emission Site from Gamma-ray Imaging

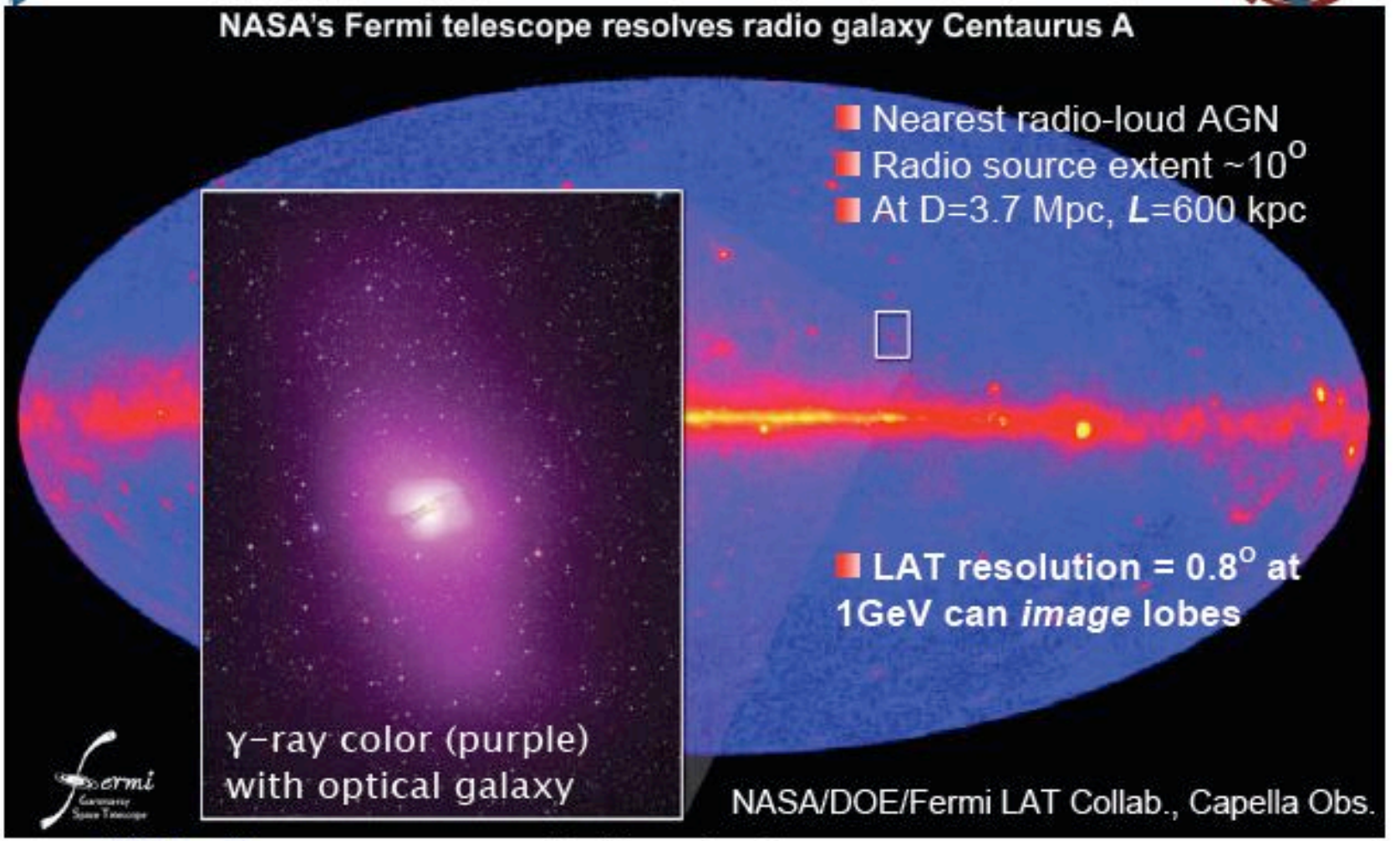

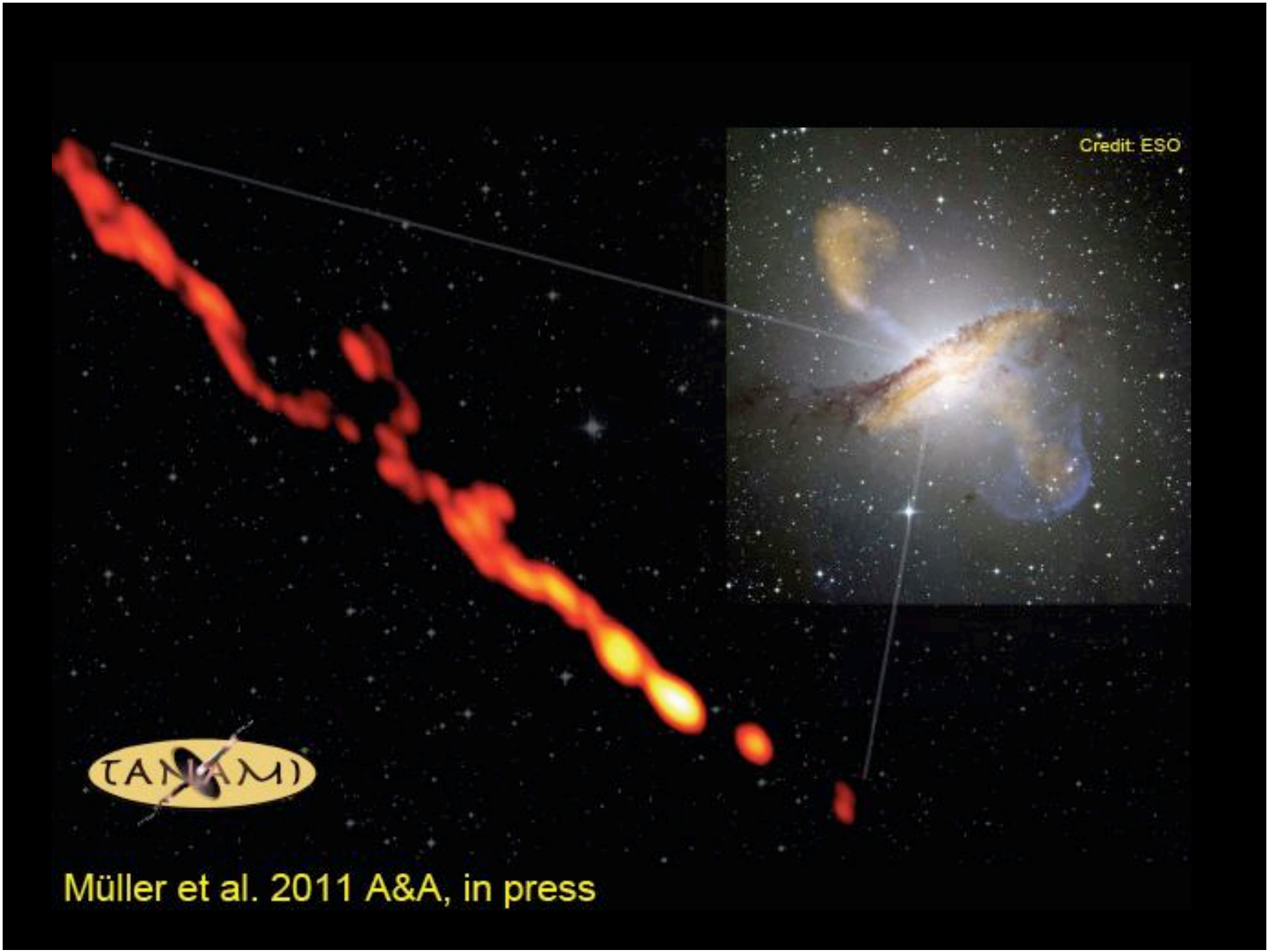
Credit: ESO
TANAMI
Müller et al. 2011 A&A, in press

Emission Site from Gamma-ray Imaging

Over ½ of the total >100 MeV observed LAT flux in the lobes

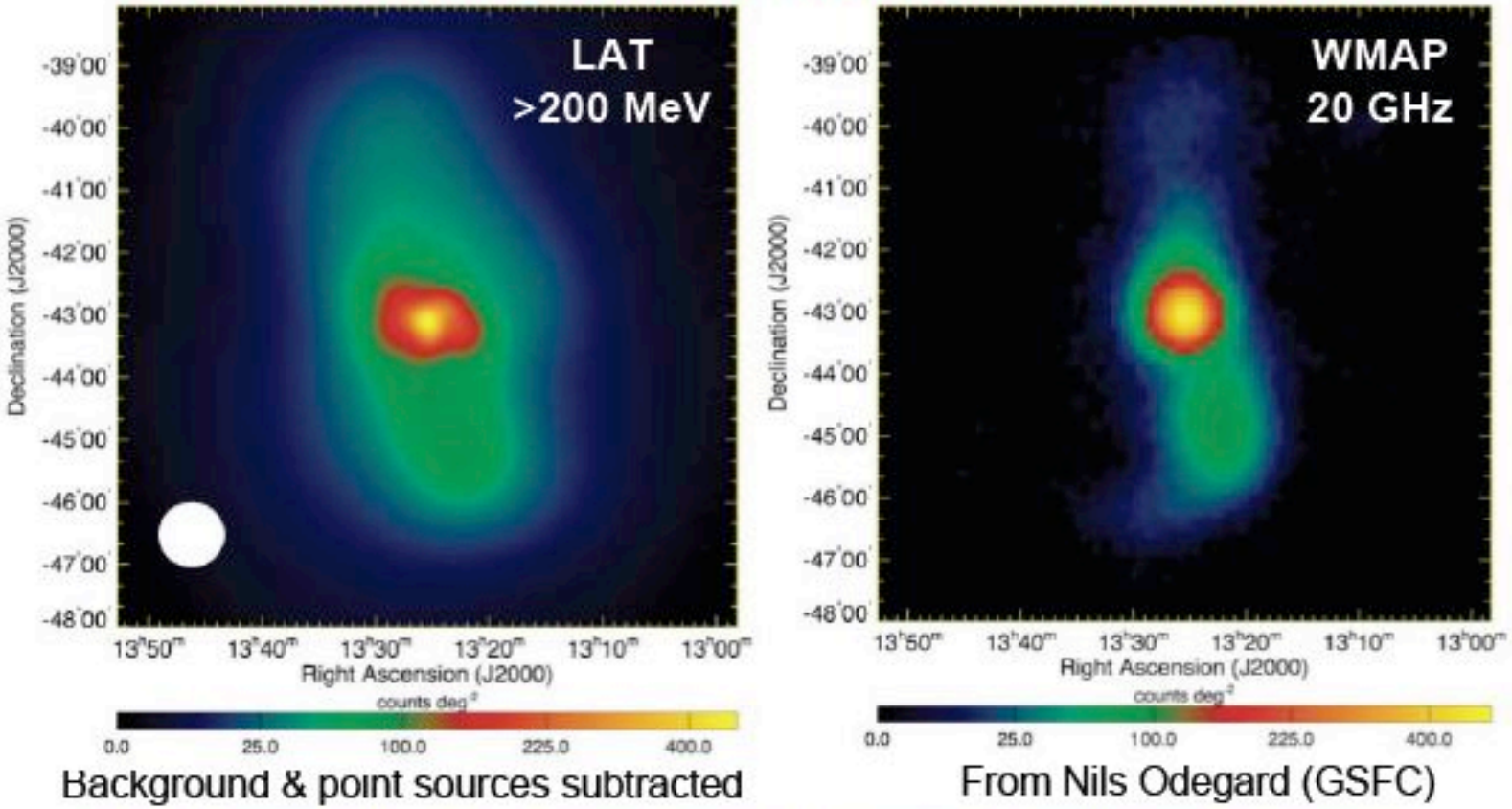

Background & point sources subtracted

From Nils Odegard (GSFC)

2010 Science, 328, 725; Leads: Cheung, Fukazawa, Knodlseder, Stawarz

Imaging Inverse Compton γ-ray Emission

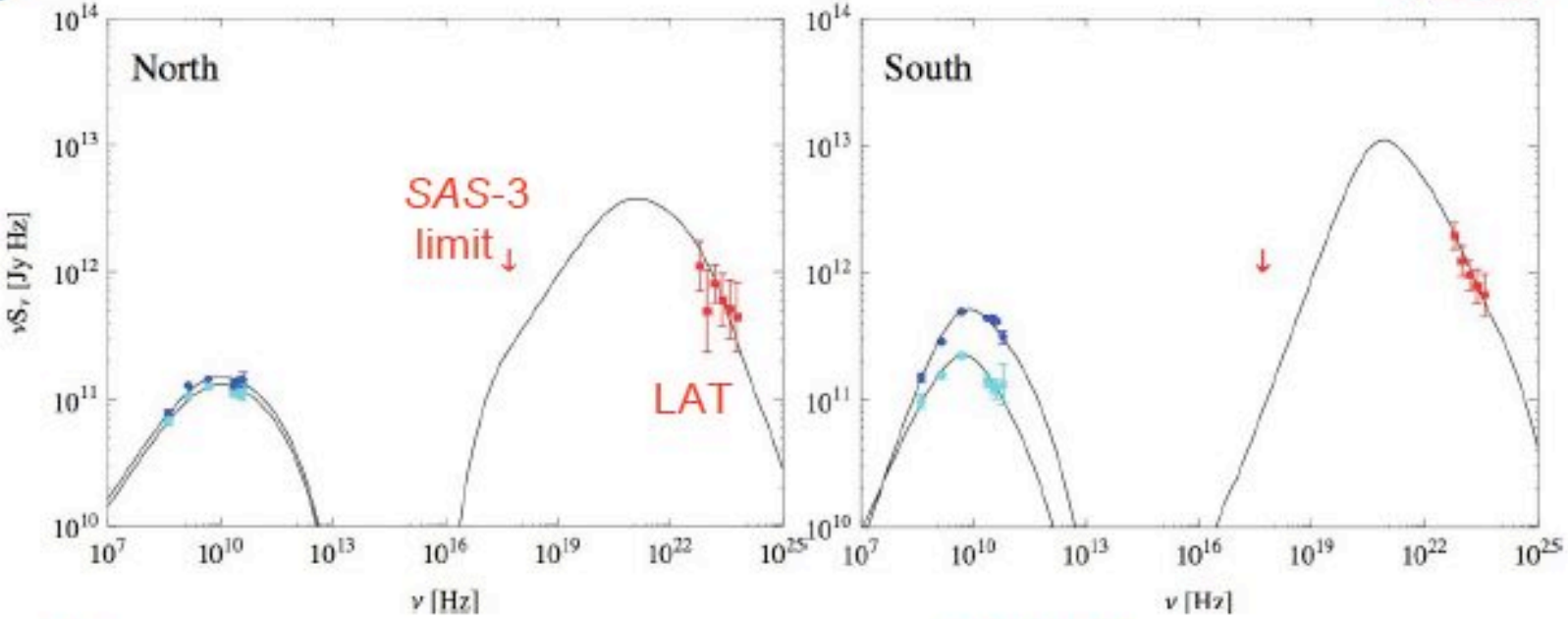

- IC (CMB+EBL) origin of LAT emission with **B ~ 1 μG** in both lobes, near equipartition
- IC component dominant, U_{CMB}/U_B ~ **10** -- 'requires' the lower *B*-field in Cen A lobes than typical in other (more powerful) examples
- Predictions for hard X-ray emission, but not yet detected by INTEGRAL (Beckmann et al. arXiv:1104.4253)

microquasars

Galactic micro-quasars

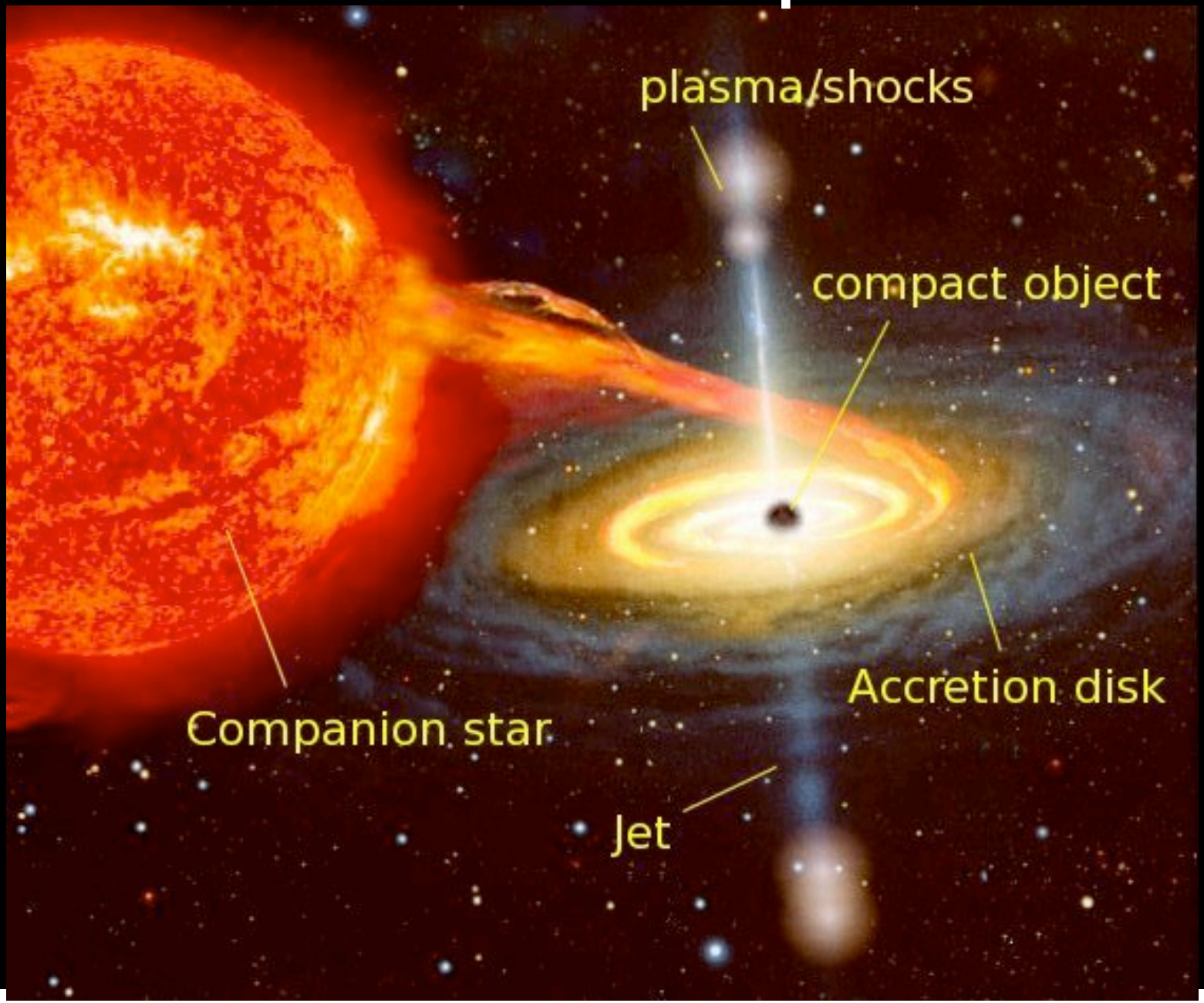

Galactic “Micro-Quasar” GRS 1915+105

(Mirabel & Rodriguez, Nature, 371, 46 (1994)

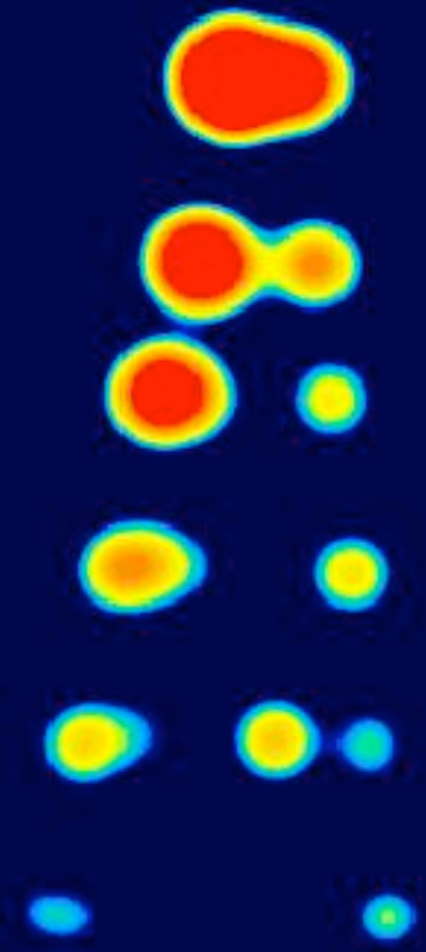

Micro-Quasar GRS 1915+105

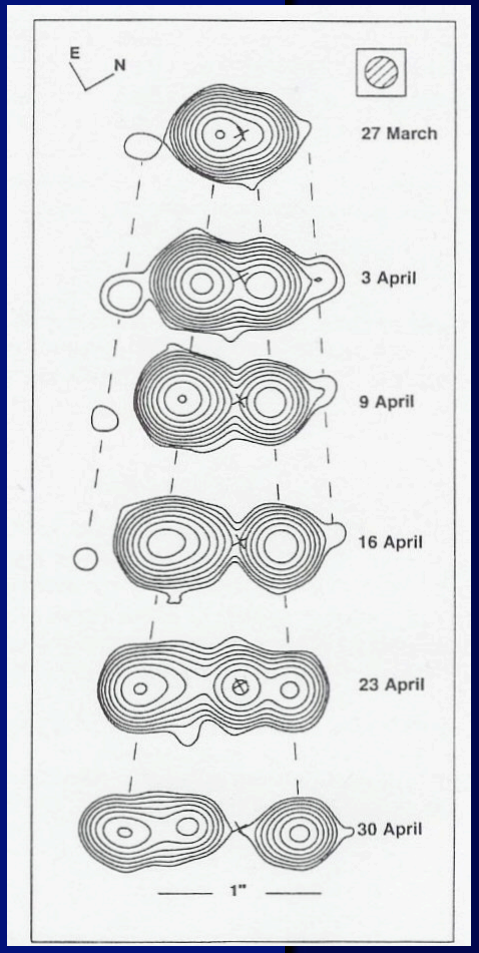

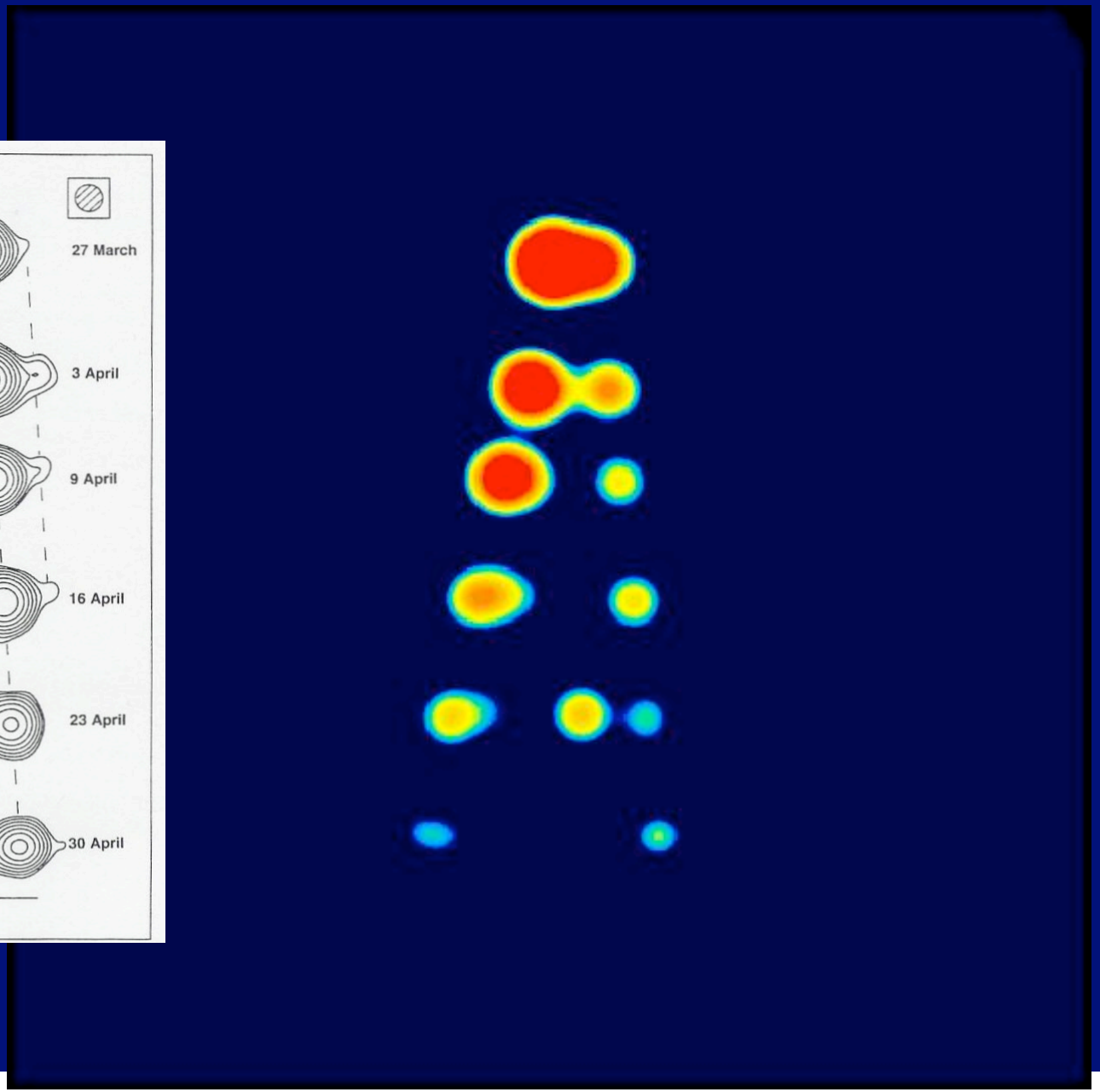

Galactic "Micro-quasars"

	Θ (degrees)	β	Γ	L_X/L_E	γ/GeV
Cyg X-1	?	?	?	0.1-1	?
Cyg X-3	< 14	> 0.8	> 1.6	0.1-1	YES
SS 433	80	0.26	1.03	0.01	no
GRS 1915+104	70	0.92	25	0.1-1	no
GRO J1655-40	> 70	0.9	2.5	1	no
GRS 1758-258	?			0.1-1	no
XTE J1550-564	60-70	> 0.8	1.5	0.1-1	no
Sco X-1	> 70	> 0.8	> 1.6	0.1-1	no
LS I 61 303	?	?	?	10^{-4}	yes
LS 5039	< 80	> 0.2	?	10^{-4}	yes

Relativistic jets from Cyg X-3

(Mioduszewski, Rupen, Hjellming, Pooley, Waltman, 2001)

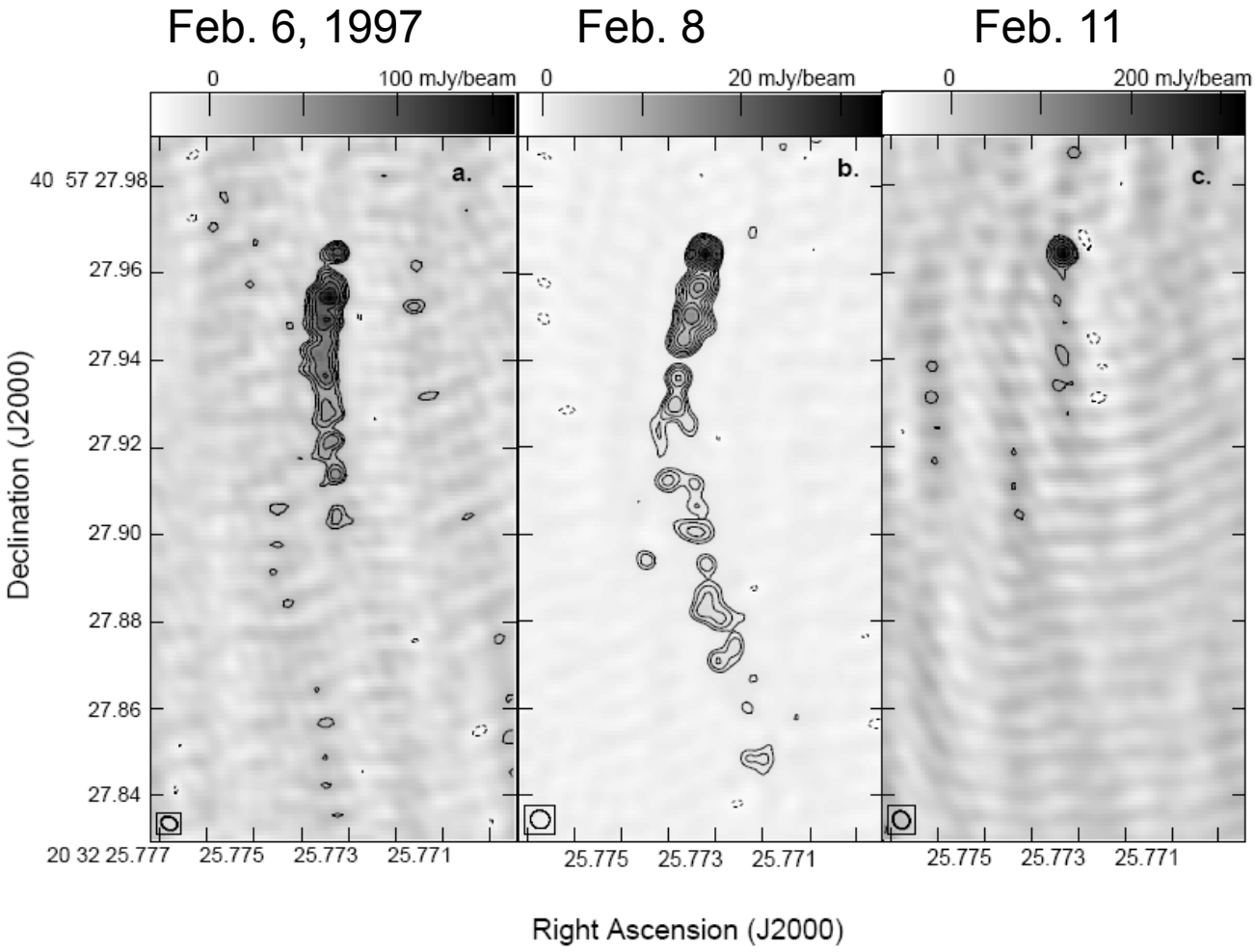

CYGNUS X-3 spectral states

(Koljionen et al., 2010 Szostek, Zdziarski, Mc Collough et al., 2008)

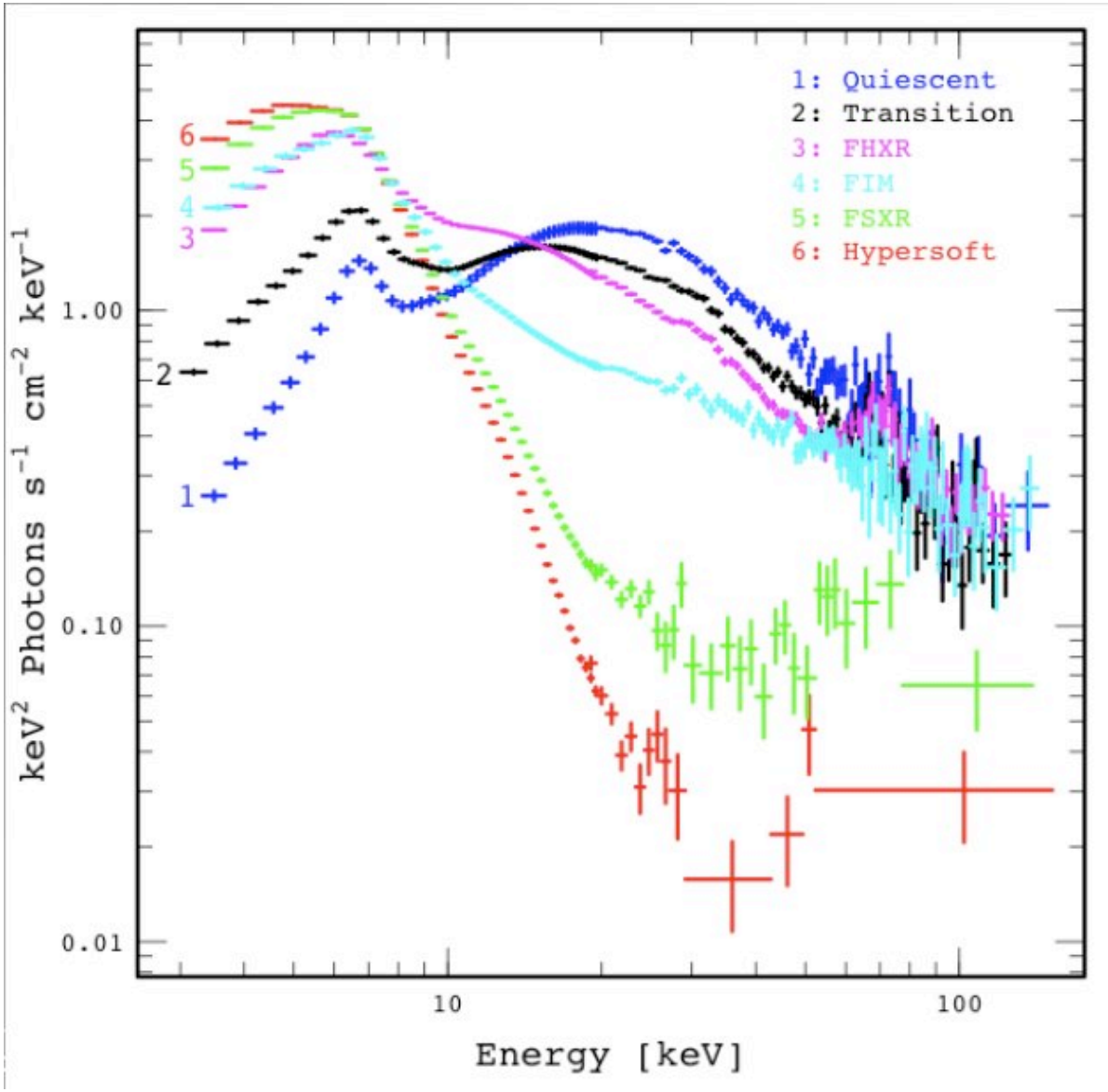

AGILE discovery of transient gamma-ray emission from Cygnus X-3 (*Nature*, 462, 620, 2009)

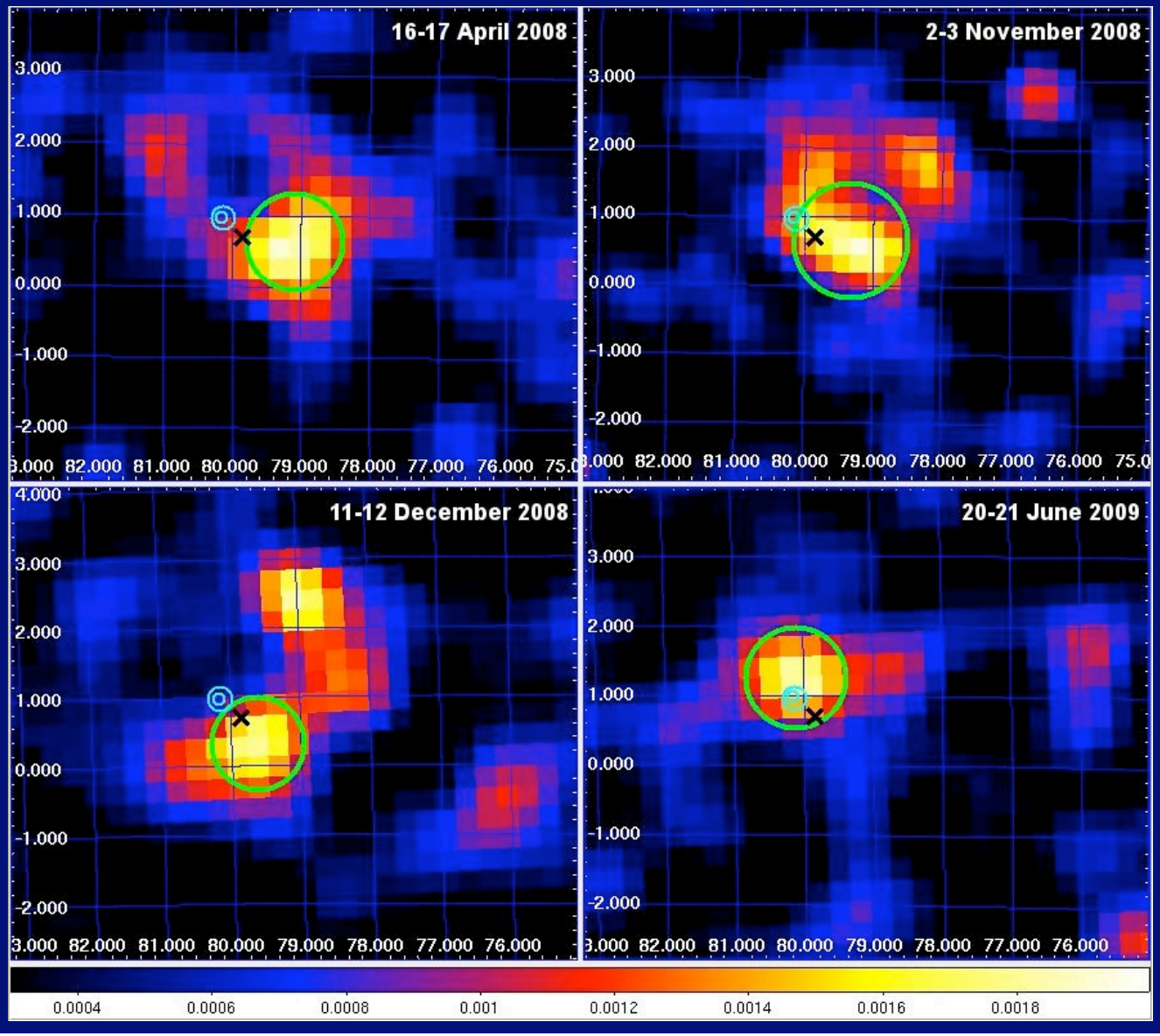

Cyg X-3 gamma-ray flares anticorrelated with hard X-rays

Plasma diagnostics with hard X-rays: acceleration with gamma-rays

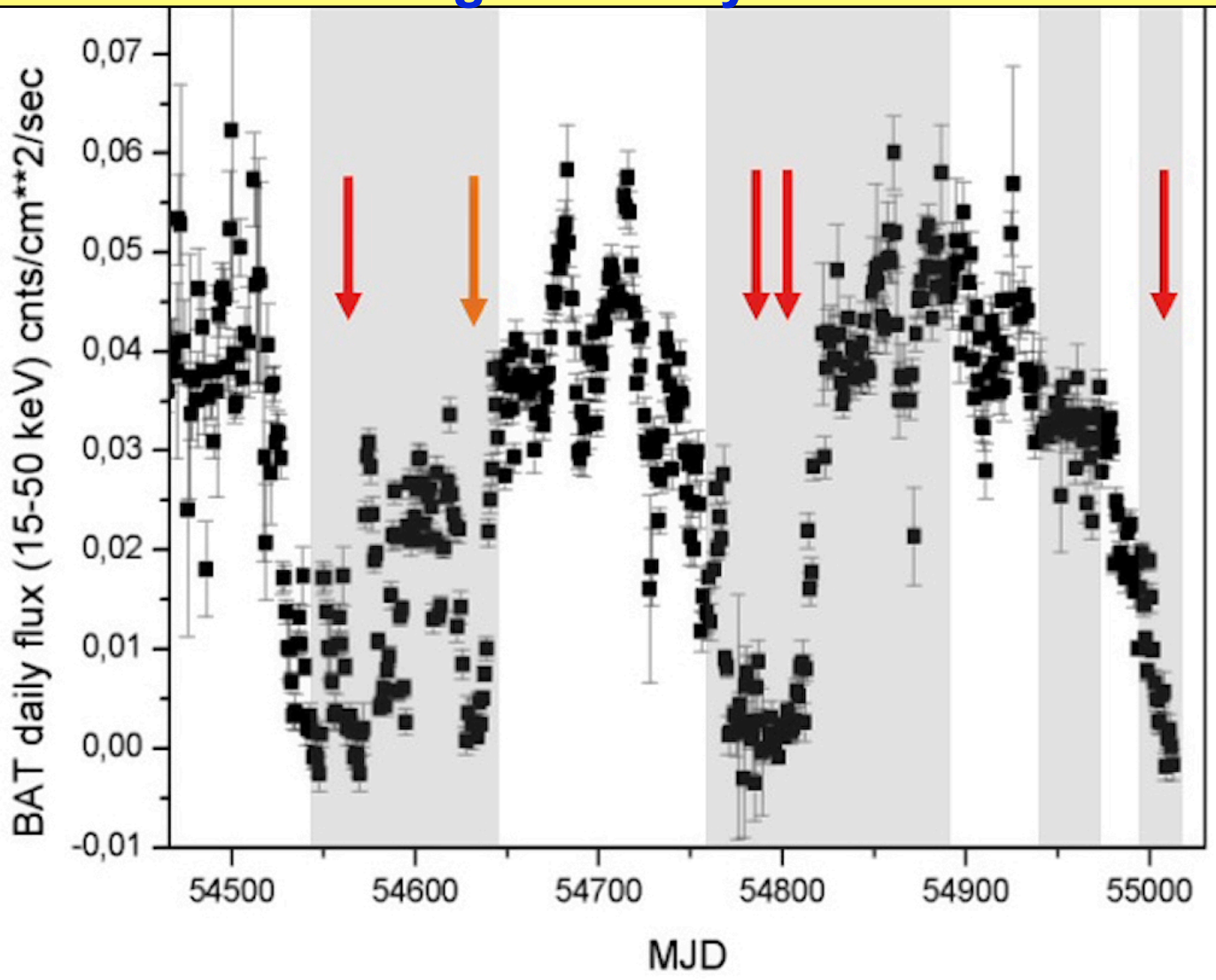

Plasma diagnostics (and acceleration) around a BH

Compton-thick cloud, $\tau = \sigma_T\, n\, R \sim 1\text{-}10$ $\quad n \sim (10^{15}\ \mathrm{cm}^{-3})\ R_8^{-1}$

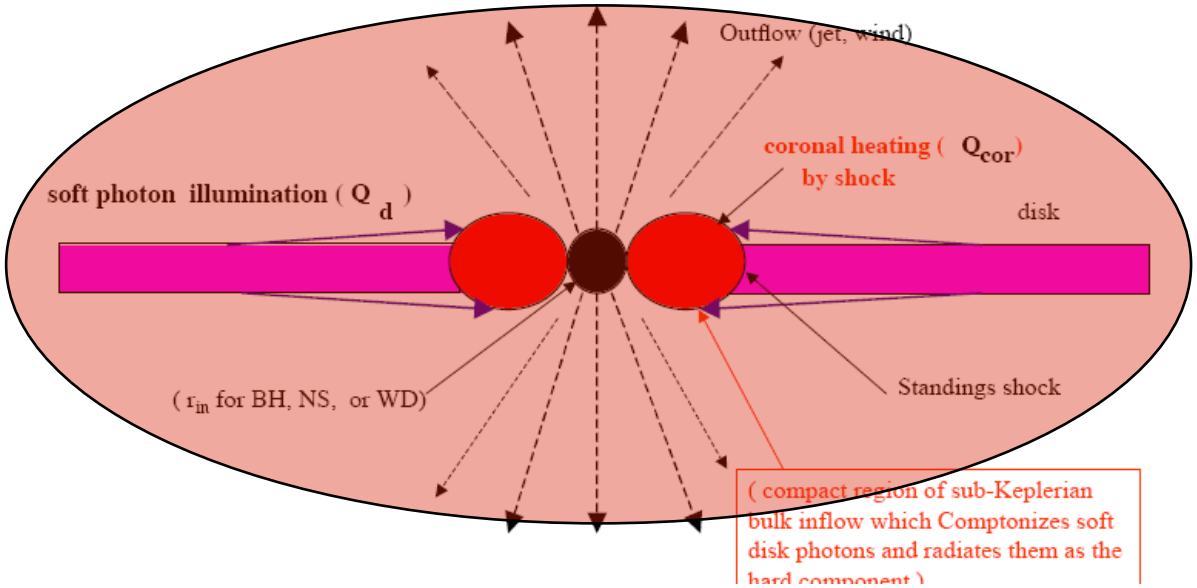

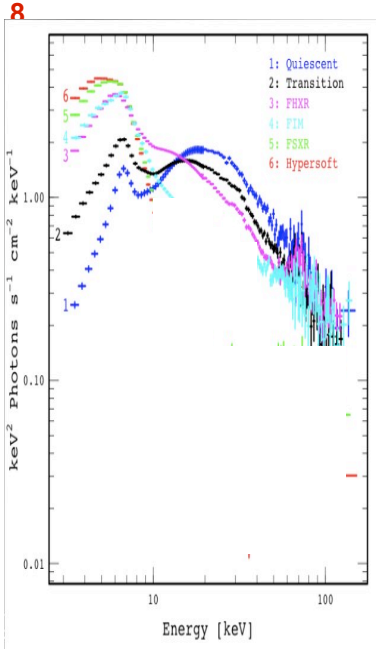

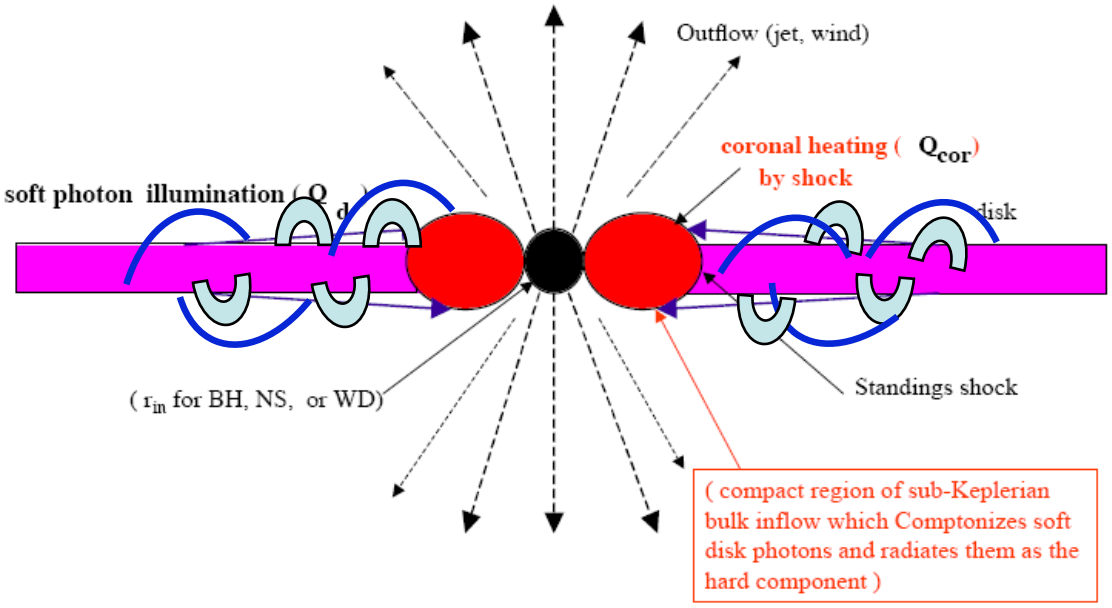

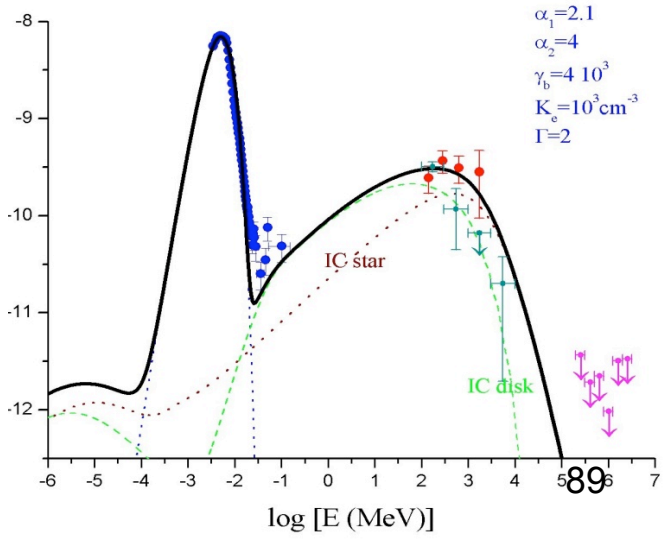

RATAN Obs. (S. Truskhin et al.) Apr. 13 – Apr. 27, 2008

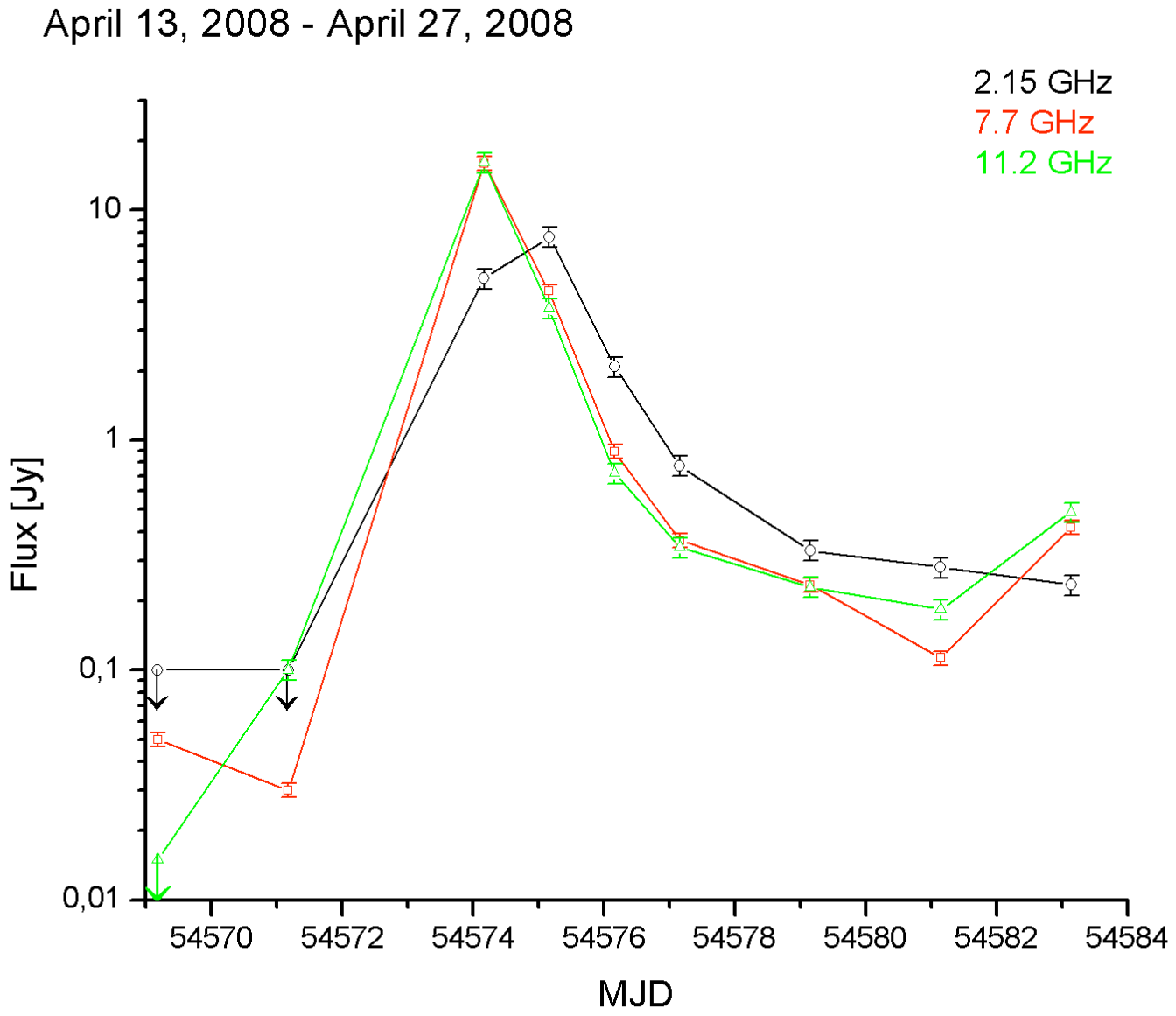

very strong radio flare, presumably with jet ejection

strong gamma-ray flare

X-ray (1-10 keV) flare

Hard X-ray flux state change (Super-A monitoring)

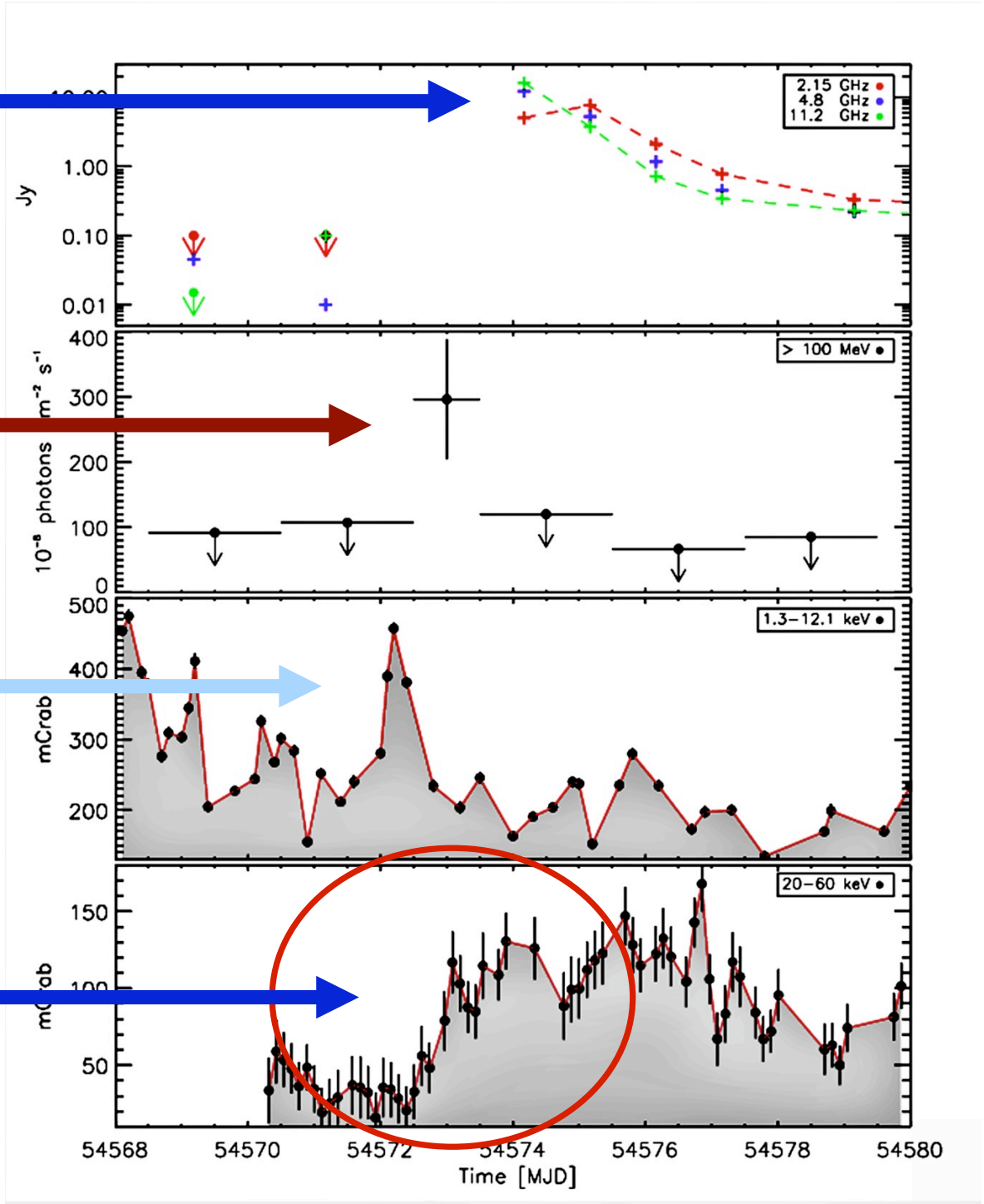

Major gamma-ray flares in special transitional states in preparation of radio flares ! (Tavani etal. Nature 2009)

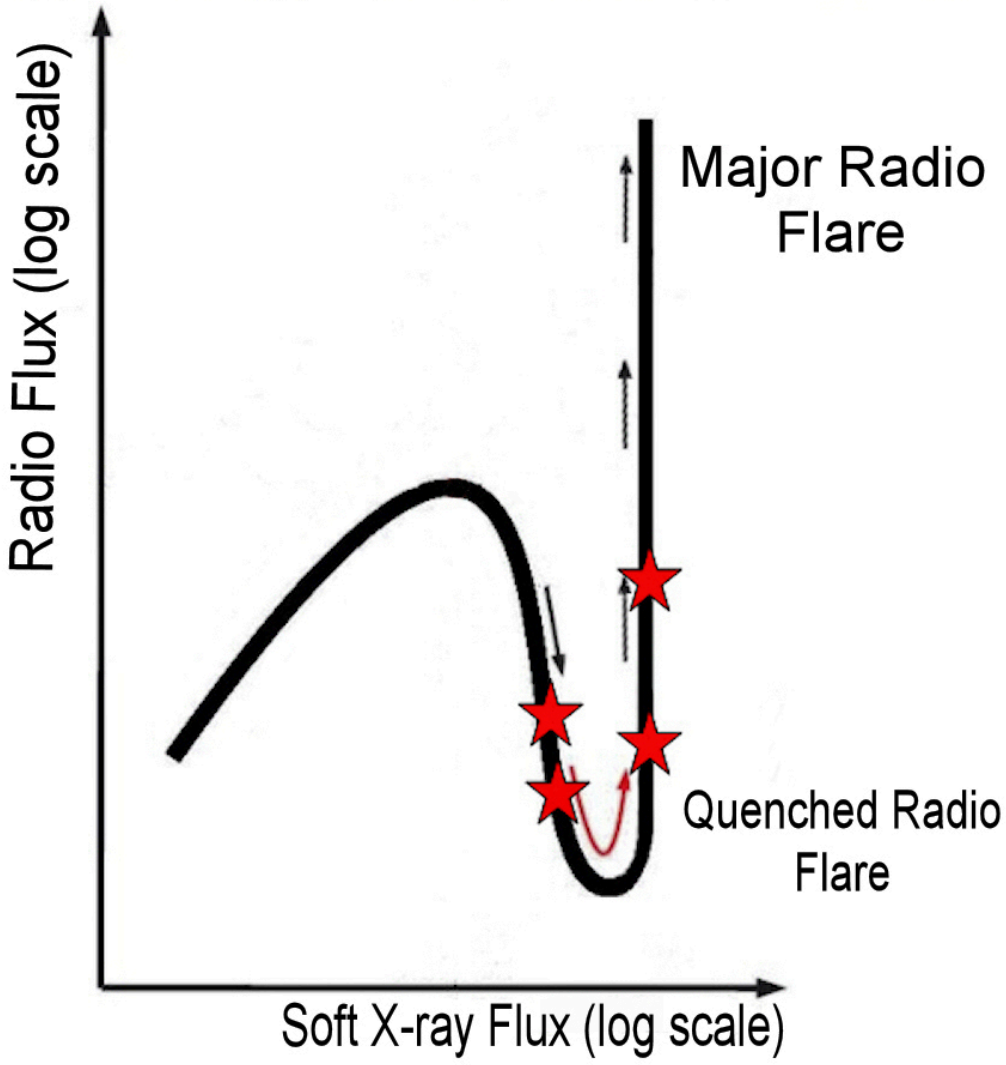

figure adapted from Szostek Zdziarski & McCollough (2008)

Plasma diagnostics in Cyg X-3

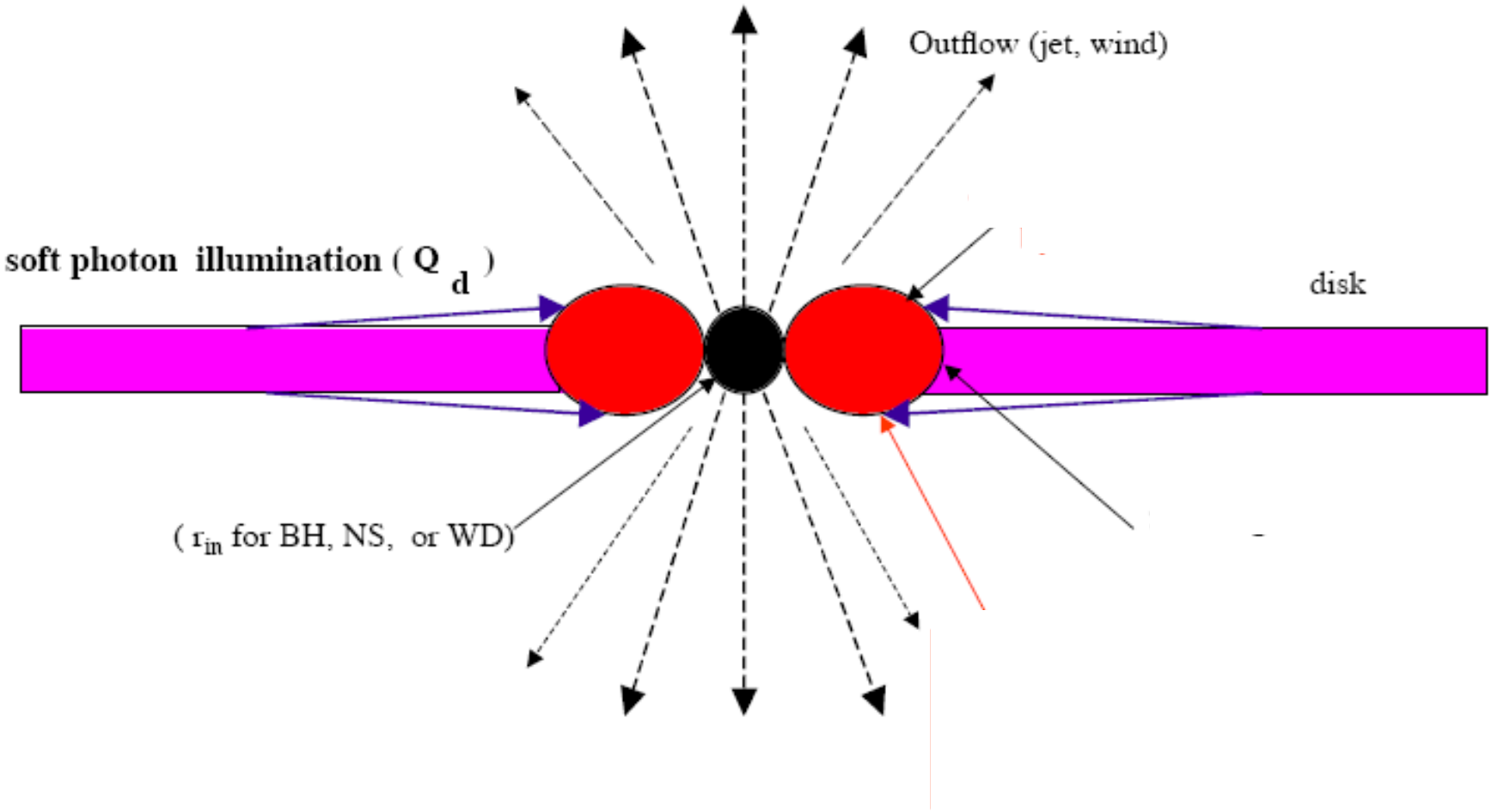

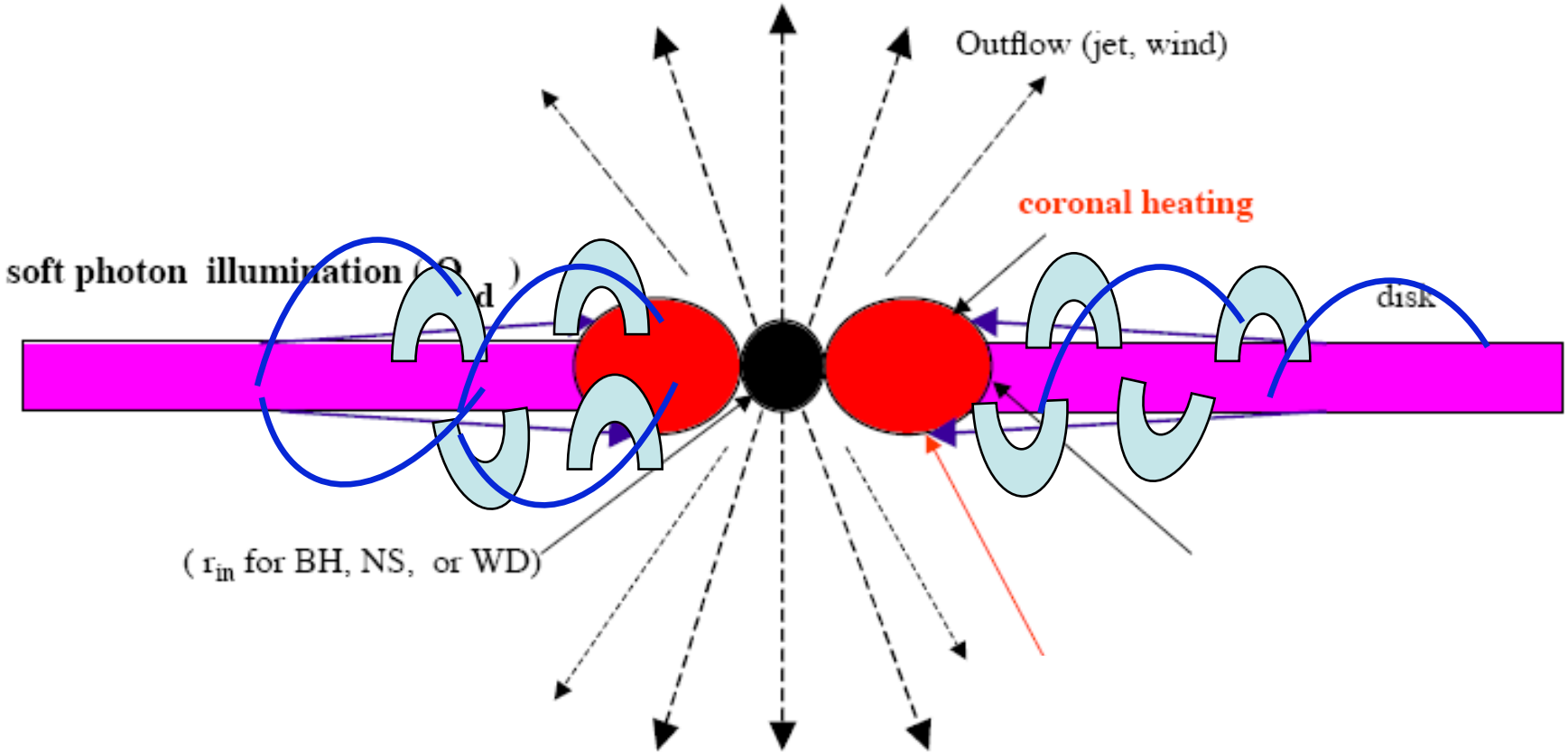
Outflow (jet, wind)
coronal heating
soft photon illumination (Θ_d)
disk
(r_{in} for BH, NS, or WD)

Comptonizing cloud

Compton-thick, $\tau = \sigma_T\, n\, R \sim 1\text{-}10$ $\qquad$ **$n \sim (10^{15}\ \mathrm{cm}^{-3})\ R_8^{-1}$**

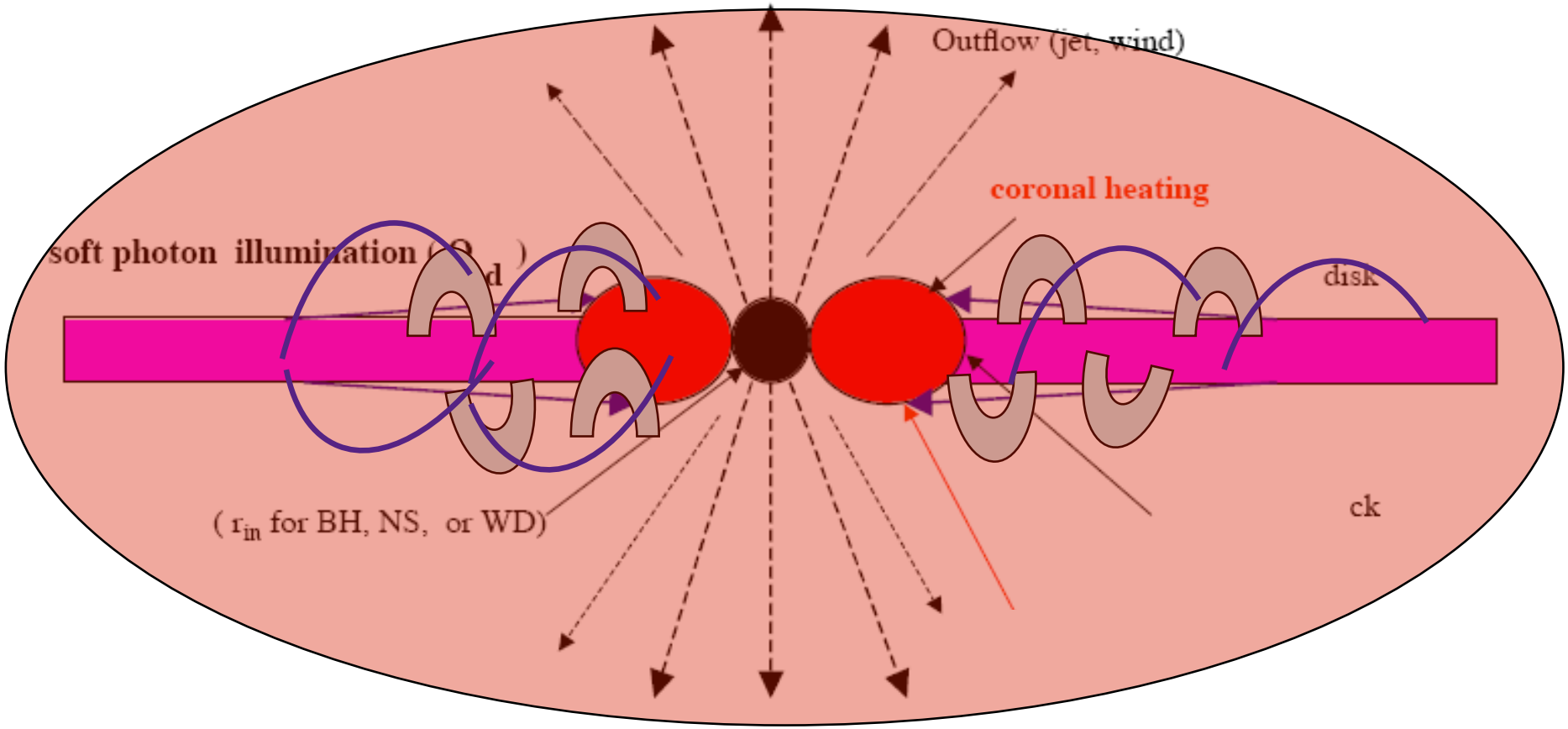

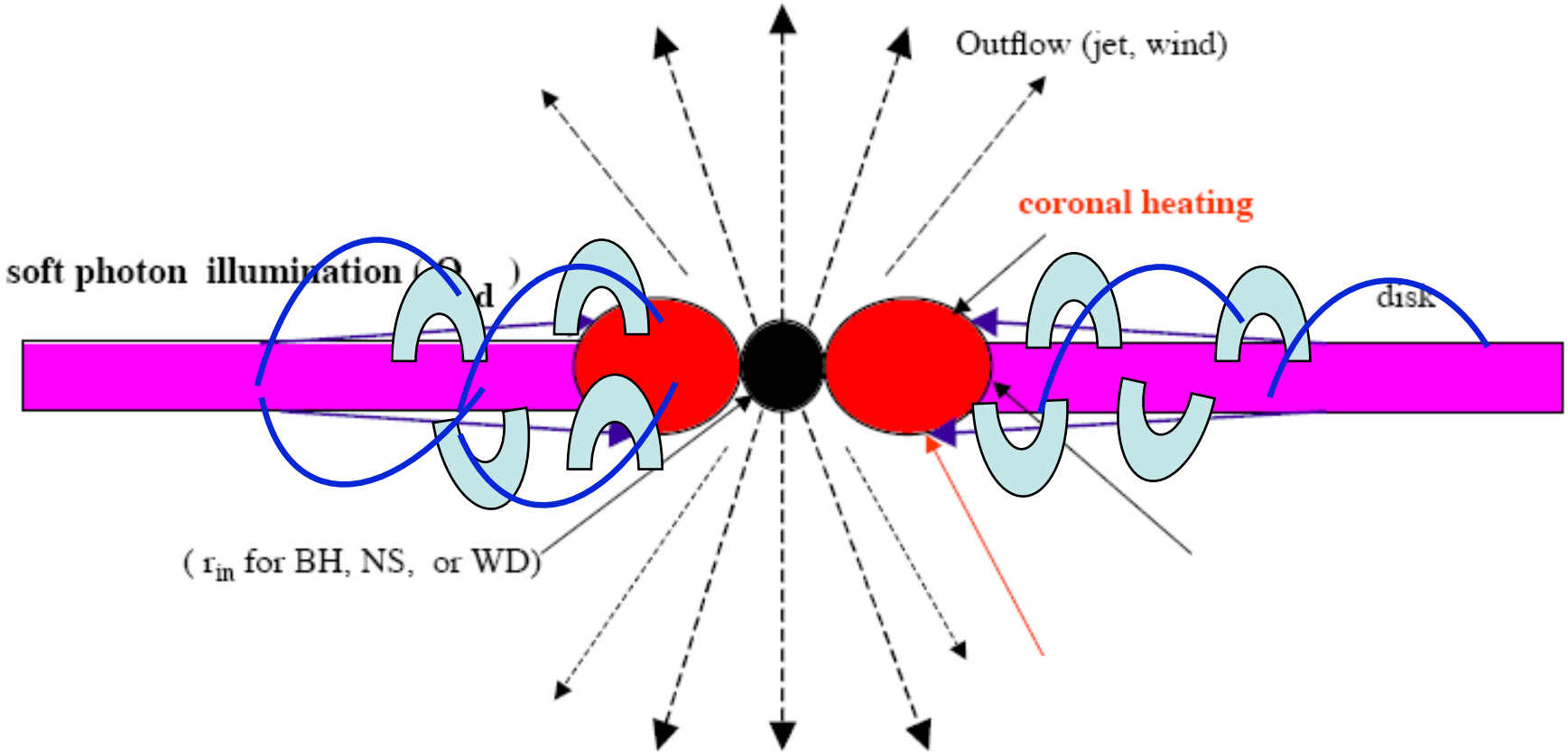
Outflow (jet, wind)
coronal heating
soft photon illumination (Θ_d)
disk
(r_{in} for BH, NS, or WD)

last pre-flare and major radio flare episode of Cyg X-3

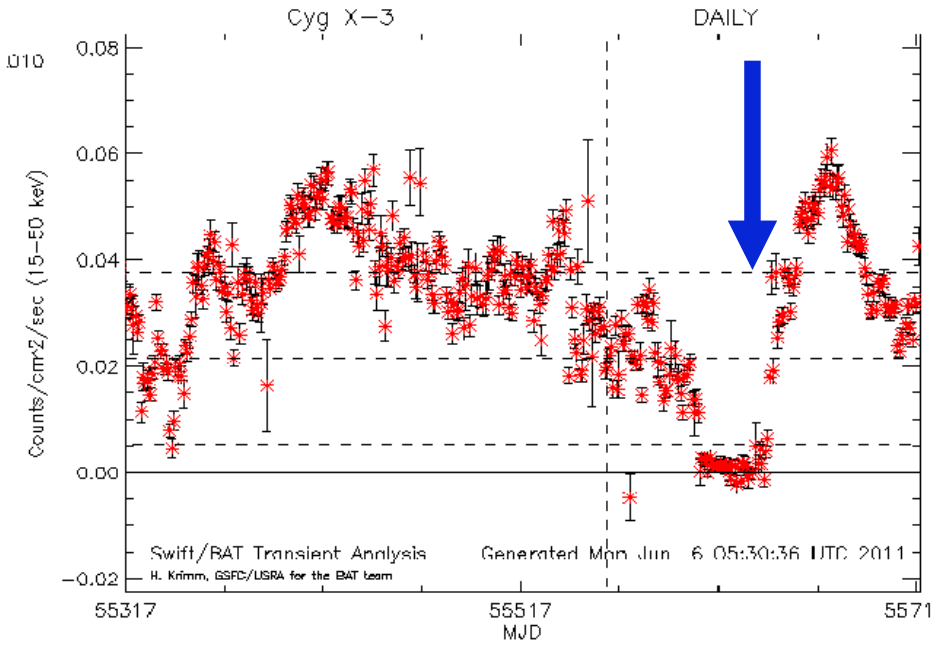

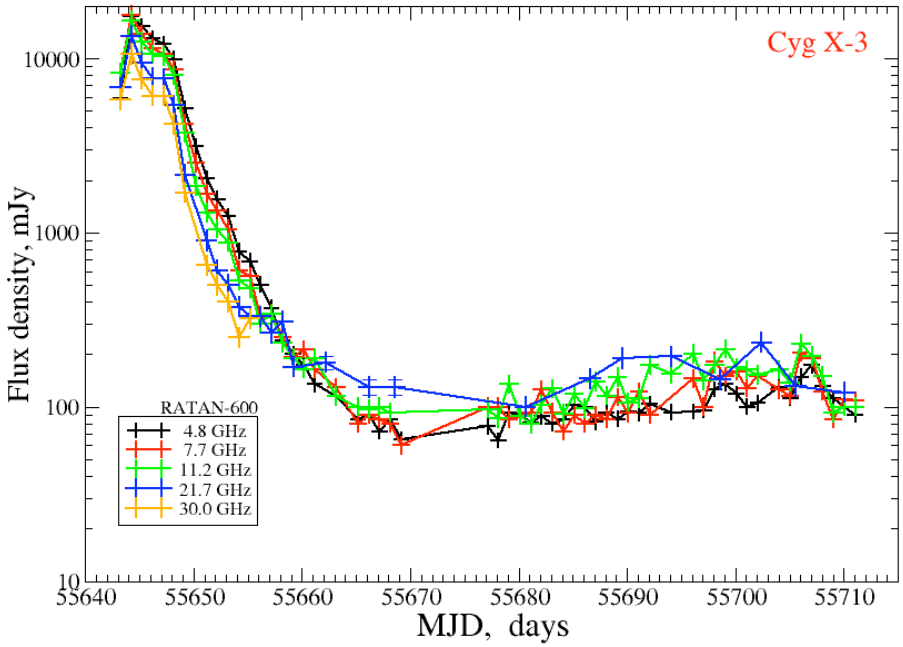

clear indication from Cyg X-3

- **particle acceleration preceding (1-2 days) jet launching**

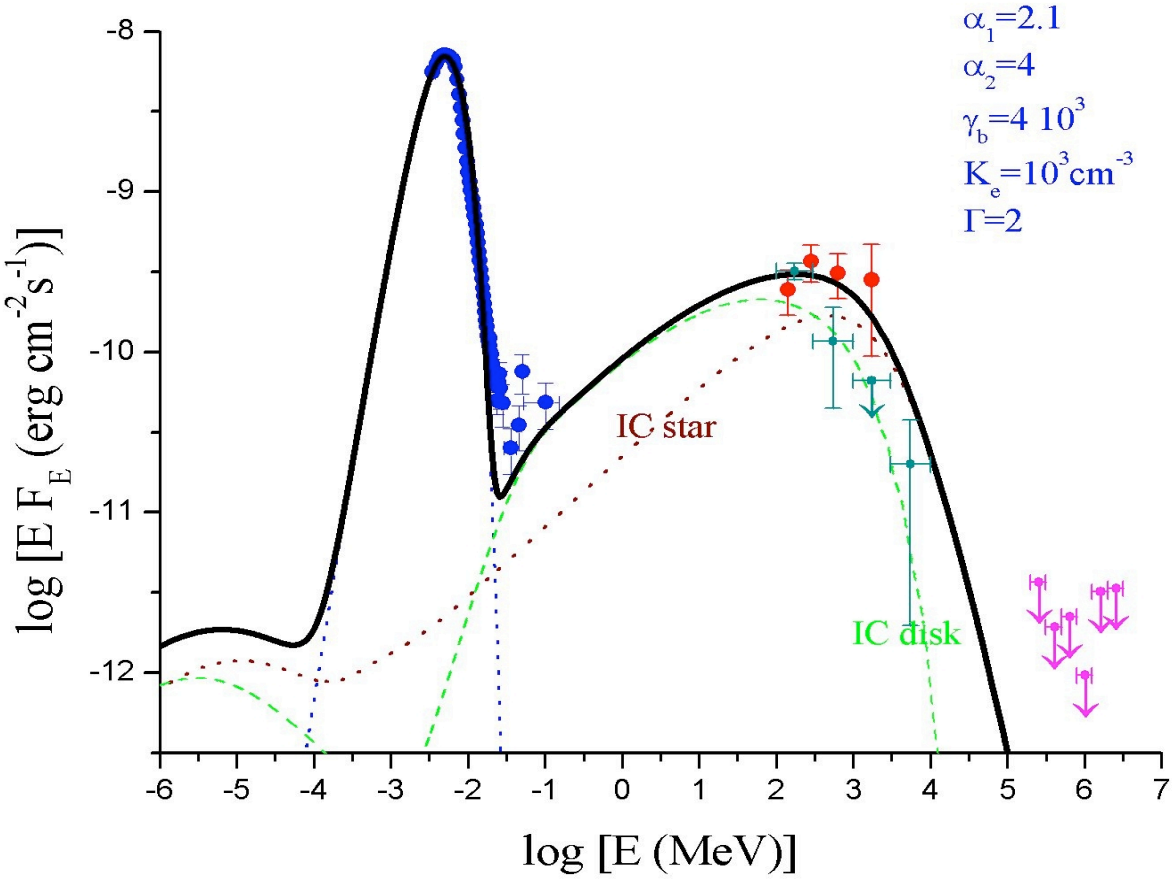

Piano, Vittorini, M.T., 2011

The puzzle of Galactic gamma-ray transients:

- GC region
- Cygnus region
- Carina region
- Crux region

- AGILE observes variability and detects new transients on time scales of 1 day at flux levels of 10^{-6} $cm^{-2}s^{-1}$, even in crowded, high diffuse emission Galactic plane regions.
- NO detectable simultaneous hard X-ray emission (F < 20-30 mCrab, 18-60 keV, 1-day integration)

Fermi-LAT detection of the symbiotic system V407 Cygni (March 2009) Abdo et al. Science 2010

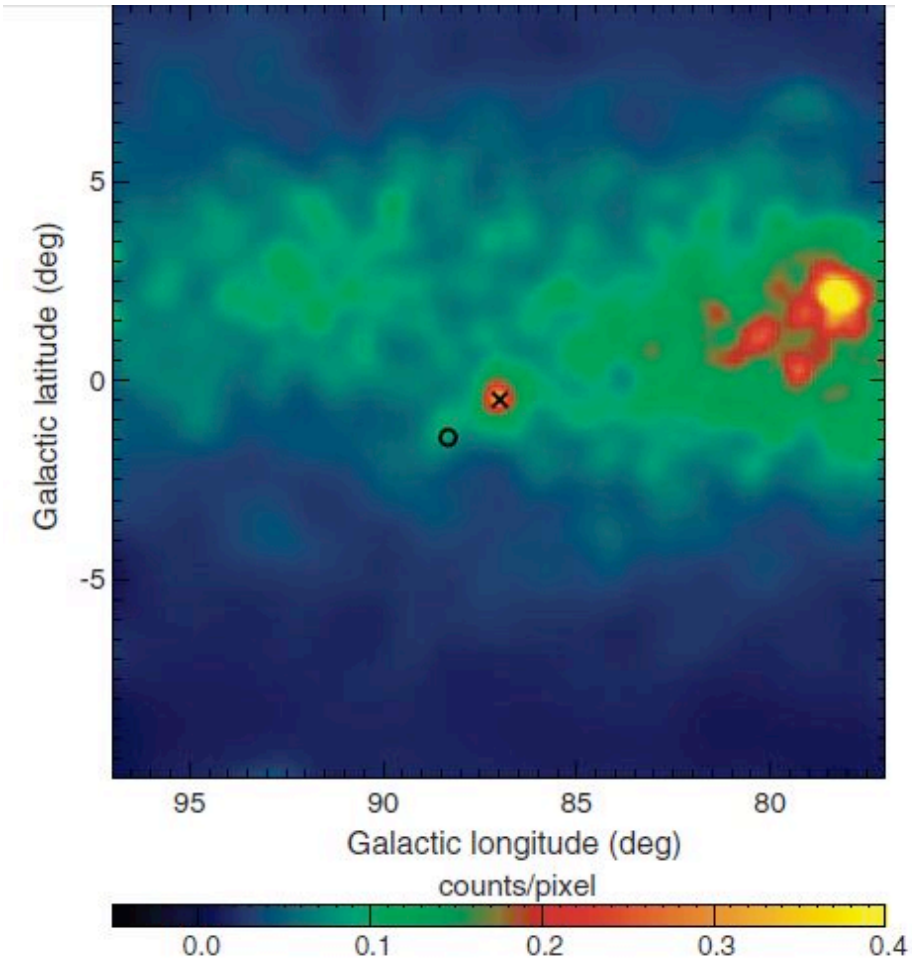

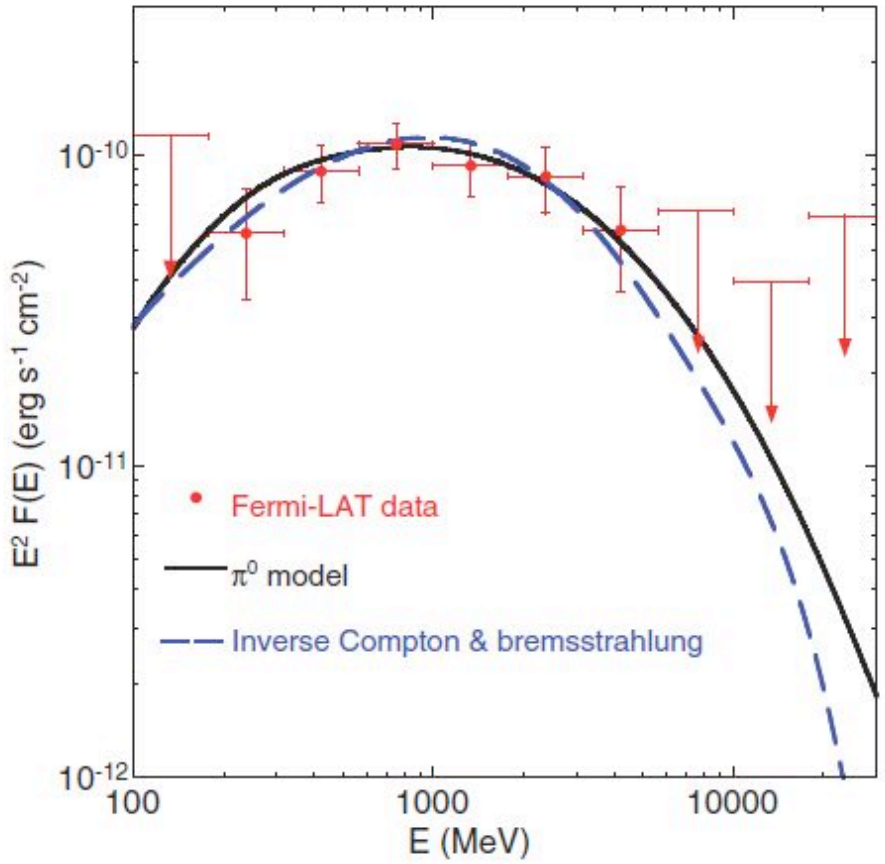

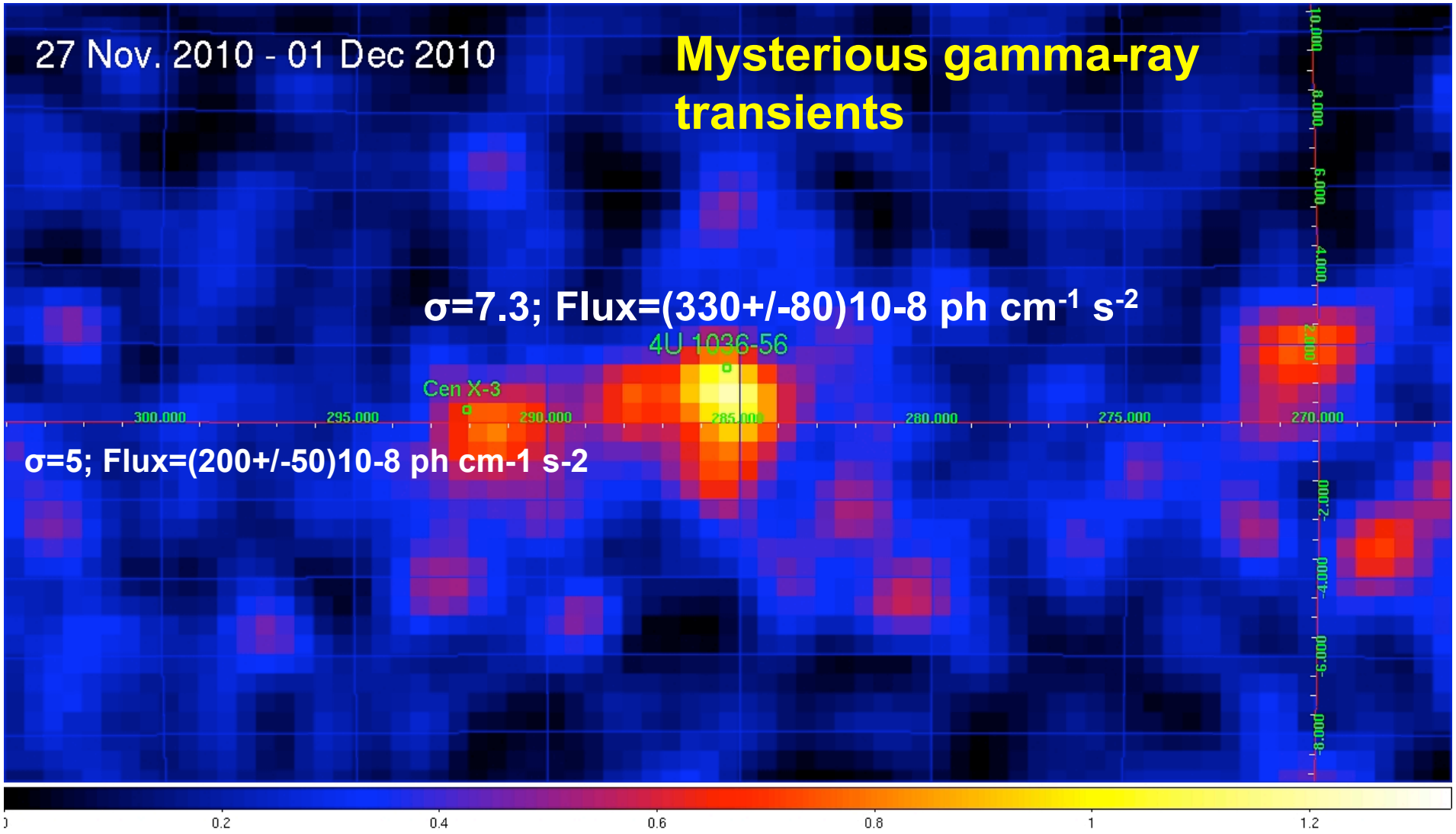

ATEL n. 3059, Bulgarelli et al., 30 Nov. 2010, 4-days integration

Crab Nebula

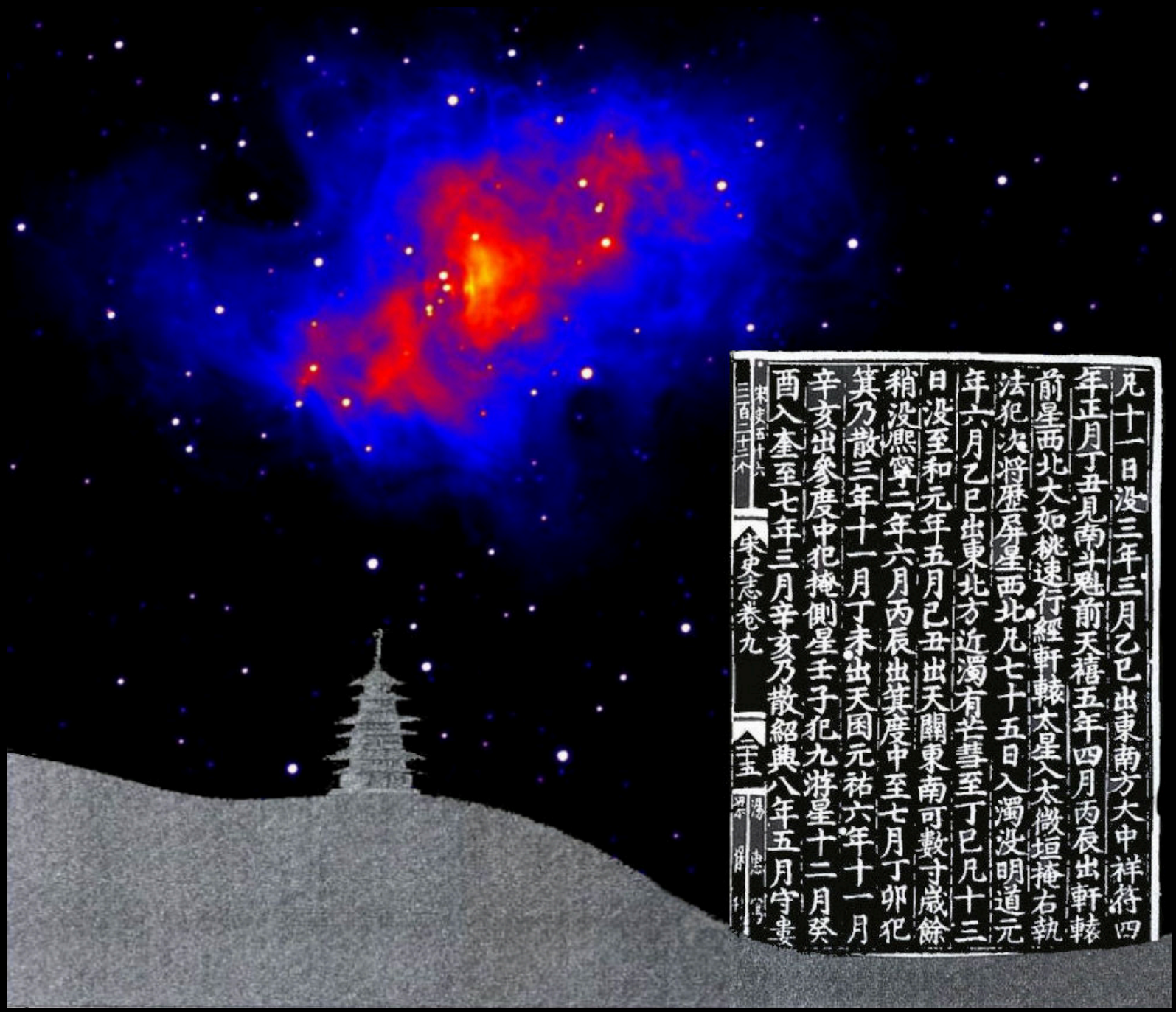

凡十一日没三年三月乙巳出東南方大中祥符四年正月丁丑見南斗魁前天禧五年四月丙辰出軒轅前星西北大如桃速行經軒轅太星入太微垣掩右執法犯次將歷屏星西北凡七十五日入濁没明道元年六月乙巳出東北方近濁有芒彗至丁巳凡十三日没至和元年五月己丑出天關東南可數寸歲餘稍没熙寧二年六月丙辰出其度中至七月丁卯犯箕乃散三年十一月丁未出天困元祐六年十一月辛亥出參度中犯掩側星壬子犯九游星十二月癸酉入奎至七年三月辛亥乃散紹興八年五月守婁

Crab Nebula (M1), named by William Parsons, Earl of Rosse (1844)

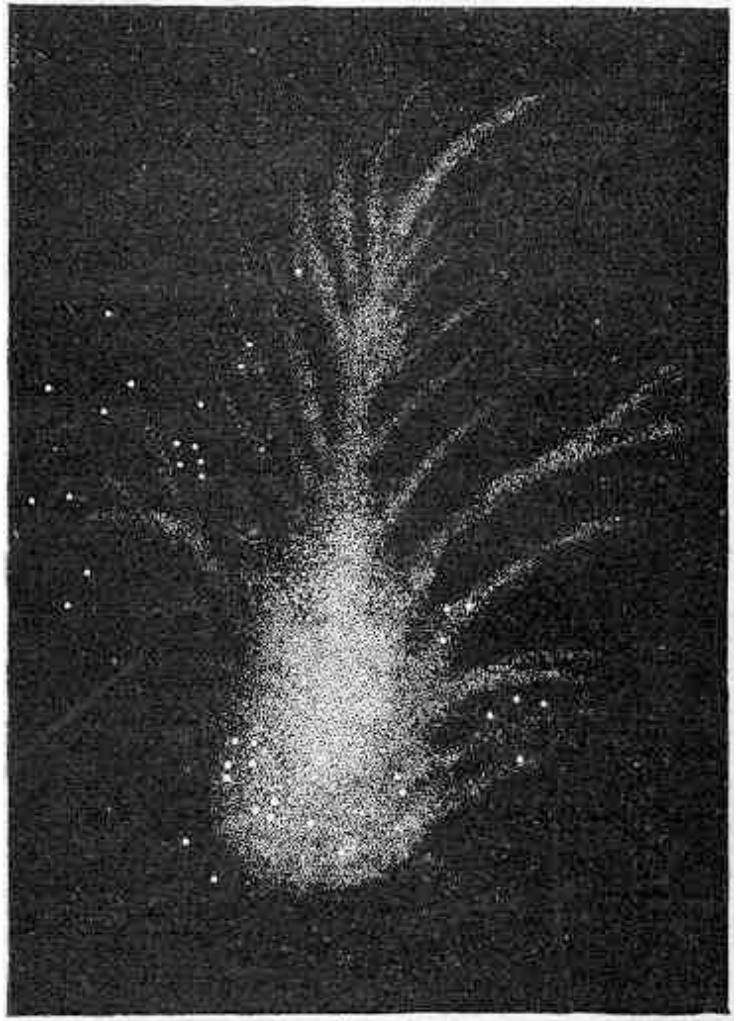

Fig. 438.

".. a cluster we perceive in this image. However, a considerable change of appearance; it is no longer an oval resolvable [mottled] Nebula; we see resolvable filaments singularly disposed, springing principally from its southern extremity, and not, as is usual in clusters, irregularly in all directions. Probably greater power would bring out other filaments, and it would then assume the ordinary form of a cluster. It is stubbed with stars, mixed however with a nebulosity probably consisting of stars too minute to be recognized. **It is an easy object,** and I have shown it to many, and all have been at once struck with its remarkable aspect. Everything in the sketch can be seen under moderately favourable circumstances."

Birr Castle, 36-inch reflector

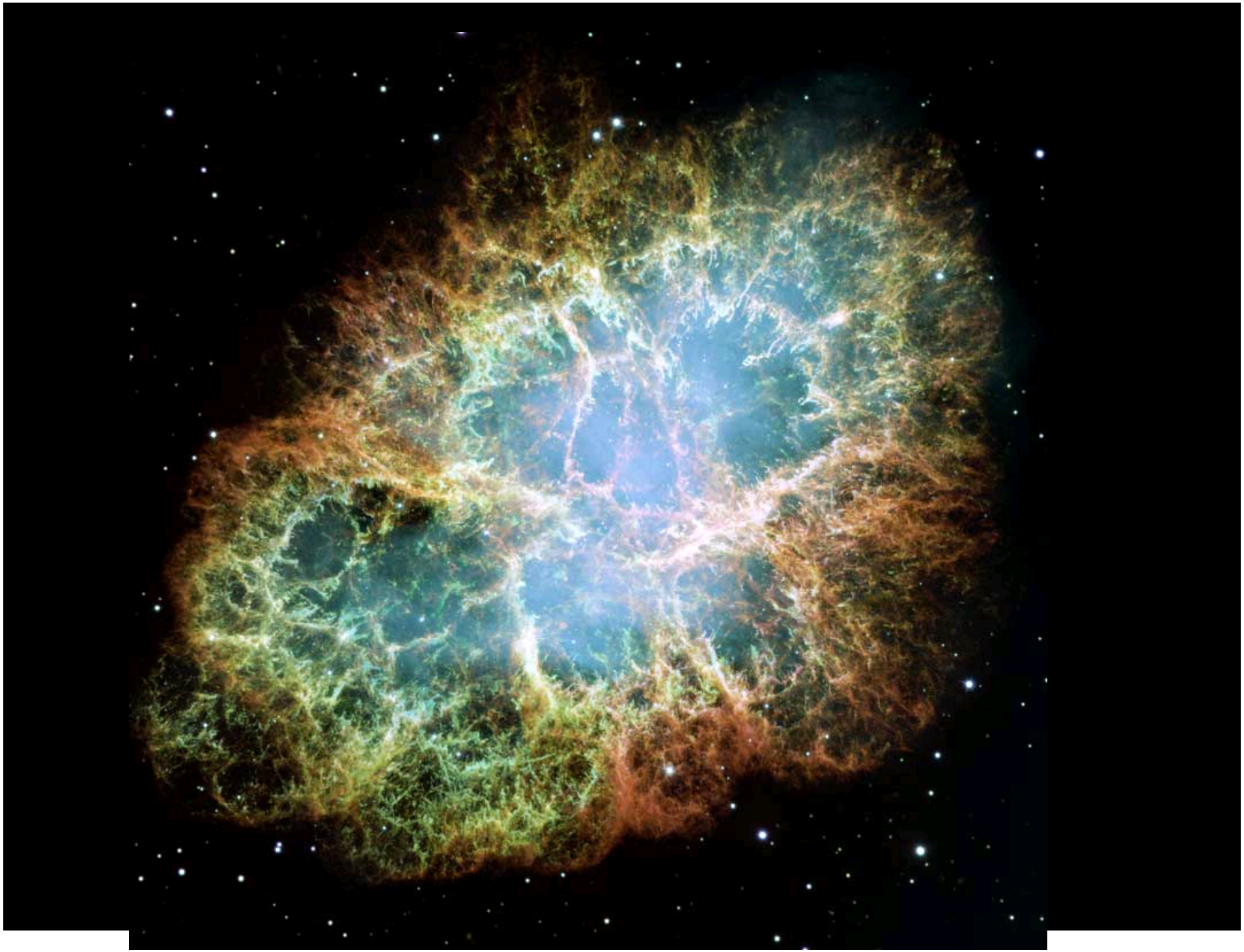

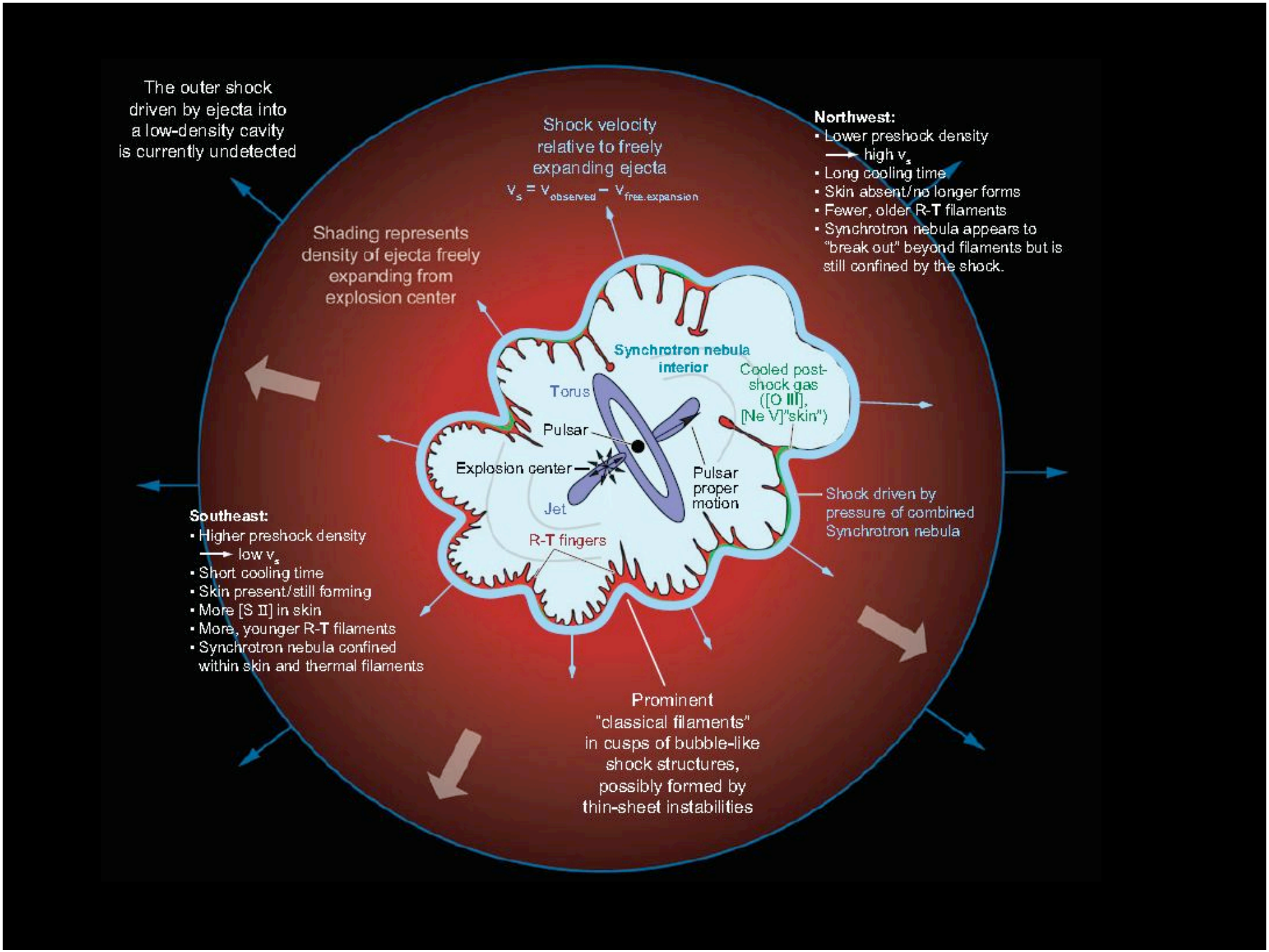
The outer shock driven by ejecta into a low-density cavity is currently undetected
Shock velocity relative to freely expanding ejecta
$v_s = v_{observed} - v_{free.expansion}$
Shading represents density of ejecta freely expanding from explosion center
Northwest:
• Lower preshock density → high v_s
• Long cooling time
• Skin absent/no longer forms
• Fewer, older R-T filaments
• Synchrotron nebula appears to "break out" beyond filaments but is still confined by the shock.
Synchrotron nebula interior
Cooled post-shock gas ([O III], [Ne V]"skin")
Torus
Pulsar
Explosion center
Pulsar proper motion
Jet
R-T fingers
Shock driven by pressure of combined Synchrotron nebula
Southeast:
• Higher preshock density → low v_s
• Short cooling time
• Skin present/still forming
• More [S II] in skin
• More, younger R-T filaments
• Synchrotron nebula confined within skin and thermal filaments
Prominent "classical filaments" in cusps of bubble-like shock structures, possibly formed by thin-sheet instabilities

The Crab Nebula: the best accelerator

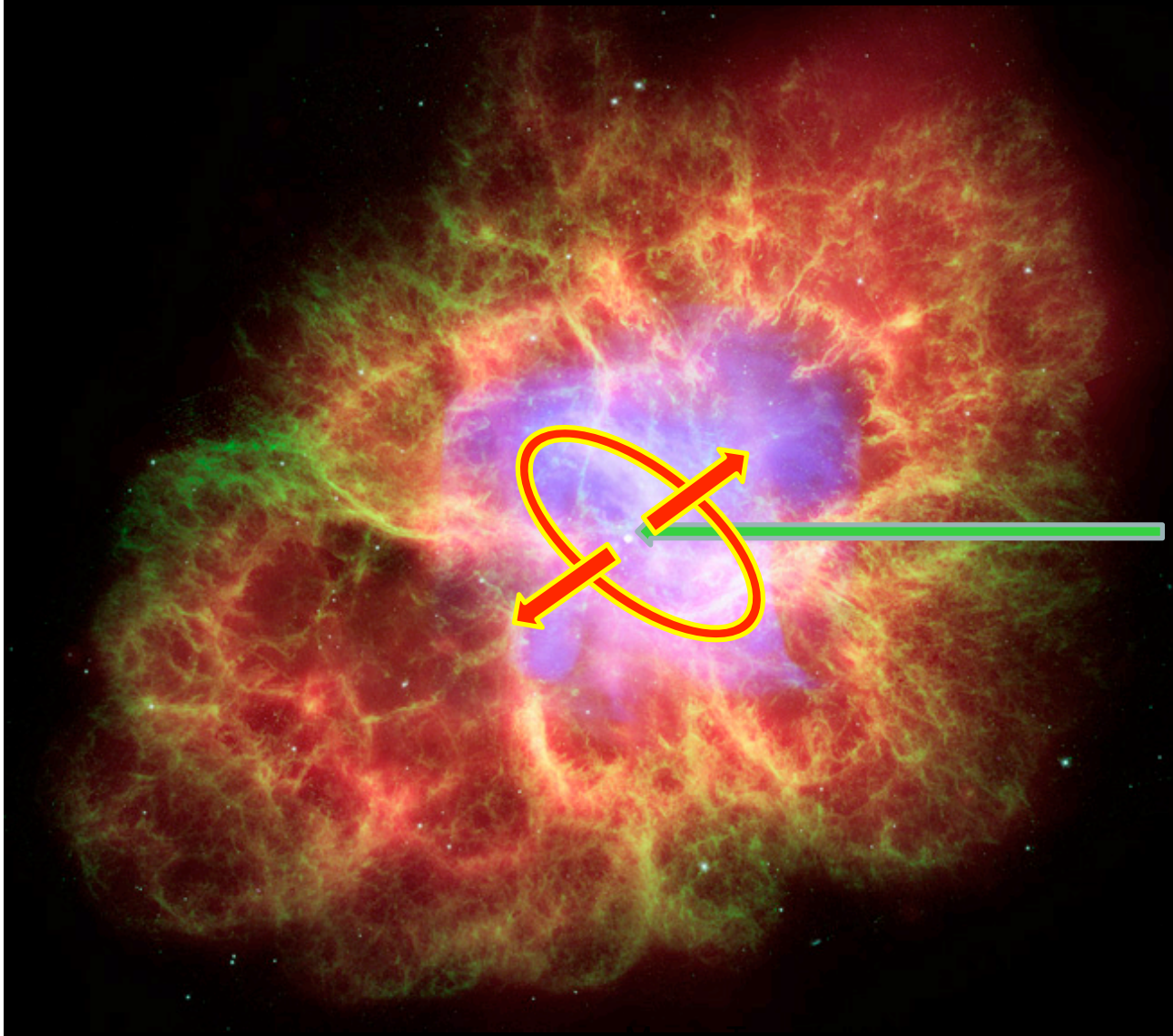

POWERFUL PULSAR
(rotating 30 times a second)

NEBULA SHOCKED BY THE PULSAR WIND

Crab Nebula

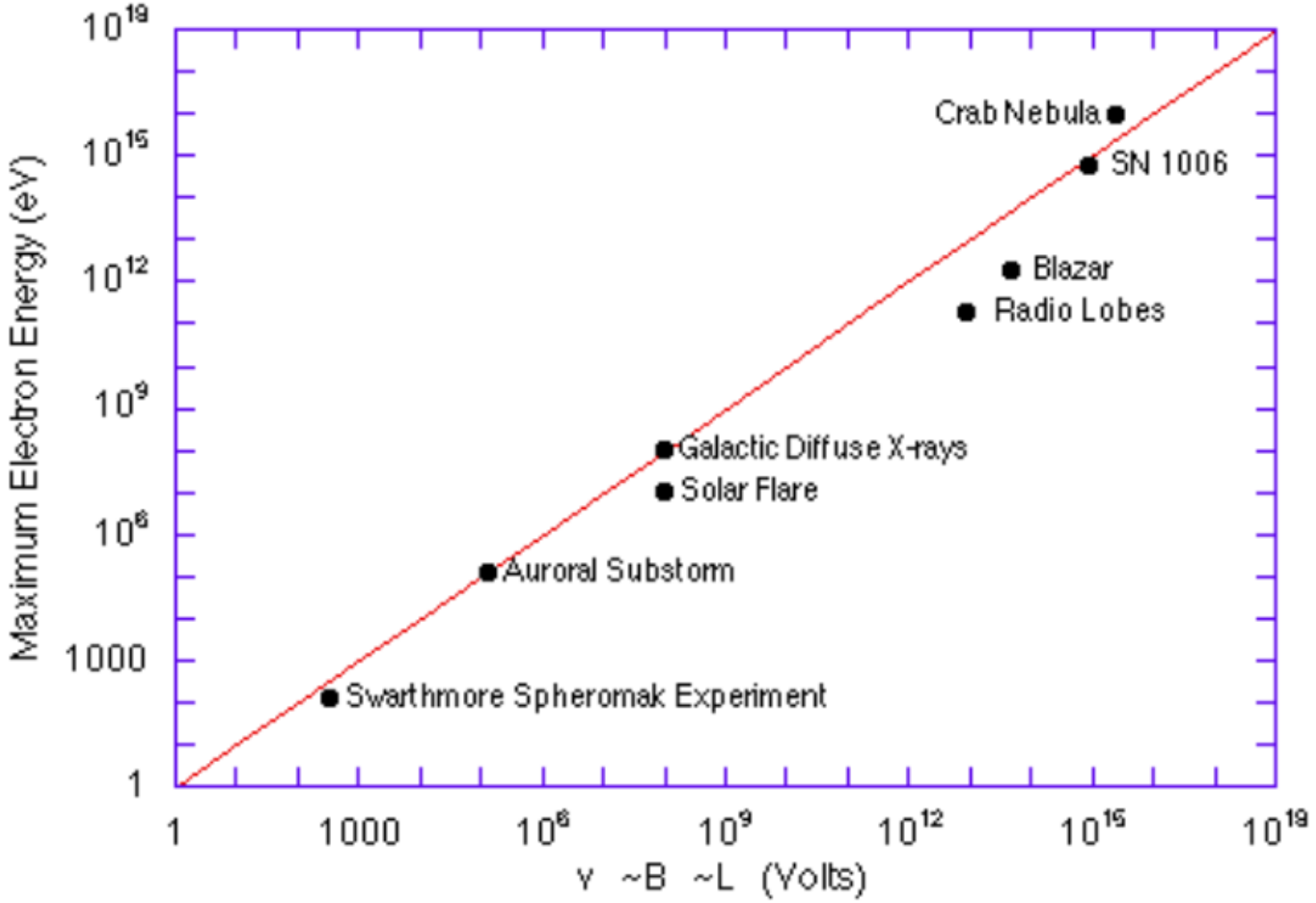

from K. Makishima, "Energy non-equipartition processes in the Universe." 1999

Crab Nebula spectrum (Hester 2008)

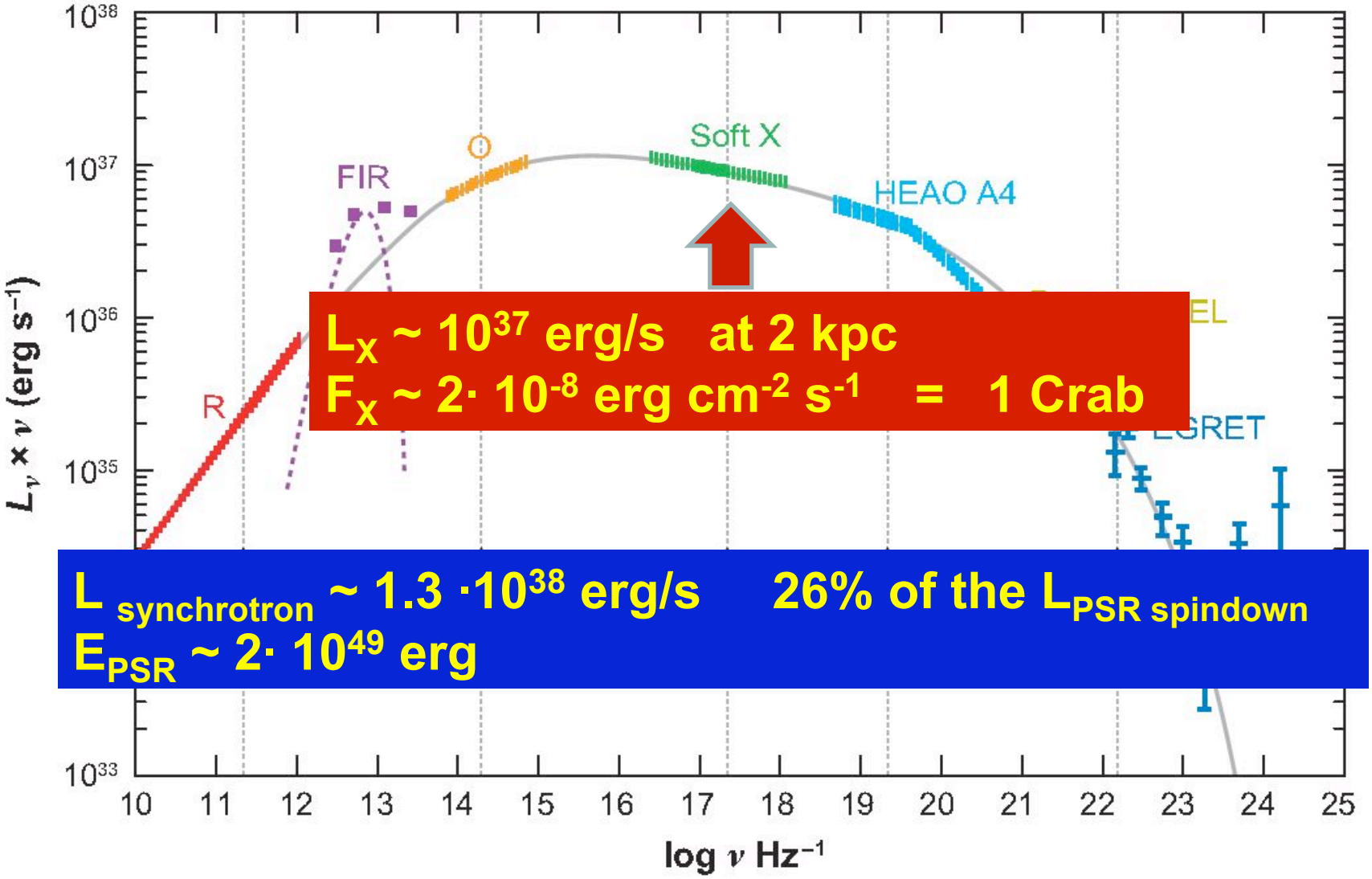

Fundamentals

- Chinese astronomers (Sung dyn.), 1054
- Messier Charles, 1758
- Parsons W. (Earl of Rosse), 1850
- Pacini, F., Nature, 1968, 219, 145
- Staelin & Reifenstein, 1968, Science, 162, 148
- Rees & Gunn, 1974, MNRAS, 167, 1
- Kennel & Coroniti, 1984, ApJ, 283, 694
- Kennel & Coroniti, 1984, ApJ, 283, 710
- deJager, Harding et al., 1996, ApJ, 457, 253
- Atoyan & Aharonian, 1996, MNRAS, 278, 525
- Arons J., 2008, Springer Lecture Notes
- Hester, J., 2008, ARAA. 46, 127

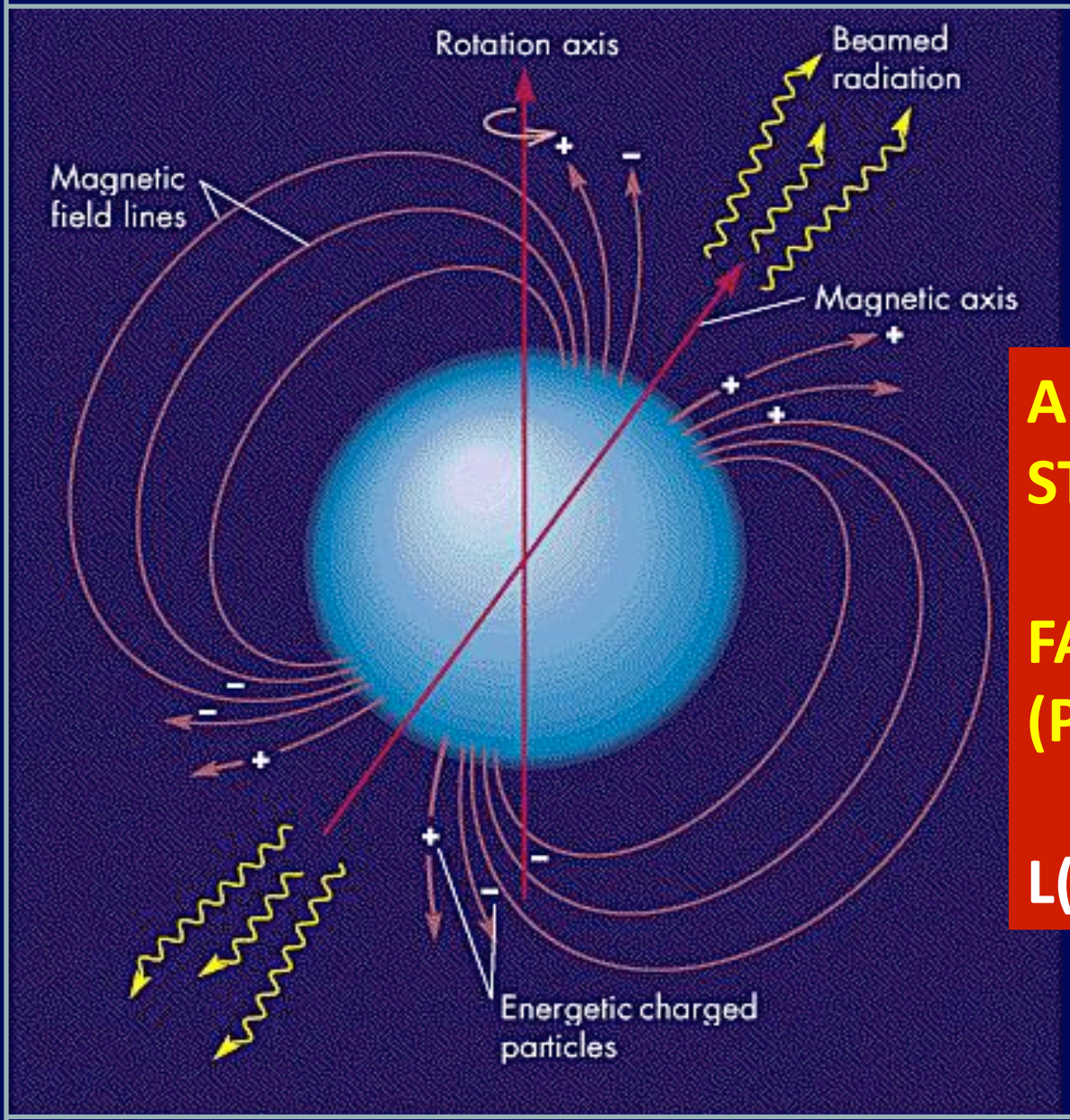

A NEUTRON STAR WITH A STRONG MAGNETIC FIELD:

FAST ROTATING PULSAR (P = 33 msec)

L(spindown) = 5 10^{38} erg/s

Crab pulsar emission (Pellizzoni et al. 2009)

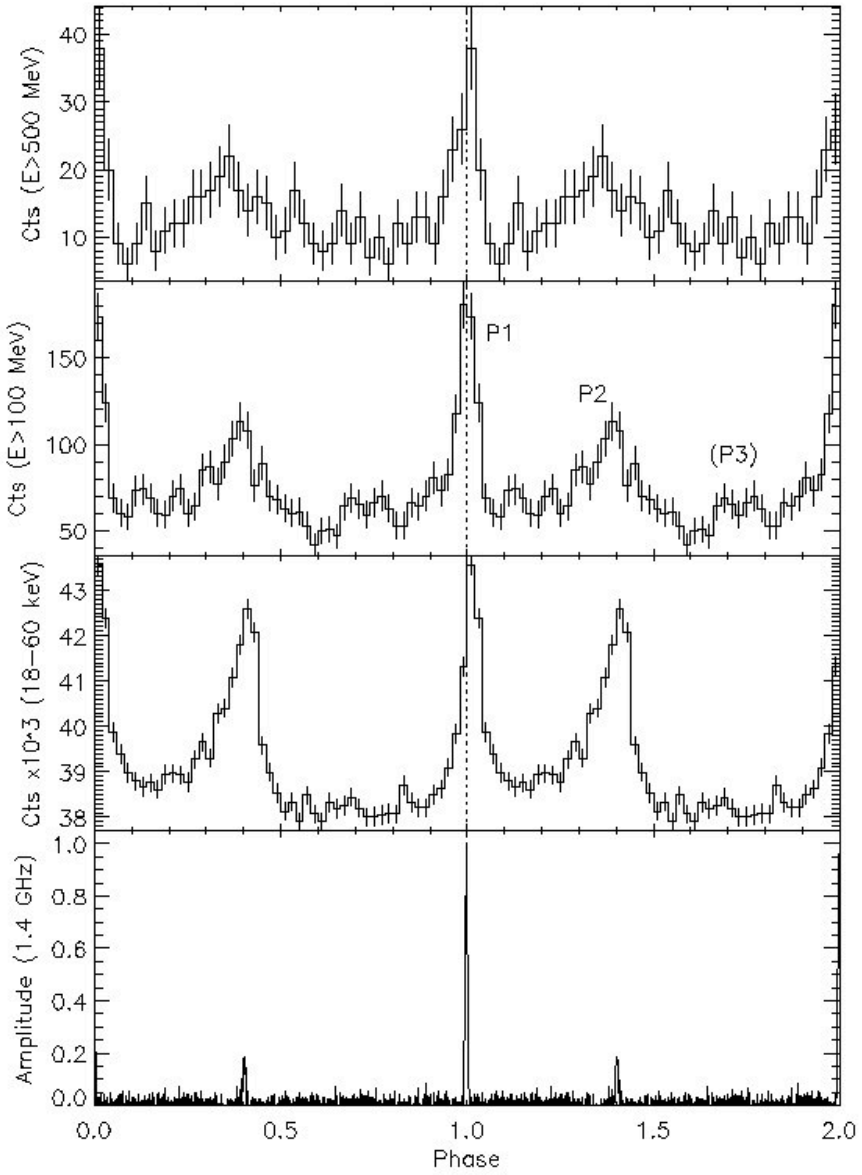

gamma-rays (> 500 MeV)
AGILE-GRID

gamma-rays (> 100 MeV)
AGILE-GRID

hard X-rays (18-60 keV)
Super-AGILE

radio (1.4 GHz)

Abdo et al. 2010

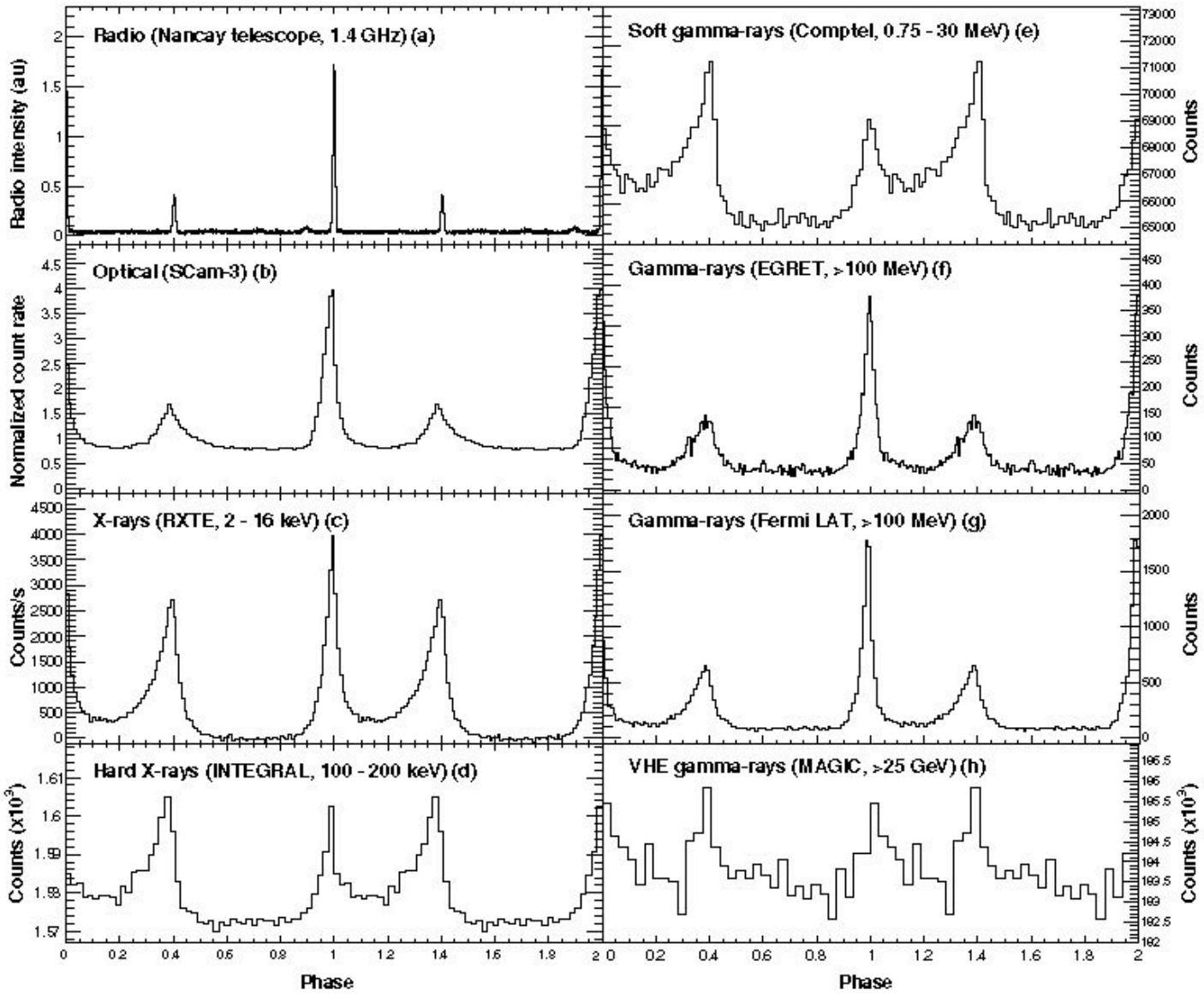

pulsed gamma-ray spectrum (Abdo et al 2010)

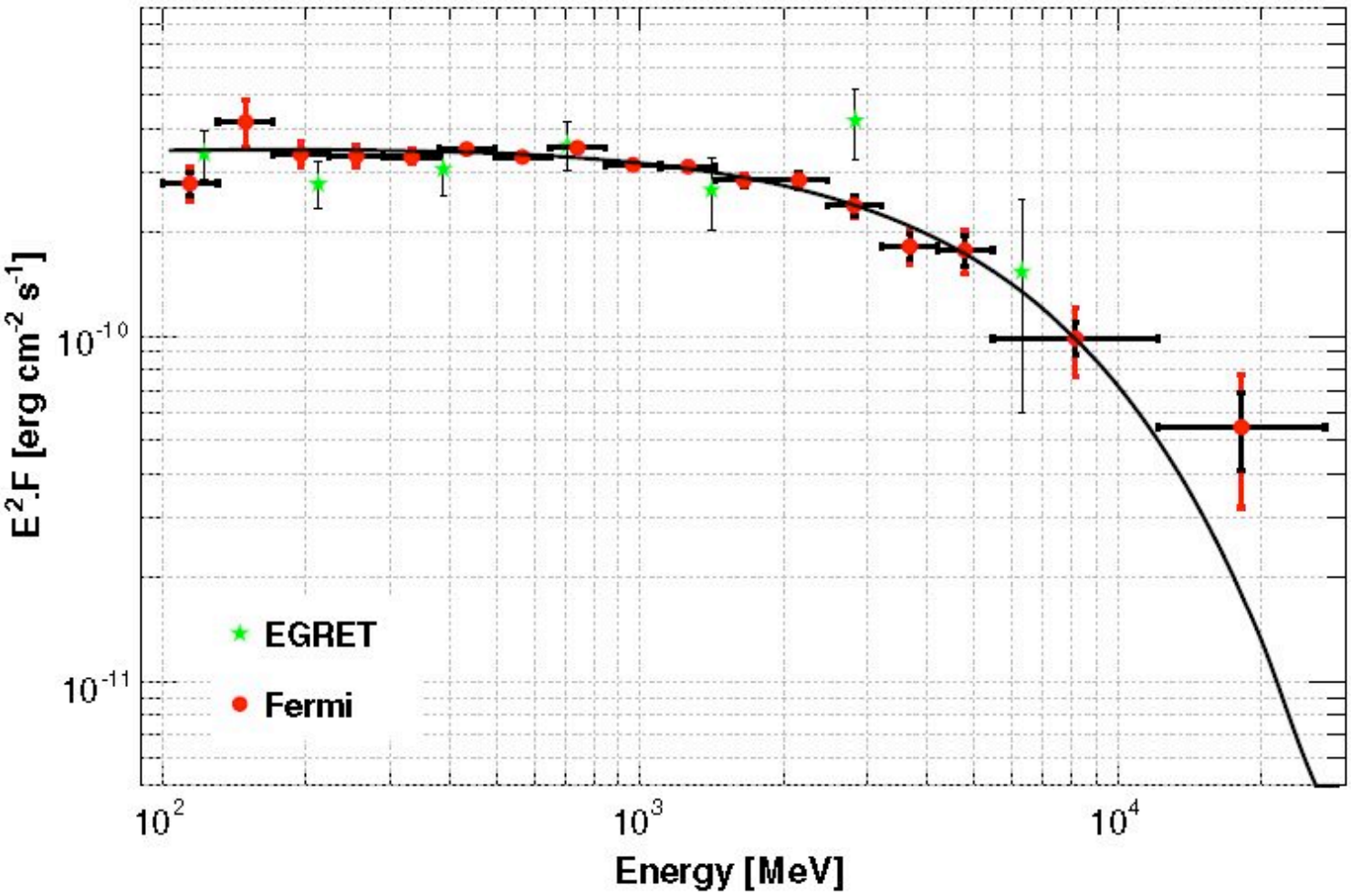

unpulsed (nebular) gamma-ray spectrum

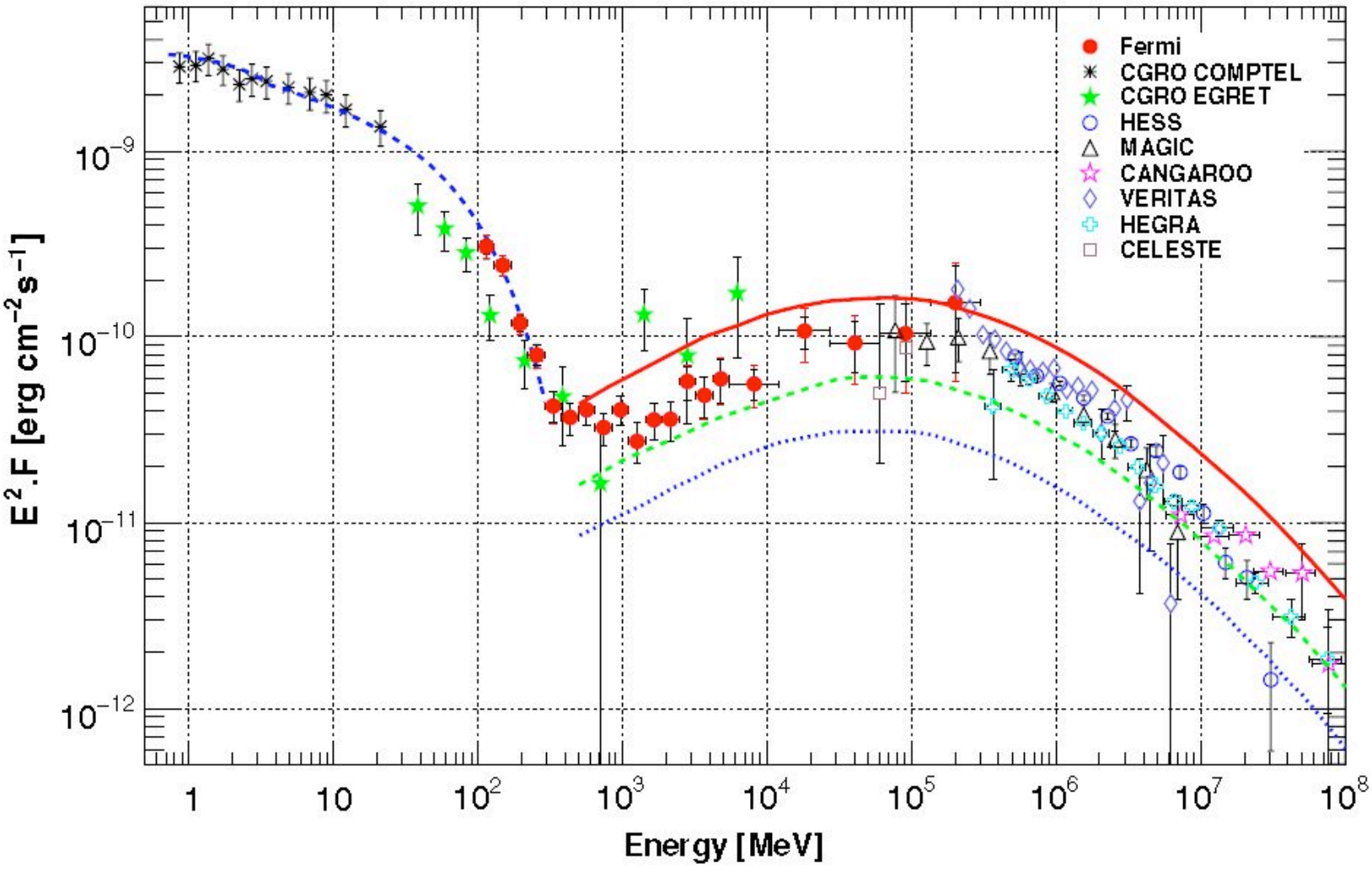

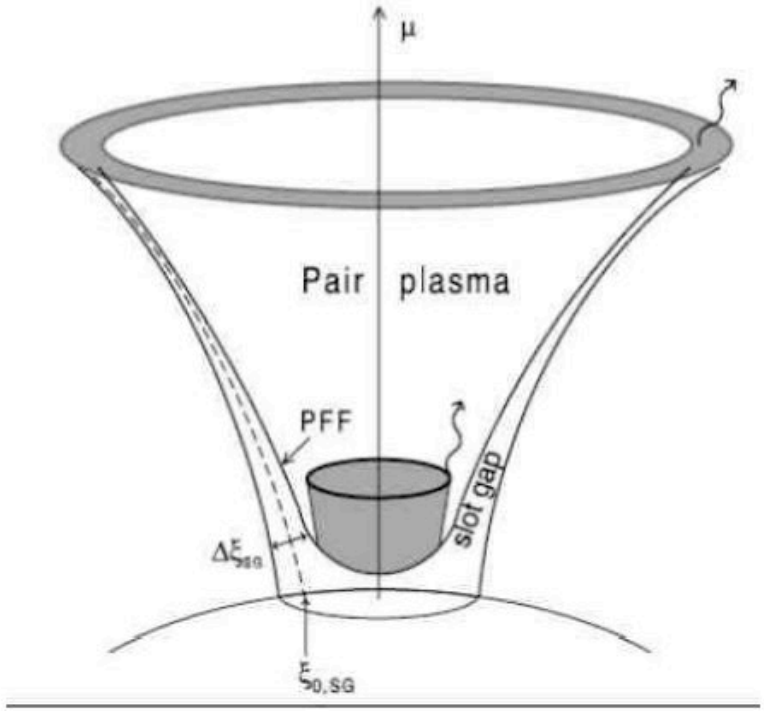

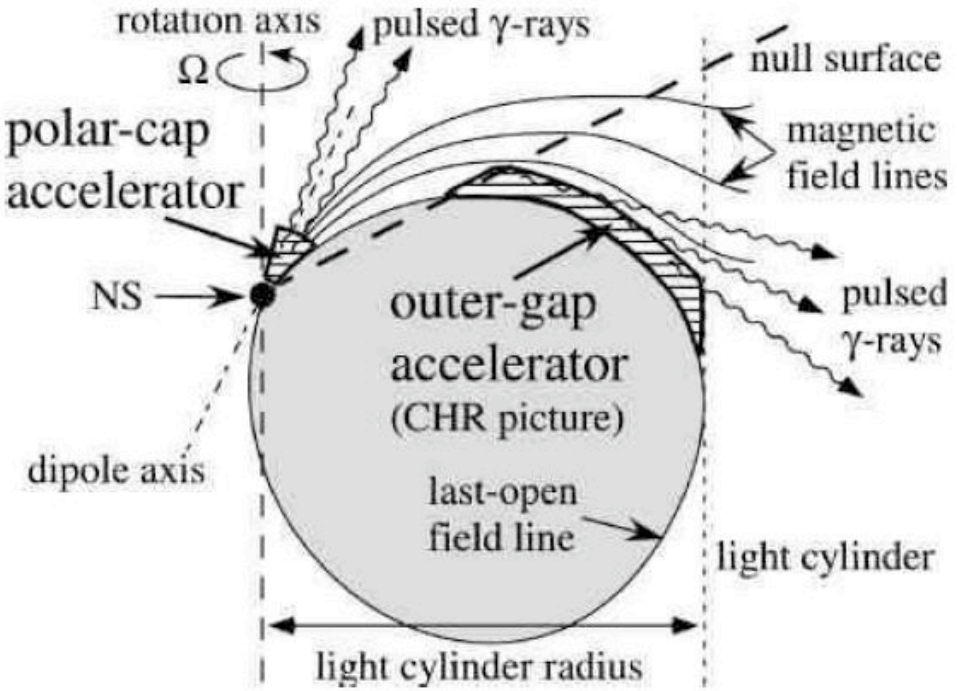

- Goldreich-Julian $n = -\mathbf{\Omega}\cdot\mathbf{B}/2\pi e$

PSR wind modelling (Spitkovsky 2006)

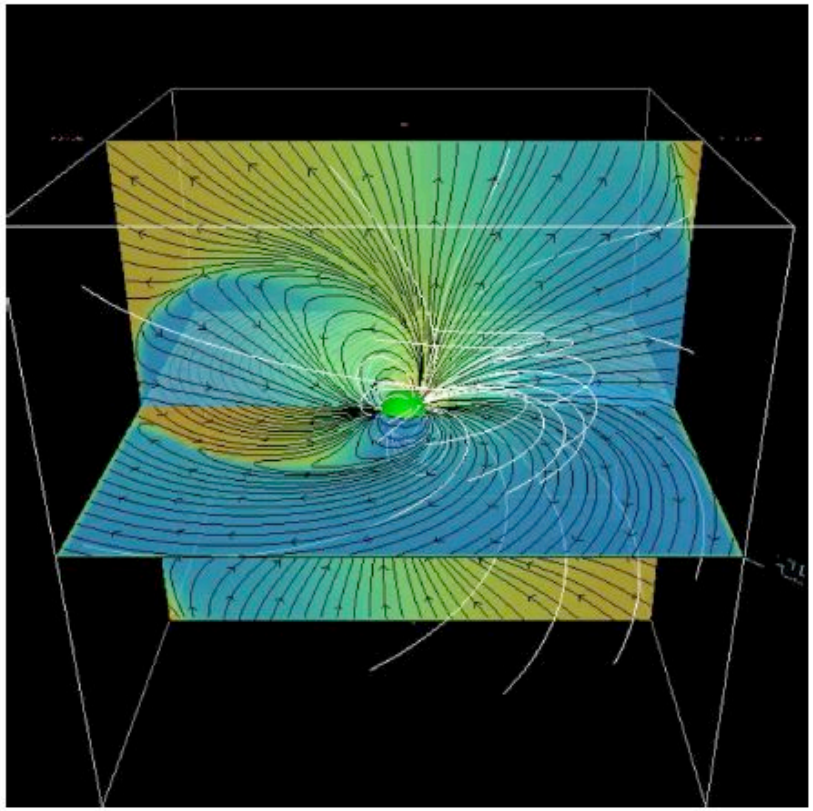

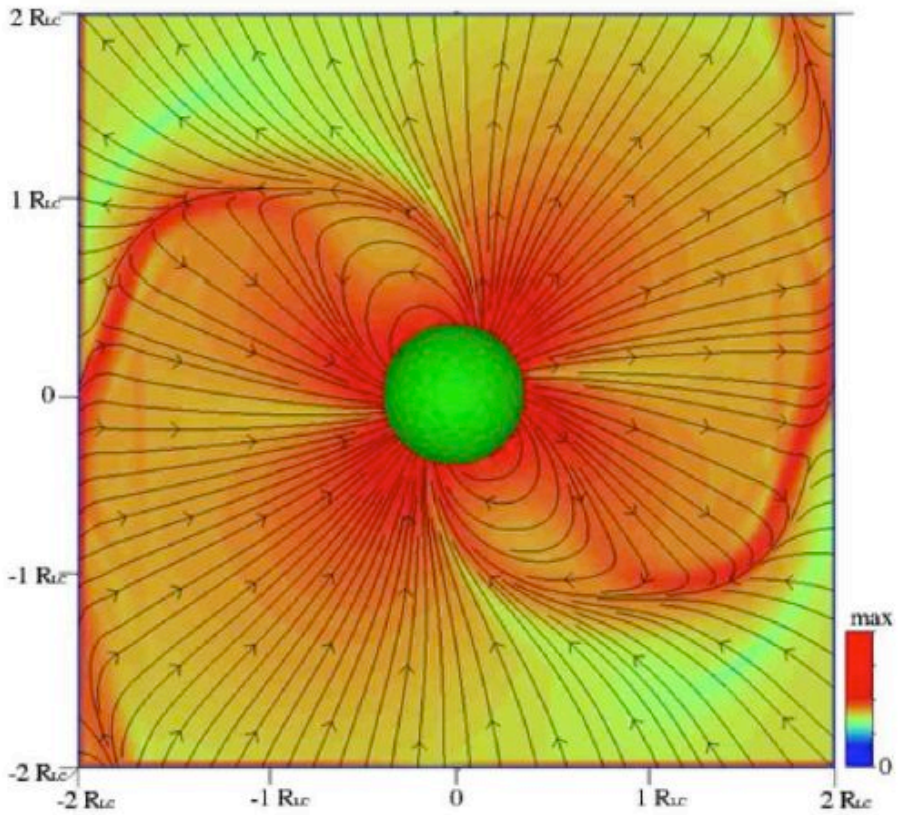

non-symmetric **PSR wind**
(relativistic e+/e-, ions (?), $\gamma_o \sim 10^2$-10^4)

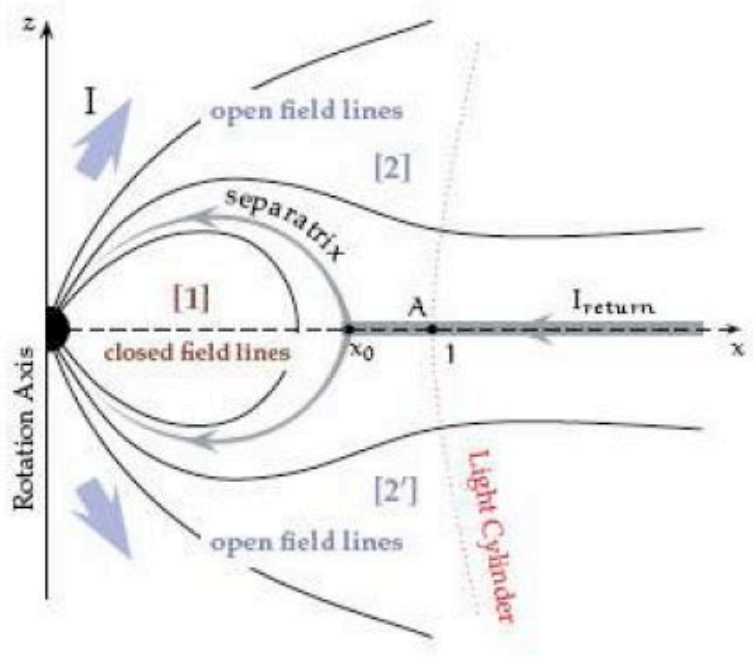

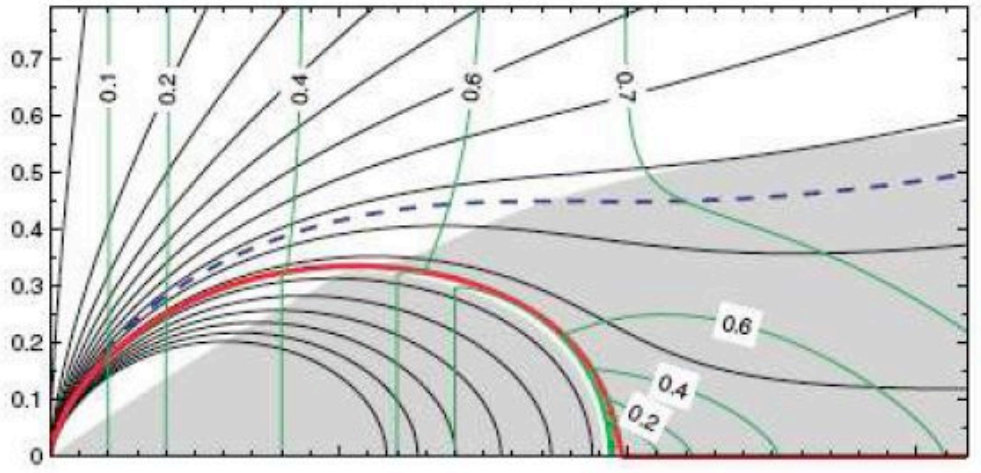

- $dN/dt = L_{sd} / (n \gamma m c^2) \sim 10^{40.5}\ s^{-1}$.
- much larger than GJ ! pair multipl. factor $\kappa \sim 10^4$

Kennel-Coroniti picture of the Crab Nebula

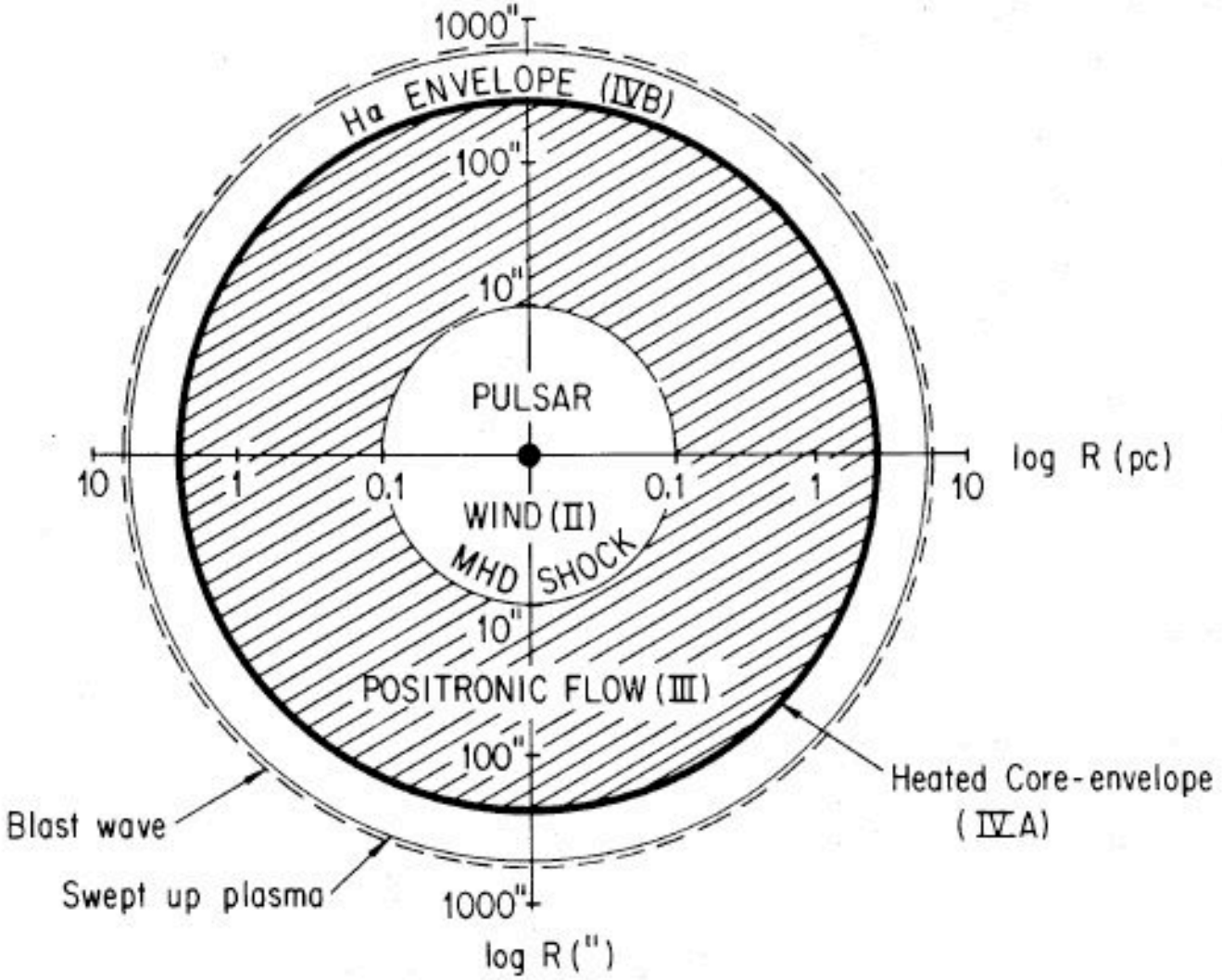

KC MHD modelling: RH eqs.

$$n_1 u_1 = n_2 u_2 \,,$$

$$E = \frac{u_1 B_1}{\gamma_1} = \frac{u_2 B_2}{\gamma_2} \,,$$

$$\gamma_1 \mu_1 + \frac{E B_1}{4\pi n_1 u_1} = \gamma_2 \mu_2 + \frac{E B_2}{4\pi n_1 u_1} \,,$$

$$\mu_1 u_1 + \frac{P_1}{n_1 u_1} + \frac{B_1^2}{8\pi n_1 u_1} = \mu_2 u_2 + \frac{P_2}{n_1 u_1} + \frac{B_2^2}{8\pi n_1 u_1}$$

KC MHD modelling: RH eqs.

the Rankine-Hugoniot relations for a strong, perpendicular shock reduce to

$$u_2^2 = \frac{8\sigma^2 + 10\sigma + 1}{16(\sigma + 1)} + \frac{1}{16(\sigma + 1)}\left[64\sigma^2(\sigma + 1)^2 + 20\sigma(\sigma + 1) + 1\right]^{1/2}$$

$$\frac{B_2}{B_1} = \frac{N_2}{N_1} = \frac{\gamma_2}{u_2},$$

$$\frac{P_2}{n_2 mc^2 u_1^2} = \frac{1}{4u_2\gamma_2}\left[1 + \sigma\left(1 - \frac{\gamma_2}{u_2}\right)\right],$$

PSR wind magnetization $\sigma = \dfrac{B^2}{4\pi nu\gamma mc^2}$

KC MHD modelling: RH eqs. solution

$$u_2^2 \approx \frac{1+9\sigma}{8}, \qquad \gamma_2^2 \approx \frac{9+9\sigma}{8}, \qquad \beta_2 = \frac{u_2}{\gamma_2} \approx \frac{1}{3}(1+4\sigma),$$

$$\frac{B_2}{B_1} = \frac{N_2}{N_1} \approx 3(1-4\sigma),$$

$$\frac{P_2}{n_1 m c^2 u_1^2} \approx \frac{2}{3}(1-7\sigma).$$

KC MHD modelling: RH eqs. solution

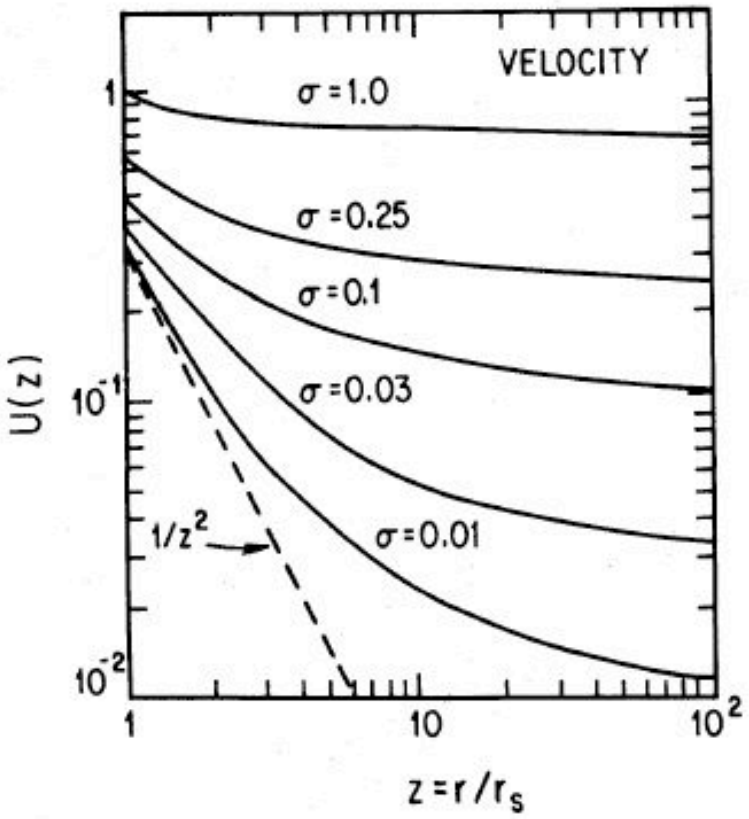

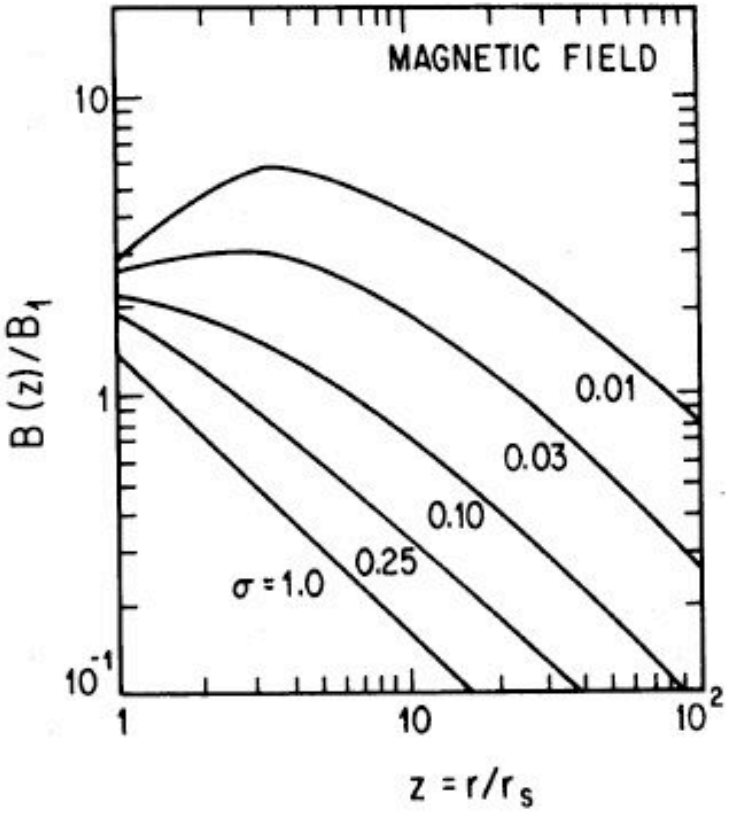

Crab Nebula modelling

- average nebular magnetic field B = 200 μ G
- PSR-injected particles dN/dt ~ $10^{40.5}$ s^{-1}
- total emitting particles, N ~ 2 ·10^{51}
- many shock accelerating sites in the Nebula
- inner Nebula variability (weeks-months)
  - **Toroidal structures (wisps)**
  - **Jet-like structures (knots)**

commonly used mechanisms

- **diffusive shock acceleration (DSA), first-order Fermi acc.**

- **shock-drift acceleration (SDA)**

results depends on particle content (ions, e+/e-), B-configuration, sigma -parameter, etc.

PARTICLE ACCELERATION IN MAGNETIZED COLLISIONLESS PAIR SHOCKS

(Sironi & Spitkovsky, 2009)

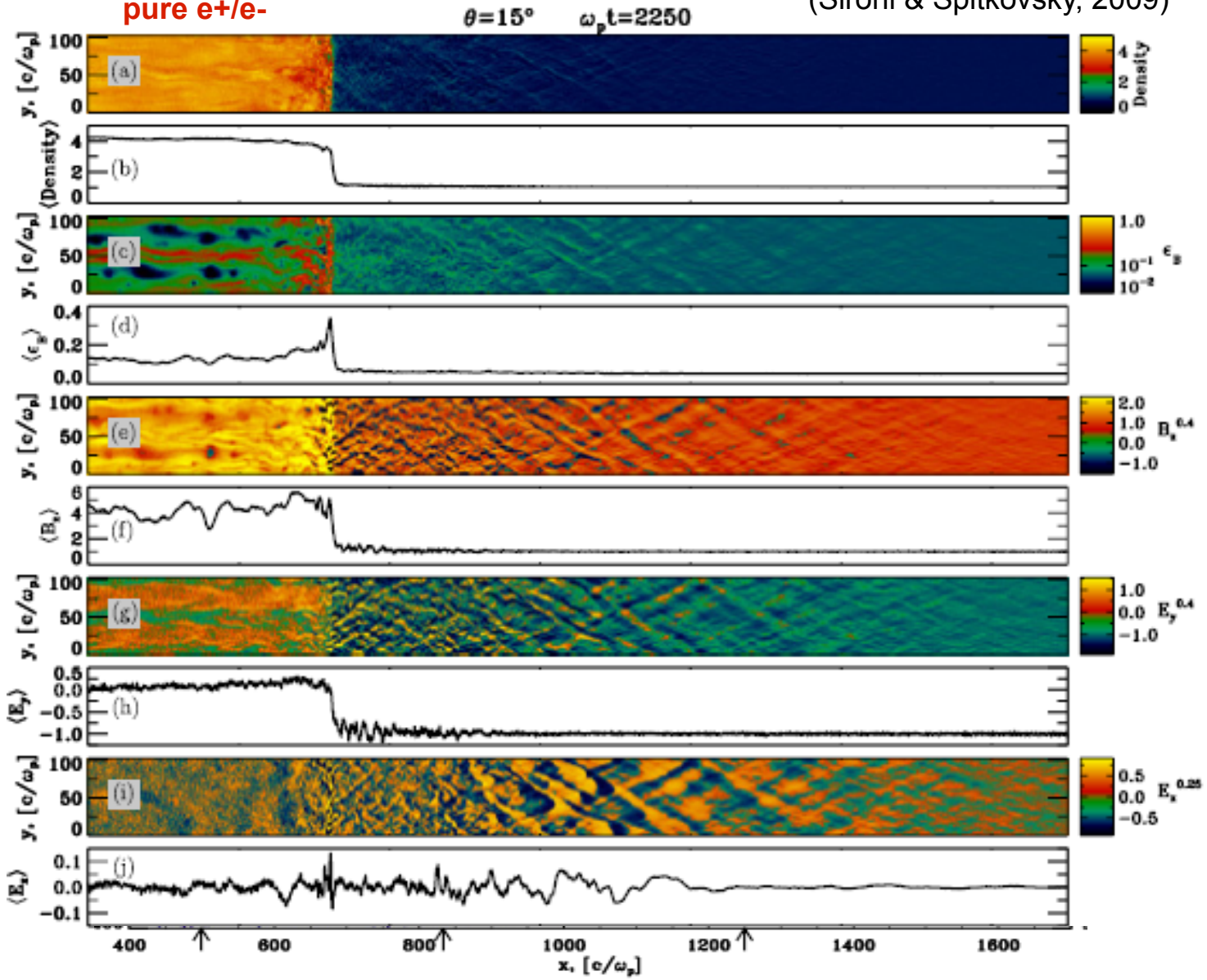

- Synchrotron cooling timescale

- $\tau_s = (30\ \text{yrs})\ B_{-4}^{-3/2}\ (E_{ph}/1\ \text{keV})^{-1/2}$

- $\tau_s = (0.1\ \text{yrs})\ B_{-4}^{-3/2}\ (E_{ph}/100\ \text{MeV})^{-1/2}$

Crab Nebula modelling

- average nebular magnetic field **B = 200 μ G**
- PSR-injected particles (e+/e- pairs)
  dN/dt ~ $10^{40.5}$ s^{-1}
- total emitting particles, **N ~ 2 ·10^{51}**
- many shock accelerating sites in the Nebula
- inner Nebula variability (weeks-months)
  - **Toroidal structures (wisps)**
  - **Jet-like structures (knots)**

possible standard mechanisms

- **diffusive shock acceleration (DSA), first-order Fermi acc.**

- **shock-drift acceleration (SDA)**

results depends on particle content (ions, e+/e-), B-configuration, sigma -parameter, etc.

the "standard" nebular model (deJager etal. 1996)

- particle acceleration by shocks or MHD/plasma instabilities, assumes E/B = 1
- $t_{acc}^{-1} \sim \alpha' \omega_B / \gamma \quad (\omega_B = eB/mc; \quad \alpha' < 1)$
- $\gamma^{-1} d\gamma/dt = (eB/\gamma mc)(\mathbf{E/B})\alpha' - (4/3)\sigma_T (B^2/8\pi)\, \gamma/mc$
- $d\gamma/dt = 0$ implies

$$\gamma_{max} \sim 10^9 (\mathbf{E/B})^{1/2} (\alpha'/\sin^2\theta\, B_{-3})^{1/2}$$

"standard" paradigm for nebular emission
(de Jager, Harding et al. 1996)

- max. emitted photon synchrotron energy is independent of the magnetic field B (for a Doppler factor δ): **synchrotron burn-off**

- $\mathbf{E_{max} = \hbar\, \omega_B\, \gamma_m^2 \sim (100\ MeV)\ (\delta\, \alpha'/\sin\theta)}$

Crab Nebula spectrum

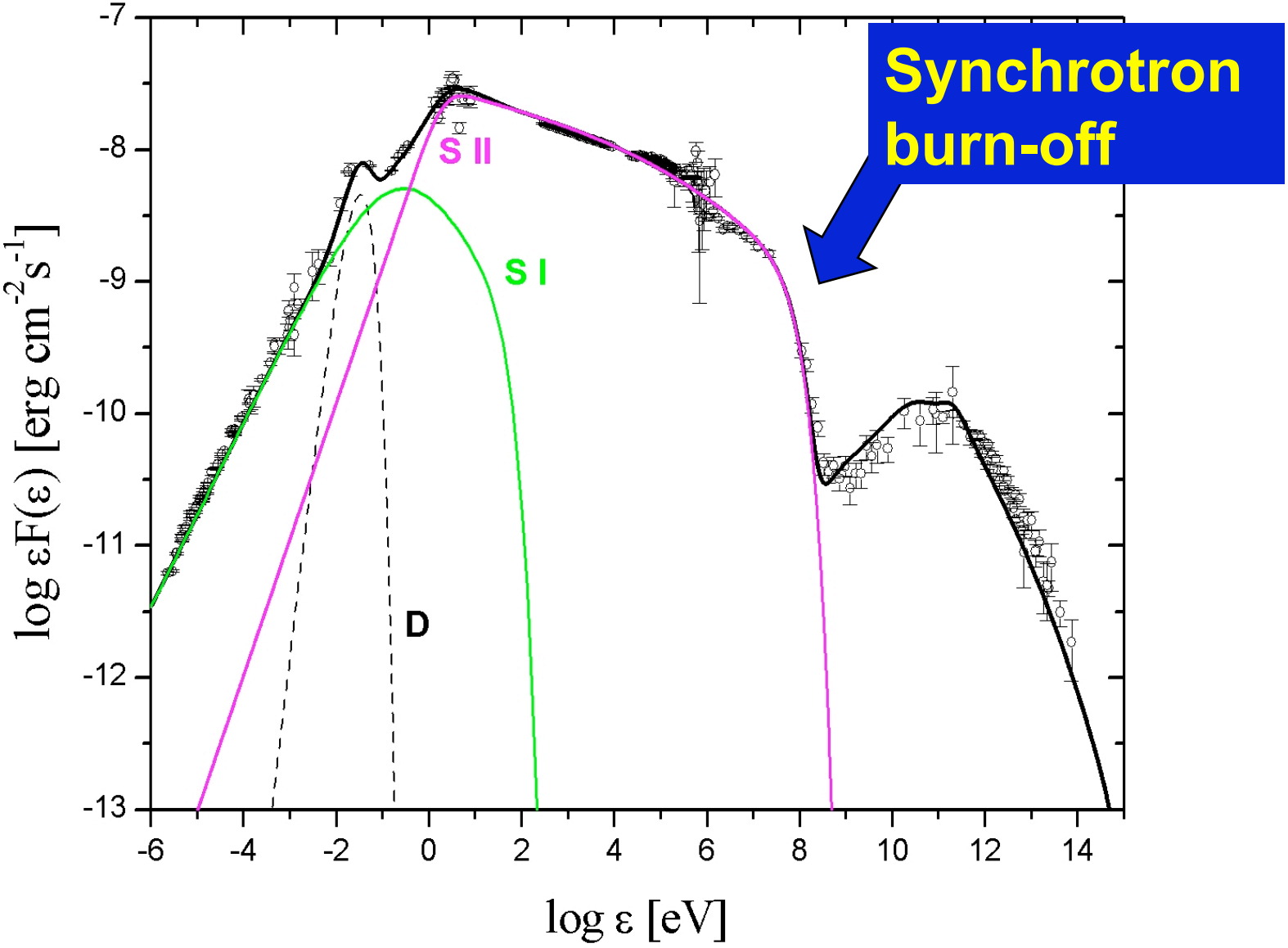

Crab Nebula spectrum

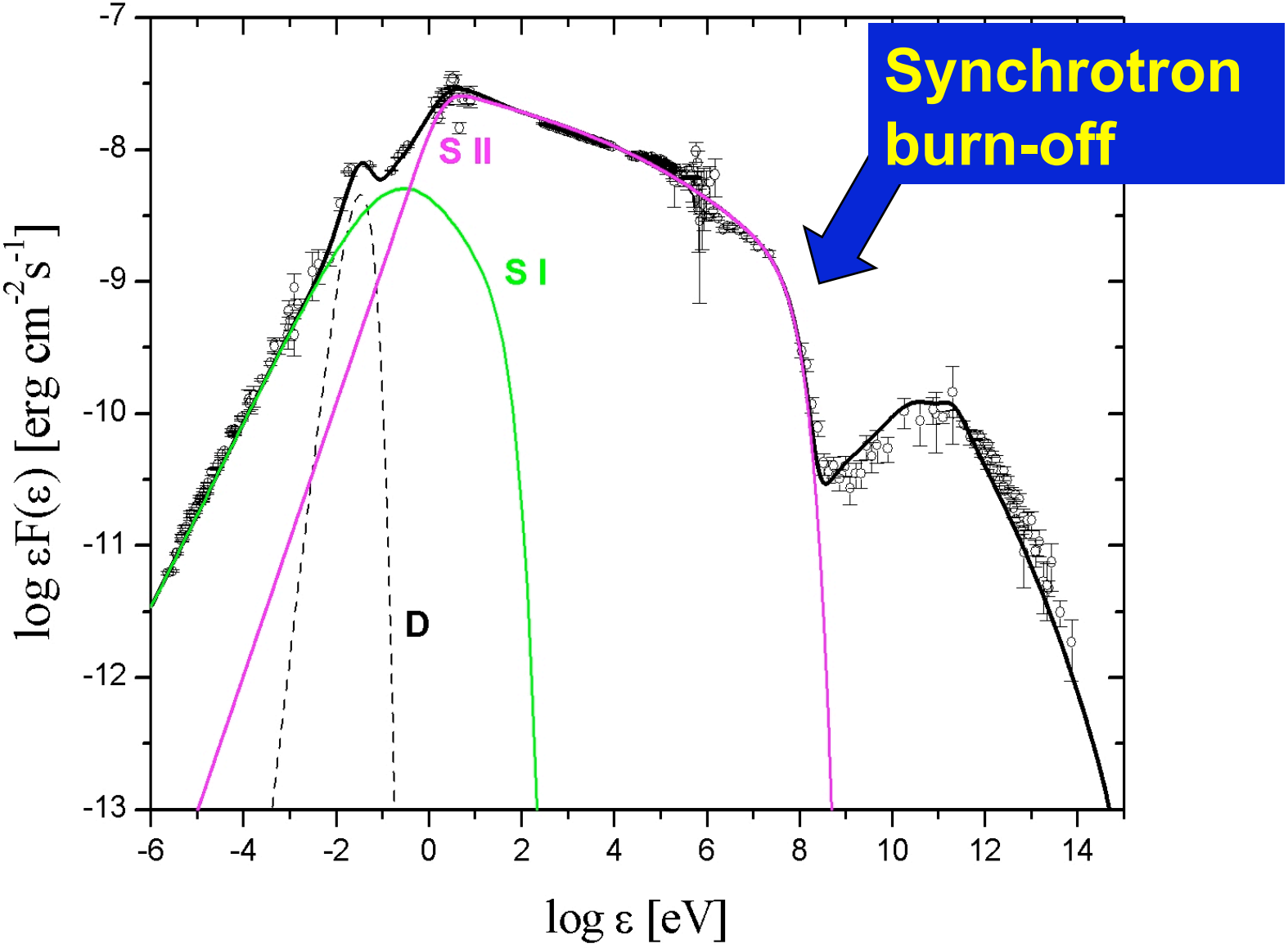

De Jager et al., 1996, Atoyan & Aronian 1996, Meyer et al. 2010,
Vittorini & M.T. 2011

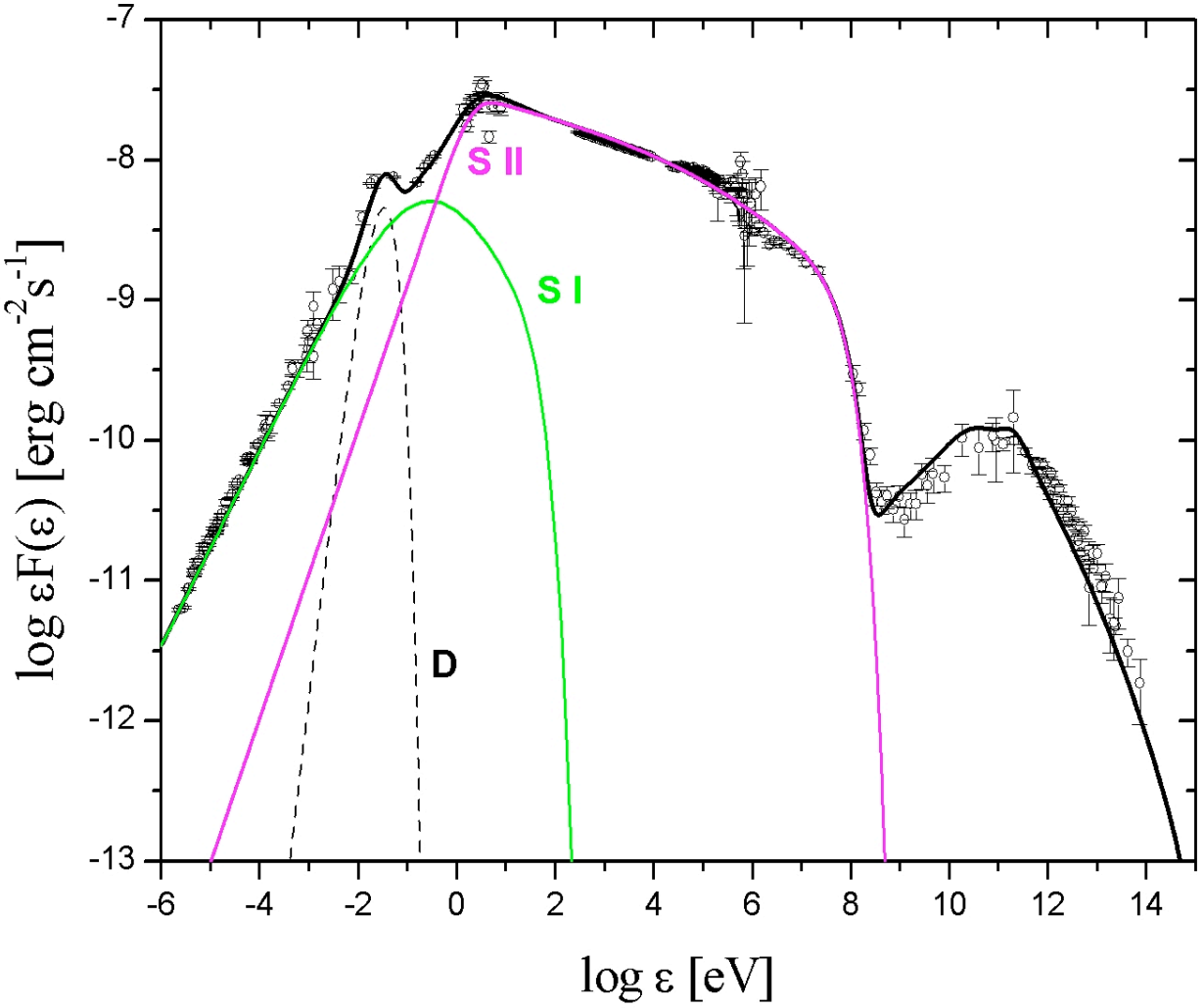

Pop. I
$60<\gamma<2.5\ 10^4$ $\alpha=1.6$
$2.5e4<\gamma<2.5e6$ $\alpha=4.0$
R=2.3e18 cm
N_{el}=2.5e51
T_{syn} ~ 10^5 years

Pop. II
$5e5<\gamma<3.8e8$ $\alpha=3.20$
$3.8e8<\gamma<3.5e9$ $\alpha=3.75$
R=2e18 cm
N_{el}=3e48
T_{syn} ~ 10 years

Dust
L=3e36 erg/s
T=100 °K

Average magnetic field
B=200 μGauss

Vittorini & M.T. 2011

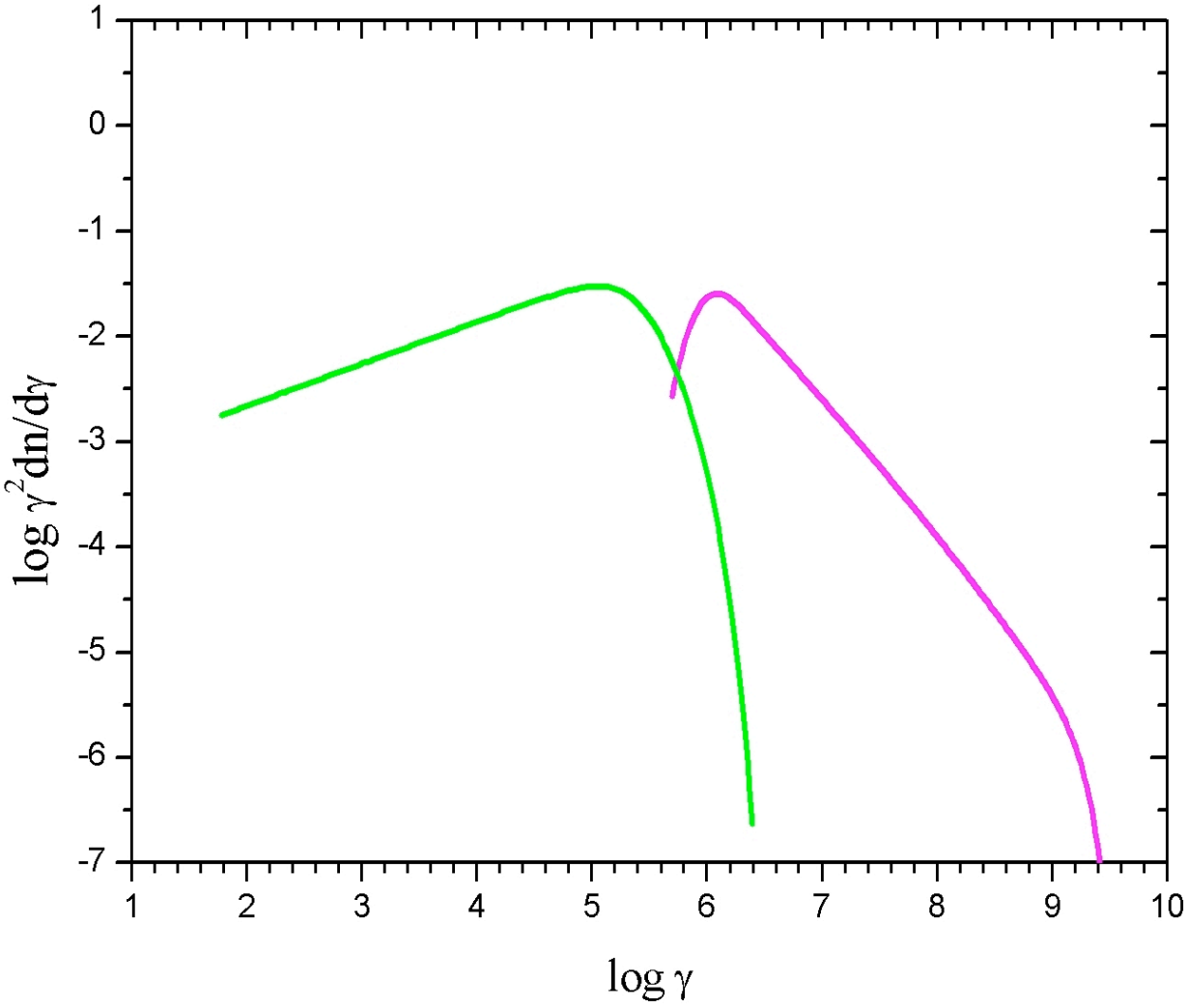

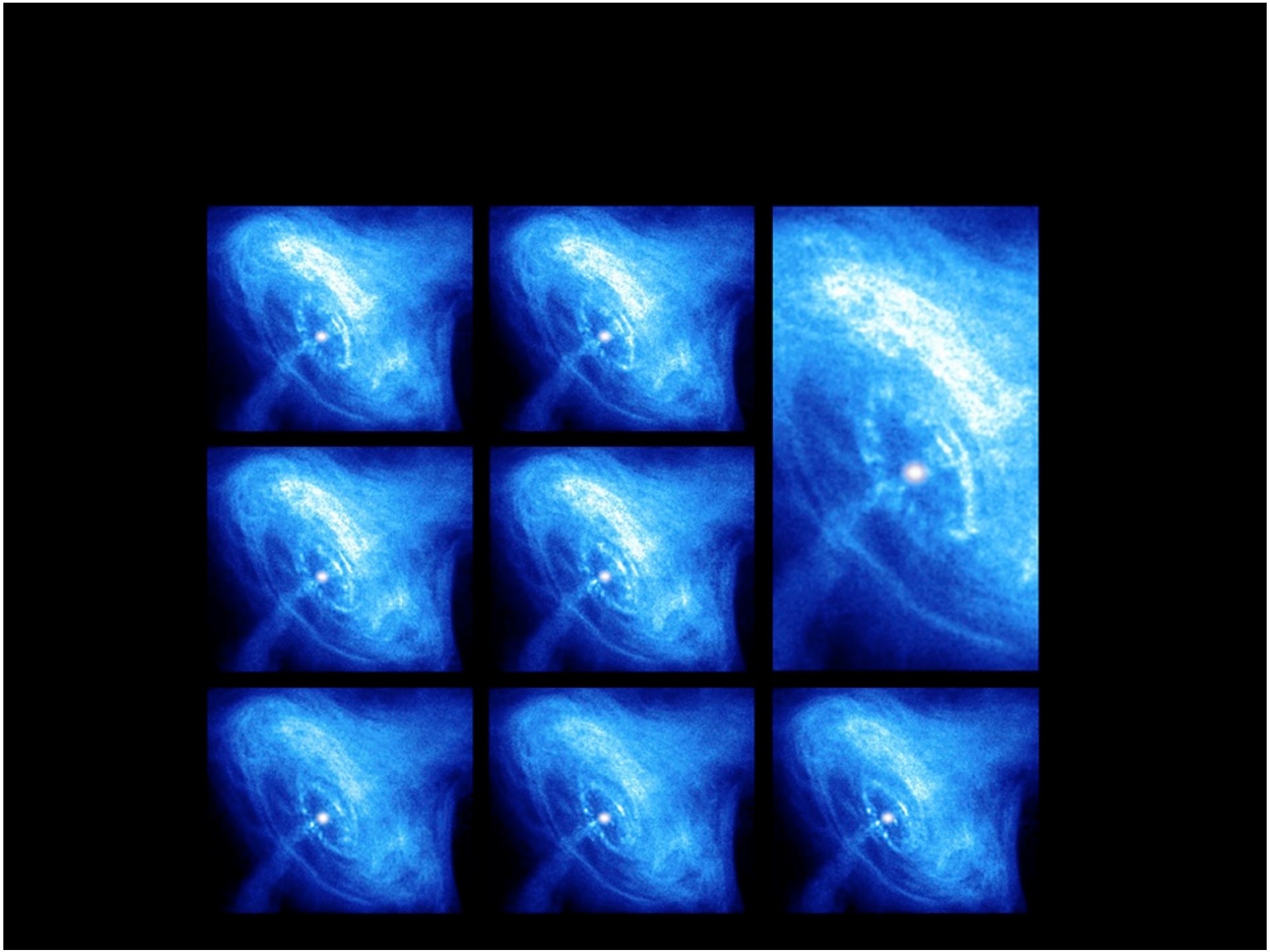

Crab Nebula MHD models

- Arons et al., 1992- 2010
- Komissarov, Lyubarsky, 2003, 2004
- Spitkowsky & Arons, 2004, ApJ, 603, 669
- Del Zanna, Volpi, Amato, Bucciantini, 2006, 2008
- Camus et al., 2009, MNRAS; 400, 1241

Camus, Komissarov, Bucciantini, Hughes, MNRAS, 400, 1241 (2009)

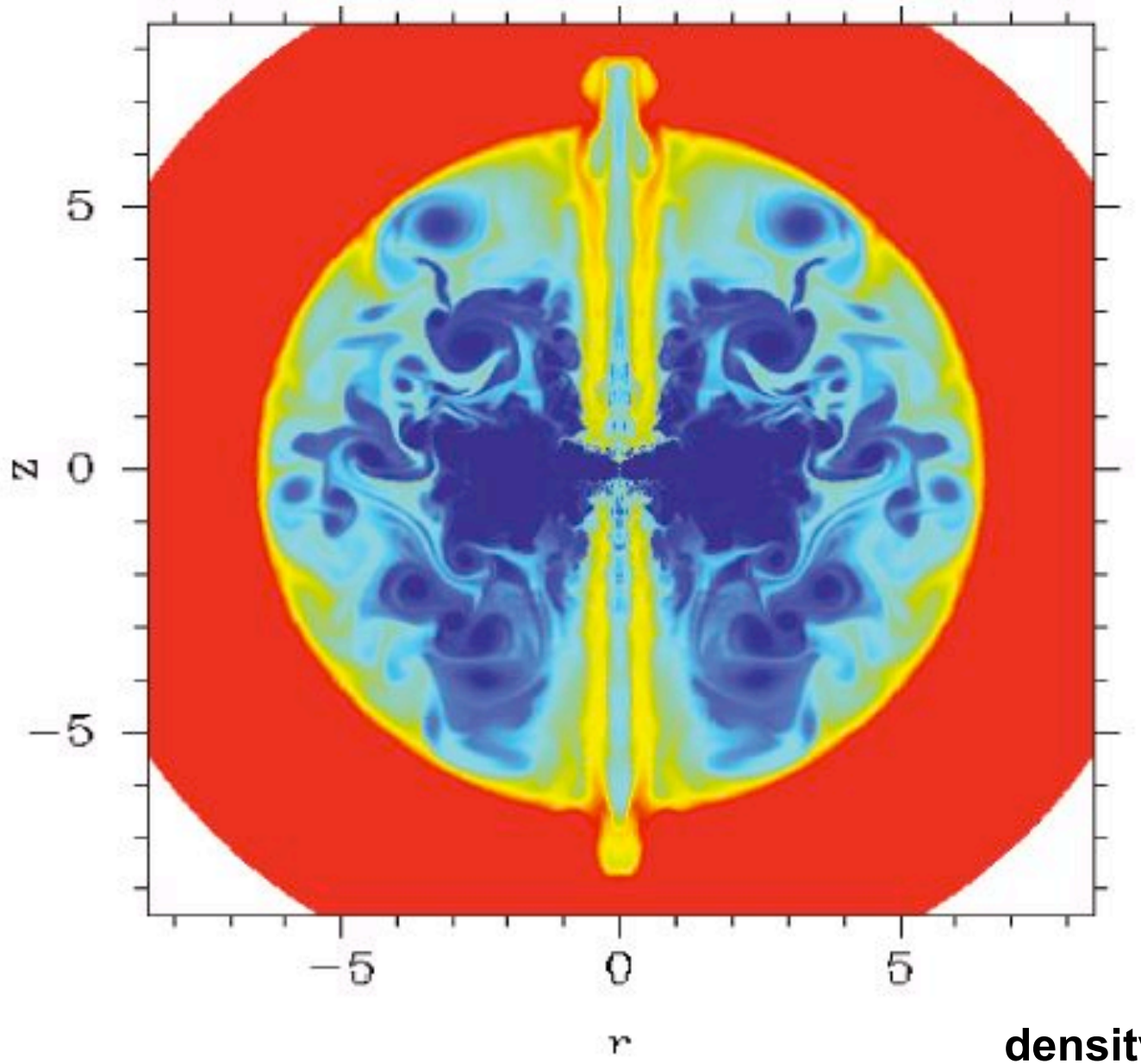

density profile

Camus, Komissarov, Bucciantini, Hughes, MNRAS, 400, 1241 (2009)

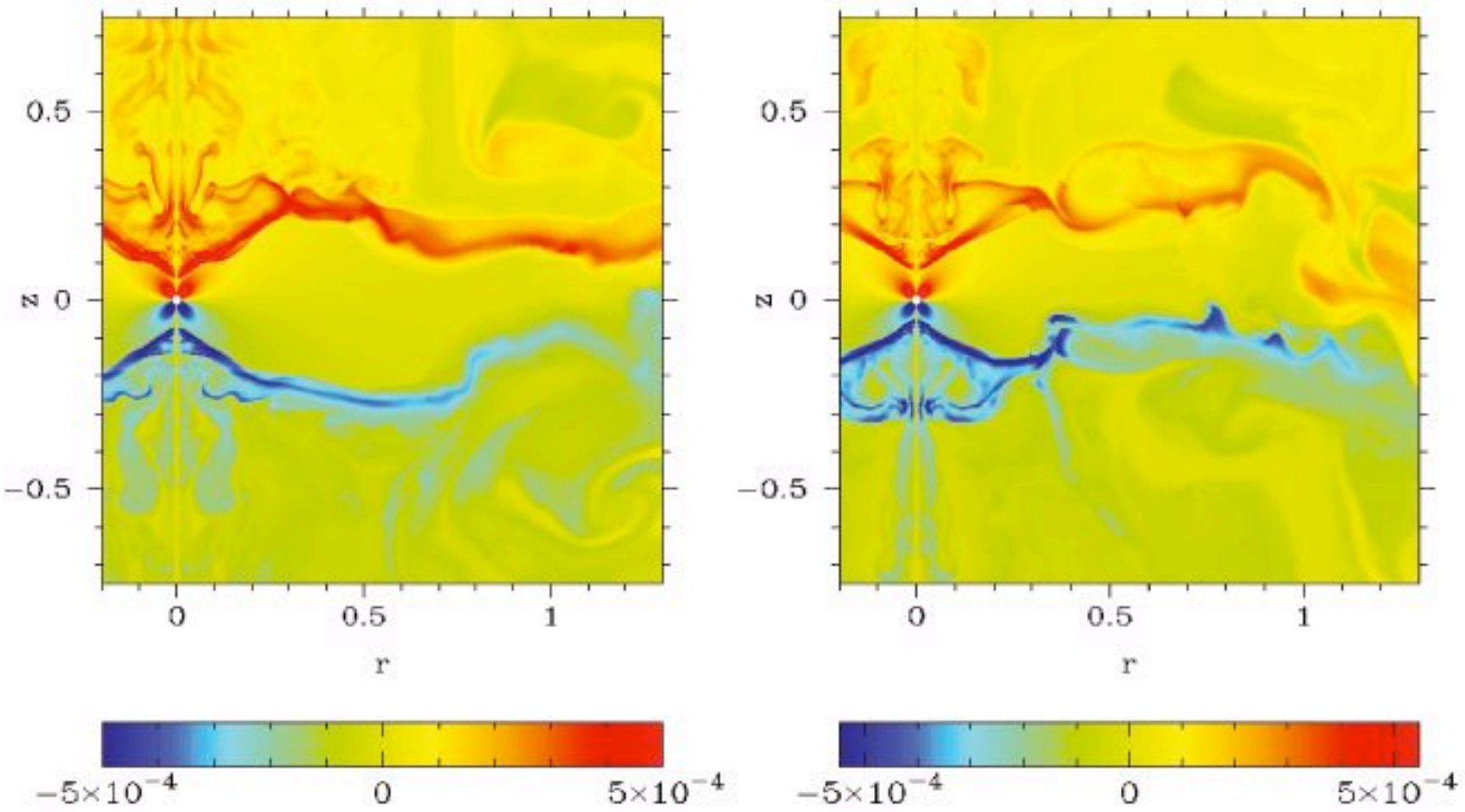

Magnetic field profile at different times

Camus, Komissarov, Bucciantini, Hughes, MNRAS, 400, 1241 (2009)

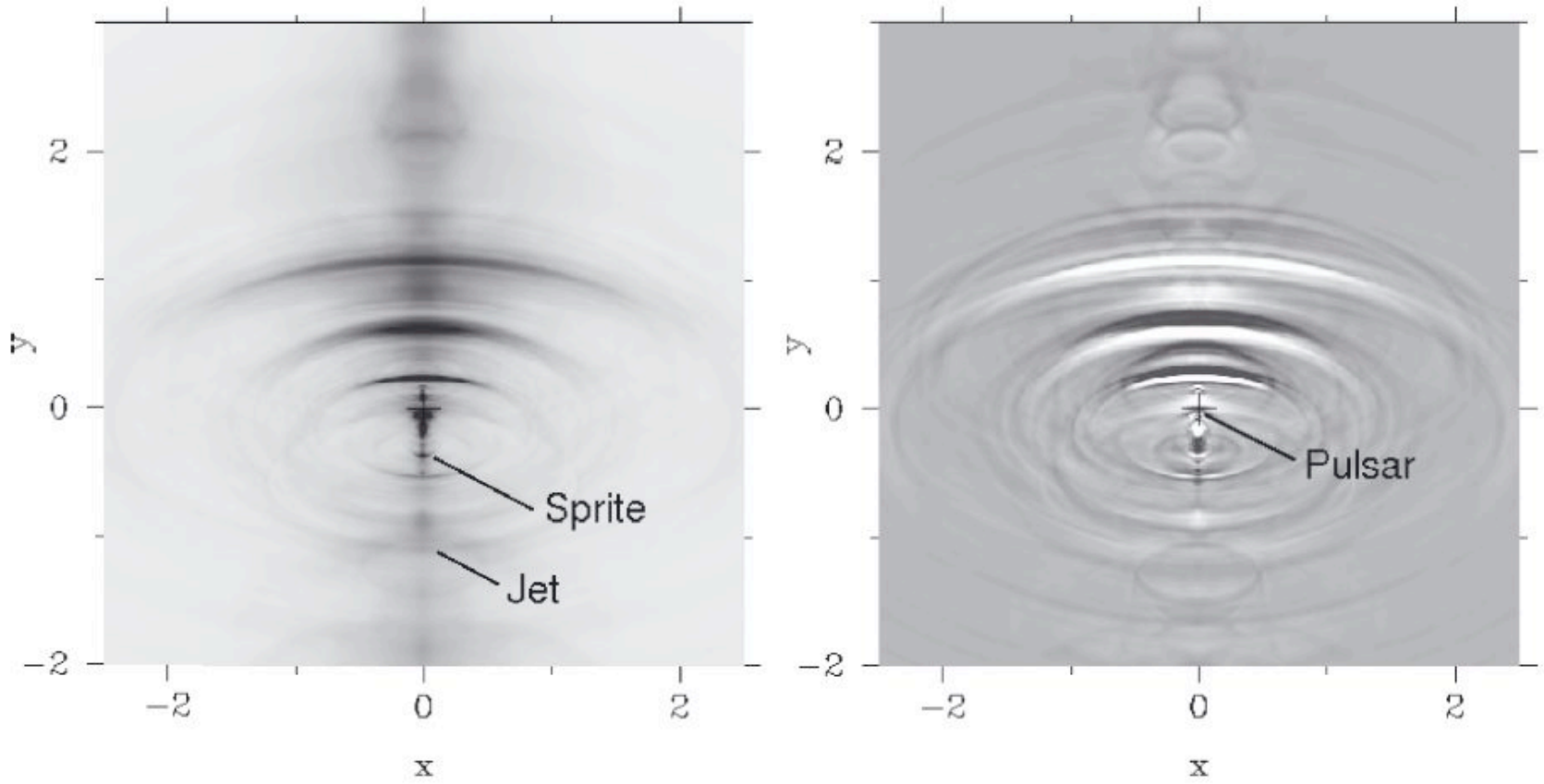

simulated synchrotron emissivity

Camus, Komissarov, Bucciantini, Hughes, MNRAS, 400, 1241 (2009)

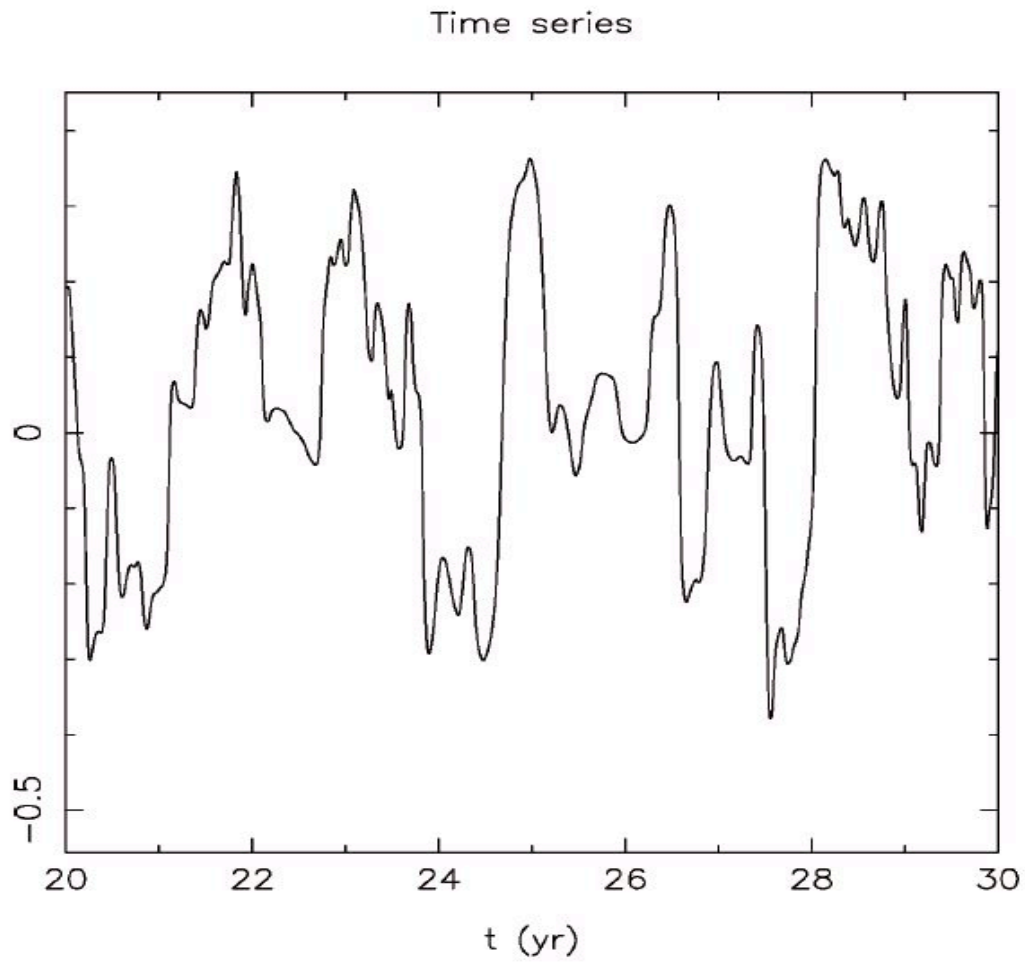

local magnetic field energy density

Variability in MHD models

From P.Blasi

Courtesy E. Amato

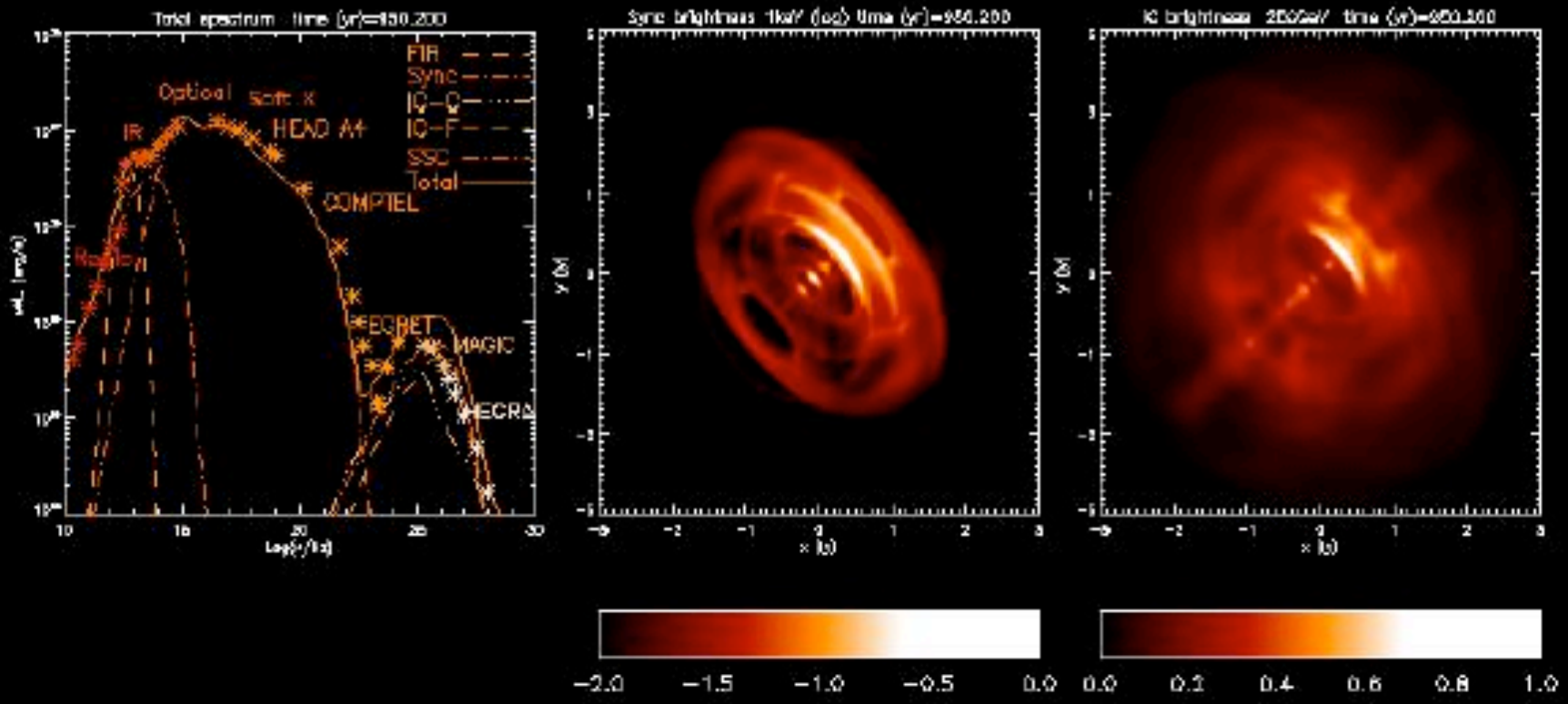

Chandra observations of the Crab Nebula

2001

Sept. 28, 2010

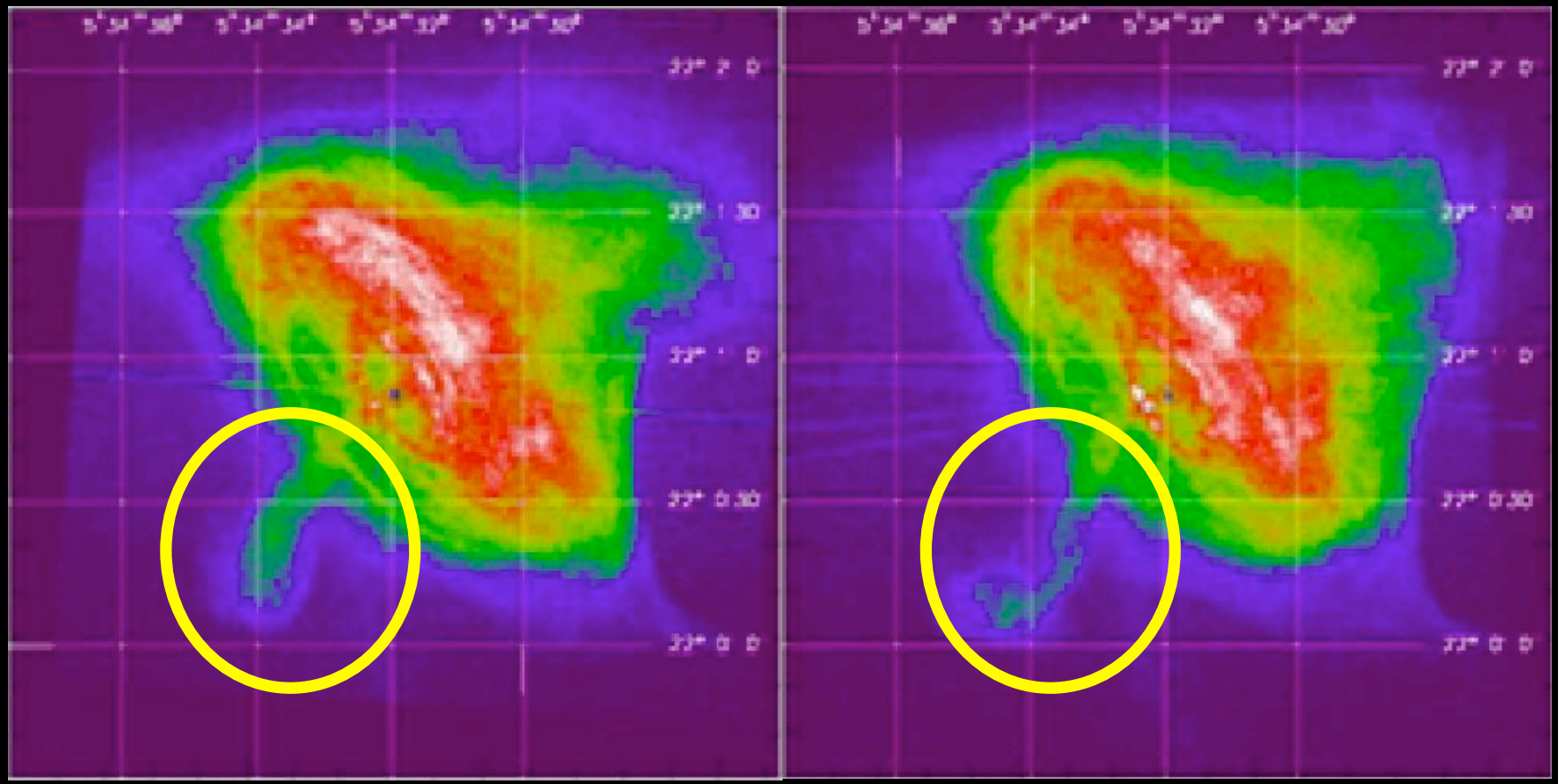

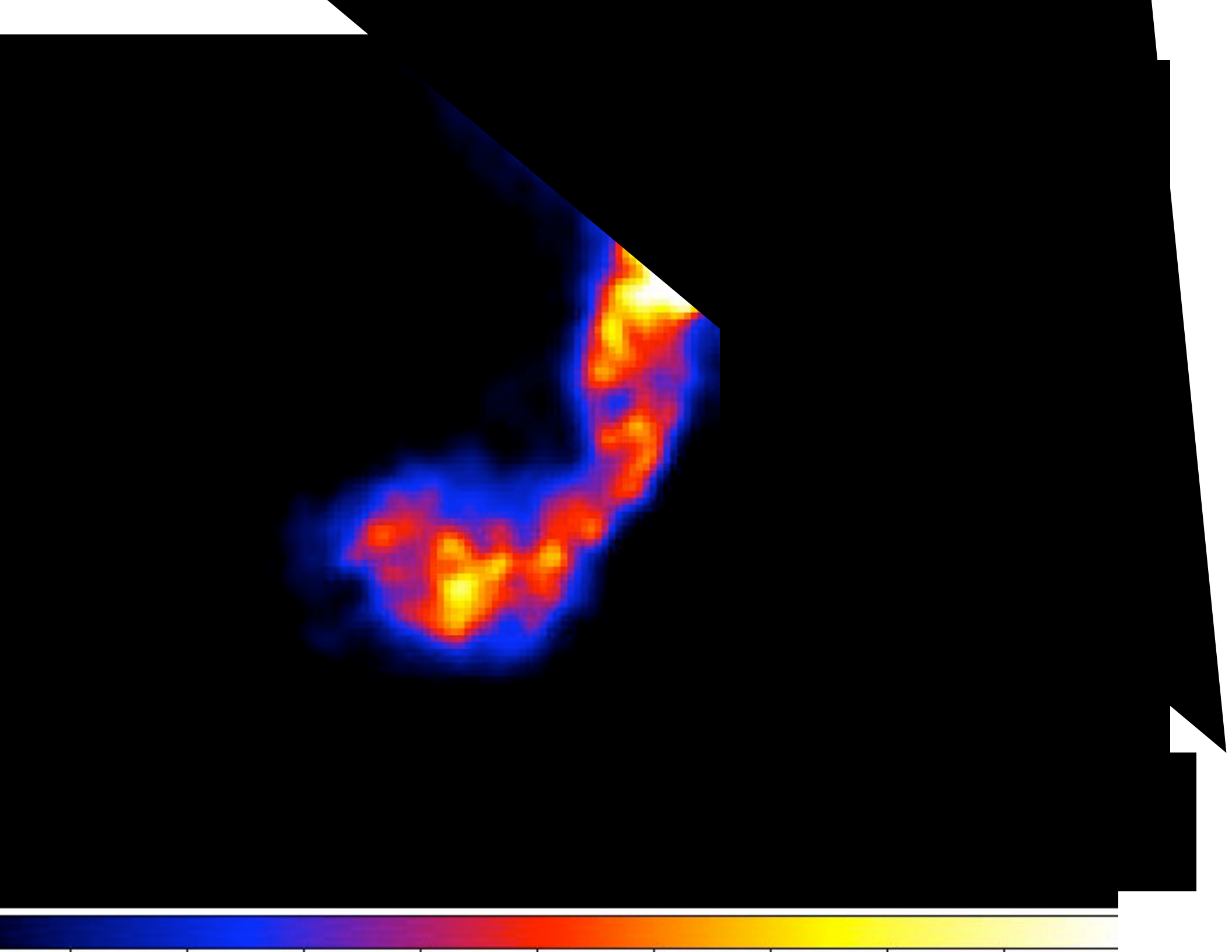

AGILE DISCOVERY OF THE CRAB NEBULA VARIABILITY IN GAMMA-RAYS

Tavani et al., Science, 331, 736 (2011)

Abdo et al., Science, 331, 739 (2011)

The Crab Nebula: a standard candle…

FIRST PUBLIC ANNOUNCEMENT Sept. 22, 2010: AGILE issues the Astronomer's Telegram n. 2855

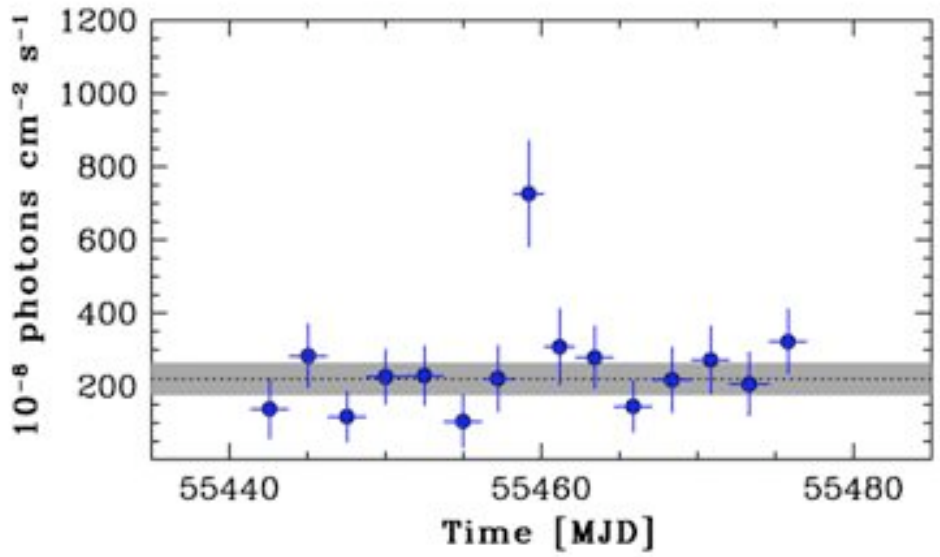

***Science Express* (6 January 2011)**

Crab Nebula

AGILE-GRID spectrum at the peak (2 days)

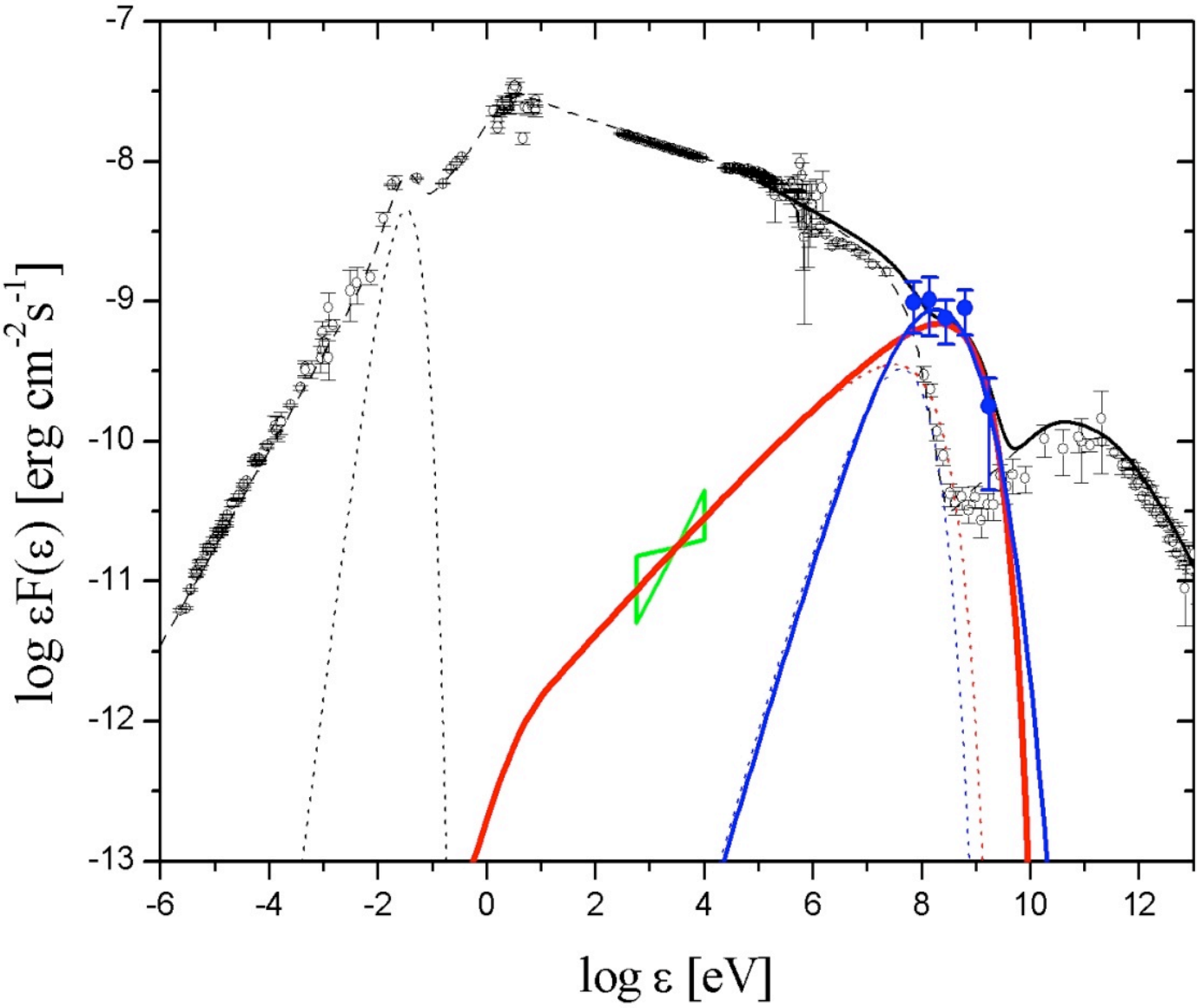

Fermi-LAT spectrum (4-day integration for Sept. 2010)

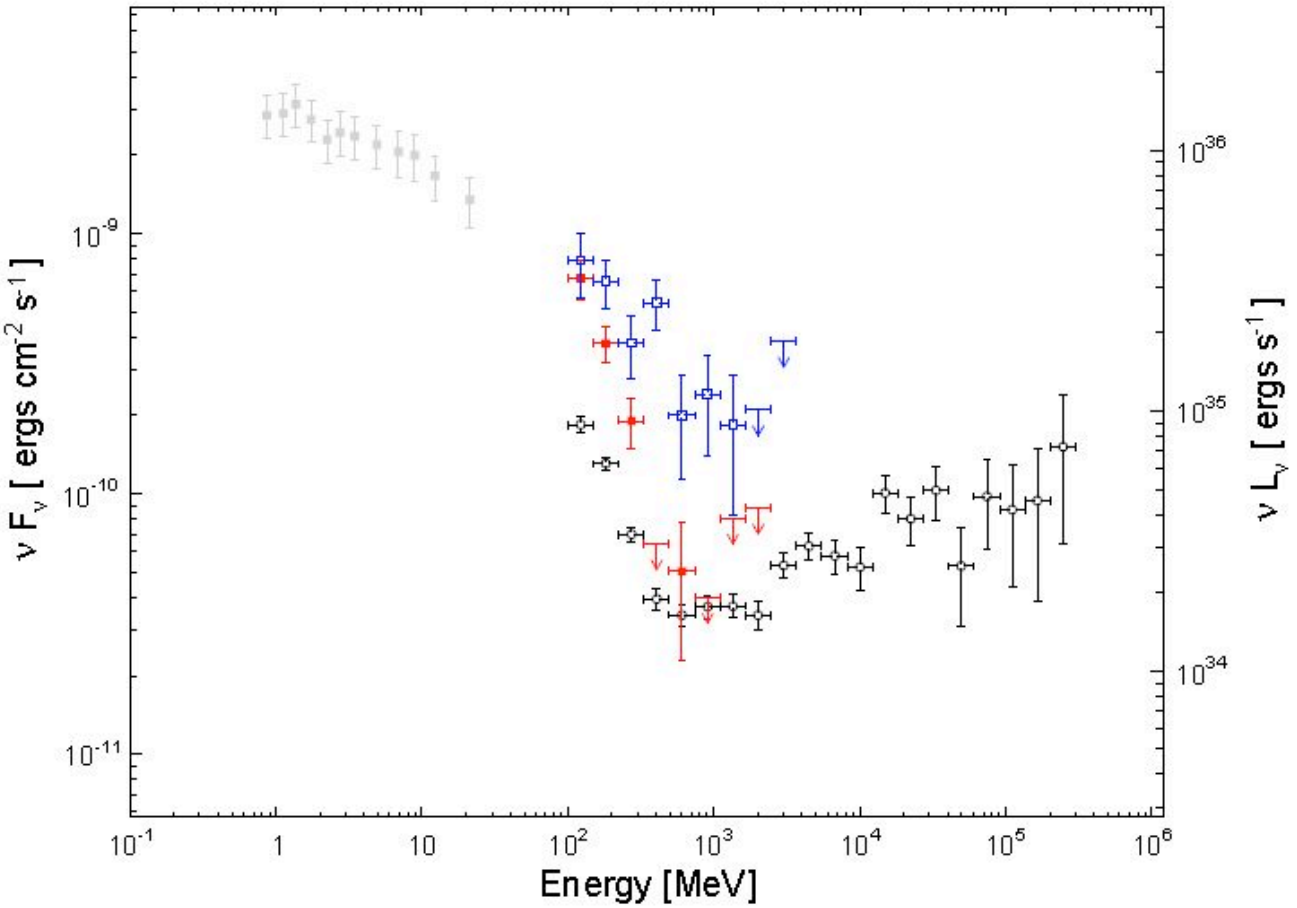

Figure 1: Spectral energy distribution of the Crab Nebula. Black open circles show the average spectrum measured by the LAT in the first 25 months of observations. Red boxes show the energy spectrum during the flare of February 2009 (MJD 54857.73-54873.73) and blue open boxes the spectrum in September 2010 (MJD 55457.73-55461.73). Gray boxes show historical data from the COMPTEL telescope (*39*). Arrows indicate 95% confidence flux limits.

post-flare excitement

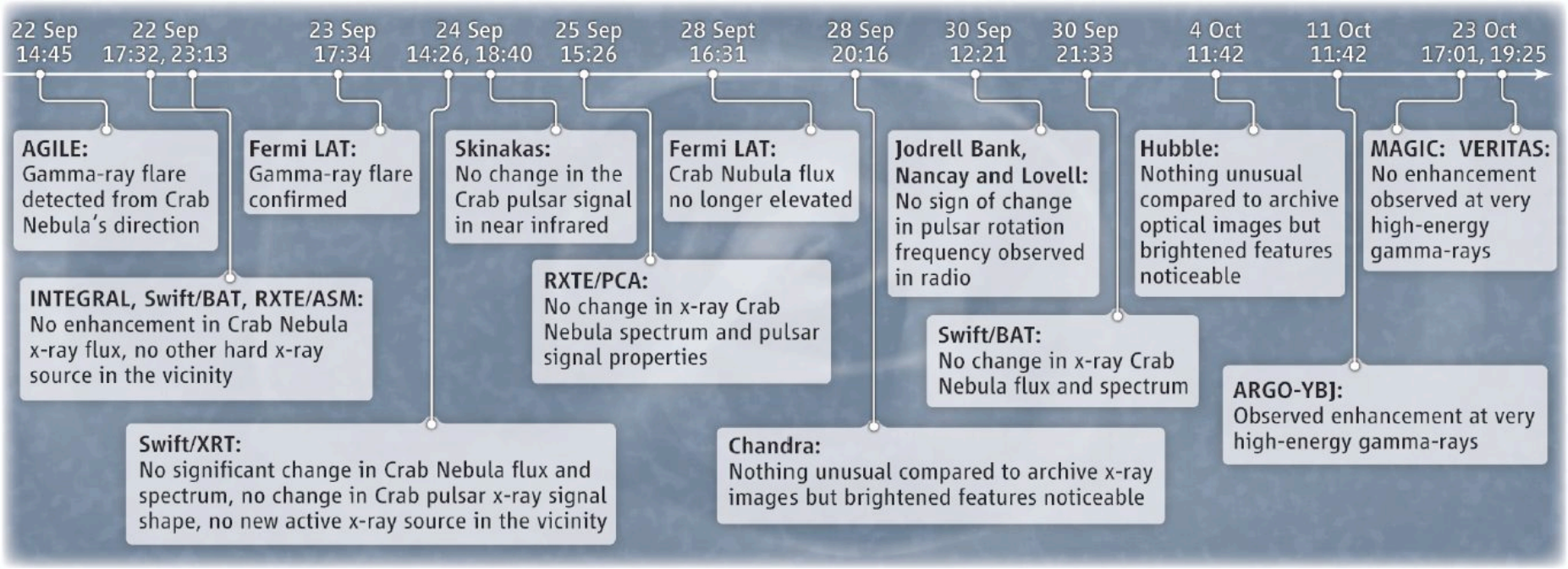

Bernardini E., 2011

- **Four major gamma-ray flaring episodes**

Flare date	Duration	Peak γ-ray flux	Instruments
October 2007	~ 15 days	~ 9 $\cdot 10^{-6}$ ph cm^{-2} s^{-1}	AGILE
February 2009	~ 15 days	~ 7 $\cdot 10^{-6}$ ph cm^{-2} s^{-1}	*Fermi*
September 2010	~ 4 days	~ 7 $\cdot 10^{-6}$ ph cm^{-2} s^{-1}	AGILE, *Fermi*
April 2011	~ 10 days	~ 30 $\cdot 10^{-6}$ ph cm^{-2} s^{-1}	AGILE, *Fermi*

major flare rate: 1-2/year

AGILE, 26 Nov. – 13 Oct. 2007

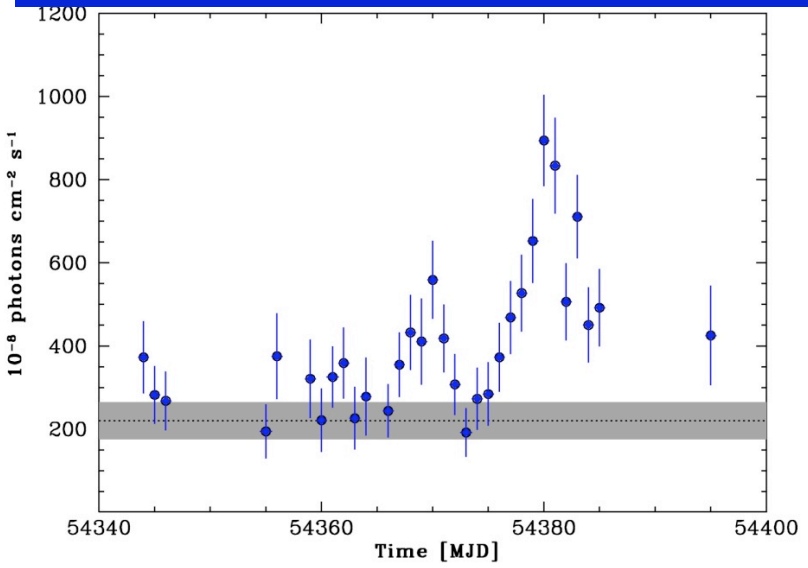

Fermi-LAT, 26 Jan. – 11 Feb. 2009

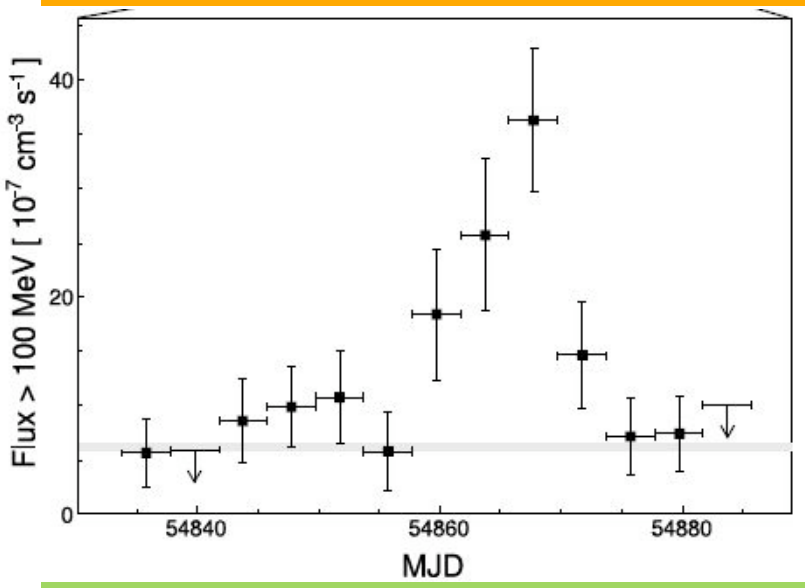

AGILE, 20-22 Sept. 2010

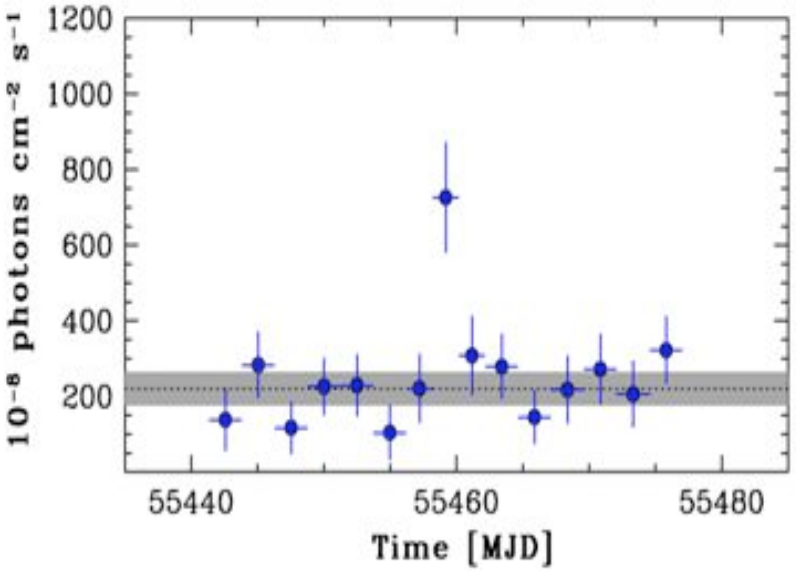

Fermi-AGILE, 12 – 20 Apr. 2011

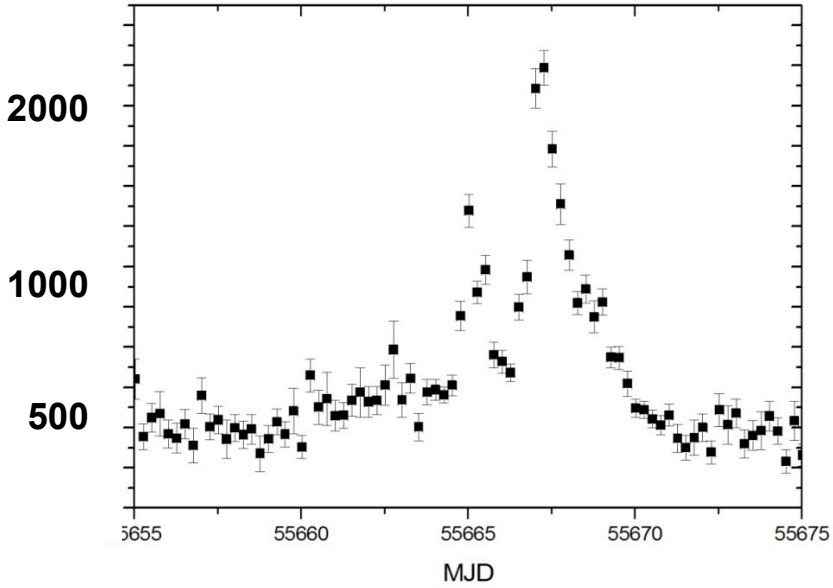

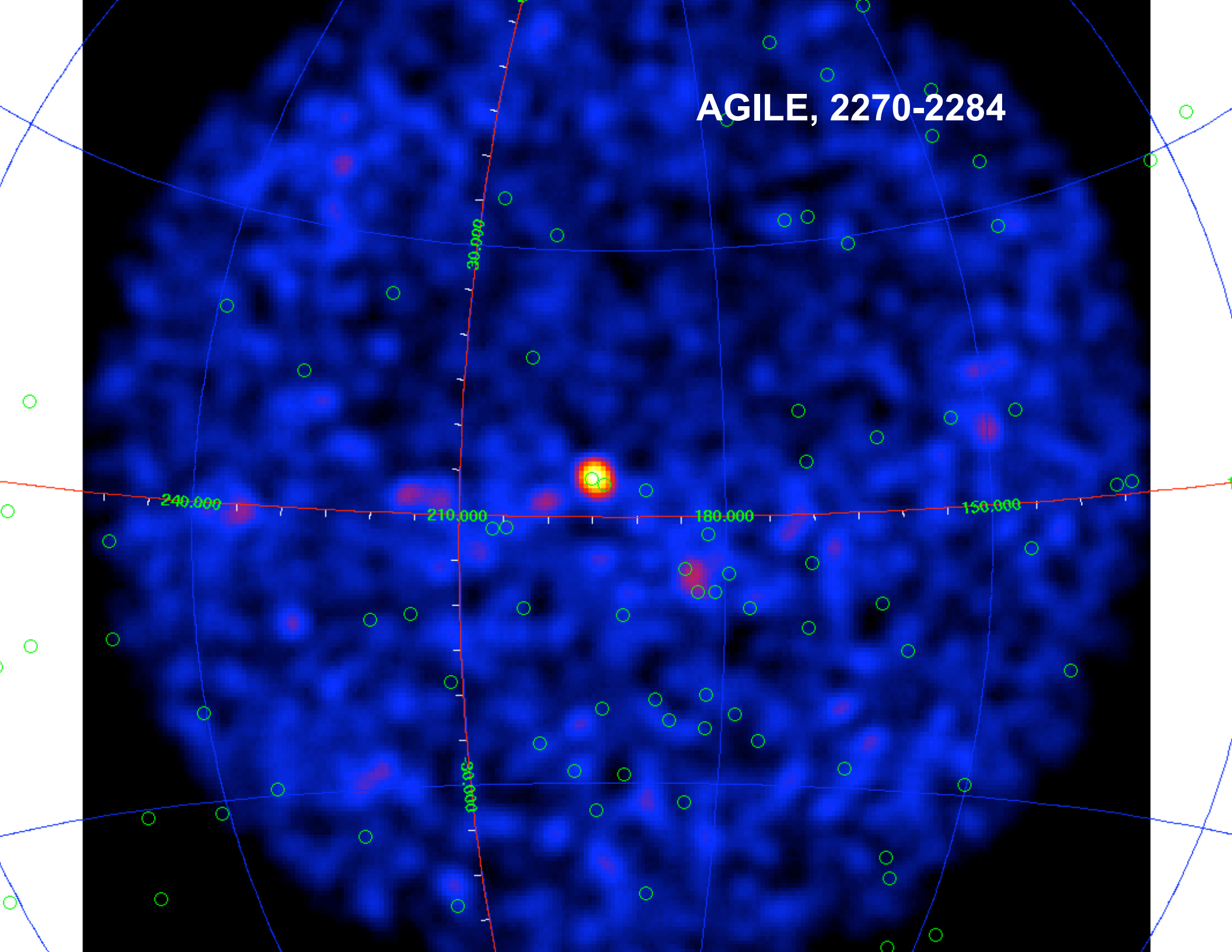
AGILE, 2270-2284
30.000
240.000
210.000
180.000
150.000
-30.000

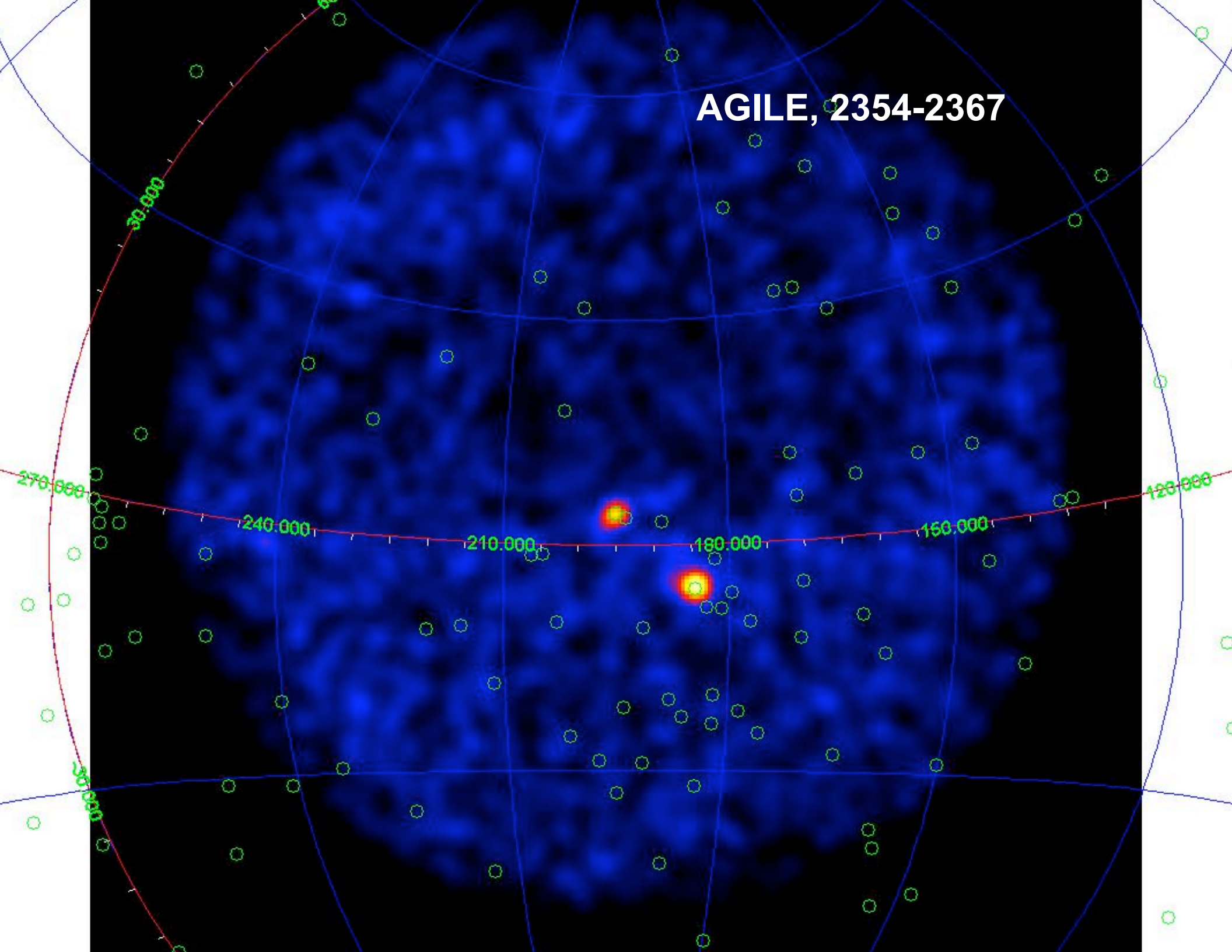
AGILE, 2354-2367
30.000
270.000
240.000
210.000
180.000
150.000
120.000
-30.000

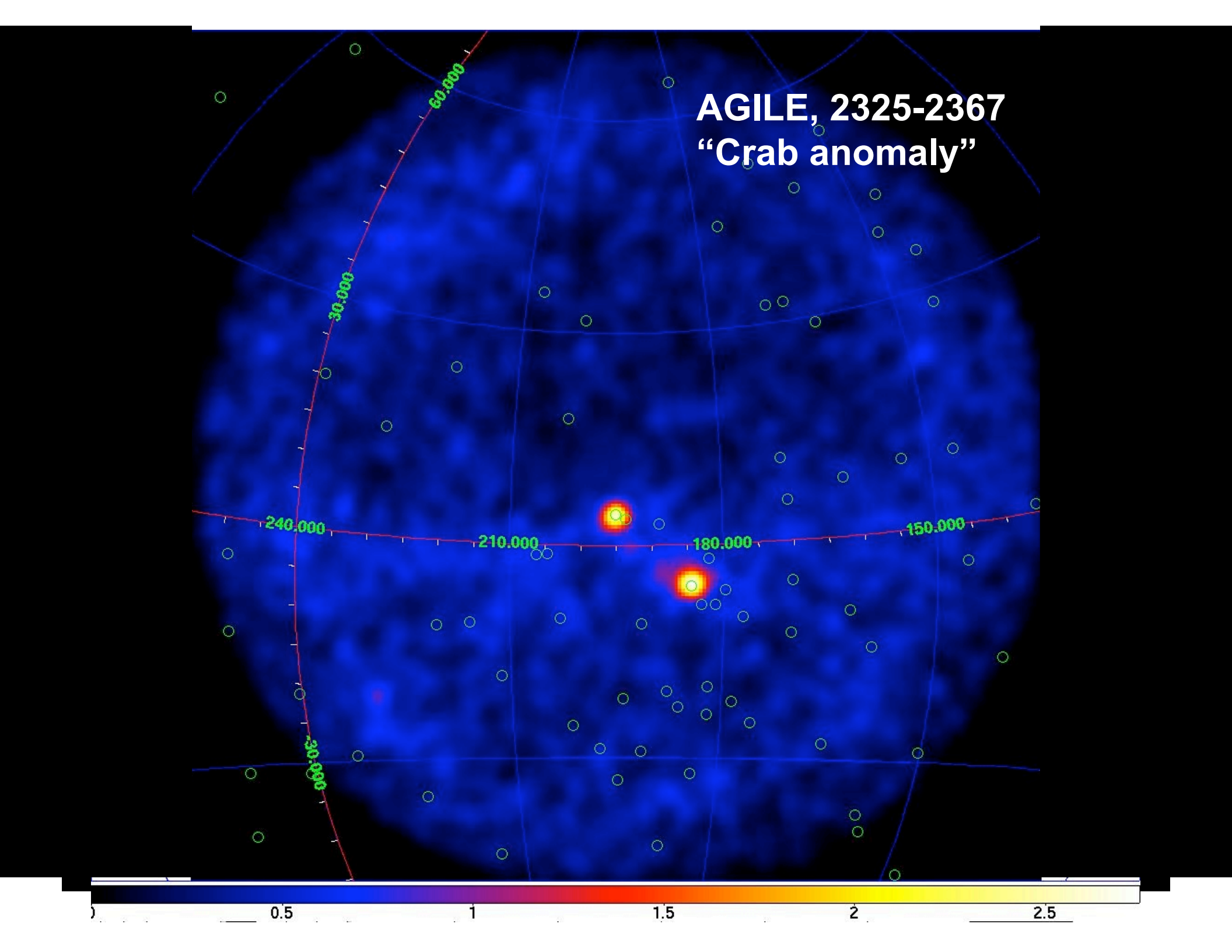
AGILE, 2325-2367
“Crab anomaly”
60.000
30.000
-30.000
240.000
210.000
180.000
150.000
0.5
1
1.5
2
2.5

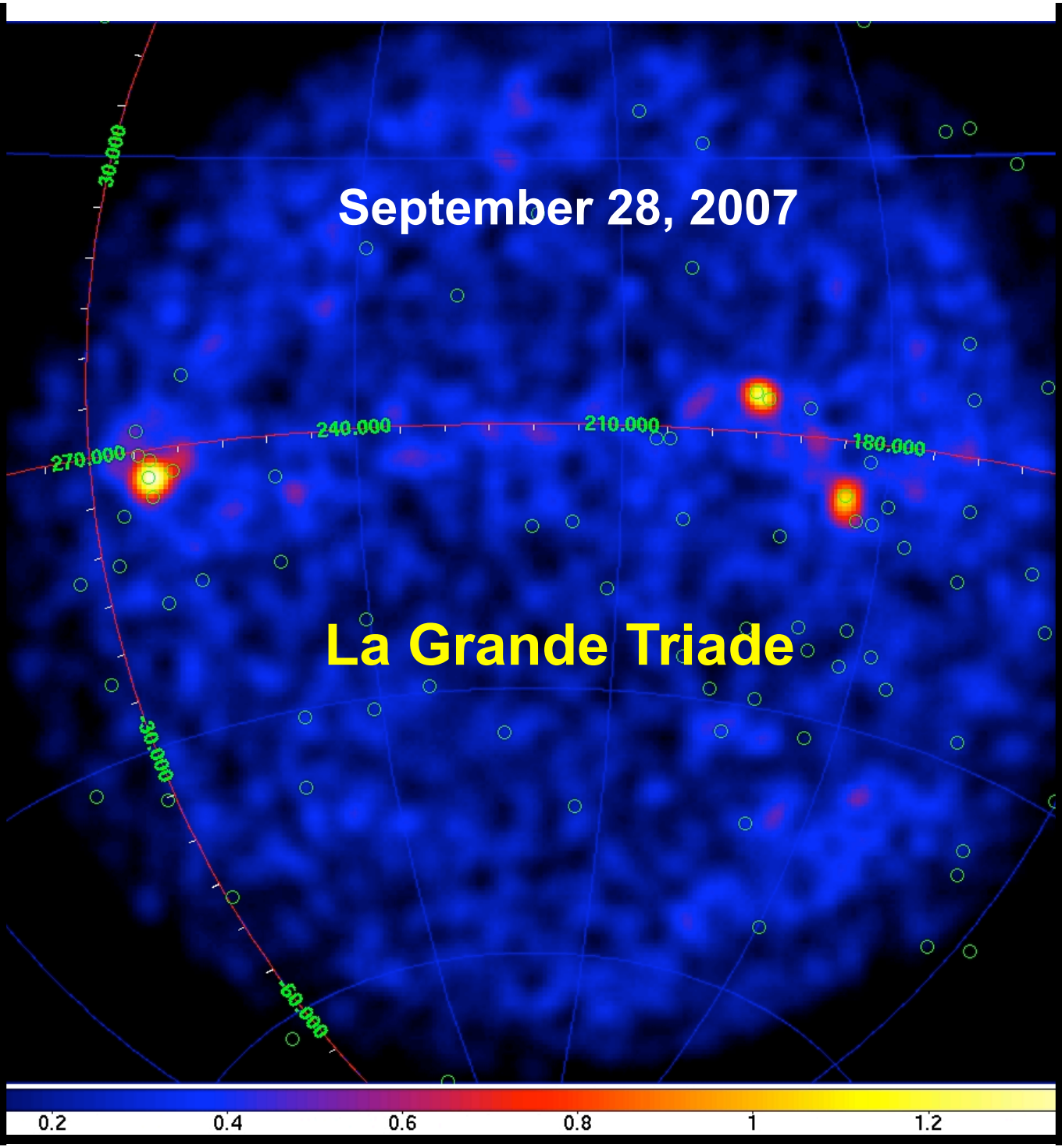
September 28, 2007
La Grande Triade
30.000
240.000
210.000
180.000
270.000
-30.000
-60.000
0.2
0.4
0.6
0.8
1
1.2

A&A 502, 995–1013 (2009)
DOI: 10.1051/0004-6361/200810527

Astronomy & Astrophysics

The AGILE Mission

M. Tavani[1,2,3], G. Barbiellini[3,4,5], A. Argan[1], F. Boffelli[13], A. Bulgarelli[8], P. Caraveo[6], P. W. Cattaneo[13], A. W. Chen[3,6], V. Cocco[2], E. Costa[1], F. D'Ammando[1,2], E. Del Monte[1], G. De Paris[1], G. Di Cocco[8], G. Di Persio[1], I. Donnarumma[1], Y. Evangelista[1], M. Feroci[1], A. Ferrari[3,16], M. Fiorini[6], F. Fornari[6], F. Fuschino[8], T. Froysland[3,7], M. Frutti[1], M. Galli[9], F. Gianotti[8], A. Giuliani[3,6], C. Labanti[8], I. Lapshov[1,15], F. Lazzarotto[1], F. Liello[5], P. Lipari[10,11], F. Longo[4,5], E. Mattaini[6], M. Marisaldi[8], M. Mastropietro[24], A. Mauri[8], F. Mauri[13], S. Mereghetti[6], E. Morelli[8], A. Morselli[7], L. Pacciani[1], A. Pellizzoni[6], F. Perotti[6], G. Piano[1], P. Picozza[2,7], C. Pontoni[3,5], G. Porrovecchio[1], M. Prest[5], G. Pucella[1], M. Rapisarda[12], A. Rappoldi[13], E. Rossi[8], A. Rubini[1], P. Soffitta[1], A. Traci[8], M. Trifoglio[8], A. Trois[1], E. Vallazza[5], S. Vercellone[6], V. Vittorini[1,3], A. Zambra[3,6], D. Zanello[10,11], C. Pittori[14], B. Preger[14], P. Santolamazza[14], F. Verrecchia[14], P. Giommi[14], S. Colafrancesco[14], A. Antonelli[17], S. Cutini[14], D. Gasparrini[14], S. Stellato[14], G. Fanari[14], R. Primavera[14], F. Tamburelli[14], F. Viola[18], G. Guarrera[18], L. Salotti[18], F. D'Amico[18], E. Marchetti[18], M. Crisconio[18], P. Sabatini[19], G. Annoni[19], S. Alia[19], A. Longoni[19], R. Sanquerin[19], M. Battilana[19], P. Concari[19], E. Dessimone[19], R. Grossi[19], A. Parise[19], F. Monzani[20], E. Artina[20], R. Pavesi[20], G. Marseguerra[20], L. Nicolini[20], L. Scandelli[20], L. Soli[20], V. Vettorello[20], E. Zardetto[20], A. Bonati[20], L. Maltecca[20], E. D'Alba[20], M. Patané[20], G. Babini[21], F. Onorati[21], L. Acquaroli[21], M. Angelucci[21], B. Morelli[21], C. Agostara[21], M. Cerone[22], A. Michetti[22], P. Tempesta[22], S. D'Eramo[22], F. Rocca[22], F. Giannini[22], G. Borghi[23], B. Garavelli[25], M. Conte[20], M. Balasini[20], I. Ferrario[25], M. Vanotti[25], E. Collavo[25], and M. Giacomazzo[25]

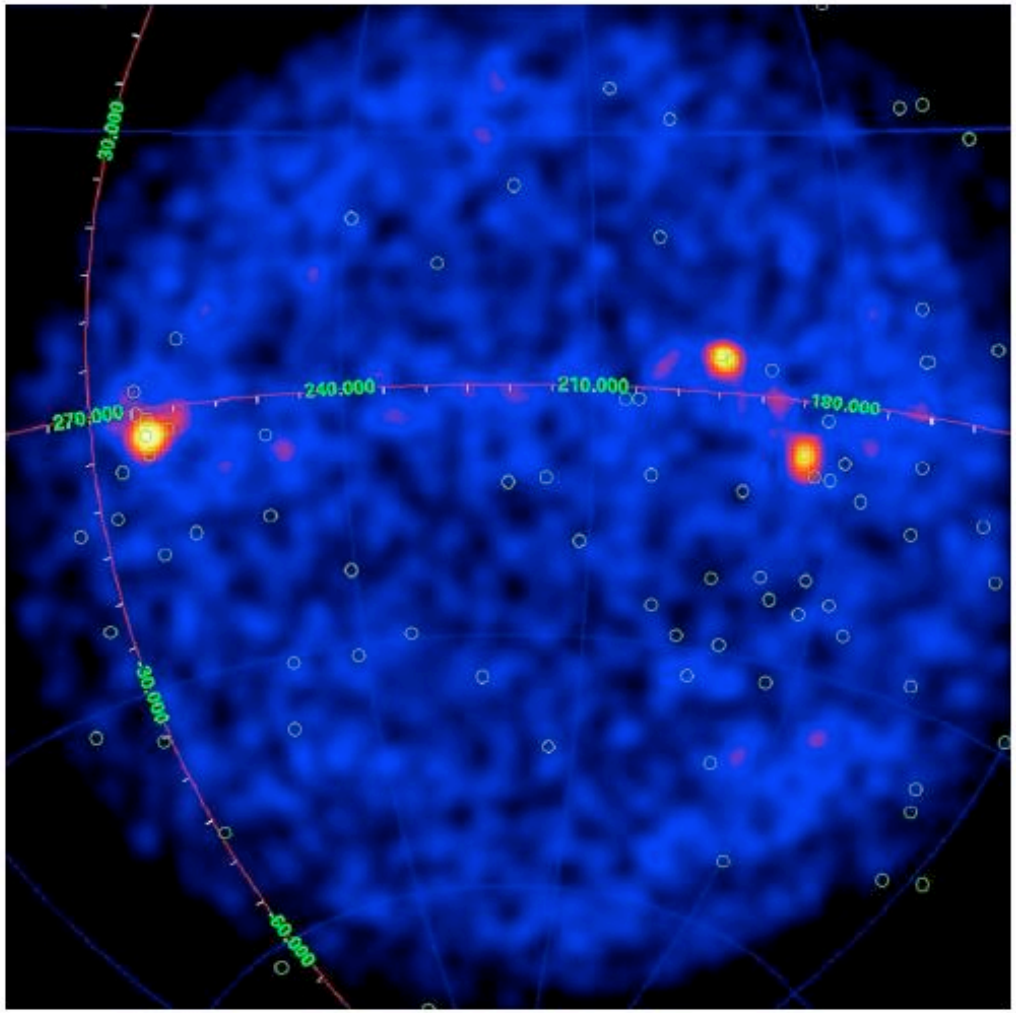

Fig. 25. The AGILE-GRID 1-day gamma-ray counts map for photons above 100 MeV obtained on 2007 September 28. The unprecedently large FOV includes for the first time in a single map all three of the most important gamma-ray pulsars: Vela, Crab, and Geminga.

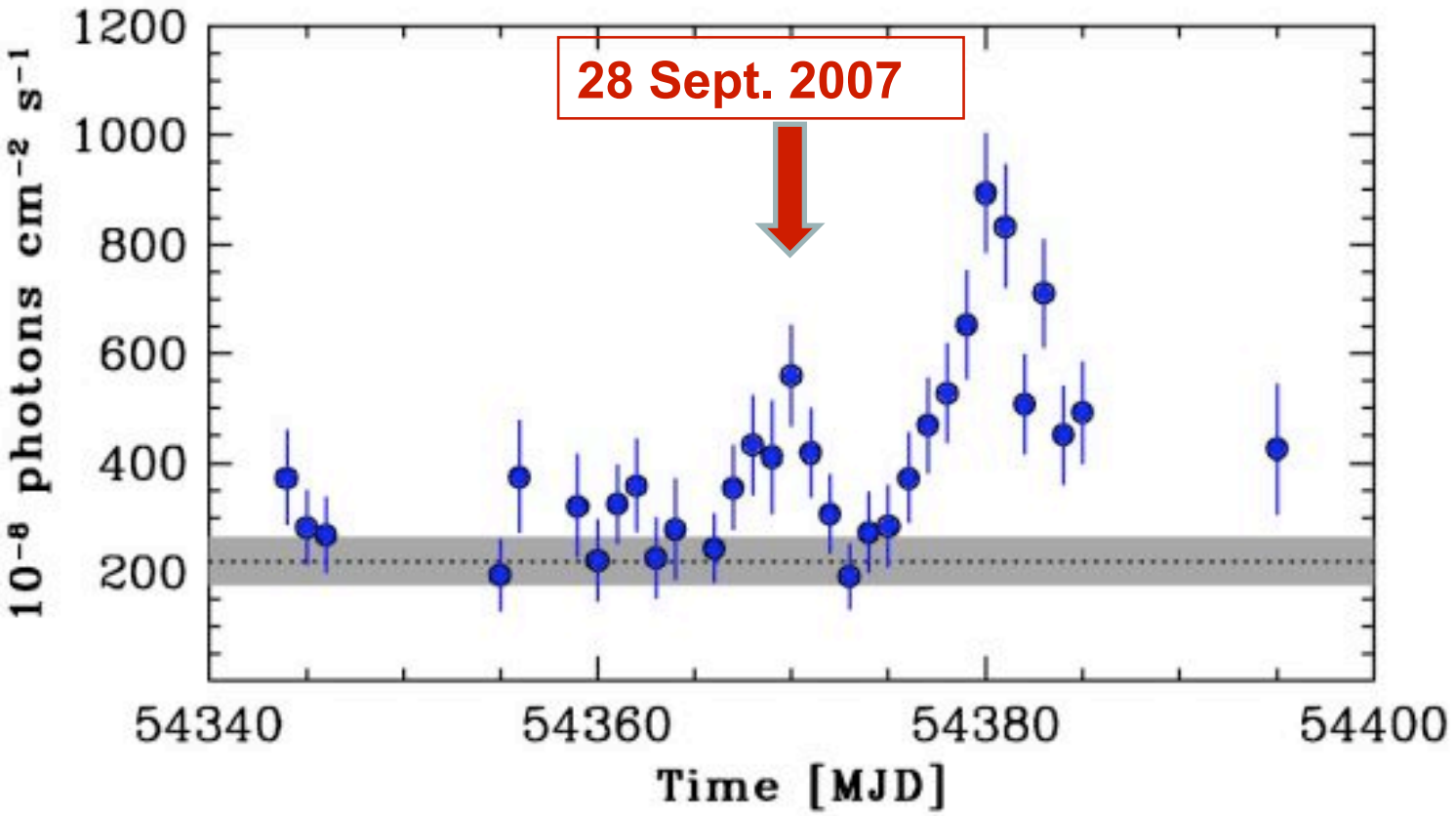
28 Sept. 2007
1200
1000
800
600
400
200
10^{-8} photons cm^{-2} s^{-1}
54340
54360
54380
54400
Time [MJD]

A&A 506, 1563–1574 (2009)
DOI: 10.1051/0004-6361/200911783

Astronomy & Astrophysics

First AGILE catalog of high-confidence gamma-ray sources

C. Pittori[1], F. Verrecchia[1], A. W. Chen[2,3], A. Bulgarelli[4], A. Pellizzoni[5], A. Giuliani[2,3], S. Vercellone[6], F. Longo[7,8], M. Tavani[9,10,11,3], P. Giommi[1,12], G. Barbiellini[7,8,3], M. Trifoglio[4], F. Gianotti[4], A. Argan[9], A. Antonelli[13], F. Boffelli[14], P. Caraveo[2], P. W. Cattaneo[14], V. Cocco[10], S. Colafrancesco[1,12], T. Contessi[2], E. Costa[9], S. Cutini[1], F. D'Ammando[9,10], E. Del Monte[9], G. De Paris[9], G. Di Cocco[4], G. Di Persio[9], I. Donnarumma[9], Y. Evangelista[9], G. Fanari[1], M. Feroci[9], A. Ferrari[3,15], M. Fiorini[2], F. Fornari[2], F. Fuschino[4], T. Froysland[3,11], M. Frutti[9], M. Galli[16], D. Gasparrini[1], C. Labanti[4], I. Lapshov[9,17], F. Lazzarotto[9], F. Liello[9], P. Lipari[18,19], E. Mattaini[2], M. Marisaldi[4], M. Mastropietro[9,21], A. Mauri[4], F. Mauri[14], S. Mereghetti[2], E. Morelli[4], E. Moretti[7,8], A. Morselli[11], L. Pacciani[9], F. Perotti[2], G. Piano[9,10,11], P. Picozza[10,11], M. Pilia[22,2,5], C. Pontoni[3,8], G. Porrovecchio[9], B. Preger[1], M. Prest[8,22], R. Primavera[1], G. Pucella[9], M. Rapisarda[20], A. Rappoldi[14], E. Rossi[4], A. Rubini[9], S. Sabatini[10], P. Santolamazza[1], E. Scalise[9], P. Soffitta[9], S. Stellato[1], E. Striani[10], F. Tamburelli[1], A. Traci[4], A. Trois[9], E. Vallazza[8], V. Vittorini[9,3], A. Zambra[2,3], D. Zanello[18,19], and L. Salotti[12]

1AGL J0535+2205 and 1AGL J0634+1748 (Crab and Geminga). These two well known strong γ-ray pulsars, together with the Vela pulsar, were used for in-flight AGILE calibrations. We report the flux values obtained during calibration subperiods. These values agree with pulsed flux values reported in (Pellizzoni et al. 2009). We note, however, that we observed higher flux values, over 1σ from the reported mean flux, for both sources when merging all the data, including shorter (1 day) integration periods during 2007. This point is under investigation.

1AGL J0617+2236. This AGILE detection provides an improved positioning compared to the 3EG J0617+2238 error box. This source is positionally coincident with the SNR IC443 (Tavani et al. 2009c). The AGILE error box also contains the PSR J0614+2229.

1AGL J0657+4554 and 1AGL J0714+3340. These two high-

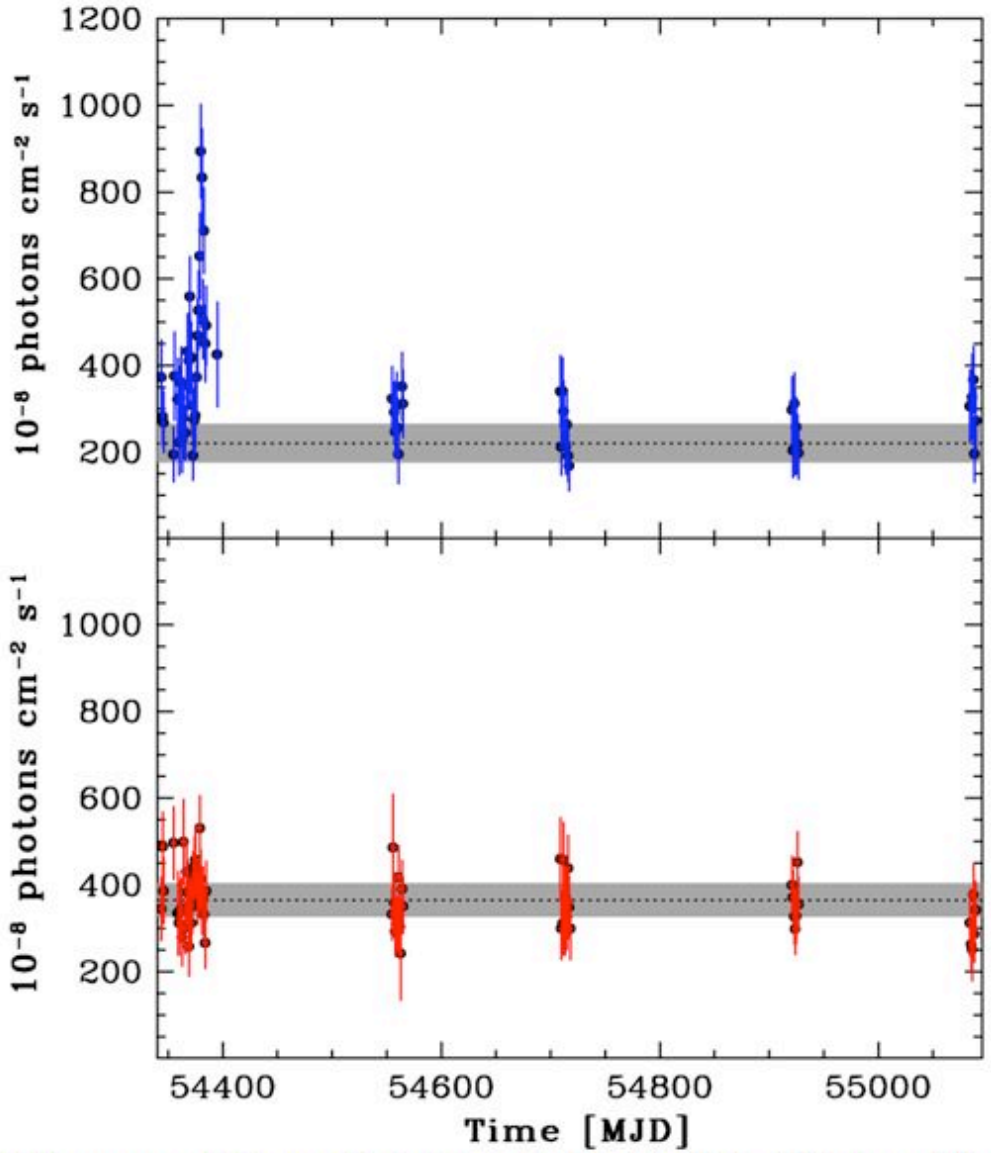

Fig. S1 – The AGILE gamma-ray light curve (1-day binning) of the Crab Pulsar/Nebula and Geminga above 100 MeV during the period **2007-09-01 – 2009-09-15** with the satellite pointing **within 35 degrees** from the source. Gaps in the light curve are due to the satellite pointing at fields different from the Crab region.

the Crab “anomaly”

- internally, since October 2007 the AGILE team discussed the anomaly tens of times because of calibration issues

- very serious problems in calibration if the anomalous 15 days were inserted !

- many internal AGILE documents showing the analyses and cure.

AGILE Discovery of Crab Nebula Variability: a Chronology

- April 2007: AGILE launch.
- October 2007: AGILE detects the first “anomalous” gamma-ray flare from the Crab.
- Oct. 23, 2007: AGILE team meeting and first discussion of the Crab event (STAG n. 39 Minutes of Meeting).
- Sept. 2009: Pittori et al. *Astron. & Astrophys*., 509, 1563, 2009:“the anomalous flux from the Crab in Oct. 2007 is under investigation.”
- Sept. 19-21, 2010: detection of the second Crab γ-ray flare by the AGILE Alert System: **evidence for a repetitive phenomenon**.
- **Sept. 22, 2010: AGILE issues Astronomer’s Telegram 2855 announcing the discovery of a γ-ray flare from the Crab.**
- **Sept. 23, 2010: *Fermi* issues ATel 2861 confirming the flare.**
- Sept. 28, 2010: first post-flare ***Chandra*** pointing.
- Oct. 2, 2010: ***Hubble*** points at the Crab; several **Swift** pointings

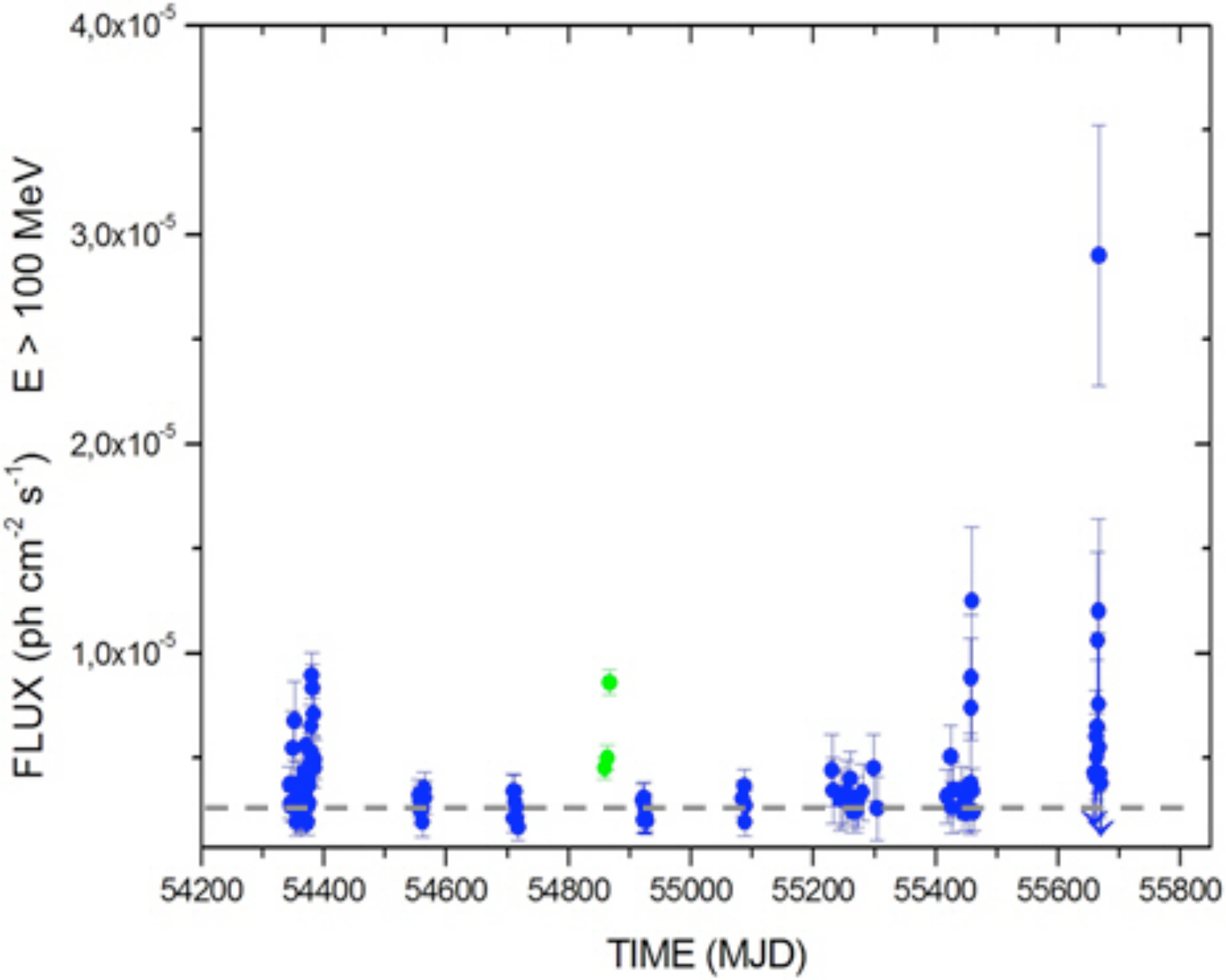
4,0x10-5
3,0x10-5
2,0x10-5
1,0x10-5
FLUX (ph cm-2 s-1) E > 100 MeV
54200
54400
54600
54800
55000
55200
55400
55600
55800
TIME (MJD)

Flare origin

- no noticeable PSR-signal variation with the current sampling, no post-flare variation
- **flare attributed to the Nebula**
- chance coincidence with another source ?
  - $F > 2 \cdot 10^{-6}$ ph cm^{-2} s^{-1}, few sources, $P < 6 \cdot 10^{-5}$
  - no known blazar in error box (0.06), X-ray observation 2 days after the Sept. Flare (ATEL 2868), $P < 10^{-4}$
  - “soft” average gamma-ray spectrum, very unusual, chance-coincidence P very small.

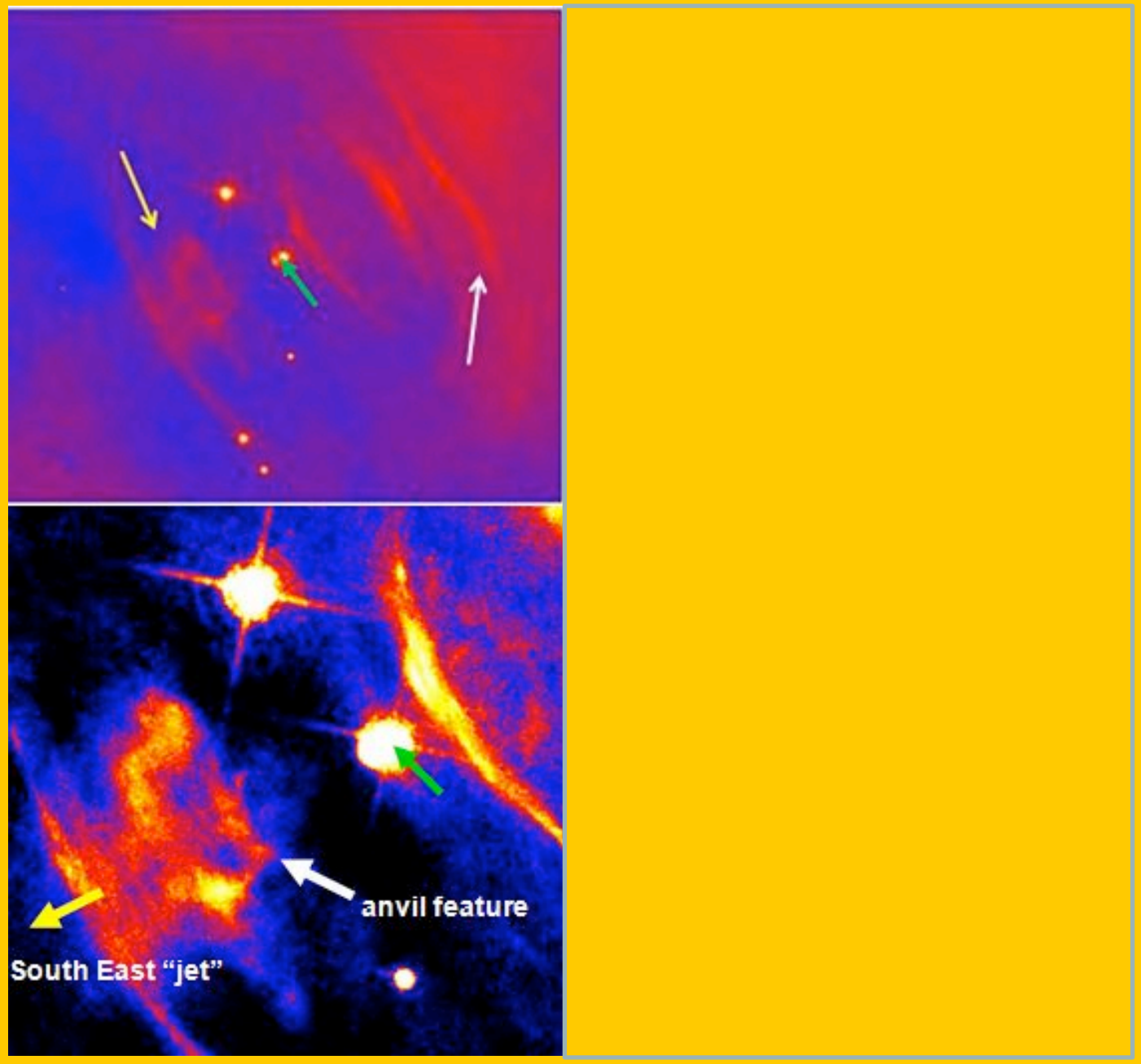
anvil feature
South East "jet"

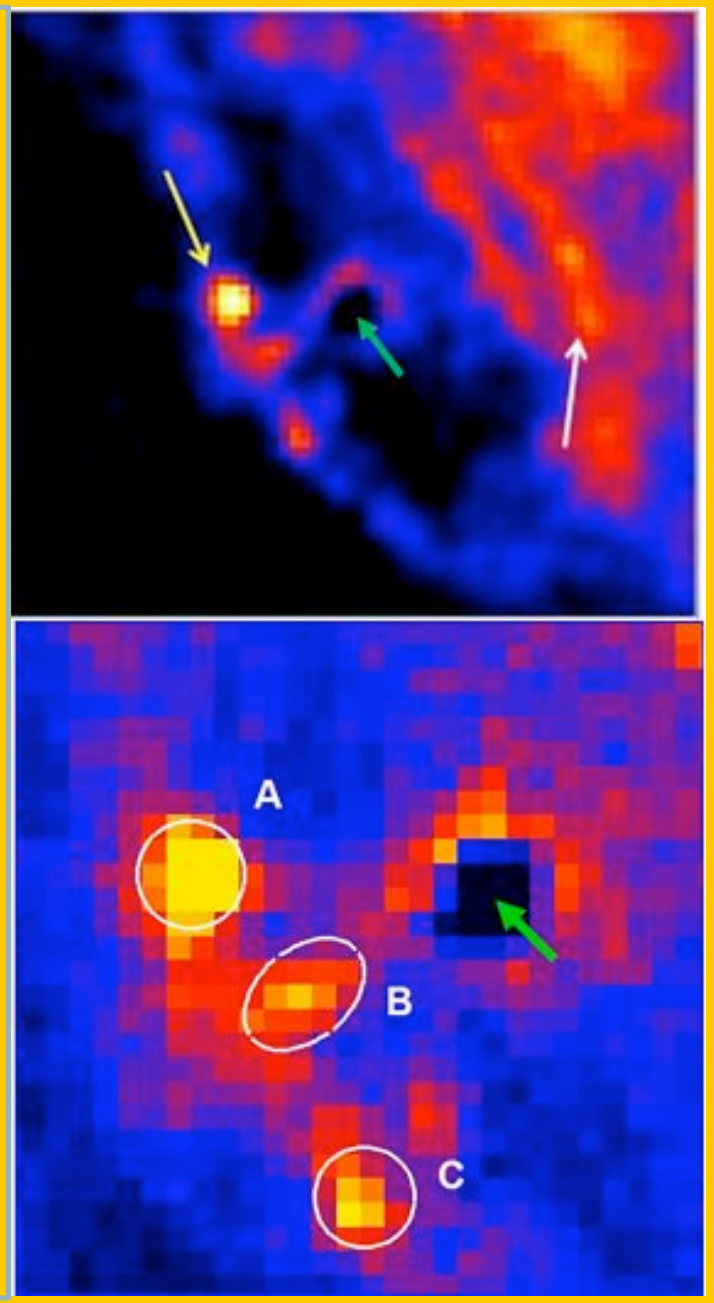
A
B
C

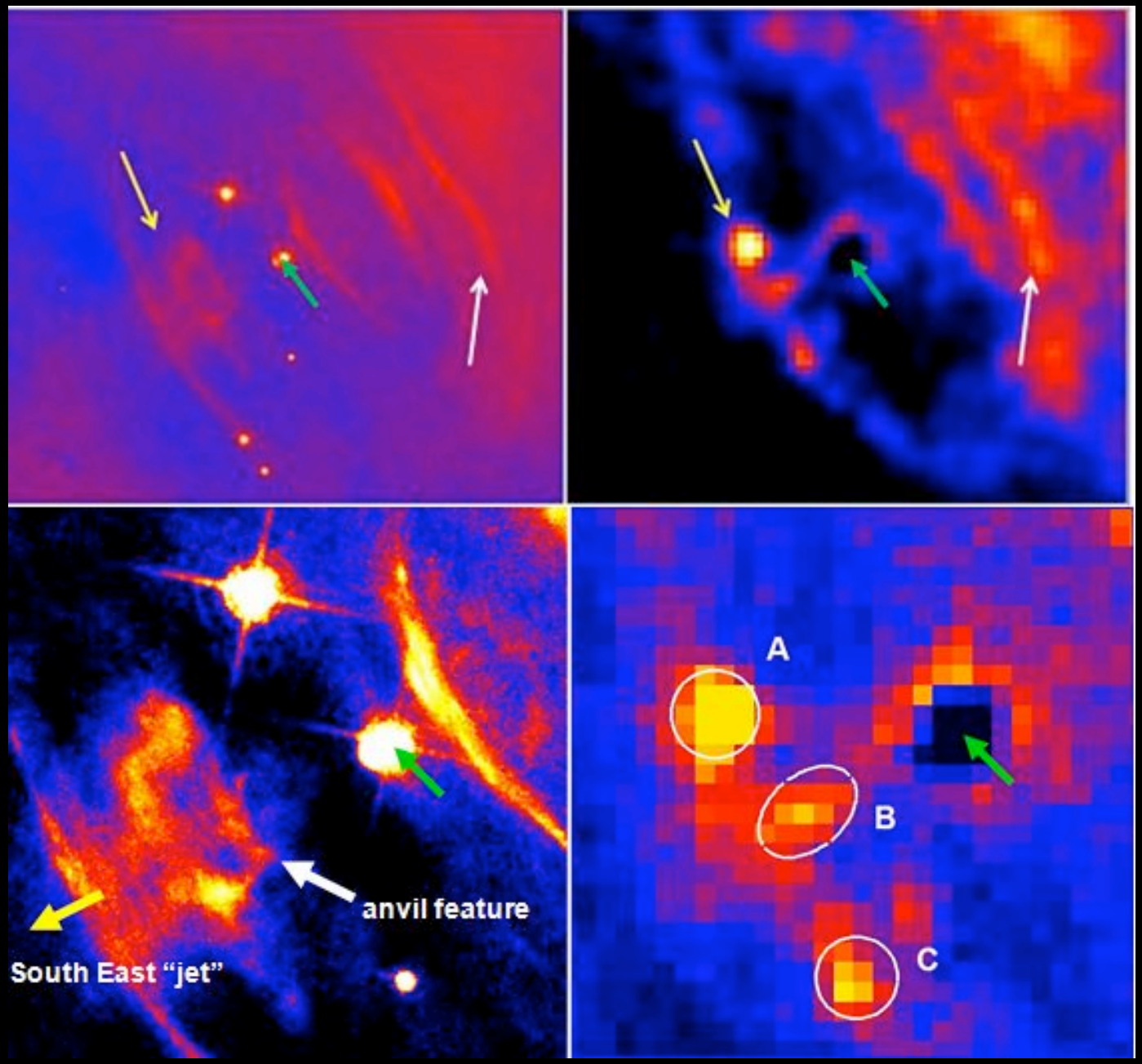
anvil feature
South East "jet"
A
B
C

a model (Vittorini V., M.T. et al., ApJ, accepted 2011)

- $dN(\gamma)/d\gamma = \gamma^{-p1}$ for $\gamma_{min} < \gamma < \gamma_{break}$
  with $p_1 = 2.1$, $\gamma_{min} = 5 \cdot 10^5$, $\gamma_{break} = 2 \cdot 10^9$
- $dN(\gamma)/d\gamma = \gamma^{-p2}$ for $\gamma_{break} < \gamma < \gamma_{max}$,
  with $p_2 = 2.7$,
- total particle number $N_{e-/e+} = 10^{42}$.
- size, Larmor radius $R \leq 10^{16}$ cm
- **local $B \approx 10^{-3}$ G**
- $\gamma_{max} \approx \gamma_{break} \leq 10^9 \, (E/B)(d\,\alpha'/\sin\theta)^{1/2} \, (B/10^{-3}\ G)^{-1/2}$
- **Doppler factor $\delta = 1$**

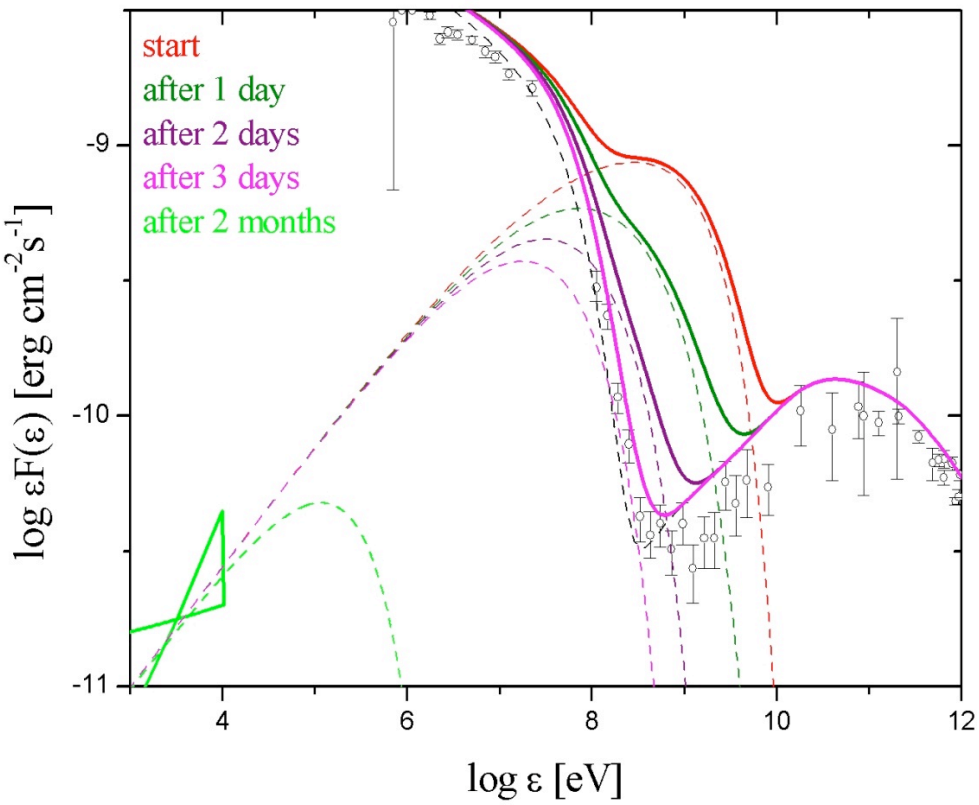
start
after 1 day
after 2 days
after 3 days
after 2 months
log εF(ε) [erg cm-2s-1]
-9
-10
-11
4
6
8
10
12
log ε [eV]

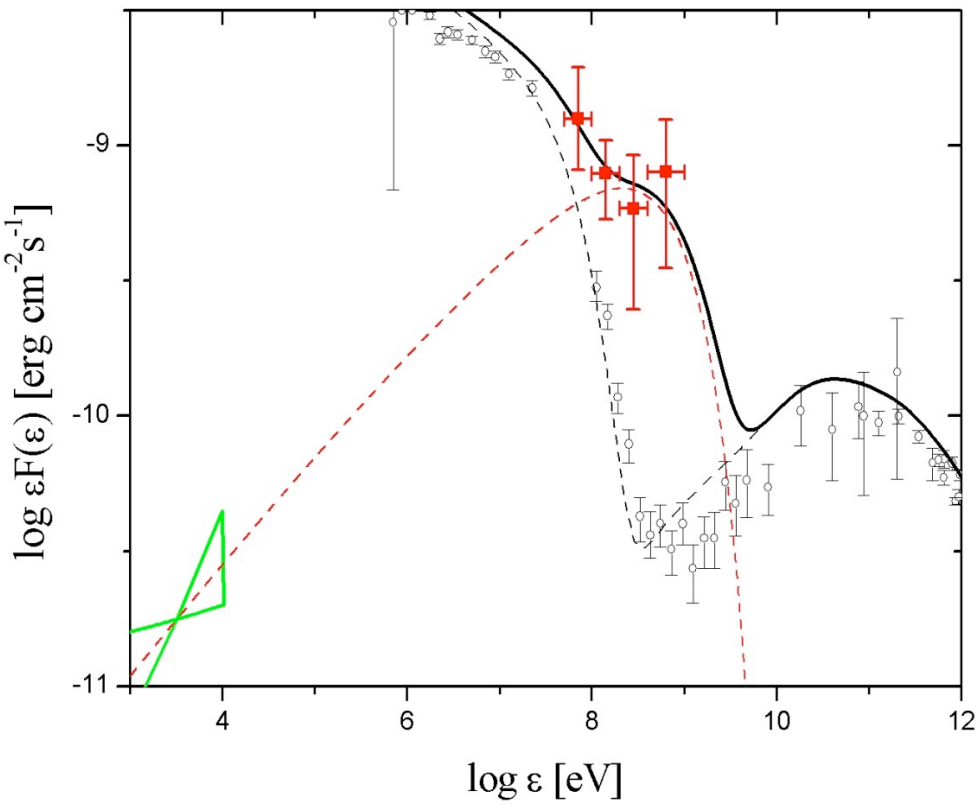
log εF(ε) [erg cm^{-2}s^{-1}]
-9
-10
-11
4
6
8
10
12
log ε [eV]

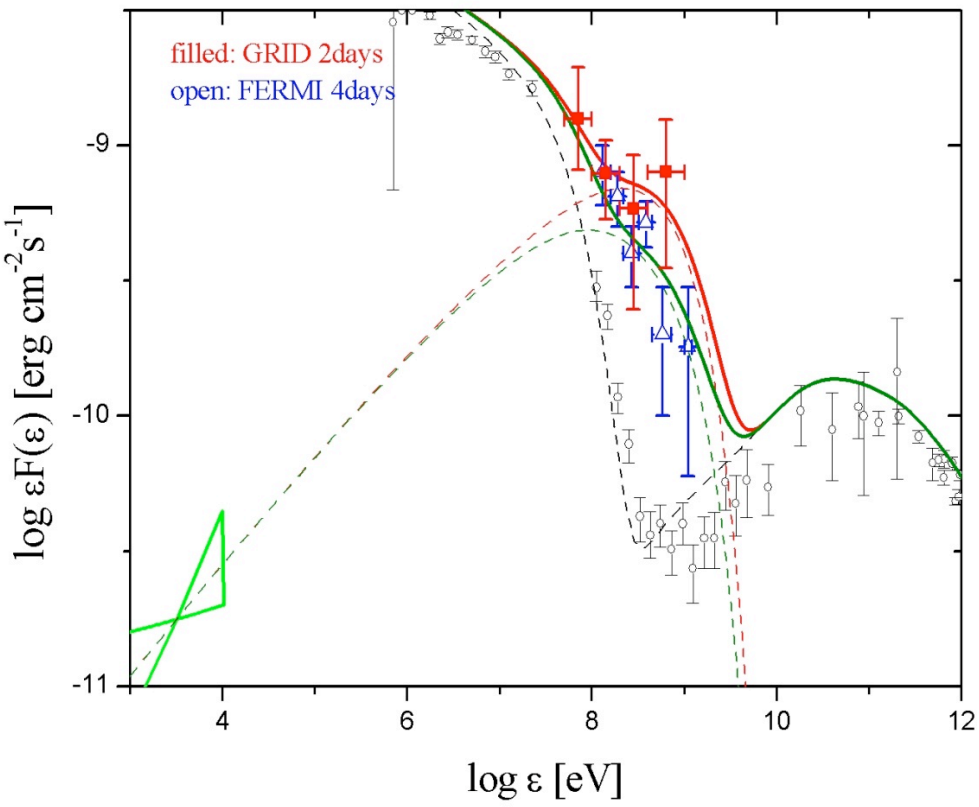
filled: GRID 2days
open: FERMI 4days
-9
-10
-11
4
6
8
10
12
log εF(ε) [erg cm-2s-1]
log ε [eV]

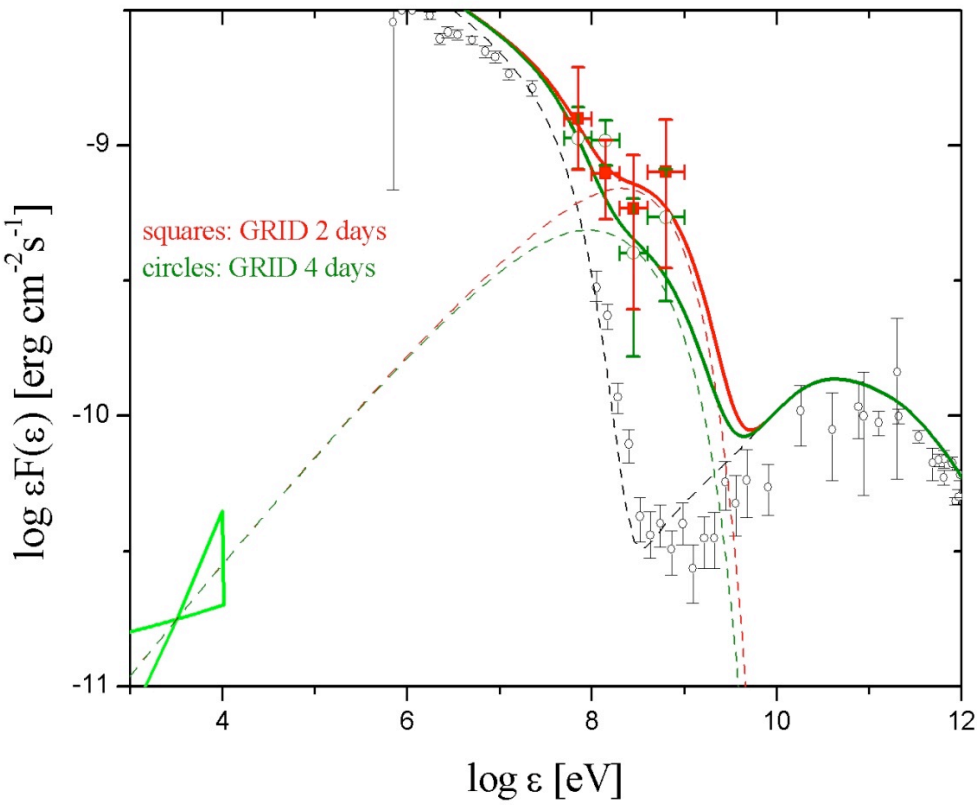
squares: GRID 2 days
circles: GRID 4 days
log εF(ε) [erg cm-2s-1]
log ε [eV]
-9
-10
-11
4
6
8
10
12

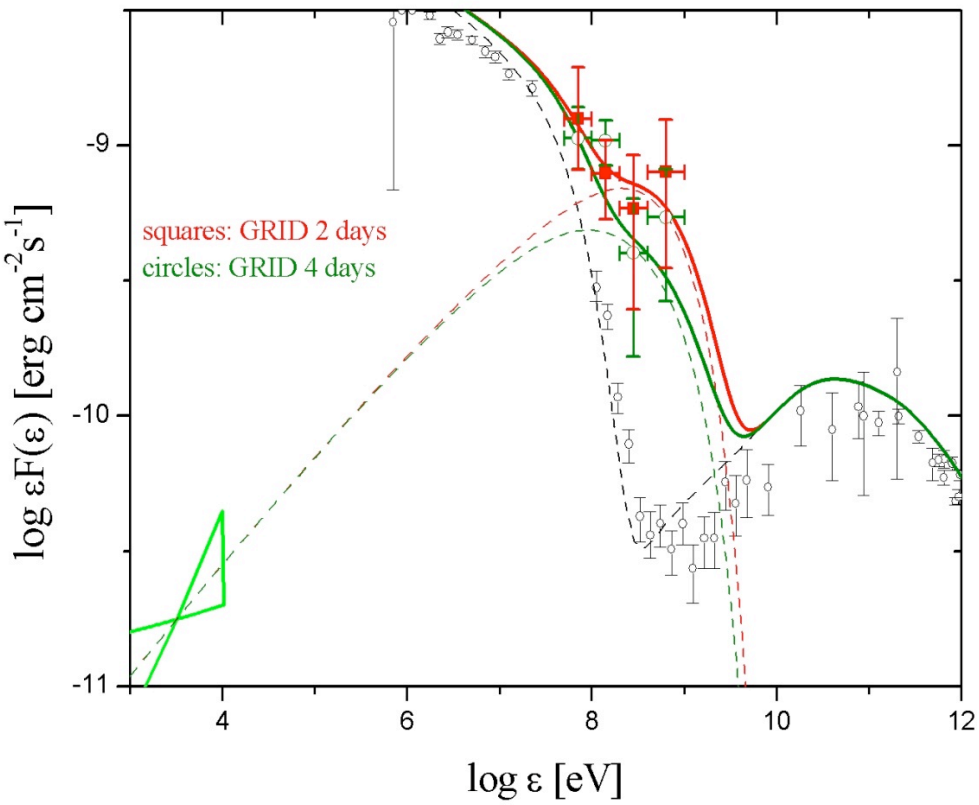
squares: GRID 2 days
circles: GRID 4 days
log εF(ε) [erg cm^{-2}s^{-1}]
log ε [eV]
-9
-10
-11
4
6
8
10
12

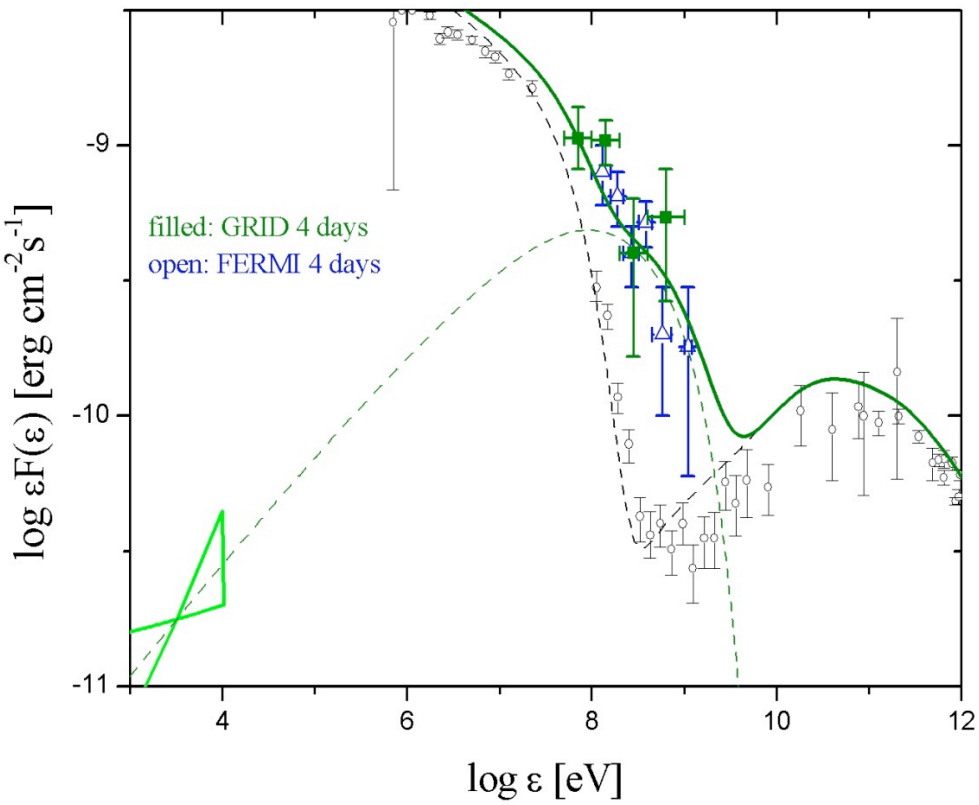
filled: GRID 4 days
open: FERMI 4 days
log εF(ε) [erg cm-2s-1]
log ε [eV]
-9
-10
-11
4
6
8
10
12

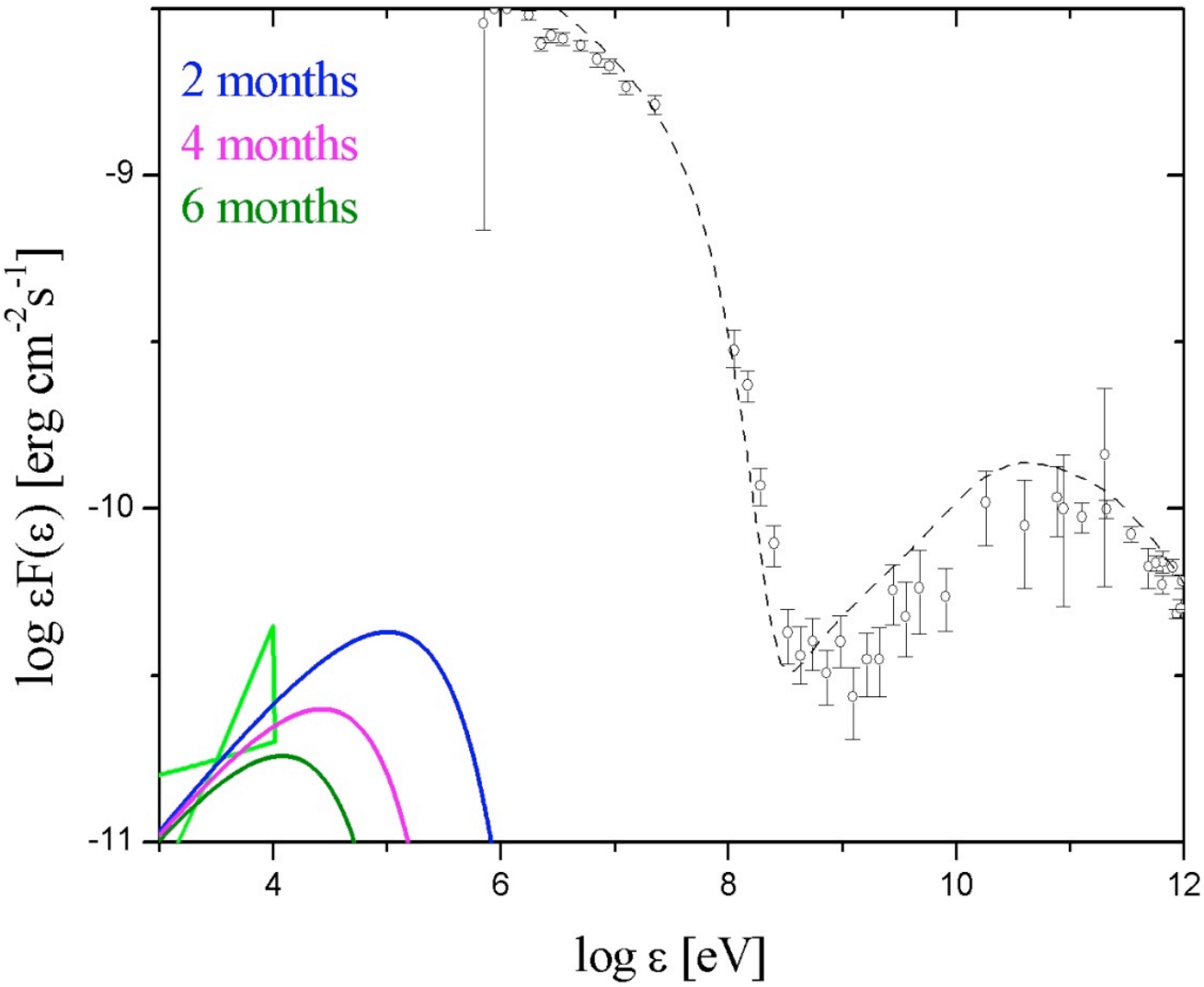
2 months
4 months
6 months
-9
-10
-11
4
6
8
10
12
log εF(ε) [erg cm-2s-1]
log ε [eV]

The Crab super-flare (12-18 April 2011)

AGILE monitoring of the Crab (April 2011)

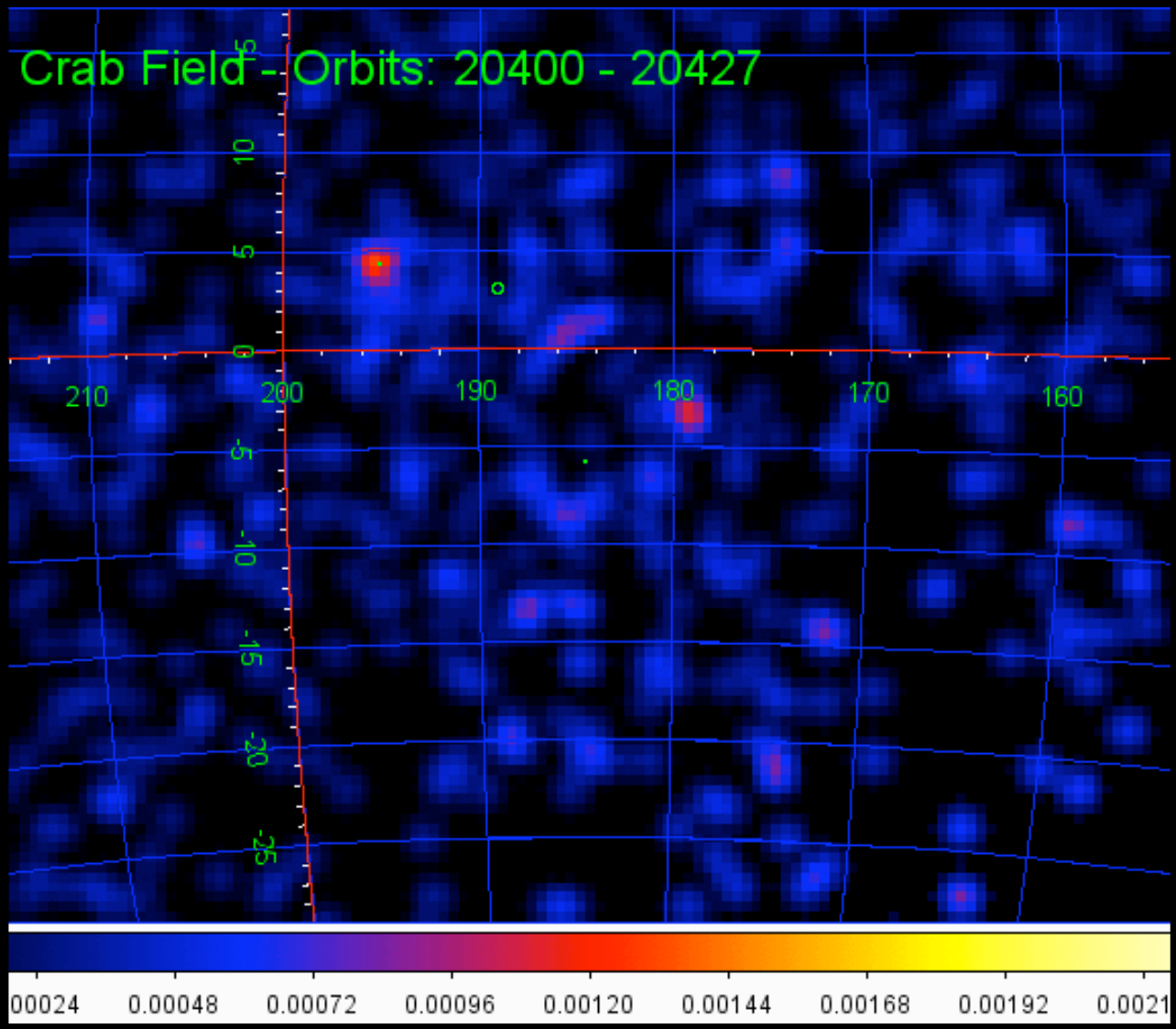

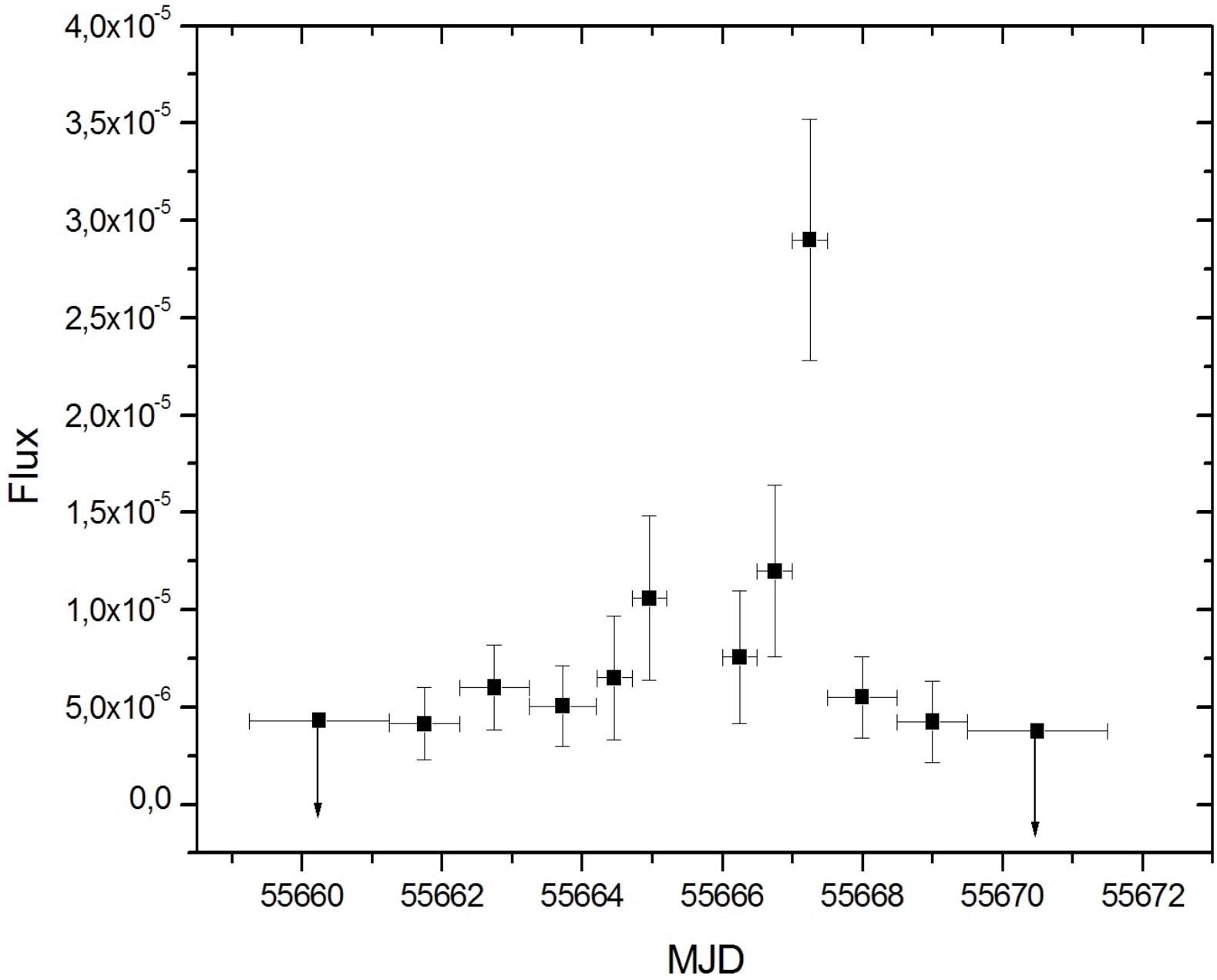
4,0x10-5
3,5x10-5
3,0x10-5
2,5x10-5
2,0x10-5
1,5x10-5
1,0x10-5
5,0x10-6
0,0
Flux
55660
55662
55664
55666
55668
55670
55672
MJD

Fermi, 6 hr.

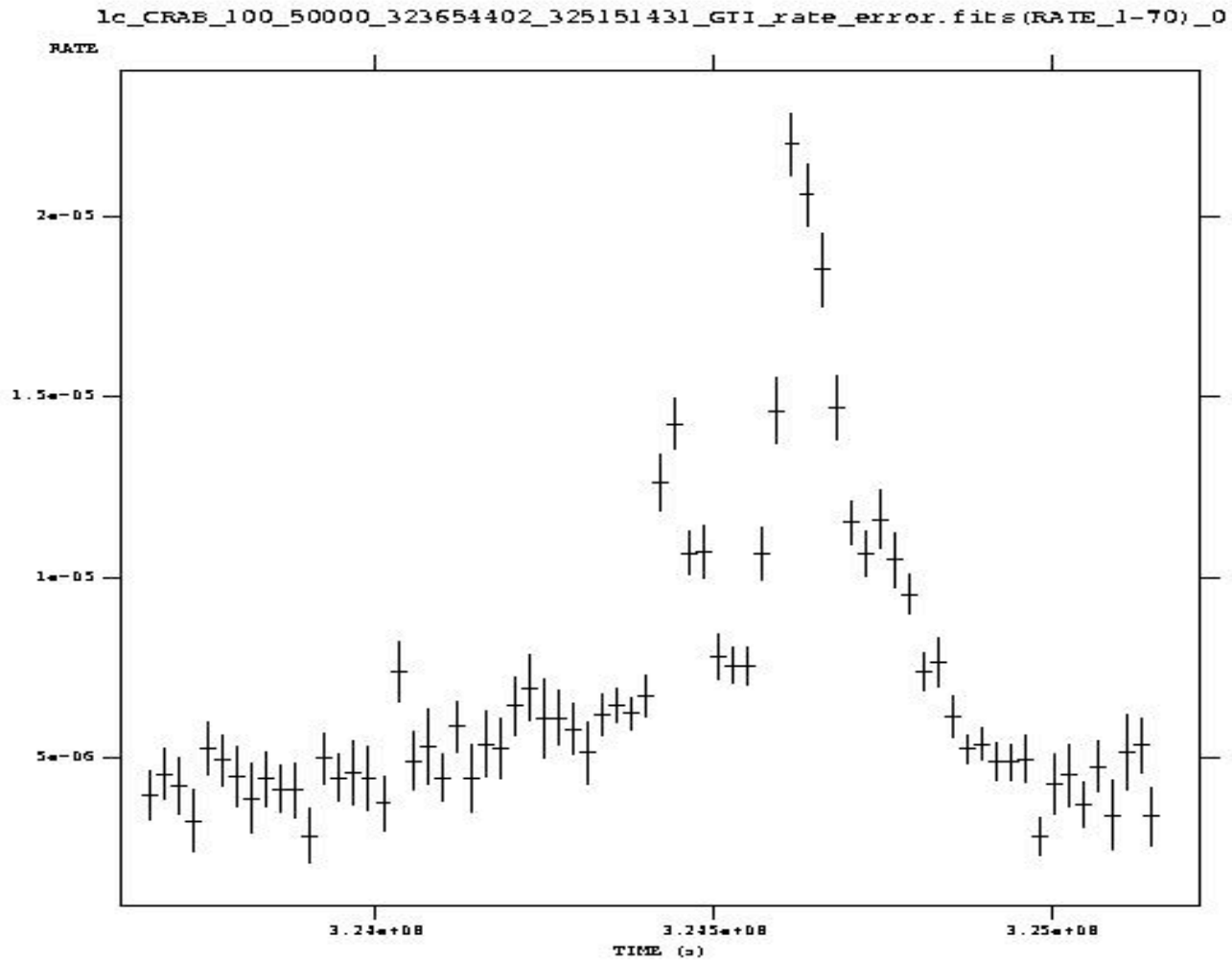
lc_CRAB_100_50000_323654402_325151431_GTI_rate_error.fits(RATE_1-70)_0
RATE
2e-05
1.5e-05
1e-05
5e-06
3.23e+08
3.235e+08
3.25e+08
TIME (s)

fermi, 4 hr.

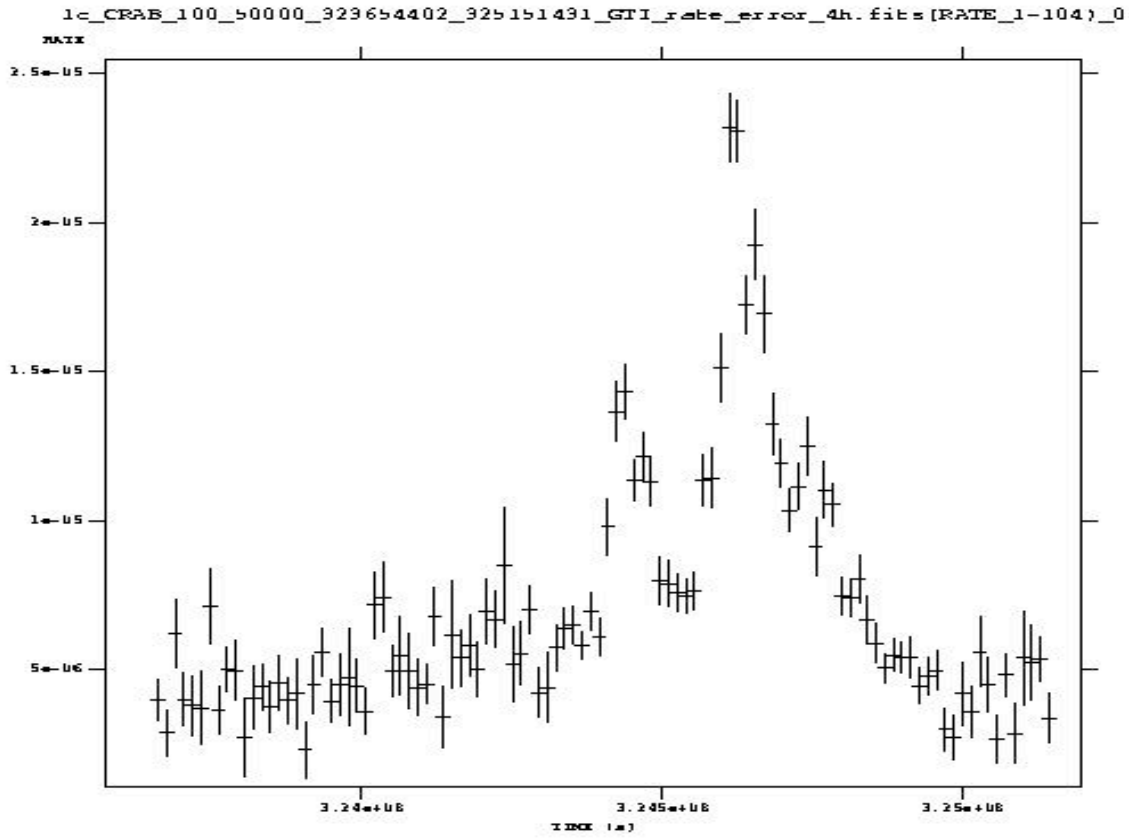
lc_CRAB_100_50000_323654402_325151431_GTI_rate_error_4h.fits[RATE_1-104]_0
RATE
2.5e-05
2e-05
1.5e-05
1e-05
5e-06
3.24e+08
3.245e+08
3.25e+08
TIME (s)

Chandra X-ray observations of the April 2011 Crab flare

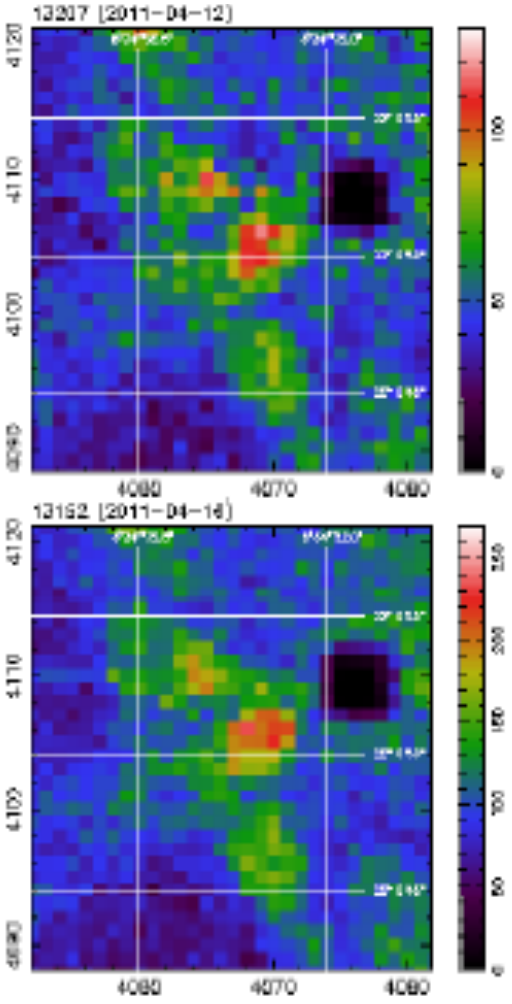

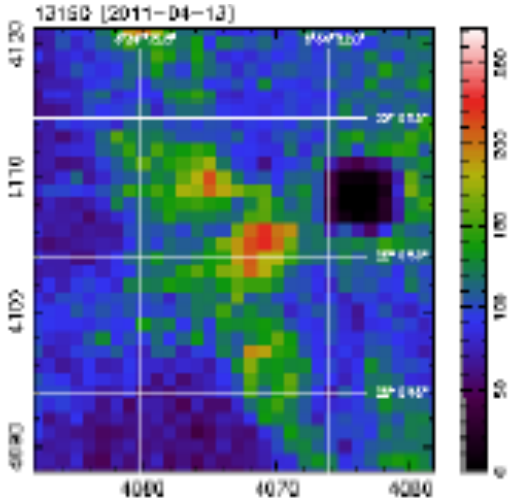

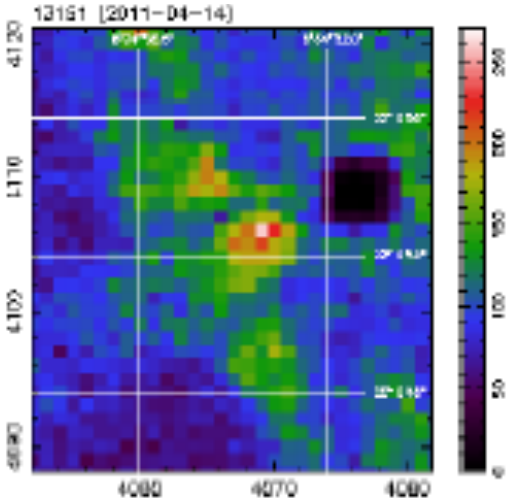

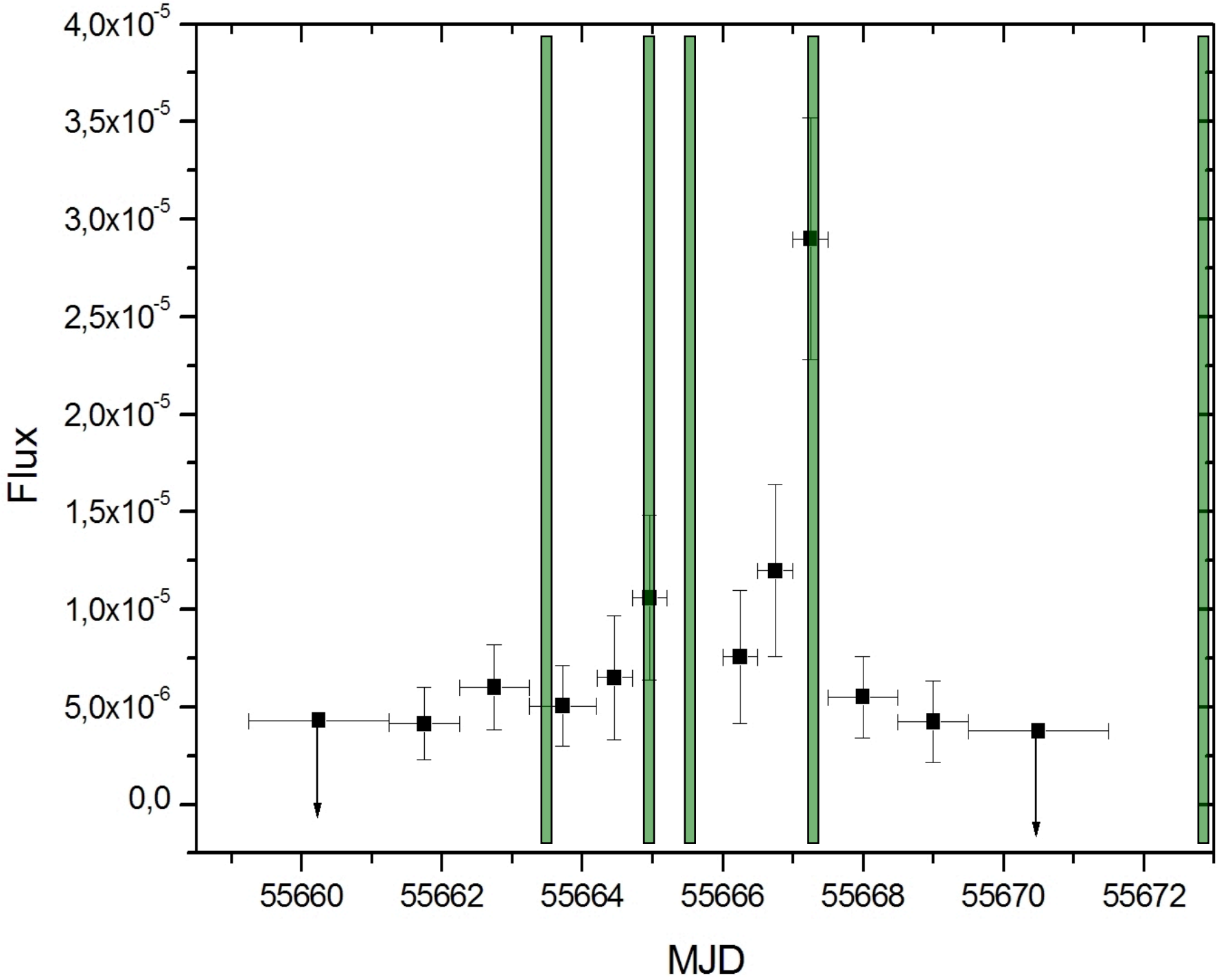
4,0x10-5
3,5x10-5
3,0x10-5
2,5x10-5
2,0x10-5
1,5x10-5
1,0x10-5
5,0x10-6
0,0
Flux
55660
55662
55664
55666
55668
55670
55672
MJD

Crab super-flare: Chandra monitoring

(12, 13, 14, 21 Apr. 2011: A. Tennant, M. Weisskopf)

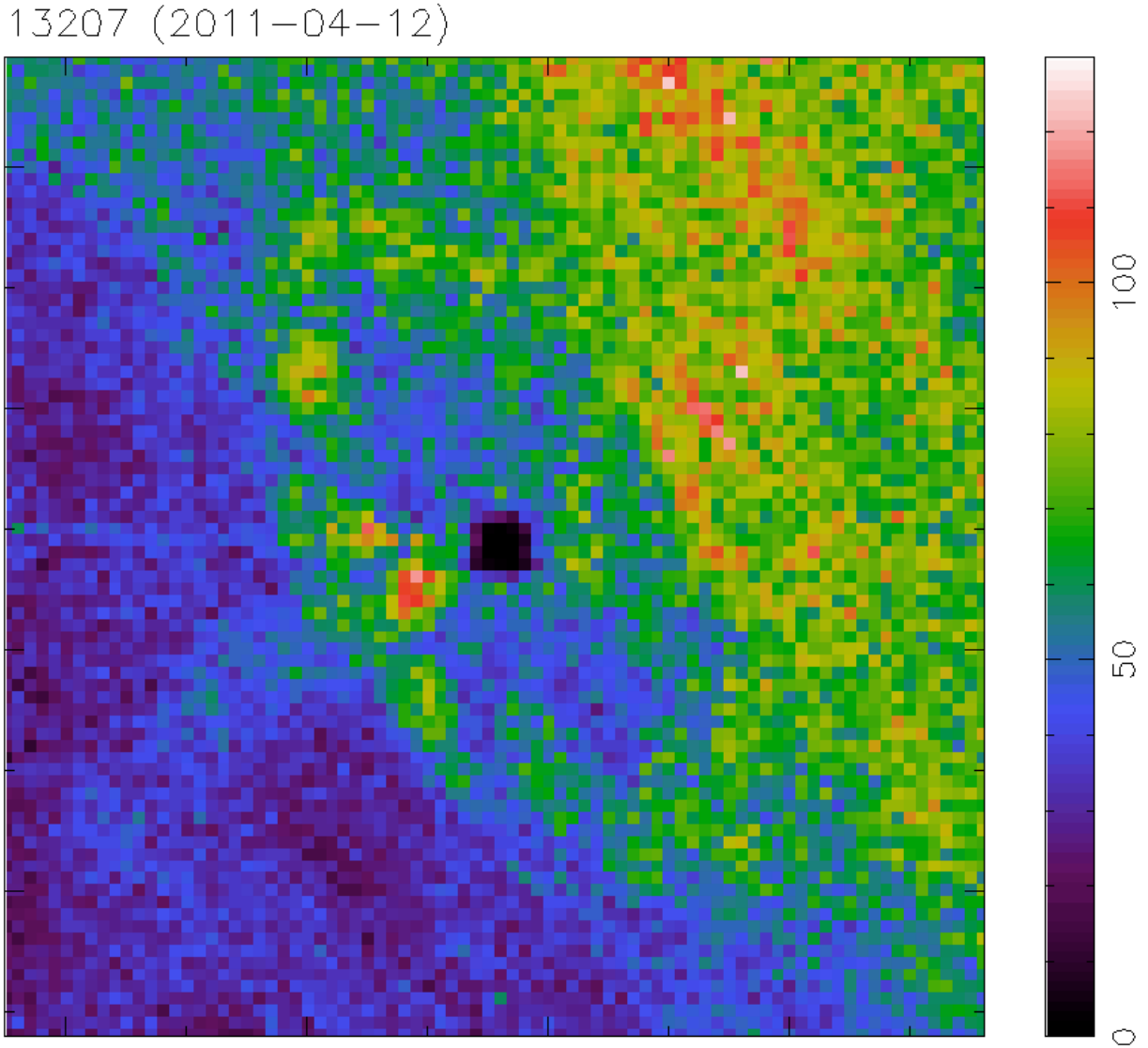

a model (Vittorini V., M.T. et al., ApJ, accepted 2011)

- $dN(\gamma)/d\gamma = \gamma^{-p1}$ for $\gamma_{min} < \gamma < \gamma_{break}$
  with $p_1 = 2.1$, $\gamma_{min} = 5 \cdot 10^5$, $\gamma_{break} = 2 \cdot 10^9$
- $dN(\gamma)/d\gamma = \gamma^{-p2}$ for $\gamma_{break} < \gamma < \gamma_{max}$,
  with $p_2 = 2.7$,
- total particle number $N_{e-/e+} = 10^{42}$.
- size, Larmor radius $R \leq 10^{16}$ cm
- **local $B \approx 10^{-3}$ G (10 times larger than average)**
- $\gamma_{max} \approx \gamma_{break} \leq 10^9 (E/B)(\delta\, \alpha'/\sin\theta)^{1/2} (B/10^{-3}\ G)^{-1/2}$

- δ = 2-3

Crab Nebula super-flare spectrum (Apr. 16, 2011)

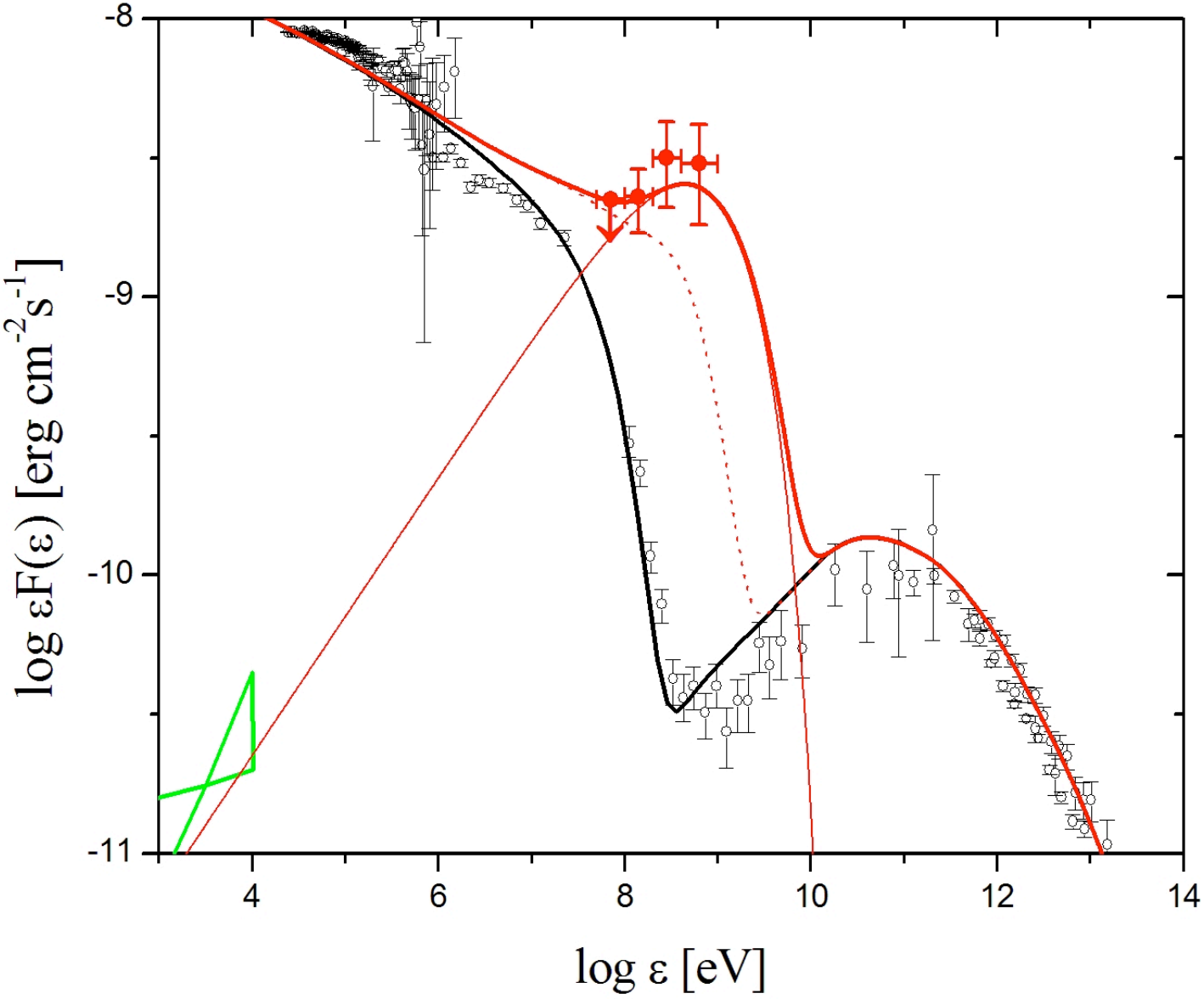

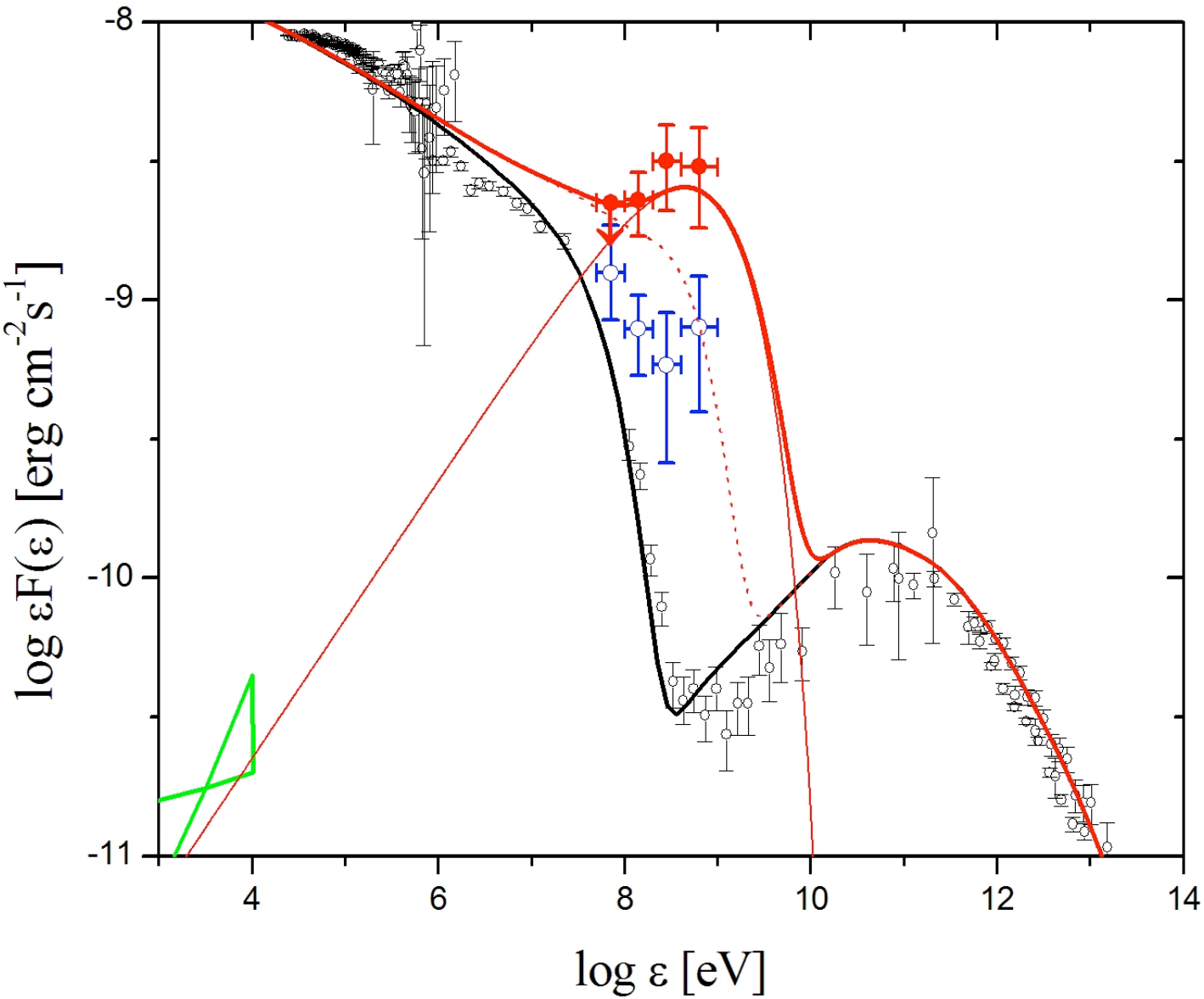
-8
-9
-10
-11
4
6
8
10
12
14
log εF(ε) [erg cm-2s-1]
log ε [eV]

- **if it's nebular emission, what is the ultimate cause of it?**
  - **PSR wind enhancement (density, local B, change of sigma)**
  - **Plasma physics, shock changes, sudden change of B-configuration, reconnection (?)**
  - **near PSR effects (?)**
  - **Knot-1 (?)**
  - **"Anvil" region (?)**

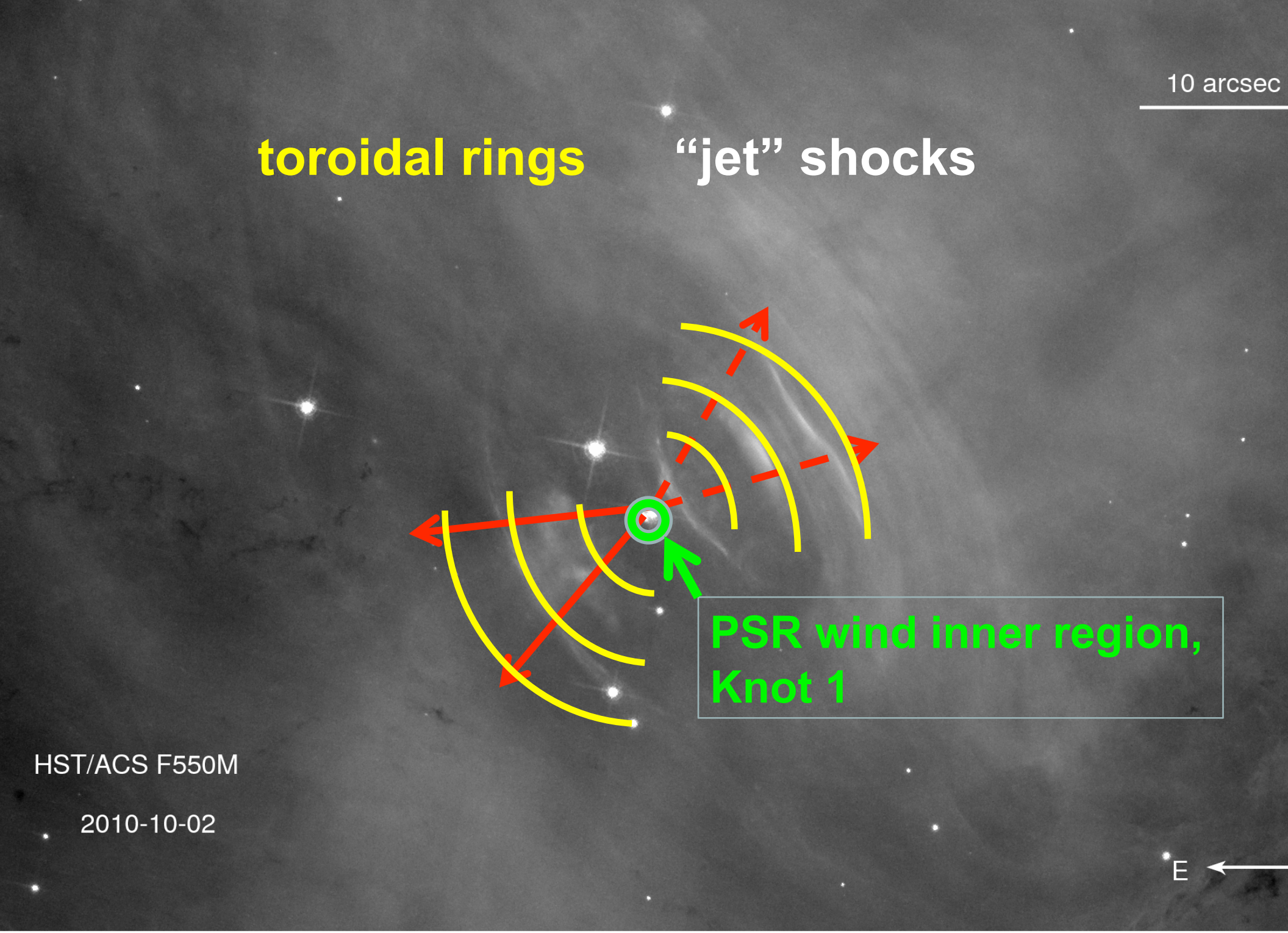
10 arcsec
toroidal rings
"jet" shocks
PSR wind inner region,
Knot 1
HST/ACS F550M
2010-10-02
E

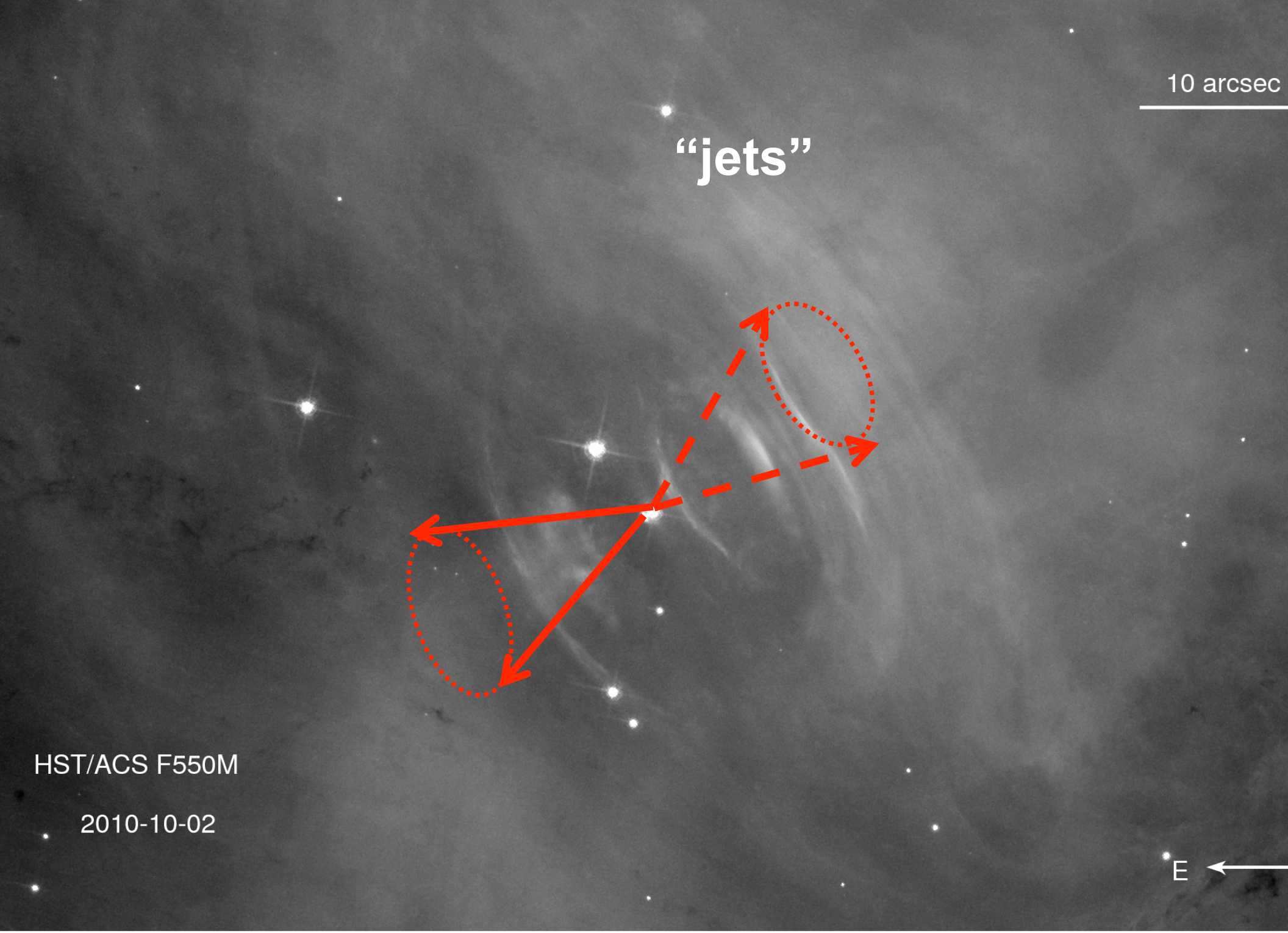
10 arcsec
“jets”
HST/ACS F550M
2010-10-02
E

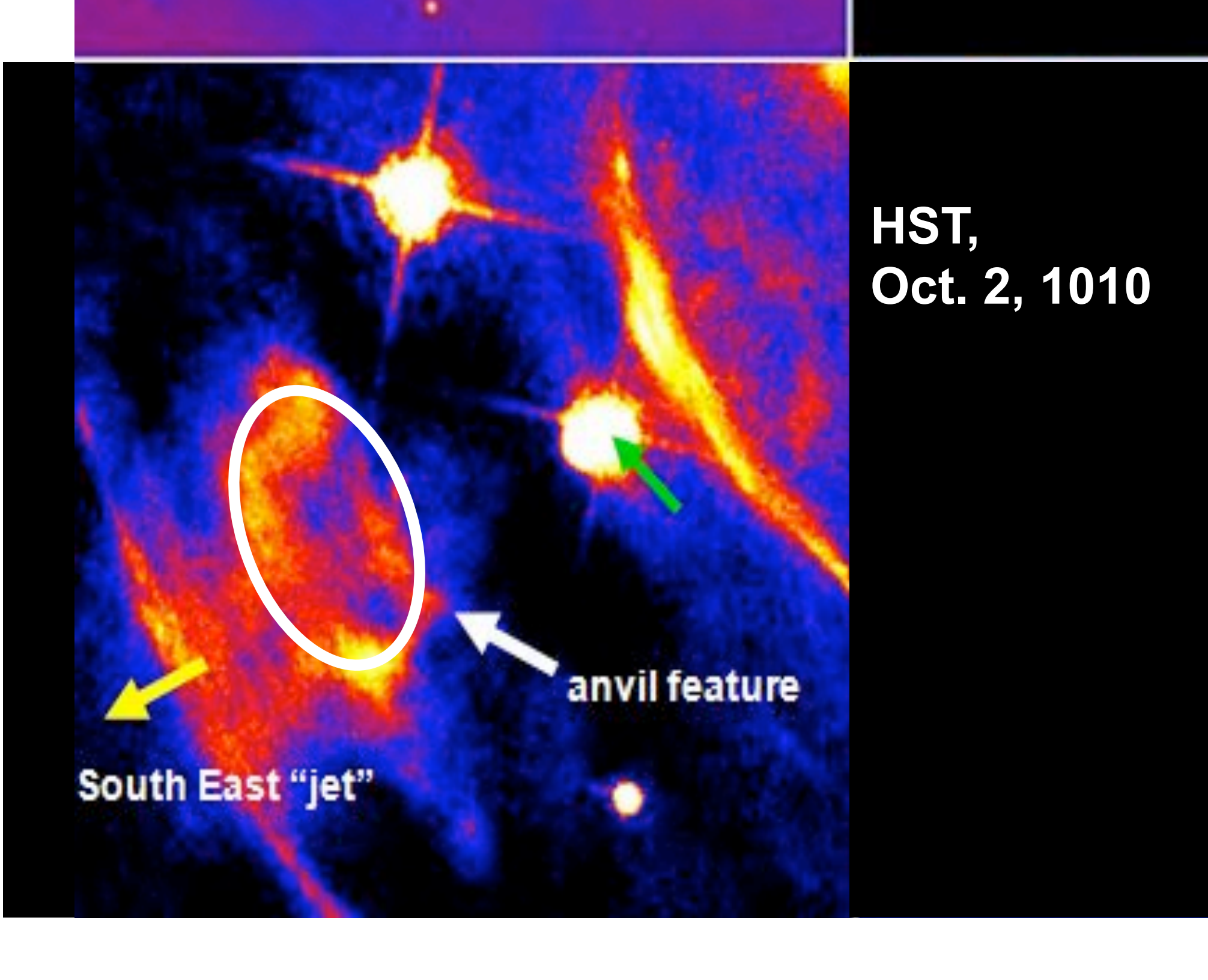
HST,
Oct. 2, 1010
anvil feature
South East "jet"

Crab Apr. 2011 flare

- gamma-ray flare peak luminosity

$$L \approx 2 \cdot 10^{36} \text{ erg s}^{-1}$$

- kin. power fraction of PSR spindown L_{sd},

$$\varepsilon \approx 0.003 \, (\eta_{-1}/0.1) \approx 0.03$$

- timescales:
  - risetime $\leq$ a few hrs ← very efficient acceleration !
  - decay: ~ 1-2-3 days ← fast cooling, B, Lorentz γ

issues

- **standard MHD simulations give too long timescales**
- **detailed acceleration mechanism to be identified**
- **not clear if a strong E-parallel is produced**

ideas

- **instability: magnetic field reconnection**
  – in the polar jet region
- **current sheet instabilities in rings**
- **relativistic shocks developing E-parallel**

Wilson-Hodge et al. 2010

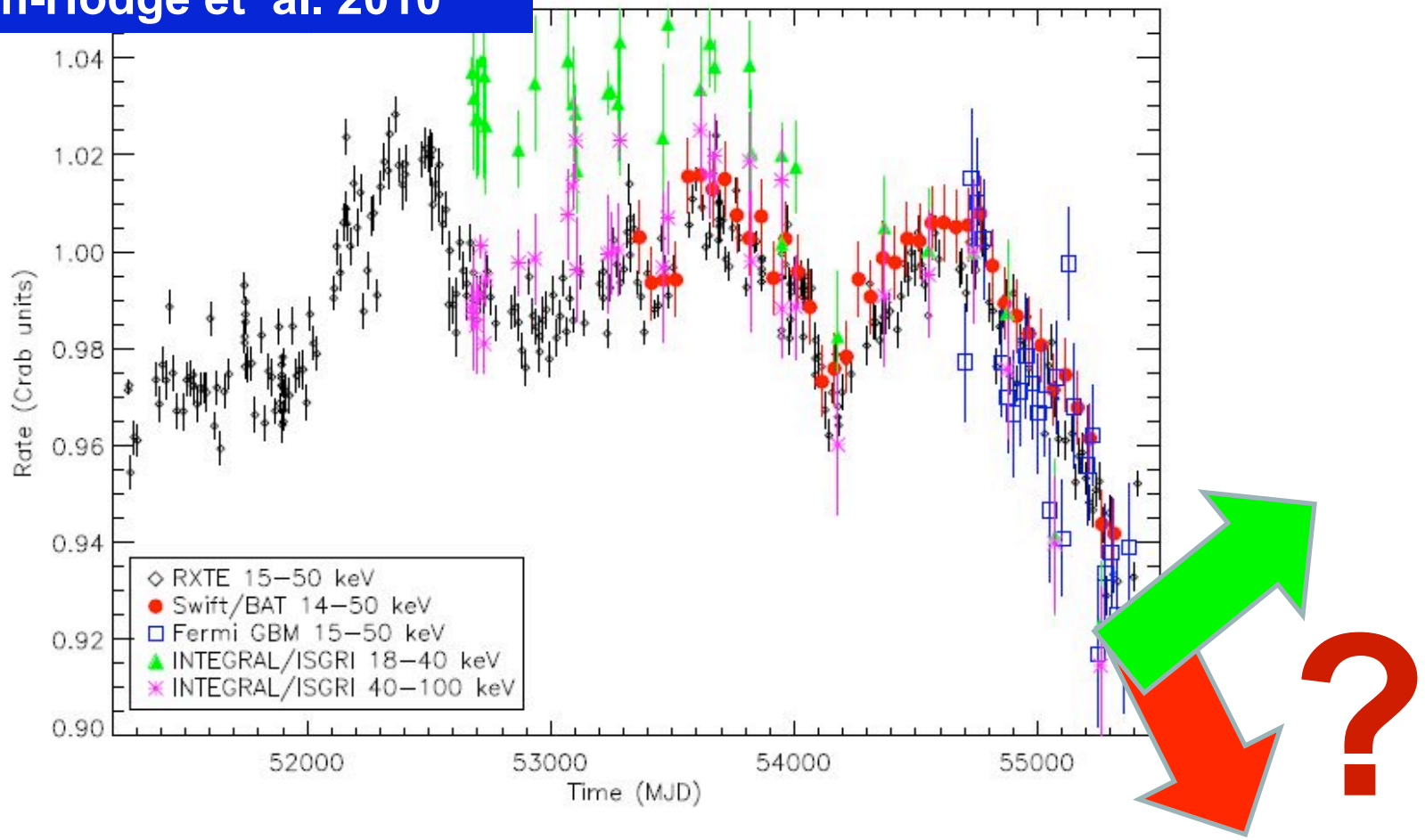

Fig. 5.— Composite Crab light curve for *RXTE*/PCA (15-50 keV - black diamonds), *Swift*/BAT (14-50 keV - red filled circles), *Fermi*/GBM (15-50 keV - open blue squares), *INTEGRAL*/ISGRI (18-40 and 40-100 keV - green triangles and purple asterisks, respectively.) Each data set has been normalized to its mean rate in the time interval MJD 54690-54790. All error bars include only statistical errors.

SNRs and the origin of cosmic rays

Cas A optical (Hubble), X-rays (Chandra), IR (Spitzer)

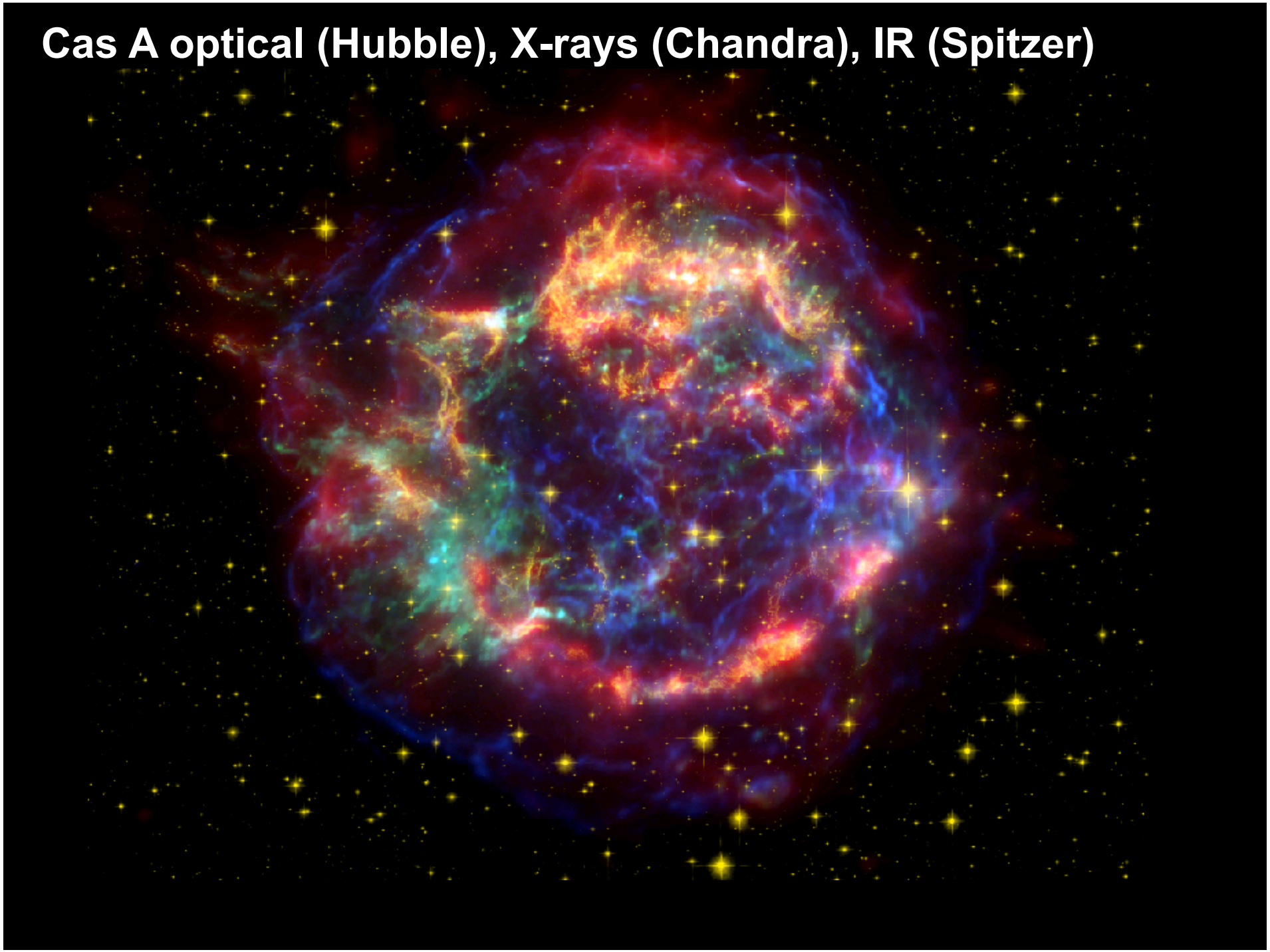

Raggi cosmici adronici (CR)

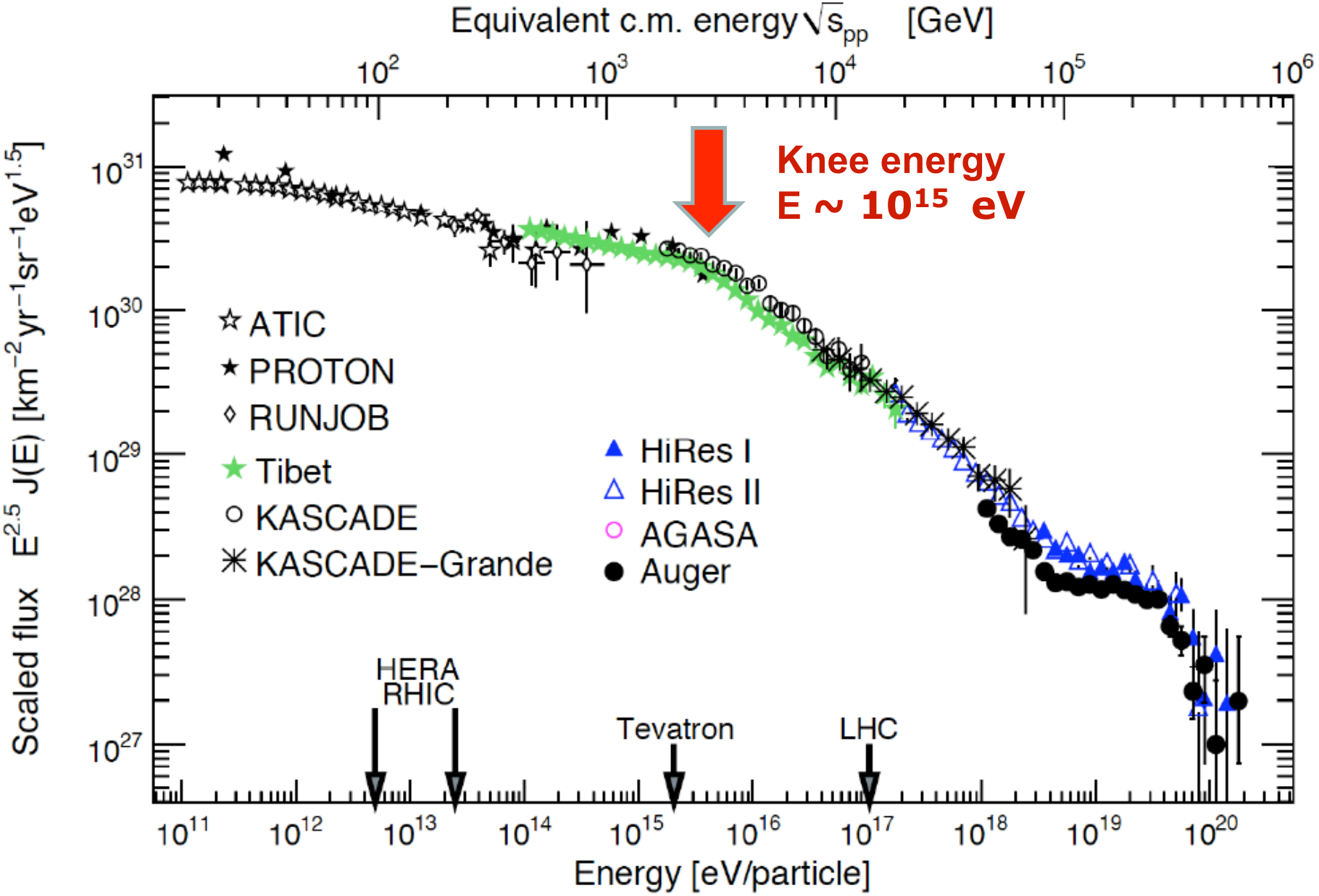

Cosmic-Ray sources and acceleration up to 10^{15} eV

- Supernova explosions and Remnants
- Fast spinning neutron stars
- Relativistic jets (microquasars, NSs)
- Exotic Objects

The big question:

Do SNe produce cosmic-rays ???

V. Ginzburg, Syrovatskii, late 50's, 1964

F. Hoyle (1960)

….

Diffusive shock acceleration (DSA) (first-order Fermi acceleration)

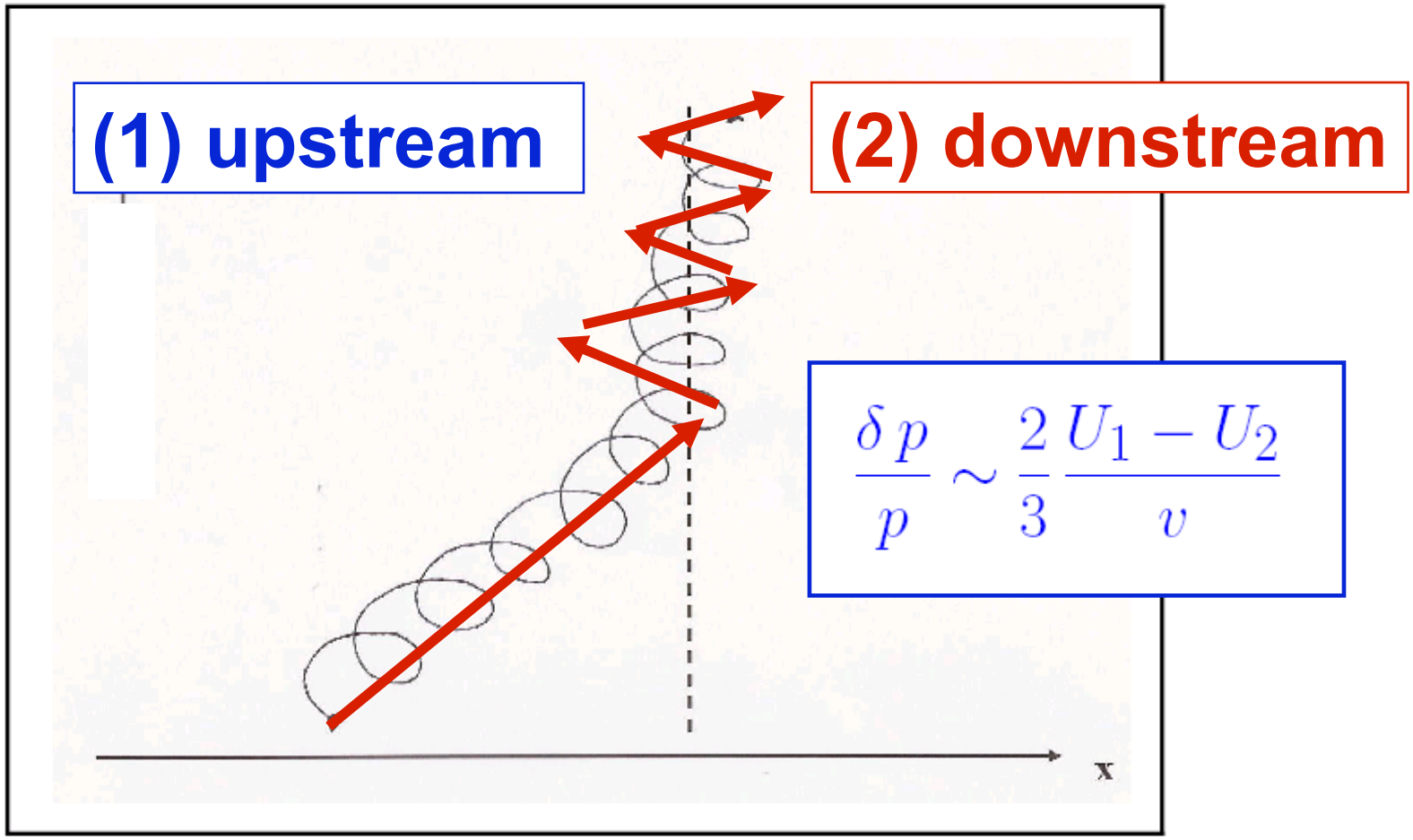

Figure 3: Particle energy gain in the case of a "parallel shock", i.e., a hydrodynamical configuration with the magnetic field parallel to the contact discontinuity's normal

- DSA shock acceleration timescale

$$\tau_{acc} \sim (10/3)\, \eta\, c\, R_g\, V_s^{-2} \approx 10^3 - 10^4 \text{ yrs}$$

- $R_g = cp/eB$ (gyroradius)
- $\eta \geq 1$ (gyrofactor)
- V_s = shock speed (10^3 km/sec)

Particle acceleration in SNRs requires a non linear theory

From P.Blasi

Analytical: Malkov(1997,1999), Blasi(2002,2004),Amato&Blasi (2005,2006)

Numerical: Berezhko & Voelk (1997),Zirakashvili&Aharonian(2010);Kang et al.

MonteCarlo: Ellison and Collaborators since 90s

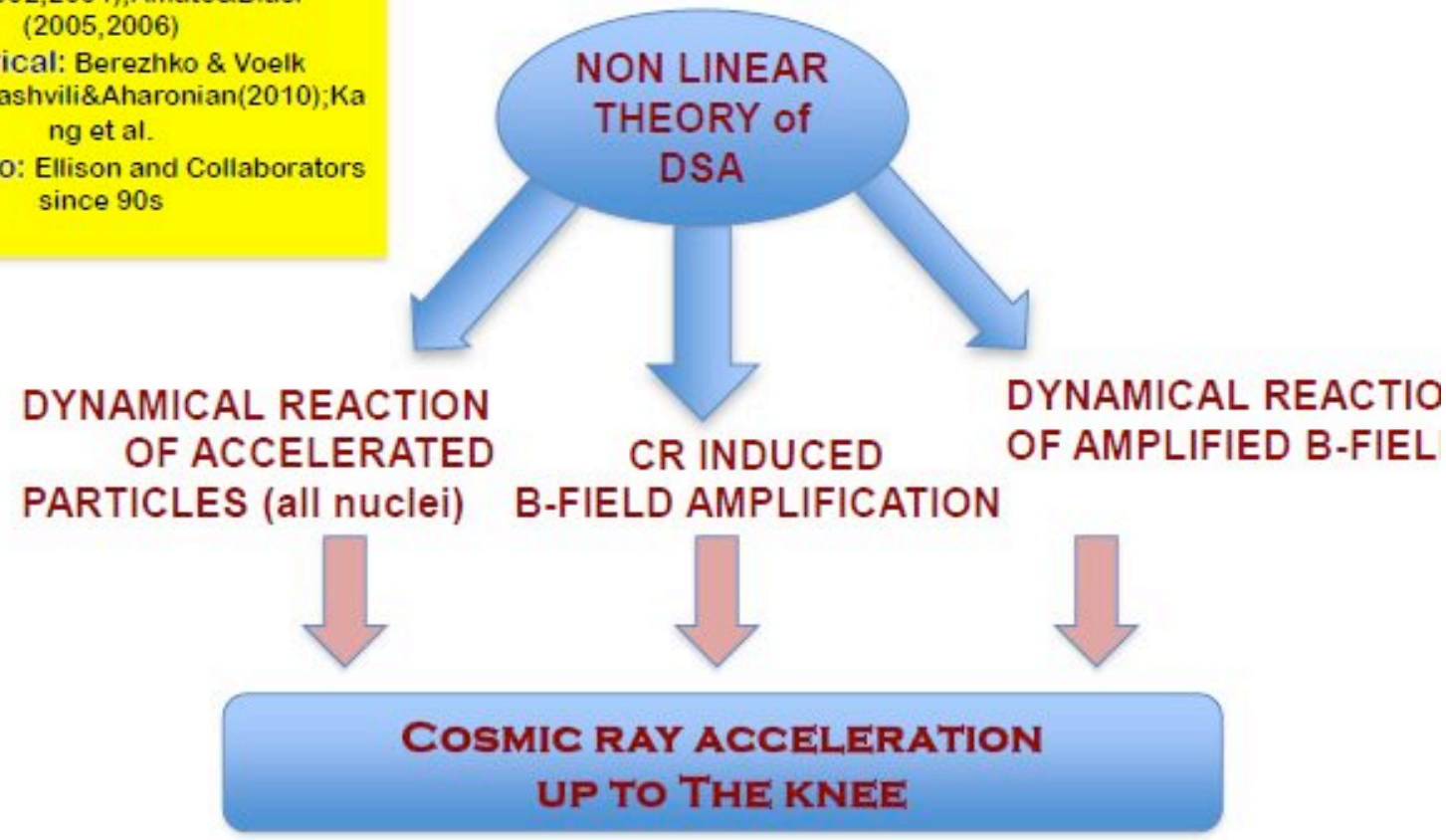

Dynamical Reaction of Accelerated Particles on a collisionless shock

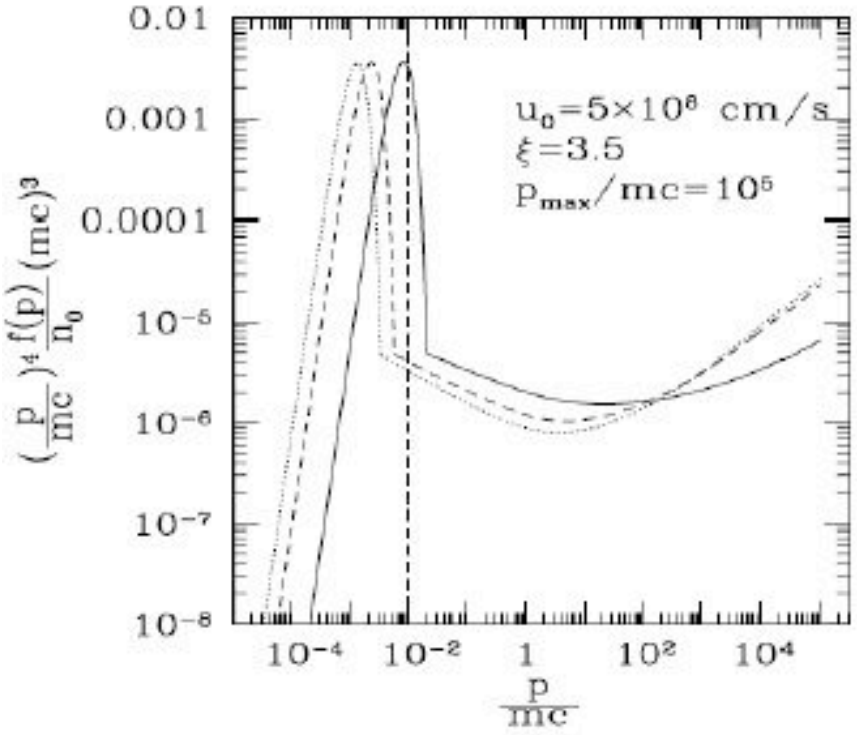

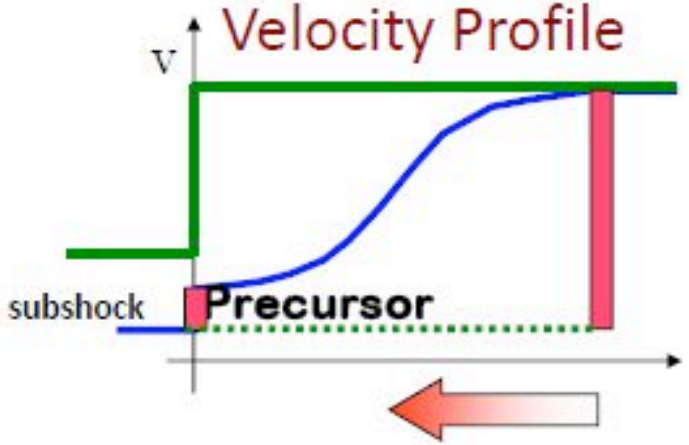

HOT: thermalization behind a collisionless shock

Supernova 1006 (Goumard et al. 2006)

First non-thermal hard X-ray SNR (1995)

Shell-type supernova

distance = 1.8 - 2.2 kpc

Winkler et al. (2003)

N_H = 0.05 - 0.3 cm^{-3}

Chandra
(X-rays)

50 light years
0.5° diameter

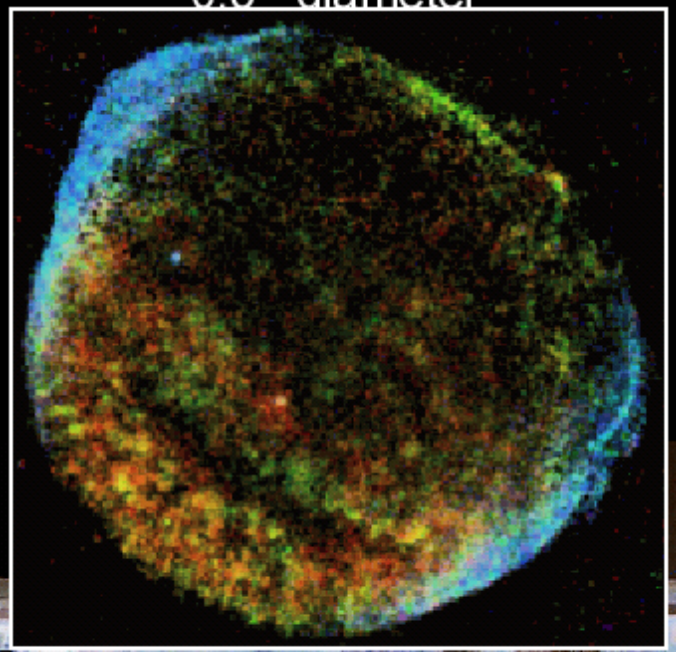

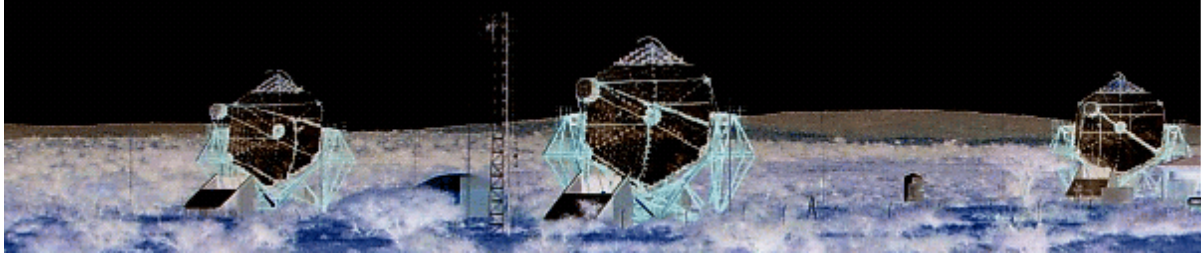

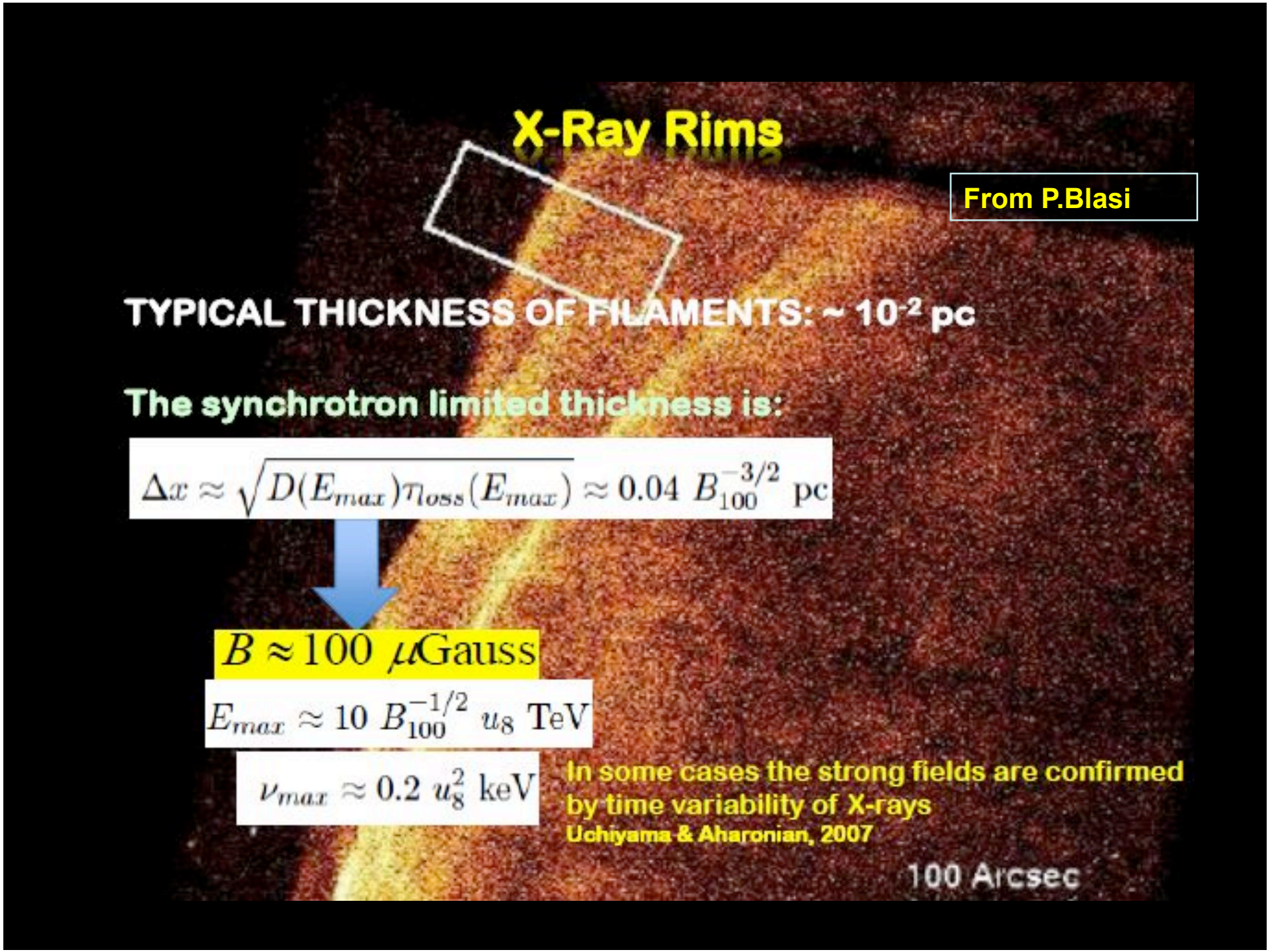
X-Ray Rims
From P.Blasi
TYPICAL THICKNESS OF FILAMENTS: ~ 10-2 pc
The synchrotron limited thickness is:
$\Delta x \approx \sqrt{D(E_{max})\tau_{loss}(E_{max})} \approx 0.04\ B_{100}^{-3/2}$ pc
$B \approx 100\ \mu$Gauss
$E_{max} \approx 10\ B_{100}^{-1/2}\ u_8$ TeV
$\nu_{max} \approx 0.2\ u_8^2$ keV
In some cases the strong fields are confirmed by time variability of X-rays
Uchiyama & Aharonian, 2007
100 Arcsec

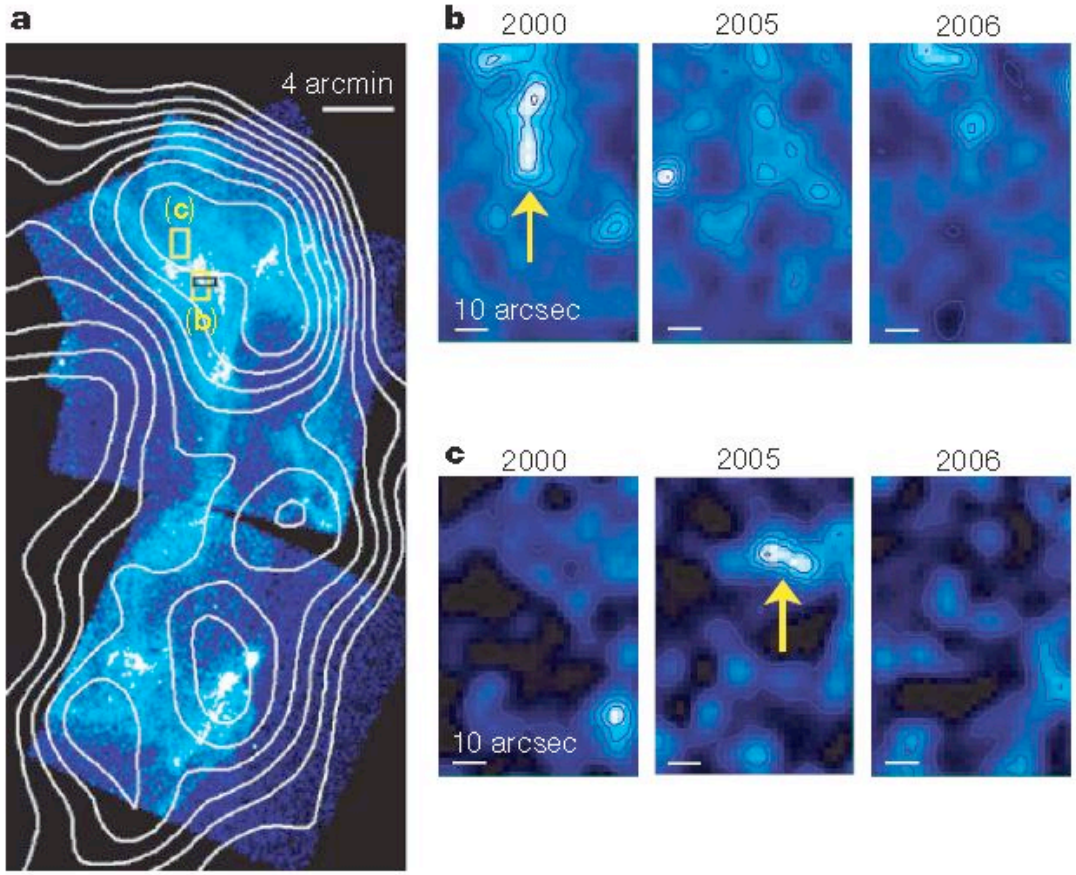

Figure 1 | Chandra X-ray images of the western shell of SNR RX J1713.7−3946. a, A Chandra X-ray mosaic image is overlaid with TeV γ-ray contours from HESS measurements[26]. North is up and east is to the

(Uchiyama, Aharonian et al. 2007)

Variable (!) and strongly enhanced X-ray features

large local magnetic field B

B-amplification by CR turbulent processes (Bell,Lucek, 2001)

B = 1 mG

proton-nuclei energies
E = 1 PeV (B/mG) (T/100 yrs)

Spectral Modelling…importance of the magnetic field

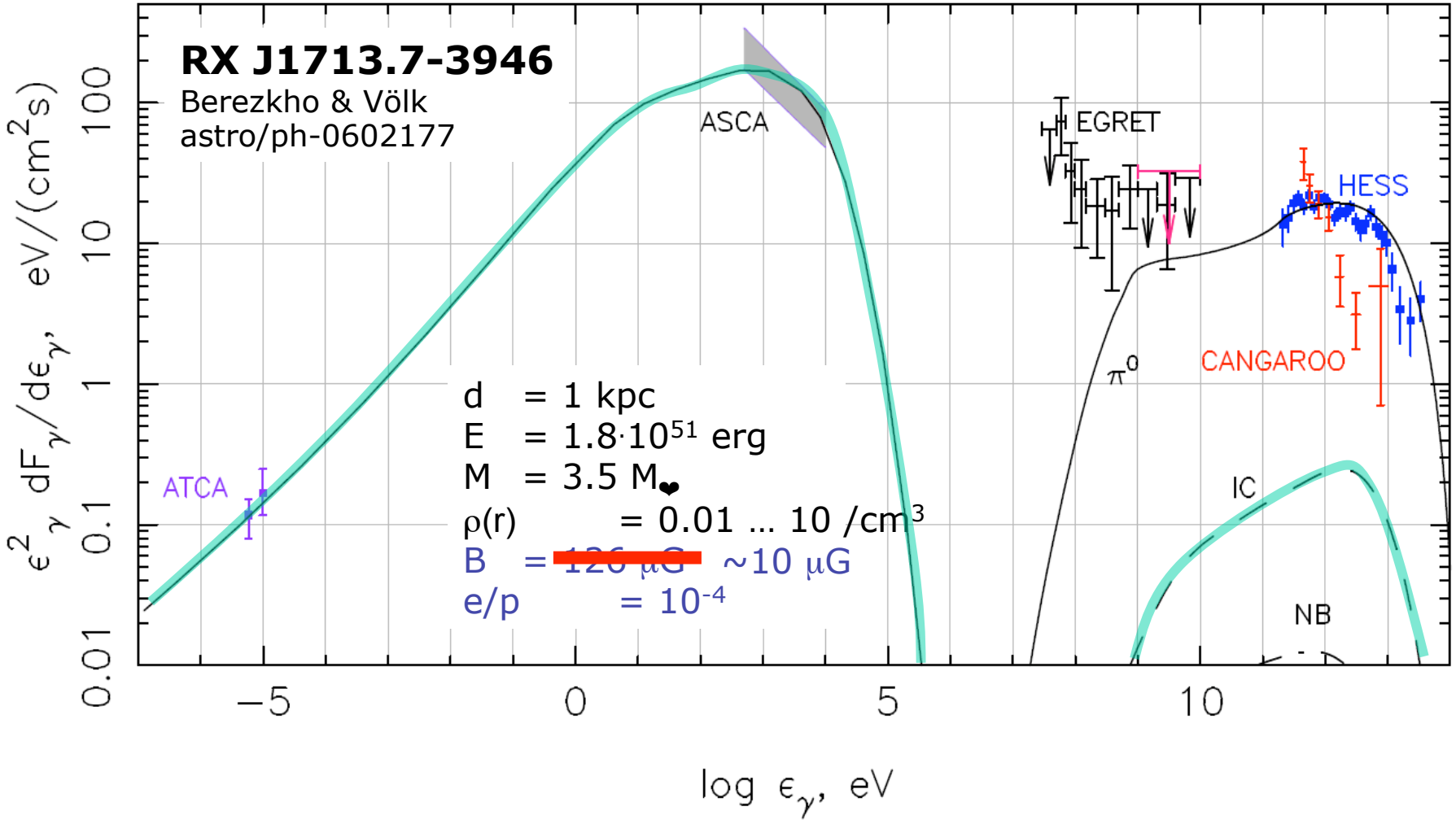

emissione di protoni/ioni

richiede un bersaglio di gas denso

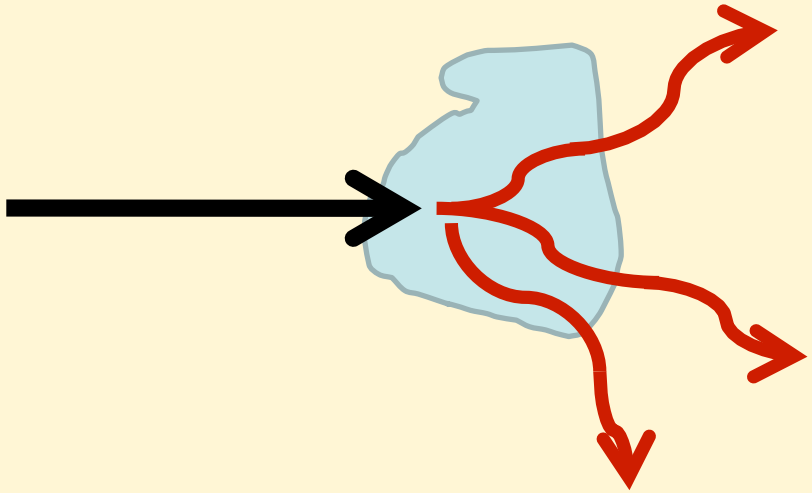

produzione di mesoni π^0

p + p → X + π^0

↳ $\gamma+\gamma$ (70+70 MeV)

emissione di elettroni

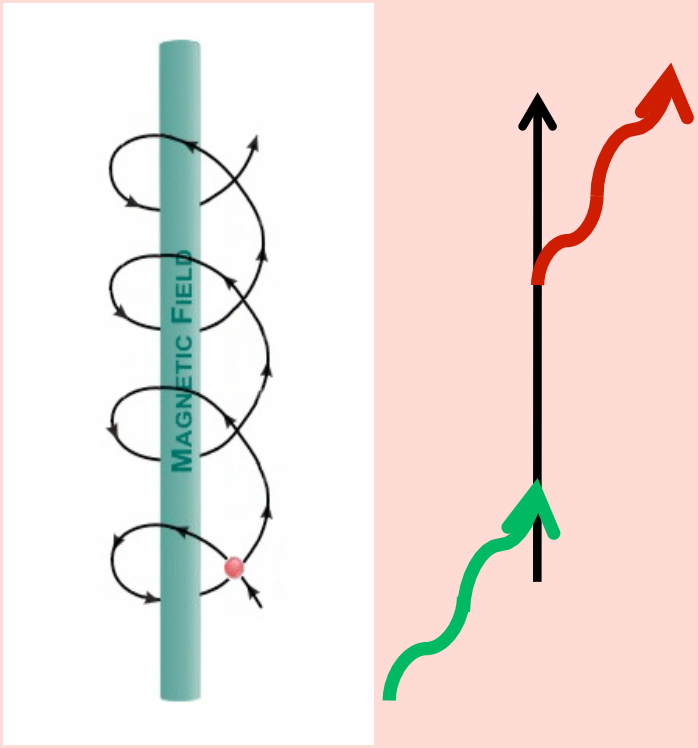

sincrotrone (campo magnetico)
Compton inverso (fotoni molli)
Bremsstrahlung (gas)

unambiguous proof of the CR origin in SNRs…

- **Electrons**
  - **Bremsstrahlung (target density)**
  - **Synchrotron emission (magnetic field)**
  - **Inverse Compton (CMB, interstellar photons)**

- **Pion production (target density)**

$$p + p \rightarrow X + \pi^0$$

$$\pi^0 \rightarrow \gamma + \gamma \quad (\sim 70+70 \text{ MeV})$$

$$\sigma_{pp} \sim 40 \text{ mbarn}$$

$$\tau \sim (\sigma_{pp}\, n\, c)^{-1} \sim (6 \cdot 10^7 \text{ yrs})\, n^{-1}$$

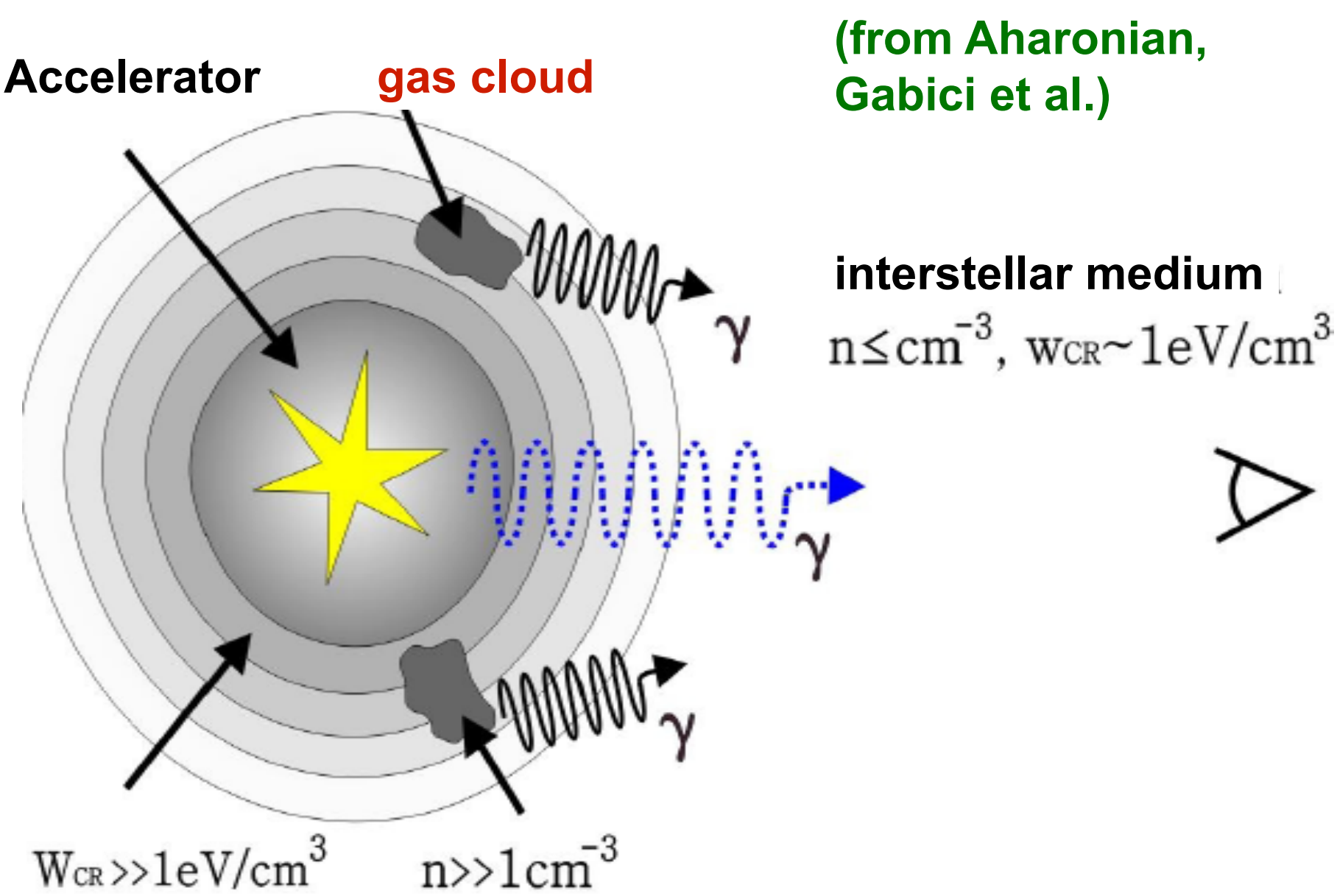
Accelerator
gas cloud
(from Aharonian, Gabici et al.)
interstellar medium
$n \leq cm^{-3}$, $w_{CR} \sim 1eV/cm^3$
γ
γ
γ
$W_{CR} >> 1eV/cm^3$
$n >> 1cm^{-3}$

gamma-rays from neutral pion production in p-p collisions (e.g. F.Aharonian)

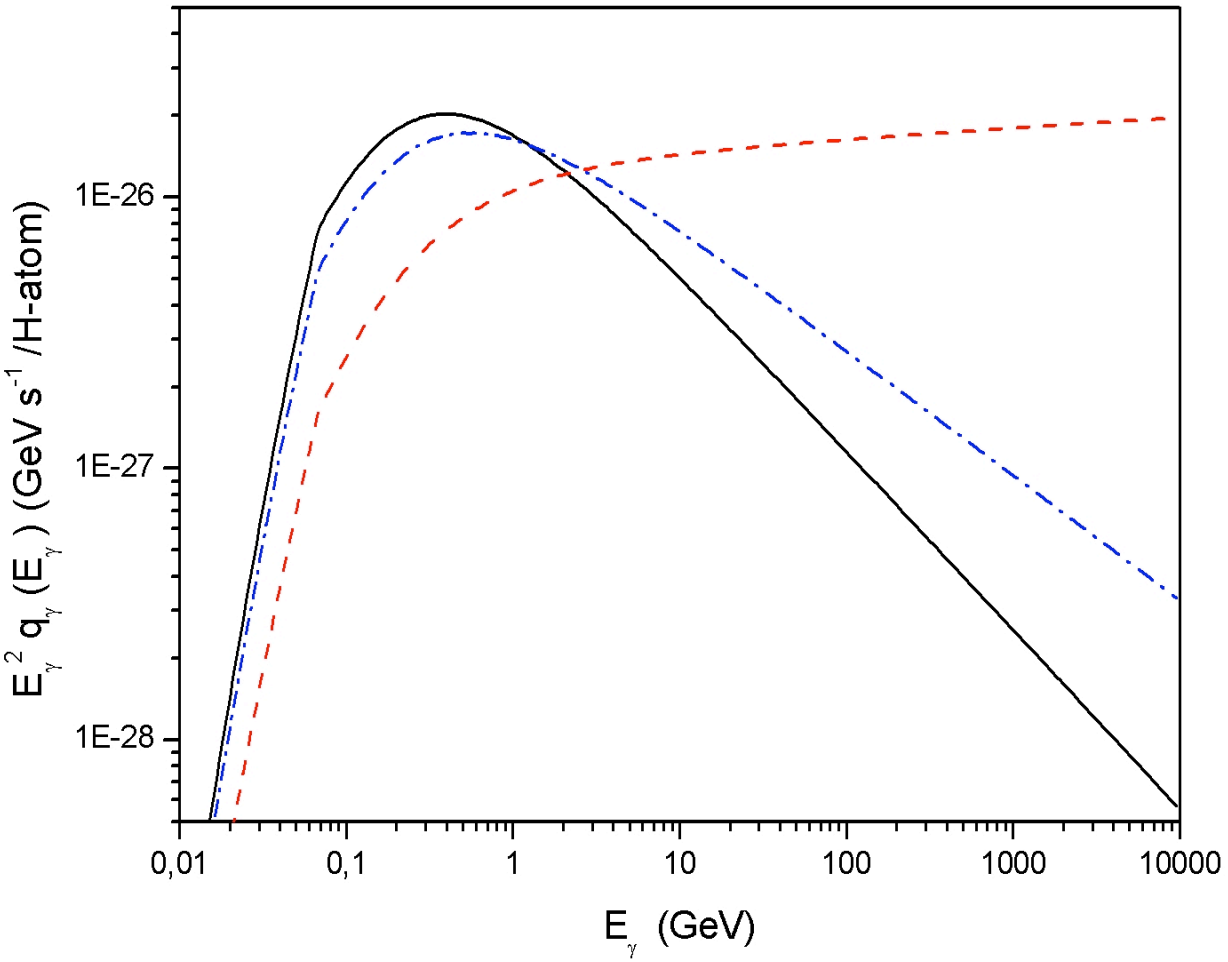

Example: SNR IC 443 electrons and protons interacting with gas $n = 1\ cm^{-3}$ and $N(p) \sim p^{-2}$ (Gaisser, Protheroe & Stanev, 1998)

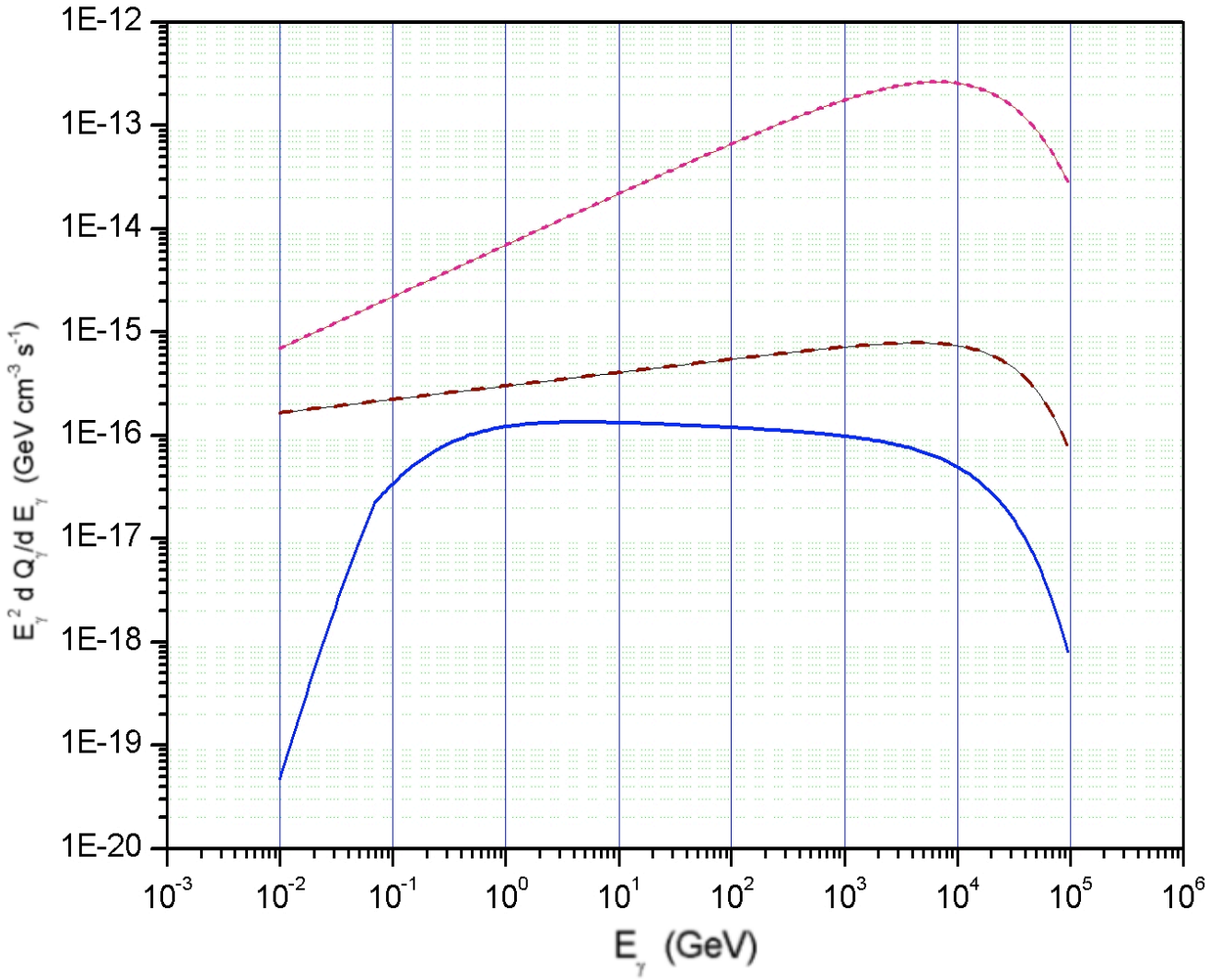

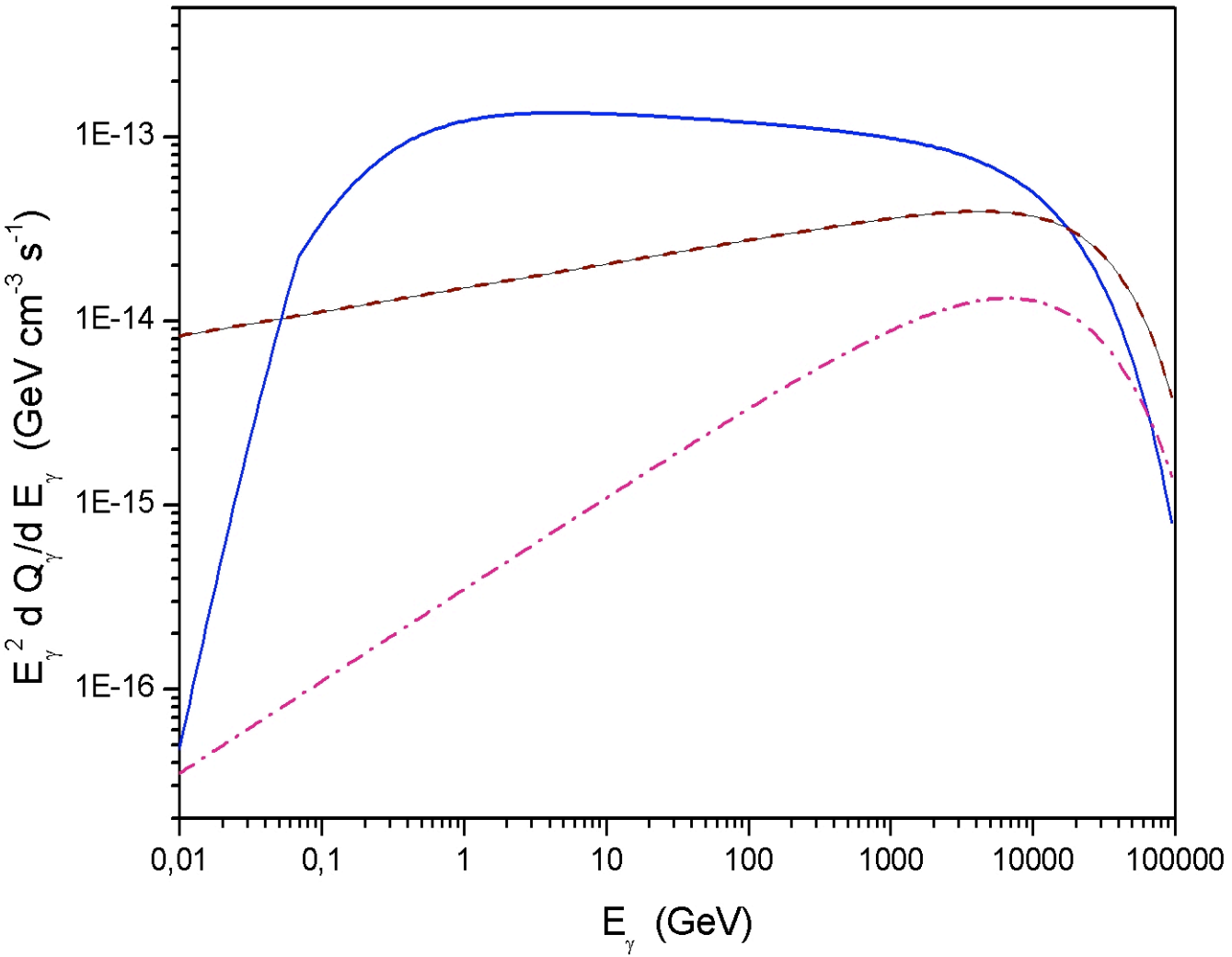
1E-13
1E-14
1E-15
1E-16
$E_\gamma^2\, d\, Q_\gamma / d\, E_\gamma$ (GeV cm^{-3} s^{-1})
0,01
0,1
1
10
100
1000
10000
100000
E_γ (GeV)

Idealized case: pion emission from accelerated CR in SNR (Caprioli et al. 2010)

the quest for a Pevatron

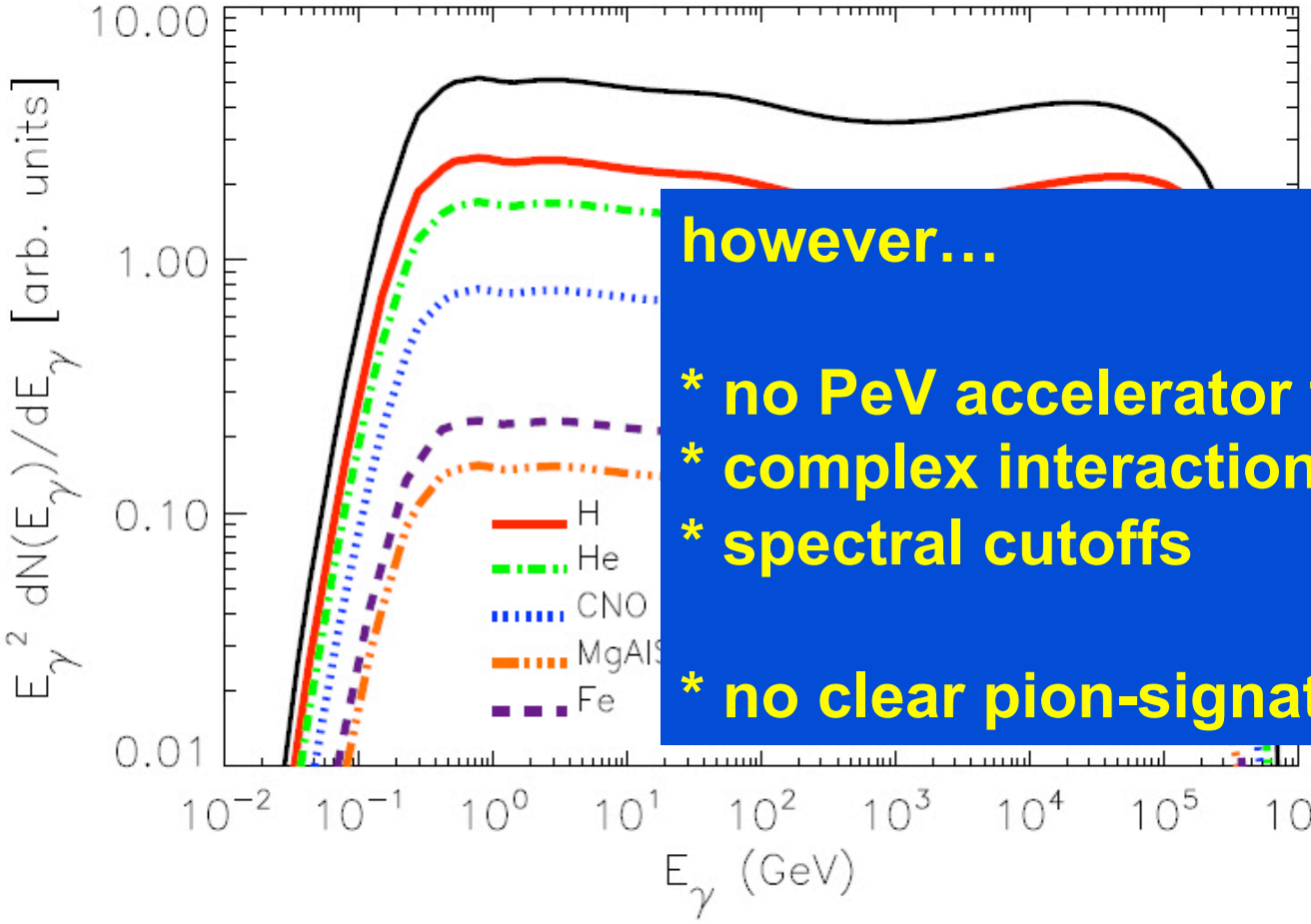

however…

*** no PeV accelerator found yet**
*** complex interaction**
*** spectral cutoffs**

*** no clear pion-signature**

Cosmic-ray origin in SNRs ?
so far, difficult to prove

- **The ideal SNR:**
  - **energetic**
  - **close to Earth**
  - **with the right dense target (molecolar cloud)**

- $f = (W_p / t_{pp})/4\,\pi\, d^2 \sim (n\, W_p)/ d^2$

- **possibly low-background**

- **not that easy…**

gamma-ray detected SNRs

SNR (l,b)	AGILE	Fermi-LAT	age[yrs]
CAS A (111.7,-2.1)	no	yes	~300
SN 1006 (327.6,+14.6)	no	no	~1,000
RXJ1713 (347.3,-0.5)	in prep.	yes	~1,600
W49B (G43.3-0.2)	no	yes	1,000-4,000
γ-Cygni (78.2,+2.1)	in prep.	no	~7,000
W51 (49.5,-0.4)	no	yes	~10,000
W44 (34.7,-0.4)	in prep.	yes	~20,000
IC443 (189.1,+3)	yes	yes	20,000-30,000
W28 (6.71,-0.05)	yes	yes	35,000-45,000

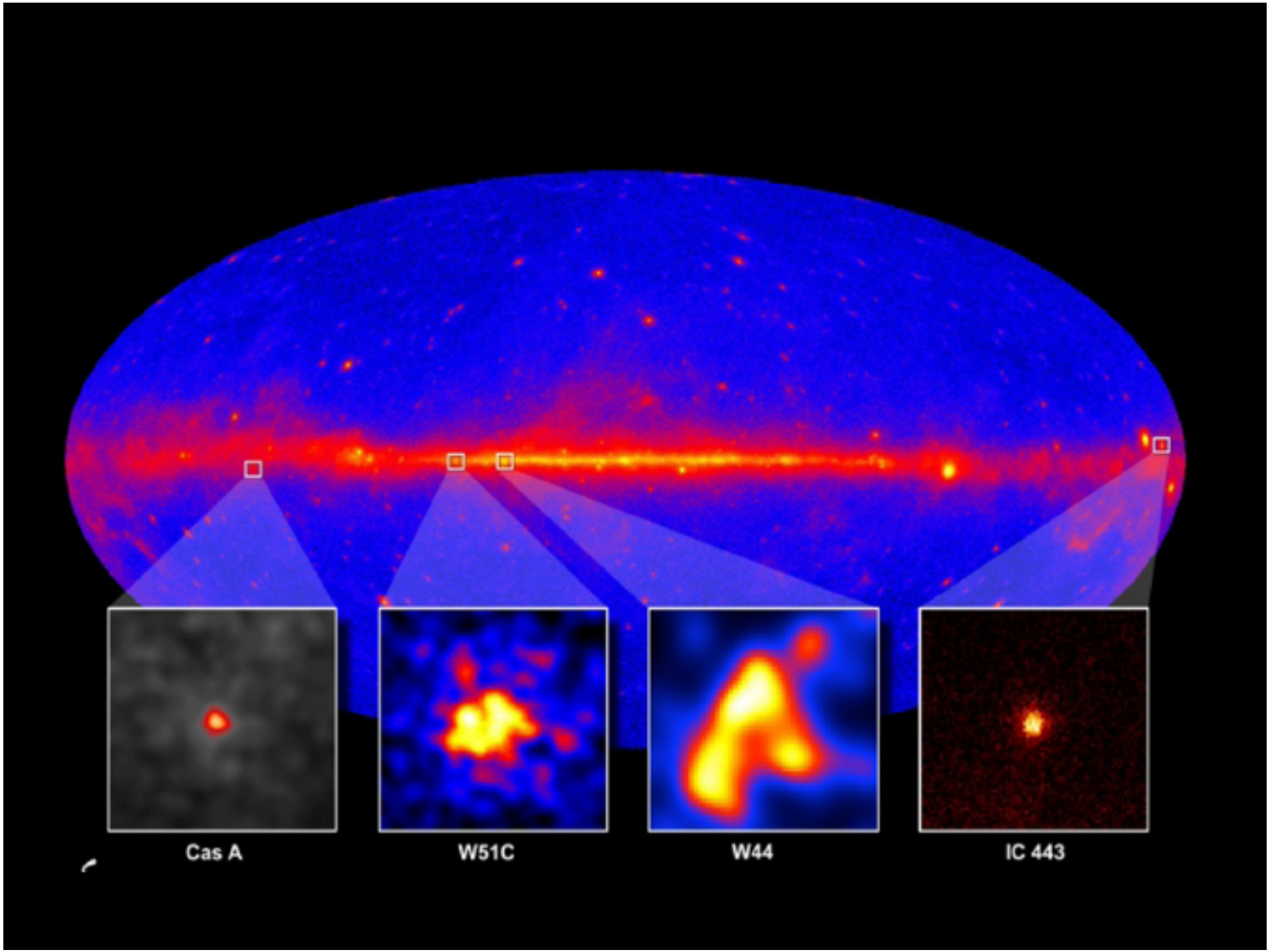
Cas A
W51C
W44
IC 443

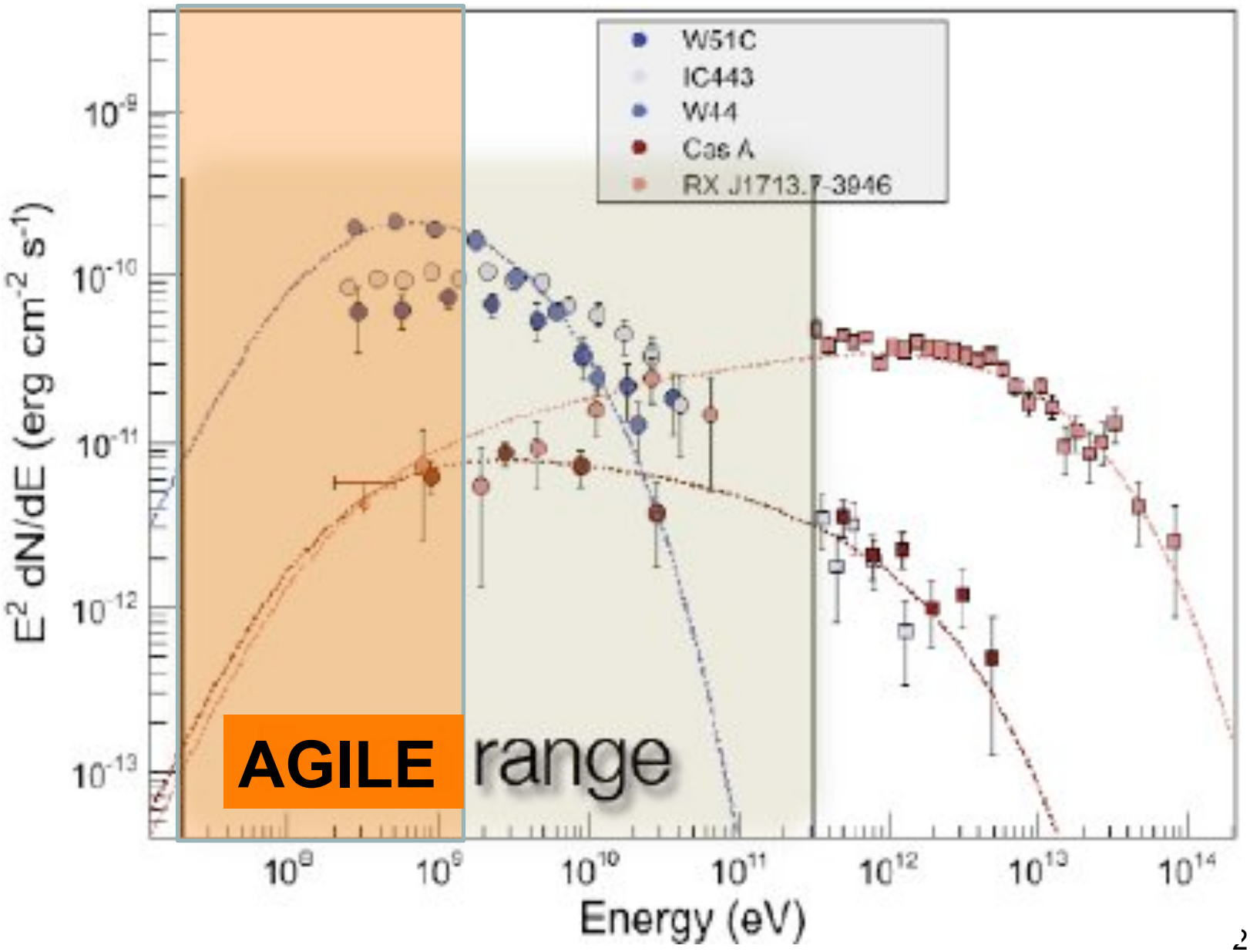
W51C
IC443
W44
Cas A
RX J1713.7-3946
AGILE range
E^2 dN/dE (erg cm^{-2} s^{-1})
Energy (eV)
10^{-9}
10^{-10}
10^{-11}
10^{-12}
10^{-13}
10^{8}
10^{9}
10^{10}
10^{11}
10^{12}
10^{13}
10^{14}

★ Tycho's SNR

- SN 1572
- SN type: Ia
- distance: ~3 kpc
- radius: ~3.7 pc

★ Cassiopeia A

- SN ~1680
- SN type: IIb
- distance: ~3.4 kpc
- radius: ~2.5 pc

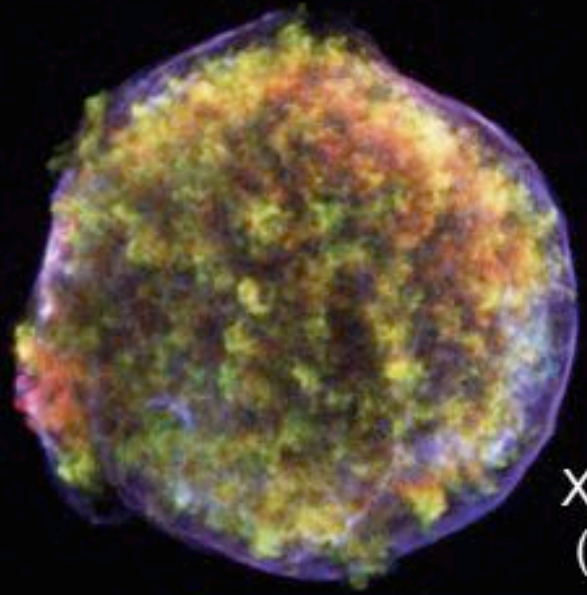

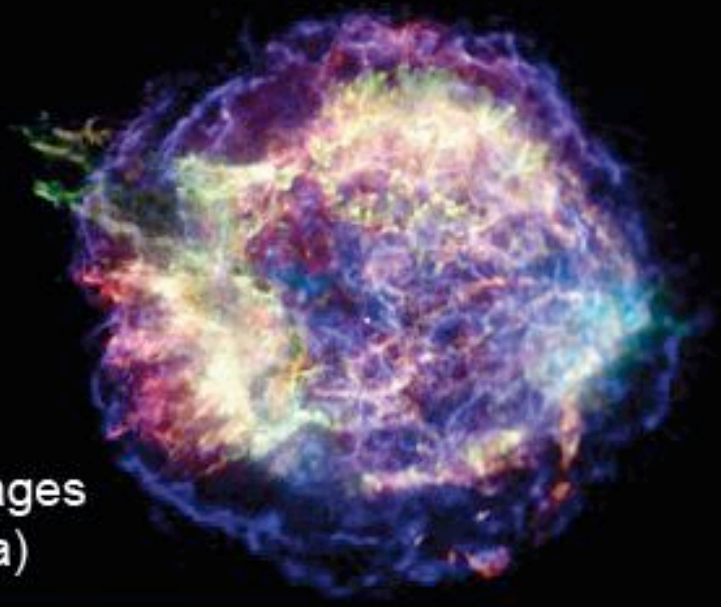

X-ray Images
(Chandra)

Most parameters are reasonably well known.
→ largely help us interpret gamma-ray results.

Tycho: New GeV Detection

Fermi-LAT Detection (5σ)

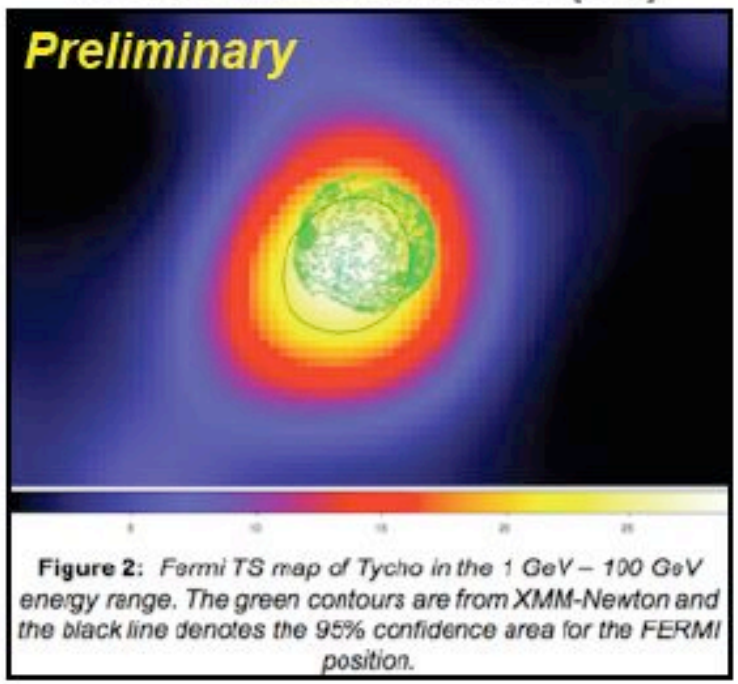

Figure 2: *Fermi TS map of Tycho in the 1 GeV – 100 GeV energy range. The green contours are from XMM-Newton and the black line denotes the 95% confidence area for the FERMI position.*

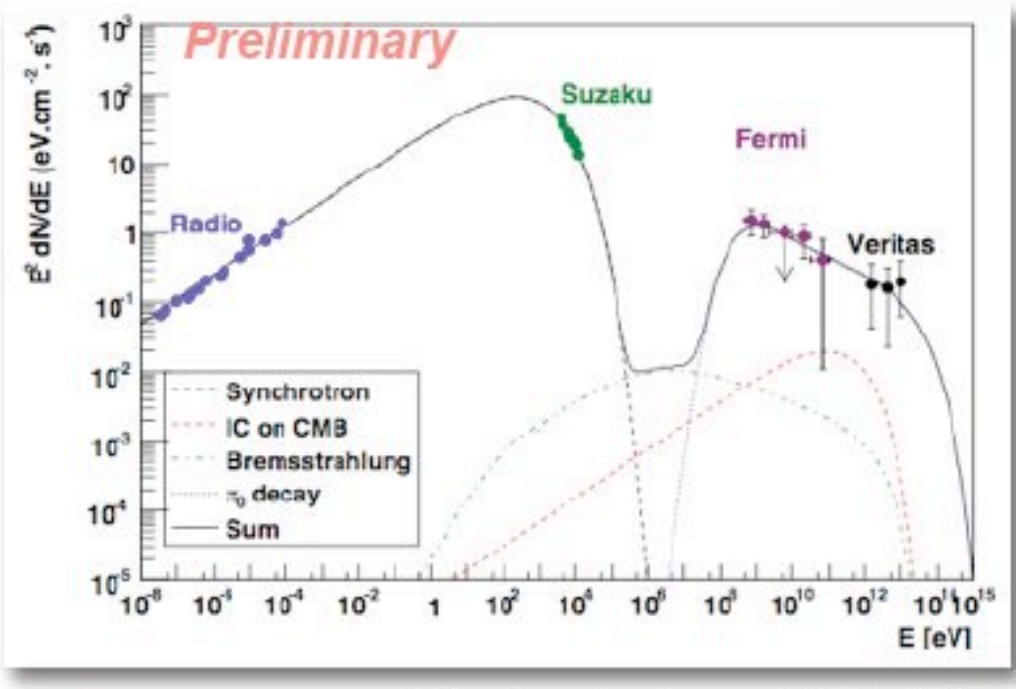

Case	D_{kpc}	n_H [cm^{-3}]	E_{SN} [10^{51}erg]	$E_{p,tot}$ [10^{51}erg]	K_{ep}
Far	3.50	0.24	2.0	0.150	4.5×10^{-4}
Nearby	2.78	0.30	1.0	0.061	7.0×10^{-4}

Photon index = 2.3 ± 0.1
(favors hadronic origin)

6-8% of E_{SN} transferred to CRs.

Cas A: GeV & TeV Detections

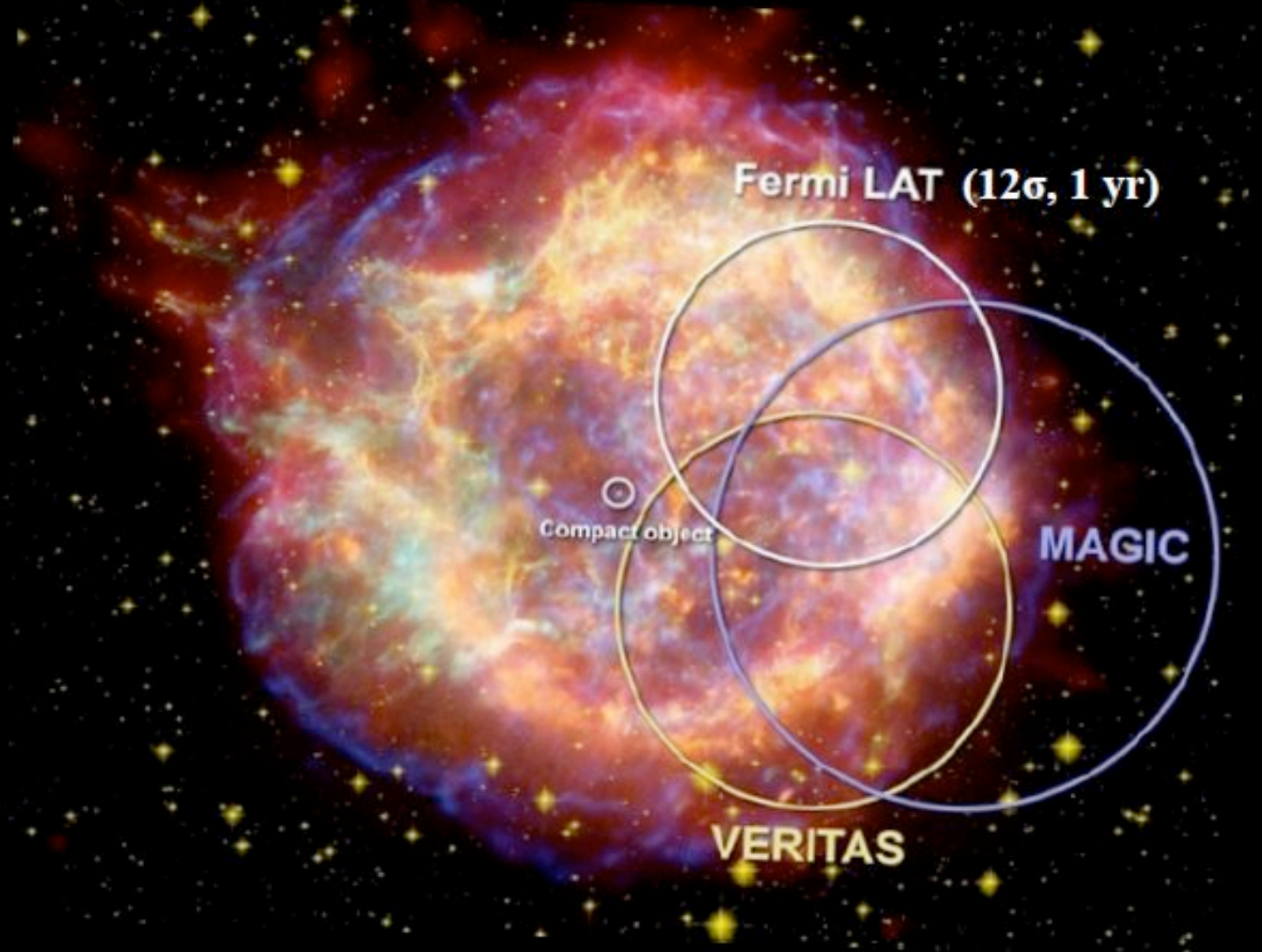

Cas A: Gamma-ray Spectrum

B_2 = 0.3-0.5 mG is inferred from the width of X-ray filaments (Vink & Laming 03; Parizot+06) **and X-ray time-variability** (Uchiyama & Aharonian 08)

π^0-decay model

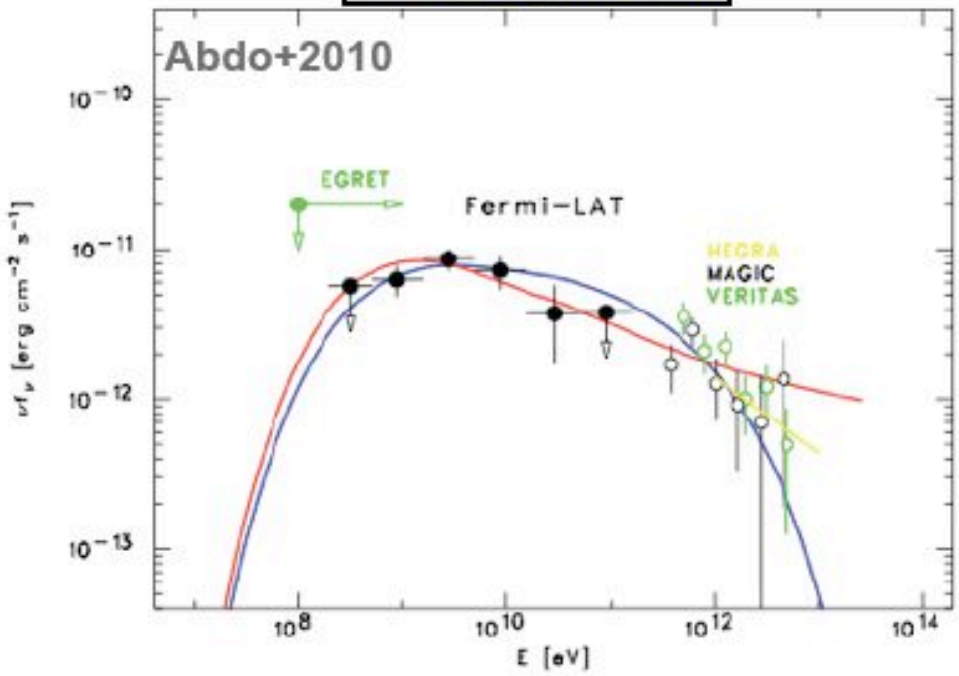

Fermi-LAT spectrum:
$\Gamma = 2.0 \pm 0.1$

CR Proton: ~0.4×10^{50} erg
E_{CR} ~ 2% of $E_{SN}=2\times10^{51}$ erg

CR spectral index = 2.3

LAT Discoveries of MC-SNRs

Fermi-LAT Collaboration (Uchiyama+) 2011

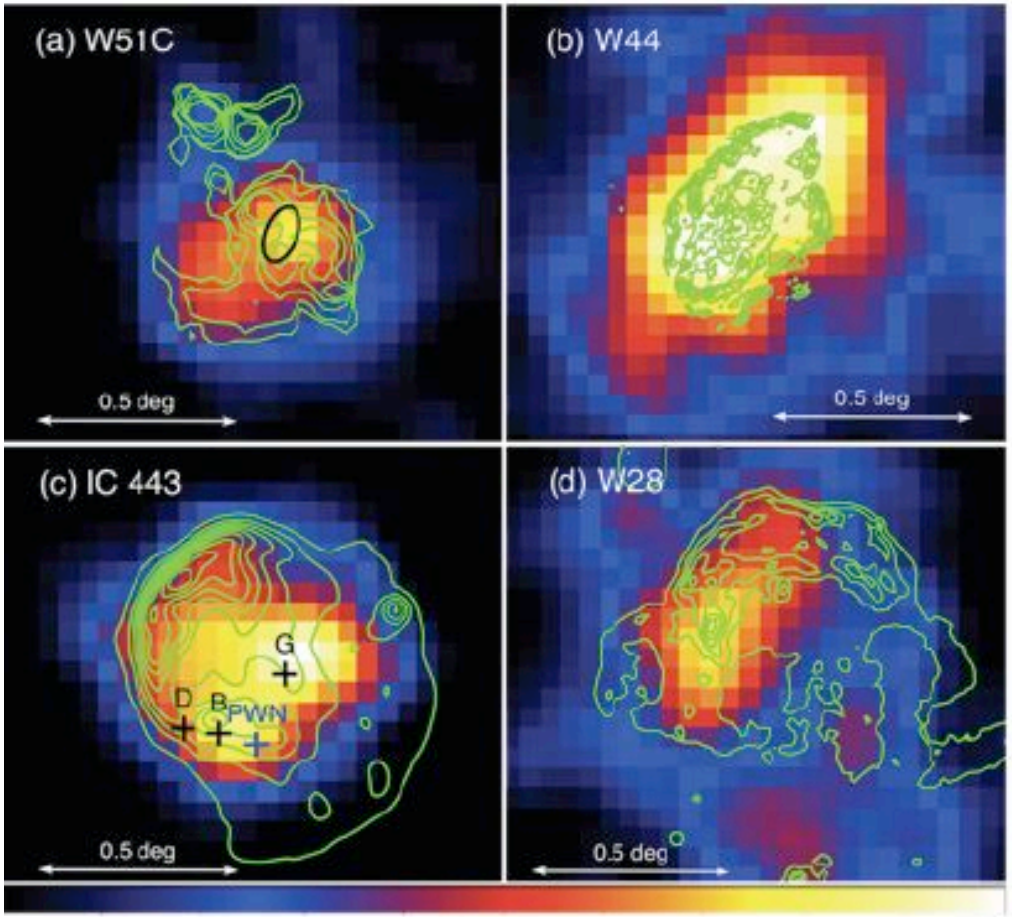

2.5 yr count maps (>2 GeV, front-converted)

Extended GeV emission has been discovered from several SNRs, with molecular cloud (MC) interactions.

GeV extension is consistent with the size of a radio remnant (except for W28).

The dominant class of LAT SNRs.

GeV Spectra of MC-SNRs

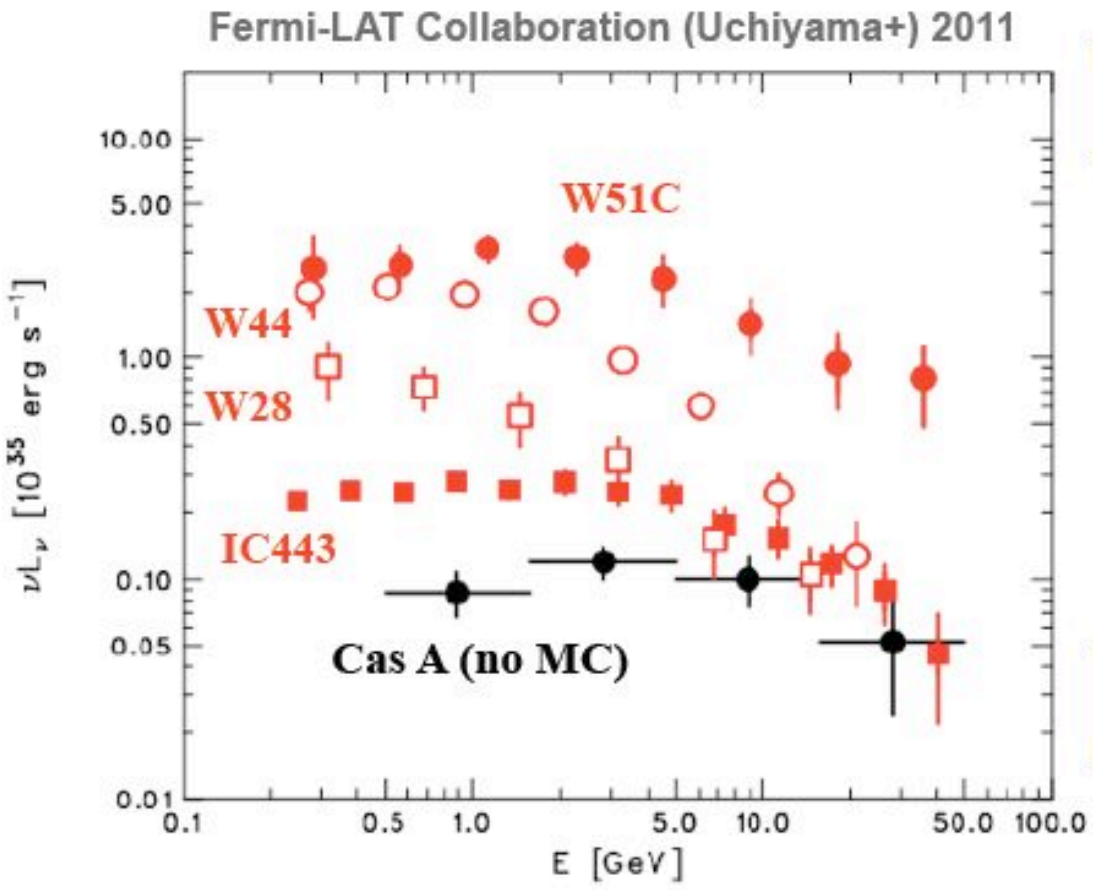

High GeV luminosity up to 10^{36} erg/s

Assuming e/p ratio less than 10%, the only way to achieve the high luminosity is:

π^0-decay γ-rays in dense gas (>10 cm^{-3}).

Spectral steepening in the GeV band

GeV luminosity >> TeV luminosity

DIFFICULT TO PROVE: Fermi paper on W51C, Abdo et al. 2010

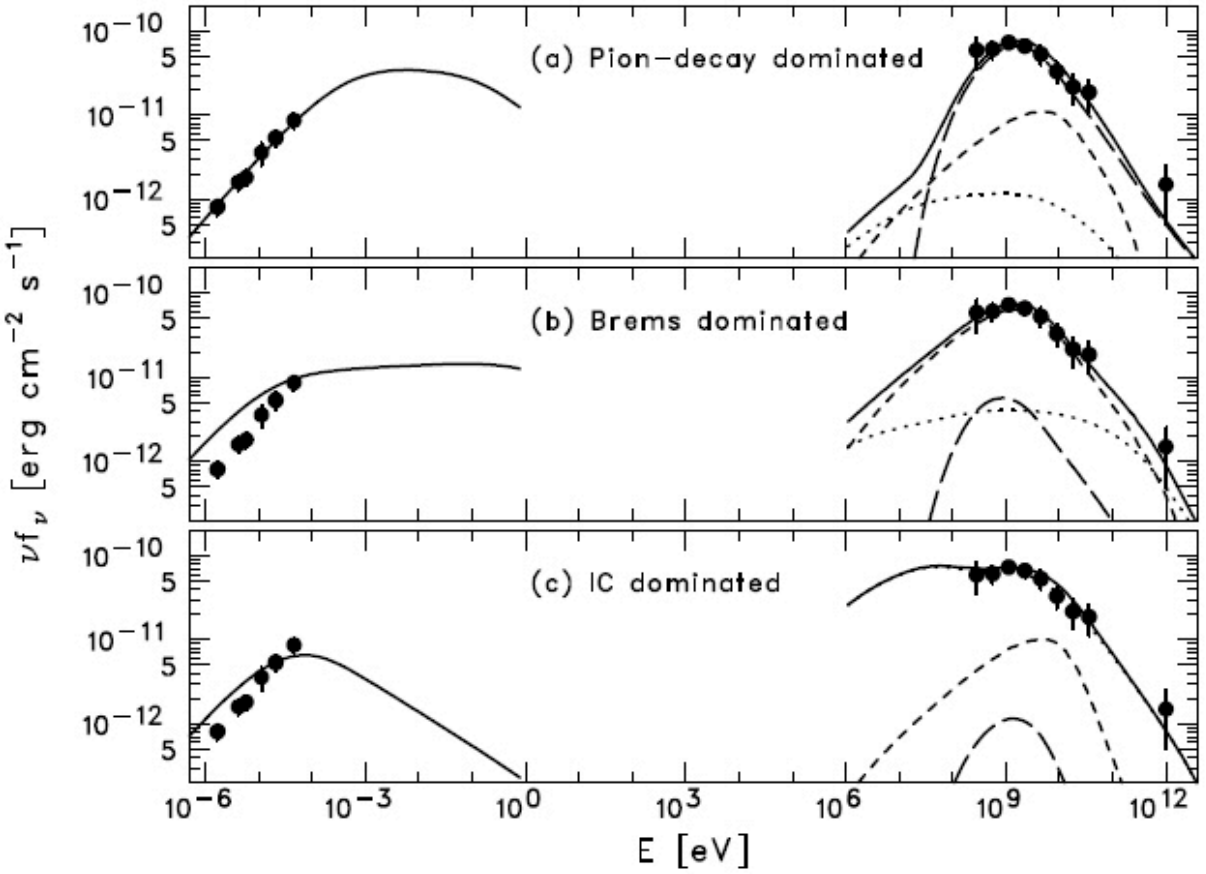

Fig. 4.— Three different scenarios for the multiwavelength modeling (see Table 1). The radio emission (from Moon & Koo 1994) is explained by synchrotron radiation, while the gamma-ray emission is modeled by different combinations of π^0-decay (long-dashed curve), bremsstrahlung (dashed curve), and IC scattering (dotted curve). The sum of the three component is shown as a solid curve.

Crushed Cloud Model

Uchiyama+2010

Re-acceleration of pre-existing CRs in MC at cloud radiative shock.
π^0-decay gamma-rays in a radiatively-compressed layer.

Naturally accounts for a gamma-ray luminosity of ~10^{35} erg/s
A slow (~100 km/s) shock explains spectral steepening in GeV range

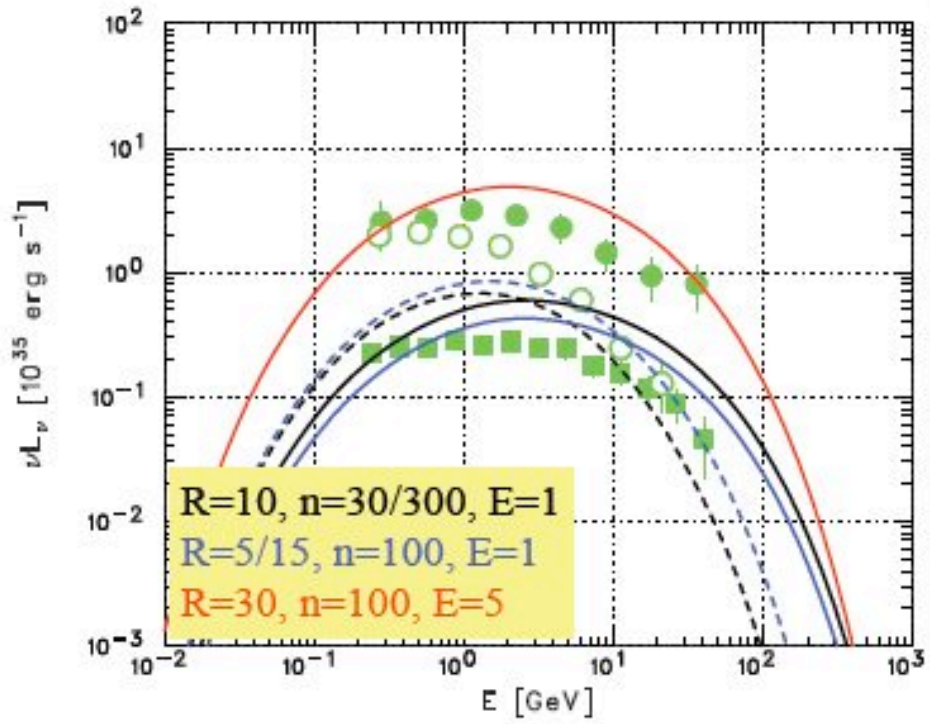

Model Parameters

f: Preshock cloud filling factor
f = 0.2 fixed

n: Preshock cloud density in cm^{-3}

B: Preshock B-field in μG
B = 2 n$^{1/2}$ fixed

R: SNR radius in pc

E: SN kinetic energy in 10^{51} erg

Crushed Cloud Model for W44

Uchiyama+2010

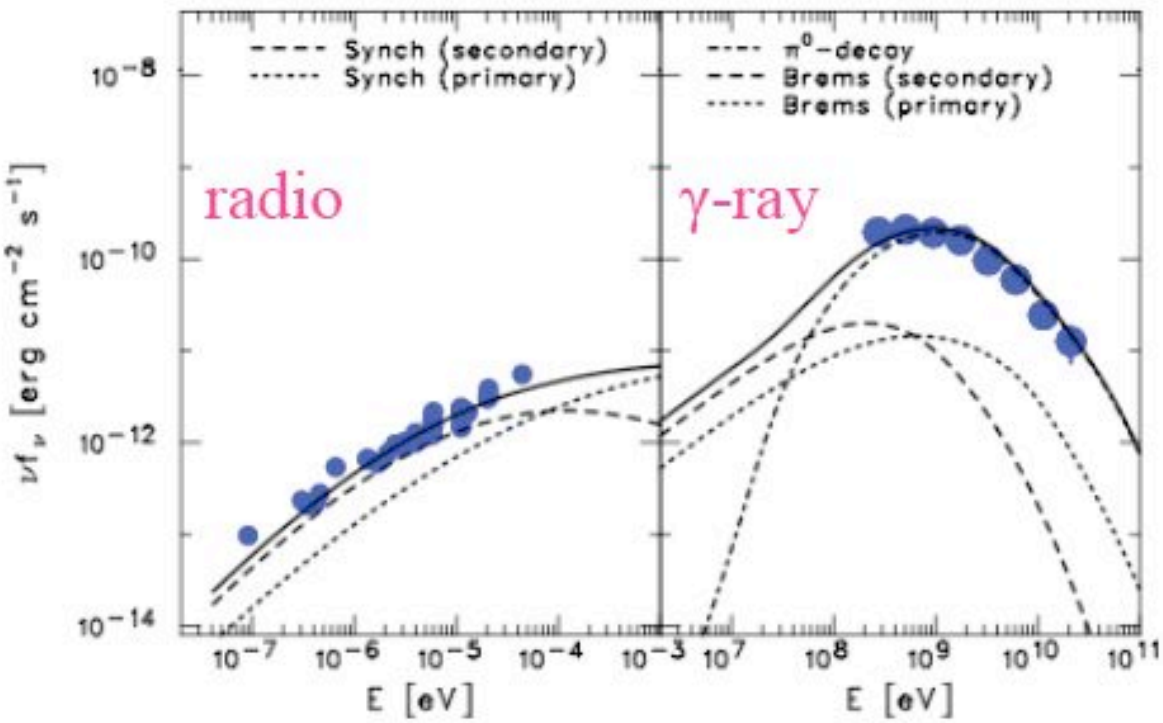

- radio & γ-ray fluxes can be explained by re-acceleration of the pre-existing GCRs

- flat radio index (α=0.37) is naturally explained

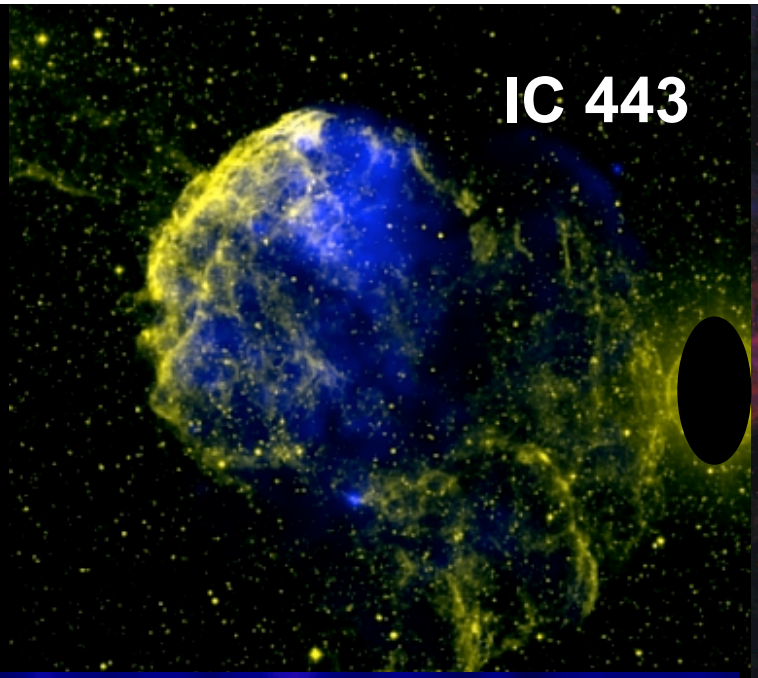
IC 443

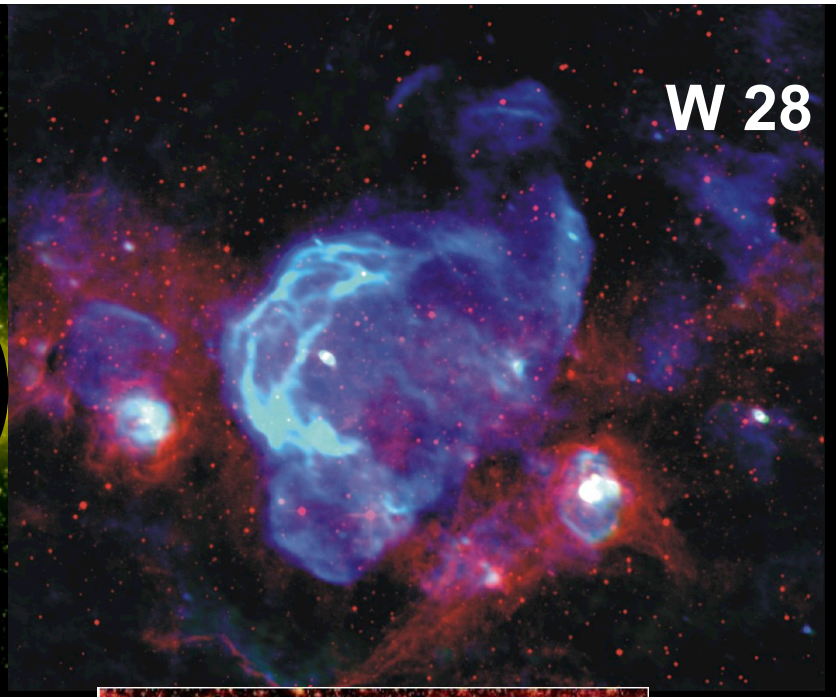
W 28

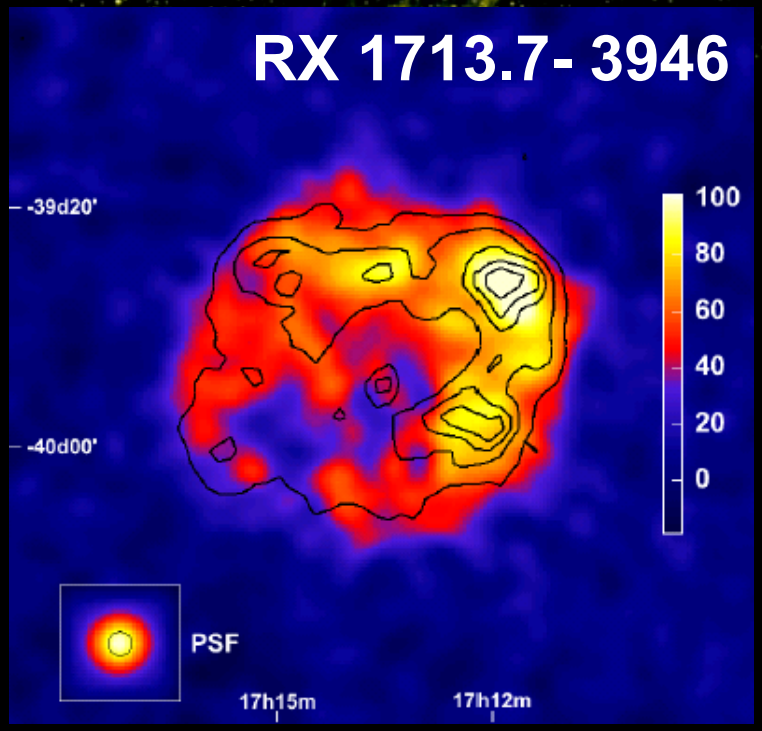
RX 1713.7- 3946
-39d20'
-40d00'
100
80
60
40
20
0
PSF
17h15m
17h12m

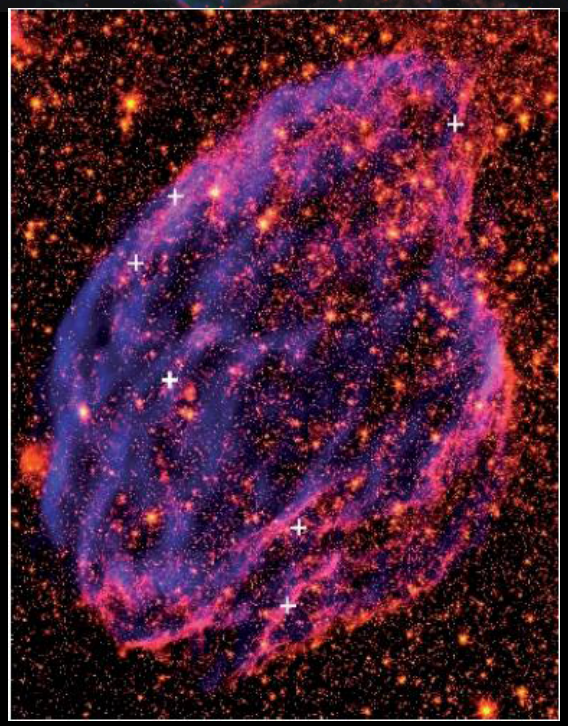
W 44

Good X-ray-TeV correlation (~80%)
ASCA-HESS data of RX 1713.7-3946 (Goumard et al. 2006)

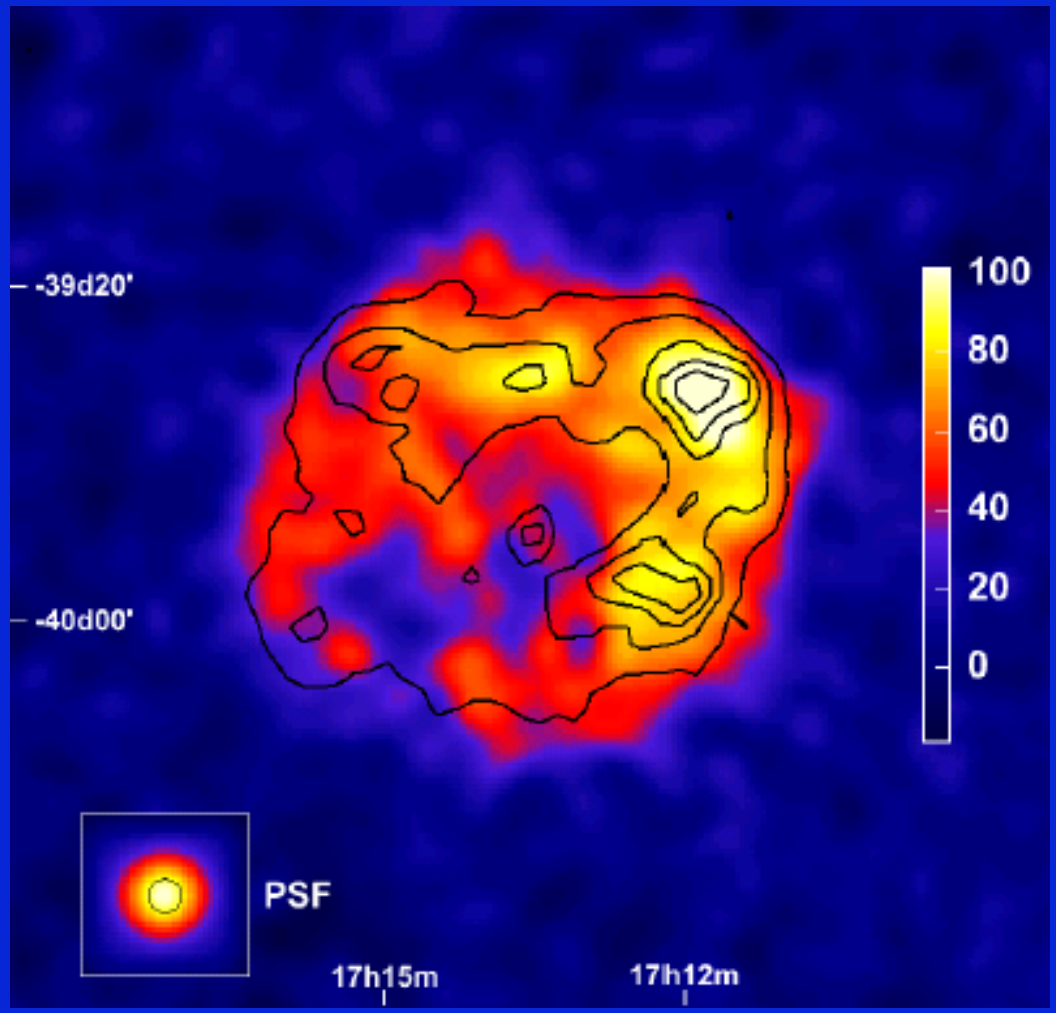

composite scenario of gamma-ray emission: forward shock in dense clouds and reverse shock

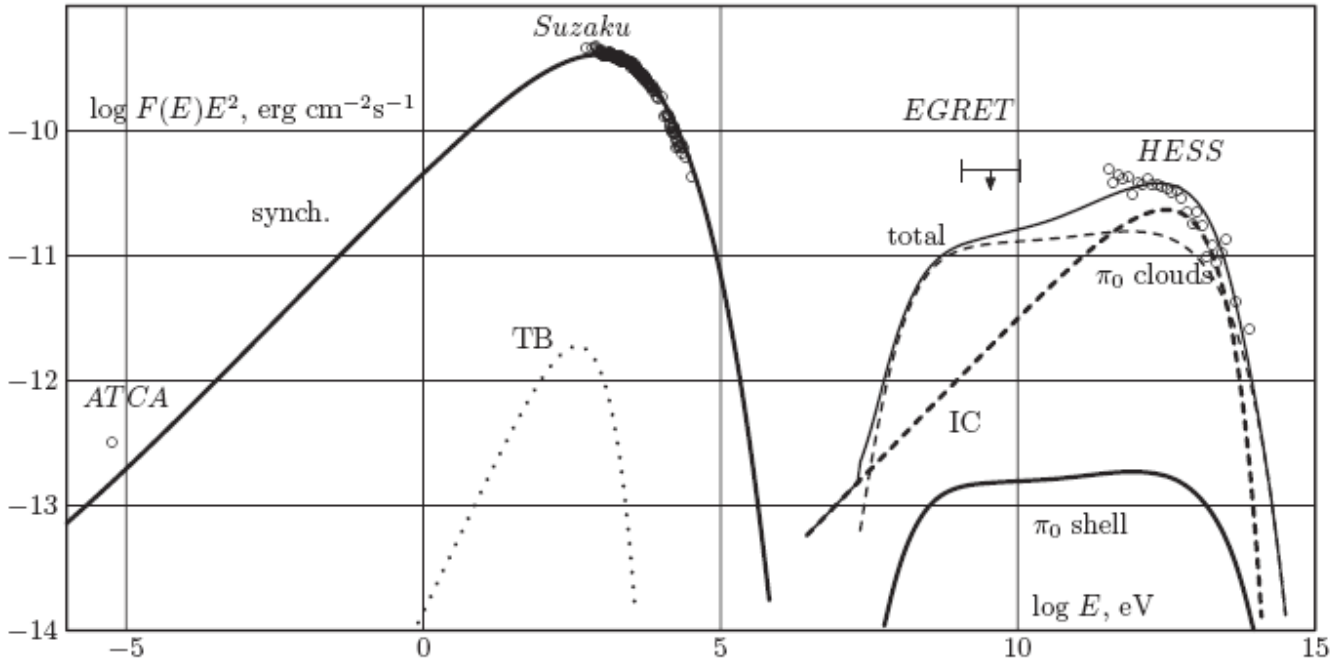

Figure 14. Broadband emission of RX J1713.7−3946 for the composite scenario of gamma rays with a non-modified forward shock and dense clouds. The principal model parameters are: $t = 1620$ yr, $D = 1.5$ kpc, $n_{\rm H} = 0.02$ cm^{-3}, $E_{SN} = 1.2 \times 10^{51}$ erg, $M_{ej} = 0.74\,M_\odot$, $M_A^f = 55$, $M_A^b = 10$, $\xi_0 = 0.1$, $K_{ep}^f = 1.4 \times 10^{-2}$, and $K_{ep}^b = 9 \times 10^{-4}$. The calculations lead to the following values of the magnetic fields and the shock speeds at the present epoch: the magnetic field downstream of the forward and reverse shocks $B_f = 22$ μG and $B_b = 31$ μG, respectively, the speed of the forward shock $V_f = 3830$ km s^{-1}, and the speed of the reverse shock $V_b = -1220$ km s^{-1}. The following radiation processes are taken into account: synchrotron radiation of accelerated electrons (solid curve on the left), thermal bremsstrahlung (dotted line), IC gamma-ray emission of the entire remnant including forward and reverse shocks (dashed line), and hadronic component of gamma-rays from the remnant's shell (solid line on the right), as well as from dense clouds assuming the factor of 120 enhancement of the flux (thin dashed line). We also show the total gamma-ray emission from the entire remnant including the dense clouds (thin solid line).

SNR RX 1713 (Abdo etal. 2011)

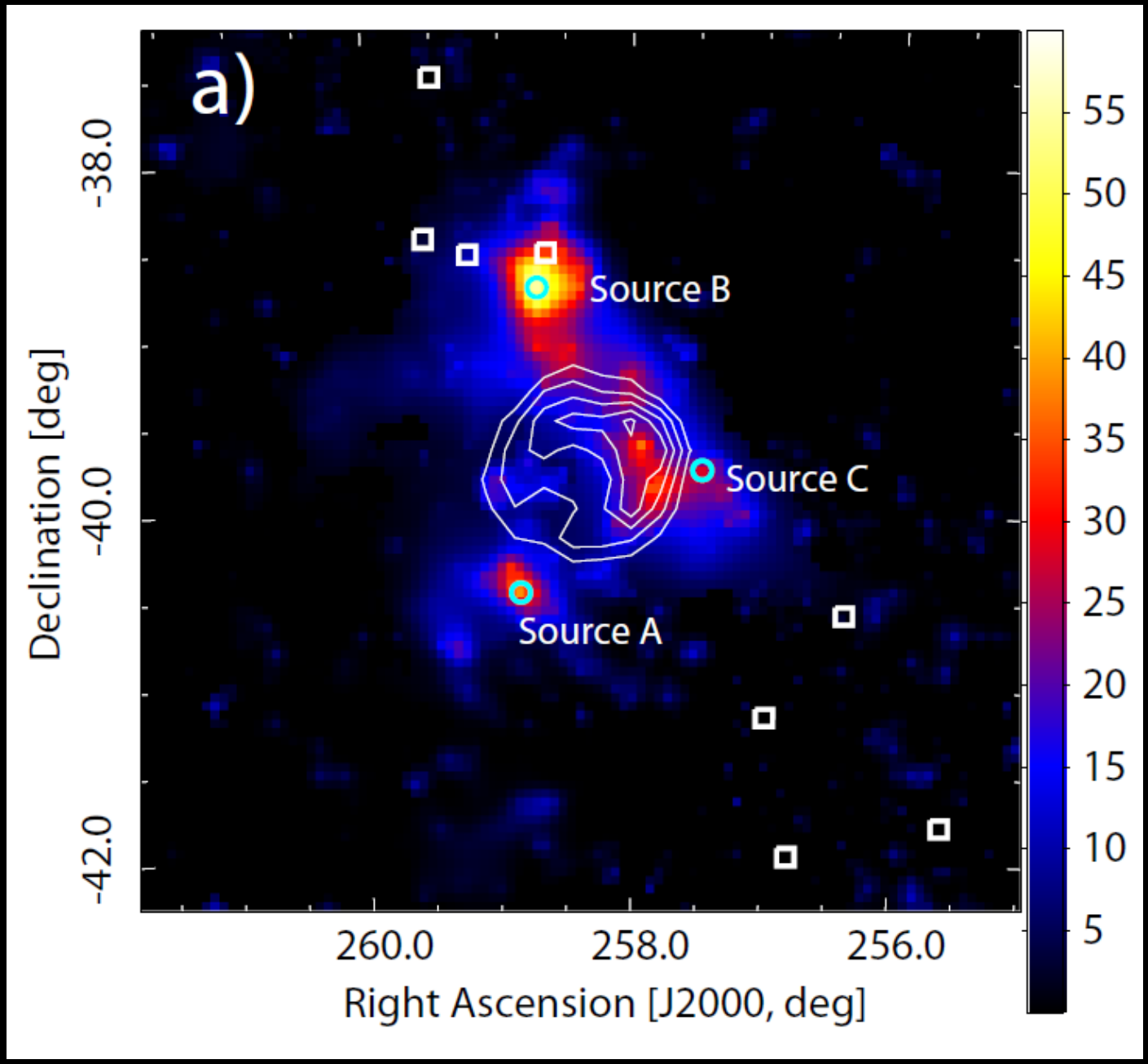

SNR RX 1713 *Fermi* 1-100 GeV
(Abdo etal. 2011)

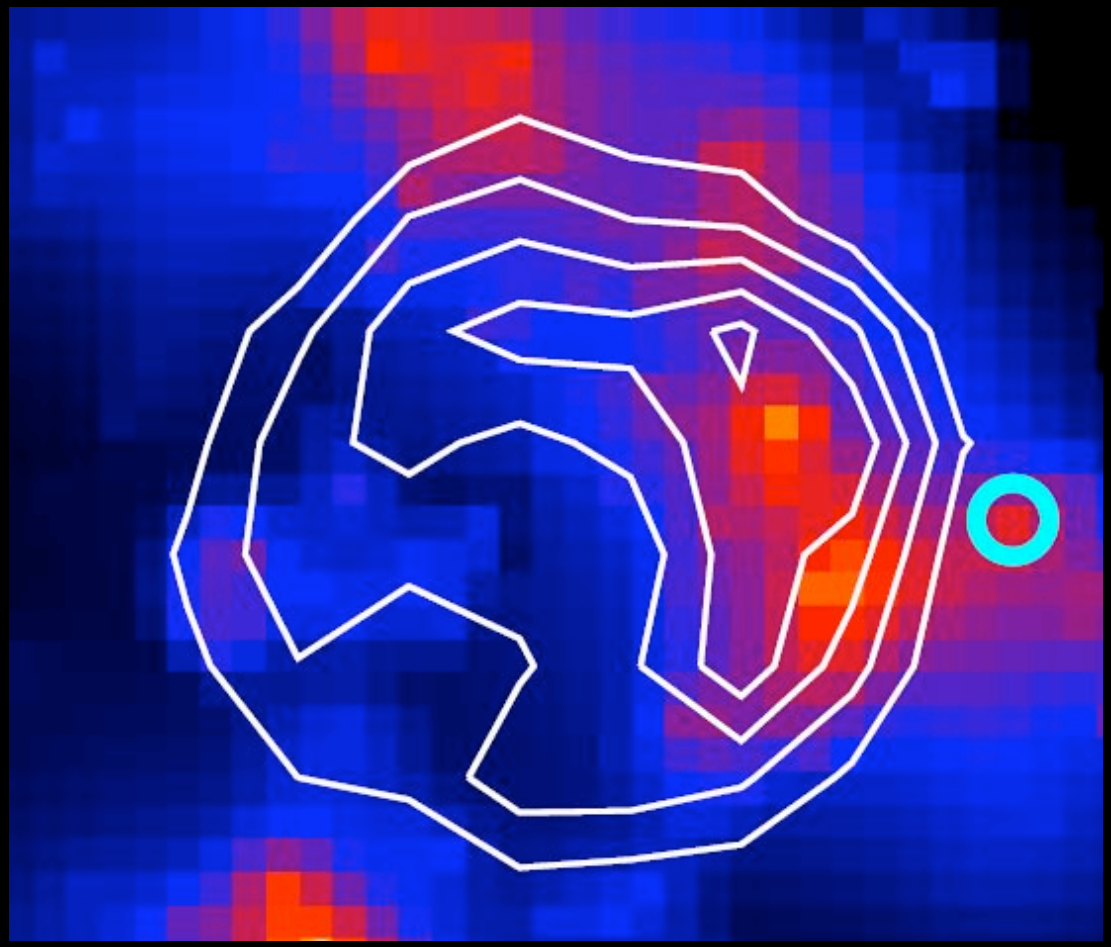

SNR RX 1713 (Abdo etal. 2011)

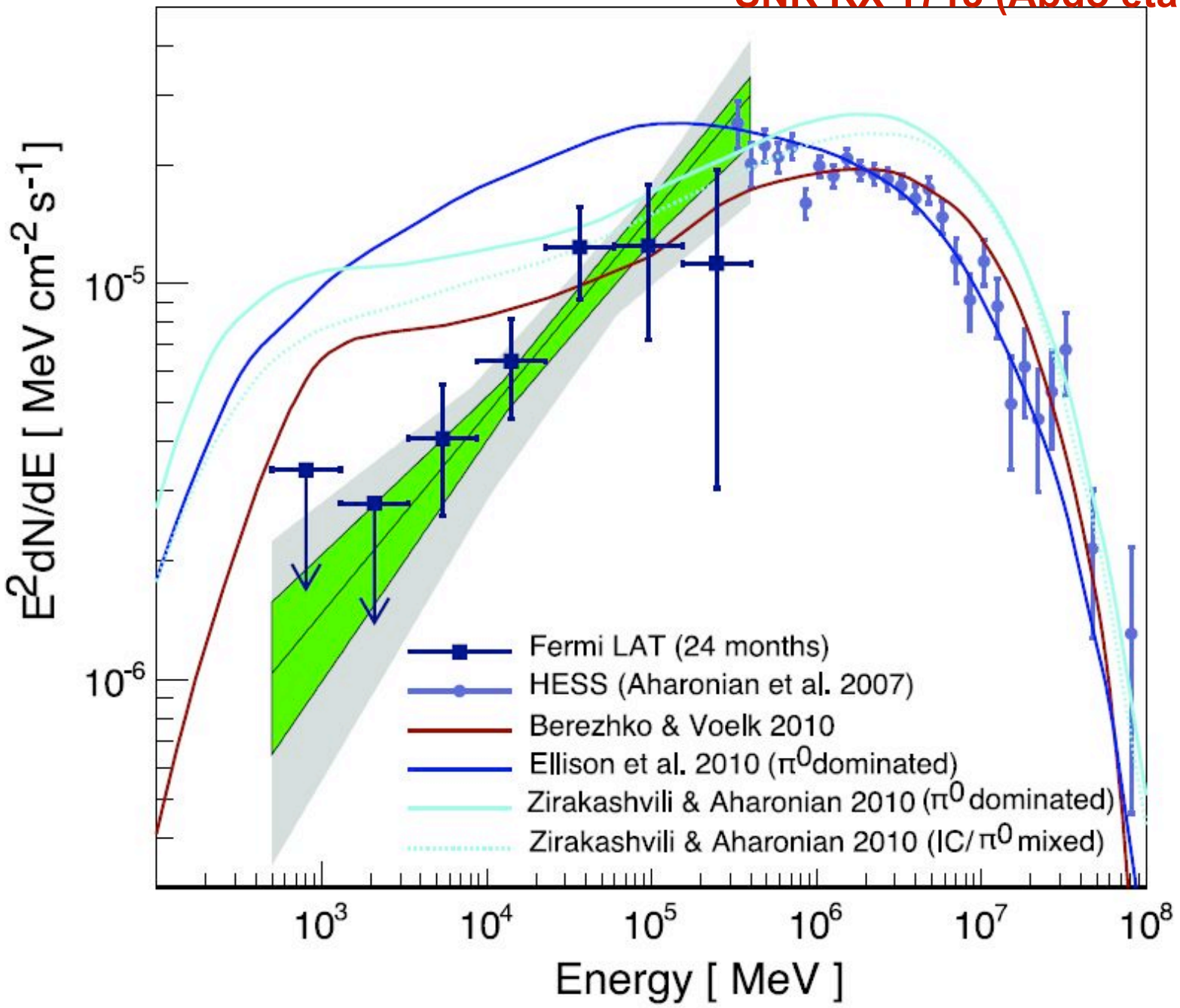

SNR RX 1713 (Abdo etal. 2011)

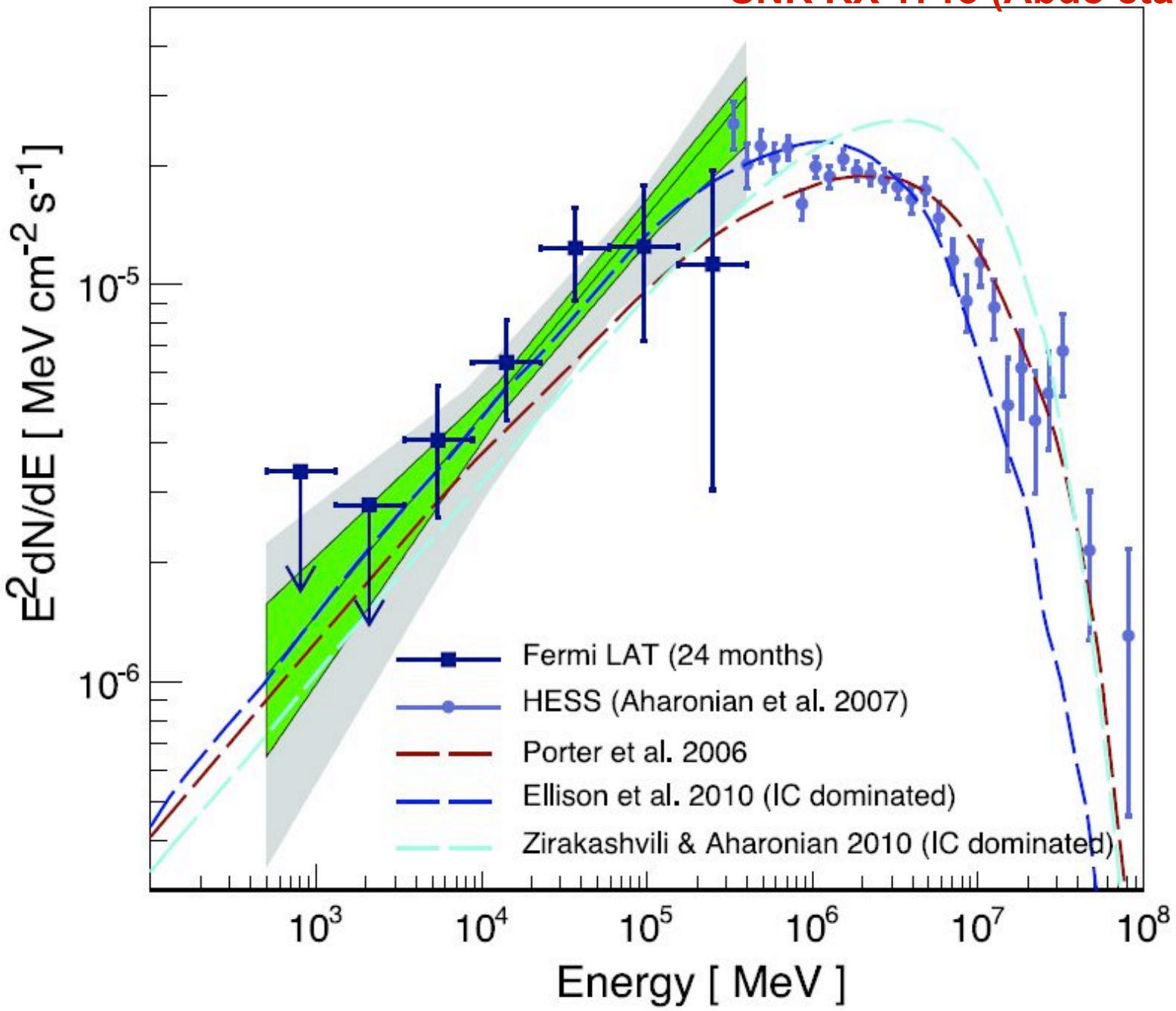

RX 1713.7-3946

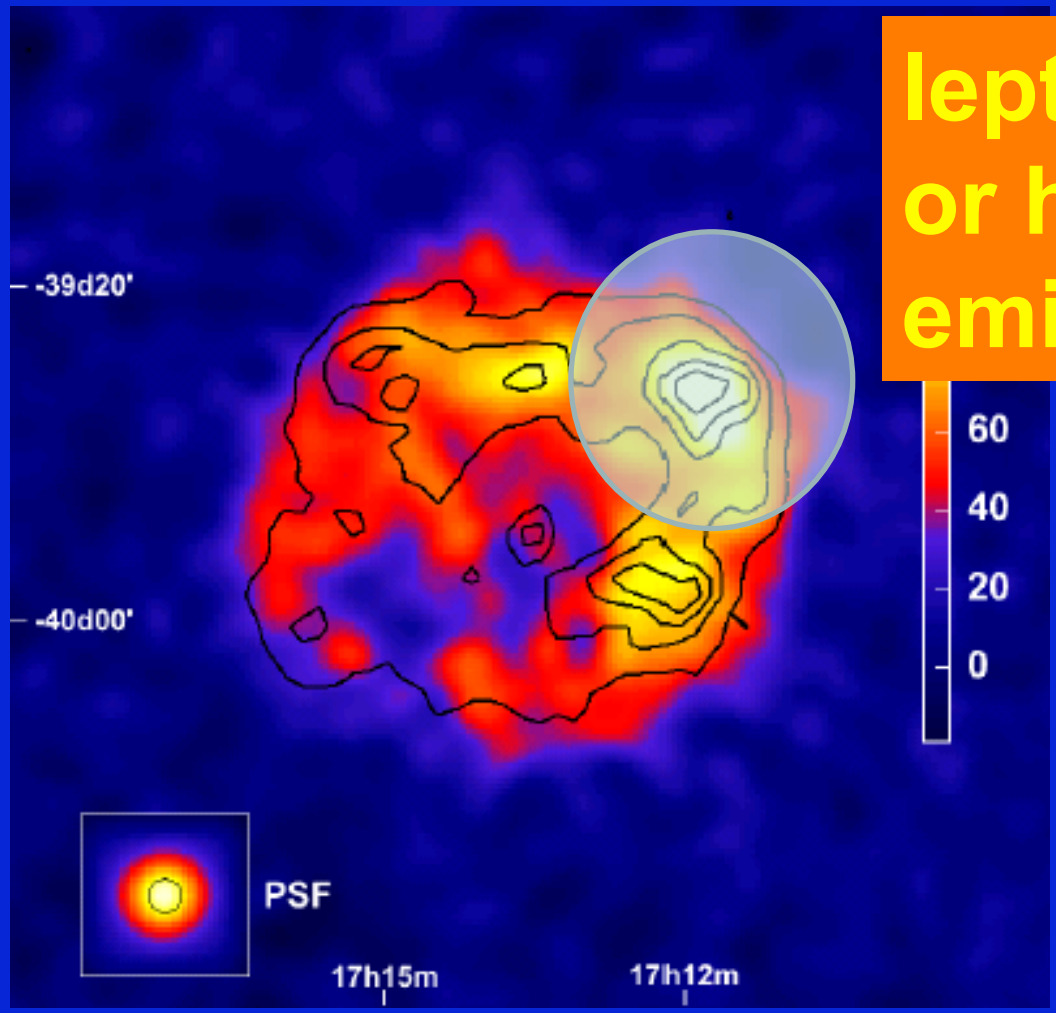

leptonic (?) or hadronic emission ?

RX 1713.7-3946

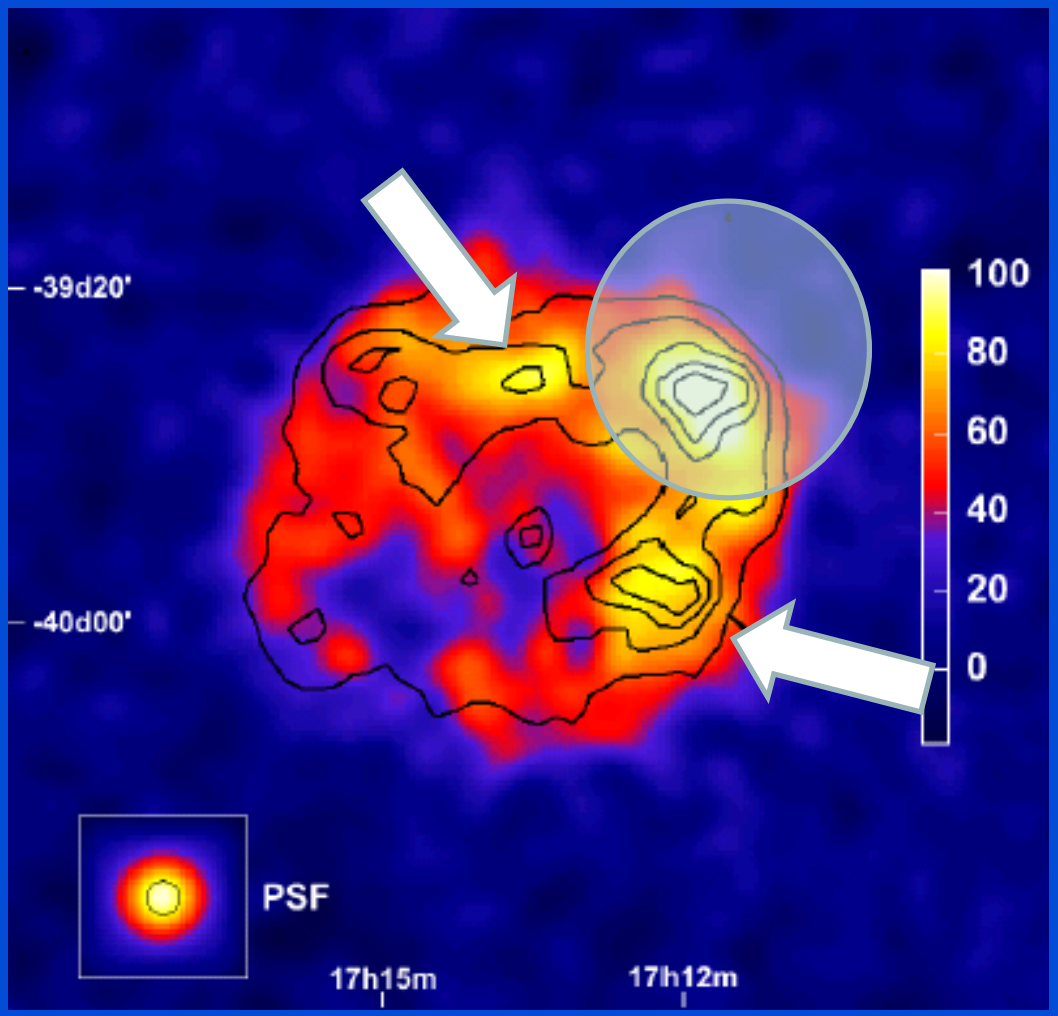

SNR RX J1713-3946

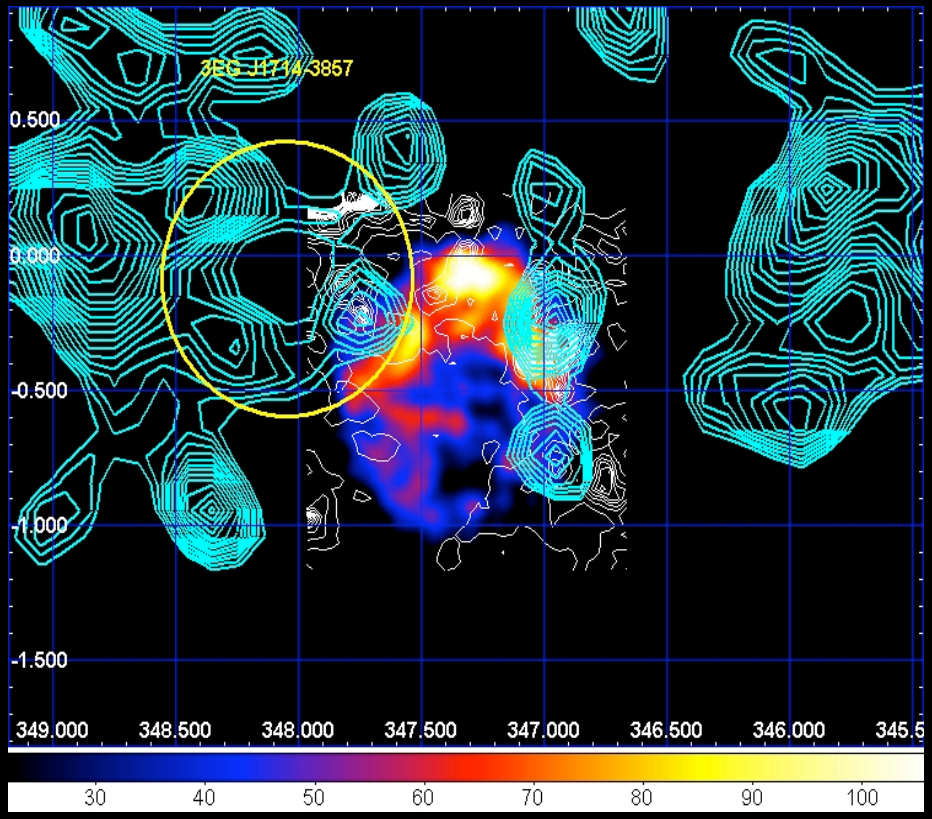

HESS map +

AGILE/GRID contours

(E> 400 MeV)

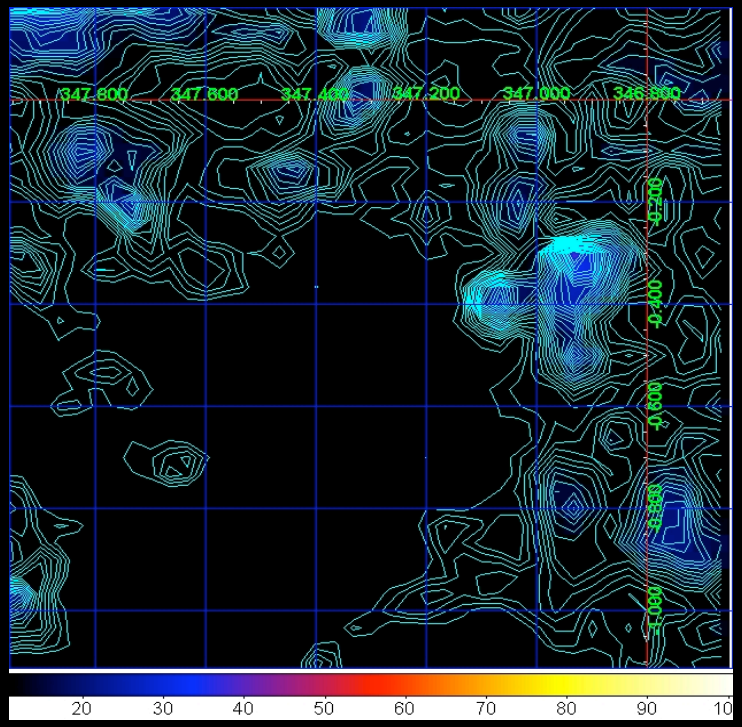

NANTEN

CO map

k to SNR W44

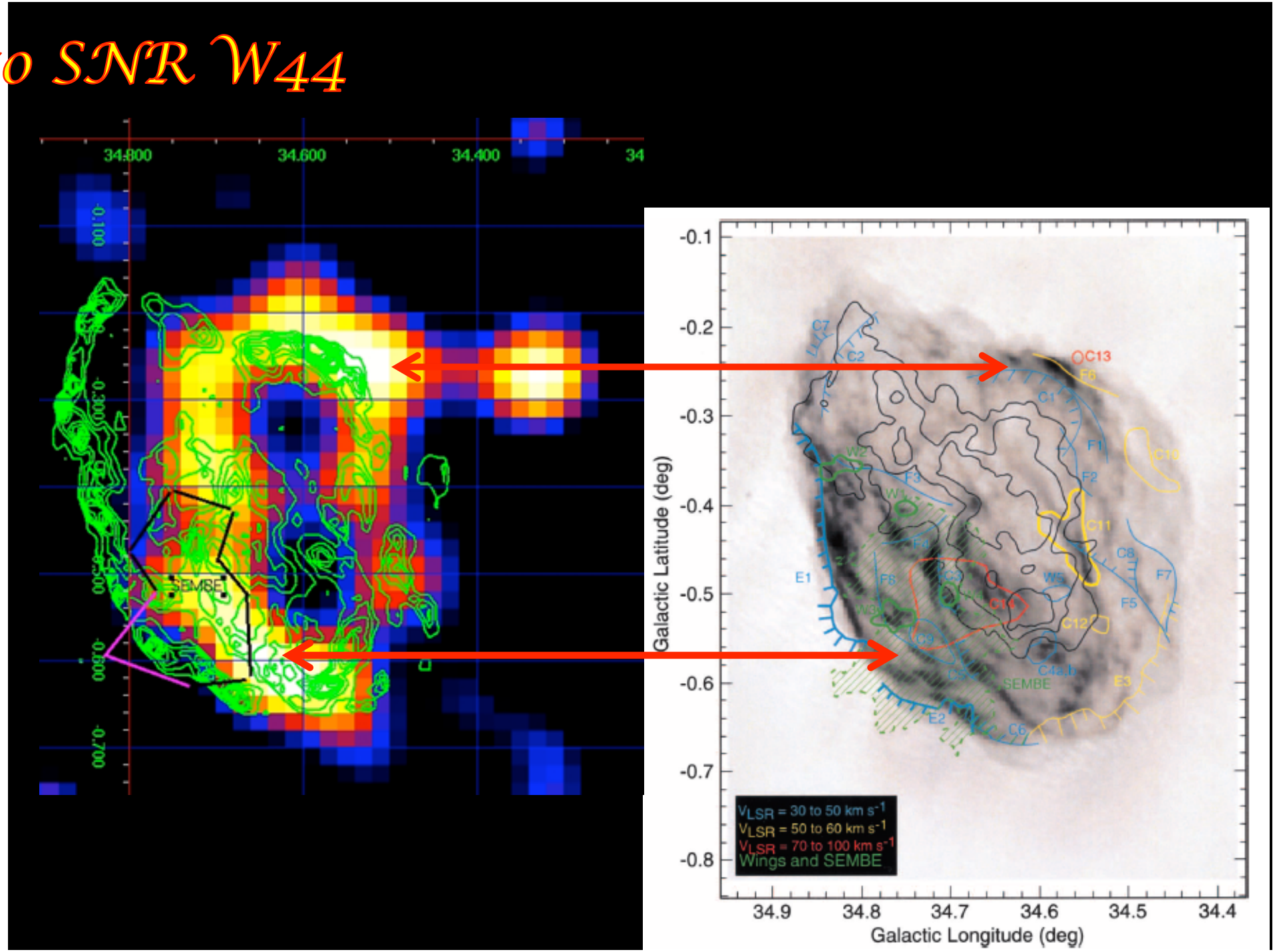
34.800
34.600
34.400
34
0.100
0.000
-0.100
-0.200
-0.300
SEMBE
-0.1
-0.2
-0.3
-0.4
-0.5
-0.6
-0.7
-0.8
Galactic Latitude (deg)
34.9
34.8
34.7
34.6
34.5
34.4
Galactic Longitude (deg)
C7
C2
C13
F6
C1
F1
C10
W2
F3
F2
W1
C11
F4
C8
E1
F8
C3
W5
F7
W3
C14
F5
C12
C9
C4a,b
SEMBE
E3
E2
C6
VLSR = 30 to 50 km s-1
VLSR = 50 to 60 km s-1
VLSR = 70 to 100 km s-1
Wings and SEMBE

The SNRW44: Fermi-LAT

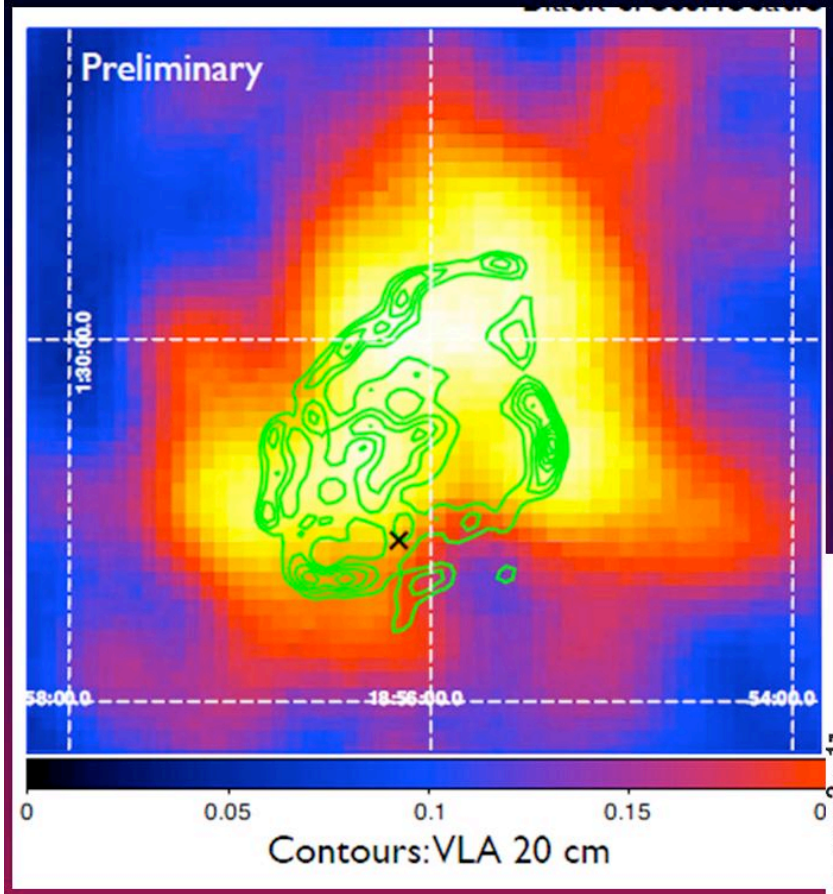

Abdo et al, 2010

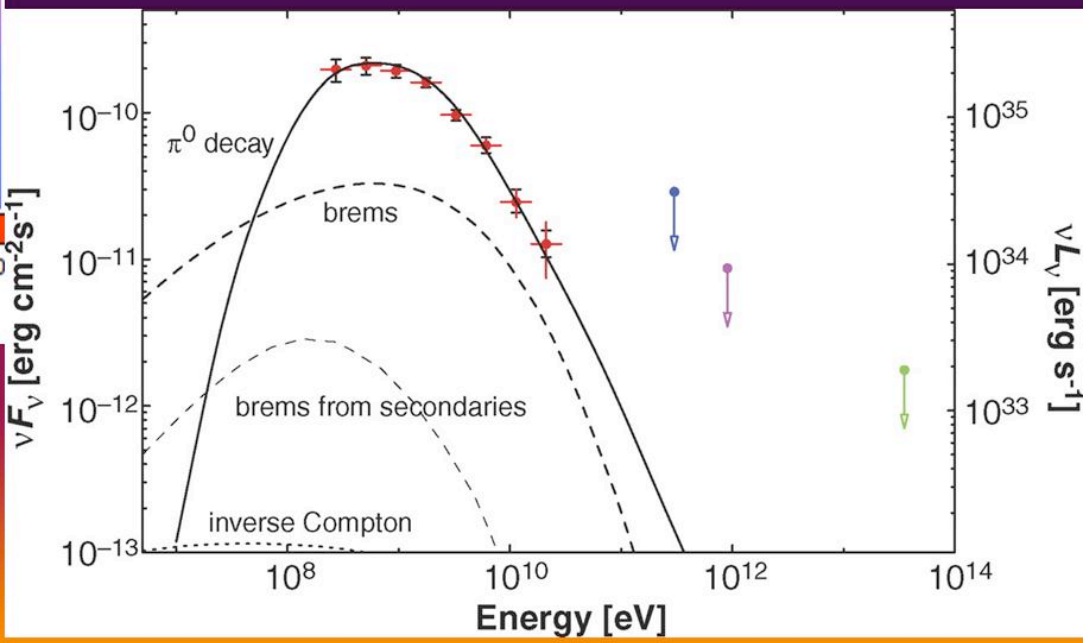

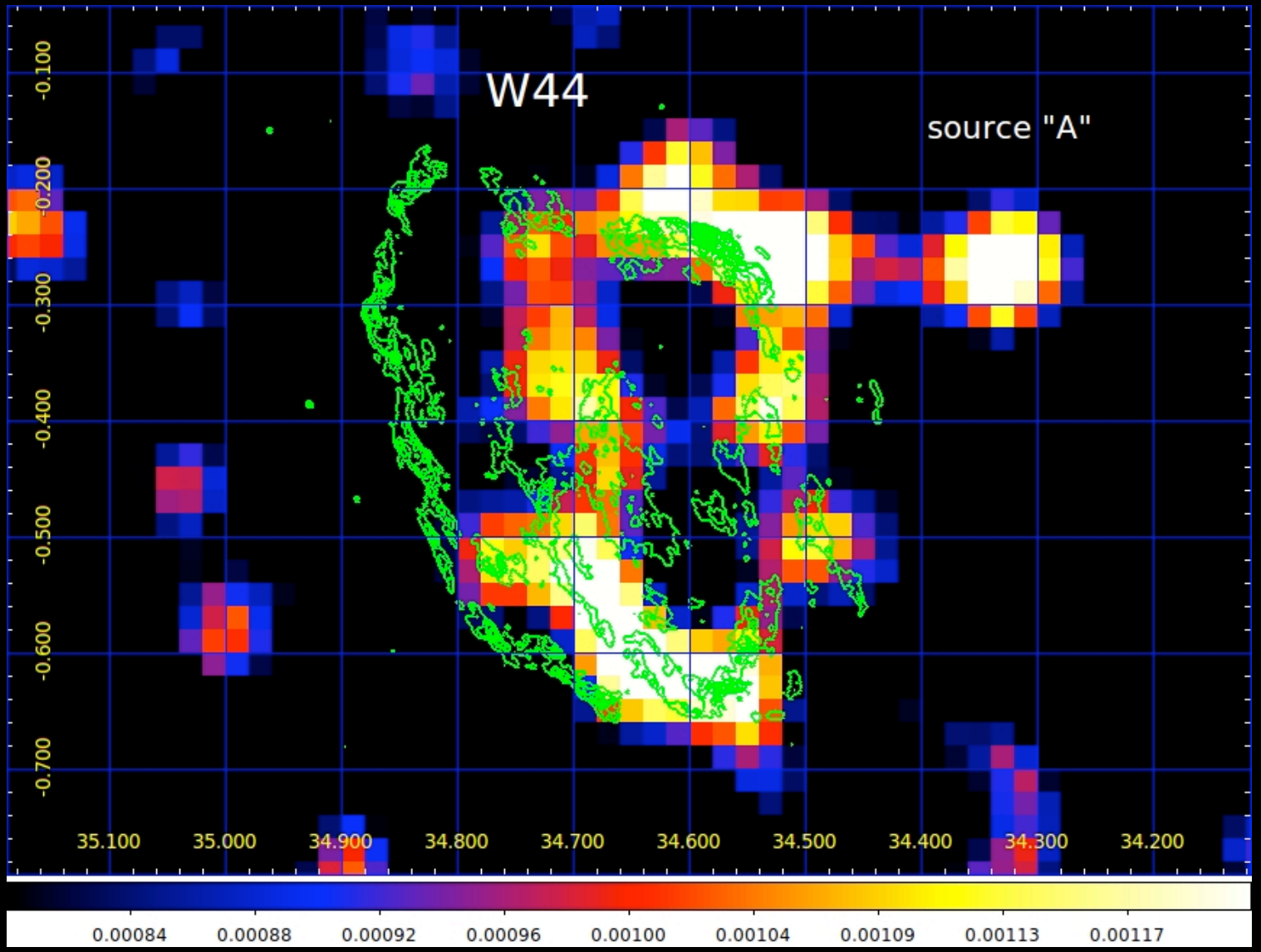
W44
source "A"
-0.100
-0.200
-0.300
-0.400
-0.500
-0.600
-0.700
35.100
35.000
34.900
34.800
34.700
34.600
34.500
34.400
34.300
34.200
0.00084
0.00088
0.00092
0.00096
0.00100
0.00104
0.00109
0.00113
0.00117

The SNR W44: AGILE

(Giuliani et al. 2011)

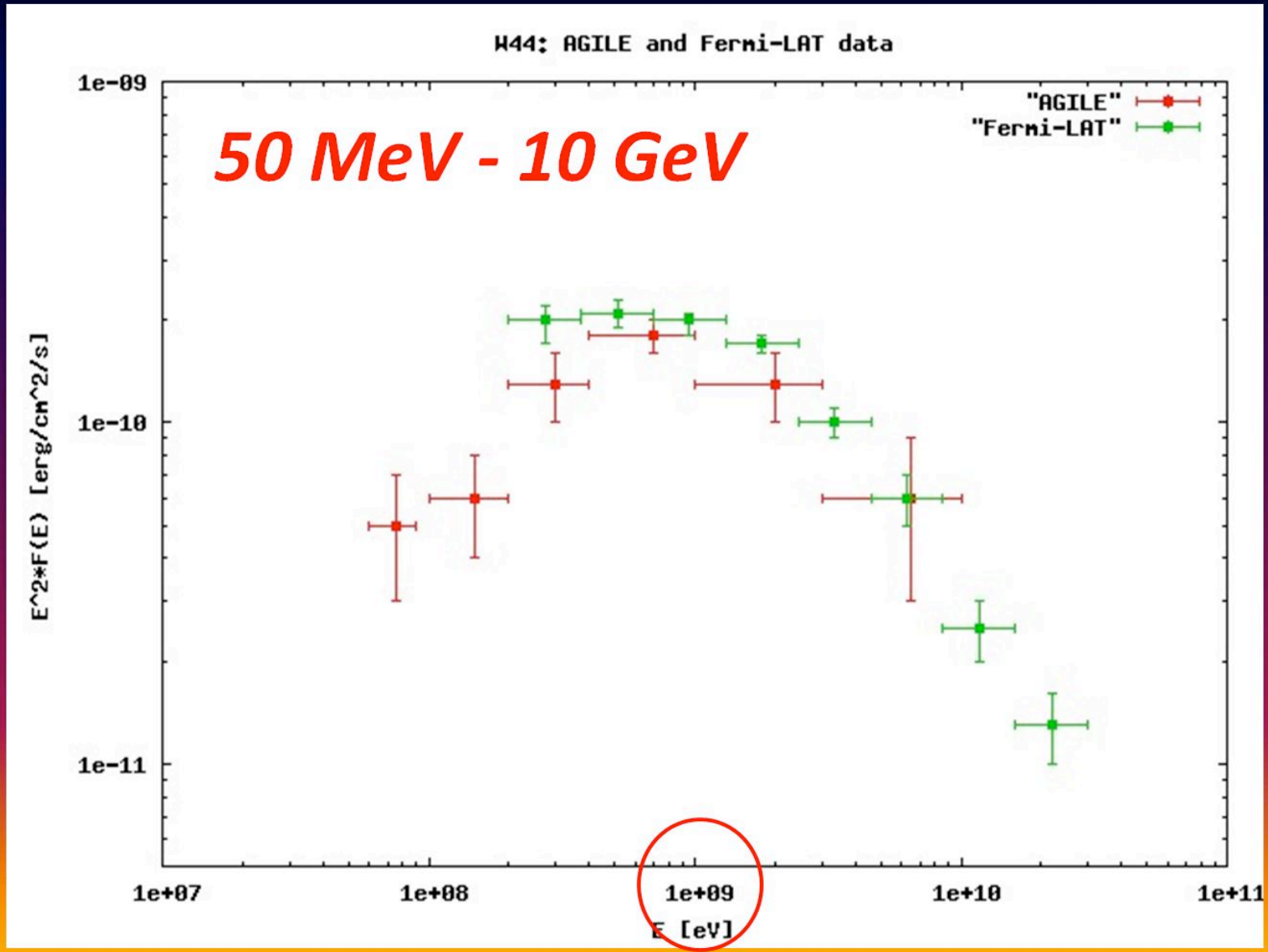

(Giuliani, Cardillo et al. 2011)

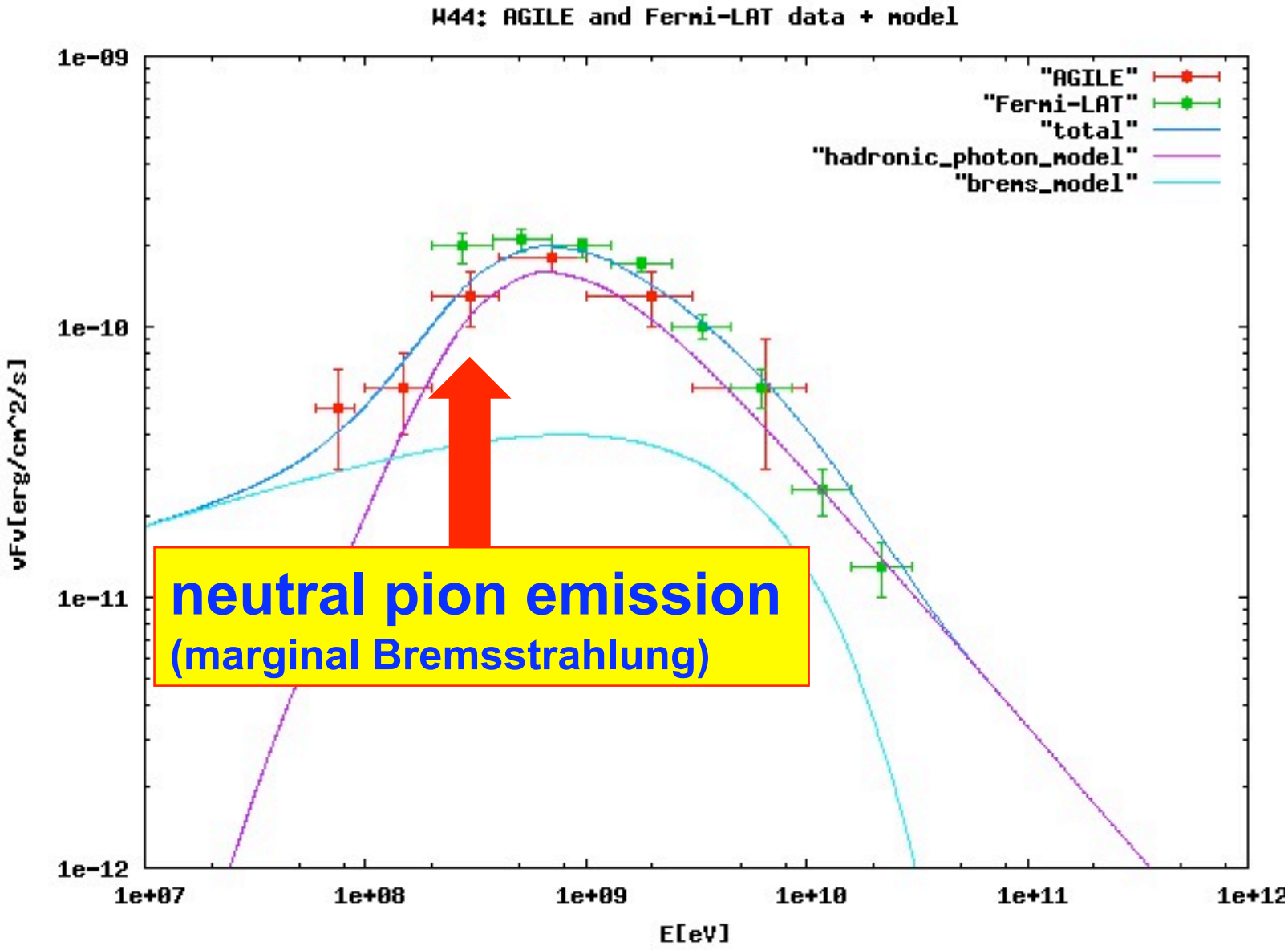

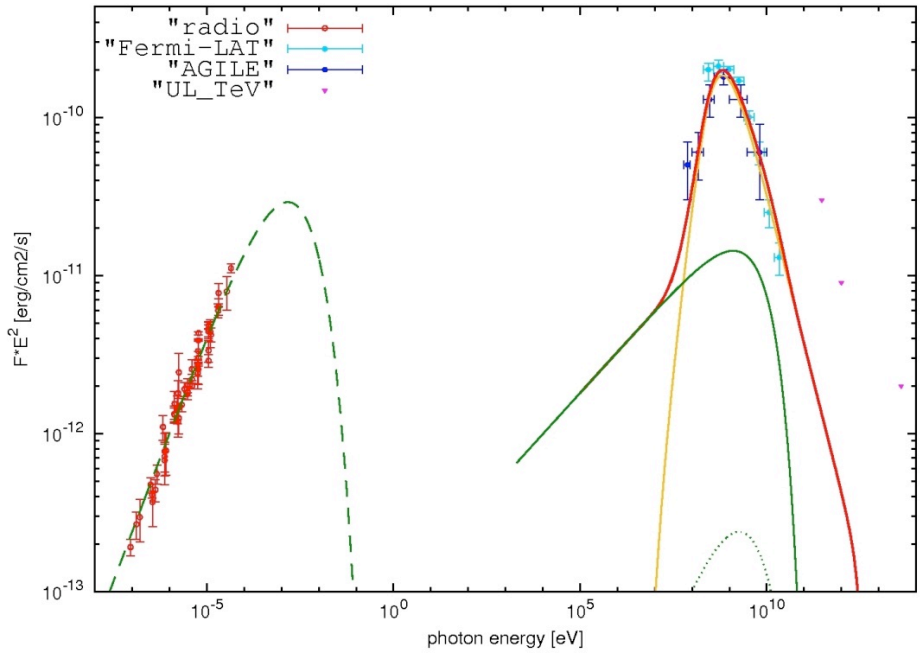

hadronic model, B = 20 μG, n = 100 cm^{-3}

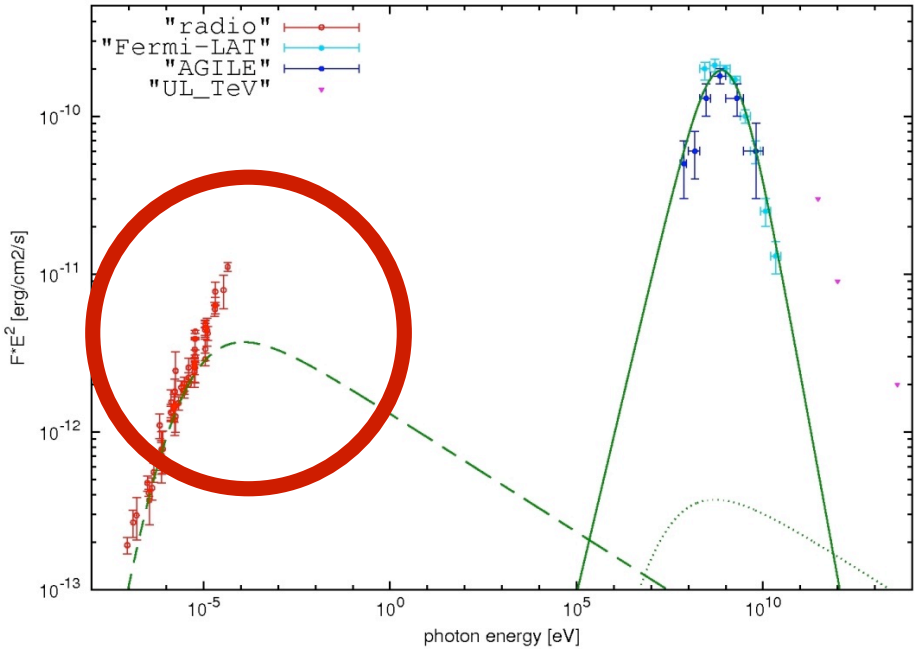

"ad hoc" e- Brems. model, B = 20 μG, n = 300 cm^{-3}

The SNR W44: AGILE

(Giuliani et al. 2011)

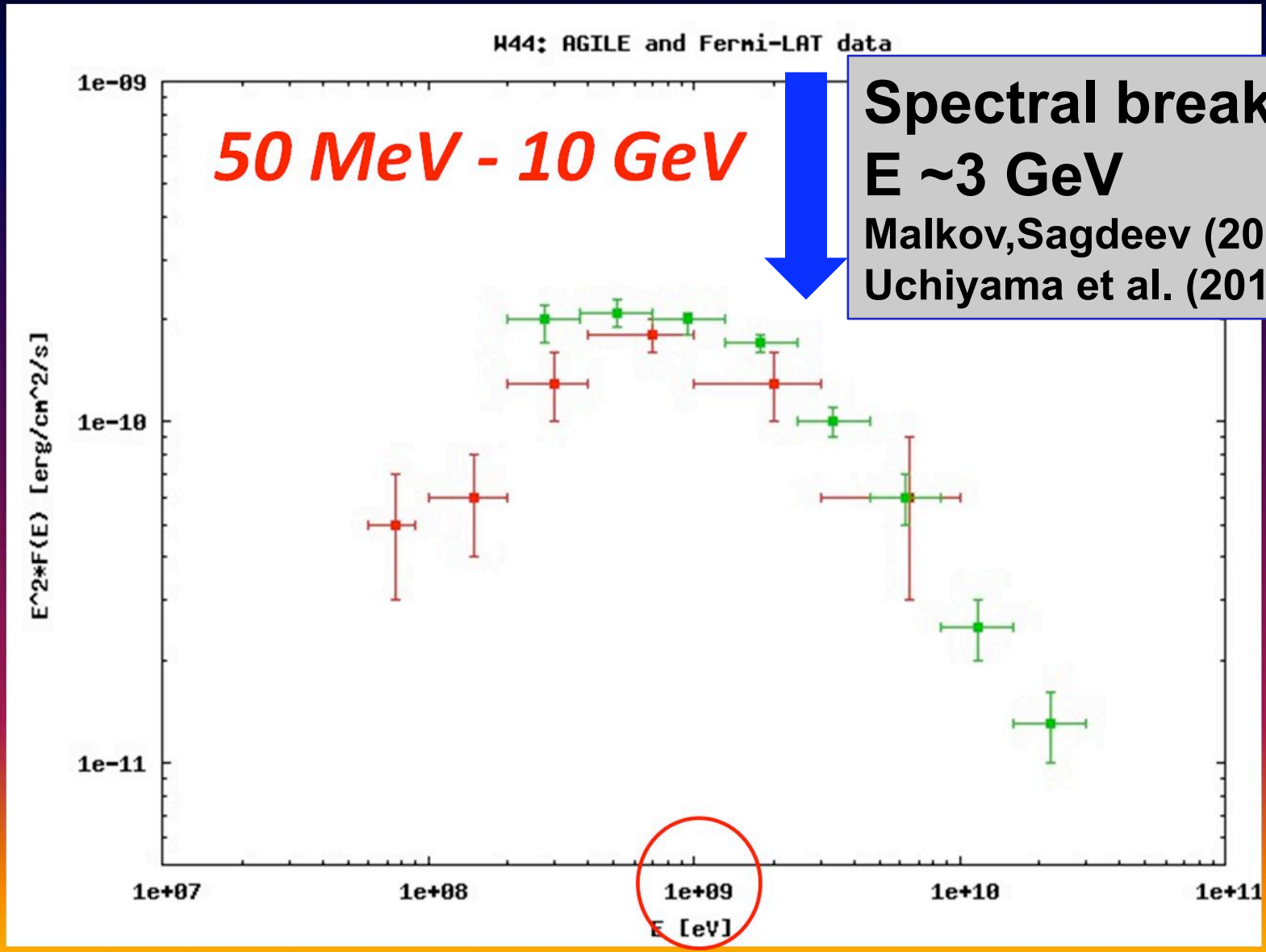

Spectral break, E ~3 GeV

Malkov,Sagdeev (2010)

Uchiyama et al. (2010)

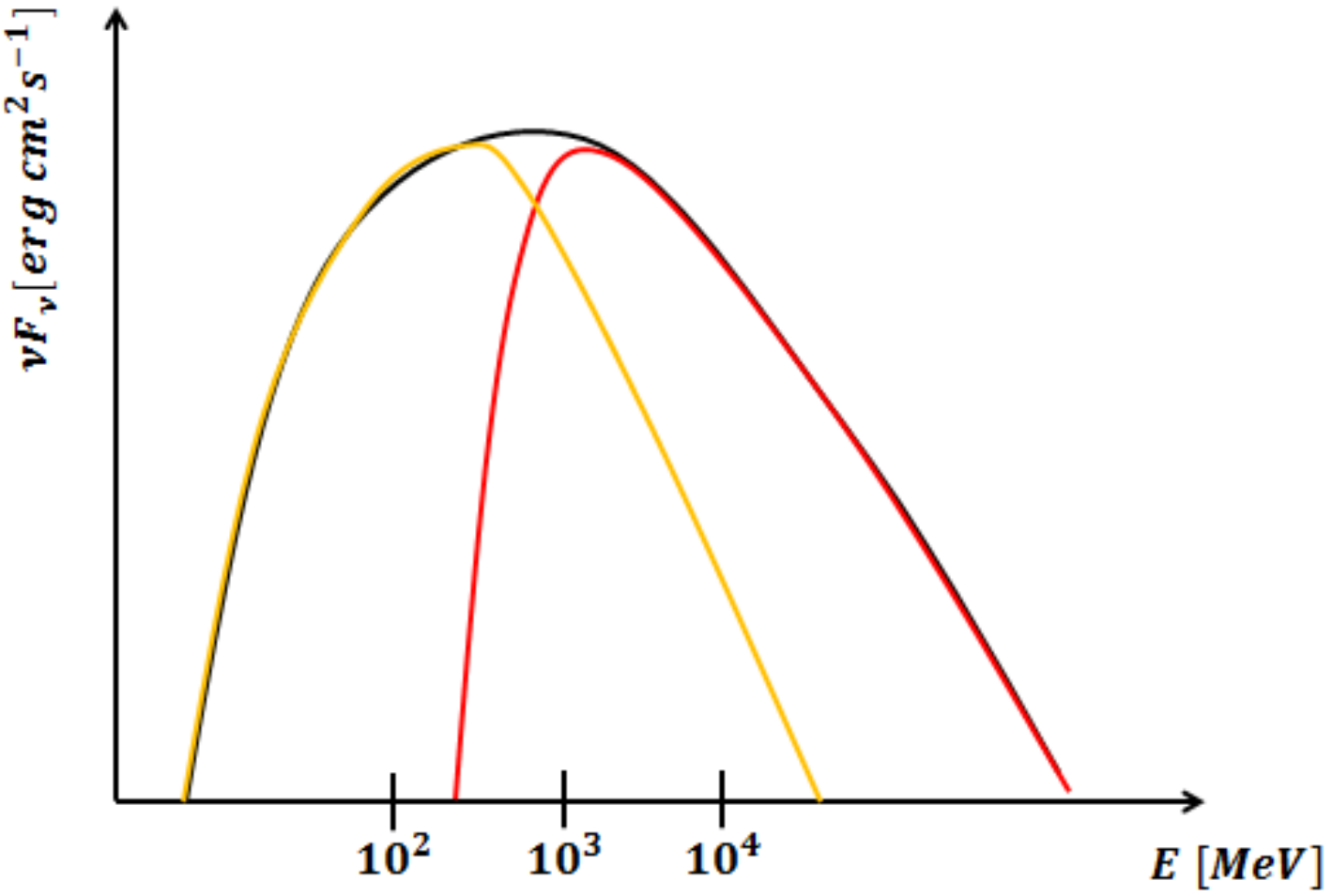
$\nu F_\nu [erg\ cm^2 s^{-1}]$
10^2
10^3
10^4
$E\ [MeV]$

lessons from RX 1713.7-3946

* complex patchy emission
* coexistence of hadronic and leptonic
* spectral cutoffs, “escape”

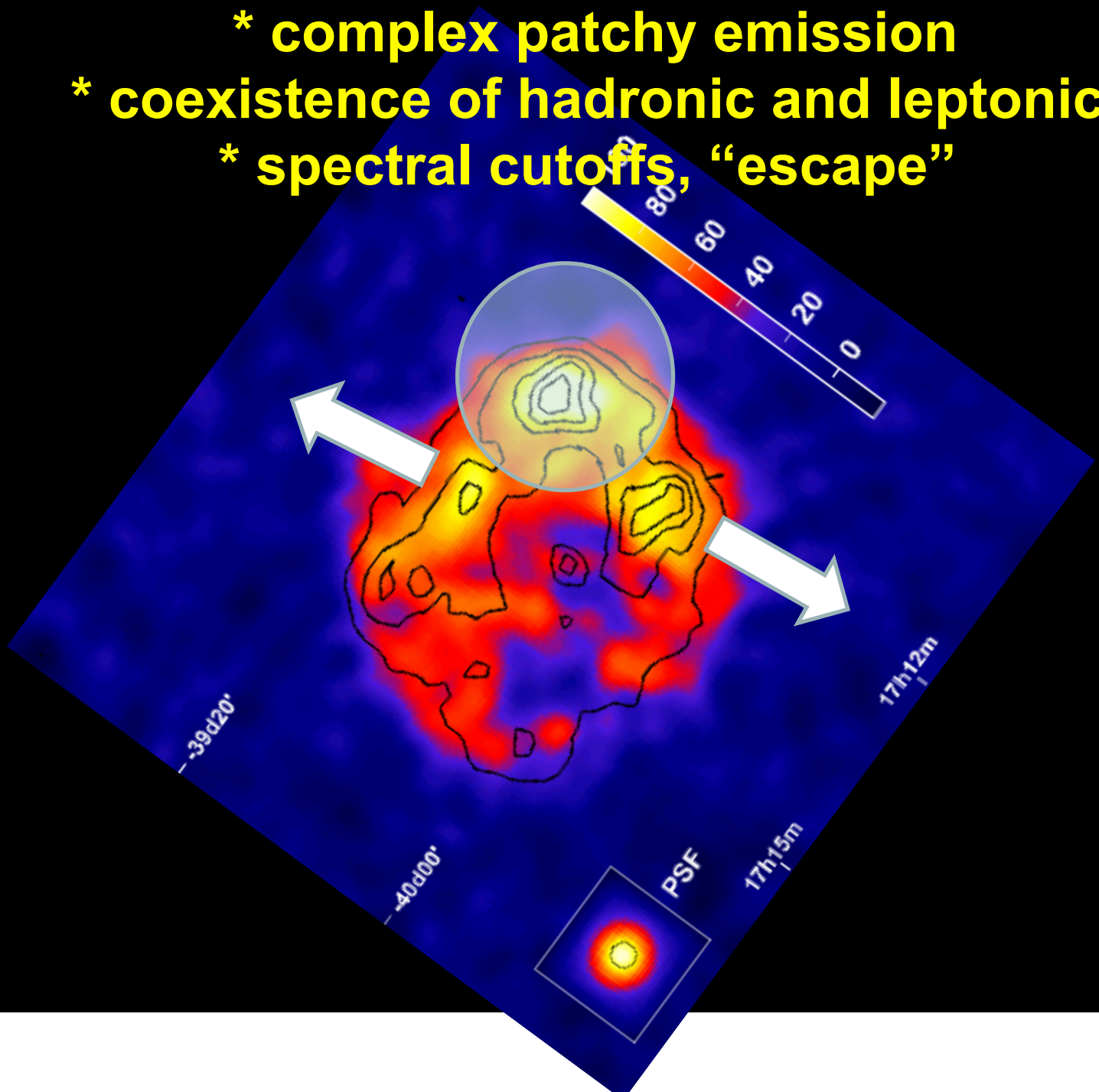

Theoretical challenges and conclusions

- a lot of progress, but also a lot of challenge for models
- Blazar-zone under discussion, fast acceleration
- jet launching in Cygnus X-3
- the surprising Crab Nebula gamma-ray flares: apparent contradiction with MHD models and DSA, probably a fast reconnection, a big challenge
- study of SNRs: direct evidence of hadronic acceleration, with challenges for current models

back-up slides

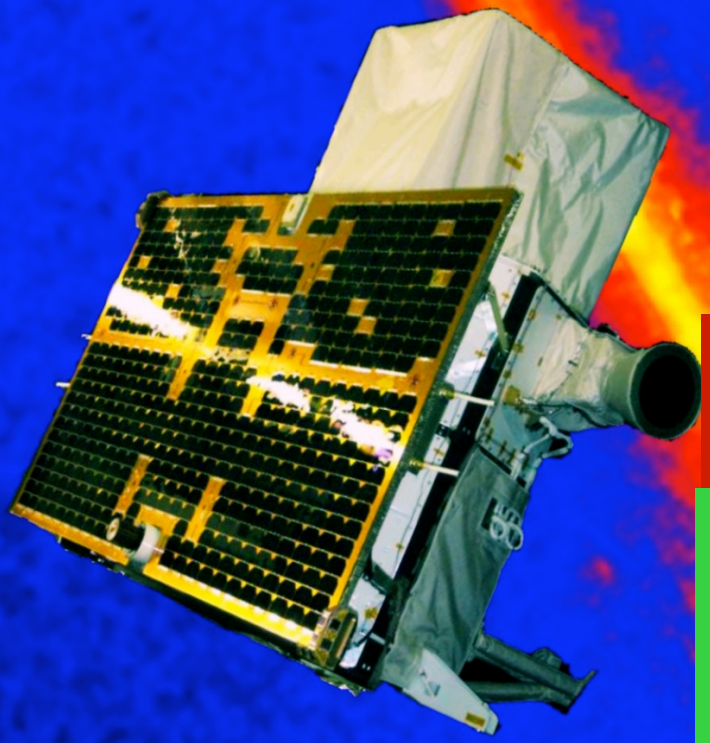

•discovery that the Crab Nebula is variable in gamma-rays !!!

• optimal sensitivity at “low” energies (E < 200 MeV)

• VERY EFFICIENT ALERT SYSTEM FOR TRANSIENTS

A quick comparison

	AGILE-1	FERMI/LAT
A_{eff} (100 MeV) (cm^2)	~ 400	~ 400-800
A_{eff} (1 GeV) (cm^2)	~ 500	~ 4000 - 8000
FOV (sr)	2.5	2.5
sky coverage	1/5	whole sky
Energy resolution (~ 400 MeV)	50 %	10 %
PSF (68 % cont. radius) 100 MeV 1 GeV	 3° - 4° < 1°	 4° - 5° < 1°

AGILE detection of enhanced gamma-ray emission from the Crab Nebula region

ATel #2855; *M. Tavani (INAF/IASF Roma), E. Striani (Univ. Tor Vergata), A. Bulgarelli (INAF/IASF Bologna), F. Gianotti, M. Trifoglio (INAF/IASF Bologna), C. Pittori, F. Verrecchia (ASDC), A. Argan, A. Trois, G. De Paris, V. Vittorini, F. D'Ammando, S. Sabatini, G. Piano, E. Costa, I. Donnarumma, M. Feroci, L. Pacciani, E. Del Monte, F. Lazzarotto, P. Soffitta, Y. Evangelista, I. Lapshov (INAF-IASF-Rm), A. Chen, A. Giuliani(INAF-IASF-Milano), M. Marisaldi, G. Di Cocco, C. Labanti, F. Fuschino,M. Galli (INAF/IASF Bologna), P. Caraveo, S. Mereghetti, F. Perotti (INAF/IASF Milano), G. Pucella, M. Rapisarda (ENEA-Roma), S. Vercellone (IASF-Pa), A. Pellizzoni, M. Pilia (INAF/OA-Cagliari), G. Barbiellini, F. Longo (INFN Trieste), P. Picozza, A. Morselli (INFN and Univ. Tor Vergata), M. Prest (Universita` dell'Insubria), P. Lipari, D. Zanello (INFN Roma-1), P.W. Cattaneo, A. Rappoldi (INFN Pavia), P. Giommi, P. Santolamazza, F. Lucarelli, S. Colafrancesco (ASDC), L. Salotti (ASI)*

on 22 Sep 2010; 14:45 UT
Distributed as an Instant Email Notice (Transients)
Password Certification: Marco Tavani (tavani@iasf-roma.inaf.it)

Subjects: Pulsars
Referred to by ATel #: 2856, 2858, 2861, 2866, 2867, 2868, 2872, 2879, 2882, 2889, 2893, 2903, 2921, 2967, 2968, 2994, 3058

AGILE is detecting an increased gamma-ray flux from a source positionally consistent with the Crab Nebula.

Integrating during the period 2010-09-19 00:10 UT to 2010-09-21 00:10 UT the AGILE-GRID detected enhanced gamma-ray emission above 100 MeV from a source at Galactic coordinates (l,b) = (184.6, -5.8) +/- 0.4 (stat.) +/- 0.1 (syst.) deg, and

Fermi LAT confirmation of enhanced gamma-ray emission from the Crab Nebula region

ATel #2861; *R. Buehler (SLAC/KIPAC), F. D'Ammando (INAF-IASF Palermo), E. Hays (NASA/GSFC) on behalf of the Fermi Large Area Telescope Collaboration*
on 23 Sep 2010; 17:34 UT
Distributed as an Instant Email Notice (Transients)
Password Certification: Rolf Buehler (buehler@slac.stanford.edu)

Subjects: >GeV, Pulsars
Referred to by ATel #: 2866, 2867, 2868, 2872, 2879, 2882, 2889, 2893, 2903, 2921, 2967, 2968, 2994, 3058

Following the detection by AGILE of increasing gamma-ray activity from a source positionally consistent with the Crab Nebula occurred from September 19 to 21 (ATel #2855), we report on the analysis of the >100 MeV emission from this region with the Large Area Telescope (LAT), one of the two instruments on the Fermi Gamma-ray Space Telescope.

Preliminary LAT analysis indicates that the gamma-ray emission (E >100 MeV) observed during this time period at the location of the Crab Nebula is (606 +/- 43) x10^ -8 ph/cm2/sec, corresponding to an excess with significance >9 sigma with respect to the average flux from the Crab nebula of (286 +/- 2) x10^ -8 ph/cm2/sec, estimated over all the Fermi operation period (only statistical errors are given). Ongoing Fermi observations indicate that the flare is continuing.

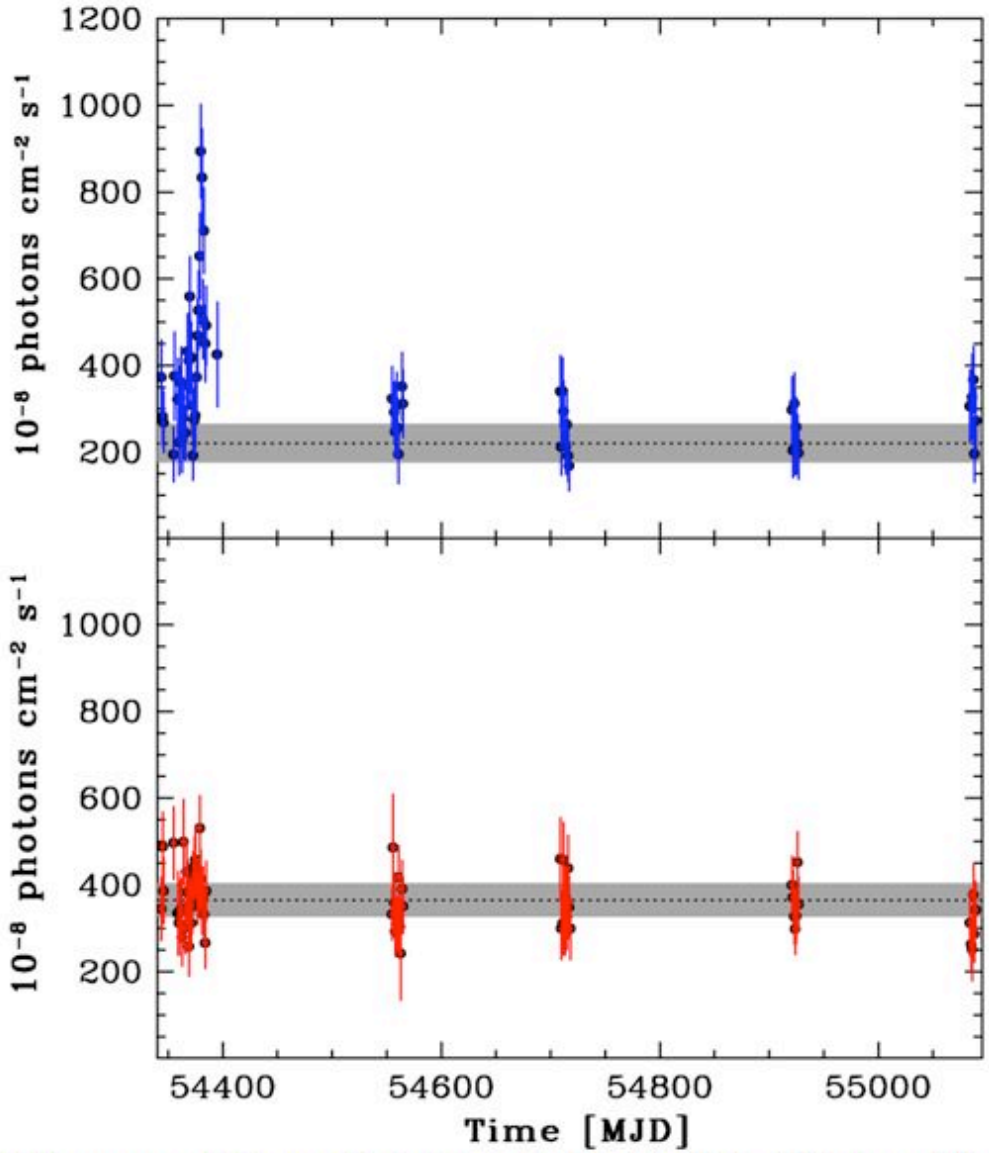

Fig. S1 – The AGILE gamma-ray light curve (1-day binning) of the Crab Pulsar/Nebula and Geminga above 100 MeV during the period **2007-09-01 – 2009-09-15** with the satellite pointing **within 35 degrees** from the source. Gaps in the light curve are due to the satellite pointing at fields different from the Crab region.

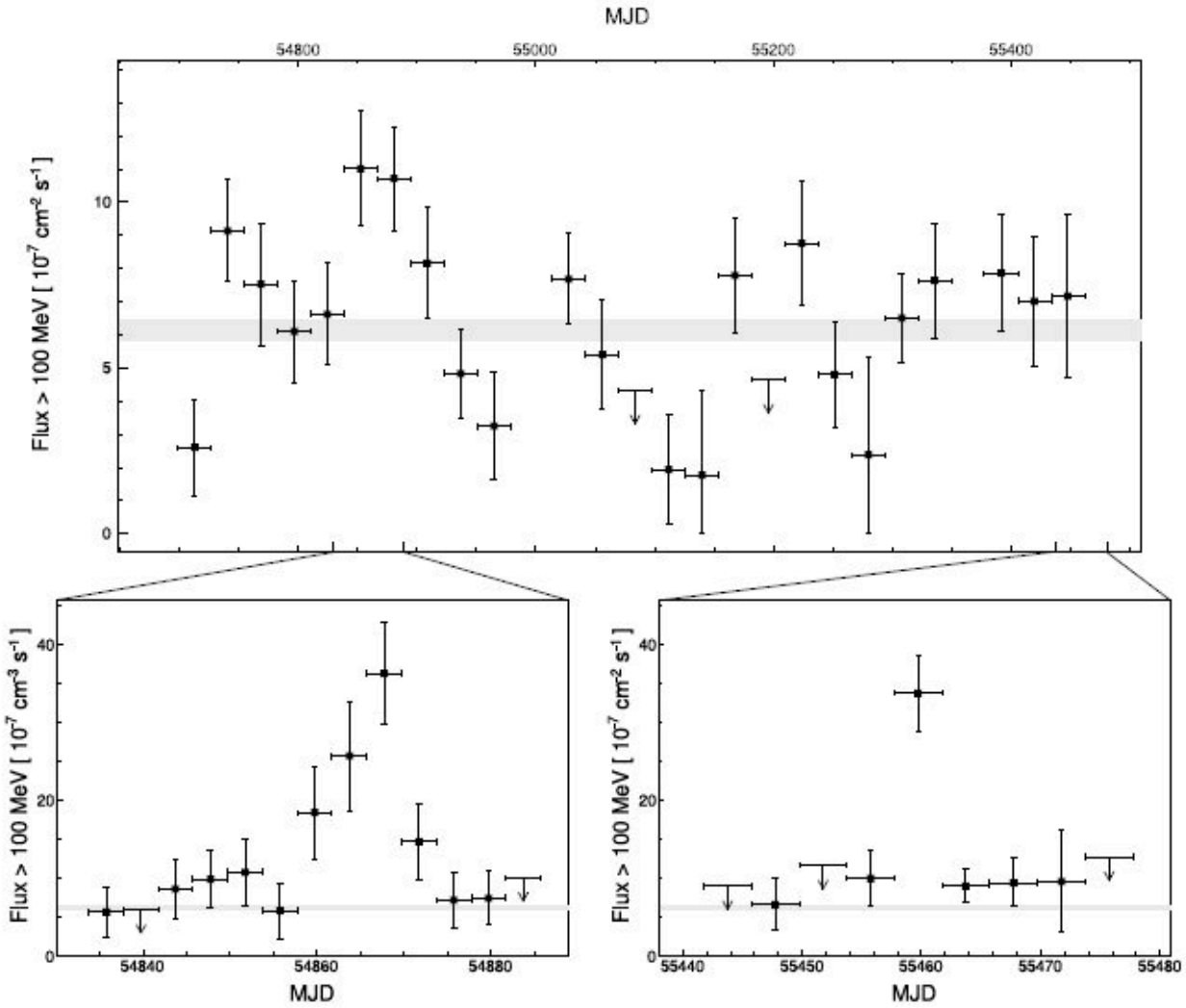

Figure 2: Gamma-ray flux above 100 MeV as a function of time of the synchrotron component of the Crab Nebula. The upper panel shows the flux in four-week intervals for the first 25 month of observations. Data for times when the sun was within 15° of the Crab Nebula have been omitted. The gray band indicates the average flux measured over the entire period. The lower panel shows the flux as a function of time in four-day time bins during the flaring periods in February 2009 and September 2010. Arrows indicate 95% confidence flux limits.

$$\varepsilon_{\gamma,max} \simeq \frac{9}{4}\left(\frac{E}{B}\right)\frac{m_e c^2}{\alpha}\left(\frac{\delta\,\alpha'}{\langle\sin(\theta')\rangle}\right)$$

$$\simeq (150\,\mathrm{MeV})\left(\frac{E}{B}\right)\left(\frac{\delta\,\alpha'}{\langle\sin(\theta')\rangle}\right)$$

De Jager et al., 1996, Atoyan & Aronian 1996, Meyer et al. 2010,
Vittorini & M.T. 2011

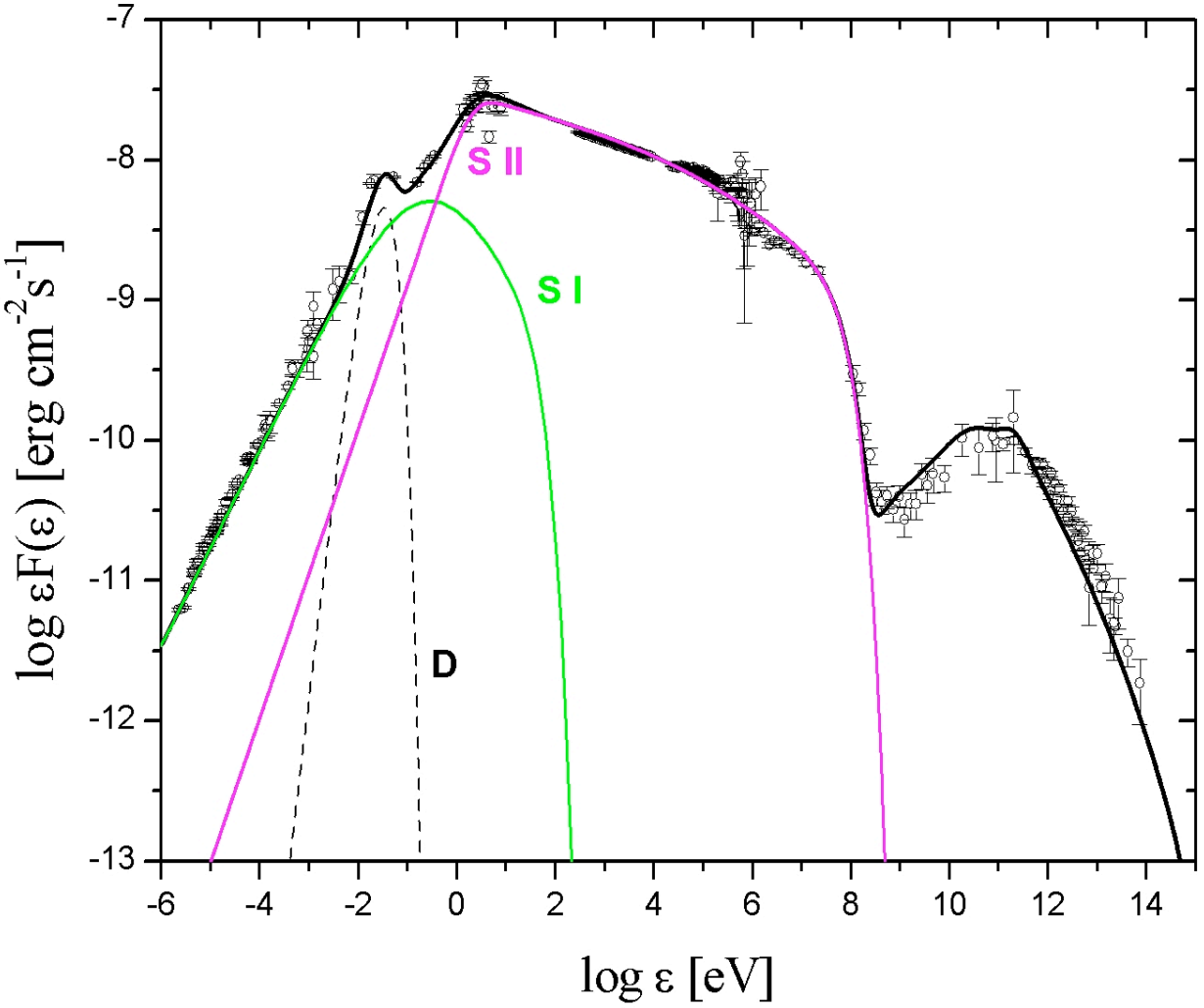

Pop. I
$60<\gamma<2.5\ 10^4$ $\alpha=1.6$
$2.5e4<\gamma<2.5e6$ $\alpha=4.0$
R=2.3e18 cm
N_{el}=2.5e51
T_{syn} ~ 10^5 years

Pop. II
$5e5<\gamma<3.8e8$ $\alpha=3.20$
$3.8e8<\gamma<3.5e9$ $\alpha=3.75$
R=2e18 cm
N_{el}=3e48
T_{syn} ~ 10 years

Dust
L=3e36 erg/s
T=100 °K

Average magnetic field
B=200 μGauss

Vittorini & M.T. 2011

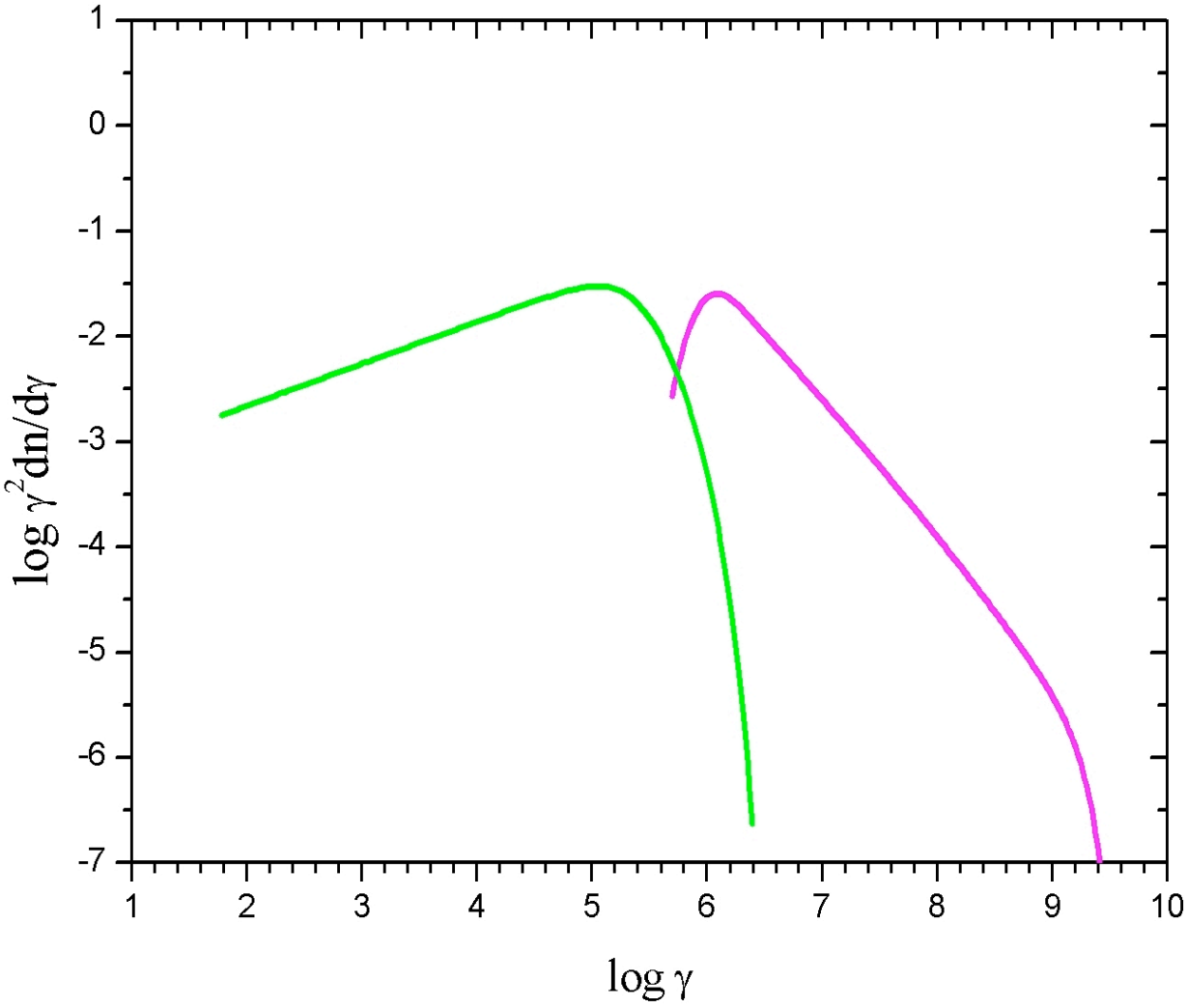

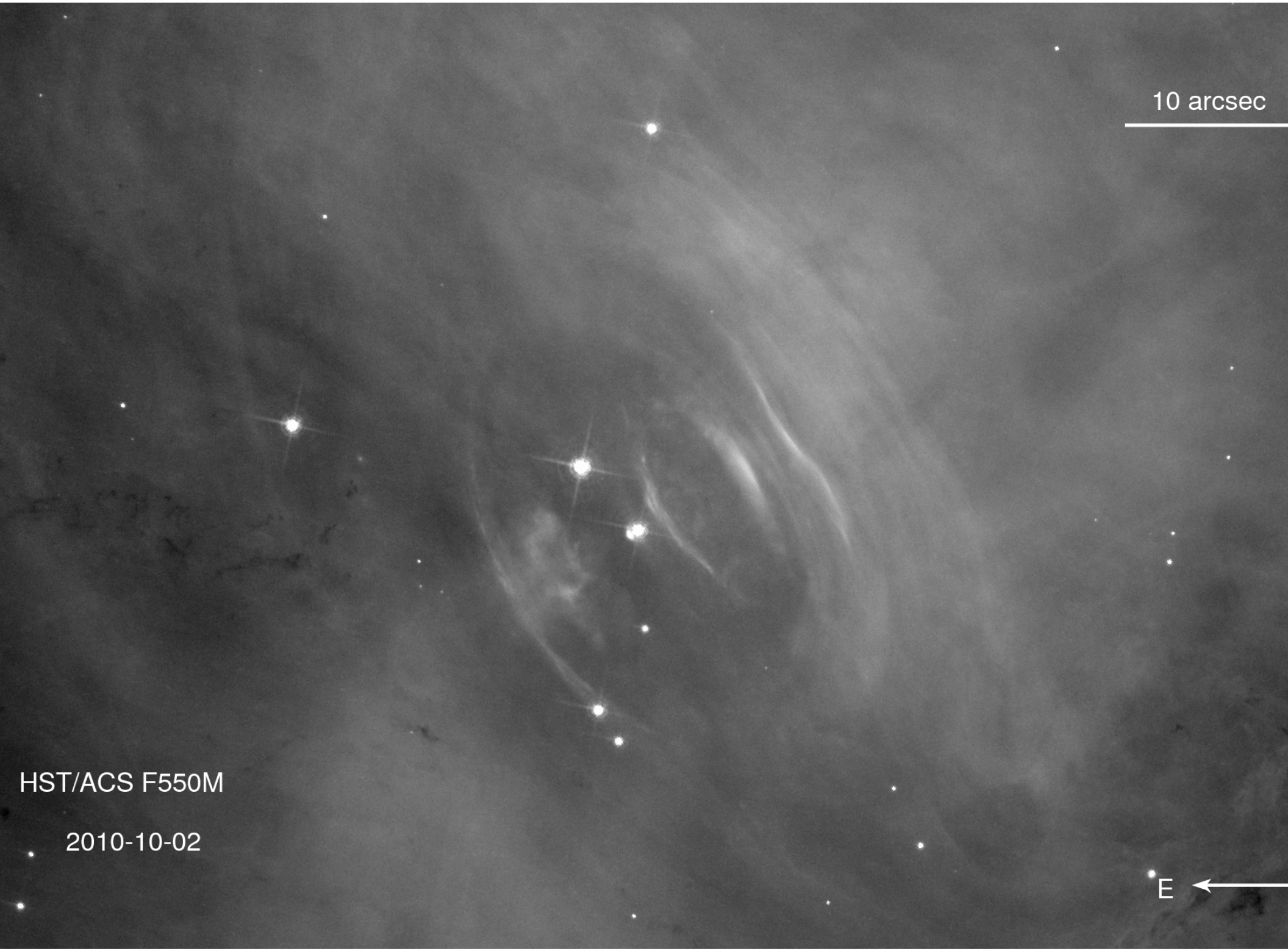
10 arcsec
HST/ACS F550M
2010-10-02
E

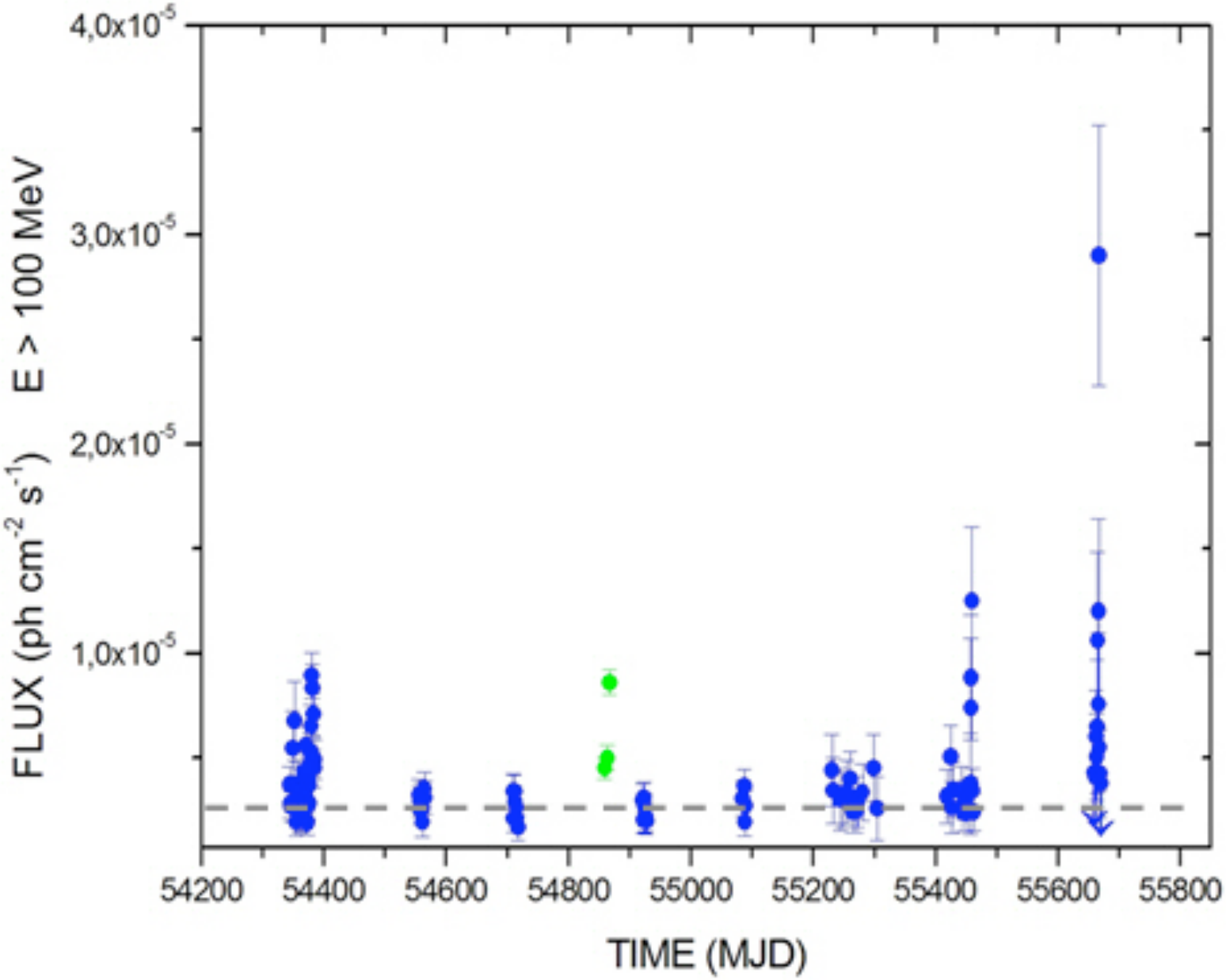
4,0x10-5
3,0x10-5
2,0x10-5
1,0x10-5
FLUX (ph cm-2 s-1) E > 100 MeV
54200
54400
54600
54800
55000
55200
55400
55600
55800
TIME (MJD)

KC MHD modelling: RH eqs.

$$n_1 u_1 = n_2 u_2 \,,$$

$$E = \frac{u_1 B_1}{\gamma_1} = \frac{u_2 B_2}{\gamma_2} \,,$$

$$\gamma_1 \mu_1 + \frac{E B_1}{4\pi n_1 u_1} = \gamma_2 \mu_2 + \frac{E B_2}{4\pi n_1 u_1} \,,$$

$$\mu_1 u_1 + \frac{P_1}{n_1 u_1} + \frac{B_1^2}{8\pi n_1 u_1} = \mu_2 u_2 + \frac{P_2}{n_1 u_1} + \frac{B_2^2}{8\pi n_1 u_1}$$

KC MHD modelling: RH eqs.

the Rankine-Hugoniot relations for a strong, perpendicular shock reduce to

$$u_2^2 = \frac{8\sigma^2 + 10\sigma + 1}{16(\sigma + 1)} + \frac{1}{16(\sigma + 1)}\left[64\sigma^2(\sigma + 1)^2 + 20\sigma(\sigma + 1) + 1\right]^{1/2}$$

$$\frac{B_2}{B_1} = \frac{N_2}{N_1} = \frac{\gamma_2}{u_2},$$

$$\frac{P_2}{n_2 mc^2 u_1^2} = \frac{1}{4u_2\gamma_2}\left[1 + \sigma\left(1 - \frac{\gamma_2}{u_2}\right)\right],$$

PSR wind magnetization $\sigma = \dfrac{B^2}{4\pi nu\gamma mc^2}$

KC MHD modelling: RH eqs. solution

$$u_2^2 \approx \frac{1+9\sigma}{8}, \qquad \gamma_2^2 \approx \frac{9+9\sigma}{8}, \qquad \beta_2 = \frac{u_2}{\gamma_2} \approx \frac{1}{3}(1+4\sigma),$$

$$\frac{B_2}{B_1} = \frac{N_2}{N_1} \approx 3(1-4\sigma),$$

$$\frac{P_2}{n_1 m c^2 u_1^2} \approx \frac{2}{3}(1-7\sigma).$$

KC MHD modelling: RH eqs. solution

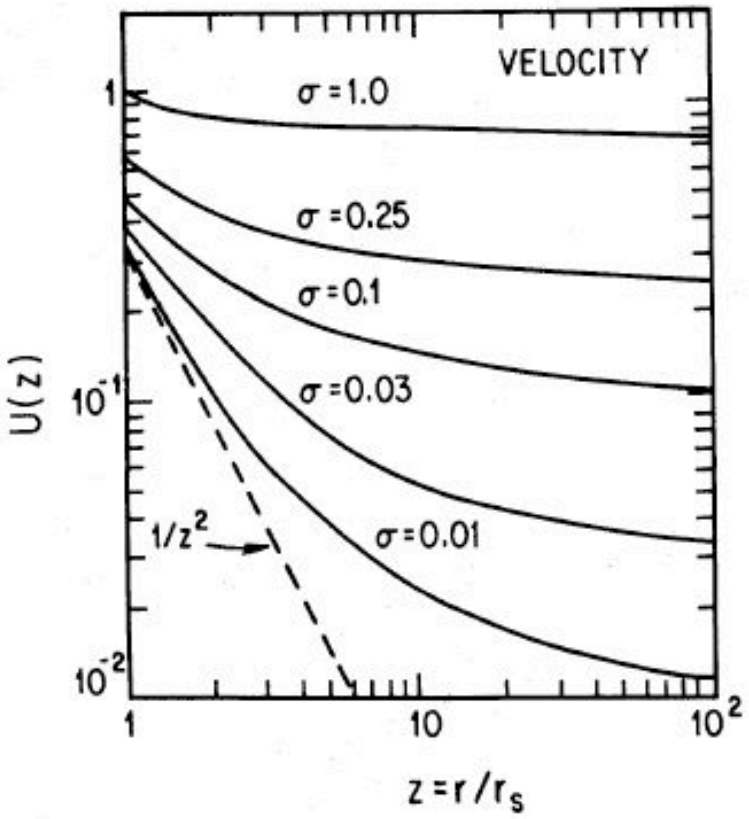

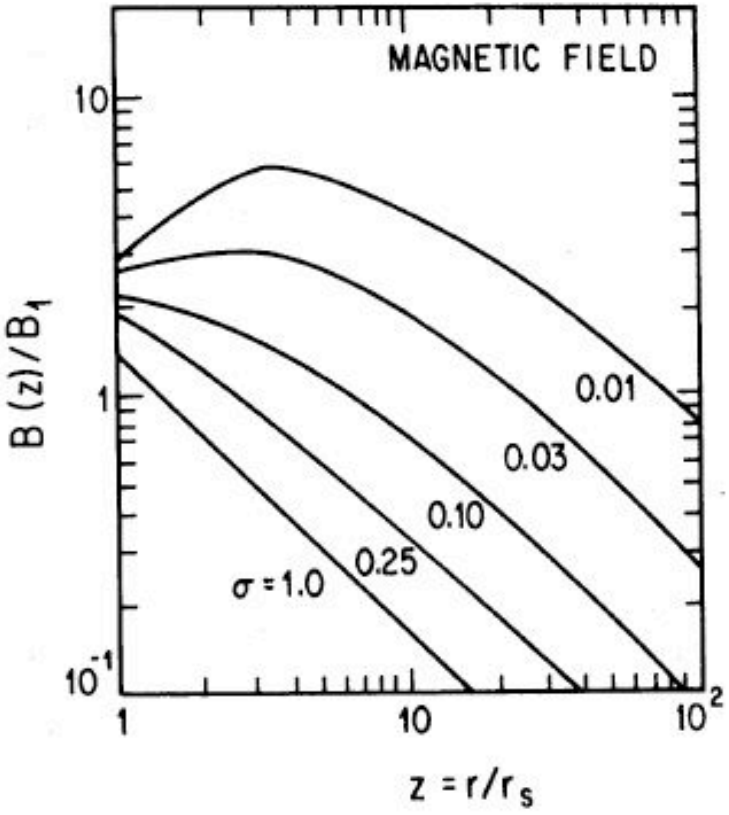

AGILE-GRID spectrum at the peak (Sept. 2010)

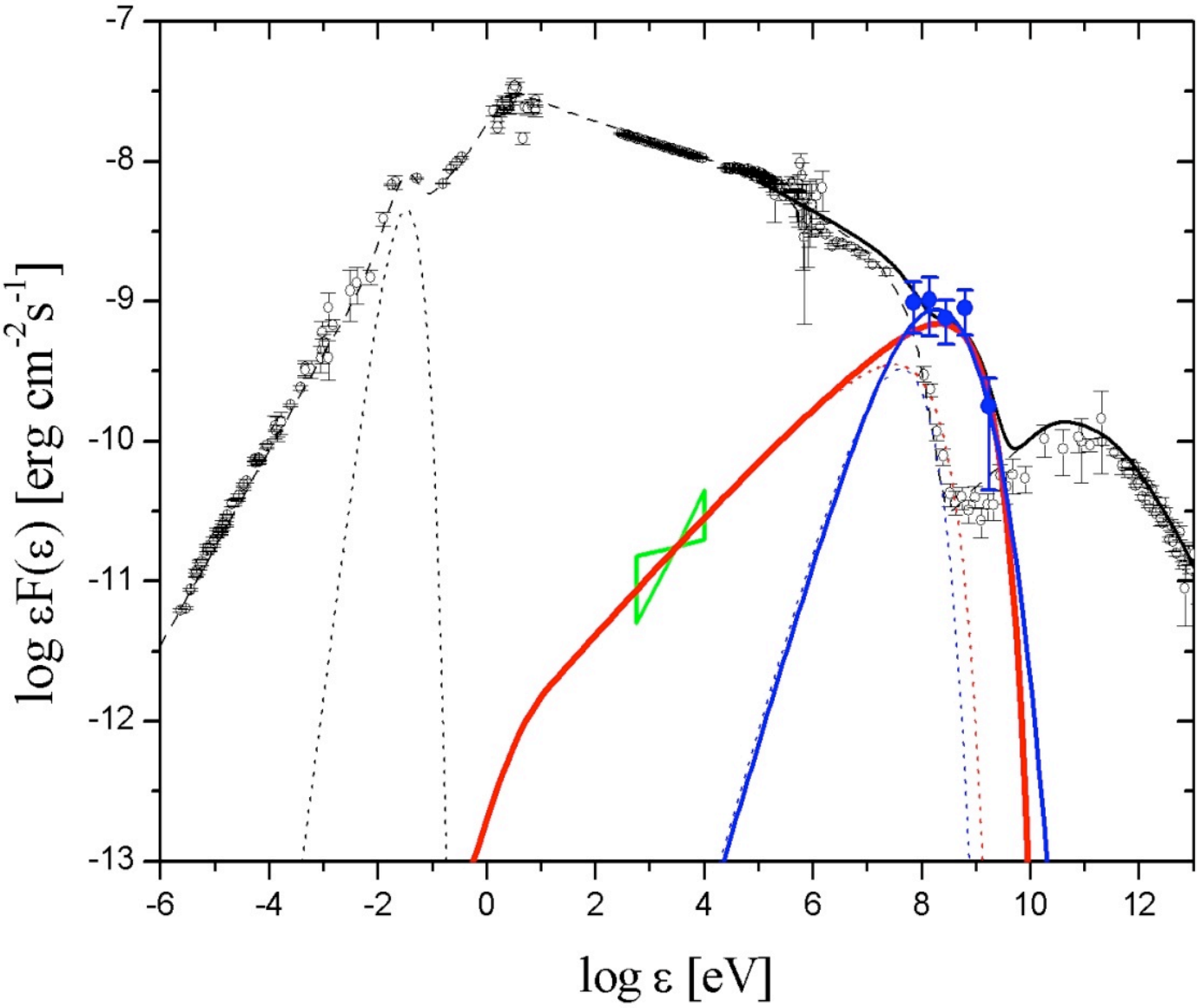

fermi, 4 hr.

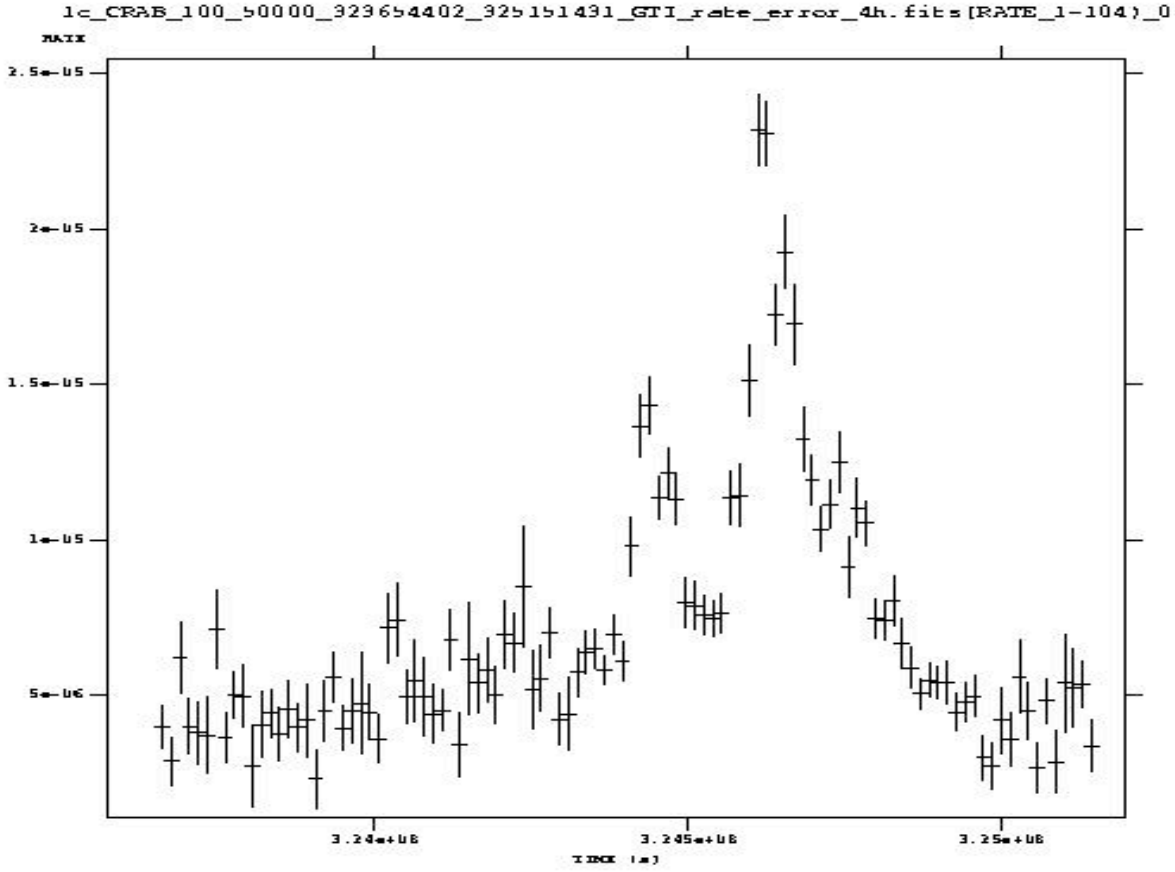
lc_CRAB_100_50000_323654402_325151431_GTI_rate_error_4h.fits[RATE_1-104]_0
RATE
2.5e-05
2e-05
1.5e-05
1e-05
5e-06
3.24e+08
3.245e+08
3.25e+08
TIME (s)

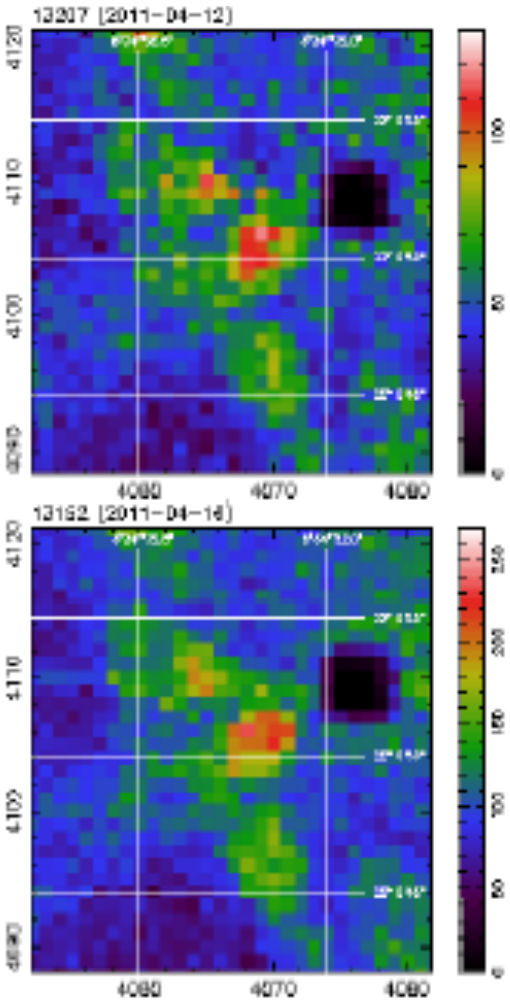
13207 [2011-04-12]
4120
4110
4100
4090
4080
4070
4060
0
50
100

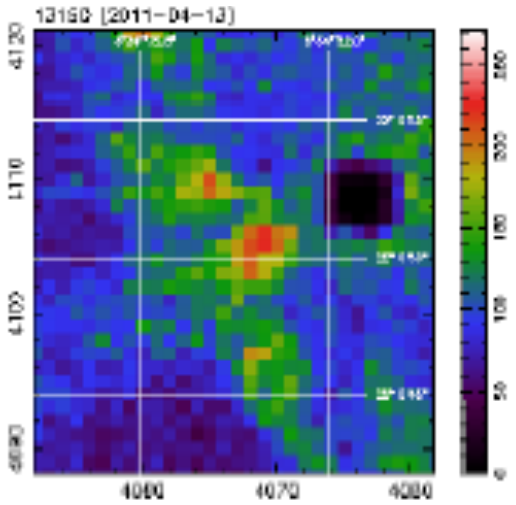
13150 [2011-04-13]
4120
4110
4100
4090
4080
4070
4060
0
50
100
150
200

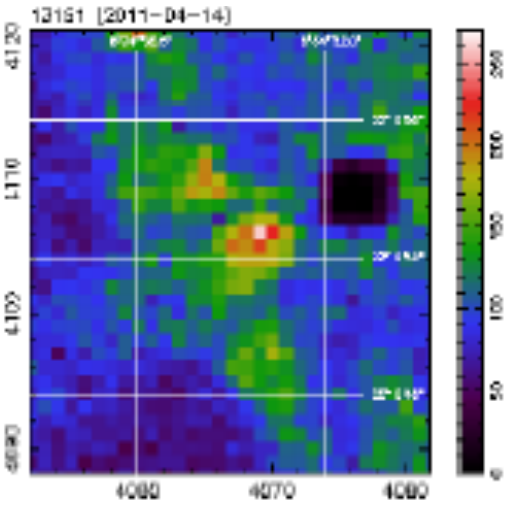
13151 [2011-04-14]
4120
4110
4100
4090
4080
4070
4060
0
50
100
150
200

13152 [2011-04-16]
4120
4110
4100
4090
4080
4070
4060
0
50
100
150
200

and also…

- X-ray (secular) variations 1-100 keV (Wilson-Hodge 2010)
- 2-3 year timescale
- a few % / year variation, 10% decrease in 4 years

Wilson-Hodge et al. 2010

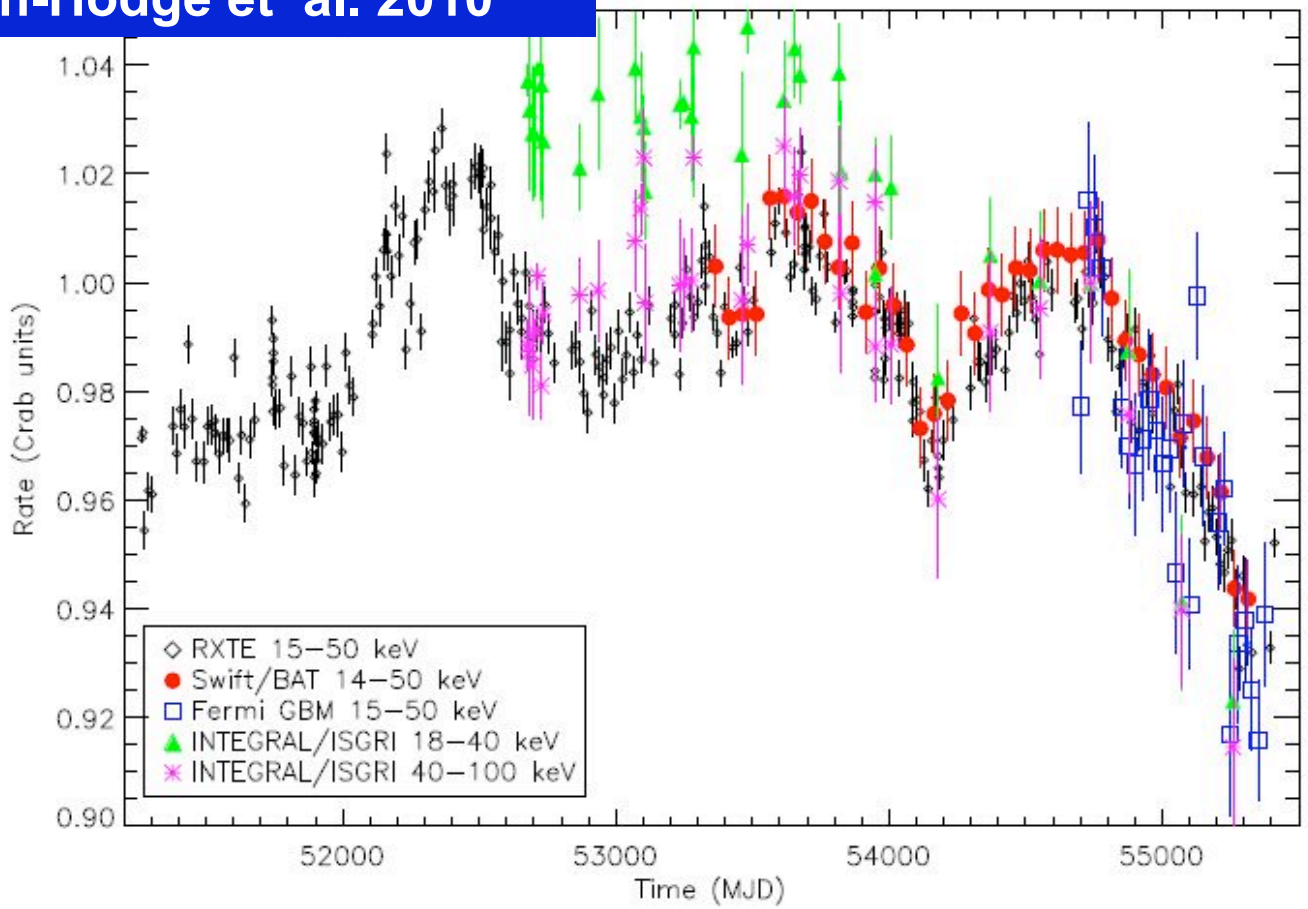

Fig. 5.— Composite Crab light curve for *RXTE*/PCA (15-50 keV - black diamonds), *Swift*/BAT (14-50 keV - red filled circles), *Fermi*/GBM (15-50 keV - open blue squares), *INTEGRAL*/ISGRI (18-40 and 40-100 keV - green triangles and purple asterisks, respectively.) Each data set has been normalized to its mean rate in the time interval MJD 54690-54790. All error bars include only statistical errors.

- **short timescale Crab variability (Sept. 2010):**

  - **currently published data:**
    - **2-day integration (AGILE)**
    - **4-day integration (Fermi)**

  - **study 1-day and 12-hr integrations**

  - **are AGILE and Fermi data consistent with 12-hr variability ?**

1-day bin lightcurves (AGILE and Fermi)

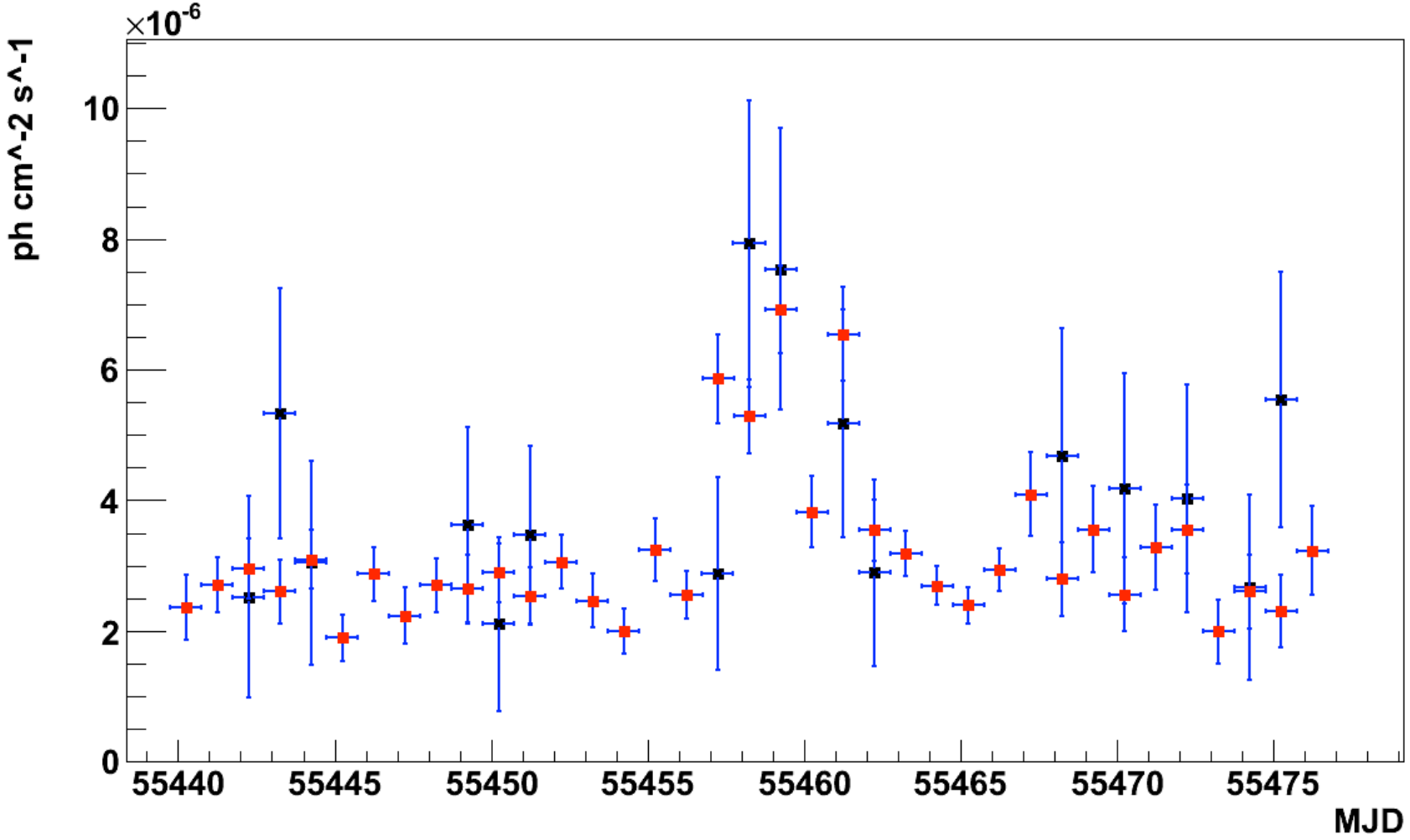

12-hr bin lightcurves (AGILE and Fermi)

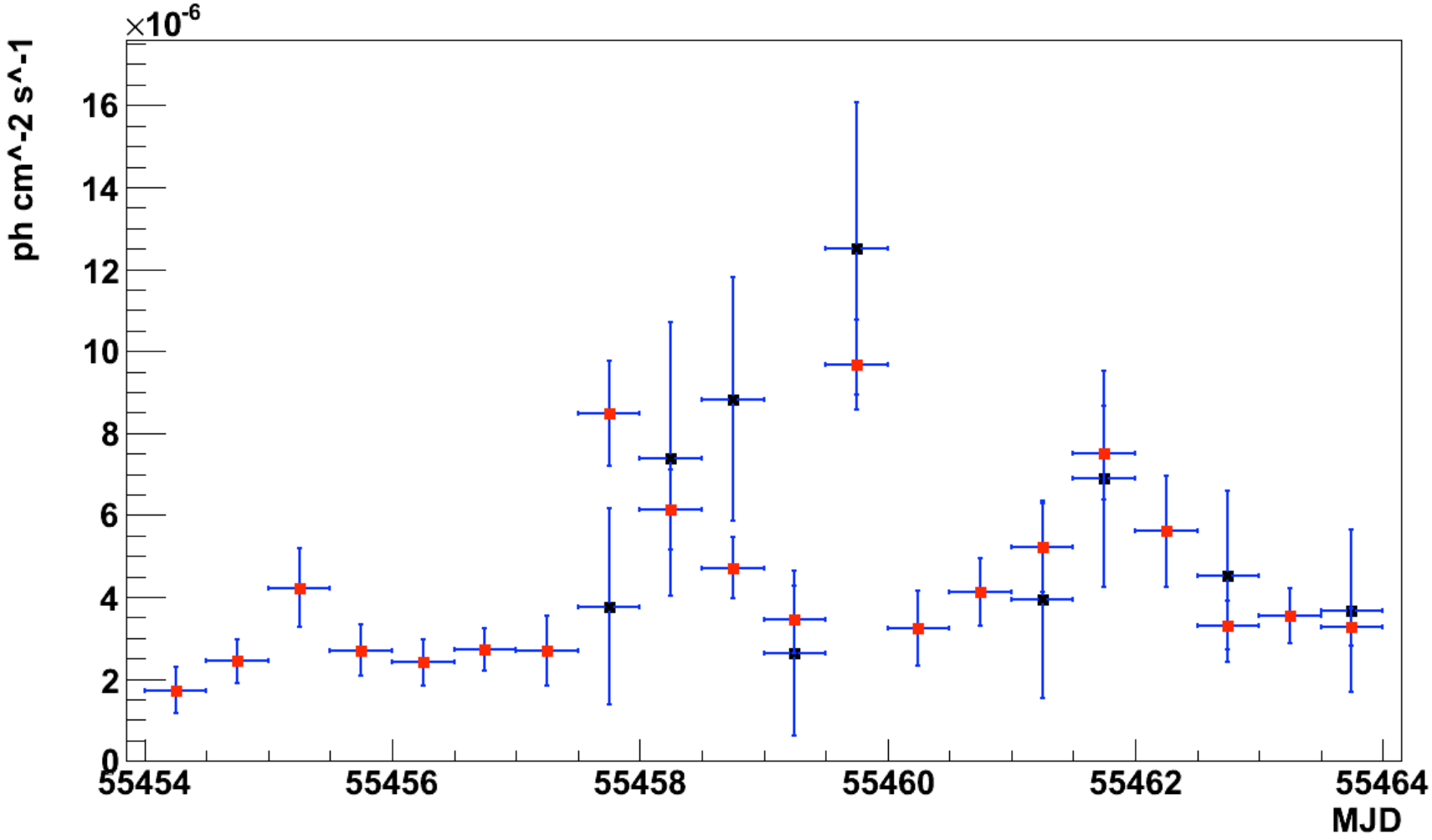

12-hr bin lightcurves (AGILE and Fermi)

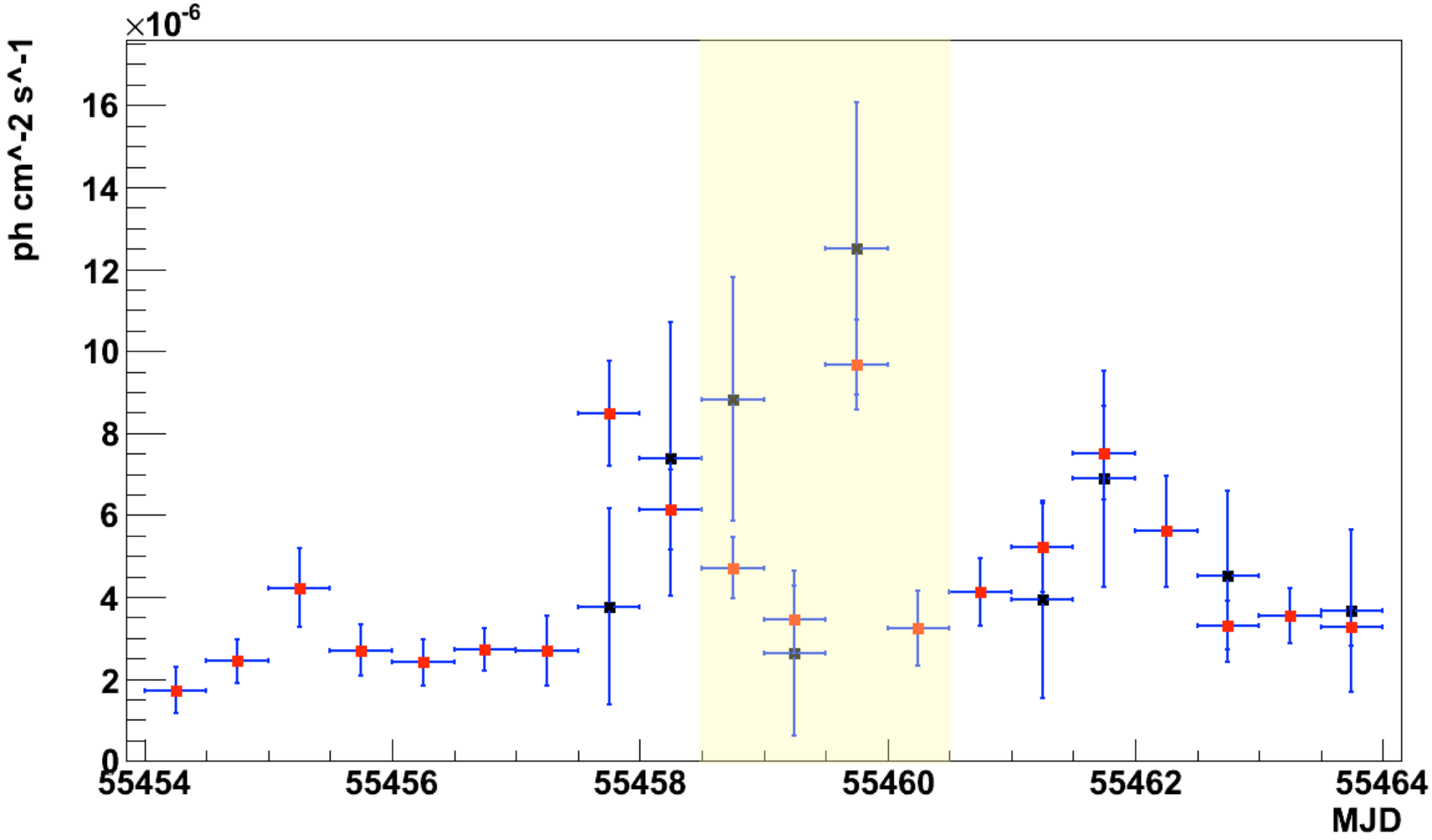

12-hr bin lightcurves (AGILE and Fermi)

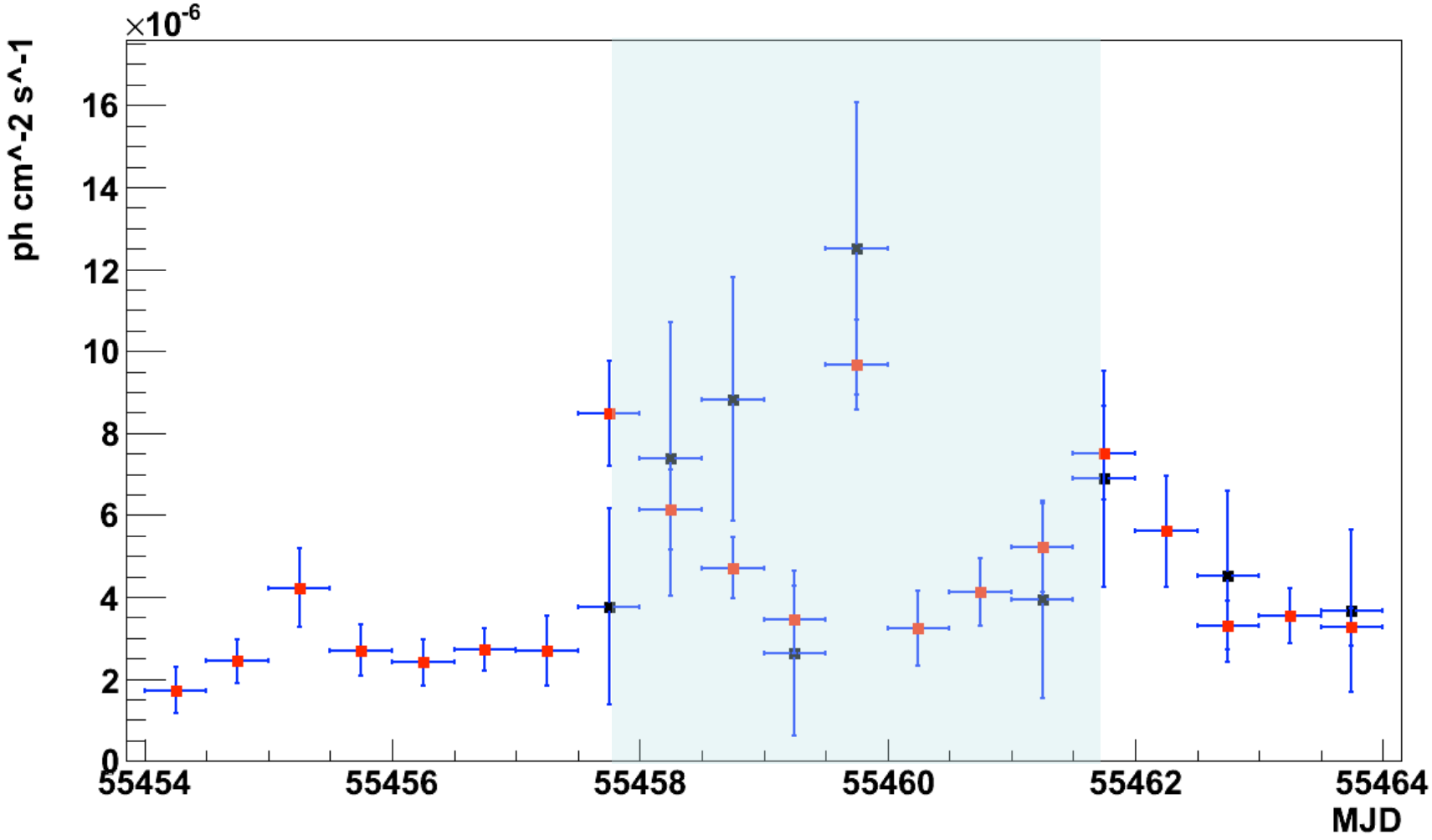

independent Fermi data analysis (Balbo et al., A&A, 527, L4, 2011)

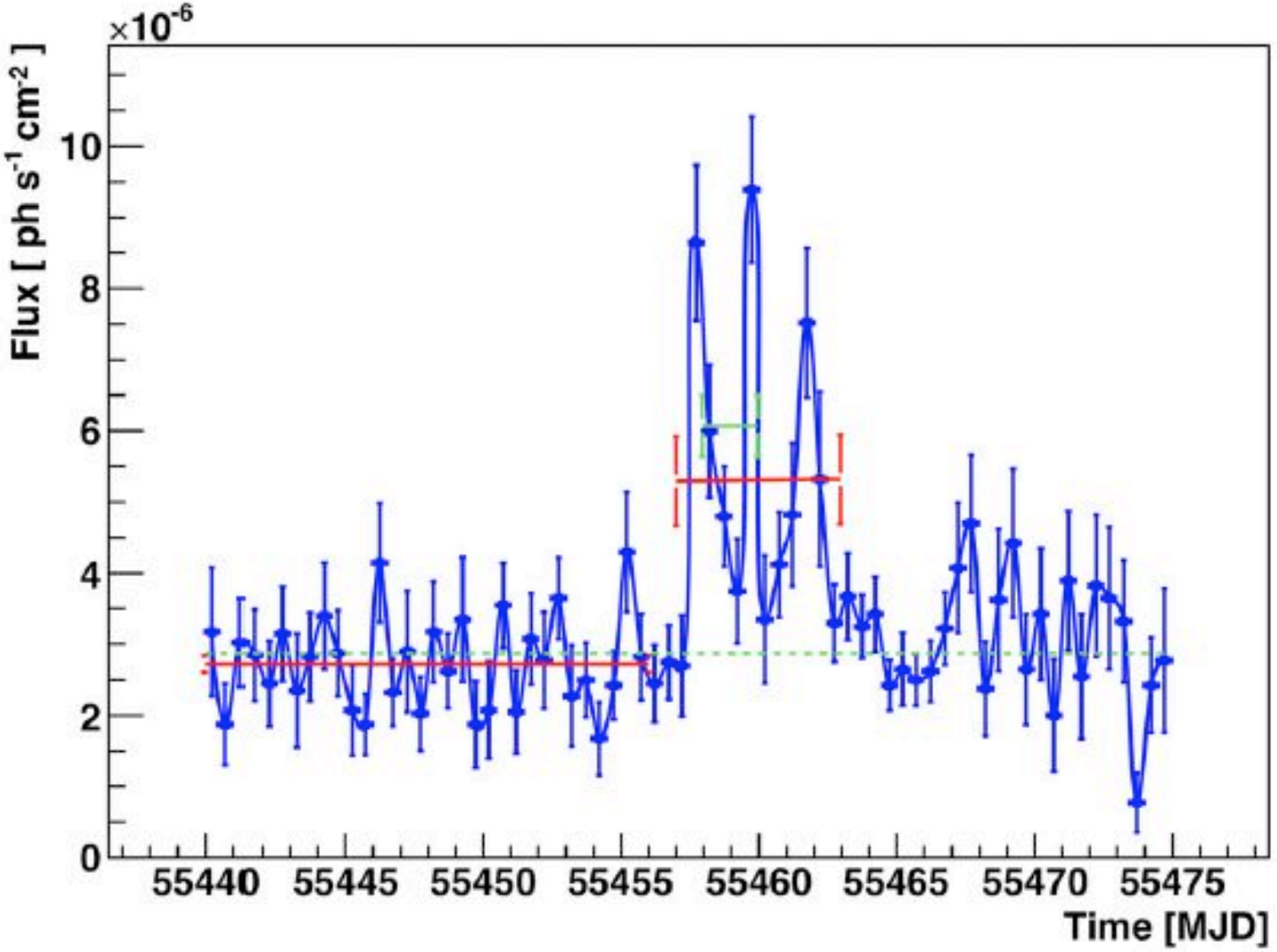

- evidence for very short (12 hrs or less) variability detected both by AGILE and Fermi

- **not the end of the story…**

still more surprises..!

- **TeV observations and ARGO-YBJ detection in Sept. 2010 (ATEL 2921)**

- **see also ATELs by VERITAS and MAGIC**

TeV nebular emission

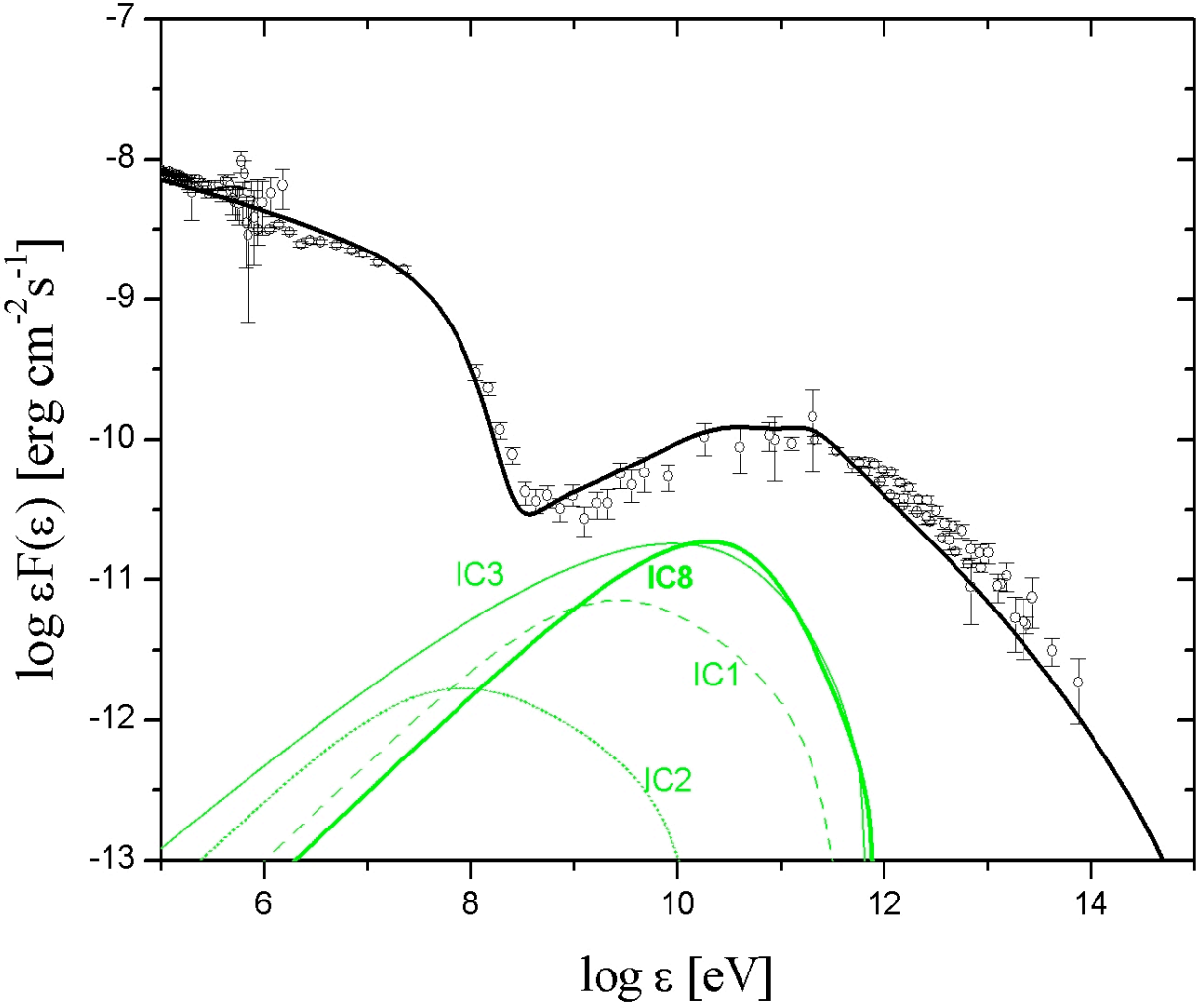

Inverse Compton contribution from **pop I** electrons scattering:

IC1 dust ph
IC2 CMB ph
IC3 syn ph from **pop I**
IC8 syn ph from **pop II**

TeV nebular emission

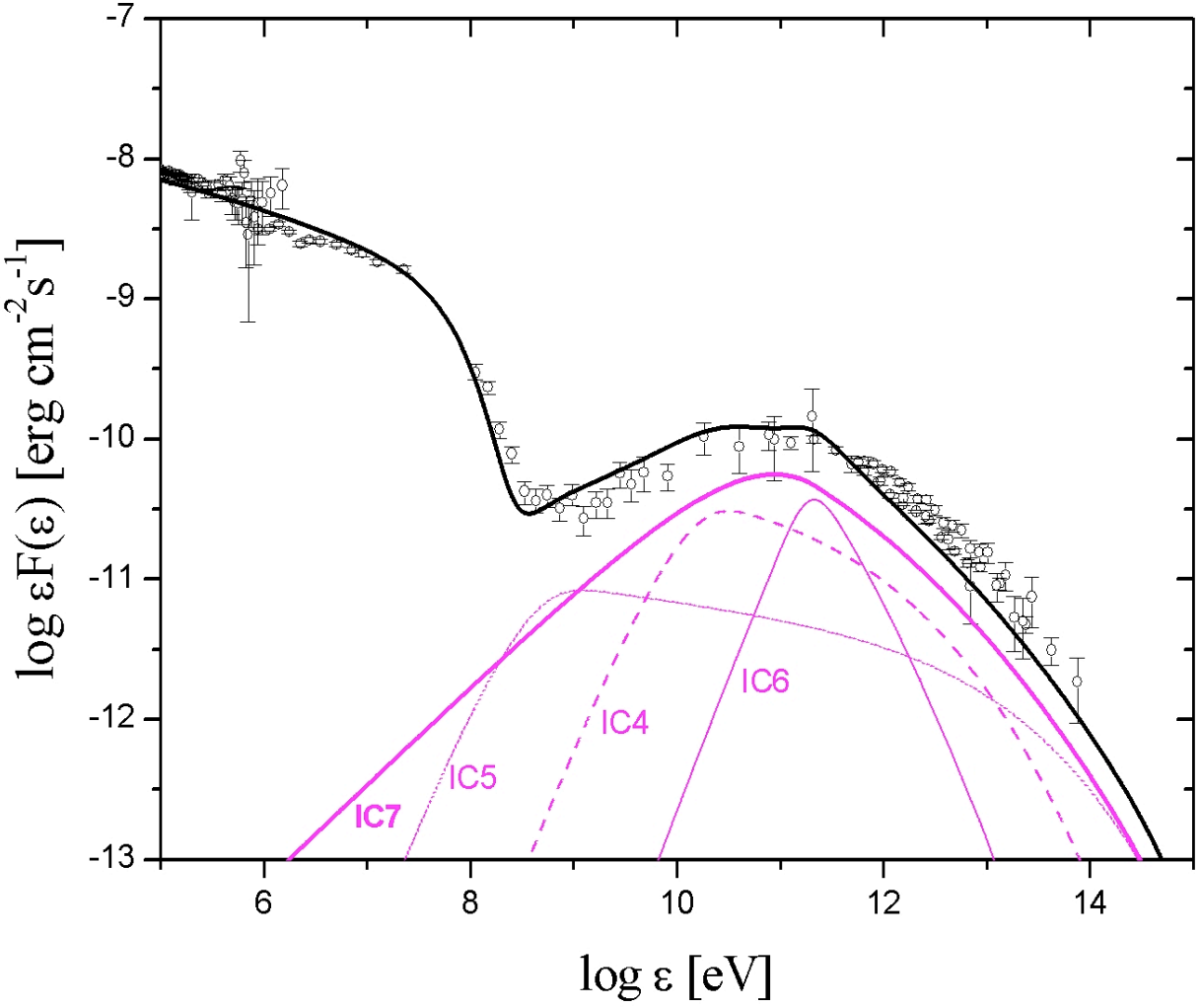

Inverse Compton contribution from **pop II** electrons scattering:

IC4 dust ph
IC5 CMB ph
IC6 syn ph from **pop II**
IC7 syn ph from **pop I**

post-flare TeV observations (ATel's: 2921, 2967, 2968)

Instrument	Epoch (MJD)	Duration	
VERITAS	55456.44	20 min.	
	55456.47	20 min.	
	55457.47	20 min.	
	55458.45	20 min.	no variation
	55458.47	20 min.	
	55459.47	20 min.	
MAGIC	55459.20	58 min.	no variation
ARGO-YBJ	55456-55461	5 days	3-4 times enhancement
	55456-55466	10 days	possible enhancement

12-hr bin lightcurves (AGILE and Fermi)

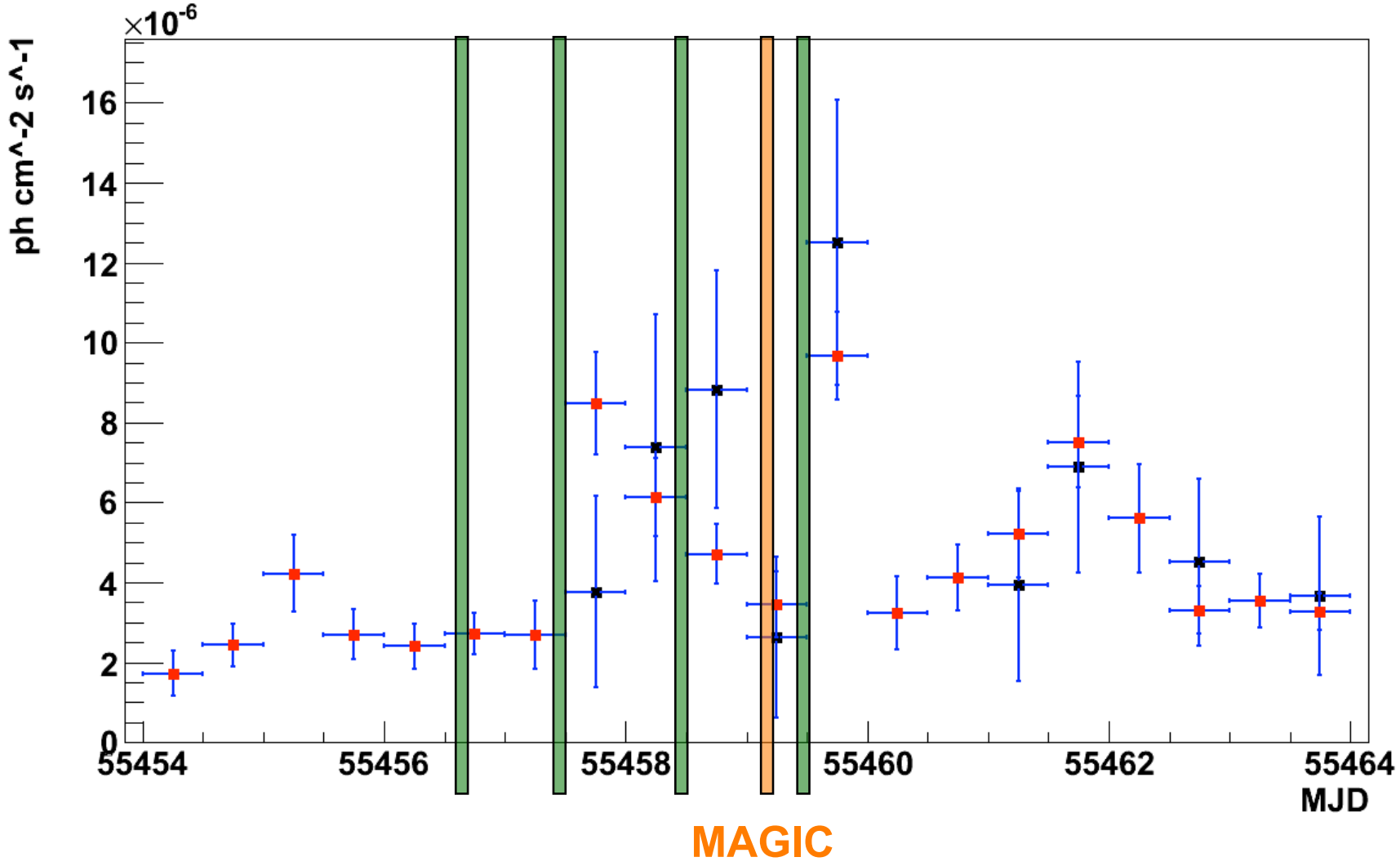

MAGIC

post-flare TeV observations

Instrument	Epoch (MJD)	Duration	
VERITAS	**55456.44**	**20 min.**	
	55456.47	**20 min.**	
	55457.47	**20 min.**	
	55458.45	**20 min.**	no variation
	55458.47	**20 min.**	
	55459.47	**20 min.**	
MAGIC	**55459.20**	**58 min.**	no variation
ARGO-YBJ	**55456-55461**	**5 days**	3-4 times enhancement
	55456-55466	**10 days**	possible enhancement

exciting prospects

- room for possible short timescale TeV emission
- test VERITAS data during the first peak of emission (MJD 55458.5)
- search for similar episodes in the past ?
- TeV emission requires enhancement !
  - favorable Doppler beaming

- very exciting results, the Crab Nebula produces ~day-long gamma-ray flares ! Not a standard candle in gamma-rays.

- nebular origin, not clear yet the association with a wisp or feature, South East “jet” base ?

- dramatic confirmation of high-efficiency relativistic particle acceleration

Conclusions

- we “lost” the stability of an ideal reference source, but gained tremendous information about the fundamental process of particle acceleration

- a big theoretical challenge
  - shock acceleration + magnetic field reconnection ?
  - current sheet and MHD instabilities
  - Doppler boosting ?

- the ultimate site of particle acceleration needs to be established: future surprises

CR physics

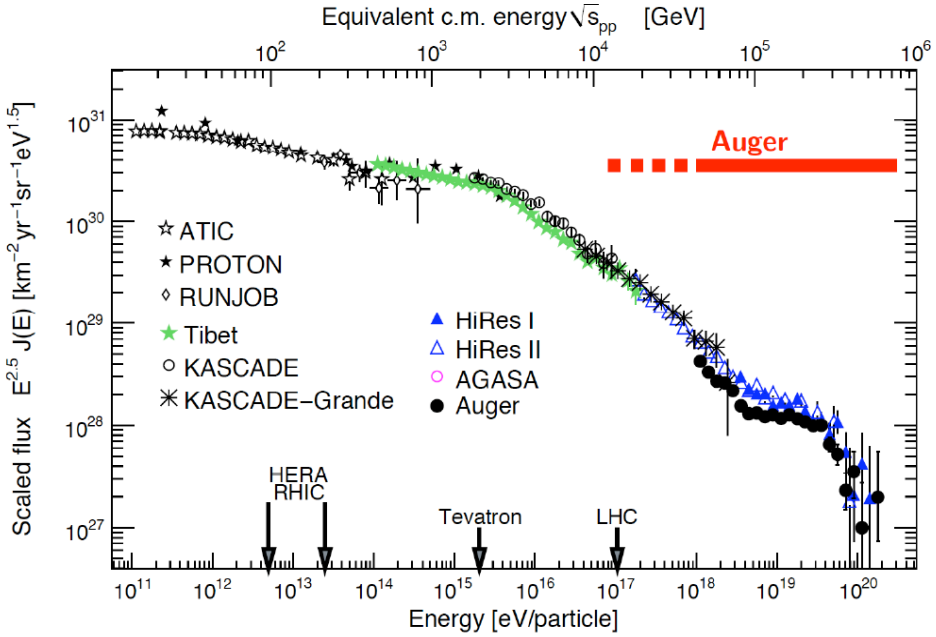
Equivalent c.m. energy $\sqrt{s_{pp}}$ [GeV]
Scaled flux $E^{2.5}$ J(E) [$km^{-2}yr^{-1}sr^{-1}eV^{1.5}$]
Energy [eV/particle]
Auger
ATIC
PROTON
RUNJOB
Tibet
KASCADE
KASCADE–Grande
HiRes I
HiRes II
AGASA
Auger
HERA
RHIC
Tevatron
LHC

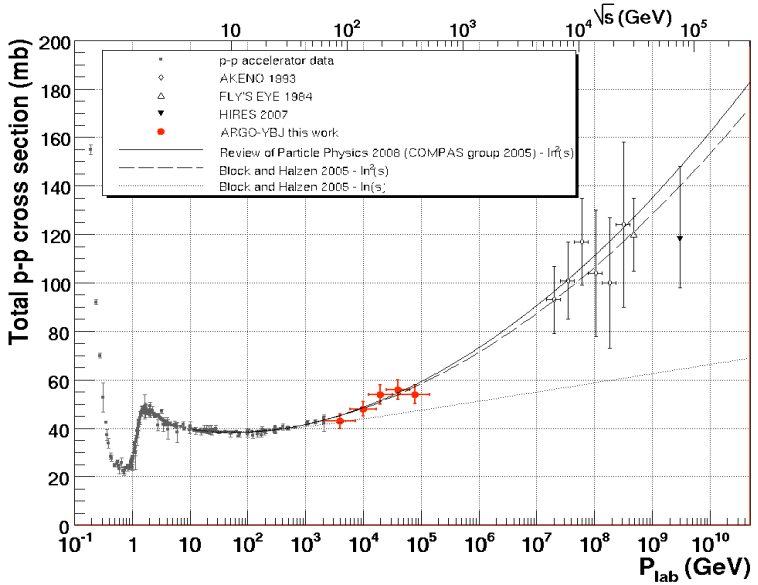
$\sqrt{s}$ (GeV)
Total p-p cross section (mb)
P_{lab} (GeV)
p-p accelerator data
AKENO 1993
FLY'S EYE 1984
HIRES 2007
ARGO-YBJ this work
Review of Particle Physics 2008 (COMPAS group 2005) - ln²(s)
Block and Halzen 2005 - ln²(s)
Block and Halzen 2005 - ln(s)

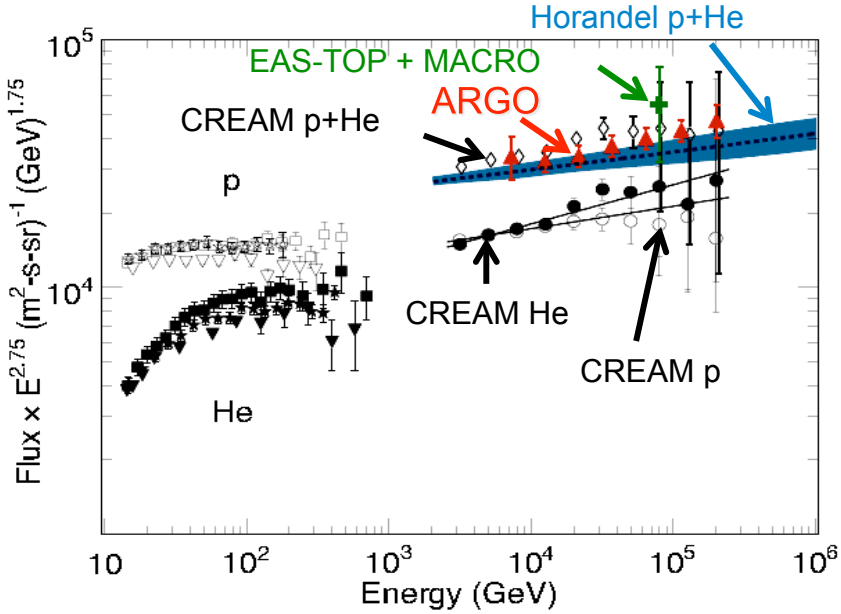
Horandel p+He
EAS-TOP + MACRO
ARGO
CREAM p+He
p
He
CREAM He
CREAM p
Flux × $E^{2.75}$ (m^2-s-sr)$^{-1}$ (GeV)$^{1.75}$
Energy (GeV)

CR physics

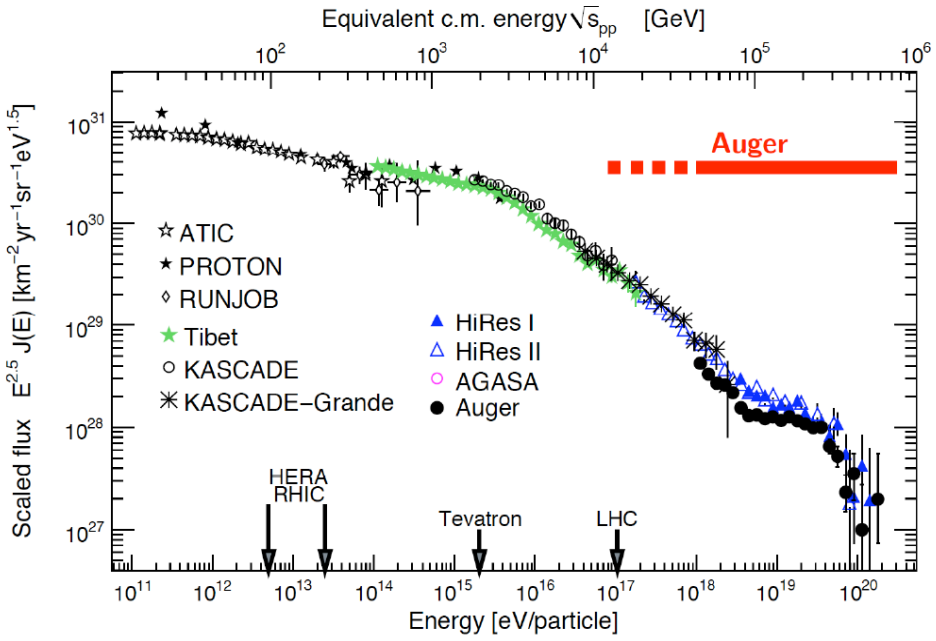

PAMELA

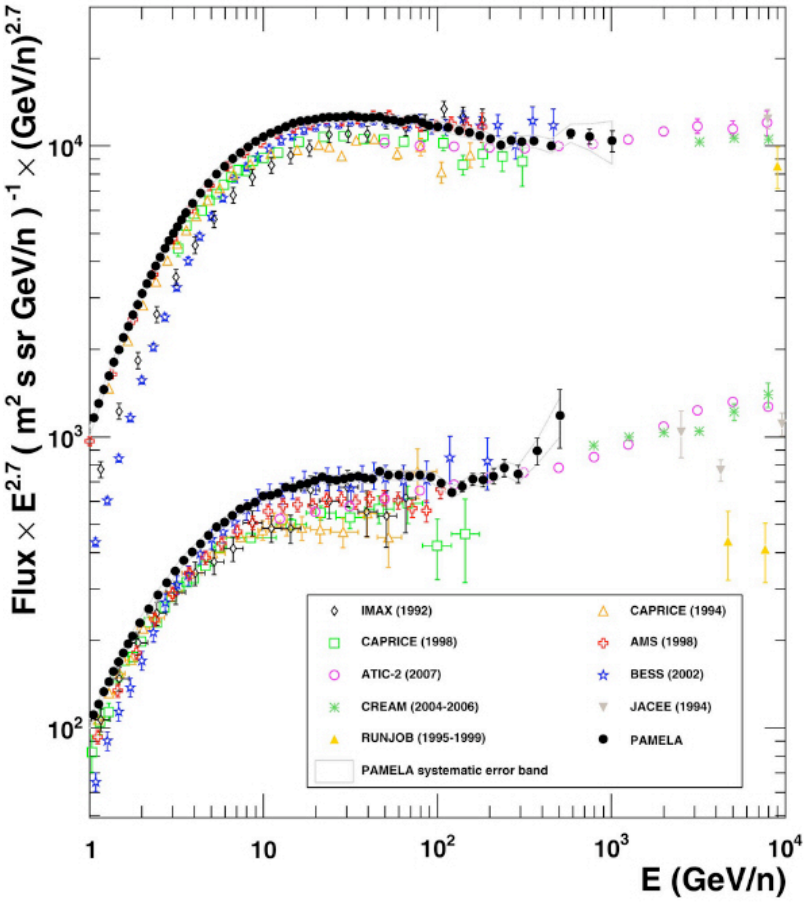

$$\frac{\partial f}{\partial t} + U\frac{\partial f}{\partial x} = \frac{\partial}{\partial x}\kappa\frac{\partial f}{\partial x} + \frac{1}{3}\frac{\partial U}{\partial x}p\frac{\partial f}{\partial p}$$

$$U(x) = \begin{cases} -u_1, & \text{if } x > 0 \\ -u_2, & \text{if } x \leq 0 \end{cases}$$

$$f = f_0(p)\exp(-u_1 x/\kappa)$$

$$\text{compression ratio, } r = \frac{u_1}{u_2}$$

$$f_0 = Q_{inj}\, p^{-q} \quad \text{where} \quad q = \frac{3r}{r-1}$$

$$t_{acc}(p) = \frac{3}{u_1 - u_2} \int_{p_0}^{p} \left(\frac{\kappa_1}{u_1} + \frac{\kappa_2}{u_2} \right) \frac{dp}{p}$$

Spectral Modelling…

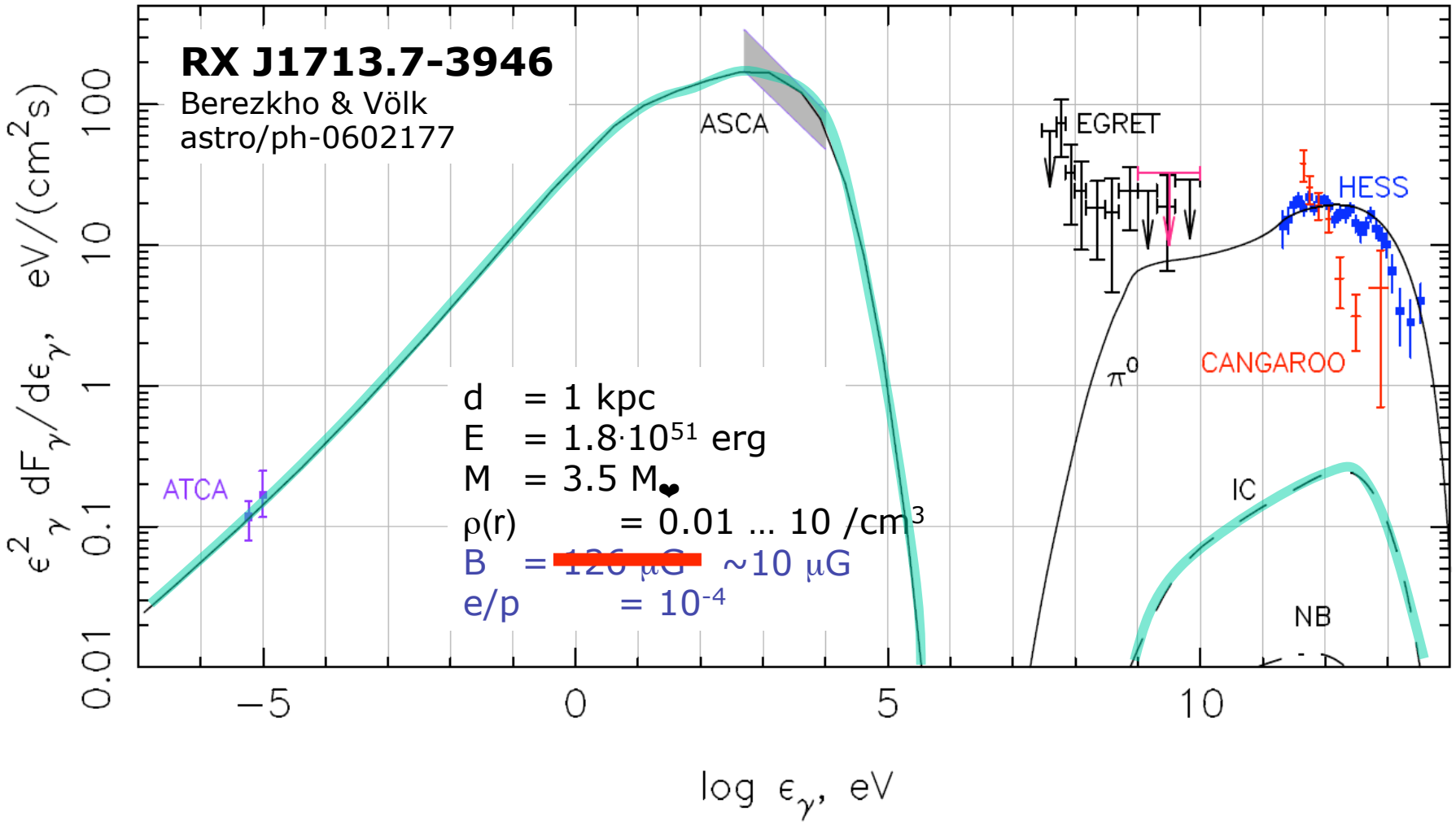

composite scenario of gamma-ray emission: forward shock in dense clouds and reverse shock

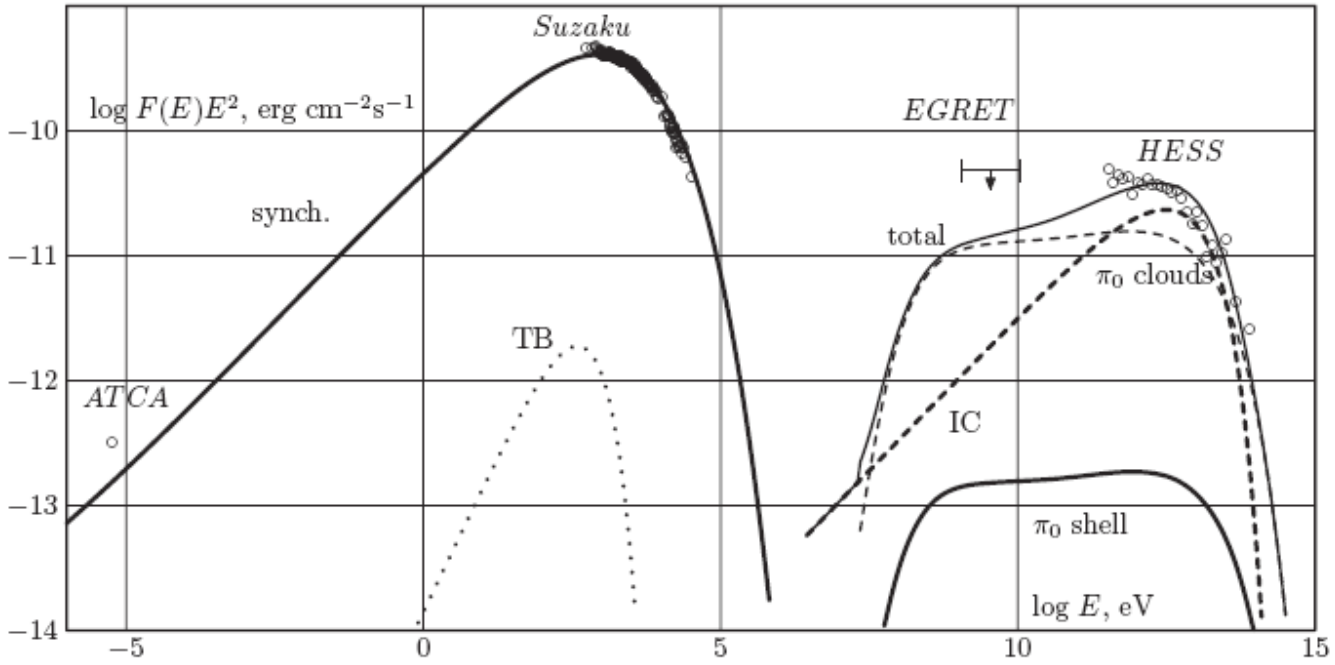

Figure 14. Broadband emission of RX J1713.7−3946 for the composite scenario of gamma rays with a non-modified forward shock and dense clouds. The principal model parameters are: $t = 1620$ yr, $D = 1.5$ kpc, $n_{\rm H} = 0.02$ cm^{-3}, $E_{SN} = 1.2 \times 10^{51}$ erg, $M_{ej} = 0.74\,M_\odot$, $M_A^f = 55$, $M_A^b = 10$, $\xi_0 = 0.1$, $K_{ep}^f = 1.4 \times 10^{-2}$, and $K_{ep}^b = 9 \times 10^{-4}$. The calculations lead to the following values of the magnetic fields and the shock speeds at the present epoch: the magnetic field downstream of the forward and reverse shocks $B_f = 22$ μG and $B_b = 31$ μG, respectively, the speed of the forward shock $V_f = 3830$ km s^{-1}, and the speed of the reverse shock $V_b = -1220$ km s^{-1}. The following radiation processes are taken into account: synchrotron radiation of accelerated electrons (solid curve on the left), thermal bremsstrahlung (dotted line), IC gamma-ray emission of the entire remnant including forward and reverse shocks (dashed line), and hadronic component of gamma-rays from the remnant's shell (solid line on the right), as well as from dense clouds assuming the factor of 120 enhancement of the flux (thin dashed line). We also show the total gamma-ray emission from the entire remnant including the dense clouds (thin solid line).

SNR 1713.7
CO map

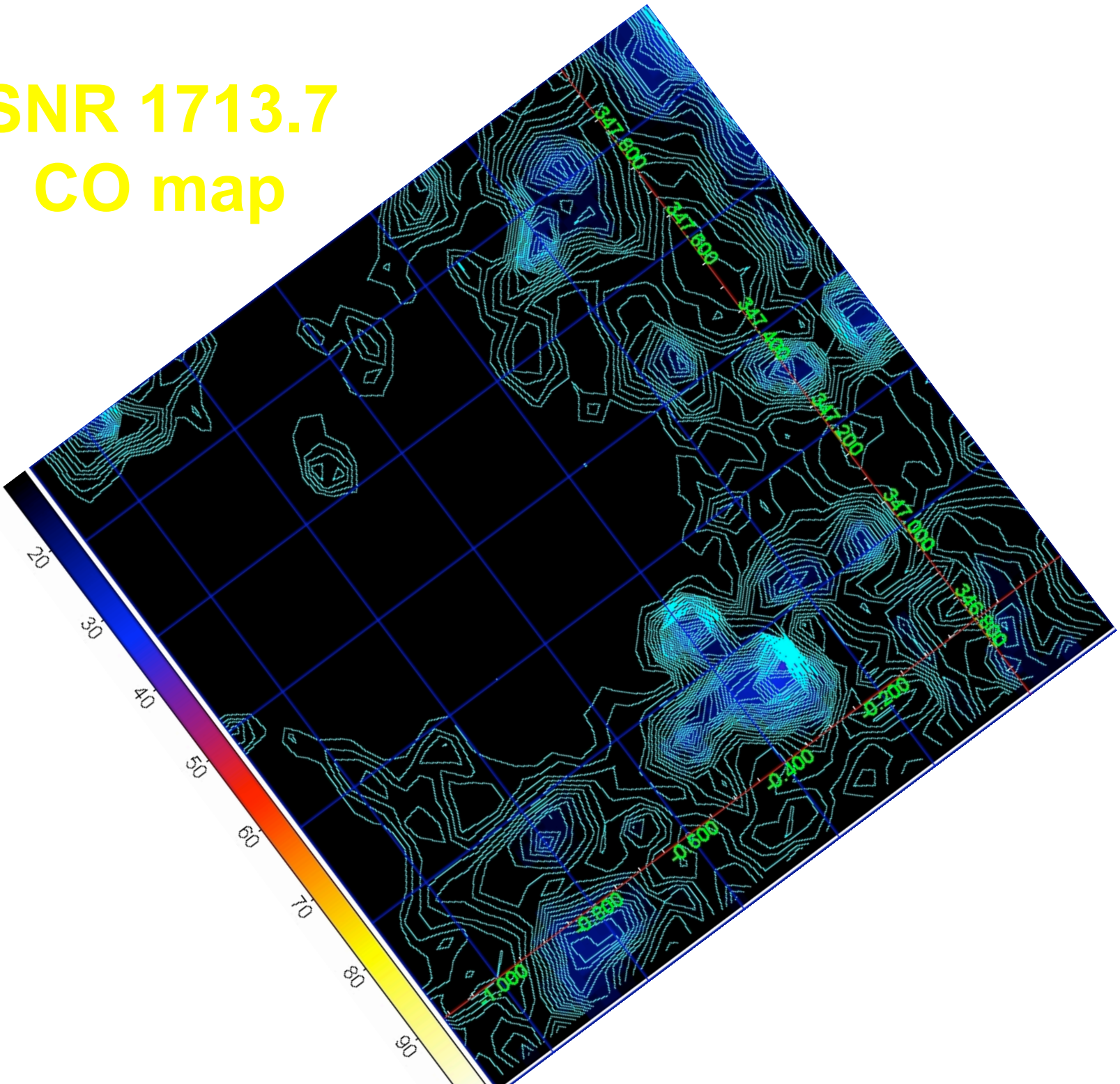

young SNRs (X-rays, Chandra)

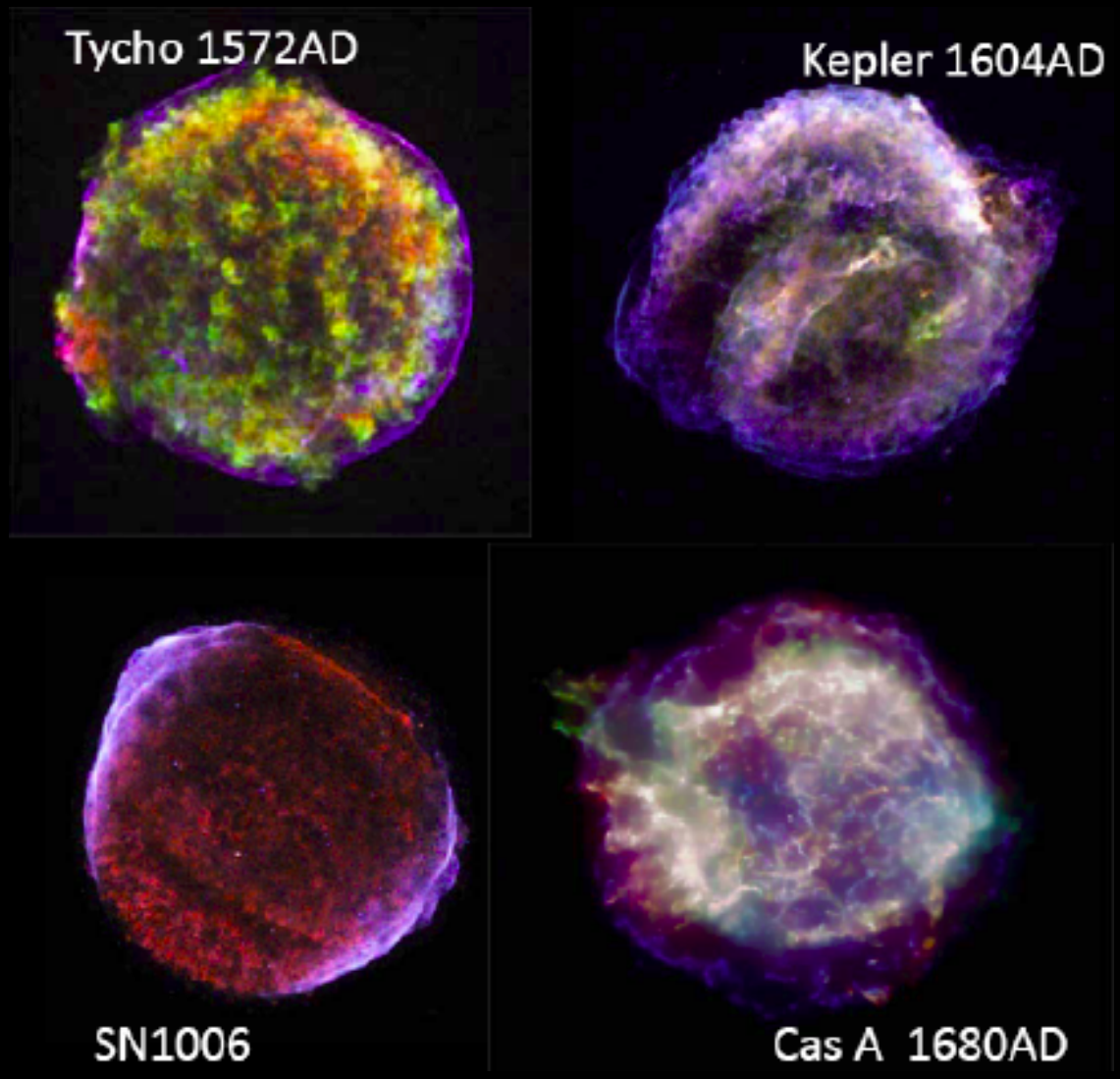

theoretical challenges

- spectral breaks near 1-10 GeV for emission associated to molecular clouds
- co-existence" (?) of *average* low-B and l*ocal* strongly enhanced-B (1 mG): filamentary structure of shocks
- no obvious sign of shock-accelerated particle concave spectra (non-linear effect)
- "escape" and propagation of hadronic CRs
- explain local anisotropies, …

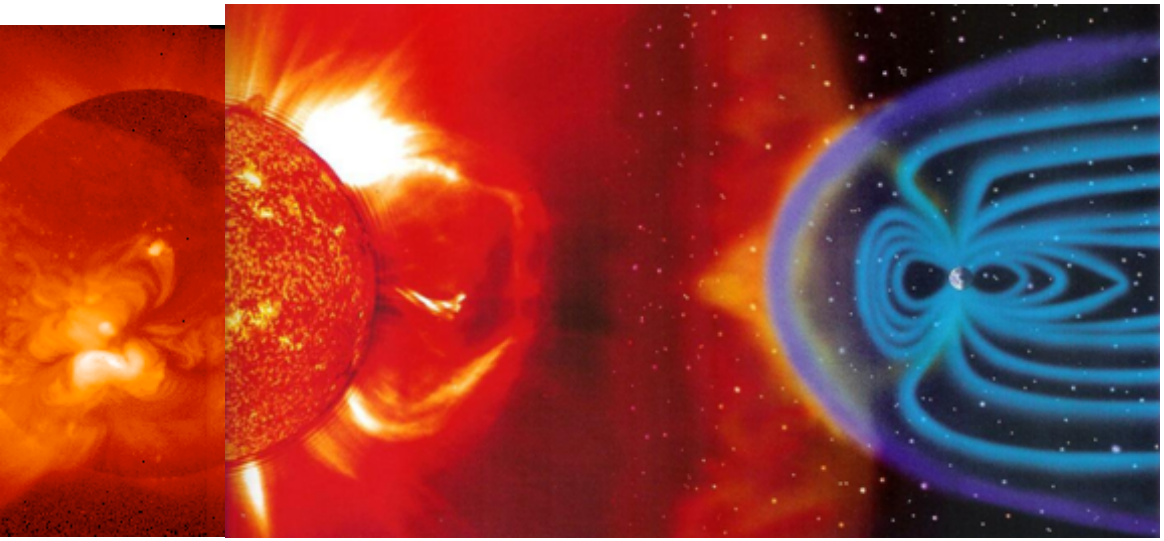

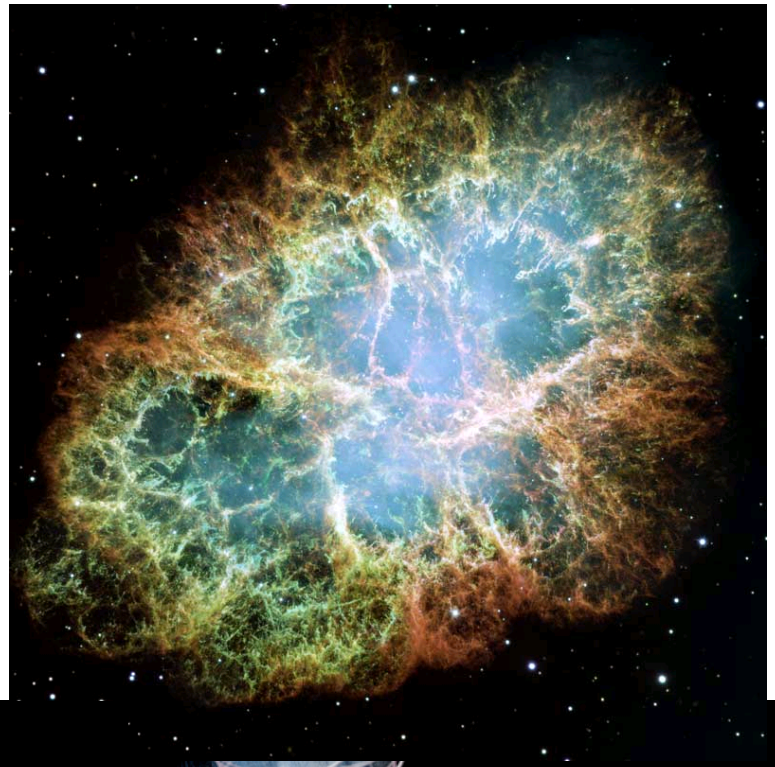

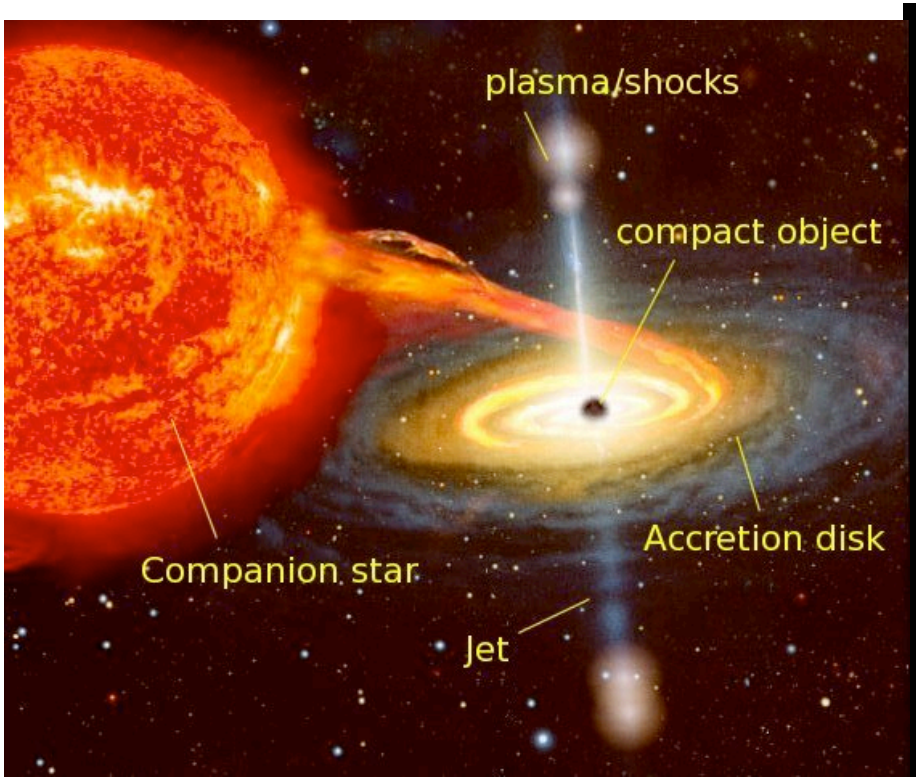
plasma/shocks
compact object
Companion star
Accretion disk
Jet

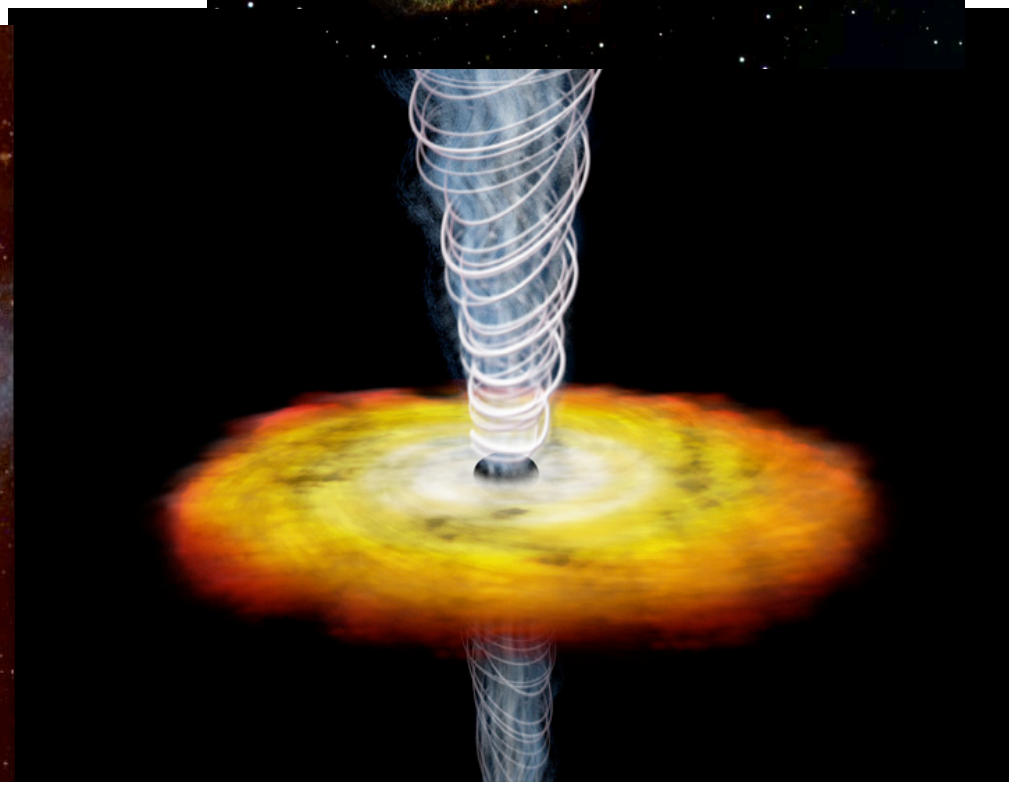

SNR 1713.7 NANTEN CO map

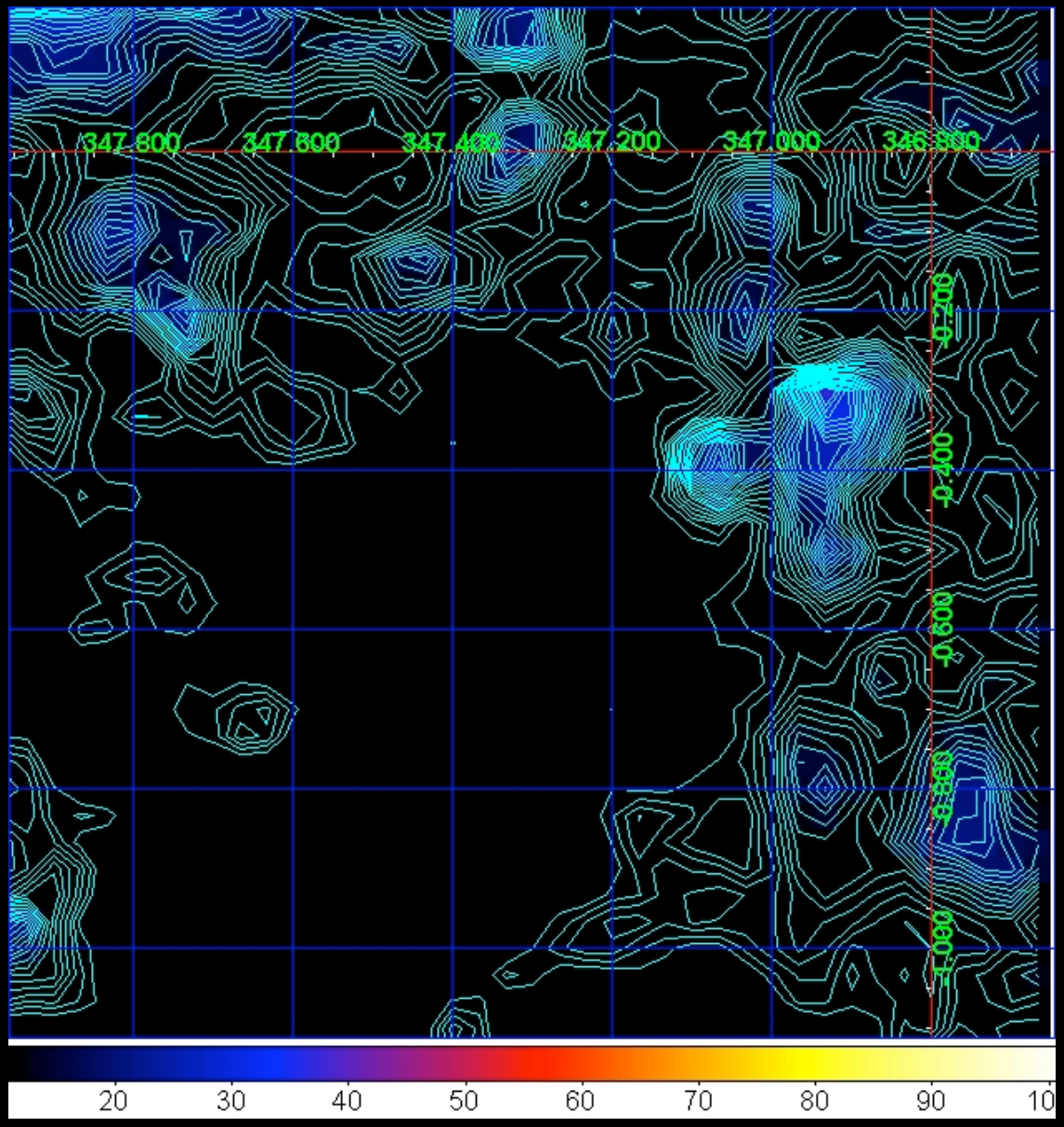

SNR RX J1713-3946
AGILE gamma-ray imaging,

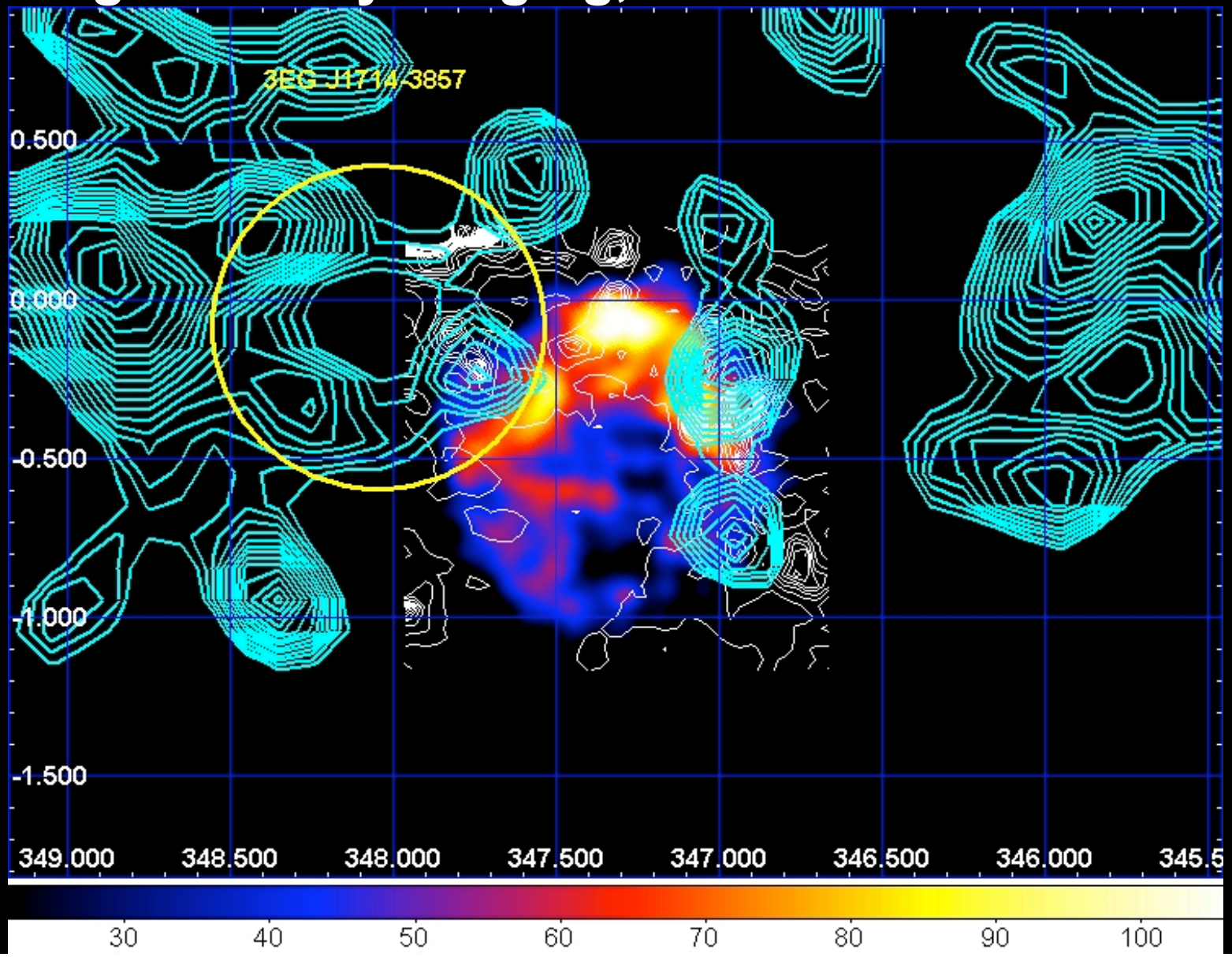

SNR RX J1713-3946

AGILE gamma-ray imaging,

E> 400 MeV

Intensity map

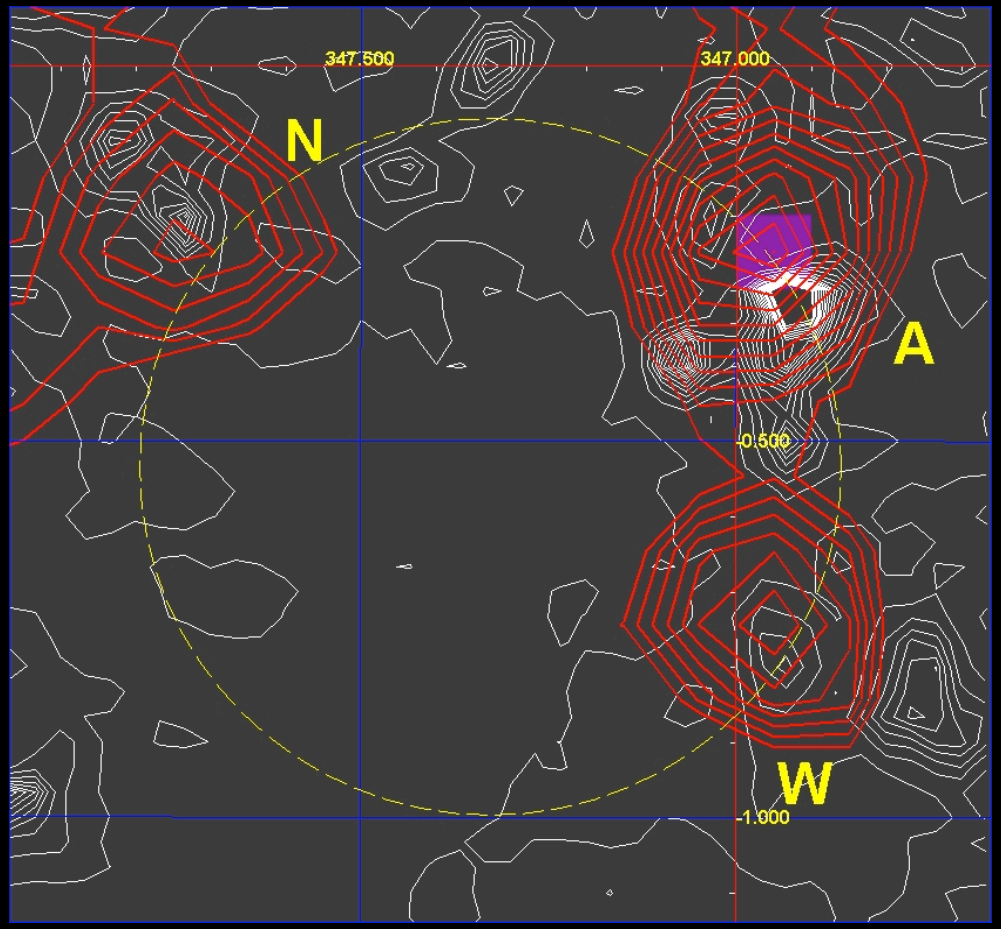

Tavani et al. 2011 in prep.

SNR RX J1713-3946

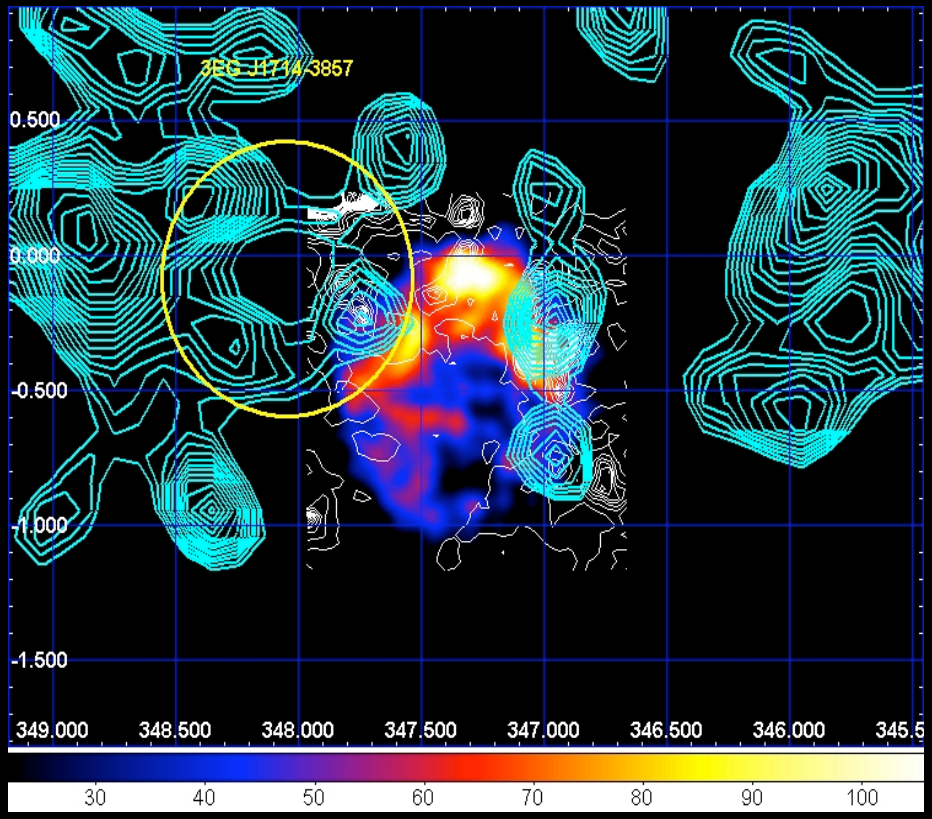

HESS map +

AGILE/GRID contours (E> 400 MeV)

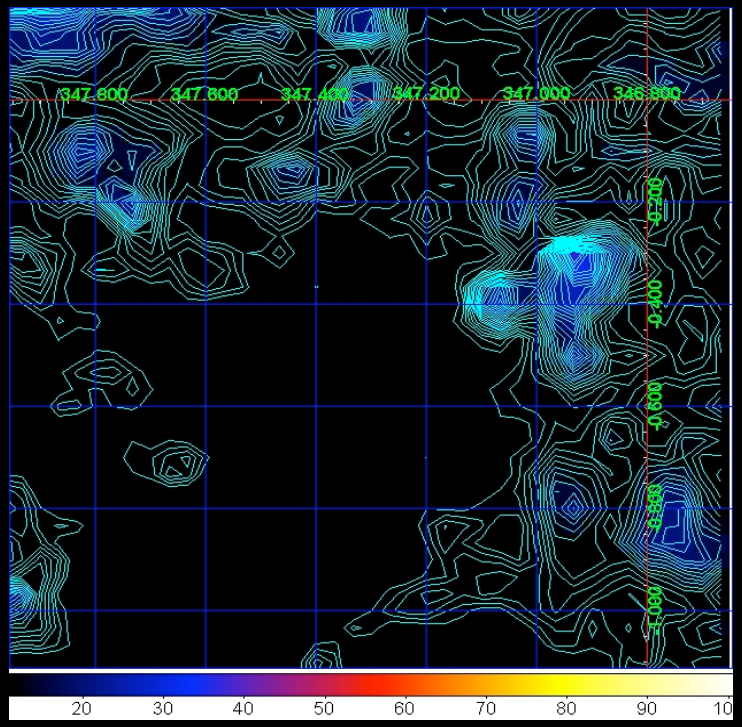

NANTEN

CO map

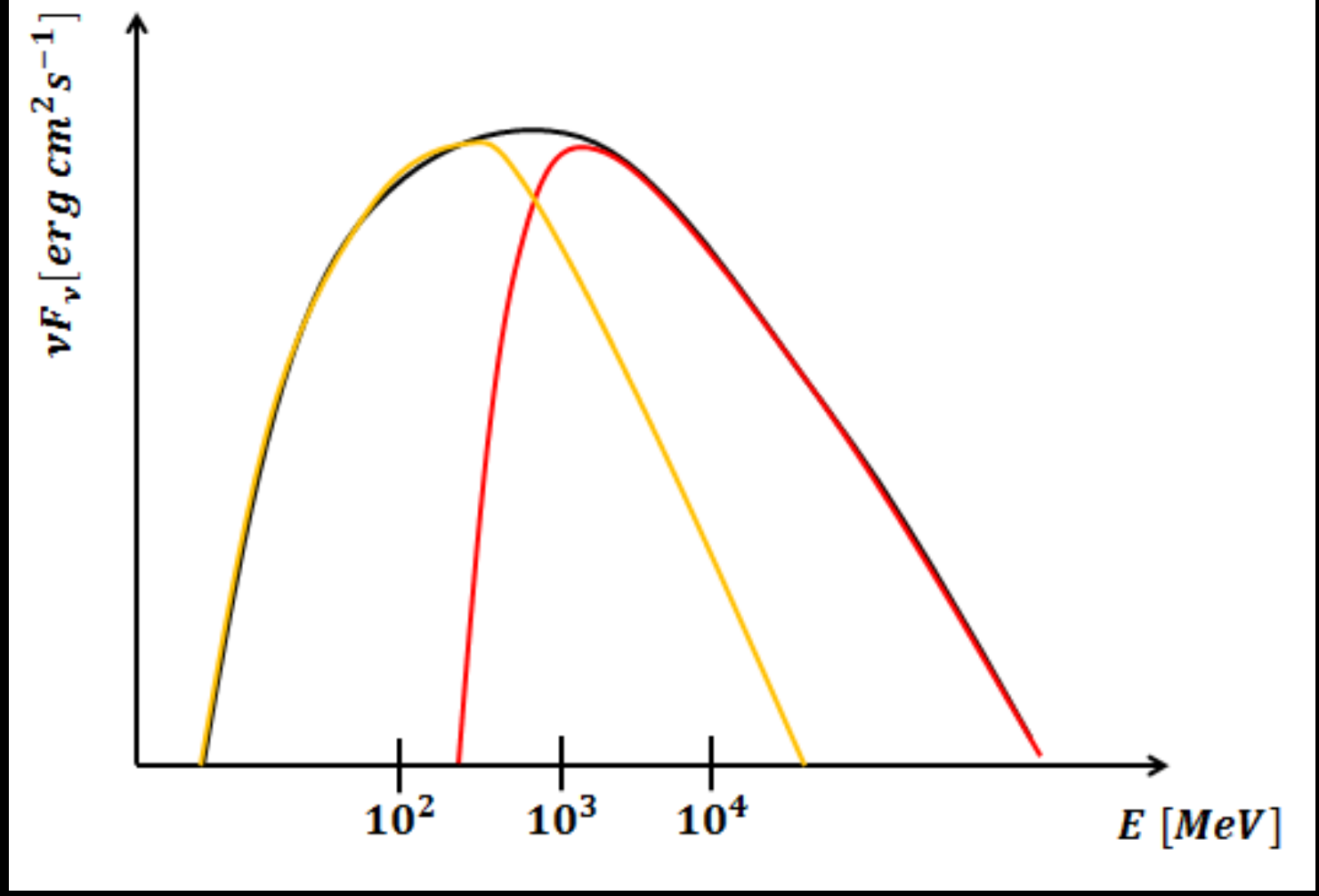
$vF_v[erg\ cm^2 s^{-1}]$
10^2
10^3
10^4
$E\ [MeV]$

lessons from RX 1713.7-3946

* complex patchy emission
* coexistence of hadronic and leptonic
* spectral cutoffs, “escape”

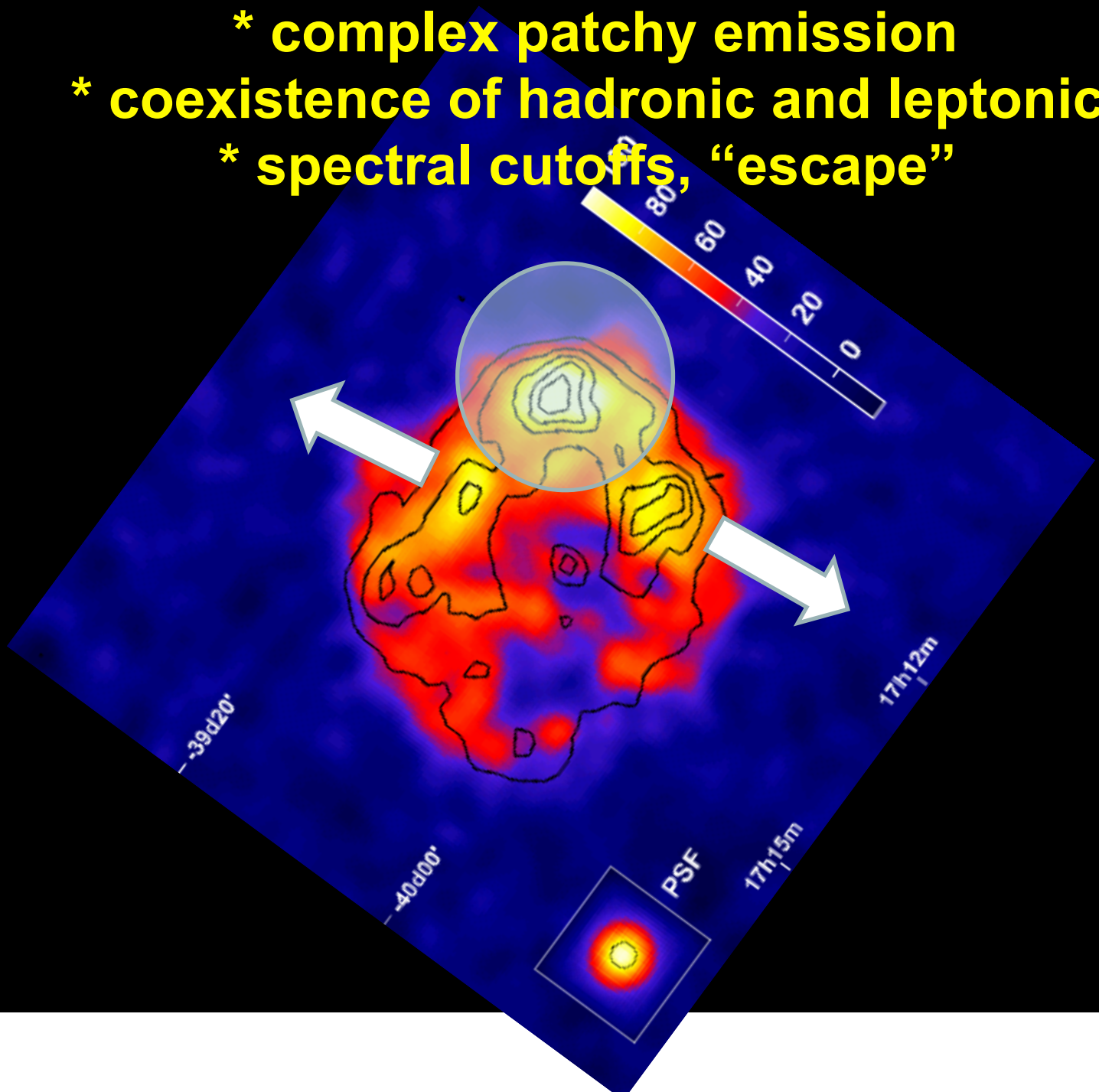

DIFFICULT TO PROVE: Fermi paper on W51C, Abdo et al. 2010

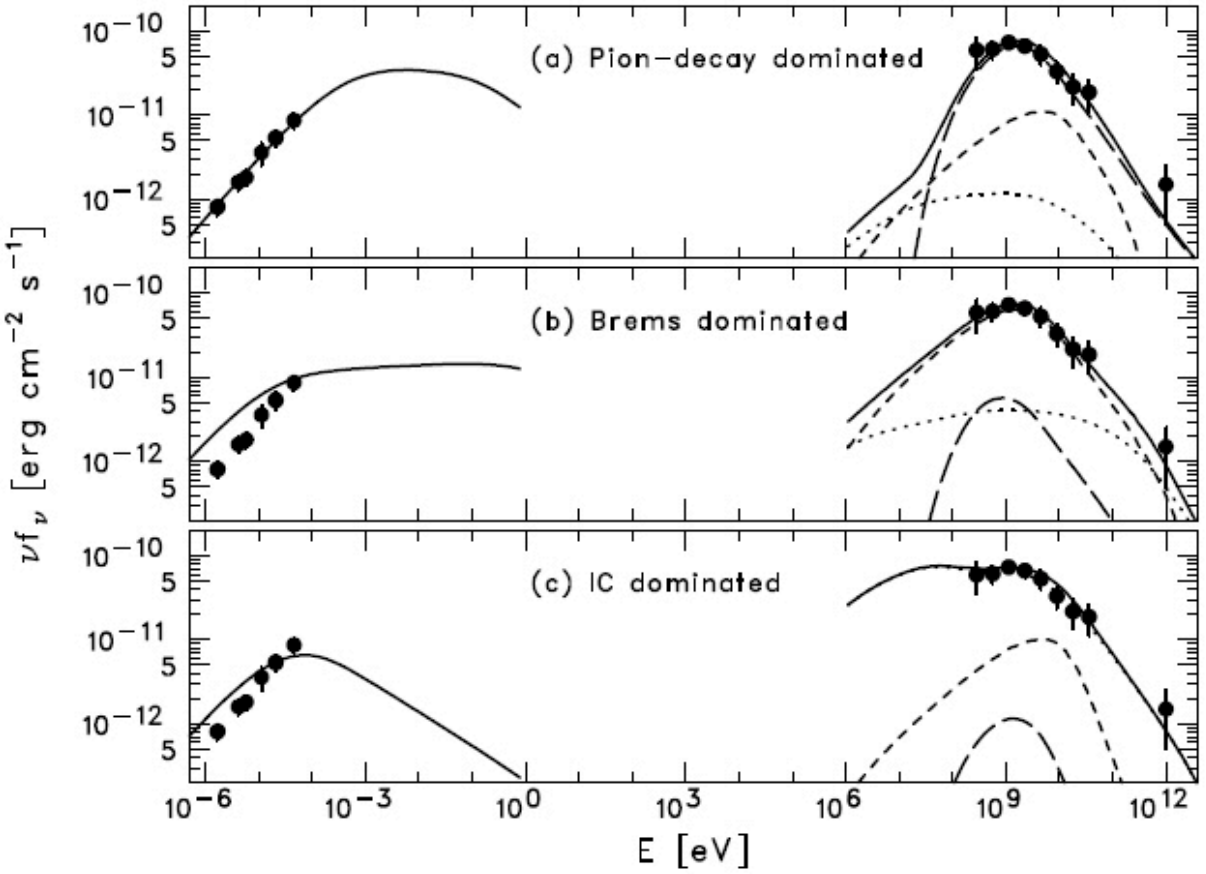

Fig. 4.— Three different scenarios for the multiwavelength modeling (see Table 1). The radio emission (from Moon & Koo 1994) is explained by synchrotron radiation, while the gamma-ray emission is modeled by different combinations of π^0-decay (long-dashed curve), bremsstrahlung (dashed curve), and IC scattering (dotted curve). The sum of the three component is shown as a solid curve.

SNR	Age (yrs)	distance
IC 443	~ 30.000	~ 1.5 kpc
W28	~ 35.000	~ 1.8-3.3 kpc
W44	~ 20.000	~ 3 kpc
1713.7-3946	1.000-3.000	~ 1 kpc

advancement in CR astrophysics

- about 10 SNRs detected in gamma-rays *Fermi* and AGILE
- complex interaction with the surroundings
- acceleration and “escape” of accelerated CRs play a crucial role
- co-existence of leptonic and hadronic emission
- so far, only 1 case of clear pion emission (W44) unveiled by AGILE

- **Synchrotron cooling timescales**

- $\tau_s = (30\ \text{yrs})\ B_{-4}^{-3/2}\ (E_{ph}/1\ \text{keV})^{-1/2}$

- $\tau_s = (0.1\ \text{yrs})\ B_{-4}^{-3/2}\ (E_{ph}/100\ \text{MeV})^{-1/2}$

- **short timescale Crab variability (Sept. 2010):**

  - **currently published data:**
    - **2-day integration (AGILE)**
    - **4-day integration (Fermi)**

  - **study 1-day and 12-hr integrations**

  - **are AGILE and Fermi data consistent with 12-hr variability ?**

1-day bin lightcurves (AGILE and Fermi)

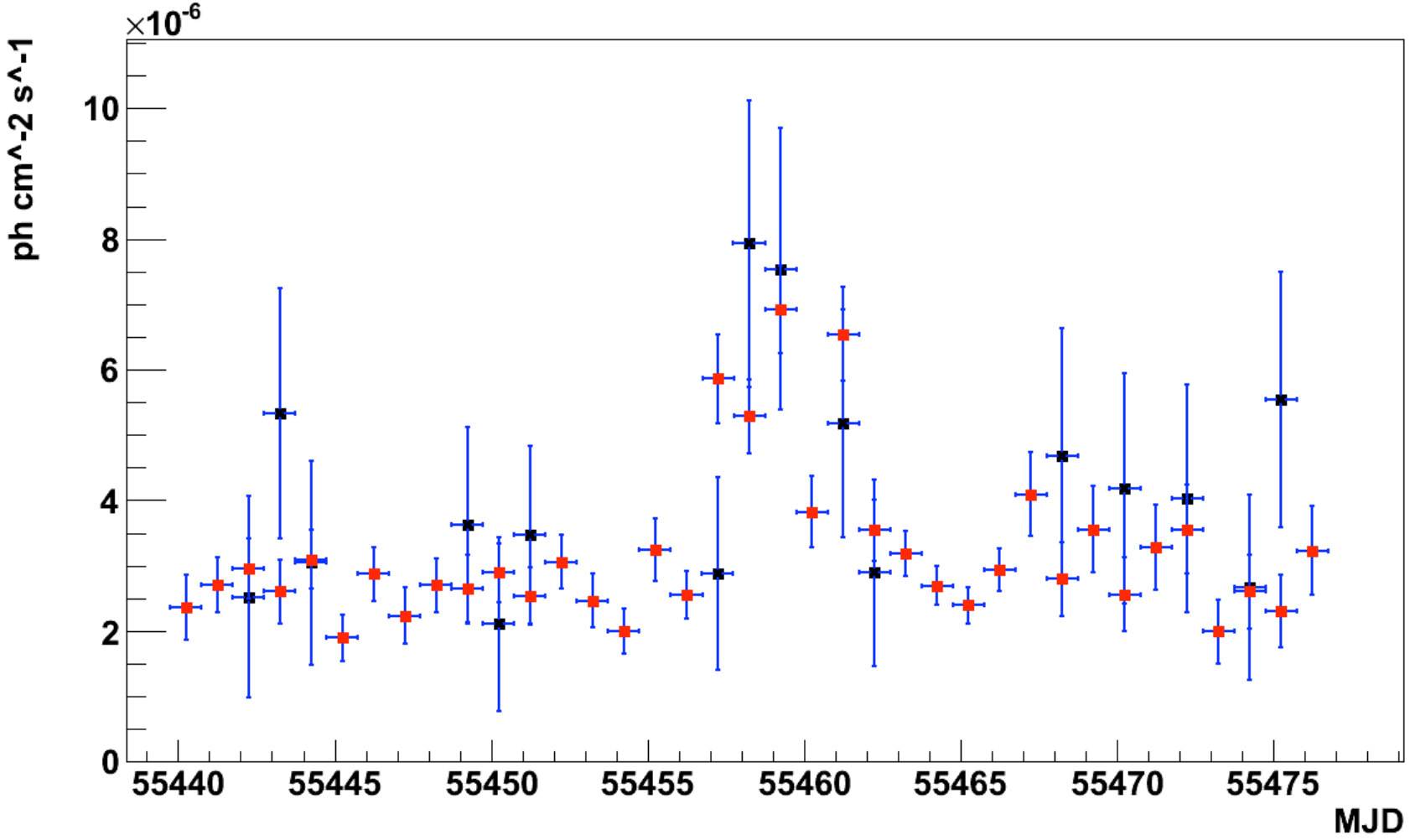

12-hr bin lightcurves (AGILE and Fermi)

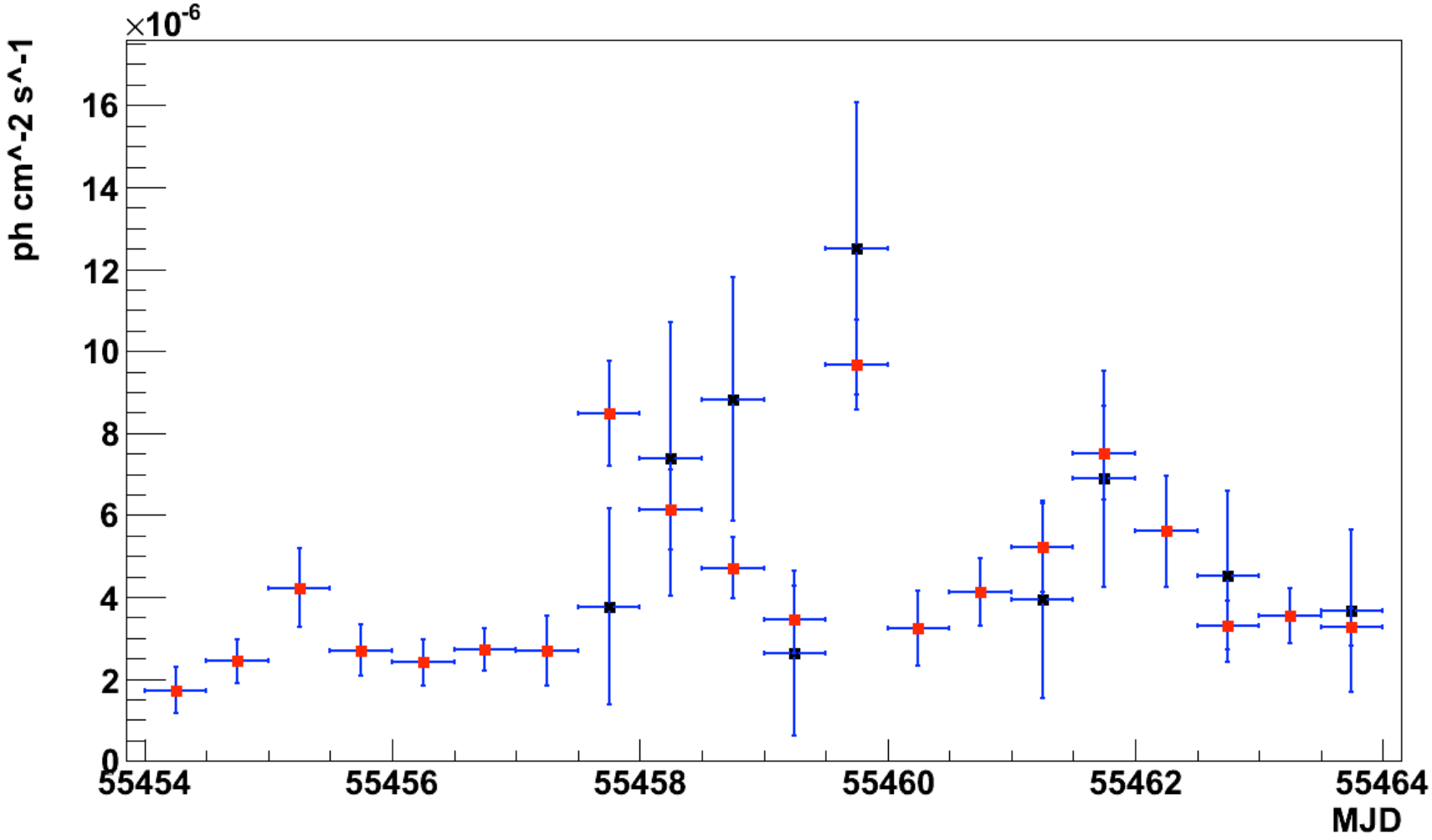

12-hr bin lightcurves (AGILE and Fermi)

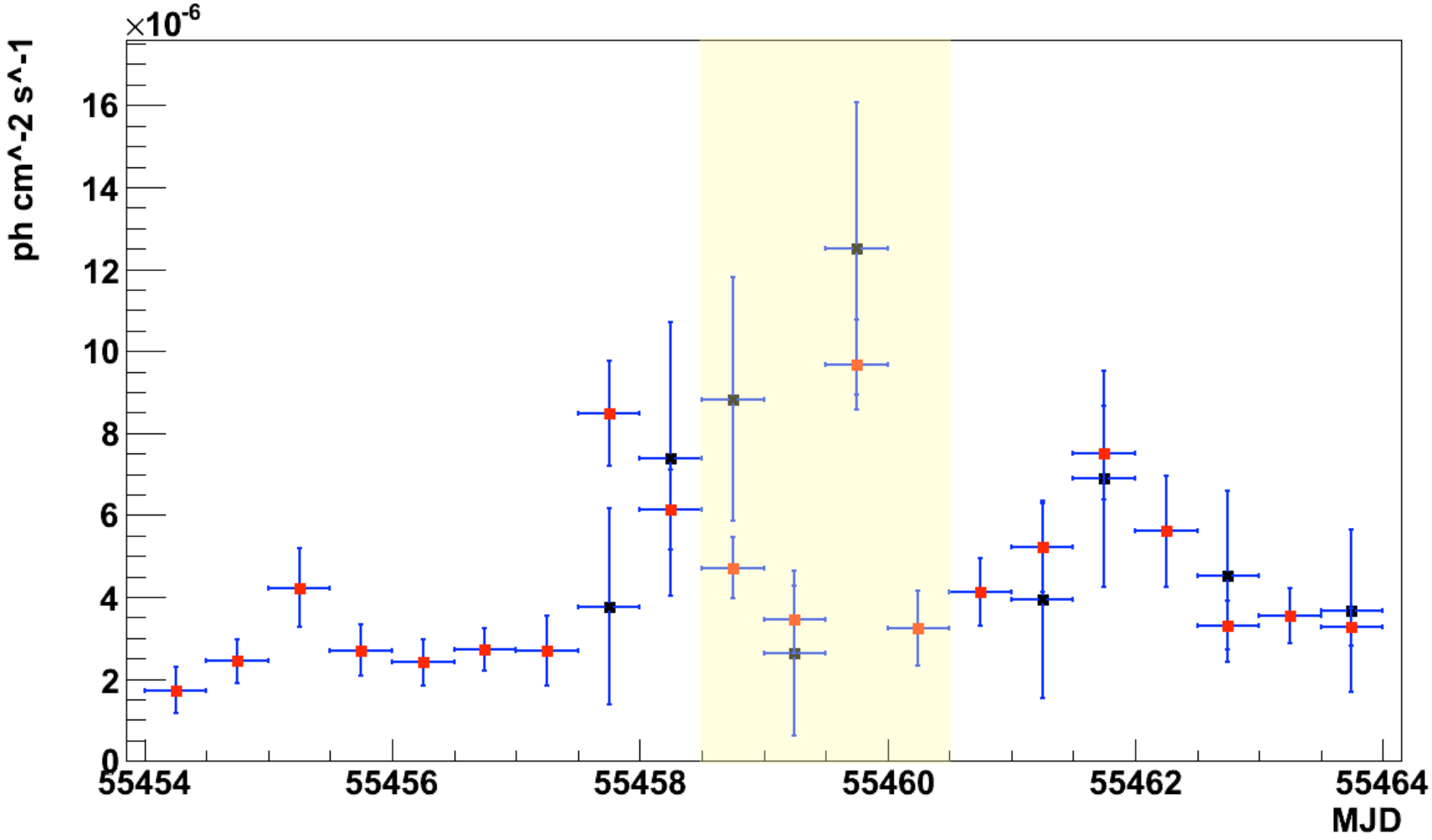

12-hr bin lightcurves (AGILE and Fermi)

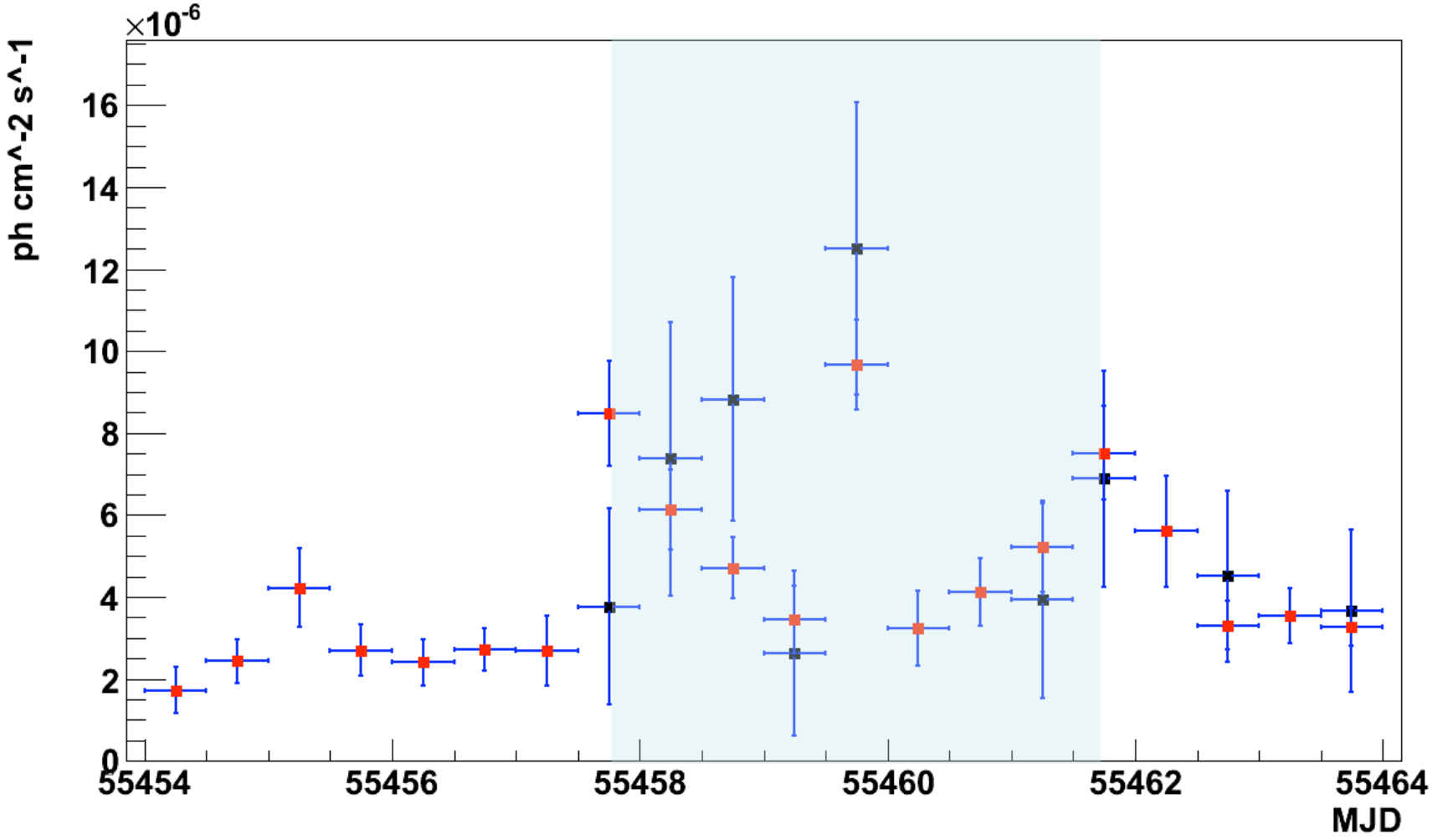

independent Fermi data analysis (Balbo et al., A&A, 527, L4, 2011)

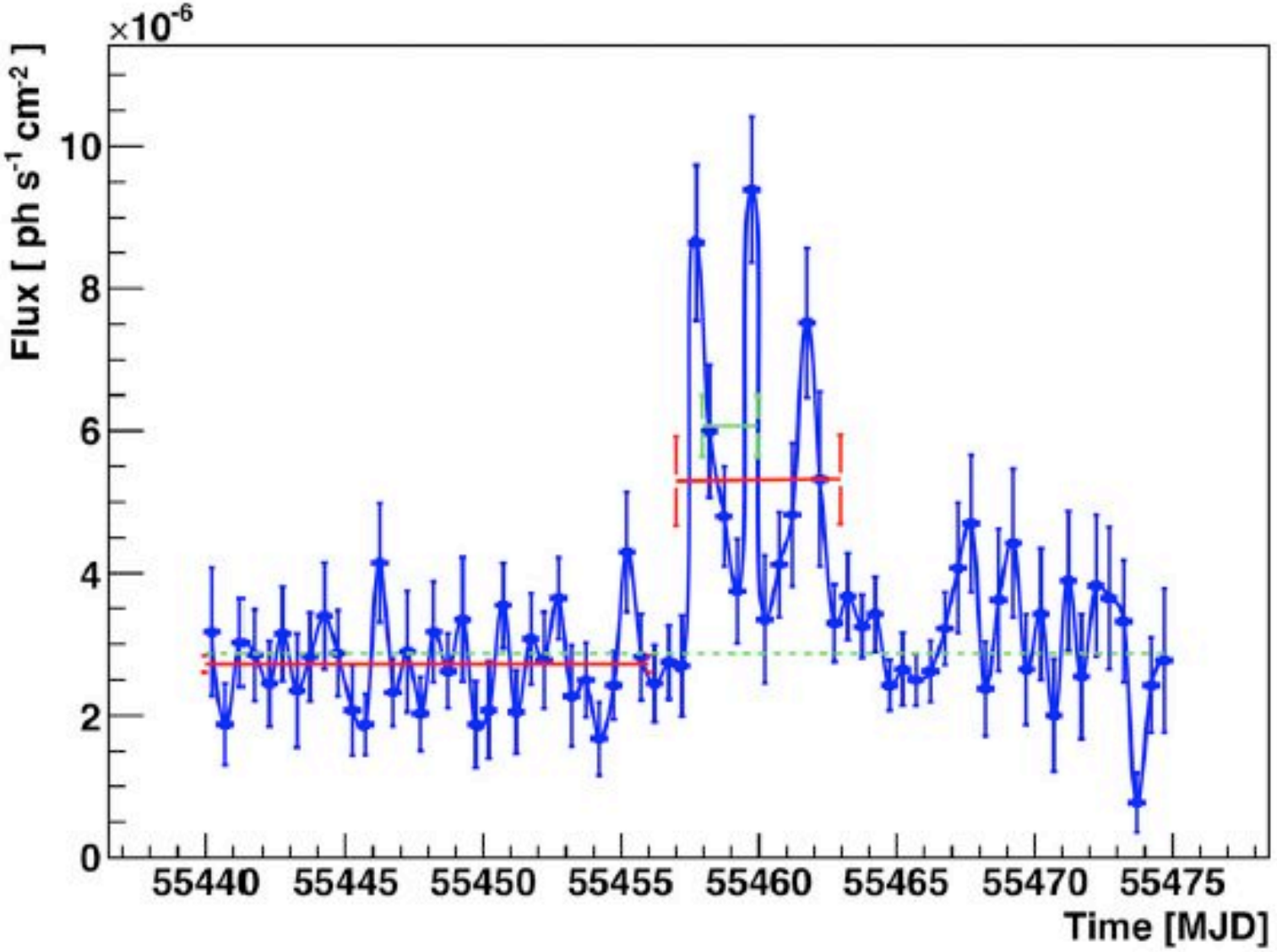

- evidence for very short (12 hrs or less) variability detected both by AGILE and Fermi

- **not the end of the story…**

still more surprises..!

- **TeV observations and ARGO-YBJ detection in Sept. 2010 (ATEL 2921)**

- **see also ATELs by VERITAS and MAGIC**

TeV nebular emission

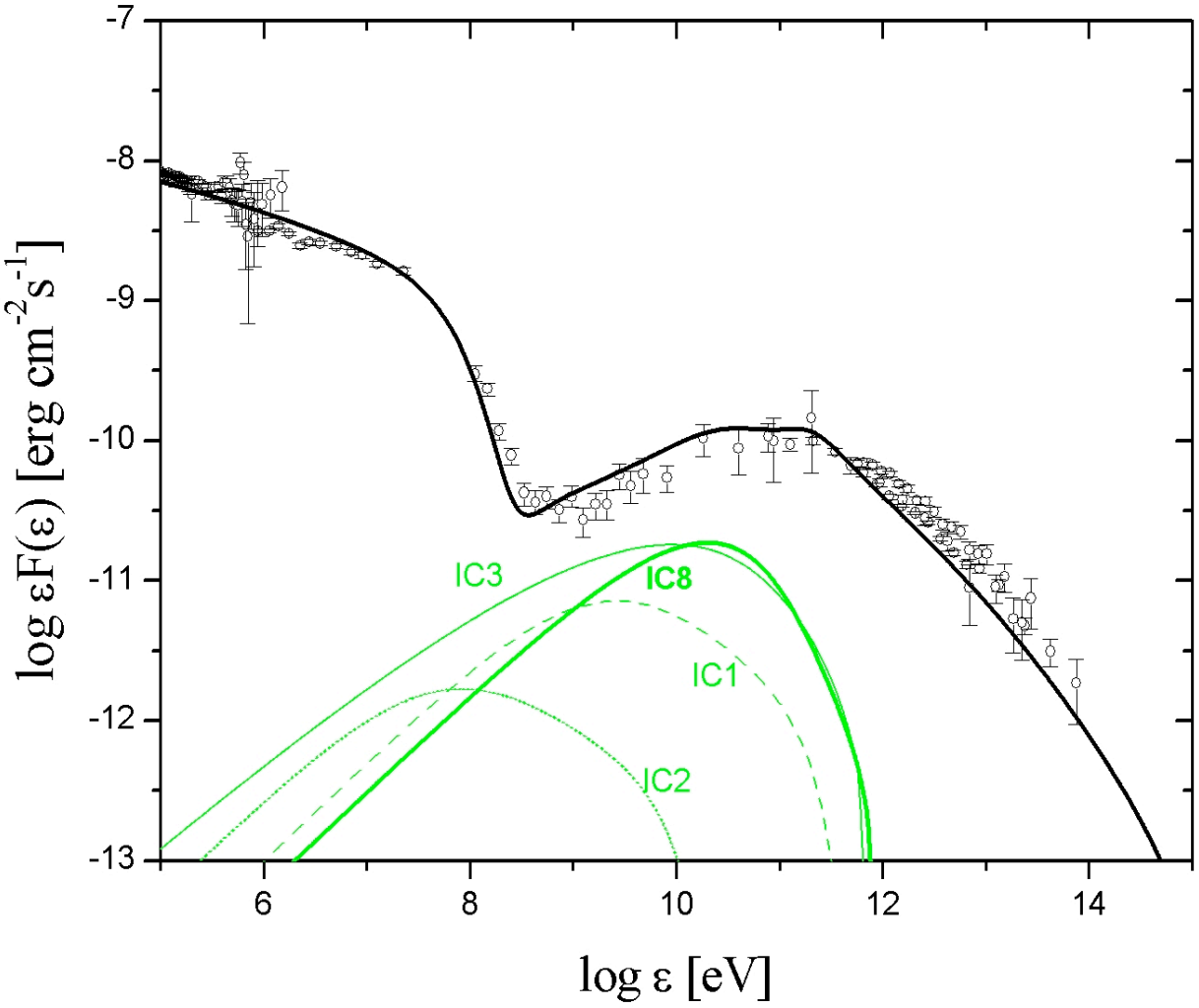

Inverse Compton contribution from **pop I** electrons scattering:

IC1 dust ph
IC2 CMB ph
IC3 syn ph from **pop I**
IC8 syn ph from **pop II**

TeV nebular emission

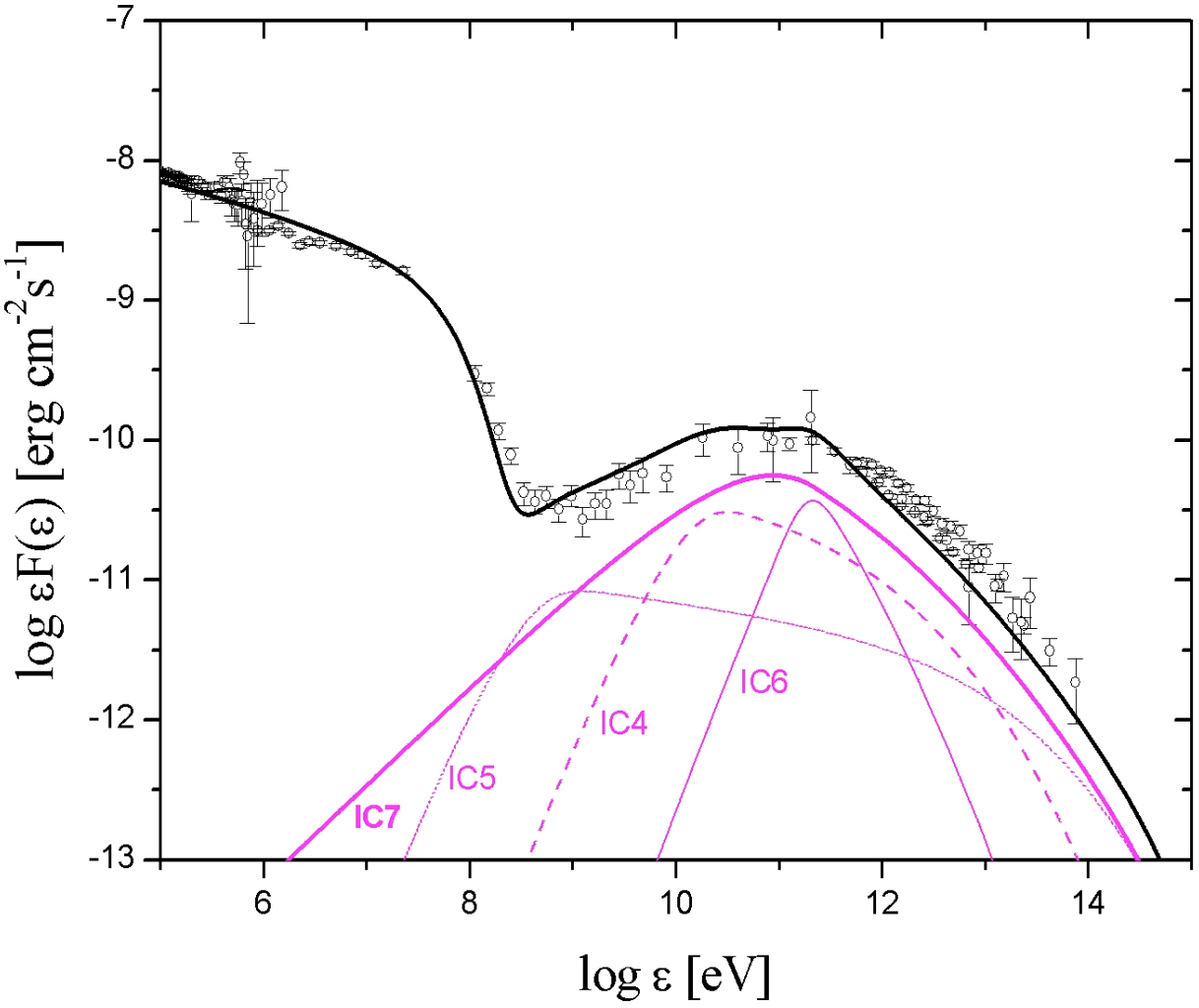

Inverse Compton contribution from **pop II** electrons scattering:

IC4 dust ph
IC5 CMB ph
IC6 syn ph from **pop II**
IC7 syn ph from **pop I**

post-flare TeV observations (ATel's: 2921, 2967, 2968)

Instrument	Epoch (MJD)	Duration	
VERITAS	55456.44	20 min.	no variation
	55456.47	20 min.	
	55457.47	20 min.	
	55458.45	20 min.	
	55458.47	20 min.	
	55459.47	20 min.	
MAGIC	55459.20	58 min.	no variation
ARGO-YBJ	55456-55461	5 days	3-4 times enhancement
	55456-55466	10 days	possible enhancement

12-hr bin lightcurves (AGILE and Fermi)

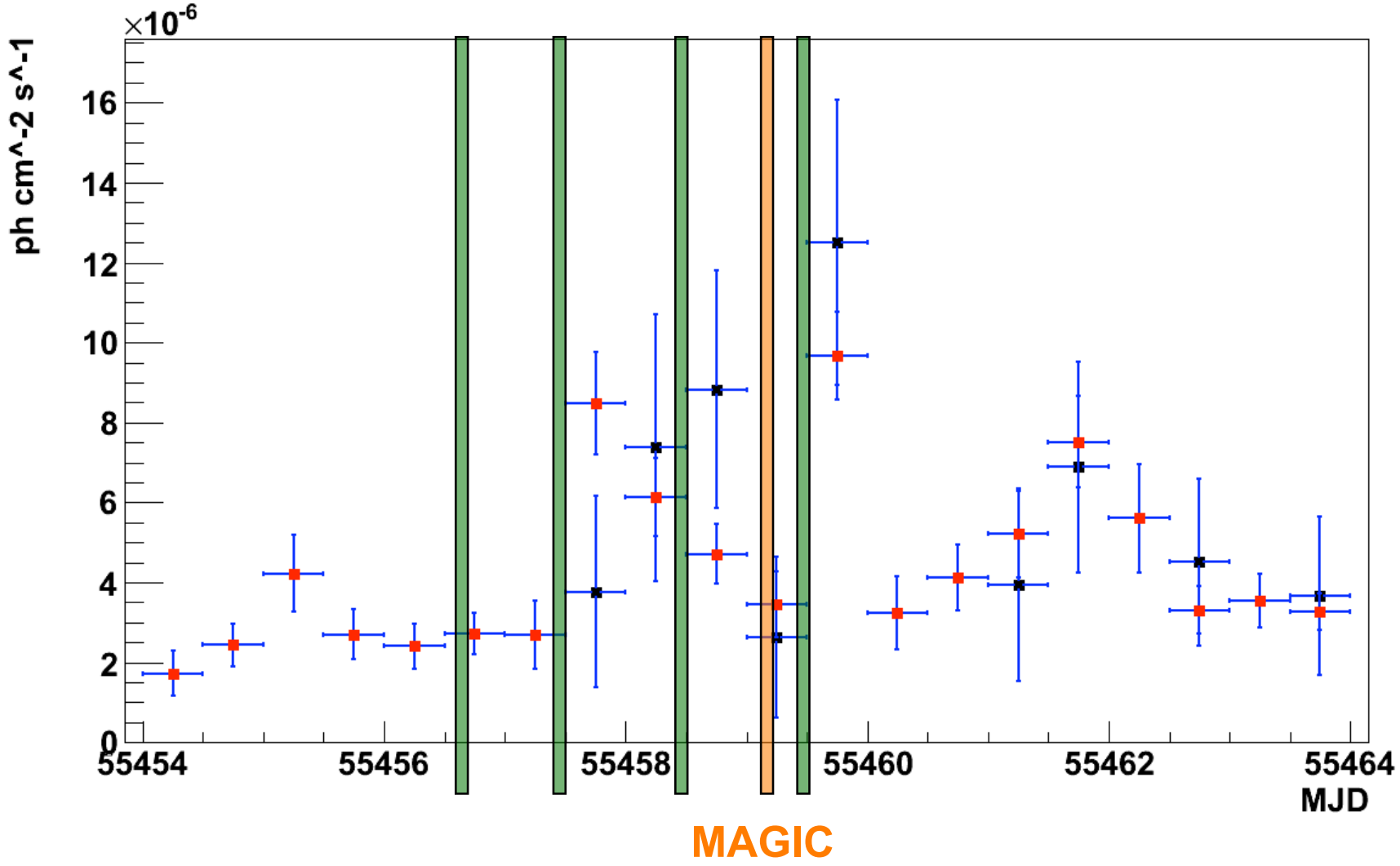

post-flare TeV observations

Instrument	Epoch (MJD)	Duration	
VERITAS	**55456.44**	**20 min.**	no variation
	55456.47	**20 min.**	
	55457.47	**20 min.**	
	55458.45	**20 min.**	
	55458.47	**20 min.**	
	55459.47	**20 min.**	
MAGIC	**55459.20**	**58 min.**	no variation
ARGO-YBJ	**55456-55461**	**5 days**	3-4 times enhancement
	55456-55466	**10 days**	possible enhancement

exciting prospects

- room for possible short timescale TeV emission
- test VERITAS data during the first peak of emission (MJD 55458.5)
- search for similar episodes in the past ?
- TeV emission requires enhancement !
  - favorable Doppler beaming

- very exciting results, the Crab Nebula produces ~day-long gamma-ray flares ! Not a standard candle in gamma-rays.

- nebular origin, not clear yet the association with a wisp or feature, South East “jet” base ?

- dramatic confirmation of high-efficiency relativistic particle acceleration

Conclusions

- we “lost” the stability of an ideal reference source, but gained tremendous information about the fundamental process of particle acceleration

- a big theoretical challenge
  - shock acceleration + magnetic field reconnection ?
  - current sheet and MHD instabilities
  - Doppler boosting ?

- the ultimate site of particle acceleration needs to be established: future surprises

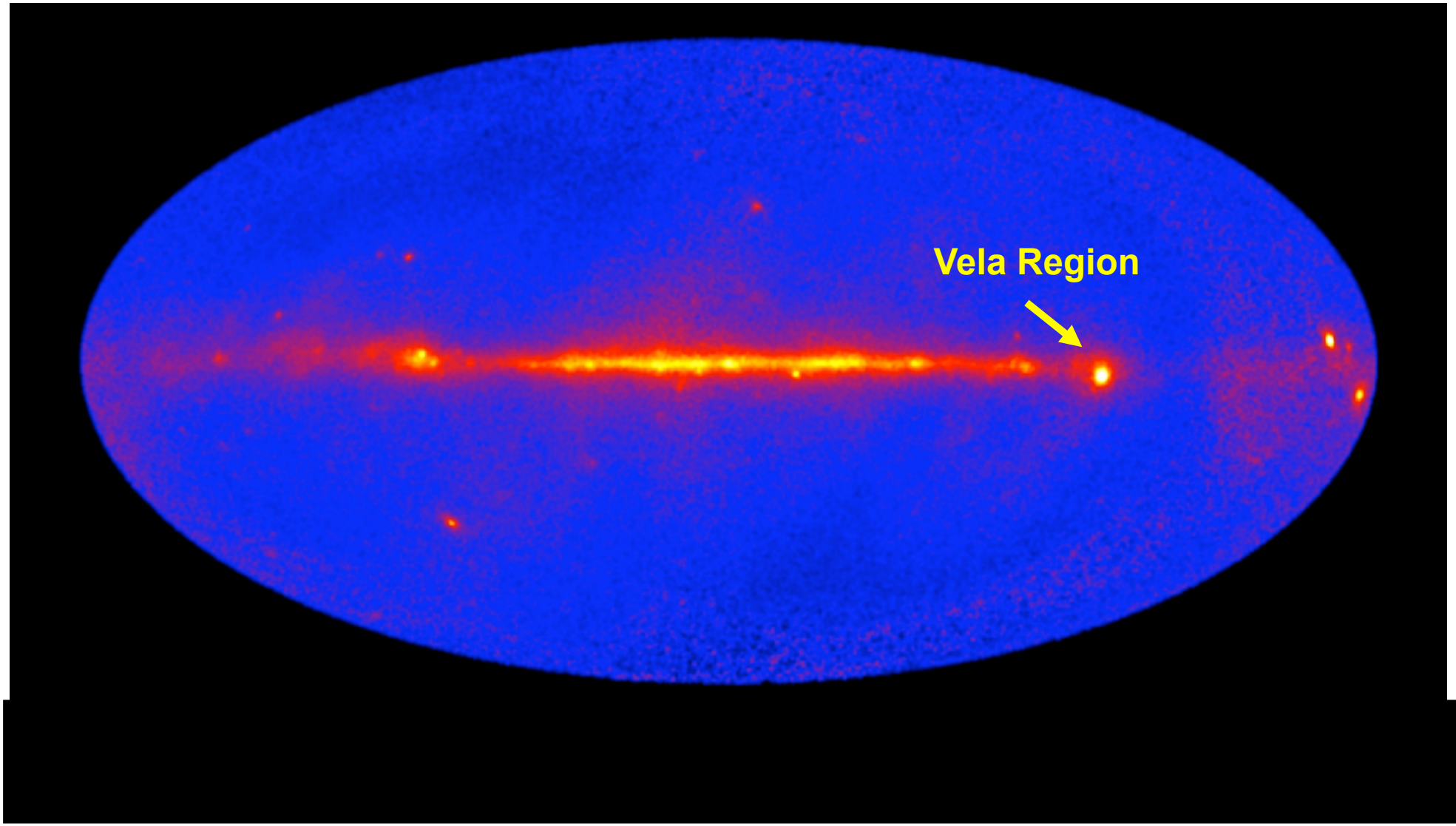
Vela Region

Vela X pulsar wind nebula

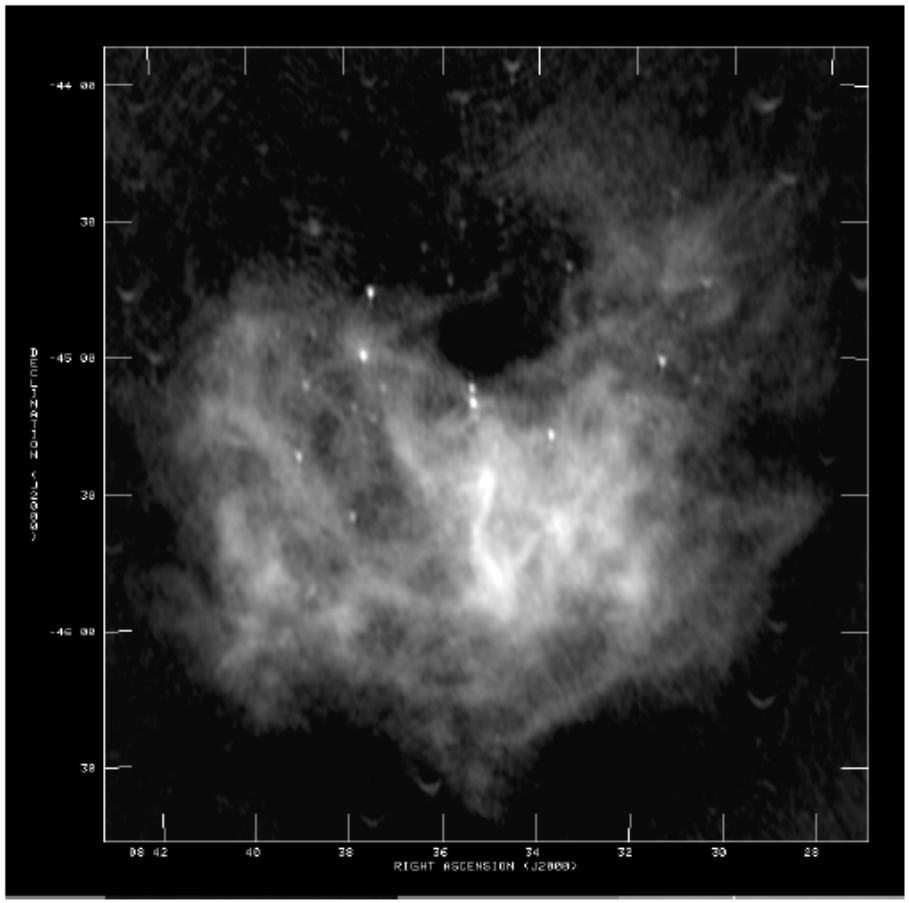

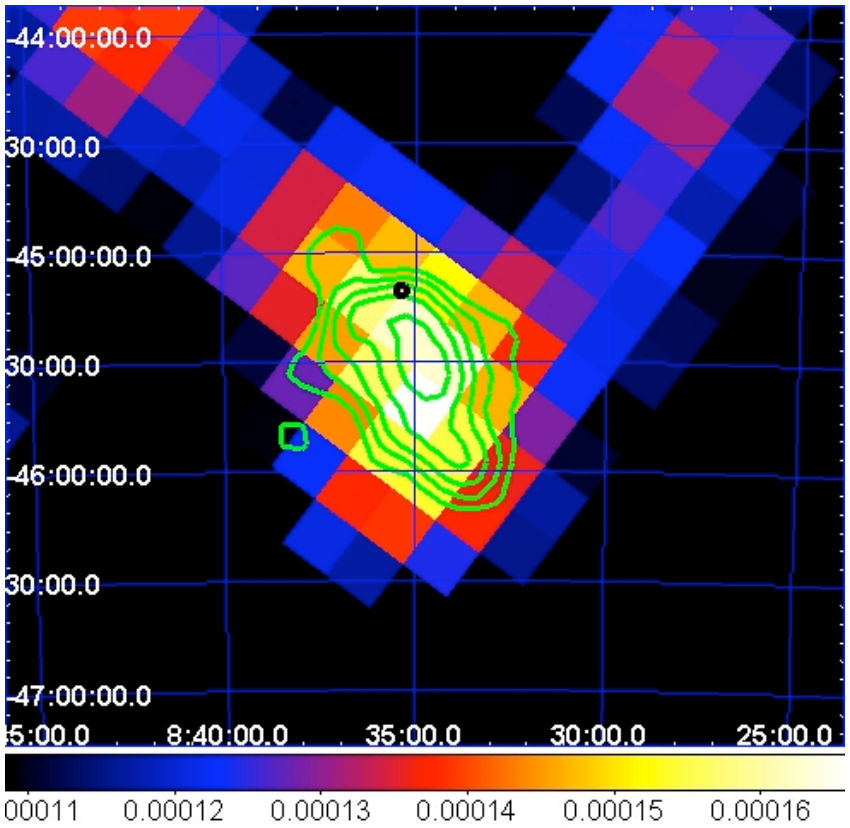

1.—A 90 cm radio continuum image of the Vela X remnant. No correction has been made for the attenuation pattern of the individual antennas, elds of view (at half maximum) are approximately 2°. The rms noise is 3.1 mJy beam^{-1}.

t al. (see 475, 225)

Fermi-LAT observation of Vela-X

- extended emission in the off-pulse emission
  - 9 σ above 800 MeV
  - not a point-source at the pulsar position
  - uncertainties in the diffuse emission

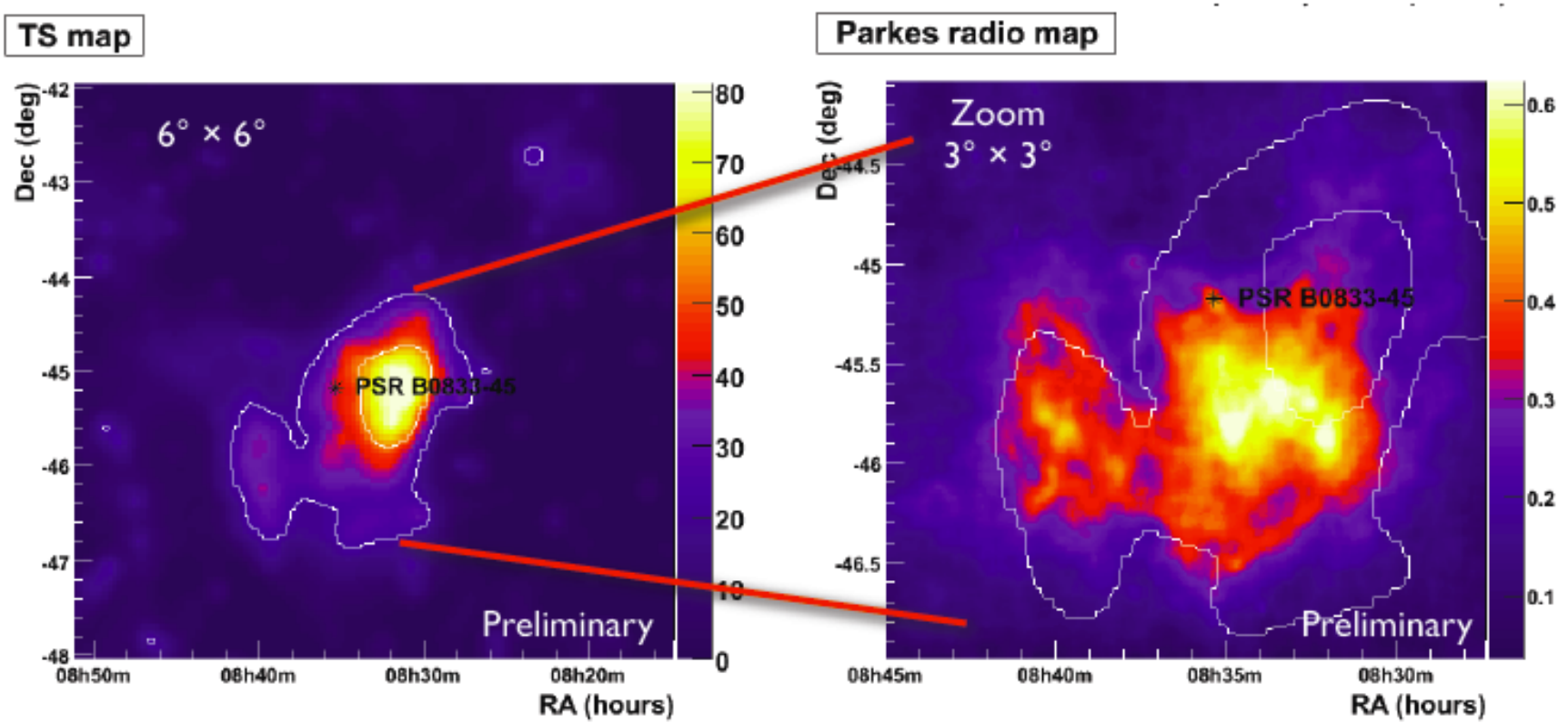

Vela-X, Fermi-AGILE comparison